IAEA-TECDOC-361

VEIN TYPE URANIUM DEPOSITS

REPORT OF THE WORKING GROUP ON URANIUM GEOLOGY
ORGANIZED BY THE
INTERNATIONAL ATOMIC ENERGY AGENCY

A TECHNICAL DOCUMENT ISSUED BY THE
INTERNATIONAL ATOMIC ENERGY AGENCY, VIENNA, 1986

VEIN TYPE URANIUM DEPOSITS
IAEA, VIENNA, 1986
IAEA-TECDOC-361

Printed by the IAEA in Austria
January 1986

PLEASE BE AWARE THAT
ALL OF THE MISSING PAGES IN THIS DOCUMENT
WERE ORIGINALLY BLANK

FOREWORD

The great surge of interest and activity in exploration for uranium deposits over the last decade has added significantly to our knowledge of uranium geology and the nature of uranium deposits. Much of the information that has been developed by government and industry programmes has not been widely available and in many cases has not had the benefit of systematic gathering, organization and publication. With the current cut-back in uranium exploration and research efforts there is a real danger that much of the knowledge gained will be lost and, with the anticipated resurgence of activities, will again have to be developed, with a consequent loss of time, money and effort. In an effort to gather together the most important information on the types of uranium deposits, a series of reports is being prepared, each covering a specific type of deposit. These reports are a product of the Agency's Working Group on Uranium Geology. This group, which has been active since 1970, has gathered and exchanged information on key questions of uranium geology and co-ordinated investigations on important geological questions.

The projects of the Working Group on Uranium Geology and the project leaders are:

Sedimentary Basins and Sandstone-type Deposits
- Warren Finch -

Uranium Deposits in Proterozoic Quartz-Pebble Conglomerates
- Desmond Pretorius -

Vein-type Uranium Deposits
- Helmut Fuchs -

Proterozoic Unconformity and Stratabound Uranium Deposits
- John Ferguson -

Surficial Deposits
- Dennis Toens -

The success of the projects is due to the dedication and efforts of the project leaders and their organizations, and the active participation and contribution of world experts on the types of deposits involved. The Agency wishes to extend its thanks to all involved in the projects for their efforts. The reports constitute an important addition to the literature on uranium geology and as such are expected to have a warm reception by the member states of the Agency and the uranium community worlwide.

Dr. Helmut Fuchs, who guided the work of this project on vein-type deposits, his employer, Urangesellschaft mbH in Frankfurt am Main, Federal Republic of Germany, and his colleagues who assisted, deserve special recognition for their efforts in the preparation of this volume.

John A. Patterson
Scientific Secretary

NOTE

Special thanks are given to all the authors participating in this project, and to their organizations which permitted the publication of their work. It is hoped that the additional information published in this volume will help to ever better understand the origin and formation of vein-type uranium deposits around the world.

I am very much indebted to Mrs. Gundula Merwald-Kollmann for typing the manuscript, to Mrs. Elfriede Friedrich for proofreading, and to Lincoln Page and Dr. George Strnad for helping to improve the English of some papers.

Helmut Fuchs
Project Manager
Editor

EDITORIAL NOTE

In preparing this material for the press, staff of the International Atomic Energy Agency have mounted and paginated the original manuscripts as submitted by the authors and given some attention to the presentation

The views expressed in the papers, the statements made and the general style adopted are the responsibility of the named authors The views do not necessarily reflect those of the governments of the Member States or organizations under whose auspices the manuscripts were produced

The use in this book of particular designations of countries or territories does not imply any judgement by the publisher, the IAEA, as to the legal status of such countries or territories, of their authorities and institutions or of the delimitation of their boundaries

The mention of specific companies or of their products or brand names does not imply any endorsement or recommendation on the part of the IAEA

Authors are themselves responsible for obtaining the necessary permission to reproduce copyright material from other sources

CONTENTS

INTRODUCTION

H.D. Fuchs

Urangesellschaft mbH

Frankfurt am Main

Federal Republic of Germany

About 15 years ago, in the light of an assumed substantially increased demand for uranium worldwide, the International Atomic Energy Agency established the idea of creating a Geological Working Group on Uranium Geology to study the different types of uranium deposits, their formation processes, and to work out their genetic concepts. As a result, individual projects were established for various types of deposits (NN (1)). During the past years, however, the approach to classify and evaluate the uranium deposits by different projects within the Working Group has changed considerably due to the discovery of new types of uranium deposits and the better understanding of their origin. This resulted in the change from the previous project 'Vein-type and Similar Uranium Deposits in Rocks Younger than Proterozoic' (NN (2)) to 'Vein-type Uranium Deposits' to be able to include all uranium occurrences and deposits of this type, but to exclude those which are directly associated with the important Proterozoic unconformity.

To avoid any controversy with respect to the genetic origin of the various deposits, it was decided to only use a descriptive definition for the different types of deposits. Nevertheless, there may occur an overlap of projects, i.e. that some occurrences or deposits can be assigned to one project or the other.

The term 'vein-type deposit' used in this publication is only a descriptive term and follows the definition of Lindgren (3), page 155: 'Veins are tabular- or sheet-like masses of minerals occupying or following a fracture or a set of fractures in the enclosing rock; they have been formed later than the country rock and fractures, either by filling of the open spaces or by partial or complete replacement of the adjoining rock or most commonly by both of these processes combined.' This definition just describes the physical properties independently of the source of uranium, the mineralizing processes and the host rocks. As already Walker and Osterwald (4) had pointed out, this definition is simple and does not lead to any misinterpretation, but is also to some extend limited to just describing the form or shape of the deposit, but does not consider other also important characteristics.

Above given definition, however, leads in some cases to an overlap to other types of uranium deposits: no sharp line can be drawn between vein-type uranium deposits and metasomatic uranium deposits. The latter or parts of them usually have a vein-type appearance as for example the uranium occurrence of Espinharas (Fuchs et al. (5)) in Brazil and the uranium deposit of Zholtye Vody (Belevtsev et al. (6)) in the USSR. In both cases, according to the above definition, we have vein-type deposits. The reason, why a uranium occurrence of the so-called metasomatic type has been included in this publication, is to show the great variety of this type of deposits. It is the uranium occurrence of Kitongo in Cameroon (Oesterlen and Vetter (7)).

Concerning the relationship between the 'classic' veins and the unconformity-related uranium deposits, it is still more difficult to draw a dividing line, since most of these deposits or parts of them are vein-type deposits. Due to their economic importance, a separation from the classic veins is justified. Artru et al. (8), however, show convincingly that also in this case a close relation exists between those two types of deposits. Even between sedimentary deposits and vein-type deposits the boundary is not always well defined as it is known from the uranium deposit of Gabon (Ampamba-Gouerangue (9)). Here, the vein-type deposits show a very close relation to stratiform deposits.

Since vein-type uranium occurrences and deposits are widely distributed with respect to time, space and rock type, it is very difficult to propose a common synthesis for such uranium concentration. To approach this problem, it may be necessary to classify the vein-type deposits by genetic sub-groups to define their common features and to compare these different sub-groups with each other. Such an approach, however, is beyond the scope of this publication.

As pointed out before, no specific classification of the various groups of vein-type uranium deposits has been proposed but to bring system into the presentation of the individual papers, the volume begins with the occurrences and deposits known from old shield areas and the sedimentary belts surrounding them. They are followed by papers describing the European deposits mostly of Variscan age, and by similar deposits known from China being of Jurassic age. The volume is completed by two papers which do not fit exactly in the given scheme.

REFERENCES

(1) NN, Discussions of the Uranium Geology Working Group IGC, Sydney, Techn. Rep. series no. 183, IAEA, Vienna (1978) 88 pp.

(2) NN, Foreword in: Vein-type and Similar Uranium Deposits in Rocks Younger than Proterozoic, IAEA, Vienna (1982) 385 pp.

(3) LINDGREN, W., Mineral Deposits, 4th Ed. McGraw-Hill Book Co. Inc., New York, London (1933) 930 pp.

(4) WALKER, G.W., OESTERWALD, F.W., Introduction to the geology of uranium-bearing veins in the conterminous United States, including sections on geographic distribution and classification of veins, in: Geology of Uranium-bearing Veins in the Conterminous United States, Geol. Surv. Prof. Paper 455-A (1963) 1-28.

(5) FUCHS, H.D., DA FONTE, J., SUCKAU, V., THAKUR, V., The Espinharas Uranium Occurrence, in: Uranium Exploration Case Histories, IAEA, Vienna (1981) 3-13.

(6) BELEVTSEV, Y.N., BATASHOV, B.G., KOVAL, V.B., The Zholtye Vody Uranium deposit and the Iron Ore Deposits of Krivoi Rog, Internat. Geol. Congress, XXVII Session, Moscow, Guide Book, Naukova Dumka Publishers, Kiev (1984) 32 pp.

(7) OESTERLEN, M., VETTER, U., Petrographic-geochemical characteristics and genesis of an albitized uraniferous granite in Northern Cameroon, Africa (1985) 121-151.

(8) ARTRU, P., BERVILLE, M., MOREAU, M., TONA, F., Geological environment of the vein-type deposits in the Aphebian basement of th- Carswell structure on the Athabasca Plateau (Northern Saskatchewan) - Comparison with other deposits of the same type (1985) 57-78.

(9) AMPAMBA-GOUERANGUE, P., Uranium in Gabon, in: Uranium and Nuclear Energy 1982, Proceedings of the 7th International Symposium held by the Uranium Institute - London, 1st - 3rd September 1982 Butterworths (1982) 93-125.

THE PROBLEM OF URANIUM MINERALIZATION IN PRECAMBRIAN METAMORPHIC SHEAR TECTONITES - WITH PARTICULAR REFERENCE TO THE SINGHBHUM COPPER-URANIUM BELT, EASTERN INDIA

S.C. Sarkar
Department of Geological Sciences
Jadavpur University
Calcutta
India

Abstract

THE PROBLEM OF URANIUM MINERALIZATION IN PRECAMBRIAN METAMORPHIC SHEAR TECTONITES - WITH PARTICULAR REFERENCE TO THE SINGHBHUM COPPER-URANIUM BELT, EASTERN INDIA

Uranium mineralization has taken place discontinuously along the 200 km long Singhbhum Copper-Uranium Belt, Eastern India, concentration being more in the central part. The early Proterozoic rocks containing the mineralization are

- chlorite-biotite quartz schist containing apatite, magnetite and tourmaline,
- quartz-chlorite schist containing apatite and magnetite,
- biotite-chlorite schist,
- brecciated quartzite and soda (-silica)-metasomatites.

The rocks are characterized by L-S type structures and zones of mylonitization

The sheet-like orebodies, sometimes occurring more than one at a place, are conformable with the compositional banding and schistosity in the host rocks. The long axis of the ore shoots are parallel to the dominant lineations in the host rocks that are almost down-dip. The principal orebody at Jaduguda extends for more than 1 km along the dip (40° to 60°). There is evidence on all scales that deformation has outlasted ore mineralization. The zones of intense copper and uranium mineralization do not coincide, although some uranium is recoverable from the tailings of the copper ores from most of the deposits mined.

The average grade of the uranium ore from the Singhbhum Belt is $< 0.01\%$ U_3O_8. The principal ore mineral, uraninite, occurs as disseminated grains and crystals. Other uranium-bearing minerals are sooty pitchblende, a complex U-Ti oxide, allanite, xenotime, davidite, pyrochlore-microlite, clarkeite, autunite, torbernite, schoepite and uranophane Ni(-Co)-Mo-S(-As-Se)-mineralization occurs close to that of uranium in the Jaduguda-Bhatin sector. The dominance of uraninite over pitchblende, the presence of several percents of REE in uraninite, the development of hematite-bearing quartz and sodic oligoclase at places, the local association of uranium mineralization and Ni(-Co)-Mo-S(-As-Se)-mineralization and the continuation of some of the ore veins to considerable depth suggest these ores formed at moderately high temperatures. The age of mineralization is 1500 to 1600 Ma.

The origin, concentration and deposition of uranium, leading to the formation of the orebodies is still unsolved. It is possible that the uranium initially came from the Singhbhum Granite to the south, was deposited in the basal sediments of the Dhanjori-Chaibasa sequence and was later mobilized during the subsequent geological evolution of the Belt. If so, the question to be solved is how the uranium initially precipitated as U (IV), became oxidized to U (VI) for

mobilization during metamorphism and why have some structures been mineralized and others of the same time not. Petrographic observations do not help locating the precipitants. In Singhbhum, as in some other shield areas, uranium mineralization took place along abyssal regional faults or shear zones, characterized by quartzo-feldspathic (Na) metasomatism. In such cases, the uranium might have migrated upward from the middle-lower crust along a deep dislocation zone during the first major tectono-thermal event, after the climacteric development of the crust at the end of the Archaean. This explanation may be an alternative to a concentration of uranium by lateral secretion at least in such situations.

1. INTRODUCTION

The Singhbhum Copper-Uranium Belt is in eastern India and runs from Duarpuram in the west to Mayurbhanj in the east. It stretches for about 200 km in an arcuate fashion and contains the most important deposits of copper and uranium in the country, the middle part of the Belt having the best mineralized sections. The copper and uranium deposits occur close to each other, but the important deposits do not coincide.

The deposits are in metamorphosed rocks and most of them underwent either partial or complete metamorphism. The primary features of the ores, orebodies, host rocks and the host-orebody relations are either obliterated or modified in varying degrees. The problem is complicated further because the mineralization is localized in metamorphic tectonites where at least some phases of the shear movement is younger than the metallization. In such metamorphic tectonites the labile nature of uranium is important in explaining the metallogenesis, especially along the Singhbhum Copper Belt.

2. REGIONAL GEOLOGICAL SETTING

The Singhbhum area, commonly subdivided into two parts, the South Singhbhum and North Singhbhum, is in general an Archaean-Proterozoic terrain. The Singhbhum Copper-Uranium Belt, a zone of intense tectonization, separates the two parts. For the most part, South Singhbhum is underlain by the Singhbhum Granite Batholith, composed mainly of biotite granodiorite, biotite-muscovite adamellite and leucogranite. The magmatic character of this massif is evident at many places. The high initial $^{87}Sr/^{86}Sr$ ratio of 0.711 $\pm$ 0.009 (Sarkar et al. (1)) in these rocks suggest that they originated by melting of pre-existing quartzo-feldsphatic material, rather than by fractionation of upper mantle or the mafic lower crust. The limited number of chemical analyses show that these, compared with granitic rocks of similar bulk composition, are richer in B, Sr, Ni and U and poorer in V, Mn, Ba and Y. In this granitic massif there are numerous bodies of biotite-tonalite gneiss that grade into granodiorite. The low initial $^{87}Sr/^{86}Sr$ ratio of 0.7018 $\pm$ 0.003 in these rocks (Sarkar et al. (1)) suggests their origin in the upper mantle. These tonalite inclusions are about 3800 Ma (Sm/Nd method: Basu et al. (2)) old and are associated with some metasediments of the same or older age. The latest estimate of the radiometric age (Rb/Sr) of the Singhbhum Granite is 2950 Ma.

The metasedimentary rocks at the eastern and western flanks of the granitic massif are more extensive to the west and consist mainly of shales, sandstones (arkose, orthoquartzite) and iron formations, a major source of iron in India.

Along the shear zone a variety of feldspathic metasomatites have developed and these are called Soda Granite and Arkasani Granophyre, depending on the petrographic details. The Chakradharpur Gneissic Complex - which may be related to

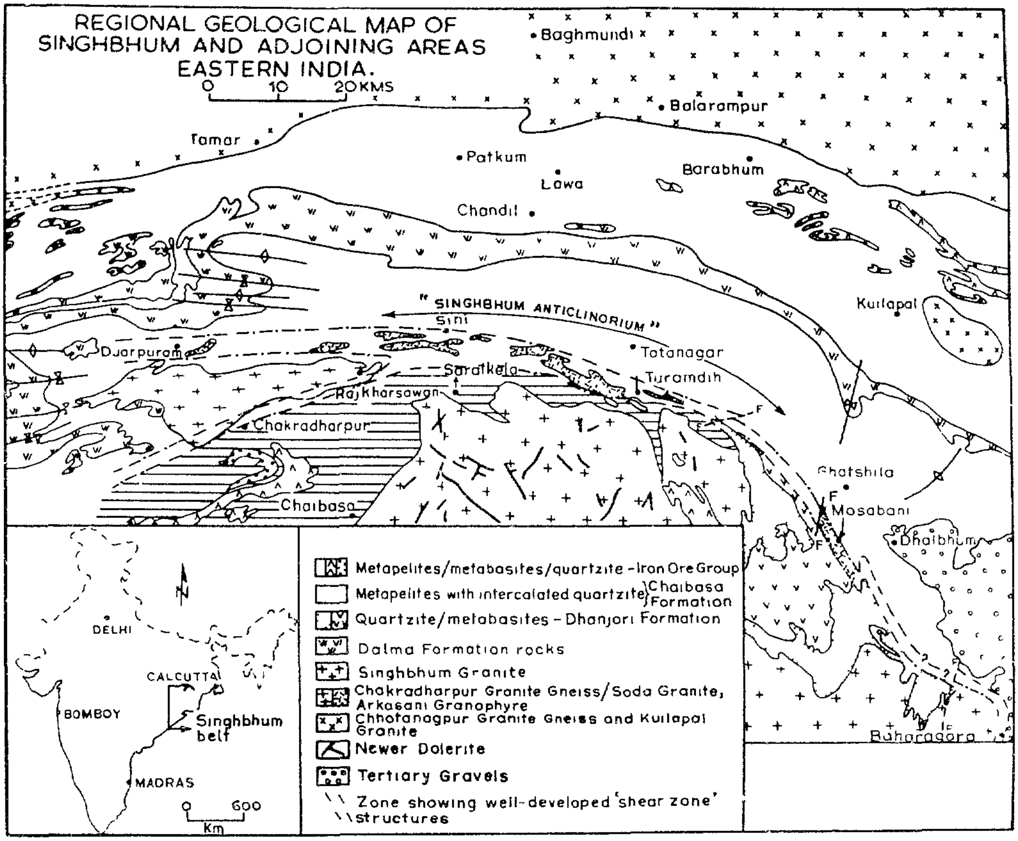

FIG. 1. A generalized geological map of the Singhbhum region.

the Singhbhum Granite - is a lensoid mass composed primarily of banded trondhjemitic material and is intruded by a later granodiorite-quartzmonzonite. This massif, though occurring within the shear zone can be correlated with the granitic rocks further south.

The Dhanjori Volcanics, mainly tholeiitic with local ultramafic members, occur in and just south of the shear zone in the southern part of Singhbhum. These are underlain by and interlayered with clastic sediments.

The rocks to the north of the shear zone are pelitic except in the Dalma volcanic range (Fig. 1), where the rocks range from basic komatiite to tholeiite.

To the north of the shear zone the metamorphic grade is generally high, usually amphibolitic. To the south it is generally low green schist facies, except where the Older Metamorphics occur.

The Dhanjori Volcanics, if they are to be correlated with the Simlipal Complex, should be dated as Early Proterozoic (Sarkar (3)). Reliable stable isotope dating for the Soda Granite does not exist but a good part of the Soda Granite along the shear zone formed by metasomatic replacement of the basic Dhanjori Volcanics or their transformed products, the chlorite schists. The metamorphic age of the metasediments north of the shear zone ranges between 1600 Ma and 900 Ma.

The regional structures in the Singhbhum region considered from the north to south are the Dalma Syncline followed by the Singhbhum Anticlinorium in the south, ending up in a shear zone of regional dimension around the Singhbhum Granite Massif (a 'protocontinent') in the south.

The principal geological events (other than mineralization along the shear zone) in the region are outlined in Table I.

TABLE I. PRINCIPAL GEOLOGICAL EVENTS OF THE SINGHBHUM BELT

ROCK UNITS	AGE	LITHOLOGY (NAMES)
LATE MAFIC AND ULTRAMAFIC INTRUSIVES		
YOUNGER GRANITE ROCKS		SODA GRANITE, ARKASANI GRANOPHYRE, MAYURBHANJ GRANITE
	1600 - 900 MA (METAMORPHIC AGE)	SINGHBHUM OROGENY (CULMINATING IN THE DEVELOPMENT OF THE SINGHBHUM SHEAR ZONE)
SINGHBHUM GROUP		CHAIBASA FORMATION: MAINLY PELITIC SEDIMENTS DHANJORI FORMATION: VOLCANO-SEDIMENTARY PILE (DALMA, SIMPLIPAL, JAGANNATHPUR)
		UNCONFORMITY
SINGHBHUM GRANITE	~2950 MA	(ALSO CHAKRADHARPUR GNEISSIC COMPLEX ?)
		IRON ORE OROGENY
IRON ORE GROUP	(NOT CLEAR, MAY BE EVEN PROTEROZOIC)	PELITIC SEDIMENTS, BANDED IRON FORMATION ± MAFIC VOLCANICS
		UNCONFORMITY
TONALITIC GNEISS	~3800 MA	
		OLDER METAMORPHIC OROGENY
OLDER METAMORPHIC GROUP		METASEDIMENTS

3. GEOLOGICAL SETTING OF THE DEPOSITS

The Singhbhum Copper-Uranium Belt coincides with a uniquely tectonized zone known as the Singhbhum Thrust Belt (STB), Singhbhum Shear Zone (SSZ) or the Copper Belt Thrust (CBT).

This zone, from the structural point of view, is characterized by rocks in which the compositional banding is subparallel to the dominant planar structures of thermo-tectonic to tectonic origin. Large-scale fold structures with subhorizontal to low-dipping axes are common in the north. In this zone, however, almost down-dip folds and warps of various size, and different linear structures of tectonic origin are characteristic. The dominant secondary planar structure in the shear zone is schistosity. But shear planes subparallel with the schistosity or making acute angle with it are also common. Movements along those structures are limited. Mylonites and phyllonites are common. In short the rocks can be referred to L-S type tectonites.

There are several post-mineralization transverse faults in the zone with conspicuous slip, but there is no proof of large scale lateral movement along the Belt or across its length and, therefore, it should not be called thrust zone. At the existing erosion level this zone would better be called a zone of ductile shear (Sarkar (3)).

The dominant rock types along the Belt are mafic schists, pelitic schists, albite-bearing gneisses and granitoids known as the Soda Granite and quartzite or quartz schists. The mafic schists originated from the Dhanjori Volcanics during shearing and metamorphism. The so-called Soda Granite formed mainly from the mafic schists by metasomatism (Sarkar (3)). The Arkasani Granophyre occurring at the western part of the Belt in the same strike-continuation of the Soda Granite also appears to be of metasomatic origin. Some of the quartzose rocks could be originally volcanogenic (chert) but some are obviously of clastic origin. Arkose-conglomerate is found towards the base of the Dhanjori Volcanics.

The shear zone rocks show evidence of both progressive and retrogressive metamorphism. The grade of progressive metamorphism in the central part of the belt is upper green-schist facies whilst it rises to low amphibolite facies near its two ends.

4. ORE DEPOSITS AND THEIR HOST ROCKS

The entire shear zone is characterized by abnormal radioactivity but only at a few places the mineralization is significant enough to justify detailed investigations. These are (Fig. 2):

(i) Khadandungri-Purandungri

(ii) Bagjata-Moinajharia

(iii) Bhalki-Kanyaluka

(iv) Badia-Mosabani

(v) Surda-Rakha Mines

(vi) Jaduguda-Bhatin

(vii) Naroapahar

(viii) Turamdih-Keruadungri

In the Khadandungri-Purandungri, Bagjata-Moinajharia and Bhalki-Kanyaluka regions the tabular orebodies are of up to 800 m in strike length and 3 m in thickness. They lie conformable to the ambient schistosity and have been found

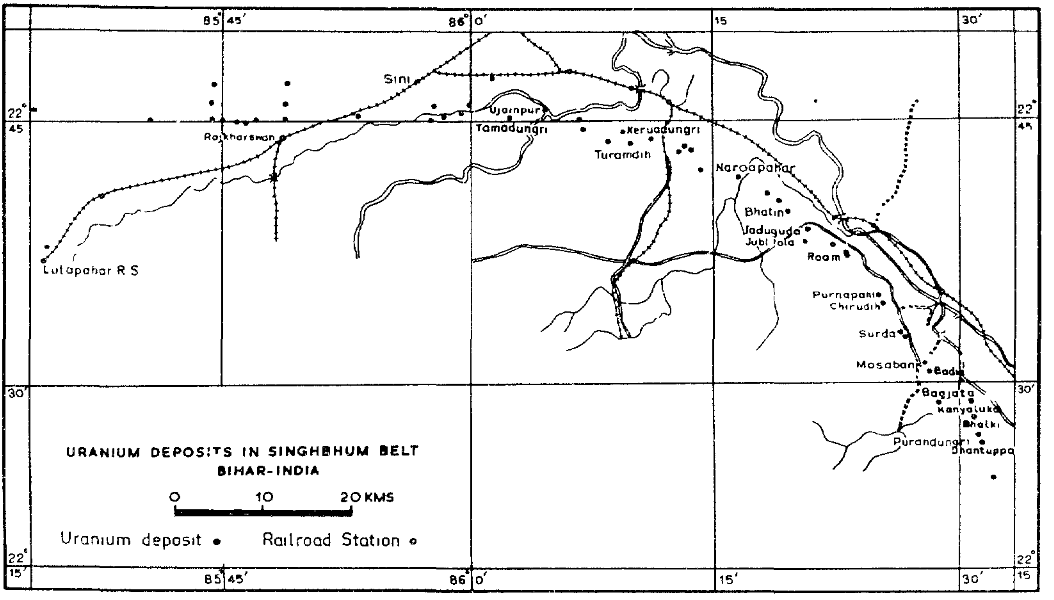

FIG. 2. Map showing the distribution of the uranium deposits along the Singhbhum Belt.

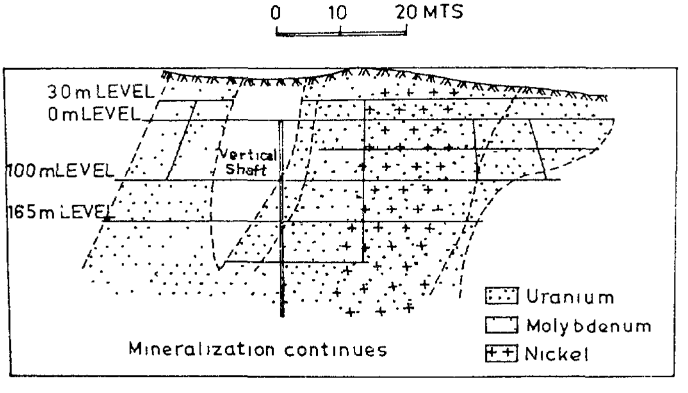

FIG. 3. A longitudinal section of the Jaduguda Mine.

in biotite schists, chlorite-biotite schists and quartz-muscovite-biotite schists. At the first two locations the ore is associated with apatite and magnetite whilst in the last one the ore zones are separated by a barren zone of about 30 m. Patches of albitic schists or of Soda Granite are present in the ore zone. The deposit has an average grade of 0.05 % U_3O_8. No wall-rock alteration was noted.

The Badia-Mosabani region is known for the mining of copper ore, that occurs mainly in the so-called Soda Granite, near its border with the metamorphosed Dhanjore Volcanics. In these mines bulk samples were collected that contained about 0.05 % U_3O_8 and in a few places as much as 0.09 % U_3O_8 (Bhola (4)).

The Surda-Rakha Mines sector is also important for copper. Here the ore lenses may contain as much as 0.08 % U_3O_8. The uranium occurs in close association with copper-ore bodies, but they are not necessarily coincident. The host rock for both the copper and uranium is chloritic quartz schist with apatite, magnetite, biotite, and tourmaline.

Until now the most important deposit of the Belt is located at Jaduguda where mining has been in progress for more than a decade. Two subparallel ore bodies, 60 m apart across strike, have been located. The larger one, i.e. the 'foot-wall lode', varies in thickness from about 6 m in the upper levels to about 20 m at a depth of about 300 m and then starts thinning again. Along strike, its existence has been proven for a distance of over 1 km with an intermediate barren zone of about 100 m that disappears down-dip (Fig. 3). The ore bodies lie conformable within the rocks which dip at an angle of 40° to 60°. Ore shoots are parallel to the down-dip lineations. The foot-wall orebody has been traced for more than 1 km down-dip. Below a vertical depth of 425 m the grade of ore improves to an average of 0.067 % U_3O_8. The rocks that host the uranium mineralization are chlorite- and biotite-bearing quartz schists, with apatite, magnetite, and tourmaline as accessories, biotite-chlorite schists, brecciated quartzites and conglomerates (autoclastic ?). The adjoining Bhatin deposit is more or less similar except that the mineralization was less intense. The deposits are separated by a post-mineralization transverse fault.

At Naroapahar exists a low grade but large tonnage deposit extending for a strike length of over 3 km. There are two subparallel orebodies in this deposit, conformable to the dominant planar structures of the host rock. The more important lower one has an average thickness of 5 m and has been traced over a vertical depth of over 500 m. The average grade is 0.058 % U_3O_8. The ore shoots follow the down-dip lineations. The host rock is a sericitic chlorite schist with abundant introduced quartz and some feldspar. Dusty hematite in quartz and feldspar can be seen at places.

At Turamdih, south of Tatanagar, a zone of uranium minerals has been detected 30 m above the zone of copper mineralization. The deposit occurs in sericitized chlorite schists. Its average grade is 0.04 % U_3O_8 (Fig. 4). At Keruadungri, 1 km to the north of Turamdih, a leaner zone of uranium minerals of the same type has been recognized.

5. MINERALOGY OF THE URANIUM ORE

Uraninite as discrete disseminated grains (Fig. 5) is the principal uranium mineral. Near surface pitchblende is common together with autunite (metaautunite), torbernite, schoepite (metaschoepite) and uranophane (Sarkar (5)). Allanite and xenotime are reported from several places. Rao (6) reported clarkeite, davidite, and brannerite from some localities. The Singhbhum uraninite is low in thorium (UO_2/ThO_2 = 70-150), high in lead (PbO = 14-15 %) (Rao (6)) and moderate in REE content (Shankaran et al. (7)). Limited determinations of cell dimension give values ranging between 5.42 and 5.55 Å.

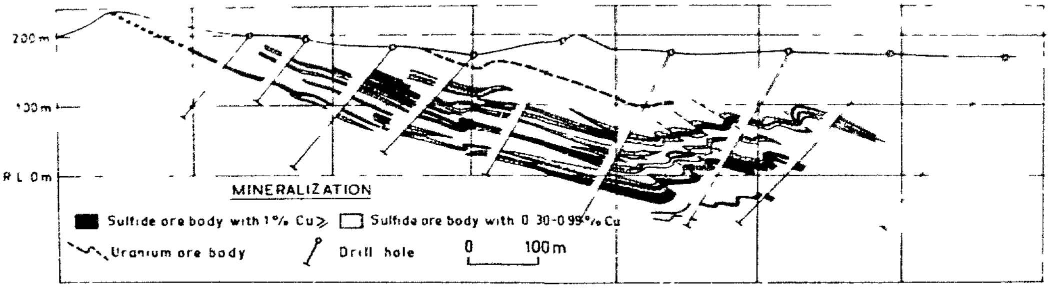

FIG. 4. A transverse section across the Turamdih ore zone.

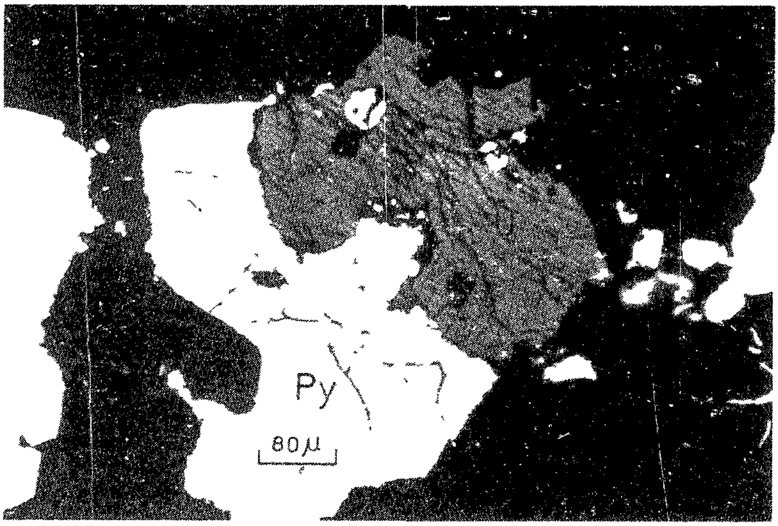

FIG. 5. A photo-micrograph showing isolated nature of the grains of uraninite in the Singhbhum ores.

Chlorite, biotite, tourmaline, apatite, magnetite, and quartz in the ore zone have been found to be radioactive. The source of radioactivity is uranium in the structural sites of these minerals or as inclusions of uraninite, or both (Sarkar (5)).

Nickel and molybdenum are obtained as by-products from the Jaduguda-Bhatin ore. Nickel occurs principally as millerite and as ferruginous heazlewoodite. Melonite is a rare phase. Pyrite, chlorite and biotite within the ore contain a small proportion of nickel. At some places molybdenite is disseminated with magnetite but the bulk of it occurs in late veins.

6. AGE OF MINERALIZATION

Vinogradov et al. (8) and Rao et al. (9) studied the Pb-isotope geochronology of these ores from several places in the Belt. The age obtained from the Pb^{207}/Pb^{206} ratio and the Concordia method (Fig. 6) are close to each other and may be taken as the age of deposition of uranium in the Singhbhum Belt. They

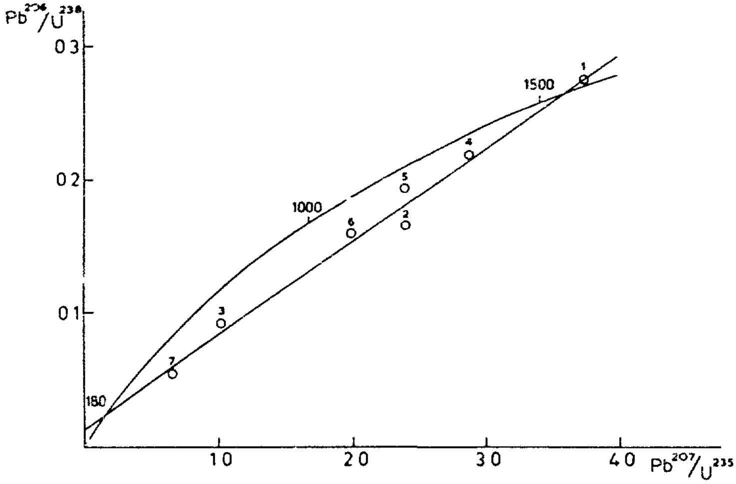

FIG. 6. Concordia plots of uraninite and apatites from the Singhbhum Belt. Data from Vinogradov et al. (8) and Rao et al. (9).

suggest that most of the Singhbhum uranium has an age of 1500 to 1600 Ma, an age not much different from the uranium of vein-type deposits in parts of the Precambrian shields of Canada and Australia (1700 - 1800 Ma).

7. ORE GENESIS

The metallogenesis of the Singhbhum Belt is controversial - whether one refers to base metal deposits or to the uranium deposits. The balance of evidence supports an initial volcanic hydrothermal deposition with subsequent modifications (Sarkar (3)) for the base metal (Cu-rich) deposits. This is more or less true for the less important apatite-magnetite deposits. But this does not seem valid for the radioactive ores because

(i) the country rocks that host the important uranium deposits of the Belt are biotite and/or chlorite rich (± apatite, magnetite) metamorphosed rocks which originated from either graywackes (Surda-Bhatin sector) or mafic volcanics, known for their low contents of uranium.

(ii) the orebodies are tabular and more or less concordant with secondary planar structures within the country rocks.

(iii) The ore shoots, where defined, are sub-parallel to the down-dip lineations.

(iv) Typical wall rock alterations are absent. The hematitization noted in Jaduguda-Bhatin and Naroapahar is neither intense nor correlatable with the intensity of uranium mineralization. Late fluorite veins and veinlets seen at Naroapahar are also not correlatable with the uranium.

(v) The principal uranium mineral is a low Th-uraninite with high Pb content.

(vi) The continuation of some of the orebodies up to considerable depth.

(vii) Nickel and molybdenum minerals are also noted within the principal orebodies at Jaduguda and Bhatin.

The question arises, do the above characteristics of the uranium ore deposits of the Singhbhum Belt qualify them to be grouped under vein or vein-type deposits? They will, if we define a vein deposit as follows:

> A vein deposit is one that has been emplaced in a deformational structure by processes such as precipitation from hydrothermal solutions, deposition from diffusing ions, or consolidation of plastic flow of mineral matter. The deposits may vary from a more or less sheet-like to an irregular body. It is epigenetic with respect to the initial formation of the host rock but may be contemporaneous with its recrystallization during diagenesis or metamorphism. Wall rock alterations may or may not be conspicuous.

Banerjee (10) suggested that the radioactive elements were partly indigneous to the rock material that was migmatized and partly extraneous, having been introduced from shear zone during migmatization i.e. formation of the Soda Granite. In a later contribution (Banerjee et al. (11)) this was modified and it was suggested that uranium originated from the migmatized material.

Bhola et al. (12) believed that the ore-bearing hydrothermal solutions emanated from a cooling magma that led to the formation of the Soda Granite.

Mookerjee (13), Rao (6) and Rao et al. (14) suggested that uranium was originally distributed in the country rocks, particularly the metasediments (Chaibasa Formation) lying north of the shear zone, and was later mobilized during deformation and metamorphism.

Sarkar (5) discussed this problem extensively. Some of the points raised are repeated and some new ones added here. It seems possible that uranium, disseminated in the basal sediments of the Singhbhum Group, was mobilized and precipitated again during the tectono-thermal evolution of the Singhbhum shear zone. This does not exclude, however, the introduction of metals and the exchange of rock constituents during the operation of an early hydrodynamic system that might have developed along the dislocation zone. The ultimate source of uranium may be located in the Singhbhum Granites in the south. A few analyses of these granites show local above average uranium content (Bhola (4), Saha et al. (15)).

It is difficult to explain how the metamorphogenic hydrothermal solutions will be oxidizing enough to leach U (IV) from its original state, to mobilize and then remobilize it into an ore deposit. Rich et al. (16) suggested that the presence of red beds in the right hydrologic position is apparently required to solve this problem. Such a situation apparently did not exist in Singhbhum. Another suggestion is that migration of a large volume of fluid along shear zones is involved and that in such a situation the fluid is likely to be oxidizing (Fyfe et al. (17)). If these fluids were involved in the deposition of uranium, then the mobilization and remobilization of uranium took place entirely during retrogressive metamorphism. Although there have been several metamorphic events in the Belt, uranium was not regenerated after its initial formation during the first metamorphic episode.

As shown in the earlier part of this discussion, mafic schists are the common host for uranium mineralization in the Belt.

Now coming to the problem of uraninite precipitation in the ore, one would, in the absence of carbonate in the ores, conjecture that the element was introduced in the form of uranyl ions from which uranium precipitated due to cooling of the fluid, reaction of uranyl with Fe (II) in the silicates of the zone, or by some other mechanism not understood at the moment. There is no petrographic evidence to support that the magnetite and the sulfides present in the zone played any important role in precipitating uraninite through reaction with the uranyl ions.

It is interesting to note that in Singhbhum, as in some other shield areas (Abou-Zied et al. (18), Kazdan (19)) uranium minerals are concentrated along absyssal faults or shear zones of regional scale, characterized by sodium (Na) metasomatism. In such cases a migration of uranium upwards from the middle-lower crust along deep reaching dislocation zones may be possible. This may have happened during the first major tectono-thermal event after the climacteric development of the crust at the end of the Archaean. This would be an alternative to or complementary to a concentration of uranium by lateral secretion during progressive or retrogressive metamorphism.

The base metal, uranium and apatite-magnetite mineralization took place in distinct but different metallogenic episodes because the main concentrations of these three elements are not coincident. There is also a difference in the genetic processes of ore formations. It is difficult to pin point the sequence, although the sulfide mineralization, being of volcanogenic hydrothermal origin (Sarkar (3)), is possibly the earliest. Direct evidence of intersection of one body by another, or mineralization of structures of different generations by different ore types, are lacking. Petrographic features such as 'replacement' of uraninite by chalcopyrite etc. locally seen are unreliable in such a situation since the Belt has a history of repeated deformation and metamorphism when diffusion and plastic flowage of some minerals would be easy, obscuring the early relationship amongst the minerals in an assemblage.

ACKNOWLEDGEMENTS

Exploration of the Singhbhum uranium deposits was done mainly by the Department of Atomic Energy. The author is obliged to it for its cooperation during the present work.

REFERENCES

(1) SARKAR, S.N., SAHA, A.K., BOELRIJK, N.I.A.M., HOBEDA, E.H., New data on the geochronology of Older Metamorphic Group and the Singhbhum Granite of the Singhbhum-Keonjhar-Mayurbhanj region, eastern India, Ind. Jour. Earth Sciences 6 (1979) 32-51.

(2) BASU, A.R., RAY, S.L., SAHA, A.K., SARKAR, S.N., Eastern Indian 3800 million years old crust and early mantle differentiation, Science 212 (1981) 1502-1505.

(3) SARKAR, S.C., Geology and ore mineralization of the Singhbhum Copper-Uranium Belt, eastern India (a monograph under publication)

(4) BHOLA, K.L., Radioactive deposits in India, Symp. Vol., uranium prospecting and mining in India, DAE, Jaduguda (1965) 1-45.

(5) SARKAR, S.C., Uranium (nickel-cobalt-molybdenum) mineralization along the Singhbhum copper belt, India and the problem of ore genesis, Mineral Deposita 17 (1982) 257-278.

(6) RAO, N.K., Mineralogy, petrology and geochemistry of uranium prospects from parts of Singhbhum shear zone, Bihar (Ph.D. thesis, Banaras Hindu University) (1977).

(7) SHANKARAN, A.V., BHATTACHARYYA, T.K., DAR, K.K., Rare earth and other trace elements in uraninites, Jour. Geol. Soc. India 11 (1970) 205-216.

(8) VINOGRADOV, A., TUGARINOV, A., ZHYKOV, C., SPANIKOVA, N., BIBIKOVA, E., KHORRE, K., Geochronology of Indian Precambrians, Rept. 22nd Intern. Geol. Cong. 10 (1964) 553-567.

(9) RAO, N.K., AGGARWAL, S.K., RAO, G.V.U., Lead isotope ratios of uraninites and the age of uranium mineralization in Singhbhum shear zone, Bihar, Jour. Geol. Soc. India 20 (1979) 124-127.

(10) BANERJEE, A.K., Cross folding, migmatization and ore localization along part of the Singhbhum shear zone, south of Tatanagar, Bihar, India, Econ. Geol. 57 (1962) 50-71.

(11) BANERJEE, A.K., TALAPATRA, A.K., SHANKARAN, A.V., BHATTACHARYYA, T.K., Ore genetic significance of geochemical trends during progressive migmatization within part of the Singhbhum shear zone, Bihar, Jour. Geol. Soc. India 13 (1972) 39-50.

(12) BHOLA, K.L., RAMA RAO, Y.N., SURI SASTRY, C., MEHTA, N.R., Uranium mineralization in Singhbhum thrust belt, Bihar, India, Econ. Geol. 61 (1966) 162-173.

(13) MOOKERJEE, D., Geokhimicheskiye cherti orudeniya v granitakh Dhabi (Avtoreferat Ph.D. thesis, Moscow State University) (1975)

(14) RAO, N.K., RAO, G.V.U., Uranium mineralization in Singhbhum shear zone, Bihar, Jour. Geol. Soc. India 24 (1983) 615-627.

(15) SAHA, A.K., SHANKARAN, A.V., BHATTACHARYYA, T.K., A preliminary study of the distribution of uranium and thorium in the granitic rocks of Singhbhum, Proc. Ind. Nat. Sci. 36A (1970) 392-397.

(16) RICH, R.A., HOLLAND, H.D., PETERSON, U., Hydrothermal uranium deposits, Elsevier, Amsterdam (1977) 264 pp.

(17) FYFE, W.S., PRICE, N.J., THOMPSON, A.B., Fluids in the earth's crust, Elsevier, Amsterdam (1978) 383 pp.

(18) ABOU-ZIED, S., KERNS, G. (eds.), Albitized uranium deposits: Six articles translated from Russian literature, U.S. Department of Energy (Colorado) Publication (1980) 114 pp.

(19) KAZDAN, A.B., Associational assignment of commercial types of uranium deposits, Intern. Geol. Rev. 20 (1978) 1389-1401.

URANIUM GENESIS WITHIN THE ARJEPLOG-ARVIDSJAUR-SORSELE URANIUM PROVINCE, NORTHERN SWEDEN

U. Hålenius, J.A.T. Smellie, M.R. Wilson
Swedish Geological Company
Luleå
Sweden

Abstract

URANIUM GENESIS WITHIN THE ARJEPLOG-ARVIDSJAUR-SORSELE URANIUM PROVINCE, NORTHERN SWEDEN

The Arjeplog-Arvidsjaur-Sorsele uranium province in Northern Sweden represents a new crustal addition along the southern margin of the Svecokarelian Archaean 'Karelian Continent' with extensive granitoid formation at 1900 - 1850 Ma from igneous sources with a very short crustal history. Emplacement of the magmas has been strongly controlled by deep marginal faults. The more acid varieties of the igneous rocks can be uranium-enriched.

Granite intrusion can be considered coeval with regional metamorphism and has probably provided the driving mechanism to cause hydrothermal fluid movement. During the passage of these fluids through the volcano-sedimentary and granitic country rocks, elements such as Ca, Na, U and Ti were mobilized, concentrated and transported. Movement of these hydrothermal solutions has been facilitated by pre-existing faults and more permeable lithological horizons. Eventually, under favourable physico-chemical conditions, the precipitation of certain elements and removal of others has resulted in the formation of alkali metasomatites and later uranium mineralization.

1. INTRODUCTION

The Arjeplog-Arvidsjaur-Sorsele uranium province lies immediately south of the Arctic circle and north of the well known sulphide ore province, the Skellefte district (Fig. 1). Since geological investigations, including uranium prospecting, were initiated in the early seventies by the Swedish Geological Survey, considerable progress has been made in attempting to explain the existence of not only the many uranium mineralizations, but also spatially associated enrichments of Mo, Sn and W.

The uranium province is characterized by thirty known mineralizations, the most important of which are epigenetic in type (Adamek et al. (1), (2)) and were emplaced towards the end of metamorphism during the Svecokarelian orogeny at about 1750 Ma. In the Sorsele area, important strata-bound mineralizations occur within rhyolitic ignimbrites and porphyries which comprise part of a volcanic sequence formed during the termination of the Svecokarelian orogeny (Lindroos et al. (3), Smellie (4)). The investigated uranium occurrences, characterized mostly by uraninite, are in the form of vein and fracture infillings and disseminations, and occur in a wide variety of Proterozoic arenites, acid volcanics and granites. In addition to these minerlizations, the host rocks, which have been formed by a variety of geological processes over a very wide range of time, are also characterized by enhanced uranium contents. In other words, the province has been anomalous with respect to uranium over a long period of time.

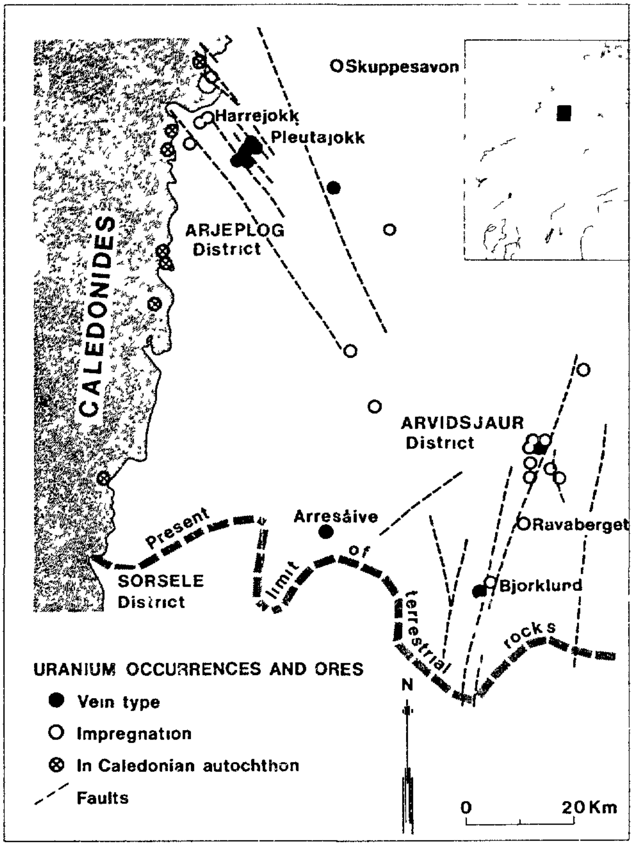

FIG. 1. The Arjeplog-Arvidsjaur-Sorsele uranium province (modified after Adamek et al. (2))

Much of the description and many of the conclusions presented in this paper are based mainly on the works of Adamek et al. (1), (2), Einarsson (5), Lindroos et al. (3), Guzman et al. (6), Gustafsson (7), Wilson (8), Smellie (4), Walser et al. (9), Wilson et al. (10), Wilson et al. (11), Wilson (12), Hålenius et al. (13), Öhlander (14), Smellie et al. (15), Smellie et al. (16) and Wilson et al. (17).

New data involving quantitative microprobe analysis of the major uranium-bearing mineral phases (i.e. uraninite and uranotitanate) are also presented, together with up-dated isotopic data on the major mineralizations and new isotopic data on genetically related granitoid intrusions which are a characteristic feature of the uranium province.

2. GEOLOGICAL SETTING

The geology and geological evolution of the uranium province (Fig. 1 and 2) has been described by Adamek et al. (1), (2), Einarsson (5), Lindroos et al. (3) and referred to by Gustafsson (7). The province is located at the southern

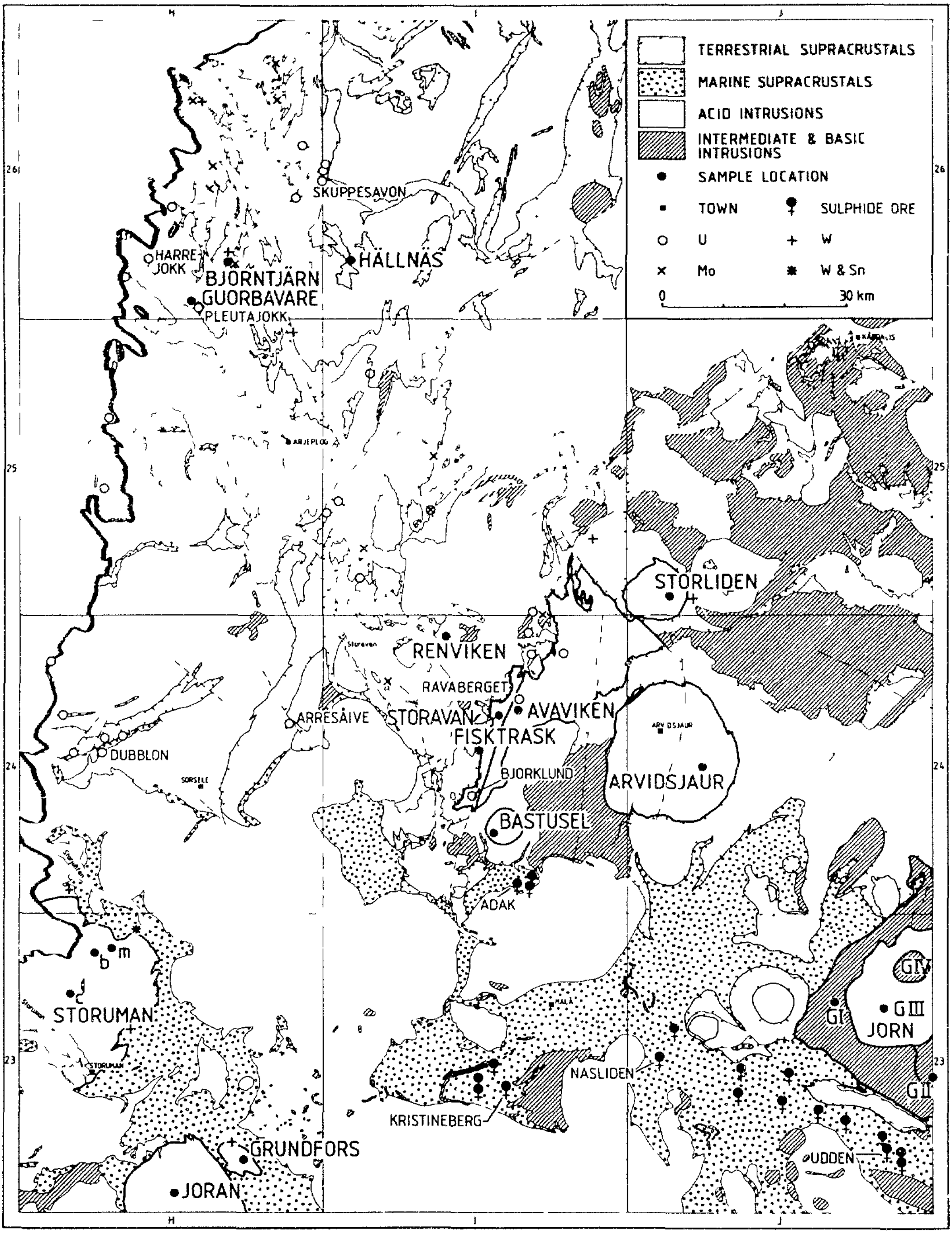

FIG. 2. Geological map of the S. Norrbotten - N. Vasterbotten region showing locations of the investigated mineralizations and granites (modified after Quesada et al. (27)).

margin of an important divide in the structure of the Baltic Shield; a transition between a northern continent and a southern ocean in Svecokarelian times (i.e. Middle Precambrian of 1950 - 1700 Ma). Along the transition between the terrestrial environment and the marine sediments is located the Skellefte sulphide province which possesses many characteristics of an island arc environment. It has been postulated that these features could be the result of subduction in a plate-tectonic model (Adamek et al. (1), (2), Rickard et al. (18), Lundberg (19), Claesson (20)).

During different stages of the Svecokarelian orogeny, the continental supracrustal rocks have been folded, faulted, recrystallized and intruded by plutonites. The investigated uranium occurrences (Fig. 1 and 2), characterized mostly by uraninite and are epigenetic in type, are associated with these supracrustal varieties and related granites. The most favourable host rocks are acid volcanic types (e.g. rhyolites at Pleutajokk) or granites from the oldest group of plutonic rocks (e.g. Björklund and Rävaberget). Uranium mineralization is rarely associated with rocks of intermediate or basic composition. Dolerite dikes often occur in the vicinity of the mineralizations but are younger; dike intrusion has been facilitated by the tectonic pattern.

The regional zones of structural weakness and bedrock lithology have played a major part in the transport of the earlier Ca- and Na-rich hydrothermal fluids and the later uranium-bearing mineralizing fluids. This has resulted in the precipitation of uranium along fractures and joints (vein-type) and as marginal dispersed concentrations (impregnation-type). Some of the uranium occurrences are dominantly vein-type (e.g. Pleutajokk), some dominantly impregnation in type (e.g. Rävaberget), whilst others exhibit both characteristics (e.g. Björklund).

3. GEOCHEMISTRY AND MINERALOGY OF THE URANIUM OCCURRENCES

Six mineralizations have been investigated in detail: Arresåive, Björklund, Harrejokk, Pleutajokk, Rävaberget, and Skuppesavon (Fig. 1 and 2).

(i) The Arresåive occurrence is associated mainly with acid volcanic porphyries although particulate tuffaceous varieties are also present. Superimposed on the primary rock fabrics is a concentrated system of veins and microfractures which contain uraninite aggregates.

(ii) The Björklund mineralization occurs within a leucocratic granite as uraninite disseminations together with fracture and fissure infillings. The uranium stage has been preceded by an episyenitization phase of local extent.

(iii) At Harrejokk, the mineralization is hosted within granites of a leucocratic nature, the uranium occurring mostly as uraninite disseminations; some fracture concentrations have also been observed.

(iv) The Pleutajokk occurrence is associated with metamorphosed acid volcanics of rhyolitic composition. Here, the uraninite is observed as concentrations along fractures and fissures.

(v) The Rävaberget mineralization is impregnation in type and occurs within a leucocratic granite. The mineralization is confined to irregular zones of episyenitized granite, the extent of which is governed by the regional joint and fracture patterns.

(vi) Lastly, Skuppesavon represents uraninite disseminations emplaced within a sequence of metavolcanics dominated by rocks of rhyolitic to trachytic composition.

TABLE 1. SUMMARY OF THE MINERALOGY AND PARAGENETIC STAGES FOR HARREJOKK, BJÖRKLUND, RÄVABERGET, PLEUTAJOKK, ARRESÅIVE AND SKUPPESAVON.

LOCALITY / PARAGENETIC STAGES	HARREJOKK Granite	BJÖRKLUND Granite	RÄVABERGET Granite	PLEUTAJOKK Acid Volcanics	ARRESAIVE Acid Volcanics	SKUPPESAVON Acid Volcanics
Metamorphic stage	Amphibole + biotite Symplectic biotite + quartz Myrmekitic K-feldspar + quartz or albite + quartz	1) Albitisation 2) Garnet + biotite 3) Amphibole + sphene + epidote + magnetite + calcite 4) Sulphides + calcite	1) Albite episyenitisation 2) Biotite + calcite + Ti-oxides + sulphides	Albite + augite + riebeckite + epidote	1) Biotite + amphibole + sphene + apatite + magnetite 2) Sphene + calcite + magnetite + sulphides	1) Albitisation 2) Pyroxene + garnet + sphene + magnetite 3) Epidote 4) Amphibole + calcite + sulphides
Hydrothermal uranium mineralisation stage	1) Uraninite + calcite + fluorite + hematite + FeOOH Oxidation and alteration of mafic minerals 2) Uranotitanates					
	Dissemination type Initial part characterised by sphene and magnetite	Different types of fracture infillings Garnet association	Dissemination type Latter stages accompanied by sphene + pyrite + epidote + magnetite	Different types of fracture infillings accompanied by sphene	Fracture mineralisations and minor disseminations	Dissemination type Latter stages accompanied by sphene + epidote
Late-stage Low-temperature hydrothermal stage	Remobilised radiogenic galena, chlorite, hematite and FeOOH Alteration of uraninite to complex uranotitanates and secondary uranium silicates					
	Pyrite	Pyrite	Pyrite + Fluorite	Pyrite		

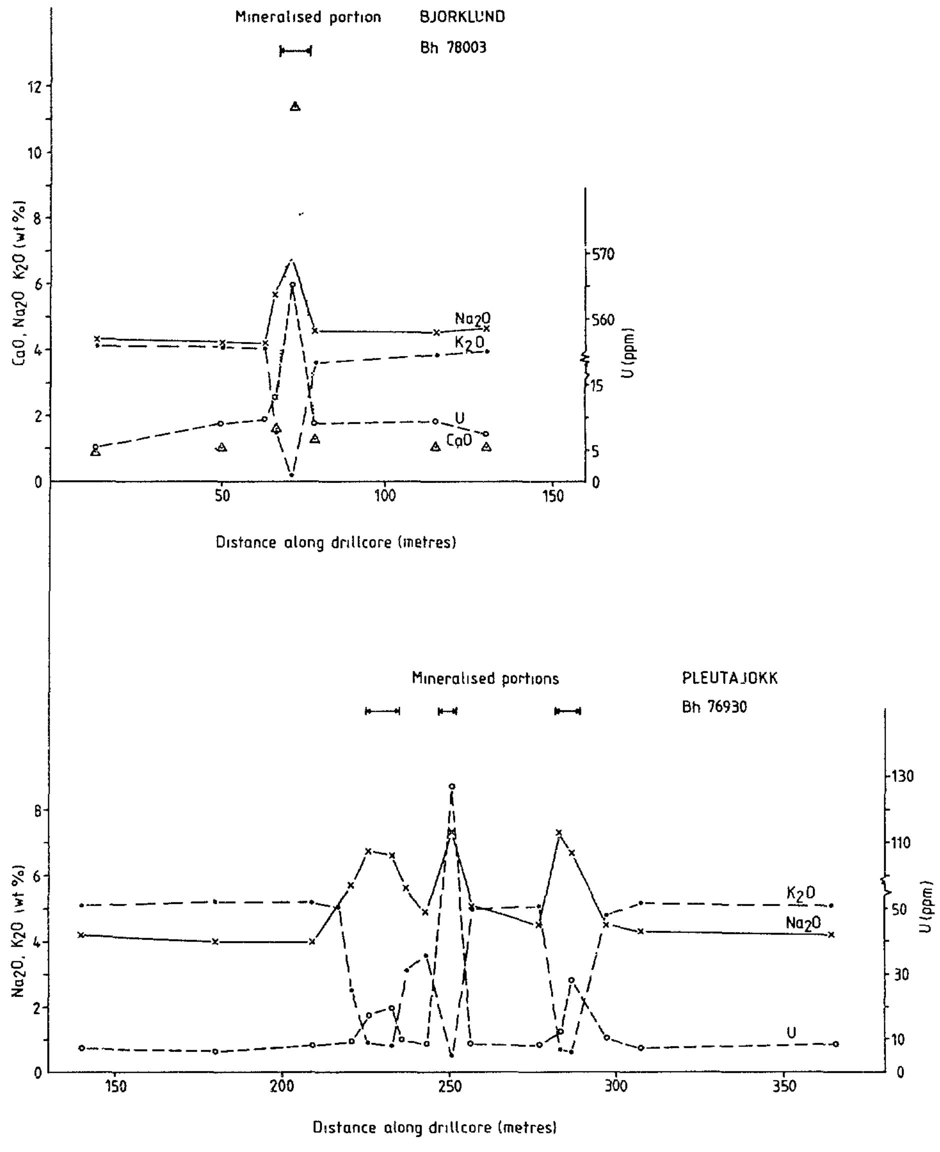

FIG. 3. Sampled profiles along drill core 78003 (Björklund) and 76930 (Pleutajokk) showing the chemical variations across the mineralized zones.

A general summation of the main mineralogical characteristics of the investigated uranium occurrences is presented in Table I. Irrespective of the host rock, the mineral evolution of the six mineralizations are all characterized by a metasomatic stage involving the introduction of solutions rich in variable amounts of Na, Ca and base metal sulfides. These solutions have preceded the hydrothermal uranium mineralization stage. It is quite clear that metasomatism is contemporaneous at all six localities and is of a regional character, occurring towards the latter stages of the Svecokarelian orogeny.

3.1. Metasomatic wall-rock alterations

A common feature of all the mineralizations is an initial pervasive metasomatic phase, the extent of which is controlled by local structural weakness and rock permeability variations. These metasomatic alterations (Fig. 3) are characterized by enrichments of sodium (e.g. Pleutajokk), sodium and calcium (e.g. Björklund) and a general depletion of potassium; sometimes silica also shows appreciable depletions (e.g. Skuppesavon and Rävaberget).

Mineralogically, increases in calcium have resulted in the formation of Ca-amphiboles (e.g. hastingsite, hornblende, and actinolite), Ca-pyroxenes (e.g. hedenbergite), Ca-rich garnets (mostly andraditic in composition), sphene and epidote. Increases in sodium are indicated by marked albitization and the presence of occasional riebeckite (only at Pleutajokk) and Na-bearing hedenbergite. Texturally, these mineral assemblages partly compensate for the absence of quartz (e.g. Rävaberget and Skuppesavon).

3.2. Mineralogy of the uranium occurrences

Following metasomatism, oxidizing uraniferous hydrothermal solutions have penetrated along the zones of weakness previously opened by the Ca- and Na-rich fluids. Not all metasomatized zones are mineralized with respect to uranium, which indicates that there was a temporary abatement in hydrothermal activity prior to uranium mineralization during which some of the transportation pathways became sealed. When possible, the precipitation of uranium has resulted in uraninite formation, which occurs as vein/fracture infillings (e.g. up to 2 mm in width at Björklund and Pleutajokk) and as disseminated impregnations (e.g. Rävaberget and Skuppesavon).

The uraninite grains are usually rounded to subheral in shape and only rarely are euhedral varieties observed; some characteristic textures are illustrated in Fig. 4. The crystalline habit of uraninite samples taken from most mineralizations within the province has been confirmed by unit cell length measurements (written commun. S. Sandbacka, 1983, personal commun. B. Gustafsson, 1984). These show a general range of 5446 - 5494 Å.

The uraniferous solutions have also been rich in Ca and Ti so that precipitation of uranium has often been followed by the formation of sphene which has locally formed reaction zones of complex uranotitanates around completely to partly resorbed uraninite grains and aggregates. Common to all mineralizations is the discontinuous precipitation of calcite, radiogenic PbS, FeOOH-oxides and sometimes chlorite and quartz. Sulphide occurrences are very minor and irregularly distributed, sometimes indicating local remobilization. Secondary uranium minerals and some continuation of uranotitanate formation characterize the late-stage, low temperature phase of the mineral parageneses.

3.2.1. Redox precipitation of uraninite

Throughout the province uranium has been transported predominantly as uranyl carbonate complexes. At Pleutajokk, fractures containing especially chlorite with subordinate Fe-oxides and amphiboles (e.g. riebeckite), have provided a suitable redox environment for uraninite precipitation. At Björklund, uraninite precipitation has occurred as disseminations and fracture infillings associated with one or more of the phases amphibolite, sphene and magnetite. At Rävaberget, the episyenitization process preceding the uranium precipitation has provided

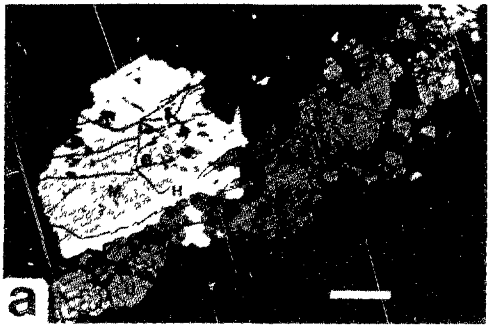

FIG. 4a. Pleutajokk mineralization: microphotograph showing local redox reactions between magnetite (M) and oxidizing uraniferous solutions which have resulted in oxidation of magnetite to hematite (H) and marginal precipitation of uraninite (U). Associated phases include sphene. Reflected light (scale-bar is 100 µm)

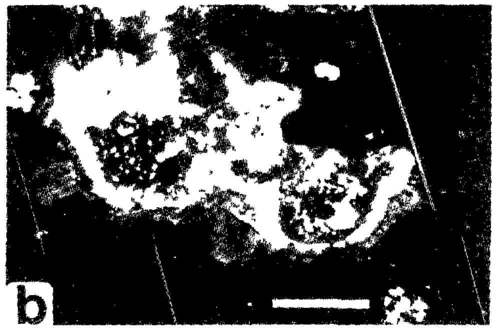

FIG. 4b: Harrejokk mineralization: microphotograph showing complex uranotitanate reaction rims (diffuse white) marginal to partly resorbed uraninite grains (bright white). Peripheral to the uranotitanates is sphene (grey). Reflected light; oil (scale-bar is 25 µm).

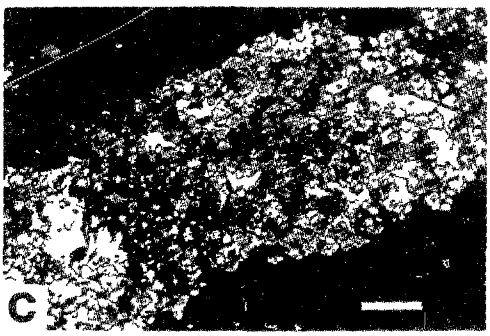

FIG. 4c: Pleutajokk mineralization: microphotograph featuring a uraninite infilled fracture. The uraninite aggregates (dark grey) are partly altered to uranium secondary phases and remobilized radiogenic galena (white) commonly forms a matrix cement. Reflected light (scale-bar is 100 µm).

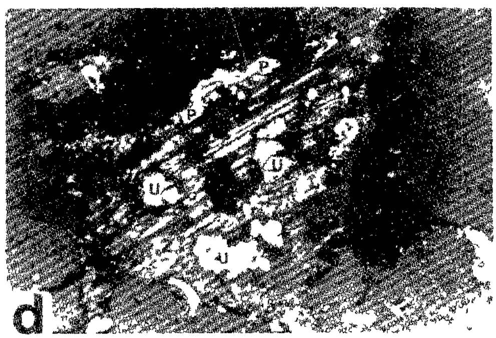

FIG. 4d: Ravaberget mineralization: microphotograph illustrating orientated ilmenite lamellae (after titanomagnetite) hosting uraninite (U), zircon (Z). Pyrite (P) occurs marginally. Reflected light (scale-bar is 25 µm).

a porous medium rich in magnetite/ilmenomagnetite (altered to Fe-Ti oxides) which has resulted in a widespread uraninite impregnation. At Arresâive, which represents mainly an impregnation-type of mineralization, the mineral phases aiding uraninite precipitation consist mainly of magnetite with subsidiary amphibole and sphene. At Harrejokk, which is impregnation in type, amphibole and biotite are the main agents aiding redox precipitation of uraninite. Lastly, at Skuppesavon, uranium precipitation has occurred in those parts of the pre-existing metasomatites that contain the greatest percentage of mafic mineral phases (e.g. pyroxene, amphibole, epidote, garnet and magnetite).

TABLE II. MICROPROBE ANALYSIS* OF URANINITE GRAINS FROM SELECTED MINERALIZATIONS IN THE ARJEPLOG-ARVIDSJAUR-SORSELE URANIUM PROVINCE, NORTHERN SWEDEN.

Analysis	1	2	3	4	5	6	7	8	9	10
SiO_2	5.95	-	0.21	0.10	0.16	0.22	0.04	0.01	0.36	0.23
TiO_2	0.59	0.13	0.10	0.10	0.23	0.58	0.08	0.07	0.11	0.28
Fe_2O_3	0.60	0.11	0.70	0.12	0.16	0.28	0.39	0.10	0.05	0.76
CaO	0.68	1.02	1.44	0.17	0.67	1.09	1.01	0.97	0.54	1.20
PbO	18.61	20.71	19.96	19.93	18.47	20.24	17.55	22.67	21.31	18.72
ThO_2	0.29	0.42	0.22	6.29	0.90	0.32	0.47	0.26	0.20	0.63
U_3O_8	69.07	68.96	70.14	66.61	73.39	74.85	73.96	76.53	73.72	74.82
Total	95.79	91.35	92.77	93.32	93.98	97.58	93.50	100.61	96.29	96.64
CA-range (Ma)	1710-1774	1890-1903	1811-1826	1820-1897	1641-1642	1699-1811	1553-1572	1833-1918	1788-1865	1564-1668

1 - Arresaive: reaction between Fe-Ti oxides and uraninite in the section.
2 - Harrejokk: large idiomorphic uraninite grains
3 - Harrejokk: uraninite inclusions in sphene. Marked reaction zone.
4 - Pleutajokk: fine-grained uraninite as a fracture infilling. FeS_2 and PbS occur in a zone between uranotitanate and the fracture edge.
5 - Pleutajokk: fine-grained uraninite disseminations within a fracture zone. Evidence of uraninite - sphene reaction in the section.
6 - Bjorklund:
7 - Bjorklund: } large aggregate of small uraninite grains.
8 - Ravaberget:
9 - Ravaberget: } reaction between Fe-Ti oxides and uraninite in the section.
10 - Skuppesavon: uraninite inclusions in sphene. Marked reaction zone.

(*Microprobe analyses were carried out by Micro-Analysis Consultants, St. Ives, U.K.)

3.2.2. Uraninite analysis

Selected uraninite and uranotitanate grains from each mineralization were analysed by the microprobe and the results are presented in Tables II and III. In general, the uraninites are characterized by uniformly low ThO_2 (0.20 - 0.90 wt.%), significant CaO (0.56 - 1.44.wt %), and high PbO (17.55 - 22.67 wt.%). Analysis 1 (Table II) from Harrejokk is anomalous, showing a high ThO_2 content (6.29 wt.%) and a much lower CaO content (0.17 wt.%). Furthermore, variation in thorium content between grains in the same specimen range from 1 - 7 % ThO_2. Texturally, the uraninite crystals in this specimen are large idiomorphs which contrast with the other investigated samples in which the uraninites are usually partly resorbed by reaction with sphene. Some localized effects of this reaction are indicated in Table II (e.g. anals. 1, 3, 6, 9, and 10) whereupon small increases in TiO_2, Fe_2O_3 and/or SiO_2 can be observed.

Excluding analysis 1, the compositional ranges obtained are fairly typical of vein-type uraninites (Snelling (21)). The generally high PbO content (17.55 - 22.67 wt.%) is due to the accumulation of radiogenic lead since Precambrian times, and this reflects the considerable age of these uraninites. The ranges

TABLE III. MICROPROBE ANALYSIS* OF COMPLEX URANO-TITANATES FROM SELECTED MINERALIZATIONS IN THE ARJE-PLOG-ARVIDSJAUR-SORSELE URANIUM PROVINCE, NORTHERN SWEDEN.

Analysis	1	2	3	4	5	6
SiO_2	-	27 38	20 50	2 06	4 28	28 42
TiO_2	6 10	35 12	30 25	85 19	55 25	30 66
Fe_2O_3	59 44	1 96	4 27	4 56	11 15	6 29
CaO	0 40	20 08	17 07	0 51	0 86	17 42
PbO	7 75	0 66	2 79	2 06	4 81	1 82
ThO_2	0 18	0 20	0 06	0 99	0 09	0 22
U_3O_8	25 96	8 02	19 62	6 81	20 66	7 56
Total	99 83	93 42	94 56	100 19	97 10	92 39

1 - Arresåive reaction between Fe-Ti oxides (mostly magnetite) and uraninite

2 - Harrejokk reaction between uraninite and sphene

3 Pleutajokk reaction between uraninite and sphene

4 - Ravaberget
5 - Ravaberget } reaction between Fe-Ti oxides (mostly ilmenomagnetite) and uraninite

6 - Skuppesavon reaction between uraninite and sphene

(* Microprobe analyses were carried out by Micro-Analysis Consultants, St Ives, U K)

of chemical ages obtained from the uraninites (Table II), calculated from the uranium and lead contents according to Pavshukov et al. (22), give a spread of 1533 - 1918 Ma. Allowing for the ease with which lead (common and radiogenic varieties) can be mobilized in metamict phases containing as much lead as shown by these uraninite analyses, the recorded ages must be regarded as minimum ages. It is noticeable that the two texturally distinct Harrejokk varieties (i e. anals. 4 and 5) show a consistent difference in chemical age. This, together with the high ThO_2 contents of the idiomorphic type, might suggest two separate generations of uraninite crystallization, one older high temperature variety (anal. 4) and a younger lower temperature type (anal. 5).

3.2.3. Uranotitanate analysis

Texturally, sphene commonly surrounds and shows reaction with the uraninite resulting in a wide range of complex uranotitanate compositions (e.g. Harrejokk, Pleutajokk and Skuppesavon) which are presented in Table III. Other uranotitanate compositions (e.g. Arresåive and Ravaberget) have formed from the reaction of primary Fe-Ti oxides (magnetite and ilmenomagnetite) with the oxidizing uranium-bearing hydrothermal fluids. This can be clearly seen from analysis 1 (Table III) which is typical of magnetite reaction, and analyses 4 and 5 which represent reaction with ilmenomagnetite.

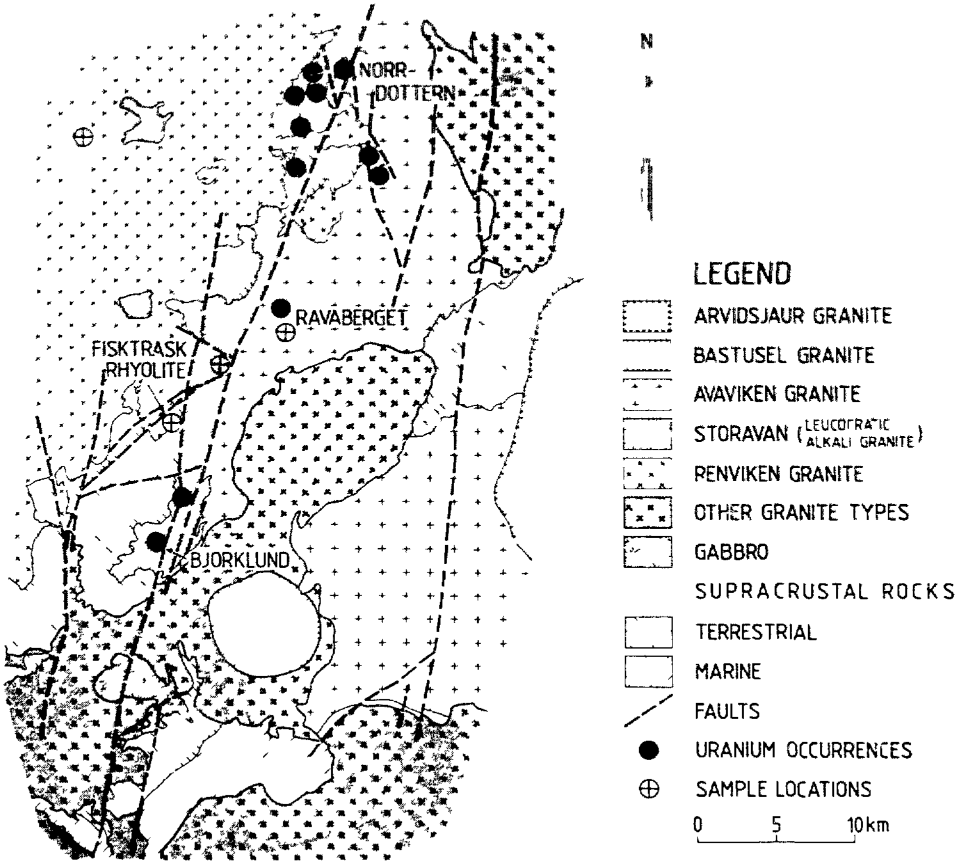

FIG. 5. Detailed geological map of the Arvidsjaur district showing locations of studied granites and the relationship between uranium mineralization and regional structures.

4. Pb-U DATING OF THE URANIUM OCCURRENCES

Pb-U dating of separated uraninite grains and/or whole-rock material has been carried out on Arresâive, Bjorklund, Harrejokk, Pleutajokk and Ravaberget (Fig. 5). Some of this work has already been presented by Adamek et al. (1), (2) but the data have been recalculated (Table IV) using common lead corrections $^{206}Pb/^{204}Pb$ = 15.312 and $^{207}Pb/^{204}Pb$ = 15.525 and the following constants: ^{238}U = 1.55125 x 10^{-10}/yr, ^{235}U = 9.8485 x 10^{-10}/yr, atomic ratio $^{238}U/^{235}/U$ = 137.88 (IUGS convention).

4.1. Arresâive mineralization

The isotopic analyses of samples selected from a vein system are presented in Table IV and Fig. 6a and 6b. Sample 7578:007 (point 7) lies well off the best

TABLE IV. NEW PB-U DATA FROM SELECTED URANIUM MINERALIZATIONS IN THE ARJEPLOG-ARVIDSJAUR-SORSELE URANIUM PROVINCE, NORTHERN SWEDEN

Mineralisation Sample	Lead Isotopic Composition			Concentration		Atomic Ratios			Ages in Ma		
	$^{204}Pb/^{206}Pb$	$^{207}Pb/^{206}Pb$	$^{208}Pb/^{206}Pb$	%U	%Pb	$^{206}Pb/^{238}U$	$^{207}Pb/^{235}U$	$^{207}Pb/^{206}Pb$	$^{206}Pb/^{238}U$	$^{207}Pb/^{235}U$	$^{207}Pb/^{206}Pb$
ARRESAIVE+											
7578 001	0 000143	0 1098	0 00413	3 67	0 938	0 2665	3 965	0 1079	1523	1627	1763
002	0 000199	0 1071	0 00522	3 04	1 04	0 3567	5 136	0 1044	1966	1842	1702
003	0 000048	0 0826	0 00168	13 84	1 31	0 1018	1 150	0 0819	625	777	1243
004	0 00023	0 1115	0 00437	1 68	0 589	0 3625	5 386	0 1077	1994	1883	1760
005	0 00049	0 1154	0 0242	0 645	0 251	0 3943	5 911	0 1087	2143	1963	1776
006	0 00026	0 1105	0 01339	0 333	0 128	0 3973	5 859	0 1069	2156	1955	1747
007	0 00031	0 1004	0 01362	2 49	0 820	0 3422	4 440	0 0962	1897	1738	1550
008	0 000514	0 1180	0 02718	0 132	0 0342	0 2605	3 991	0 1111	1493	1632	1816
BJORKLUND*											
7776 502	0 004204	0 602	0 13719	0 208	0 093	0 3748	5 181	0 1015	2052	1850	1650
503	0 000300	0 1121	0 01237	6 12	2 03	0 3415	5 021	0 1079	1894	1822	1764
504	0 000681	0 1047	0 02379	2 03	0 384	0 1929	2 498	0 0951	1136	1272	1528
505	0 000415	0 1065	0 02391	17 63	3 19	0 1850	2 538	0 1007	1094	1284	1636
506	0 000376	0 1135	0 01455	2 01	0 623	0 3177	4 687	0 1083	1778	1764	1770
507	0 000862	0 1196	0 02928	3 44	1 02	0 2961	4 339	0 1076	1672	1700	1758
508	0 000197	0 1089	0 00670	3 98	1 14	0 2978	4 306	0 1062	1680	1694	1734
509	0 000407	0 1135	0 01571	0 466	0 147	0 3235	4 755	0 1079	1808	1778	1784
RÅVABERGET*											
7676 030	0 004689	0 1605	0 1764	0 2425	0 0758	0 2509	3 311	0 09565	1443	1484	1540
031	0 050327	0 7941	1 9642	not determined							
032	0 039573	0 6379	1 5045	not determined							
033	0 00148	0 12867	0 05295	0 9189	0 3548	0 3709	5 548	0 1084	2033	1908	1772
034	0 006075	0 1919	0 22513	2 7403	0 9624	0 2596	3 910	0 1092	1488	1616	1785
035	0 03751	0 61971	1 3270	1 1389	2 0920	0 2987	3 489	0 08466	1685	1525	1307
036	0 05618	0 8988	2 1292	not determined							
7383 323	0 000455	0 1134	0 01569	5 671	1 7003	0 3066	4 533	0 1072	1724	1737	1751
404	0 000314	0 1129	0 00940	61 719	19 3633	0 3235	4 850	0 1087	1807	1794	1776
407	0 0000992	0 1098	0 00332	59 768	17 7414	0 3098	4 635	0 1085	1740	1756	1773

+Analysis by Teledyne Isotopes (U S A)

*Analysis by the British Geological Survey (London, U K) fit line on both the Pb-U and Pb-Pb plots, while sample 7578:003 (point 3) lies well off the Pb-Pb plot and is highly discordant on the Pb-U plot. In consequence, sample 7578:007 was not used in the age calculation. Comparison of Fig. 6a and 6b shows that the Pb-Pb plot does not give a satisfactory fit (1800 ± 80 Ma; MSWD 8.2) in contrast to the Pb-U plot (1750 ± 80/70 Ma; MSWD 1.54) which is much more acceptable.

4.2. Björklund mineralization

Twelve samples from Björklund have been investigated (Table IV). The four analyses reported by Adamek et al. (1) (samples 7373:636, 638-640) were from blasted outcrop portions. Uraninite, sometimes contaminated by magnetite, was separated from these samples. This present paper contains isotopic data for additional eight samples obtained from drill cores representing both vein and impregnation mineralization types.

Combining all the available Björklund data (Table IV, Fig. 6c and 6d) the best fit chord gives 1724 ± 52/38 Ma, and a MSWD of 0.9 (12 points). The whole-rock data shows more discordance than the separated minerals and four samples lie above the concordia indicating some loss of uranium. Omitting samples 7776: 502/503 results in a better fit giving 1748 ± 84/60 Ma, and a MSWD of 0.3 (Fig. 6c). A Pb-Pb model age for nine of the Björklund samples (Fig. 6d) give 1750 ± 100 Ma, which is in general agreement with the Pb-U data although the MSWD is high (4.8). This suggests that the correction applied for common lead is correct.

4.3. Harrejokk and Pleutajokk mineralizations

Uraninite grains (95 - 99 % pure) were separated from these respective mineralizations; five samples from Harrejokk and eight samples from Pleutojokk. The results are presented in Fig. 6e and the analytical data published earlier (Table III, Adamek (1)). From the $^{206}Pb/^{238}U$ vs. $^{207}Pb/^{235}U$ plot, the samples are slightly discordant with one sample lying above the concordia (uranium loss). Upper intercepts are 1738 ± 20 Ma (MSWD 1.4), for Pleutajokk and 1738 ± 18 Ma (MSWD 1.7) for pooled data from Harrejokk and Pleutajokk.

4.4. Rävaberget mineralization

Four high purity uraninite concentrates from blasted outcrop samples were previously analysed (Table III in Adamek et al. (1)). Three of these samples have been re-analysed (samples 7383:323/404/407; Table IV) together with seven new whole-rock samples taken from drill core material representing impregnation mineralization. Unfortunately, uranium and lead contents were not determined on all of the samples.

On the Pb-U plot (Fig. 6f) seven of the samples define a concordia with an upper intercept of 1767 ± 8/6 Ma (MSWD 2.4). Two of these samples lie above the concordia (7383:322/323) indicating uranium loss. However, samples 7676:030/035 lie a long way from the discordia. From the Pb-Pb plot (Fig. 6g) the samples define a model age of 1767 ± 12/18 Ma (MSWD 0.8), with two samples (7676:407) somewhat displaced. The close agreement between these precise dates indicates that the common lead correction is correct.

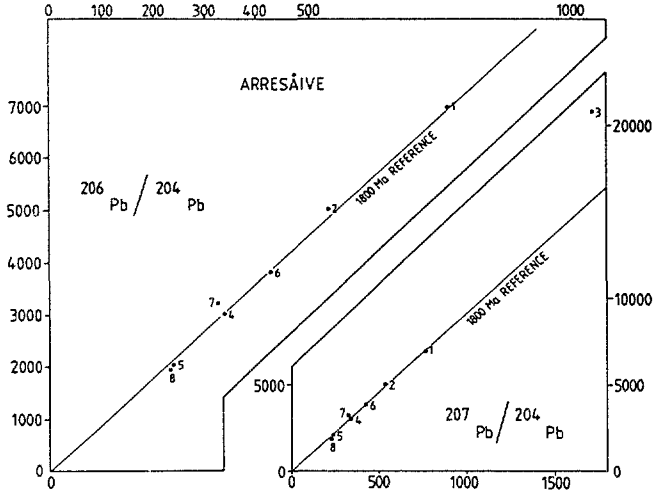

FIG. 6a. Arresåive Pb-Pb plot

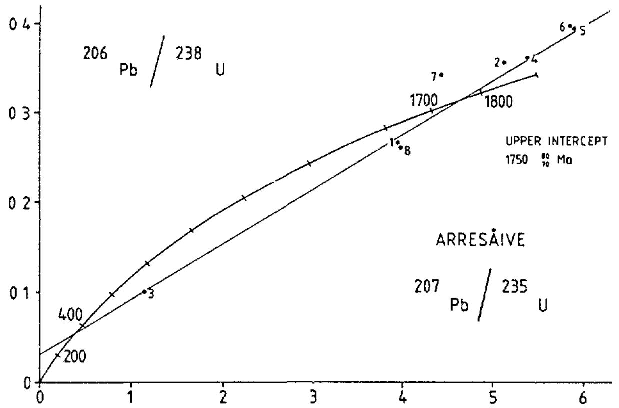

FIG. 6b. Arresåive Pb-U plot

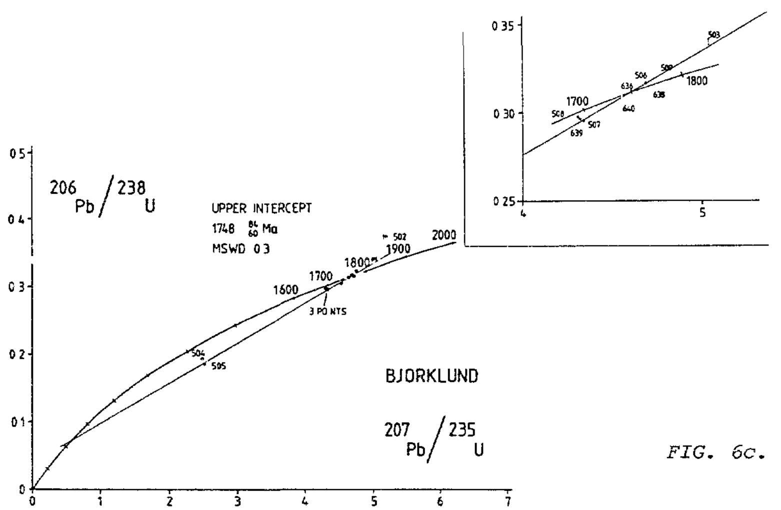

FIG. 6c. Bjorklund Pb-U plot

FIG. 6. Pb-U and Pb-Pb isotopic plots for the investigated mineralizations (see text for explanation)

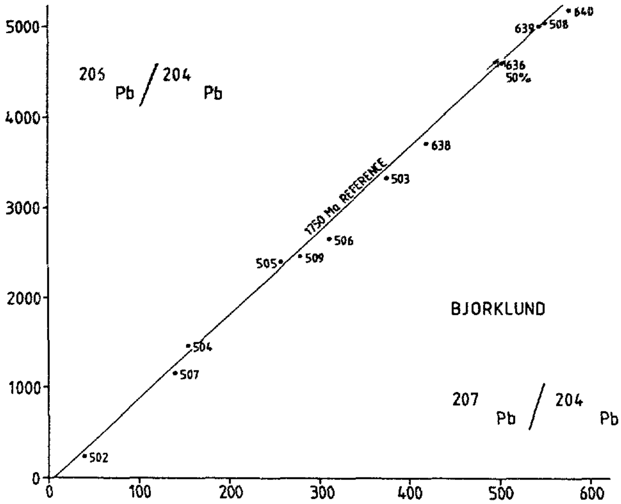

FIG. 6d. Bjorklund Pb-Pb plot

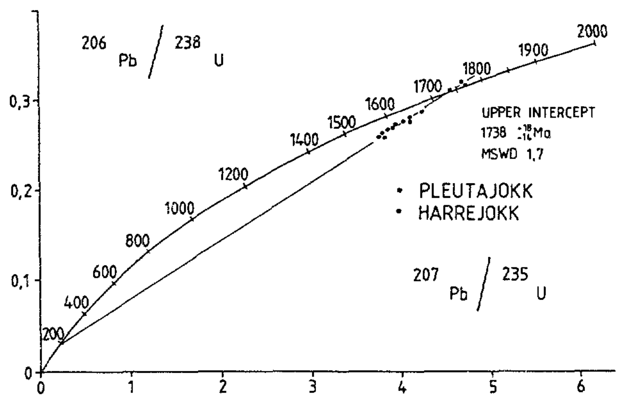

FIG. 6e. Harrejokk and Pleutajokk Pb-U plot

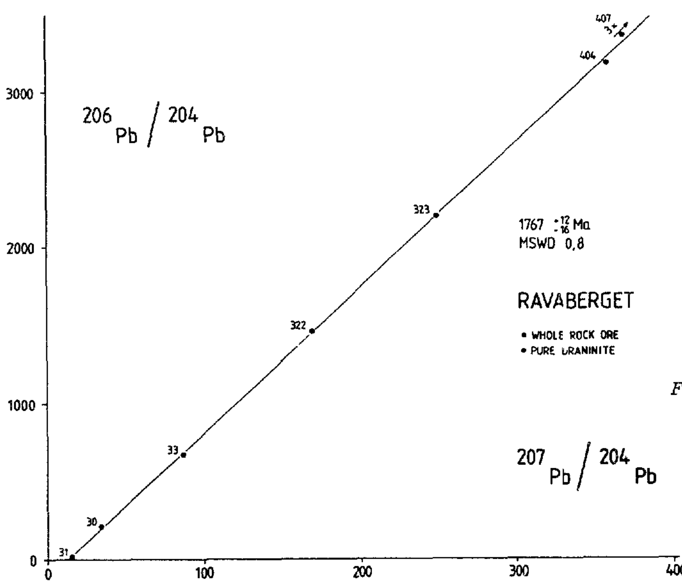

FIG. 6f. Rävaberget Pb-Pb plot

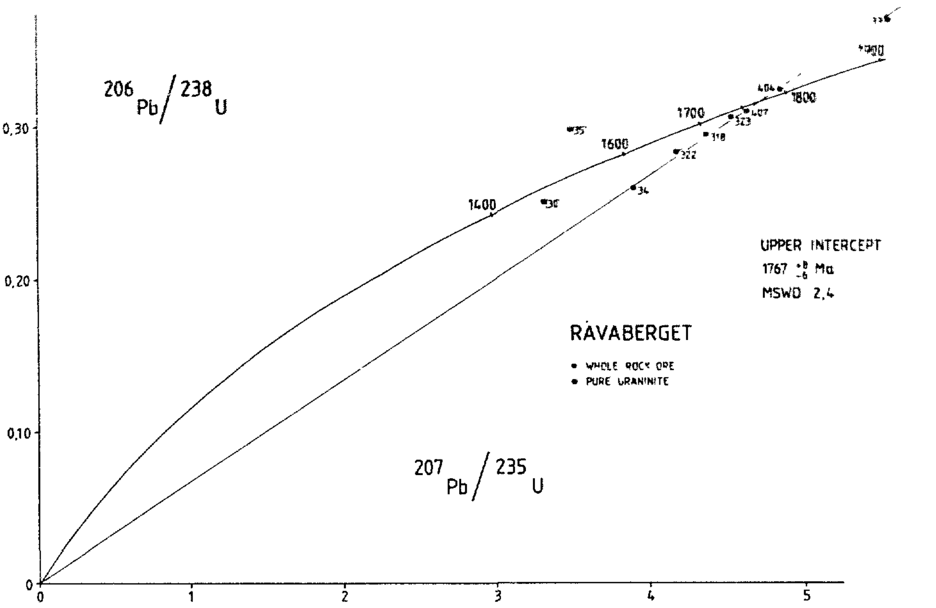

FIG. 6g. Rävaberget Pb-U plot

A summary of the Pb-U data on these mineralizations is presented in Table V. In general the MSWD values are sufficiently low for the calculated ages to be considered meaningful; however, in several cases the calculated error is unsatisfactorily large. Nevertheless, the five mineralizations all give apparent ages that are remarkably similar at around 1750 Ma. It is doubtful whether the Pleutajokk-Harrejokk mineralizations (from the Arjeplog region) are significantly younger than Rävaberget (from the Arvidsjaur region).

Secondary uranium minerals from Pleutajokk and Norr Döttern (ca. 15 km north of Rävaberget, Fig. 5) and other Swedish uranium occurrences were dated by the Pb-U method by Löfvendahl et al. (23). The minerals almost certainly post-date the Quaternary glaciation and in many cases can be demonstrated to have formed since prospecting started in the early 1970's. Unexpectedly, the Pleutajokk secondaries give apparent Pb-U ages in good agreement with the ages on the primary uraninite minerals indicating that the lead in these secondaries is derived from the uraninite. This is supported by the mineralogical investigations. Isotopic data show that the uranium secondaries are concordant or reversely discordant (uranium loss). The present authors would suggest that this result confirms the reliability of the uraninite ages as reflecting primary mineralization; a slight recrystallization of uraninite without total loss of radiogenic lead would not reset the system.

5. RELATIONSHIP BETWEEN URANIUM MINERALIZATION AND URANIUM-ENRICHED GRANITES

The Arjeplog-Arvidsjaur-Sorsele uranium province is characterized by enhanced uranium and thorium contents in many of the granites and volcanics. There is a clear genetic relationship between occurrences of Mo, W and Sn and the uranium-enriched granites (Walser et al. (9), Wilson et al. (11), Öhlander (14)). The connection between U-rich granites and volcanics and uranium mineralizations is not so clear. For example, although Pleutajokk lies near the U- and Th-enriched Guorbavare granite (Fig. 2), Rb-Sr dating suggested that the granite was

TABLE V. SUMMARY OF Pb-U AGE DATA ON SELECTED URANIUM MINERALIZATIONS FROM THE ARJEPLOG-ARVIDSJAUR-SORSELE URANIUM PROVINCE, NORTHERN SWEDEN

Mineralisation	U-Pb Age	n	MSWD	Pb-Pb Age	n	MSWD
Arresålve	1750^{+80}_{-70}	7	1.54	1800±160	7	8.19
Bjorklund	1748^{+84}_{-60}	10	0.32	1750+100	9	4.8*
Pleutajokk Harrejokk	1738±18	13	1.7			
Pleutajokk	1738±20	9	1.4			
Ravaberget	1767^{+8}_{-7}	6	2.5	1767^{+12}_{-14}	6	0.8*

*Non-fit geological error.

Dates are expressed in Ma with an error of 2σ.

TABLE VI. SUMMARY OF AGE AND ISOTOPE DATA ON MINERALIZATION RELATED GRANITES IN THE ARJEPLOG-ARVIDSJAUR-SORSELE URANIUM PROVINCE, NORTHERN SWEDEN

Granite	Mineralisation	U-Pb Zircon Age			Rb-Sr Age	$^{87}Sr/^{86}Sr$	$\delta^{18}O$	ε_{Nd}	T_{DM}
		Ma	n	MSWD	Ma	Initial	‰		Ga
Guorbavare	Pleutajokk (U)	1864^{+20}_{-19}	3	0 93	1590±35	0.712±2	+7.89 +8.24	+2.09 +1 49	2.0 2.0
Bjorntjarn	Allabouda (Mo,U)	See Figure	7		-	-	+8.46	-	2.3
Hallnas	Skuppesavon (U)	-	-	-	1698±25	0.708±2	+8 33	-	2.2
Avaviken	Ravaberget (U)	1840±9	12	3 9	1789±36	0.7024+2	+6 66 +7.69 +5 84	+1.14 +2.85 +3.42	2.1 1.9 1.9
Storavan	Bjorklund (U)	1893^{+42}_{-27}	-	0.09	-	-	-	-	
Storliden	(W)	1868^{+39}_{-22}	-	0.005	1678±56	0 709+6	+7.80	+2.13	2.0
Fisktrask Rhyolite		-	-	-	1750	-	+5.65	-	2.0
Hydrothermal vein associated with the Bjorklund mineralisation (Storavan granite).					Sm-Nd isochron 1845±67 Ma		$\delta^{18}O$ +5.8 +7.7	ε_{Nd} +2.8±1.2	

(Analysis carried out at the Scottish Universities Research and Reactor Centre, East Kilbride, Scotland).

much younger than the mineralization. However, Rb-Sr isochron ages in Precambrian terrains are commonly much lower than Pb-U zircon ages and therefore several of the granites have recently been Pb-U zircon dated. Adamek et al. (1), (2) speculated on the relationship between uranium and Archaean basement. Although no Archaean dates are reported from South Norbotten it is quite possible that Archaean forms a basement to this southern part of the "Karelian Continent" and that several of the more gneissic rock units could actually represent Archaean. Sm-Nd and O isotope studies have therefore been carried out to determine whether or not the granites could represent recycled Archaean basement. These results are summarized in Table VI.

5.1. Arjeplog Region

The Guorbavare granite (Fig. 2) is a large U- and Th-enriched intrusion whose contact lies some 600 m west of Pleutajokk. The Rb-Sr isochron age of 1590 ± 35 Ma (initial $^{87}Sr/^{86}Sr$ 0.712 ± 2) (Welin et al. (24)) is significantly younger than the Pb-U age of 1738 ± 20 Ma for uraninites from Pleutajokk. Three zircon concentrates from Guorbavare were recently Pb-U dated (Fig. 7). They are extremely discordant but fit a discordia with an upper intercept of 1864 ± 20/19 Ma and lower intercept of 286 ± 27 Ma (MSWD 0.39). This is by far the most common upper intercept age for granites from Norrbotten (Skiöld (25), Wilson et al. (17)) and clearly refers to a major period of formation of granitoid crust. However, it is well documented (Pidgeon et al. (26)) that zircons can survive a partial melting and still preserve an isotopic memory. This means that a zircon age may not always represent the actual intrusion age for the specific granite. In the case of Guorbavare the zircons are so discordant that this is a possibility. It would be desirable to carry out complementary dating by the Pb-U or Sm-Nd method on mineral phases clearly related to crystallization or emplacement.

An alternative possibility is that the granite has been strongly affected by movement of groundwater either during Late Precambrian peneplanation and sedimentation or during the Late Silurian phases of the Caledonian orogeny. The granite does lie only a few kilometres from the Caledonian Front.

The Guorbavare granite was therefore either intruded at 1864 ± 20/19 Ma, (about 120 Ma before the Pleutajokk mineralization) or intruded at an unknown time between 1864 and 1590 Ma.

The oxygen isotopic composition of two whole-rock samples from Guorbavare are $\delta^{18}O$ = + 7.8 ‰ and 8.2 ‰, i.e. normal values for an igneous provenance. Sm-Nd analyses give ϵ_{Nd} values of + 1.5 and + 2.1 indicating that the source material for the granite was derived from a light rare earth element (LREE) depleted mantle with a minimum contribution of older (Archaean) crust and a relatively short crustal residence time (Wilson et al. (11), Wilson et al. (17)). These samples give a T_{DM} model age of 2.0 Ga, a typical value for South Norrbotten.

A nearby U-enriched granite Björntjärn (Fig. 2) has Mo-bearing aplites (Allabouda occurrence) (Walser et al. (9), Öhlander (14)) and was regarded, like Guorbavare, to be an example of the 'younger granites' in the Arjeplog area. Zircons from Björntjärn (Fig. 7) do not lie on the same discordia as the Guorbavare and other 1.9 Ga granites, but could be slightly younger. The zircons are quite discordant and form a tight cluster, which does not allow an upper intercept age to be calculated. It is apparent from Fig. 7 that the zircons could be of about the same generation as the Arvidsjaur zircons (1.79 Ga). As with Guorbavare the possibility also exists that the zircons are recycled.

An oxygen isotope analysis gives $\delta^{18}O$ = 8.5 ‰ (Wilson et al. (11)) and Sm-Nd data on Björntjärn give a clear indication that the source material for the granite could contain an important Archaean component. The T_{DM} model age is 2.3 Ga, in marked contrast to the majority of granites sampled in South Norrbotton (Wilson et al. (17)).

A similar T_{DM} model age was obtained from the U-rich Hällnäs granite (Fig. 2) which lies very near the Skuppesavon uranium mineralization. This granite has given a Rb-Sr whole rock age of 1698 Ma (Welin (24)). It has an $\delta^{18}O$ value of

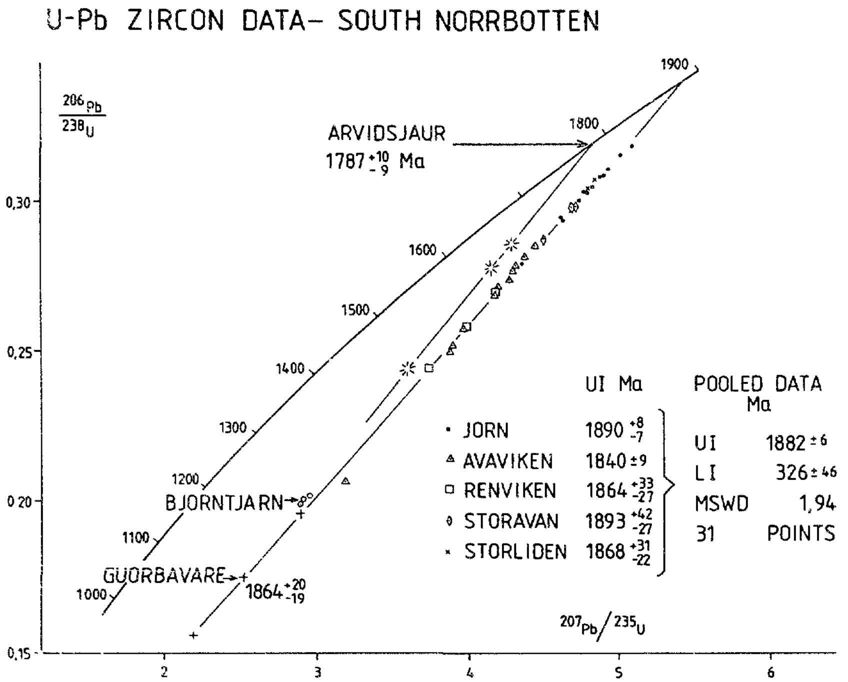

FIG. 7. Pb-U isotopic plot for selected granitoids in the Arjeplog-Arvidsjaur-Sorsele area (after Wilson et al., in preparation (17)).

+ 8.3 ‰ and T_{DM} model age of 2.2 Ga. It is thought that these two T_{DM} model ages are geologically meaningless as ages, but represent an average of the crustal residence times of the different components, i.e. a mixture of Archaean with a crustal residence time of about 2.8 Ga with new Proterozoic material with a crustal residence time of 2.1 to 1.9 Ga. Assuming ages between 1.9 and 1.7 Ga, these granites give ϵ_{Nd} values between 0 and -2.

5.2. Arvidsjaur Region

The Rävaberget uranium mineralization lies within a granodioritic to granitic massif, the Avaviken granite (Fig. 2). Twelve Pb-U zircon analyses on two adjacent samples (Fig. 7) give upper intercepts of 1832 ± 7 Ma (MSWD 1.83) and 1850 ± 13/12 Ma (MSWD 1.08), the pooled data giving 1840 ± 9 Ma (MSWD 3.87). Rb-Sr whole rock analyses do not define a true isochron but give a reference of 1789 ± 36 Ma (MSWD 19). The Pb-U data is significantly older than the Pb-U data on the uranium mineralization (1767 ± 8/6 Ma). Oxygen isotope values vary from + 5.5 ‰ to + 7.7 ‰ and ϵ_{Nd} from + 1.1 to + 3.4. T_{DM} model ages are 1.9 to 2.1 Ga. These values are similar to those from the Guorbavare granite and indicate an igneous source with minimum contribution of Archaean material. The Björklund uranium mineralization lies within a leucocratic alkali granite described in Adamek et al. (2) and termed here the Storavan granite. Three zircons (Fig. 7) give a Pb-U upper intercept of 1893 ± 42/27 Ma (MSWD 0.09). Sm-Nd whole rock analyses were made on the mineralized hydrothermal vein system in this granite at Björklund (samples described in Smellie et al. (15)). The four samples give a perfect isochron with an age of 1845 ± 67 Ma and initial $^{143}Nd/^{144}Nd$ of 0.510394

$\pm$ 64 corresponding to ϵ_{Nd} + 2.8 $\pm$ 1.2. The hydrothermal vein is rich in garnet; this is probably responsible for the extreme Sm/Nd ratios that have allowed whole rock dating.

The Pb-U age on the Björklund mineralization is 1748 $\pm$ 84/60 Ma. Interpretation of these three dates must take into account that the calculated analytical error for each determination is sufficiently large to allow overlap between the mineralization and the hydrothermal vein on the one hand, and the vein and the granite on the other. However, the MSWD values on the determination are $\sim$1 which suggests that they are reliable. In addition, both the mineralization and the granite give apparent ages that fit the regional pattern. Bearing in mind these characteristics, the Sm-Nd data suggest the following:

- The Pb-U zircon date relates to intrusion of the Storavan granite; the zircons are not relict.
- The date of the hydrothermal vein system, characterized by Na and Ca metasomatism (which includes the growth of garnet), represents the stage at which hydrothermal fluids were active in the region.
- The initial Nd isotope ratio of the hydrothermal altered zone (ϵ_{Nd} + 2.8) indicates a LREE depleted source and a minimal crustal residence time. The ϵ_{Nd} value is comparable to those from the 1.9 Ga granitoids.
- Oxygen isotope values for the hydrothermal vein range between 5.7 and 7.6 ‰. These suggest igneous origin with slight lowering through interchange with meteoric water. This is in accordance with the above interpretation.

A rhyolitic ash flow tuff (termed the Fiskträsk rhyolite) from the Arvidsjaur district has also been studied (Fig. 2). This rhyolite, described by Adamek et al. (2) has considerable extent and is uranium-enriched. The role of this and similar continental rhyolites has been discussed by Adamek et al. (1) and Gustafsson (7). The Norr Döttern occurrence, from which Löfvendahl et al. (23) determined 1.87 - 1.88 Ga $^{207}Pb/^{206}Pb$ ages on secondary kasolite, lies within the same volcanic suite.

Extracting zircons from these fine-grained rocks has not yet been successful but the volcanics are considered to predate the Avaviken and Storavan granites. Their Sm-Nd systematics (T_{DM} 2.0 Ga) are comparable to the Avaviken granite and the Björklund hydrothermal veins, indicating a short crustal residence time and a source derived from LREE depleted mantle.

5.3. Discussion

The Pb-U zircon ages quoted here and others from South Norrbotten (Wilson et al. (17) and North Norrbotten (Skiöld (25)) indicate clearly that 1900 - 1850 Ma was a major period for the formation of granitoid crust. The O and Sm-Nd data quoted indicate that the source of the granites and volcanics of South Norrbotten had not gone through a sedimentary cycle and, with the exception of Björntjärn and Hällnäs, did not include a significant Archaean component. Apart from these two exceptions there is no significant difference in zircon Pb-U, O or Sm-Nd systemtatics between U-rich and normal granite.

In the case of Storavan, it is reasonably certain that the zircon upper intercept ages do represent the time of intrusion. Only slight discordance is seen in the Avaviken and several other granites which suggests that these are also intrusion ages. For Guorbavare and Björntjärn there remains the possibility that the granites have a younger intrusion age than that represented by the zircon Pb-U ages, although it is considered unlikely that they post-date the uranium mineralizations.

6. CONCLUSIONS

The Arjeplog-Arvidsjaur-Sorsele uranium province represents a new crustal addition along the southern margin of the Svecokarelian-Archaean 'Karelian Continent' with extensive granitoid formation at 1900 - 1850 Ma from igneous sources with a very short crustal history. The most probable sources are the basic to acid volcanics of the types preserved in the area. The presence of a characteristic volcanic arc to the south, succeeded southwards by a major greywacke basin, has suggested parallels with modern destructive plate boundaries. Emplacement of the magmas has been strongly controlled by deep marginal faults, possibly of a transform nature. The more acid varieties of the igneous rocks can be strongly enriched in uranium.

Granite intrusion in the province can be considered coeval with the regional metamorphism and has probably provided the necessary temperature gradient to cause hydrothermal fluid movement. During the passage of these fluids through the volcano-sedimentary and granitic country rocks, elements such as Ca, Na, U and Ti were mobilized, concentrated and transported. Movement of these hydrothermal solutions has been facilitated by pre-existing faults and more permeable lithological horizons. Eventually, during the latter stages of metamorphism, and under favourable conditions of temperature, pressure, oxidation and redox potential and pH, the precipitation of certain elements and removal of others have resulted in the formation of alkali metasomatites and later uranium mineralization.

ACKNOWLEDGEMENTS

The authors wish to express their thanks to Dr. I. Swainbank (British Geological Survey) and Drs. P.J. Hamilton, A.E. Fallick and M. Aftalion (Scottish Universities Research and Reactor Centre) for isotopic data and helpful discussions. In addition, gratitude is extended to colleagues at the Swedish Geological Company who have contributed to the geological background of the studied region.

REFERENCES

(1) ADAMEK, P.M., WILSON, M.R., Recognition of a new uranium province from the Precambrian of Sweden, Recognition and evaluation of uraniferous areas, IAEA-TC-25/1b, Vienna, (1977) 199-215.

(2) ADAMEK, P.M., WILSON, M.R., The evolution of a uranium province in northern Sweden, Proc. R. Soc. Lond. 291 (1979) 355-368.

(3) LINDROOS, H., SMELLIE, J.A.T., A stratabound uranium occurrence within Middle Precambrian ignimbrites at Duobblon, northern Sweden, Econ. Geol. 74 (1979) 1118-1130.

(4) SMELLIE, J.A.T., The mineralogy and genesis of uranium in rhyolitic ignimbrites of Precambrian age from Dubblon, Sweden, Mineralog. Mag. 46 (1982) 187-199.

(5) EINARSSON, Ö., The Precambrian rocks of the Dubblon area, Västerbotten County, Sver. Geol. Undersök. Ser. C. 748 (1979) 123 pp.

(6) GUZMAN, M., HÅLENIUS, U., SMELLIE, J.A.T., Selected uranium mineralizations in the Arjeplog-Arvidsjaur-Sorsele area, Geol. För. Stockh. Förh. 102 (1980) 288-290.

(7) GUSTAFSSON, B., Uranium exploration in the N. Västerbotton province, northern Sweden, Uranium exploration case histories (IAEA-AG-250/2), Vienna (1980) 333-352.

(8) WILSON, M.R., Granite types in Sweden, Geol. For. Stockh. Forh. 102 (1980) 167-176.

(9) WALSER, G., EINARSSON, O., The geological context of molybdenum occurrences in the southern Norrbotton region, northern Sweden, Geol. Rdsch. 71 (1982) 213-229.

(10) WILSON, M.R., ÅKERBLOM, G.V., Geological setting and geochemistry of uranium-rich granites in the Proterozoic of Sweden, Mineralog. Mag. 46 (1982) 235-247.

(11) WILSON, M.R., FALLICK, A.E., The relationship between uranium-enriched granites and hydrothermal mineralization in northern Sweden, NEA-IAEA Symposium on uranium exploration methods, OECD, Paris (1982) 293-306.

(12) WILSON, M.R., Magma types and the tectonic evolution of the Swedish Proterozoic, Geol. Rdsch. 71 (1982) 120-129.

(13) HÅLENIUS, J., SMELLIE, J.A.T., Mineralizations of the Arjeplog-Arvidsjaur-Sorsele uranium province, Mineralogical studies of selected uranium occurrences, N. Jb. Miner. Abh. 147.3 (1983) 229-252.

(14) OHLANDER, B., Geochemical characteristics of granites associated with Proterozoic molybdenum mineralization in northern Sweden (in preparation).

(15) SMELLIE, J.A.T., ROSHOLT, J.N., Radioactive disequilibria in mineralized fracture samples from two uranium occurrences in northern Sweden, lithos (in press).

(16) SMELLIE, J.A.T., LAURIKKO, J., Skuppesavon, northern Sweden, a uranium mineralization associated with alkali metasomatism, Mineralium Deposita (in press).

(17) WILSON, M.R., HAMILTON, P.J., FALLICK, A.E., AFTALION, M., MICHARD, A., Sn-Nd, U-Pb and O systematics and the Proterozoic crustal evolution of part of Sweden (in preparation).

(18) RICKARD, D.T., ZWEIFEL, H., Genesis of Precambrian sulphide ores, Skellefte district, Sweden, Econ. Geol. 70 (1975) 255-274.

(19) LUNDBERG, B., Aspects of the geology of the Skellefte field, northern Sweden, Geol. For. Stockh. Forh. 102 (1980) 156-166.

(20) CLAESSON, L.Å., Stratigraphy and petrochemistry of the ore-bearing Skellefte group volcanics, Geol. For. Stockh. Forh. 104 (1982) 378-379.

(21) SNELLING, A.A., Uraninite and its alteration products, Koongarra uranium deposit, Proc. Int. Uranium Symposium on the Pine Creek Geosyncline (1980) 487-498.

(22) PAVSHUKOV, V.V., KOMLEV- L.V., ANDERSON, Ye B., SMYSLOVA, I.G., X-ray microprobe data on the state of the U-Pb system in uranium ores, Geokhim. 4 (1975) 603-613.

(23) LOFVENDAHL, R., ÅBERG, G., An isotopic study of Swedish secondary U-Pb minerals, Geol. For. Stockh. Forh. 103 (1982) 331-342.

(24) WELIN, E., EINARSSON, O., GUSTAFSSON, B., LINDBERG, R., CHRISTIANSSON, K., NILSSON, O., Radiometric ages of intrusive rocks in northern Sweden, 2, Sver. Geol. Undersok. Ser.C.731 (1977) 33 pp.

(25) SKIOLD, T., Chronostratigraphic correlations based on radiometric data from northern Sweden, Geol. For. Stockh. Förh. 103 (1981) 523-524.

(26) PIDGEON, R.T., AFTALION, M., Cogenetic and inherited zircon U-Pb systems in granites, Palaeozoic granites of Scotland and England, in: Crustal Evolution in Northwestern Britain and Adjacent Regions, Eds. D.R. Bowes and B.E. Leake, Geological Journal Special Issue 10 (Seel House Press, Liverpool) (1977) 183-220.

(27) QUESDA, R., IHRE, P., Domstukterer prospektering efter legeringsmetaller, Del. 1 & 2, SGAB Interal Report (BRAP 83030/31) (1983).

VEIN-TYPE URANIUM MINERAL OCCURRENCES IN SOUTH GREENLAND

P. Nyegaard, A. Armour-Brown, A. Steenfelt
The Geological Survey of Greenland
Copenhagen
Denmark

Abstract

VEIN-TYPE URANIUM MINERAL OCCURRENCES IN SOUTH GREENLAND

Many vein-type uranium mineral occurrences are located in South Greenland. These veins lie in what is termed the "Granite Zone" within the Proterozoic Ketilidian mobile belt (1900 - 1600 Ma). In this area the crystalline rocks were subjected to a period of faulting accompanied by the cratonic depositional and alkaline igneous activity of the Gardar period (1150 - 1350 Ma). The faulting is intensive and in many different directions, but is interpreted as being caused by a regional, EW orientated, sinistral stress system.

The pitchblende veins and the many minor radioactive mineral occurrences are located in or associated with fault zones. U-Pb isotope analyses of the pitchblende indicate a Gardar age of 1180 ± 15 Ma.

In the most extensive occurrences pitchblende and secondary uranium minerals are the most common radioactive minerals. In many of the minor occurrences brannerite is found. The gangue minerals are mainly quartz and calcite with varying amounts of specular hematite, fluorite and minor sulphides.

The fractured wall rock - granite or dike - is normally altered and often red coloured, and several different types of alteration are recognized, but none can be specifically related to the pitchblende occurrences.

Reconnaissance exploration results revealed that there are also uranium mineral occurrences in the Ketilidian rocks to the south of the Granite Zone. Isotopic contents of this uraninite gives an age corresponding to the Ketilidian metamorphism. Consequently, uranium was present in South Greenland before the Gardar. It is suggested, therefore, that the Granite Zone is a uranium geochemical district within a larger uranium geochemical province.

The genesis of the uraniferous veins is believed to have been controlled by the Gardar faulting, which facilitated the hydrothermal circulation of the volatiles derived from the Gardar igneous activity. The uranium itself is believed to have been derived to some extent from the highly differentiated alkaline units, but probably mostly from the older Ketilidian occurrences.

1. INTRODUCTION

Geochemical drainage and airborne gamma-spectrometry surveys demonstrated high levels of uranium in South Greenland (Armour-Brown et al. (1)). Follow-up field work resulted in the finding of many uranium mineral occurrences of different ages (Armour-Brown et al. (2)), and it became clear that the area could be characterized as an uranium geochemical province. Prospecting, concentrated in the most promising central district of the province, the Granite Zone (Fig.1), has shown a wide distribution of uranium occurrences of late Proterozoic age in the many faults and fractures there. Age determinations have been carried out on pitchblende samples from three different localities in the zone. The isotopic data indicate an age of 1180 ± 15 Ma (Armour-Brown et al. (3)), which falls within the limits of the Gardar igneous activity. In the Migmatite Complex to the south (Fig. 1) uraninite also occurs in metasediment units, but there it is of early Proterozoic age (about 1700 Ma) corresponding to the last stage of Ketilidian metamorphism. These occurrences are believed to have been formed penecontemporaneously with the deposition of the sediment (Armour-Brown et al. (1)).

This contribution will discuss the occurrences in the central Granite Zone, which are characteristically of the vein-type associated with fractures and faults.

2. GEOLOGY OF SOUTH GREENLAND

South Greenland comprises a part of the Precambrian shield of Greenland, which consists mostly of the Proterozoic Ketilidian 'Mobile Belt'. This belt has been divided into four major structural zones (Allaart (4)): the 'Border Zone' in the north, the 'Granite Zone' in the centre and the 'Folded Migmatite Zone' and the 'Flat-lying Migmatite Zone' in the south. The last two zones have been combined for the purpose of this paper into the 'Migmatite Complex' (Fig.1).

(i) In the Border Zone Ketilidian supracrustal units unconformably overlie the Archaean basement of granodioritic gneisses. The supracrustal units are composed of basic metavolcanics with mixed metasedimentary rocks of early Proterzoic age.

(ii) The Migmatitic Complex is composed of migmatized supracrustal rocks intruded by late to post-kinematic granite and a late rapakivi granite all of early Proterozoic age. The supracrustal units are composed of pelitic to semipelitic gneiss, arkosic quartzite and basic metavolcanics.

(iii) The Granite Zone is underlain by a complex of granite, diorite and gneissose granite in an 80 - 150 km wide belt trending in a northeast to southwest direction known as the Julianehåb Granite. This granite has been divided into early and late members. The early members are along the margins and the younger members in the central parts of the zone. The early granite members are foliated, inhomogeneous, often nebulitic rocks of adamellitic to granodioritic composition with supracrustal relics. The late granite is less foliated, coarser grained, often porphyritic, adamellitic to granodioritic in composition having more pronounced intrusive relationships. Basic and intermediate rocks (appinitic suite) are scattered throughout the Granite Zone. The age of the metamorphism forming the early granite is early Proterozoic approximately 1840 Ma, and the late granites approximately 1776 Ma according to Rb-Sr isotopic age dates (Van Breemen et al. (5)).

After the Ketilidian diastrophism the crystalline rocks were subjected to a period of intense faulting accompanied by the cratogenic depositional and igneous activity of the Gardar period (1330 - 1150 Ma), (Blaxland et al. (6)). The Gardar supracrustal rocks, the Eriksfjord Formation, consisting mainly of sandstone and basic lava, unconformably overlie the Ketilidian Granite (Poulsen (7), Stewart (8)). They are now largely confined to fault bounded outliers, which probably approximate the general NE-SW trend of the graben structure into which they were deposited. Upton et al. (9) have in fact proposed that this graben was bounded by NE striking faults along Eriksfjord and Bredefjord (Fig. 2). Small remmants of the formation have been found, however, up to 10 km to the north of the present mapped outcrops, and structural evidence along the present

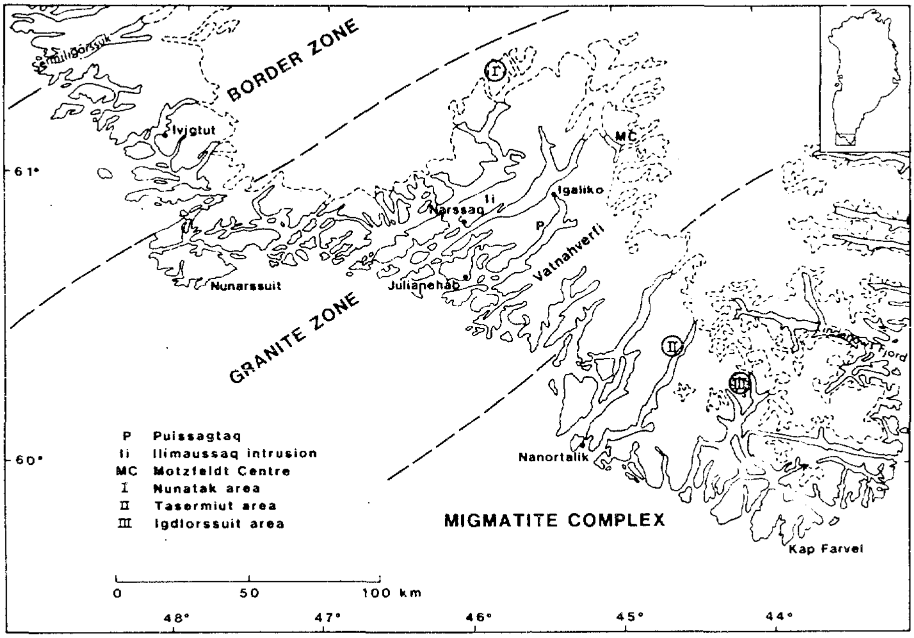

FIG. 1. Locations in South Greenland with major structural zones

southern boundary of the formation, in the vicinity of Igaliko, suggest that the original southern boundary of the graben was further to the south (Harrison et al. (10)). The original width of the graben and extent of sedimentation was, therefore, probably considerably greater although the general NE-SW trend was the same.

Both the Gardar supracrustal rocks and the basement were intruded by a variety of Gardar dikes and alkaline complexes. The dikes commonly strike in a NE-SW direction particularly when they occur in swarms, but they are also found striking EW to ESE-WNW. Basaltic and gabbroic dikes are the most common type but felsic dikes of phonolite, trachyte, and comendite form dense swarms in the zone extending throughout the islands southwest from Narssaq (Emeleus et al. (11)). Some 'Giant Dikes' are composite consisting of dolerite, syenite and nepheline syenite or granite. There are several major Gardar intrusive complexes in the Granite Zone all composed of alkaline rocks with the individual centres showing a variable degree of silica saturation. In the Ilímaussaq (Fig. 1, Ii) an extensive low grade Th-U mineral occurrence has been proven (Sørensen et al. (12), Nielsen (13)) and in the Motzfeldt Centre (Fig. 1, MC) an even more extensive Th-U-Zr-Nb-Ta-REE mineral occurrence has lately been found (Tukiainen et al. (14), Bradshaw et al. (15).

Mesozoic basic dikes and lamprophyric sills, which have been related to the opening of the Labrador Sea, intrude on a very limited scale along the coast (Watt (16)).

3. TECTONIC SETTING OF THE GRANITE ZONE DURING THE GARDAR PERIOD

Previous workers have all recognized that the Granite Zone is highly faulted and fractured. This can be particularly well seen from the high frequency of lineaments on aerial photographs and satellite imagery. Mapping has shown

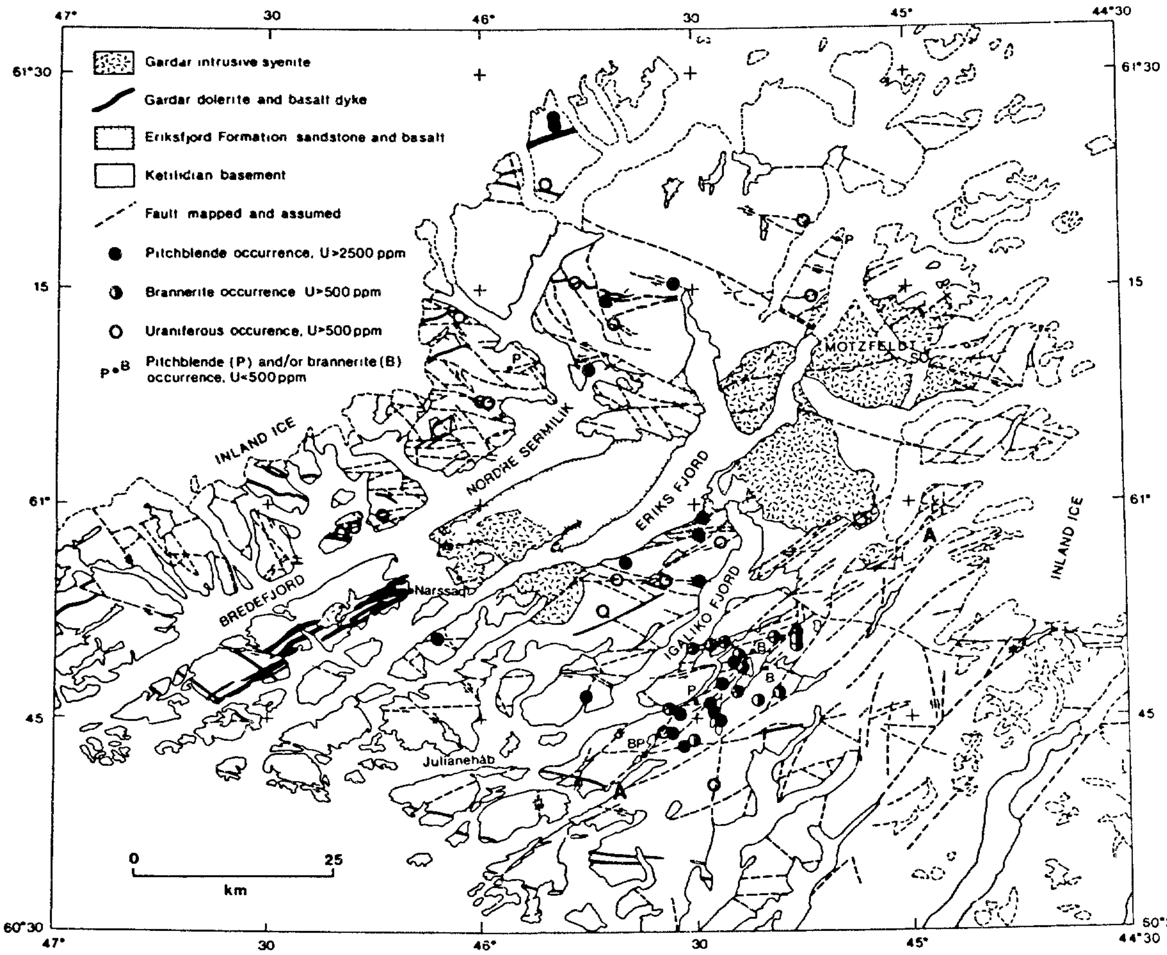

FIG. 2. Geology of the Granite Zone with uraniferous localities. The fault marked with A-A is the suggested southern limit of the Gardar graben.

that the most important faults have left-lateral movements along ESE-WNW to EW striking faults. These have been mapped at fairly regular intervals of 10 - 18 km (Allaart (17), (18), Stephenson (19)). A total sinistral displacement of between 15 and 20 km has been calculated for the central part of the area (Stephenson (19)). This pattern of faulting has been recognized at least 150 km to the northwest (Berthelsen et al. (20), Higgins (21)), and south of the area shown in Fig. 2. Movement along these faults have taken place throughout the Gardar period. This is established by the progressively greater displacements that have been noted of the older Gardar dikes (Henriksen (22), Allaart (4)). Similarly Stephenson's (19) explanation of the rather unusual elliptical shape of most of the large Gardar syenite intrusions, with their long axes oriented in a NW-SE direction, being due to ductile deformation of the hot intrusions undergoing simple sinistral shear along EW faults also establishes the Gardar age of these faults.

There are also faults and fractures in ENE-WSW and NW-SE directions. The ENE-WSW faults are strongly emphasized because the topography, the fjords, and the Gardar dike swarms strike in this direction. No significant lateral displacements, however, have been recorded along them. Vertical movements can be assumed on the faults bounding the areas where the Eriksfjord sediments have been preserved, and 2 - 3 km vertical downthrow along Bredefjord is postulated around Narssaq with a rapid diminishing to the ENE at the head of the fjord (Emeleus et al. (11)). The satellite imagery indicates a sharp southeastern limit to the fracturing of the basement along a NE striking lineament, which dissects the Vatnahverfi peninsula (Fig. 2, A-A). This lineament also marks a sharp fall of geochemical tenor of notably U, Nb and Y to the southeast (Armour-Brown et al. (23)).

The displacements along the NW-SE faults and fractures have only been rarely recognized and mapped, but they are usually lateral with sinistral sense. There are also some NS to NNE-SSW striking faults, both vertical and dipping from 30° to 50° to the east. Very little is known of these faults. Overthrusting on a minor scale of a few tens of metres has been noted along one of them, but otherwise no relative movements associated with them have been noted in this area (Fig. 2).

Our interpretation of the main tectonic features of the region is that throughout the Gardar period the area was subjected to a regional, sinistral, simple shear with a ESE-WNW to EW orientation. Such a stress field would account for all the main fault directions and most of the minor ones. Firstly it gave rise to the important sinistral EW strike slip faults. The direction of tensional strain features in such a stress field will be oriented in a NE-SW direction. The weakening and the thinning of the crust in this direction is evident from the NE-SW orientation of the dike swarms and larger dikes, and the graben in which the Eriksfjord Formation was deposited (Upton et al. (9). This hypothesis also explains why there have not been any major lateral movements noted along the well defined NE-SW linear features. The NW-SE faults are interpreted as second order faults to the main EW shears. The minor sinistral displacements that have been noted along them would confirm such an interpretation.

The NE trending lineament (Fig. 2, A-A) mentioned above, which marks the southeast limit of the more intensive fracturing, is believed to be the southern boundary fault of the NE trending graben. The numerous curved faults just to the northwest of it suggest the scalloped shaped faults, which characteristically develop along a normal fault. Its apparent function as a geochemical barrier reflects the reduced permeability of the less fractured rocks to the southeast.

4. RADIOACTIVE MINERAL OCCURRENCES

Over 200 radioactive occurrences with more than 100 ppm U or Th have been found so far in the Granite Zone, of which the majority are dominated by uranium. They can be classified into five types of occurrences:

(i) Pitchblende associated with faults, fractures and related joints.

(ii) Brannerite, is also associated with fractures and disseminated in altered granite along them. This type occurs particularly in the southern part of the Granite Zone.

(iii) Thorium dominated fenitized veins. These veins are found in ENE-WSW striking tension fractures and show a strong sodium metasomatism.

(iv) Allanite associated with pegmatites in the late Julianehåb Granite. These are Th dominated.

(v) Uraninite disseminated in the pre-Julianehåb Granite metasediments. These have only been found so far at two localities in the north of the Granite Zone and appear to be similar to those found in the Migmatite Complex.

These latter two types of radioactive mineral occurrences are not of interest here and will not be discussed further except to note that at least the latter type could constitute a source of U in the younger vein-type uranium occurrences.

The third type has been described by Hansen (24) and Steenfelt et al. (25) and are related to the alkaline Gardar intrusion. This type may have some bearing on the discussion of the formation of the uraniferous showings described below.

The first two categories constitute the vein-type uranium occurrences referred to in the title and will be described in more detail below.

4.1. Pitchblende vein occurrences and description of the Puissagtaq prospect

Pitchblende occurrences are distributed widely throughout the Granite Zone (Fig. 2). So far they have tended to be rather small lenses along the fractures, but they can be found along the same fracture sometimes for distances of up to 10 km. The most dense distribution of pitchblende veins has been found at Puissagtaq (Fig. 1, P), and this showing is described below as an example of the pitchblende type of occurrence.

Four pitchblende veins lie in the northern part of a 150 - 200 m wide, EW, sinistral, strike slip, fault zone within 1 km of each other and found between 100 to 200 m above sea level. The veins are not exposed, and were found by tracing radioactive boulders back to their source. They are up to 11 m long. Two of them follow the EW fault zone with a dip close to vertical. One of them is 'en echelon' with two shorter veins. The other two strike NE-SW, which is the direction of the tension fractures in the fault zone. The wall rock is altered and brecciated dolerite or granite. One vein is found in a 5 m wide red felsic dike and is more like a joint filling a few metres long, but also with many radioactive spots located for 50 m along its strike in fractures in the dike.

The pitchblende is massive 1 - 10 cm thick and may be slightly brecciated. Fluorite and secondary uranium minerals occur in a zone up to 10 cm adjacent to the pitchblende. Specular hematite, fluorite and minor sulphides with malachite are also present.

Gamma-spectrometer assays of 12 representative samples collected in trenches over a width of 0.5 m of these showings have a mean of 3.25 % U ranging between 0.75 to 9.08 % U with very little Th.

Four other uranium mineral showings are found in the fault zone about 600 m west of the pitchblende veins. Two of them are found in small joints 3 - 6 m long and 1 - 3 cm wide in altered granite striking EW and SSE-NNW and containing 2827 ppm U and 739 ppm U respectively. Investigations of polished thin sections, and confirmed by microprobe investigations, show that the uranium is contained in the U-Ti mineral brannerite. The two other localities are found in felsic dikes. One is very small (10 x 10 cm) and with 3938 ppm U. It is found in a cavity filling with barite, quartz, hematite, ilmenite, pyrite and bornite, but the uranium mineral has not been identified. The other occurrence is found in a 1 - 2 m wide quartz cemented, brecciated felsic dike striking EW. The mineralization can be followed for about 10 m. It is low in uranium (147 ppm), and is mainly a sulphide mineralization with galena and bornite and some digenite, covellite, chalcopyrite and tetrahedrite. No uranium minerals were identified.

Mineralogical studies show that pitchblende occurs as botryoidal masses often displaying cataclastic texture. Cracks in the pitchblende frequently contain small grains of galena which is probably radiogenic in origin. It is associated with specular hematite and minor pyrite and chalcopyrite. The pyrite is cataclastic and partly altered to limonite and may be replaced by hematite. Veinlets of pitchblende are noticed to cut specular hematite and to form pseudomorphs after pyrite. The pitchblende can be slightly brecciated indicating some fault movement after its deposition. The gangue minerals are calcite, quartz and fluorite.

4.2. Brannerite type occurrences, Vatnahverfi area

Brannerite occurrences are also associated with the faults and fractures, but it tends to be disseminated in drusy cavities in the altered granite wall-rock. It is occasionally found with the pitchblende, but more commonly alone. Most of the occurrences are in the Vatnahverfi area, where over 50 have been found with more than 100 ppm U.

The majority of the radioactive showings are small, less than one square metre, but several have been found to extend from 50 to 150 metres along the fault zones. In many cases a lineament has several localities with radioactive occurrences along its trend. A good example is a 5 km long, ENE striking fracture zone intruded by a 5 - 7 m wide lamprophyric dike found to the north in the Vatnahverfi area close to the Igaliko Fjord (Fig. 2). In the contact zone between granite and dike many uraniferous occurrences were found. The mineralized zone varies between 0.5 and 1 m in width, and contains 500 - 2100 ppm U and very little Th. The rock is brecciated, strongly altered and red-brown, with fluorite, hematite and disseminated sulphides.

The radioactive minerals commonly occur with fluorite, calcite and hematite, and in some cases limonitized sulphides. Quartz and carbonate veining is normal.

Mineralogical studies show that brannerite is disseminated in the rock associated with chlorite or following fracture fillings of calcite, quartz or chlorite. It is found as disseminated yellow grains, as radiating greenish yellow needles with metamict brown centres, brownish metamict fracture fillings or very small disseminated brown metamict grains. Associated with brannerite are minor pitchblende, coffinite, uraniferous titanite and zircon. Hematite is the most widespread associated gangue mineral, and fluorite commonly occurs. In some samples ilmenite together with rutile is seen, and are probably remnants of altered titanomagnetite. Pyrite, often altered to limonite, is the most common sulphide mineral with some chalcopyrite and galena.

Semi-quantitative electron microprobe analyses (energy dispersive - EDX) of the brannerite gave an average composition of 36.4 % UO_2, 32.2 % TiO_2, 5.4 % SiO_2, 3.2 % CaO, 2.7 % FeO and 1.0 % Al_2O_3. The amount of UO_2 varies from 25 to 55 % and TiO_2 from 22 to 43 %. Back scatter images normally show two phases with the highest UO_2 values in the center of the grain and 3 - 5 % less in the margins. Normally the ThO_2 content of the brannerite is low (less than 0.5 %) with the exception of one sample in which 8 to 11 % ThO_2 was found and an unusually low UO_2 content of 17 - 30 %. The colour of this type of brannerite is dark orange-brown in contrast to the normal type, which is yellow or brown (metamict). A few percent of REE (La, Ce, Nd) and Y is also found in the different types of brannerite with the highest values (4 - 7 %) in the Th-rich type. The PbO_2 content varies from 3.3 to 0.3 %, but is often not detected.

Several types of mineral inclusions in the brannerite have been identified which were presumably present before the brannerite formed including uraniferous zircon, rutile, titanite, galena and pitchblende. The zircon contains up to 10.0 % UO_2 with less than 0.5 % ThO_2, differing markedly from the original zircon in the granite, which has up to 7.5 % ThO_2 with very little UO_2.

There are also other uraniferous mineral phases one of which is a Ca-Ti silicate with up to 30 % UO_2, which is possibly a titanite. Another uranium mineral phase is found as very fine-grained inclusions concentrated at the apical parts of radiating aggregates of apatite. This radioactive 'dust' is a U-Ca phosphate with a UO_2 content varying between 17 and 61 %. The apatite itself has about 1.5 % UO_2. In the same apatite rich sample a calcium phosphate rich in ThO_2 (8 - 48 %) and low in UO_2 (4 - 5 %), brannerite and bastnaesite were found.

5. ALTERATION OF THE WALLROCK

Alteration of the wallrock, not only along radioactive mineral occurrences but also associated with the fractures, has been observed throughout the Granite Zone. From superficial studies this alteration appears to affect the granitic rocks more than the dikes. Presumably this is partly due to the fact, that the dikes are of alkaline composition and are more in equilibrium with the hydrothermal activity, since they are both derived from the same magmatic sources and in many cases the same late stage differentiates. In any event, there is no chemical data relating the alteration of dikes to mineralization, so the following discussion refers only to the granite.

Two types of alteration have previously been recognized. Albitization accompanied by desilicification is the most commonly recognized and is usually related to the Gardar magmatic activity (Allaart (17)). It is associated with radioactive green veins intruded along NE-SW trending tension fractures east of the Ilímaussaq intrusion (Hansen (24)). The veins are characterized by a considerably higher Th than U content, a high Na content (5 - 12 %), and a depletion of K (mostly <0.10 %). These green veins have been related to hydrothermal activity associated with the intrusion of the Ilímaussaq intrusion. In the Qagssiarssuk area, on the other hand, a progressive K-feldspathization of the basement granite adjacent to carbonatite plugs has been noted (Stewart (26)). The eventual outcome of this alteration is the more or less complete removal of Na, desilicification and the introduction of K up to 11.57 %.

The alteration of the Julianehåb granite in the Puissagtaq area has taken place in three different ways. The most common type is associated with a reddening of the granite, but there is also a greenish alteration and an albitization. Mineralogical changes start with an alteration of the mafic minerals biotite and hornblende to chlorite, epidote and hematite. The next step is a sericitization of the plagioclase, often accompanied by a reddening of the feldspars by fine hematite 'dust'. The microcline is normally only little affected by the metasomatism but may also be totally altered to sericite (greenish alteration). Calcite and sometimes fluorite are introduced.

Chemically all three types of alteration are characterized by a depletion of Si, an increase in Ca and volatiles and an oxidation of Fe (Table I, 3-5). The differences between the three types are the following:

(i) Increase of K and a depletion of Na in the granite suffering the reddening

(ii) Depletion of K and an increase of Na in the albitized sample

(iii) Depletion of Na and only small variations in K in the green altered samples

Alteration has been noted in many other places during the course of the exploration. Some of them have been confirmed, by major element analyses, to be similar to those above, and it appears, that all radioactive albitized veins are Th dominated, but not all albitization is radioactive.

There are, however, other types of altered zones. Among these is a 2 m wide alteration zone, which is typical of a series of parallel NNE trending fractures in the northern part of the Granite Zone. The granite wallrock is rusty and hard, but becomes more friable towards the centre of the altered zone before it turns into a purplish clay with bleached patches. A narrow (2 - 5 cm) sericitic quartz vein runs down the centre. Chemically, the granite affected by this alteration progressively looses Na and Ca, Si increases towards the centre accompanied by an oxidation of Fe and K remains constant (Tab. I, 6 - 8). This particular zone is not itself uraniferous or radioactive but the streams draining the area contain high levels of U both in the water and the sediment, suggesting the presence of U minerals, which have not yet been found.

TABLE I. MAJOR ELEMENT ANALYSES OF ALTERED SAMPLES FROM THE GRANITE ZONE.

GGU NO.	(1) 304281	(2) 304525	(3) 304278	(4) 304524	(5) 304523	(6) 304539	(7) 304540	(8) 304541	(9) 304585	(10) 304863
SiO_2	69.92	73.60	56.20	59.19	63.93	63.18	63.31	71.30	36.20	25.75
TiO_2	0.56	0.21	0.40	0.88	0.85	0.51	0.51	0.51	0.43	0.21
Al_2O_3	14.56	13.71	16.35	17.38	15.63	15.16	15.47	14.80	2.68	5.68
Fe_2O_3	1.07	0.37	2.28	2.07	2.77	1.90	2.22	5.71	1.32	5.64
FeO	1.56	1.33	0.31	2.44	1.49	2.19	1.25	0.36	5.16	0.12
MnO	0.04	0.04	0.14	0.10	0.11	0.07	0.09	0.00	0.68	0.20
MgO	0.78	0.09	0.82	1.69	2.00	1.51	1.34	0.17	1.64	0.17
CaO	1.38	0.74	4.93	2.51	2.15	3.28	4.20	0.33	23.21	31.06
Na_2O	4.14	3.68	1.00	8.51	0.10	5.45	0.23	0.16	0.03	0.57
K_2O	4.61	5.40	12.43	1.33	6.16	1.39	4.06	4.02	0.03	3.74
LOI	0.86	0.54	4.84	3.03	4.15	4.49	7.10	2.29	19.78	0.98
P_2O_5	0.18	0.04	0.11	0.41	0.45	0.21	0.22	0.21	2.06	24.70
SUM	99.66	99.75	99.81	99.54	99.79	99.34	100.00	99.86	93.22	98.82

MAJOR ELEMENTS IN WEIGHT PERCENT OF TOTAL, ANALYSED BY X-RAY FLUORESCENCE AT GGU

1. MEDIUM GRAINED BIOTITE-HORNBLENDE GRANITE, FRESH, PUISSAGTAQ
2. APLITIC BIOTITE GRANITE, FRESH, PUISSAGTAQ
3. RED ALTERED GRANITE, PUISSAGTAQ
4. ALBITIZED GRANITE, PUISSAGTAQ
5. GREEN ALTERED GRANITE, PUISSAGTAQ
6. ALTERED GRANITE, HARD, NORTHERN GRANITE ZONE
7. ALTERED GRANITE, SOFT, RUSTY, NORTHERN GRANITE ZONE
8. ALTERED GRANITE, FRIABLE, NORTHERN GRANITE ZONE
9. CARBONATITIC VEIN, NORTHERN GRANITE ZONE
10. PHOSPHATE RICH VEIN, NORTHERN GRANITE ZONE

Other types of alteration were noted in veined fractures some of which are uraniferous. These are slightly radioactive (Th dominated) calcium carbonate rich veins with very depleted Si, Na and K (Tab. I, 9), and one phosphate rich vein with depleted Si and Na and enriched in Ca, which is also radioactive but dominated by U (Tab. I, 10). This type of alteration is also found in the Vatnahverfi area.

The overall relationship of the alteration zones to the precipitation of radioactive minerals is not well understood. All that can be said about them at present is that they reflect widespread hydrothermal activity, which has been greatly helped by the fractured condition of the basement and by the many heat sources during the long history of the Gardar igneous activity. Their differing chemistry presumably reflects, both the long history of hydrothermal activity, different magmatic sources, as well as chemical changes with distance from their sources.

6. DISCUSSION OF THE GENESIS OF THE URANIUM VEIN OCCURRENCES

The genesis of the pitchblende vein occurrences can be related, without much doubt, to the hydrothermal activity associated with the Gardar igneous events. This conclusion is based on the late Gardar age which has been established by U and Pb isotope analyses on three samples from three different localities (Armour-Brown et al. (3)). The U-Pb isotopic values lie on or close to the concordia indicating that there has been no later redistribution of the isotopes, and give ages between 1096 and 1200 ± 15 Ma. Their occurrence in the Gardar related faults and fractures, and the association of the typical alkaline suite of elements also strongly suggest an affinity with this hydrothermal event. The brecciated texture of the pitchblende shows that it was deposited while the faults were still active, i.e. during the Gardar.

There is no reason to believe, that the brannerite occurrences are not similarly related although no isotopic ages are yet available. Both their chemistry and their emplacement in the Gardar fracture system suggest the same origin.

These conclusions are corroborated by the geographical distribution of the elements from the reconnaissance geochemical stream sediment samples, which reflect the Gardar alkaline igneous activity. Elements such as Y, Nb and Sr like U are all enhanced in value in the Granite Zone. They are particularly high in the northwest side of the ENE-WSW trending lineament (Fig. 2, A-A), which marks the southern boundary of the highly fractured part of the Granite Zone. It certainly shows how the fracturing of the granite controlled the distribution of the hydrothermal activity.

The source of the uranium may be derived from highly differentiated alkaline complexes. Two of these are rich in Th and U (the Ilímaussaq intrusion and the Motzfeldt Centre), a part of the U may come from this source, as may Th in the albitized veins. Uranium, however, has been found in a soluble form in the Ketilidian basement rocks. Two localities with uraninite have been found in the north of the Granite Zone in pre-granite supracrustal units (Fig. 1, I), which are believed to be of Ketilidian age (Armour-Brown et al. (2)). Also, in the Migmatite Complex to the south (Fig. 1, II, III), disseminated uraninite is located in the neosome of the migmatite, which has a supracrustal origin, and U-Pb isotopic determinations gave an age of 1728 Ma (Nielsen et al. (27)). A disseminated uraninite occurrence in supracrustal rocks has also been found at Igdlorssuit (Fig. 1, III), (Armour-Brown et al. (2)). The age of this uraninite is also Ketilidian.

Uranium was therefore present in South Greenland before the Gardar time, and at least some, if not all, of it found in the vein-type occurrences could have been derived from this source and redistributed by the hydrothermal system. The alkaline magma from the highly differentiated Gardar igneous complexes could have provided both the heat and the volatiles to produce this hydrothermal system. These volatiles would have varied in composition with source, time and place as can be surmised from the varied wallrock alteration. The only information on the chemistry of the volatiles, which have been derived from the differentiating alkaline magmas, comes from a study of fluid inclusion in alkaline rocks of various Gardar intrusions. They were all found to be aqueous with a varying composition of hydrocarbons and carbon dioxide (Konnerup-Madsen et al. (28)). Although this is only indirect evidence for the chemistry of the volatiles in hydrothermal veins outside the intrusions, they may be assumed to have been alkaline in composition with a low oxygen fugacity and possibly some hydrocarbon content. Such a composition would, following the phase diagrams of Langmuir (29), greatly facilitate the mobility of any U derived from the alkaline magmas. At the same time, meteoric waters were presumably oxidizing and possibly even acidic and would also have had no difficulty in dissolving and transporting uranium from the surrounding uraniferous Ketilidian units or even the granite. The nearness of the present land surface to the original Gardar erosion surface, which is indicated by the remnants of the Eriksfjord Formation sediments in the granite, would certainly support this possibility. Similarly the omnipresent hematite suggests a ready supply of oxygen and the open drusy character of the hydrothermal minerals suggest a relatively near surface phenomena with a low confining pressure.

The mixing of these two water sources in the fractures, would in turn be facilitated by the contemporaneous movement along them, and it is easy to imagine that they could create the physical-chemical conditions conducive to the precipitation of pitchblende. The Th dominated veins were presumably formed at a higher temperature. This is reflected in their proximity to the alkaline intrusions. The brannerite, on the other hand, appears to have formed at a lower temperature, is farther from the intrusions and contains inclusions of presumably earlier pitchblende.

7. CONCLUSIONS

U mineral occurrences have now been found from the most northern point in the Granite Zone to the most southern. The most interesting U occurrence located so far is at Puissagtaq (Fig. 1, P) where four small pitchblende veins have been found. These veins grade 0.75 - 9.0 % U, with very little Th over sampling widths of 0.5 m and are due to massive pitchblende in 2 - 5 cm wide lenses. The longest vein could be traced for 11 m. The veins occur at 100 m difference in altitude so that it may be concluded that they are not overly controlled by their depth below the erosion surface. The brannerite occurrences in Vatnahverfi are widespread but small. They may originate partly from a redistribution of uranium from pitchblende which, in some cases, is found close to them.

The pitchblende and brannerite vein occurrences are epigenetic, and their genesis and the alteration of the wallrock are related to Gardar hydrothermal activity, controlled by the Gardar faults and related fractures. Although the source of the U may be from the differentiated alkaline intrusives, it is also probable that it was also derived from earlier (Ketilidian) uranium occurrences.

ACKNOWLEDGEMENTS

We would like to thank the Director of the Geological Survey of Greenland for permission to publish this paper and W. Stuart Watt for correcting the english.

REFERENCES

(1) ARMOUR-BROWN, A., STEENFELT, A., KUNZENDORF, H., Uranium districts defined by reconnaissance geochemistry in South Greenland, J. Geochem. Explor. 19 (1983) 127-145.

(2) ARMOUR-BROWN, A., TUKIAINEN, T., NYEGAARD, P., WALLIN, B., The South Greenland Exploration Programme, Final report of progress 1980-1983, Internal report, Grønlands geol. Unders. (1984) 107 pp.

(3) ARMOUR-BROWN, A., TUKIAINEN, T., WALLIN, B., Pitchblende vein discoveries in the Proterozoic Ketilidian granite of South Greenland, Geol. Rdsch. 71 (1982) 73-80.

(4) ALLAART, J.H., Ketilidian mobile belt in South Greenland, in: A. Escher and W.S. Watt (editors), Geology of Greenland, Geol. Surv. Greenland, Copenhagen (1976) 121-151.

(5) VAN BREEMEN, O., AFTALION, M., ALLAART, J.H., Isotopic and geochronologic studies on granites from the Ketilidian mobile belt of South Greenland, Geol. Soc. Am., Bull. 85 (1974) 403-412.

(6) BLAXLAND, A.B., VON BREEMEN, O., EMELEUS, C.H., ANDERSON, J.G., Age and origin of the major syenite centres in the Gardar province of South Greenland: Rb-Sr studies, Geol. Soc. Am., Bull. 89 (1978) 231-244.

(7) POULSEN, V., The sandstones of the Precambrian Eriksfjord Formation in South Greenland, Rapp. Grønlands geol. Unders. 2 (1964) 16 pp.

(8) STEWART, J.W., The earlier Gardar igneous rocks of the Ilímaussaq area, South Greenland, Unpubl. Ph. D. Theses, Univ. Durham, England (1964) 423 pp.

(9) UPTON, B.G.J., BLUNDELL, D.J., The Gardar igneous province: evidence for Proterozoic continental rifting, in: E.-R. Neumann, I.B. Ramberg (editors), Petrology and Geochemistry of Continental Rifts, Reidel Publishing Company (Holland) (1978) 163-172.

(10) HARRISON, S.M., HESSELBO, P. (eds.), Aberdeen University, Geological Expedition to South Greenland, (unpubl.) (1983) 39 pp.

(11) EMELEUS, C.H., UPTON, B.G.J., The Gardar period in southern Greenland, In Escher, A., Watt, W.S., Geology of Greenland, Geol. Surv. Greenland, Copenhagen (1976) 154-181.

(12) SØRENSEN, H., ROSE-HANSEN, J., NIELSEN, B.L., LØVBORG, L., SØRENSEN, E. LUNDGAARD, T., The uranium deposits at Kvanefjeld, the Ilímaussaq intrusion, South Greenland; Geology, reserves and beneficiation, Rapp. Grønlands geol. Unders. 60 (1974) 54 pp.

(13) NIELSEN, B.L., Exploration history of the Kvanefjeld uranium deposit, the Ilimaussaq intrusion, South Greenland, in: Uranium exploration case histories, IAEA Vienna (1981) 353-388.

(14) TUKIAINEN, T., BRADSHAW, C., EMELEUS, C.H., Geological and radiometric mapping of the Motzfeldt Centre of the Igaliko Complex, South Greenland, Rapp. Grønlands geol. Unders. 120 (1984) 78-83.

(15) BRADSHAW, C., TUKIAINEN, T., Geological and radiometric mapping of the Motzfeldt Centre of the Igaliko Complex, South Greenland, Progress report, Internal GGU report (1983) 34 pp.

(16) WATT, W.S., The coast-parallel dyke swarm of Southwest Greenland in relation to the opening of the Labrador Sea, Can. J. Earth Sci. 6 (1969) 1320-1321.

(17) ALLAART, J.H., Descriptive text to Geological map of Greenland 1:100 000, Julianelb 60 V 2 Nord., Grønlands geol. Unders. (also Meddr Grønland 192,4) (1973) 41 pp.

(18) ALLAART, J.H., Descriptive text to Geological map of Greenland 1:100 000, Narssarssuaq 61 V 3 Syd, Grønlands geol. Unders., Copenhagen (1983) 20 pp.

(19) STEPHENSON, D., A simple shear model for the ductile deformation of high-level intrusions in South Greenland, J. geol. Soc. Lond. 132 (1976) 307-308.

(20) BERTHELSEN, A., HENRIKSEN, N., Descriptive text to Geological Map of Greenland 1:100 1000, Ivigtut, 61 V Syd, Grønlands geol. Unders., Copenhagen (also Meddr Grønland 185, 1) (1975) 210 pp.

(21) HIGGINS, A.K., The stratigraphy and structure of the Ketilidian rocks of Midternaes, Southwest Greenland, Bull. Grønlands geol. Unders. 87 (also Meddr Grønland 189, 2) (1970) 96 pp.

(22) HENRIKSEN, N., Structural analysis of a fault in Southwest Greenland, Bull. Grønlands geol. Unders. 26 (also Meddr Grønland 126, 9) (1960) 60 pp.

(23) ARMOUR-BROWN, A., TUKIAINEN, T., WALLIN, B., The South Greenland uranium exploration programme, Final report of reconnaissance results, Internal report, Grønlands geol. Unders. (1982) 95 pp.

(24) HANSEN, J., A study of radioactive veins containing rare-earth minerals in the area surrounding the Ilímaussaq alkaline intrusion in South Green-

land, Bull. Grønlands geol. Unders. 76 (also Meddr Grønland 181, 8) (1968) 47 pp.

(25) STEENFELT, A., TUKIAINEN, T., Uranium-thorium mineralization in the vicinity of the Igdlerfigssalik Centre of the Igaliko nepheline syenite complex, South Greenland, Rapp. Grønlands geol. Unders. 105 (1981) 44-47.

(26) STEWART, J.W., Precambrian alkaline-ultramafic/carbonatite volcanism at Qagssiarssuk, South Greenland, Bull. Grønlands geol. Unders. 84 (also Meddr Grønland 186, 4) (1970) 70 pp.

(27) NIELSEN, B.L., TUKIAINEN, T., Uranium-bearing metasediment and granite in the Tasermiut Area, South Greenland, Rapp. Grønlands geol. Unders. 105 (1981) 47-50.

(28) KONNERUP-MADSEN, J., ROSE-HANSEN, J., Volatiles associated with alkaline igneous rift activity: fluid inclusions in the Ilímaussaq intrusion and the Gardar granitic complexes (South Greenland), Chemical Geology 37 (1982) 79-93.

(29) LANGMUIR, D., Uranium solution-mineral equilibra at low temperatures with applications to sedimentary ore deposits. In Kimberley, M.M. (ed.): Short Course in Uranium Deposits: Their Mineralogy and Origin, Miner. Ass. Can. (Toronto) (1978) 17-55.

GEOLOGICAL ENVIRONMENT OF THE VEIN-TYPE DEPOSITS IN THE APHEBIAN BASEMENT OF THE CARSWELL STRUCTURE ON THE ATHABASCA PLATEAU (NORTHERN SASKATCHEWAN) COMPARISON WITH OTHER DEPOSITS OF THE SAME TYPE

P. Artru, M. Bervillé, M. Moreau, F. Tona

Cogéma, Branche Uranium Naturel
Département des Prospections et Recherches Minières

Vélizy-Villacoublay

France

Abstract

GEOLOGICAL ENVIRONMENT OF THE VEIN-TYPE DEPOSITS IN THE APHEBIAN BASEMENT OF THE CARSWELL STRUCTURE ON THE ATHABASCA PLATEAU (NORTHERN SASKATCHEWAN) COMPARISON WITH OTHER DEPOSITS OF THE SAME TYPE

The Athabasca Plateau, widely known for its unconformity-related high grade and massive uranium deposits, contains vein-type deposits as well: although less striking, they are nevertheless of great scientific and economic interest. Claude and N deposits are now supplemented by the Peter River discovery.

The Cluff Lake area basement deposits of the western Athabasca Plateau have been the subject of several scientific papers. This paper deals mainly with the Cluff Lake deposits but refers to other basement deposits of the Eastern Athabasca Plateau when data are available: Dawn Lake, Rabbit Lake, the deposits of the western shore of the Wollaston Lake and large parts of Key Lake are basement deposits.

Cluff Lake basement deposits are characterized by their stratigraphic position in or close to a dominantly aluminous, graphitic and pyritic metasedimentary formation (Peter River gneiss), most probably a former black shale. They are also close to an underlying unit consisting of quartzo-feldspathic gneisses (Earl River Complex) which could be a former arkosic sandstone, metamorphosed and reactivated. This latter unit is mainly found in the heart of dome shaped anticlines (mantled gneiss domes). The reactivation process created favourable conditions for mobilization of uranium into small concentrations early (1800 Ma) in the metamorphics.

The main structural control of the deposits appears to be Hudsonian mylonites and subsequent fracturation. However, it is after the deposition of the Athabasca Sandstone that the mylonites and their associated fractures were rejuvenated and invaded by hydrothermal fluids. A widespread alteration pervaded through the surrounding rocks and uranium precipitated in the open fractures.

Several phases with different paragenesis can be identified with ages spreading from 1200 Ma to 900 Ma although some remobilization occurred much later. The 480 Ma violent tectonic event associated with the formation of the Carswell structure and the injection of the Cluff Breccia further complicated the structure, partially obscuring the earlier events.

The unconformity deposits are represented in Cluff Lake by the well known D deposit. An important Hudsonian mylonite is the main link between this deposit and the Peter River basement deposit. The ages of both mineralizations are similar, leading to the conclusion that both result from the same long mineralizing process. Adaptation of this process to different lithological environments gave birth to two very different types of deposits.

1. GEOLOGICAL UNITS

1.1. Basement of Northern Saskatchewan

This crystalline basement belongs to the Churchill Province of the Canadian Shield. The Archaean basement here has been deeply involved in the Hudsonian Orogeny, and is mainly preserved as nuclei of high metamorphic rocks around which are wrapped the generally less granitized and less competent rocks of Aphebian age.

Classical subdivisions are:

- Western Craton
- Cree Lake zone
- Rottenstone Complex
- South-Eastern Complex

Known uranium deposits are located only in the two first zones (Fig. 1).

1.1.1. Western Craton

The Western Craton extends west of the main Hudsonian orogen from the Virgin River shear zone up to the Mac Donald fault in the Northwest Territories. Lewry et al. (1) distinguished three domains within the craton: the Western Granulite, the Clearwater and the Firebag domains (Fig. 2).

It seems that Aphebian rocks from the Firebag domain (Godfrey et al. (2)) and from the Western Granulite domain (Scott (3)) are similar, although structurally divided by the axis of the Clearwater domain. The metamorphic core of the Carswell circular structure belongs to the Firebag domain on the edge of the Clearwater domain (Tona et al. (4)).

The whole Western Craton is an area of indurated catazonal crustal blocks (Archaean?) with a relatively thin Aphebian cover submitted to intense brittle to ductile tectonic movements and local granitic intrusions. This mobile platform zone hosts two uranium districts: the Cluff Lake deposits in the basement core of the Carswell circular structure and the Beaverlodge deposits around Uranium City.

1.1.2. Cree Lake Zone

The Cree Lake zone is the ensialic part of the typical Hudsonian orogen. It consists of three domains: Virgin River to the West, Mudjatik in the middle and the Wollaston Belt in the East. Aphebian rocks of shelf to miogeosynclinal type cover a granitized Archaean basement. The Archaean is heavily remobilized and involved in an Hudsonian folding and metamorphism which is more intense than in the Western Craton.

The Mudjatik domain is the most remobilized heart of the Cree Lake zone, showing horizontal migmatitic lobes. It contrasts with the lower temperatured Virgin River and Wollaston Domain with their typical mantled gneiss dome systems with remobilized 'Archaean' cores.

The Wollaston Belt contains some of the largest uranium deposits in the world, associated with the Athabasca Plateau Helikian sandstones unconformity. It is characterized by the development of non magnetic metapelites or quartzo-metapelites units, rich in graphite and associated with numerous calcsilicate intercalations.

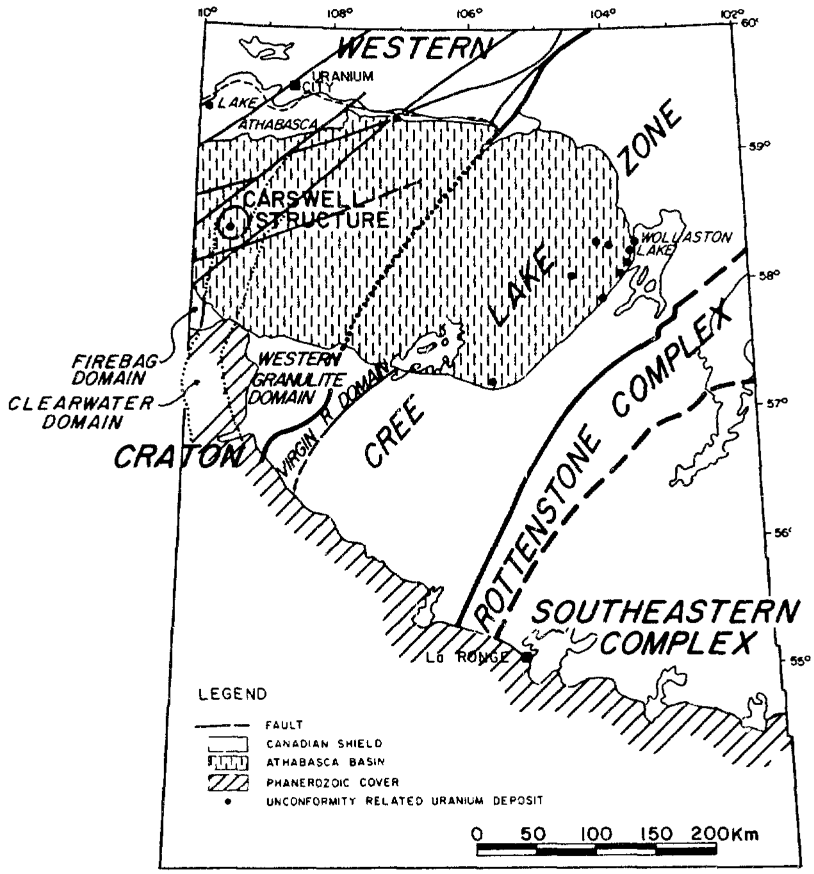

FIG. 1. Location of the Carswell structure with respect to the lithostructural subdivisions of the Western Canadian Shield (mod. after Lewry et al., (1) in Tona et al. (4))

The upper part of the Wollaston series consists in a highly magnetic unit of volcanogenic origin which develops eastward and could be an equivalent, at least chemically, of the Whataman granitization in the Rottenstone domain. Its volcanic component is proven by its particular calcoalcaline composition with low alumina and monzonitic mineral association rich in magnetic amphiboles.

A surprising characteristic of the Wollaston Belt is the absence of a detrital basal sequence. One hypothesis is that this detrital sequence was initially present but has been digested during the migmatitic reactivation of the Hudsonian Orogeny. The graphitic layers of the Aphebian pelite stopped the advance of the anatexis, giving a false impression of unconformity. However, some hold for a more sedimentary approach where the 'basal pelites' are a transgressive unit on Archaean domes. Whatever the hypothesis, it is certain that the contact between the Archaean granitized rocks and the Aphebian metapelites has undergone considerable remobilization during the Hudsonian Orogeny.

1.2. Martin Formation

The Martin Formation is a pre-Athabasca post-orogenic molasse which is found in an elongated graben close to Beaverlodge deposits. It is a typical red beds formation.

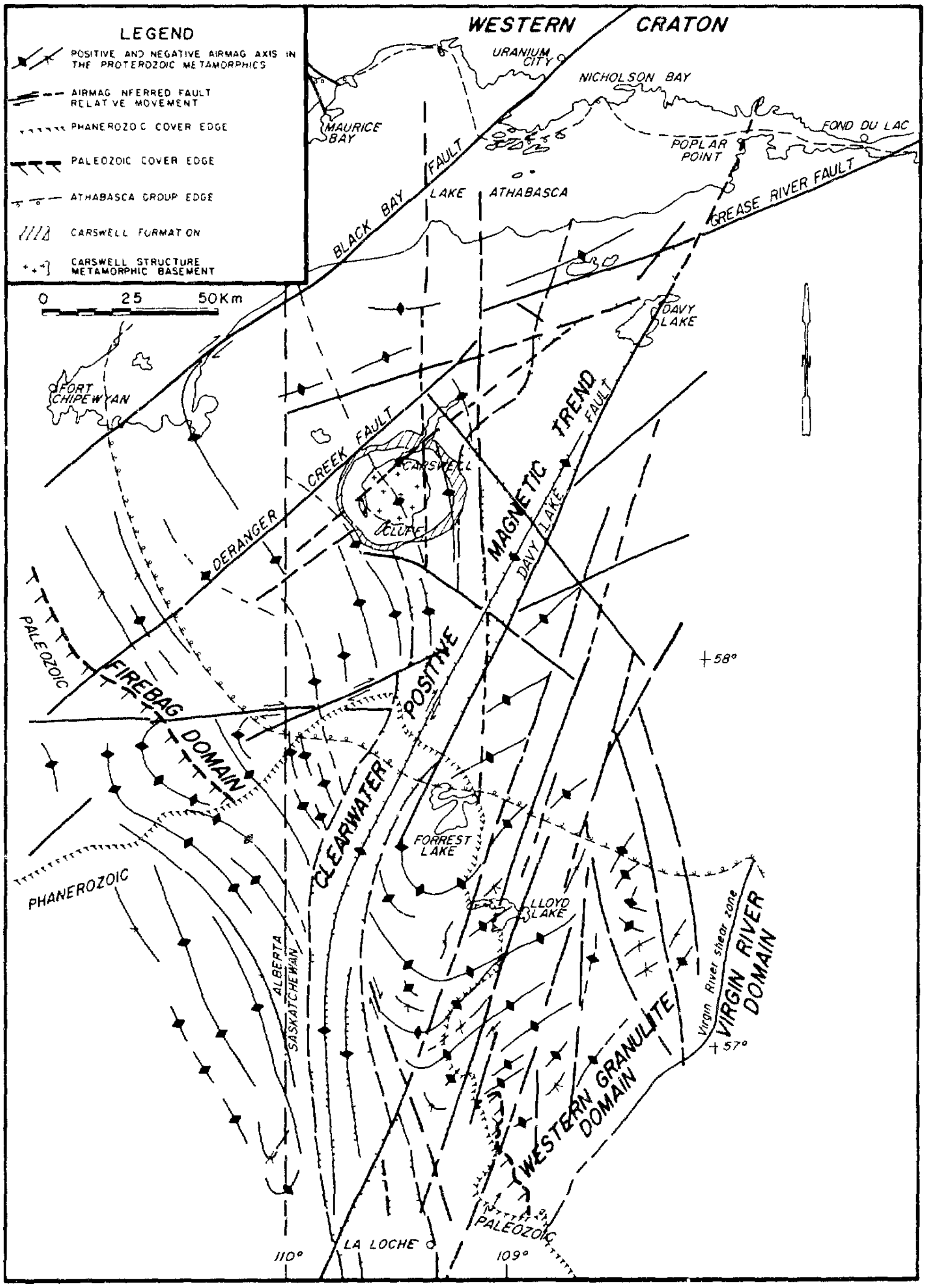

FIG. 2. Structural location of the Carswell structure (in Tona et al. (4)).

1.3. Athabasca Plateau Basin

The Helikian sandstones filling this oval-shaped basin have been studied and divided in several groups (Ramaekers (5)). Recently, clay fraction was used to refine the sandstone stratigraphy (Hoeve et al. (6)).

In the Carswell structure, Pacquet et al. (7) identified a discontinuous basal unit, up to 60 m thick, laying directly on the regolithic basement. Pe-

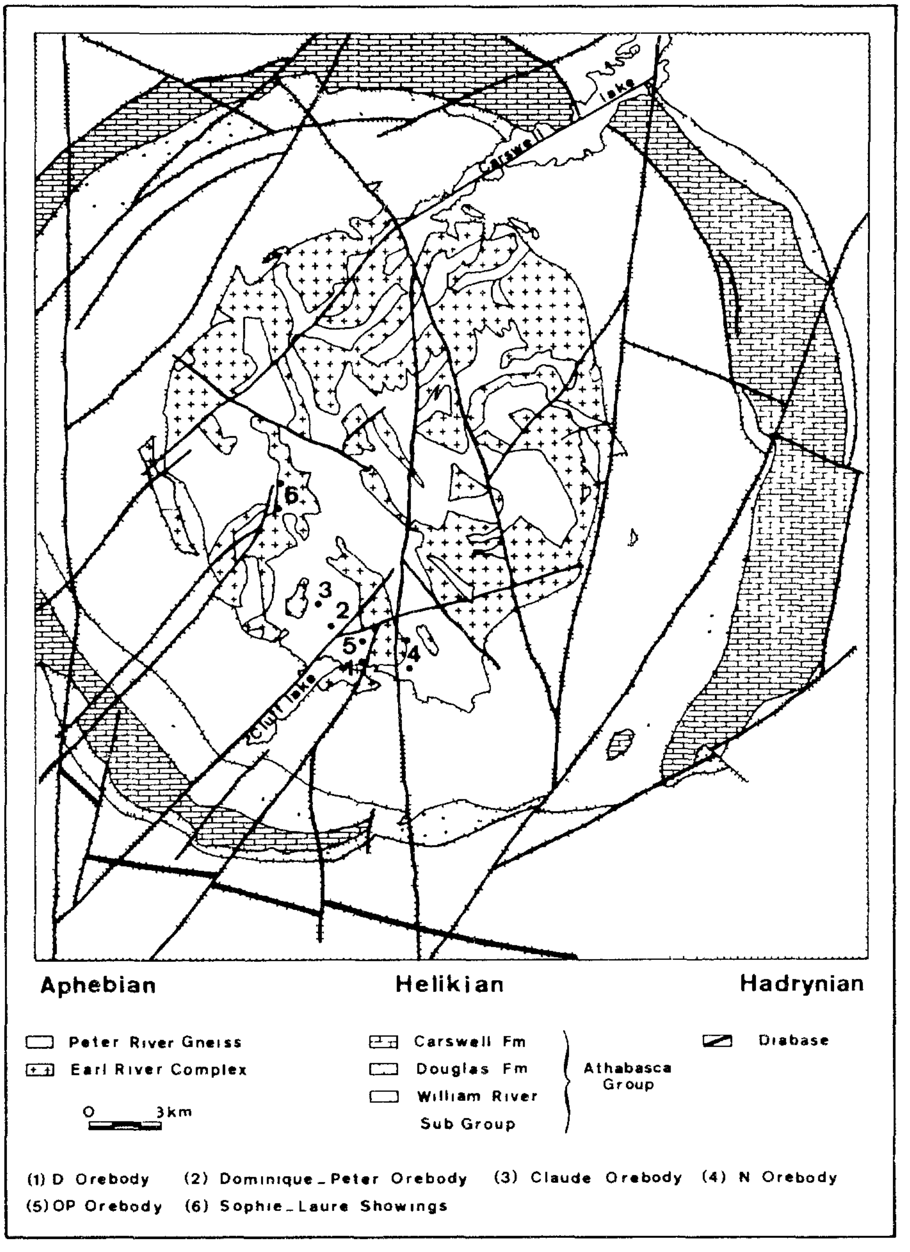

FIG. 3. Geological map of the Carswell circular structure (mod. after Amok (15)).

lites from this unit have a distinctive acid volcanic inprint. Similar palaeo-helikian red beds have been found in other places at the bottom of the Athabasca Group (Ramaekers (5)).

Monotonous sandstone formations of continental to marine origin form the main part of the present Athabasca Basin filling. However, stratigraphically higher pelitic and dolomitic formations known as the Douglas and Carswell Formations are found preserved in the circular moat of the Carswell structure (Wheatley et al. (8)). Recent dating by K/Ar method on illites, on the Douglas Formation gives an age of 1292 ± 27 Ma and 1220 ± 43 Ma (Clauer et al. (9)). Diabase dikes cutting through the Athabasca sandstones are dated from 1230 to 930 Ma (Burwash et al. (10), Wanless et al. (11)).

1.4. Carswell circular structure

The Carswell circular structure is located approximately 60 km south of Lake Athabasca and 25 km east of the Alberta/Saskatchewan border within the Athabasca Plateau (Fig. 3).

The roughly circular structure contains a 20 km diameter core of metamorphic basement assimilated to the Firebag domain within the Western Craton (Tona et al. (4)) which is unconformably in contact with the surrounding William River Subgroup sediments (Ramaekers (5), Hoeve et al. (6)).

A major event (cryptoexplosion or meteoritic impact?) dated 480 Ma (Bell (12)) brought the basement to surface and disturbed the entire Athabasca Group around the structure. This event was accompanied by swarms of 'Cluff breccia' (Pagel (13), von Einsiedel (14)).

The metamorphic basement is divided into two main units (Amok (15)):

- Peter River gneiss
- Earl River complex

It has been noted that the Peter River gneiss commonly overlies the Earl River Complex.

The Peter River gneiss is a distinct metasedimentary unit of aluminous gneisses (banded, well foliated, rich in garnet, cordierite, sillimanite, pyrite and graphite). Based on such a composition, the Peter River gneiss may represent a former sedimentary black shale. The average Rb/Sr age date on the series is 1760 $\pm$ Ma (Bell (12)).

The Earl River Complex is a mixed series of feldspathic gneisses, mafic gneisses, amphibolites, granitoids and pegmatoids. Pagel et al. (16) conclude to a metasedimentary origin (former arkose), Bell et al. (17) suggest a mafic volcanic origin (komatiites) for the mafic gneisses which possibly form part of a larger volcanic succession. The average Rb/Sr age on these series is 1870 $\pm$ 75 Ma (Bell (12)), but it cannot be excluded that the Earl River gneisses are the most remobilized part of older Archaean gneisses.

Major fault directions in the basement are NS and N 60° E while minor faults trend EW. The N 60° E directions are inherited from the Hudsonian NE compression, while the N 60° E direction corresponds to lateral faults. The general trend of the main foliation is N 140° E. Some thrust faults (N 140° E) show an important development of mylonites mainly along the interface between the Earl River Complex and the Peter River gneiss. Late Hudsonian movements are expressed in a mantled gneiss dome tectonic: the lighter Earl River Complex intrudes the denser Peter River gneiss which wraps itself around Earl River Complex cores.

2. BASEMENT DEPOSITS

2.1. Cluff deposits

Uranium in the Carswell circular structure has been found in both basement rocks and Athabasca sediments. At present, the D orebody having been mined, all economic deposits are located in the basement. The D deposit was in the Athabasca sandstones, at the unconformity (Ey et al. (18)).

Basement hosted mineralizations, like Dominique-Peter, N, and OP are usually found near the interface between the Peter River gneiss and the Earl River Complex. This interface is typically a ductile active zone (mylonite) where later fracturing facilitated circulation of hydrothermal fluids and uranium deposits formation (Fig. 4).

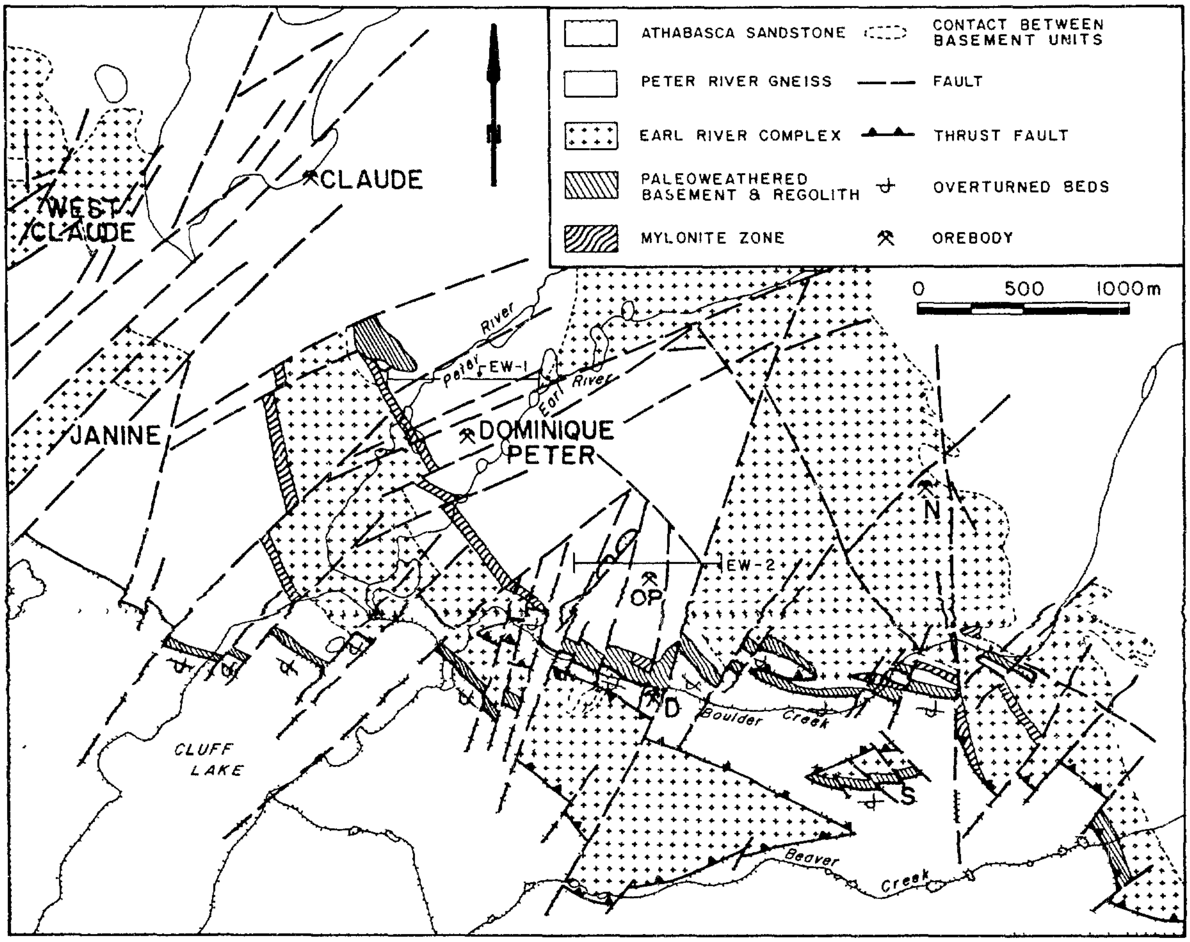

FIG. 4. Subsurface geology of the Cluff Lake Area (from Tona et al. (4)).

The oldest mineralizations are Hudsonian preconcentrations dated at 1800 Ma by chemical age (Pagel (19)). They were found at Sophie at the contact between pegmatoids and mafic gneisses in the Earl River Complex, and are comparable to the Uranium City mineralizations (Tremblay (20)). Apart from these uneconomic occurrences, datations of the three main episodes in the history of the Athabasca Basin deposits cluster around three dates: 1100 Ma, 850 Ma, and 300 Ma (Ruhlmann (21), Bell (12)).

2.1.1. Dominique-Peter orebody

The mineralization of this important deposit is entirely contained within the basement gneisses; controlling factors include structure, lithology, alteration and proximity of the Athabasca Group unconformity (Fig. 5).

The Peter River Gneiss and the Earl River Complex in the area are commonly separated by an Hudsonian mylonite usually strongly fractured and altered to a mixture of sericite and chlorite.

The area is tectonically affected by three sets of structures trending N 60° E, NS and N 120° E. These structures displace the mylonite zone. The mineralization occurs as fracture fills, veinlets and disseminations in N 60° and NS structures dipping 45° - 55° to the west and north west (Blaise et al. (22)).

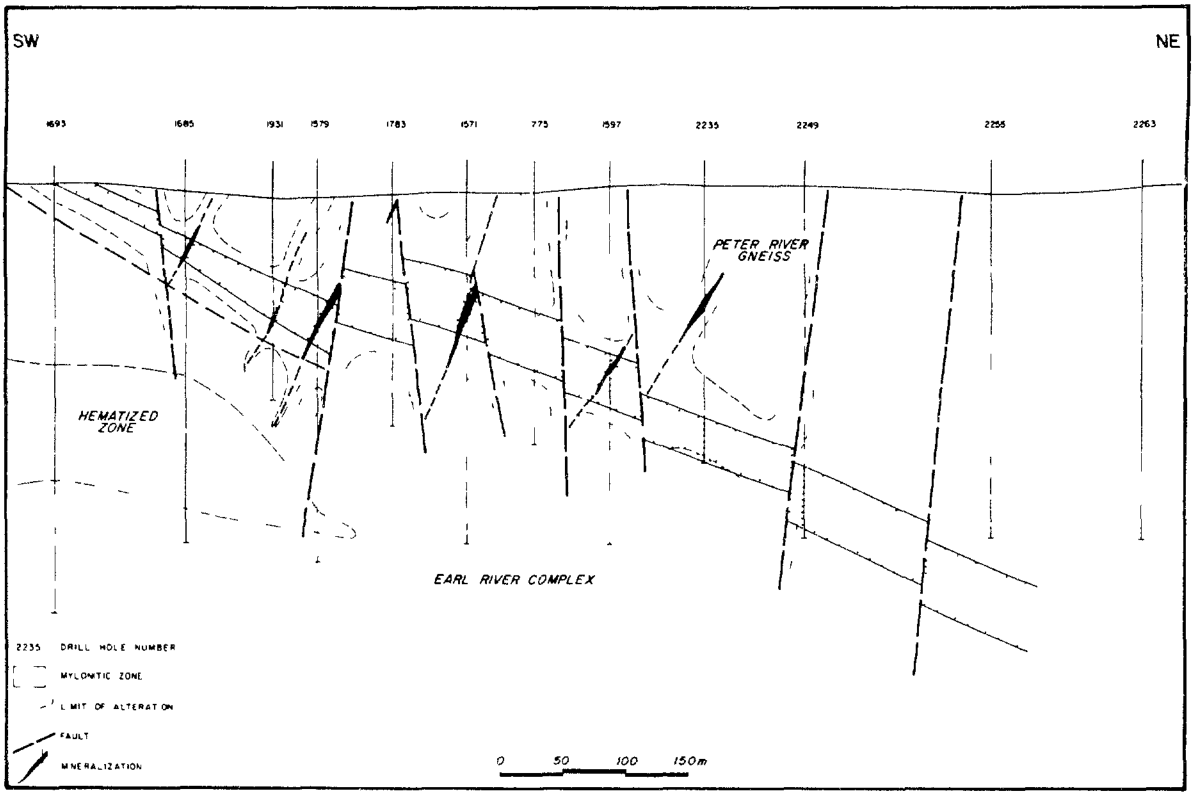

FIG. 5. Dominique-Peter deposit simplified cross-section SW-NE (from Blaise et al. (22)).

Two main parageneses have been observed: an uraninite-polymetallic sulphide assemblage dated between 1050 and 950 Ma (U/Pb; Bell (12)) and an uraninite-dravite simple sulphide assemblage dated by analogy with the OP deposit between 820 and 890 Ma (Bell (12)). Tectonic breccia zones often contain a secondary paragenesis where coffinite is the principal uranium mineral.

2.1.2. Claude orebody

The mineralization is entirely contained within the Peter River gneiss, the main control being a EW trending vertical tectonic zone with rotated fault blocks ('zones à boules'). Some younger NE-SW structures have displaced the EW mineralization.

The host rocks consist of Peter River Gneiss with several interfoliated granitoids. The gneiss is strongly altered around the mineralization, chloritization is ubiquitous and overprints a variable sericitization. Sericitization and chloritization of the biotite are accompanied by anatase aggregates. Tourmaline may be locally present.

Mineralization formed by uraninite, uranium-titanium minerals, clausthalite, galena, pyrite, chalcopyrite, sphalerite and jordesite, is located in clay zones between the elements of the 'zones à boules'. Mineralization at Claude has been dated 1050 ± 65 Ma (Devillers (23)).

Organic matter associated with the mineralization is younger than the main mineralization (Landais et al. (24)).

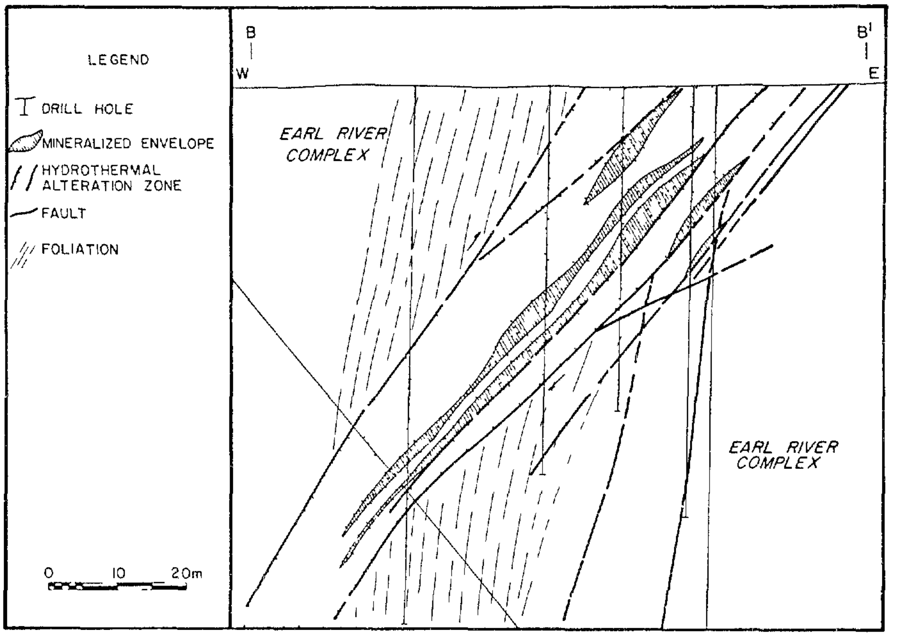

FIG. 6. 'N' orebody - north-south structures (Tona et al. (4)).

2.1.3. N orebody

The N orebody is located within strongly altered mixed gneisses and granitoids of the Earl River Complex thrusted on the Peter River Gneiss (Fig. 6). It is composed of a series of discontinuous mineralized fractures trending NS and dipping 45° to the west. These fractures are cut in the north by a N 40° E structure containing a mineralized brecciated vein. This steeply dipping N 40° E structure shows a dextral movement.

Harper (25) distinguished an old illite-kaolinite alteration associated with the regolith and later chlorite alteration due to hydrothermal fluids (1050 - 950 Ma, Bell (12)). Regolithic alteration has been observed and is a further proof of the Athabasca Sandstone cover proximity as in the Dominique-Peter orebody.

Mineralization is contained within a chloritic gouge. Uraninite is the principal uranium mineral and occurs in the phyllite cleavages or in veinlets. Galena, clausthalite, chalcopyrite, covellite, pyrite and jordisite are accessory to the uranium in the 1050 Ma mineralization. Coffinite haloes and veinlets of quartz-pitchblende could reflect the 900 Ma mineralization event. Late organic materials are also present.

2.1.4. OP orebody

The small OP orebody consists of three subvertical NS structures crosscutting the Peter River Gneiss close to the regolith and Athabasca sandstone slabs.

Uraninite is deposited around quartz crystals along with chalcopyrite, galena, clausthalite and pyrite. Magnesium-rich tourmaline with a second quartz phase commonly crystallized after the uraninite. Coffinite and magnesium chlorite have been observed in contact with the uraninite mineralization (Ruhlmann (21)). This quartz vein associated mineralization has also been observed in Dominique-Peter. A narrow alteration zone exists around these quartz veins.

Gancarz (26) dated some of the OP mineralization at 800 Ma (Pb/Pb), Bell (12) determined U/Pb ages from a uraninite-dravite assemblage between 820 and 890 Ma. This mineralization and the related hydrothermalism are therefore a well defined episode in the formation of the Cluff deposits.

2.2. East Athabasca basement deposits

They belong to two different types: deposits which are entirely included in the basement like Rabbit Lake and Eagle Point, and deposits which are located at the unconformity but extend also in the basement like Key Lake, Midwest and Dawn Lake.

2.2.1. Rabbit Lake

Several papers deal with this deposit (Dunning et al. (27), Hoeve (28), (29), Hoeve et al. (30), (31), Knipping (32), Rimsaite (33), (34), (35), Sibbald (36), (37), Tremblay (20)). Field visits allowed many geologists to make their own mind about it.

Rabbit Lake is located in the eastern part of the Athabasca Plateau in the Wollaston Group rocks. The deposit occurs in an assemblage of calcareous and siliceous rocks, calcsilicate, quartzite, graphite-bearing rocks, marble, the limit between plagioclasite and quartzo-feldspathic gneiss being intensively tectonized. The Athabasca Sandstone is overthrust by the Wollaston Group rocks: a witness of post-Athabasca compressive movements. A hydrothermal altered dike cuts through these formations.

The host rocks of the deposit are also deeply altered and disregarding retromorphism, two types of alteration can be distinguished: palaeoweathering and hydrothermal alterations, the latter being closely associated with the mineralization. There is also a late hydrothermal alteration consisting in a Mg-rich argillization (chloritization), which obliterates the first ones. Silicification and tourmalinization are associated with the mineralization and brecciation processes.

Mineralization is dated from 1075 to 1350 Ma (Cumming et al. (38), Little (39)), postdating the deposition of Helikian Athabasca Sandstones. We consider that the presence of the basic dike has a great significance as it is probably related to a tensional phase which occurred after the Athabasca deposition (Grenvillian Orogeny). This phase was most probably responsible for a reactivation of hydrothermal 'plumbing systems' throughout the basin and in the basement fractures network, leading to the formation of the main uranium economical concentrations. The same type of late diabase intrusive is also found in the Midwest Lake deposit (Wray et al. (40)) and in the Cluff Lake area (Tona et al. (4)).

Similarities between Cluff basement deposits and Rabbit Lake orebody are obvious: litho-structural location, alterations and ages.

2.2.2. Eagle Point and Collins Bay deposits

Eagle Point deposit lies in basement rocks, in the northern extension of the main structure which controls a trend of very rich deposits (Rabbit Lake, Collins Bay A and B), (Tremblay (20)).

According to Sopuck et al. (41) the orebodies are stratabound and located at the limit between biotite-cordierite garnet gneiss, very similar to the Peter River Gneiss of Cluff, and biotitic gneiss of the Aphebian Wollaston Group. They

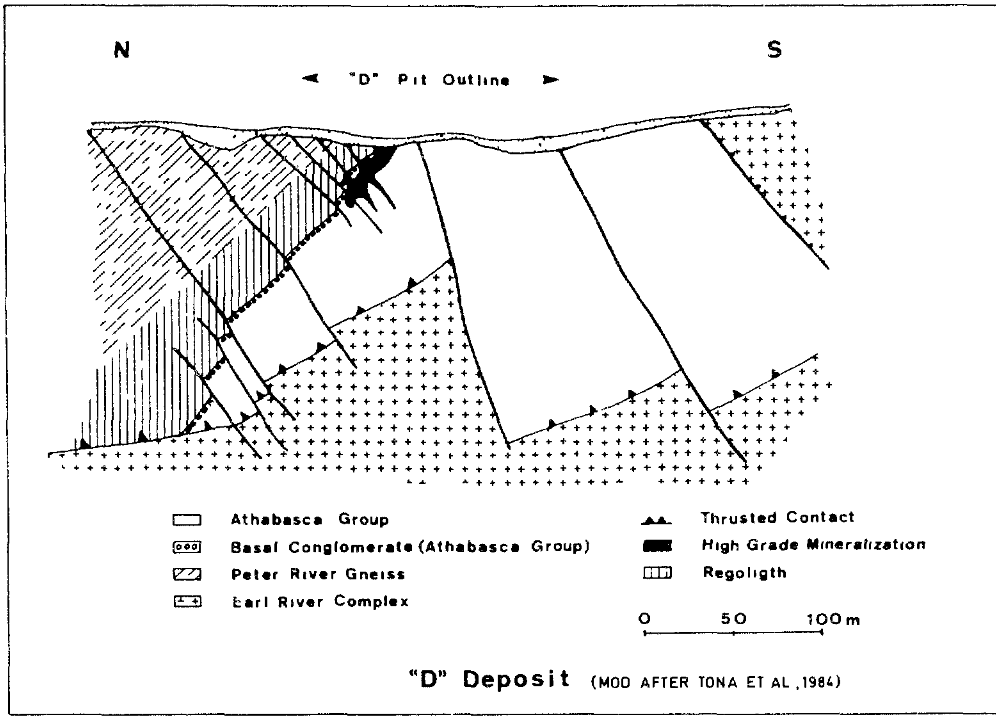

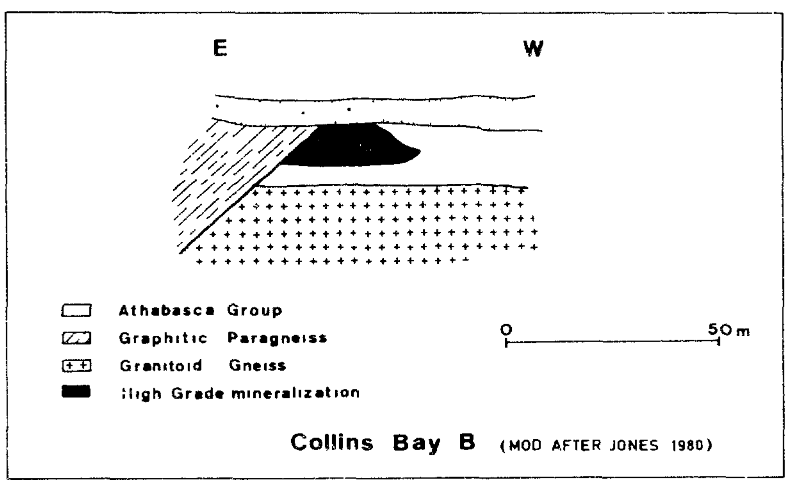

FIG. 7. Comparison between cross-sections in 'D' deposit and Collins Bay B deposit.

are also located near the Collins Bay thrust fault. Quartzo-feldspathic gneiss domes are situated west of the deposit. Mineralization is linked to bleached (Mg chlorite) graphitic conductive zones.

It is very enlightening to observe the similitude between two cross-sections drawn through the 'D' orebody of Cluff (Tona et al. (4)) and the Collins B deposit (Jones (42)), (Fig. 7). In Cluff, the mylonite located between Peter River gneiss and Earl River Complex, reactivated by mantled gneiss doming, controls both the basement deposits (Dominique-Peter) and 'D' unconformity deposit. The Eagle Point deposit location reminds the Dominique-Peter deposit at Cluff, alterations are similar (Mg chloritic halo), and the vicinity of the Athabasca Group with unconformity deposits (D and Collins Bay B) led to assume that Eagle Point is the basement expression of the metallogenic process which created Collins Bay B farther on the same main structure.

Collins Bay A is a small orebody within altered paragneiss from the Wollaston Group, close to small erosion remnants of Athabasca rocks (Tremblay (20)). The aluminous gneiss is altered by regolithic and hydrothermal processes at the limit with quartzo-feldspathic gneiss (Jones (42)). Again, these characteristics make this deposit very similar to the Dominique-Peter deposit of Cluff.

2.2.3. Dawn Lake

In a detailed paper, Clarke et al. (43) showed how these uranium deposits are located close to the unconformity but could be either in the sandstone, at the unconformity itself (zone 14) or in the basement Wollaston Group rocks (zone 11 B). The strict alignment of zones 11 B, 11 A and 11 along the same basement structure is a new example of the relationship which exists between basement deposits and unconformity deposits through a main structure of the basement affecting also the sandstone cover.

In the basement, deposits tend to be of multiple vein-type while at the unconformity, they tend to take a more massive development as illustrated by the Midwest deposit and more recently the Waterbury deposit. Clay alteration characterized the mineralization in the basement.

The stratigraphic position of the Dawn Lake (also McLean) deposists as it relates to the basement is considered higher than those of other deposits as Collins Bay, Midwest and Key Lake. The basement structures controlling these deposits located higher in the Aphebian sequence are not as individualized and apparent than for the deposits which are closer to Archaean reactivated domes.

2.2.4. Key Lake

These deposits are well described (Dahlkamp (44), De Carle (45)). They are situated within Aphebian metasediments of the Wollaston Group, close to reactivated 'Archaean' domes. The link between Deilmann and Gaertner deposits is again an important mylonitic structure. Besides the mylonite, graphitic schists constitute the major control of the mineralization which extends largely in the sandstones, close to the unconformity.

Here again, we can distinguish two trends of alteration: the palaeoweathering profile and the hydrothermal alteration, superimposed on the first one, characterized by an intense chloritization in the orebody vicinity (Sopuck et al. (41)). A strong Mg-B-SiO_2 metasomatism postdates the original feldspar and biotite alteration which is related to palaeoweathering.

3. MINERALIZATION FACTORS

3.1. Archaean factor

The metamorphic basement of the Athabasca Plateau region belongs to the Churchill Province in which the Hudsonian Orogeny inprints younger ages on older Archaean formations. Age is therefore a not too useful criteria for identifying Archaean in this region. It is also not easy to distinguish Aphebian from Archaean in the field. Generally, the ancient unconformity has been obliterated and is presently underlined by Hudsonian granitoids and shear zones. Rocks of true

Archaean age occur east of the Wollaston Belt, especially in the granulitic, high-grade metamorphic Pederson Lake Complex, intruded by 2500 Ma old Kenoran granitoids (Money (46)). Within the Wollaston folded belt, granitoids outcropping in the core of antiforms may either include Archaean material reworked during Hudsonian metamorphic events, or be the result of the complete anatexis of a basal coarse detritic Aphebian unit, which has not been identified yet.

In the Carswell structure, the Peter River aluminous gneisses may be compared to the graphitic metapelites occurring at Rabbit Lake in the Wollaston Belt, which are typical Aphebian metasediments. The Earl River Complex, rich in quartzitic and basic rocks may be equivalent to a detritic basal Aphebian unit and to the Archaean basement, reworked during the Hudsonian Orogeny. Bell et al. (17) notice that the Earl River rocks display komatiitic affinities, a typical Archaean feature.

It is assumed that the Earl River Complex stems from the anatexis of the ancient Archaean-Aphebian unconformity, the ultimate cause of the Athabasca metallogenic Province could be identified as the alteration and reworking of the uranium initially associated with the Kenoran granitoids. During the erosion process, the uranium refractory minerals were interbedded with the Aphebian basal conglomeratic sediments. These minerals were reworked and partially destroyed during Hudsonian metamorphism and anatexis. Uranium was liberated, enriching the aluminous graphitic metasediments, at the contact with the mantled gneiss domes.

3.2. Aphebian factor

3.2.1. Aphebian sedimentation

In the Carswell area the Aphebian sedimentation is marked by the deposition of arkosic sediments and black shales (Pagel et al. (16)). Compared to other rocks, black shales have a high uranium background and such a syngenetic preconcentration may represent a step in the mobilization of uranium from the hydrosphere. Another possibility is that uranium has been transferred from the stock of refractory minerals of the underlying Aphebian detritic units during the Hudsonian Orogeny, as discussed below.

In the Wollaston Lake area, the Aphebian consists of two units:

(i) A basal detritic unit with dominant graphitic pelites and semi-pelites minor quartzites, calcsilicates and carbonates; the absence of a coarse basal detritic unit is something to be noted.

(ii) An upper quartz-feldspathic unit, generally considered arkosic, but displaying a magmatic calcoalkaline potassic composition and most probably representing monzonitic volcanic tuffs and lava flows. Such a volcanism, which may be related to the Wathaman magmatism of the Rottenstone, is generally a good geochemical source of uranium and thorium. The geochemical uranium of this unit may have been depleted during Hudsonian metamorphism and partly reconcentrated in the underlying graphitic metapelites.

3.2.2. Hudsonian Orogeny

During the Hudsonian Orogeny the basement gneisses have been metamorphosed to granulite facies. Average Rb/Sr dates of 1800 Ma are found for the aluminous gneisses (Bell (12)). The most important event is the development of mylonite zones in deep ductile tectonic conditions accompanied by a retrograde metamorphic alteration. This alteration is marked by secondary amphibole, K-mica and Fe-rich chlorite as well as by local episyenitization of the feldspathic gneisses and granitoids. This phase of retrograde metamorphism released fluids and exsolved uranium, boron and fluor from the phyllites (Ahmad et al. (47)). These processes correspond to an initial redistribution of the uranium trapped in the Aphebian sediments.

During the Late Hudsonian, crustal shortening (NE compression) and diapirism lead to the formation of gneiss domes. These domes are made of quartzofeldspathic gneisses and granitoids, lighter than the metasedimentary black shales (Peter River Gneiss). In anatexitic conditions, they intruded the reducing layers up to the point where they encountered graphite concentrations and where loss of water inhibited the granitization process. Non-economic uranium concentrations observed at Sophie seem to correspond to this Hudsonian history. They are dated at 1800 Ma (Pagel et al. (19)). The concentration process involved the tectonic shear zones and the fluid circulations around the rising domes.

3.3. Unconformity factor

Although all the described deposits are located in the basement, the proximity of the Athabasca unconformity is a major factor in the formation of these deposits. Cluff deposits (Dominique-Peter, N and OP) keep relicts of the regolith as witnesses of the unconformity proximity. The unconformity is still present at Rabbit Lake, Key Lake and Collins Bay A. At Eagle Point it is assumed that the unconformity was very close but has been eroded away. The unconformity role is important in several aspects:

- The weathering stage helped in the redistribution of uranium from the basement during the lateritic episode (Tremblay (20)).

- The upper portion of the regolith is made of kaolinitic clay (upper bleached layer) and constitutes an impermeable screen which controlled most of the Helikian circulations (Mac Donald (48)).

- On the contrary, the bulk of the regolith appears to be more permeable and, after compaction and diagenesis of the Athabasca cover, it became one of the preferential drains for solutions.

3.4. Helikian factor

3.4.1. Deposition of the Athabasca Plateau basin sedimentary pile

Around 1500 to 1400 Ma, a large body of coarse continental, brackish and marine, oxidized sandstones were deposited, reaching a thickness of more than 2500 m. Finer chemical, detrital as well as organic sediments occurred after, now preserved only in the moat of the Carswell structure. New conditions were therefore created in the basement and at the unconformity.

- Subsidence enlarged the pre-existing fracture network according to a mechanism described by Bourbon et al. (49).

- A larger body of water now existed above the unconformity, impregnating also the basement fracture system.

- Above the unconformity, redox conditions were kept oxidizing as demonstrated by hematite in fluid inclusion (Pagel et al. (50)) and red coating of detrital elements (Pacquet et al. (7)). In the basement conditions were reducing, in the vicinity of graphitic metapelites.

- As depth of burying increased and cementation of the sandstone occurred, trapped connate waters became increasingly saline, as proven by fluid inclusions, and overpressured (Pagel et al. (50)).

Such hypersaline oxidizing waters can exercize a strong solubilizing effect on metals (including uranium) contained in basal coarse sediments where heavy minerals are abundant, in the regolith, and in the fractured basement. Such brines, when reduced, can still selectively dissolve some metals (White (51)).

With increasing compaction and cementation by authigenic clays of the sandstone pile, and basal pelite beds, circulation became more and more restricted to the unconformity and existing fracture networks. As long as the basin stayed tectonically inactive, waters of contrasted composition, density, pH and Eh were well stratified.

Absence of escape for the connate waters must have created, as usually, extreme overpressure conditions when lithostatic pressure became transferred to the insterstitial fluids.

3.4.2. Reactivation of the aquifers at the Grenville time

Between 1300 and 1000 Ma, probably in correlation with the Grenvillian Orogeny and movements in the Cordilleran Province, tensional and compressive constraints were exercized again in the Athabasca Plateau region. Diabase dike swarms invaded some tensional areas, whereas, in compressed areas, inverse faulting was predominant.

Dormant connate waters were remobilized and their stratification disturbed. The then well indurated basal sandstones were fractured by reactivation of old Hudsonian weakness zones, particularly along graphitic mylonites close to Archaean nuclei and mantled gneiss domes.

Fractures created pathways between depth and upper levels of the sedimentary pile where conditions were hydrothermalically normal. Overpressured waters rushed through these opening enlarging them by hydraulic fracturing, creating plumbing systems which attracted more waters from the periphery and below.

The unconformity, as demonstrated by permeability measurements, was the natural horizontal channelway for the oxidizing fluids. Reducing fluids expelled from the basement used the more vertical channels caused by fracturing.

At the chemical interfaces, uranium and other metals dissolved in the oxidized or reduced brines precipitated, following brutal changes in Eh, pH and pressure. The system worked long enough to allow the accumulation of huge amounts of metals in some very specific points. Even after the return to stable tectonic conditions, artesianism may have permitted more oxidizing waters to meet with localized flows of reducing fluids above the most important basement faults.

Reducing, acid, hot and overpressured waters dissolved large quantities of quartz, forming authigenic hydrothermal clay minerals and quartz crystals higher in the Athabasca Sandstones and causing the alteration halos which are such a useful guide for uranium exploration (Sopuck et al. (41), Hoeve (52)).

3.5. Post-mineralization factors

3.5.1. Cluff event

Despite its awesome magnitude, the Cluff event, regardless of if it has been caused by a meteor impact, a crypto-explosion or by purely tectonic forces, has not created any important mineralization. There are, however, good evidences that this event destroyed or dispersed existing deposits. Geologists are now able to reconstruct most of the pre-event structure and this has lead to important progress in exploration and understanding of the Cluff deposits.

3.5.2. Later events

At some points in the post-Cluff event history, oxidizing fluids invaded the basin and its basement and caused important remobilization of the primary deposits. The secondary mineralizations of that age, which have not yet been proved economic, are typically formed by an assembly of quartz-hematite-pitchblende. In Cluff, a boulder train called the Donna train, whose source has not been defined, is largely composed of sandstone boulders showing this mineral assemblage. Datation by U/Pb gave an age of 380 Ma (Bell (12)). Similar mineralization exists along fault, in the sandstone of the eastern Athabasca Plateau. It is not excluded that part of the Fond-du-Lac deposit, located in the northern edge of the Athabasca basin, belongs to the same category. Up to now all these uranium occurrences were found in the sandstone but they are considered a good guide toward basement or unconformity deposits.

4. CONCLUSIONS

There are still many questions left unanswered in the genesis of the Athabasca deposits and to answer these questions will mean a greater amount of laboratory, field and sub-surface studies. Nevertheless, this review of the uranium deposits found in the basement of the Athabasca Plateau region particularly in Cluff, has stressed some important facts pertaining to the localization and the metallogeny of these deposits.

- They are located in the Aphebian and preferentially in rock units consisting mainly metamorphosed black shales (often reaching amphibolite to sillimanite facies).

- They are preferentially located in mylonites or major fault zones affected by low-grade retromorphism. The fluids associated with this retromorphism displaced the uranium from refractory minerals and phyllites toward more labile positions.

- The deposits are generally, but not systematically, located close to granitoids representing reactivated lower Aphebian to Archaean formations. These older formations have often risen as mantled gneiss domes up to the point where their ascent was stopped by carbonated or graphitic rocks.

- The basement deposits are within the Helikian unconformity influence zone.

- Subsidence during Athabasca deposition and later tectonic movements (tensional and compressive) reopened or created the networks of fractures in which uranium precipitated between 1300 and 950 Ma.

- In a given area there are links between these basement deposits and the well-known unconformity deposits, even if they are disconnected. The link generally appears to be a major structure (fault or mylonite). Moreover the ages of the two types of deposits are similar. Both are resulting from the same metallogenic process applied on two different lithostructural environments. Basement deposits of the Athabasca Plateau region are typical vein-type deposits with a rather complex structure due to the low competency of their host rocks. They still represent valid economic targets.

REFERENCES

(1) LEWRY, J.F., SIBBALD, T.I.I., REAS, C.J., Metamorphic Patterns and their Relation to Tectonism and Plutonism in the Churchill Province in Northern Saskatchewan, in: Metamorphism in the Canadian Shield, Geol. Surv. Can., Paper 78-10 (1978) 139-154.

(2) GODFREY, J.D., LANGENBERG, C.N., Metamorphism in the Canadian Shield of Northern Alberta, in: Metamorphism in the Canadian Shield, Geol. Surv. Can., Paper 78-10 (1978) 129-138.

(3) SCOTT, B.P., Geology of the Upper Clearwater River Area (Southeast part of 74-F), Report 202, D.M.R. Sask. (to be published).

(4) TONA, F., ALONSO, D., SVAB, M., WHEATLEY, K., The Carswell Structure Uranium Deposits (Saskatchewan), to be published by Geol. Ass. Can. (1985).

(5) RAMAEKERS, P., Hudsonian and Helikian Basins of the Athabasca Region, Northern Saskatchewan, in: F.H.A. Campbell (editor), Proterozoic Basins of Canada, Geol. Surv. Can., Paper 81-10 (1981) 219-233.

(6) HOEVE, J., QUIRT, D., ALONSO, D., Clay Mineral Stratigraphy of the Athabasca Group in and around the Carswell Structure, to be published by Geol. Ass. Can. (1985).

(7) PACQUET, A., McNAMARA, S., Stratigraphy, sedimentology and petrography of the Athabasca Group in the D and ELF areas of the Carswell Structure, Palaeogeographical implications evidence of a contemporaneous acid volcanism, to be published by Geol. Ass. Can. (1985).

(8) WHEATLEY, K., HENDRY, H., The Dolomites of the Carswell Formation - Sedimentology and Structure, to be published by the Geol. Ass. Can. (1985).

(9) CLAUER, N., EY, F., GAUTHIER-LAFAYE, F., K-Ar Dating of Different Types of Rocks from Cluff Lake Uranium Ore Deposits, to be published by Geol. Ass. Can. (1985).

(10) BURWASH, R.A., BAADSGAARD, H., PETERMAN, Z.E., Precambrian K-Ar Dates from the Western Canada Sedimentary Basin, Journal of Geophysical Research, 67-4 (1962) 1617-1625.

(11) WANLESS, R.K., STEVENS, R.D., LACHANCE, G.R., DELABIO, R.N., Age Determinations and Geological Studies, K-Ar Isotopic Ages, Geol. Surv. Can., Paper 79-2 (1979) 67 pp.

(12) BELL, K., The Geochronology of the Carswell Area, Northern Saskatchewan, to be published by Geol. Ass. Can. (1984).

(13) PAGEL, M., Cadre géologique de gisements d'uranium dans la structure Carswell (Saskatchewan, Canada), Etude des phases fluides, Thèse de Docteur de Spécialité (3e cycle), Université de Nancy (1975) 157 pp.

(14) EINSIEDEL, C.A. von, Petrography and Geochemistry of the Cluff Lake breccias, Carswell structure, Northern Saskatchewan, B. Sc. Carleton University (1981) 44 pp.

(15) AMOK Ltd., Solid geology of the Carswell structure, Geological Map 1:50000, published by Amok Ltd., Saskatoon, Sask. (1983).

(16) PAGEL, M., SVAB, M., Petrographic and Geochemical Variations within the Carswell Structure Basement Core and its Implications with Respect to Uranium Deposition, to be published by Geol. Ass. Can. (1985).

(17) BELL, K., CACCIOTTI, A.D., SCHNESSL, J.H., Petrography and Geochemistry of the Earl River Complex, Carswell Structure Saskatchewan, to be published by Geol. Ass. Can. (1985).

(18) EY, F., GAUTHIER-LAFAYE, F., LILLIE, F., SCHUMACHER, F., WEBER, F., Le gisement d'uranium de Cluff C (Saskatchewan, Canada), Etude structurale et pétrographique, Geol. Geoch. Uranium Memoire du CREGU-Nancy (1983) 97-113.

(19) PAGEL, M., RUHLMANN, F., Chemistry of Uranium Minerals in Deposits and Showings of the Carswell Structure, to be published by Geol. Ass. Can. (1985).

(20) TREMBLAY, L.P., Geology of the uranium deposits related to the sub-Athabasca unconformity, Saskatchewan, Geol. Surv. Can., Paper 81-20 (1982) 56 pp.

(21) RUHLMANN, F., Mineralogy and Metallogeny of the Uraniferous Occurrences in the Carswell Structure, to be published by Geol. Ass. Can. (1985).

(22) BLAISE, J.R., KONING, E., The Dominique-Peter Uranium Deposit, Mineralogy and Structural Aspects, to be published by Geol. Ass. Can. (1985).

(23) DEVILLERS, C., Datation de l'Echantillon 'Claude' par la Méthode U/Pb, CEA Internal Report (1974).

(24) LANDAIS, P., DEREPPE, J.M., Chemical Study of the Carbonaceous Material from the Carswell Structure, to be published by Geol. Ass. Can. (1985).

(25) HARPER, C.T., The Geology and Uranium Deposits of the Central Part of the Carswell Structure, Northern Saskatchewan, Canada, unpublished PhD Thesis, Colorado School of Mines, Golden, Colorado, USA (1983) 337 pp.

(26) GANCRAZ, A.J., Chronology of the Cluff Lake Area Uranium Deposit, Saskatchewan, Canada, in: International Uranium Symposium on the Pine Creek Geosyncline, Extended Abstracts, IAEA Vienna (1979) 91-94.

(27) DUNNING, N., PARSLOW, G.R., Preliminary report on the geochemistry and geology of the Rabbit Lake area, Northern Saskatchewan, in: G.R. Parslow (editor), Proceedings of a Symposium on Uranium Exploration Techniques, Saskatchewan Geological Society, Special Publication No. 4 (1979) 257-280.

(28) HOEVE, J., Uranium metallogenetic studies II, Rabbit Lake: Mineralogy and geochemistry, in: Summary of Investigations 1977, Saskatchewan Geological Survey (1977) 124-135.

(29) HOEVE, J., Uranium metallogenetic studies, Rabbit Lake: Mineralogy geochemistry, in: Summary of Investigations 1978, Saskatchewan Geological Survey, Miscellaneous Report 78-10 (1978) 61-65.

(30) HOEVE, J., SIBBALD, T.I.I., The Rabbit Lake Uranium Mine, in: C.E. Dunn (editor), Proceedings of a Symposium on Uranium in Saskatchewan, Saskatchewan Geological Society, Special Publication No. 3 (1976) 331-354.

(31) HOEVE, J., SIBBALD, T.I.I., On the genesis of Rabbit Lake and other unconformity-type uranium deposits in Northern Saskatchewan, Canada, Econ. Geol. 73 (1978) 1450-1473.

(32) KNIPPING, H.D., The Concepts of Supergene Versus Hypogene Emplacement of Uranium at Rabbit Lake, Saskatchewan, Canada, in: Formation of Uranium Ore Deposits, IAEA Vienna (1974) 531-548.

(33) RIMSAITE, J.Y.H., Mineral Assemblage at the Rabbit Lake Uranium Deposit, Saskatchewan, A preliminary report, in: Report of Activities, Part B, Geol. Surv. Can., Paper 77-1B (1977) 235-246.

(34) RIMSAITE, J.Y.H., Layer Silicates and Clays in the Rabbit Lake Uranium deposit, Saskatchewan, in: Current Research, Part A, Geol. Surv. Can., Paper 78-1A (1978) 303-315.

(35) RIMSAITE, J.Y.H., Petrology of basement rocks at the Rabbit Lake Deposit and Progressive Alteration of Pitchblende in an Oxidation Zone of Uranium Deposits in Saskatchewan, in: Current Research, Part B., Geol. Surv. Can., Paper 79-1B (1979) 281-299.

(36) SIBBALD, T.I.I., Uranium Metallogenic Studies I, Rabbit Lake, Geology, in: Summary of Investigations 1977, Saskatchewan Geological Survey (1977) 111-123.

(37) SIBBALD, T.I.I., Uranium Metallogenetic Studies, Rabbit Lake, Geology, in: Summary of Investigations 1978, Saskatchewan Geological Survey, Miscellaneous Report 78-10 (1978) 56-60.

(38) CUMMING, G.L., RIMSAITE, J., Isotopic studies of lead-depleted pitchblende, secondary radioactive minerals and sulfides from the Rabbit Lake uranium deposit, Saskatchewan, Canadian Journal of Earth Sciences 16 (1979) 1702-1715.

(39) LITTLE, H.W., Uranium in Canada, in: Report of Activities, Part A., Geol. Surv. Can., Paper 74-1A (1974) 137-139.

(40) WRAY, E.M., AYRES, D.E., IBRAHIM, H., Geology of the Midwest uranium deposit, Northern Saskatchewan, in: T.I.I. Sibbald (editor), Proceedings of CIM-SEG, Uranium Geology Symposium, Saskatoon (1983) in press.

(41) SOPUCK, V.J., De CARLE, A., WRAY, E.M., COOPER, B.R., Application of Lithogeochemistry in Locating Unconformity-Type Uranium Deposits, in: G.R. Parslow (editor), Geochemical Exploration 1982. Devel. in Econ. Geol. 17, Elsevier (1984) 77-99.

(42) JONES, B.E., The Geology of the Collins Bay Uranium Deposit, Saskatchewan, Canadian Institute of Mining Bull. 73- No. 818 (1980) 84-90.

(43) CLARKE, P.J., FOGWILL, W.D., Geology of the Asamera Dawn Lake Uranium Deposits, Athabasca Basin, Northern Saskatchewan, in: Canadian Institute of Mining and Metallurgy Geology Division Uranium Field Excursion Guidebook, September (1981) 8-13.

(44) DAHLKAMP, F.J., Geological Appraisal of the Key Lake U-Ni Deposits, Northern Saskatchewan, Econ. Geol. 73 (1978) 1430-1449.

(45) De CARLE, A.L., Geology of the Key Lake Deposits, Saskatchewan, reprint from a talk given at the CIM District Meeting, Flin Flon, Manitoba (1980) 36 pp, in pre-print.

(46) MONEY, P.L., The Geology of the Daly Lake Area (east half) Saskatchewan, Saskatchewan Department of Mineral Resources, Rep. 108 (1966) 48 pp.

(47) AHMAD, R., WILSON, C.J.L., Uranium and boron distributions related to metamorphic microstructures evidence for metamorphic fluids activity, Contrib. Mineral. Petrol. 76 (1981) 24-32.

(48) McDONALD, C.C., Mineralogy and geochemistry of a precambrian regolith in the Athabasca Basin, M. Sc. Thesis University of Saskatchewan (1980) 151 pp.

(49) BOURBON, M., GRACIANSKY, P.C., L'enregistrement d'un épisode de tectonique cassante par un système de filons synsédimentaires en Briançonnais, in: Abstracts Thème 4, Tome I, Nice (1975) 27-32.

(50) PAGEL, M., POTY, B., SHEPPARD, S.M.F., Contribution to some Saskatchewan uranium deposits mainly from fluid inclusions and isotopic data, in: International Symposium on the Pine Creek Geosyncline, IAEA Vienna (1980) 639-654.

(51) WHITE, D.E., Environments of Generation of Some Base-Metal Ore Deposits, Econ. Geol. 63 (1968) 301-355.

(52) HOEVE, J., Host Rock Alteration and its Application as an Ore Guide at the Midwest Uranium Deposit, Northern Saskatchewan, Saskatchewan Reserach Council Publication (1982) 1-44.

THE PANDANUS CREEK URANIUM MINE, NORTHERN TERRITORY, AUSTRALIA

B.D. Morgan
Triad Minerals N.L.
Melbourne

D. Campi
Metals Exploration Limited
Melbourne
Australia

Abstract

THE PANDANUS CREEK URANIUM MINE, NORTHERN TERRITORY, AUSTRALIA

The Pandanus Creek Uranium Mine was discovered in 1958 and selectively mined between 1960 and 1962 for a yield of 26 t U_3O_8.

The mine is situated on a tectonic ridge of Lower Proterozoic metamorphics intruded by a granite complex with comagmatic acid volcanics of basal Middle Proterozoic age (1770 Ma). The volcanics are the mine host rocks.

The primary ore consists of lenses of pitchblende along shears developed within a meta-quartzite adjacent to a granite intrusion. The pitchblende has suffered extensive supergene alteration due to tropical weathering since Mesozoic times. The ore contains significant gold and silver.

The pitchblende was emplaced 850 Ma ago, after widespread faulting of overlying Middle Proterozoic rocks. The source of the uranium is believed to be the basement rocks of the tectonic ridge. Hydrothermal solutions ascended along the major faults and deposited pitchblende preferentially in adjacent minor structures within the volcanics.

1. INTRODUCTION

The Pandanus Creek Uranium Mine is situated at latitude 17°41'S, longitude 137°50'E in the Northern Territory of Australia, approximately 15 km west of the Queensland border and 374 km NNW of Mt. Isa (Fig. 1). It is also known as the Eva Mine.

The climate is sub-tropical with a warm dry winter and a hot humid summer. The rainfall averages 600 mm p.a. mainly as storms between December and March. The average maximum temperature is 32°C.

The orebody was discovered by local prospectors in 1958. Percussion and diamond drilling of 148 holes totalling 2809 m during 1958 and 1959 indicated ore reserves of 55,000 t averaging 0.56 % U_3O_8 (309 t contained U_3O_8) to a depth of 42 m. High grade ore shoots were selectively mined by open cuts and underground workings from 1960 to 1962. Some 3400 t of ore and waste containing 57 t U_3O_8 was extracted, of which 311 t averaging 8.37 % U_3O_8 were hauled 1850 km by road to a treatment plant for a yield of 26 t U_3O_8.

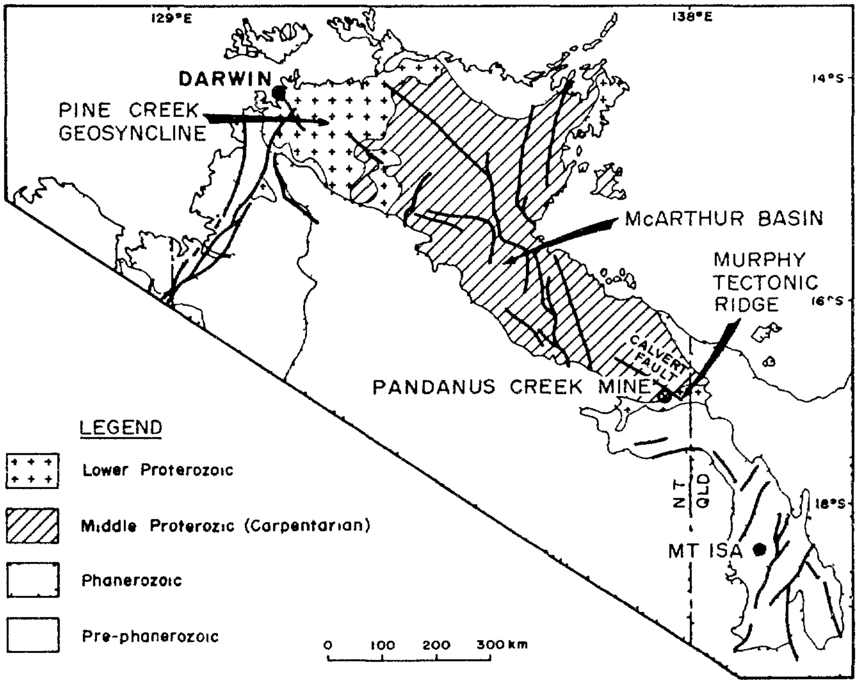

FIG. 1. Location and tectonic setting

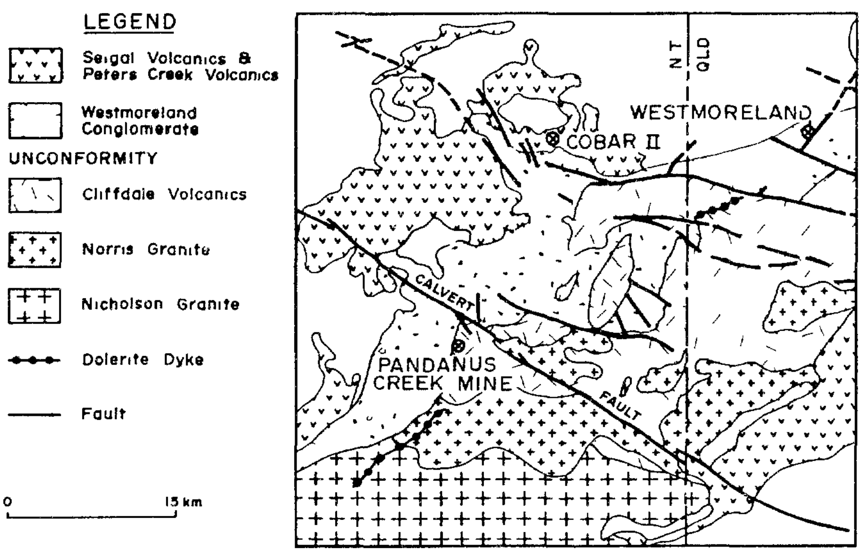

FIG.2. Regional geology of Pandanus Creek Area

2. REGIONAL GEOLOGY

2.1. Tectonic setting

The mine is situated on the Murphy Tectonic Ridge which is a north-easterly trending belt 150 km long and 25 km wide composed of Lower Proterozoic schists intruded by a granite complex with comagmatic acid volcanics of basal Middle Proterozoic age which are the host rocks of the orebody (Fig. 2).

The structure is dominated by east-northeast trends reflecting primary fault control of the Murphy Tectonic Ridge and a younger northwest trend dominated by the Calvert Fault which is a major transverse strike slip fault running across the Murphy Tectonic Ridge for 175 km displacing all Proterozoic formations 7 km horizontally and 750 m vertically. The mine site is 2 km south of the Calvert Fault.

The Murphy Tectonic Ridge was a basement high during widespread Middle Proterozoic sedimentation. It formed the southern flank of the McArthur Basin which is a relatively undeformed structure covering an area of 17,000 km² and extending 600 km northwest to the Lower Proterozoic Pine Creek Geosyncline where the majority of the known uranium deposits in the Northern Territory are located.

The McArthur Basin sediments overlie the Murphy Tectonic Ridge formations unconformably with an erosion time gap of 50 to 100 million years. The basal quartz arenite formation outcrops as a prominent escarpment up to 200 m high dipping 60° to 70° north off the Murphy Tectonic Ridge indicating a continuation of fault movements along the margin of the Ridge after Middle Proterozoic sedimentation. The orebody lies approximately 30 m stratigraphically below the unconformity.

2.2. Stratigraphy

The stratigraphic units outcropping in the area were described by Roberts et al. (1) with later modifications by Grimes et al. (2).

The local basement rocks are the Lower Proterozoic Murphy Metamorphics which consist of quartz albite-biotite-chlorite schists and quartz-albite-muscovite schists.

These are intruded by the Nicholson Granite Complex which consists of a series of eight related intrusions emplaced at successively higher crustal levels (Gardner (3)). The early intrusions are massive porphyritic biotite granite and adamellites collectively termed the 'Nicholson Granite'. The later intrusions are finer grained leucogranites called the 'Norris Granite'. Webb (4) dated a suite of 22 samples of the granites at ages ranging from 1860 ± 103 Ma to 1773 ± 56 Ma.

The mine host rocks are the Cliffdale Volcanics, a sequence of rhyolitic to andesitic ignimbrite, lavas and tuffs which have been dated at 1770 ± 20 Ma (Webb (5)) and here define the base of the Middle Proterozoic Carpentarian System (Dunn et al. (6)). The Cliffdale Volcanics are intruded by the later discordant phases of the Nicholson Granite Complex so it is believed that the volcanics are comagmatic with the granites. The volcanics are not regionally metamorphosed and primary structures are well preserved, but contact metamorphic development of chlorite, epidote, albite, biotite and actinolite occurs near the discordant granite intrusions. Steeply dipping north trending joints and horizontal joints are well developed.

The overlying Middle Proterozoic Tawallah Group deposited in the McArthur Basin consists essentially of quartz rich arenites and subordinate basic volcanics, carbonates and lutites up to 6 km thick. The basal formation is the Westmoreland Conglomerate, a formation 1500 m thick of quartz and felspathic sandstones including near shore conglomerates and arkoses. This is overlain by 1000 m of flood basalts constituting the Seigal Volcanics (previously included in the Peters Creek Volcanics).

The Middle Proterozoic formations are capped unconformably by remnants of undeformed shallow water Mesozoic sediments.

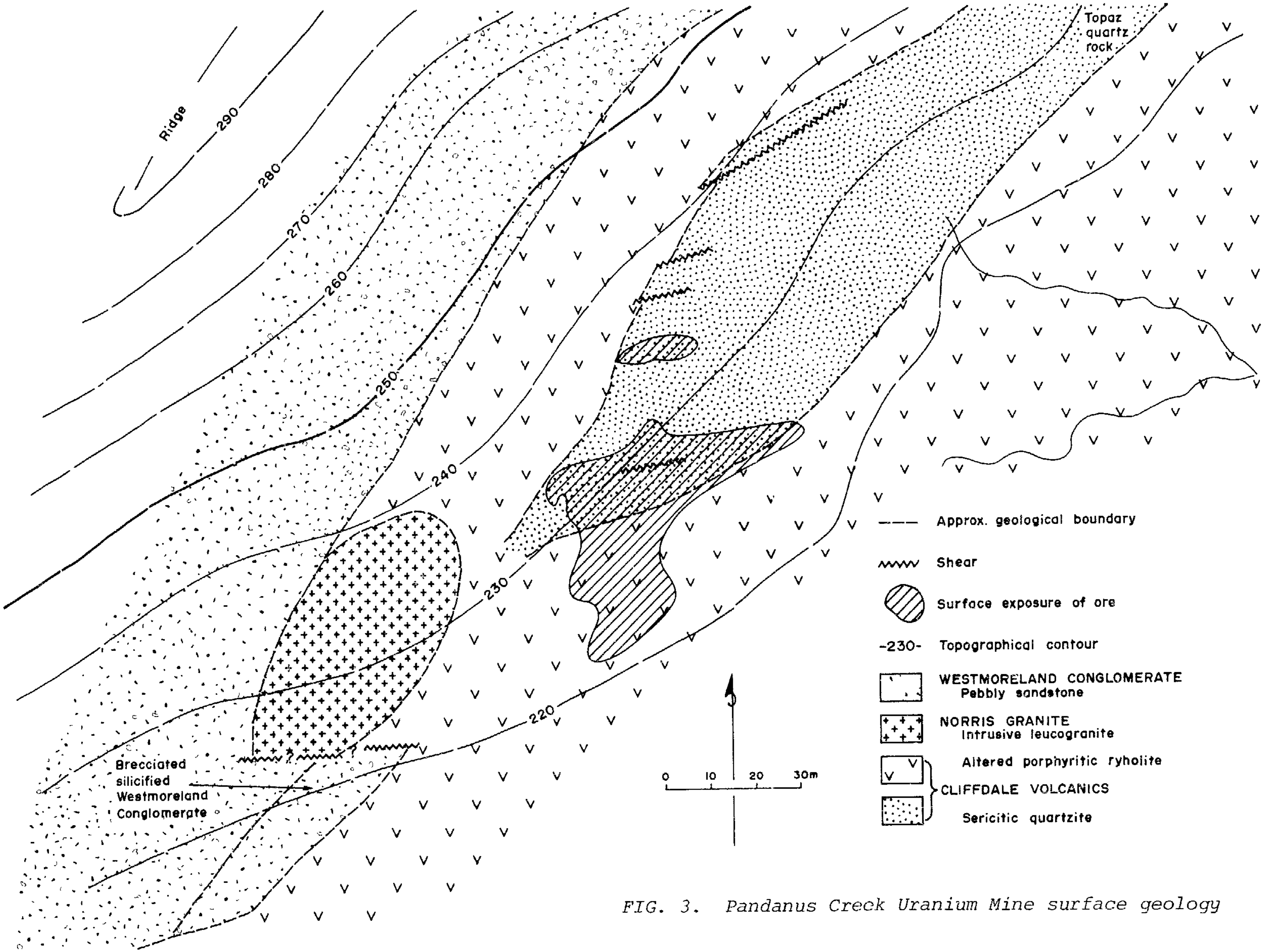

FIG. 3. Pandanus Creek Uranium Mine surface geology

2.3. Mineralization

Numerous small copper and uranium prospects have been found in shears and fault zones within the volcanics. The Calvert Fault has expression in a major quartz reef containing sporadic copper and uranium mineralization.

Tin and tungsten occurs in quartz veins and greisens associated with the later granite intrusions ('Norris Granite').

Newton et al. (7) have described shear controlled uranium deposits in the Seigal Volcanics 20 km north of the Pandanus Creek Mine. Hills et al. (8) have described fault controlled uranium mineralization in the Westmoreland Conglomerate at Westmoreland 35 km northeast of the mine. Here the mineralization occurs adjacent to dolerite dikes which may be feeders of the Seigal Volcanics.

The Pandanus Creek deposit has many similarities in terms of geological setting to the numerous deposits in the Pine Creek Geosyncline. Common factors as described by Dodson et al. (9) are:

(i) The deposit is situated on the edge of a granite complex.

(ii) The mineralization occupies fractures and shears.

(iii) The deposit is exposed at the present land surface in close proximity to the unconformity with basal McArthur Basin sediments.

3. MINE GEOLOGY

3.1. Host rocks

The orebody occurs in the Cliffdale Volcanics on a steep scree covered slope 30 m below an escarpment formed by pebbly sandstone of the Westmoreland Conglomerate.

It is in the contact aureole of a small stock of intrusive granite exposed 15 m west of the orebody. The granite is a medium grained pink leucogranite consisting of subhedral pink felspar, quartz, and green mica with veins of chert. No uranium mineralization has been detected in the granite.

The bulk of the ore occurs in a band of sericitic quartzite within porphyritic lavas (Fig. 3). The quartzite consists of 75 % sub-angular to sub-rounded quartz grains without preferred orientation averaging 0.2 mm in diameter set in a patchy matrix of fine flaky sericite and intergrown anhedral epidote. The rock is probably a metamorphosed tuff or rhyolite. Near the granite contact it has been extensively felspathized, and 100 m north-east of the orebody the quartzite has been locally metasomatized with the development of topaz. The quartzites commonly have a purple brown discolouration in the vicinity of uranium mineralization.

The surrounding volcanics are mottled green or grey rhyolites, often iron and manganese stained, containing phenocrysts of felspar completely altered to sericite which range from 0.3 to 3 mm in size and show remnants of Carlsbad and occasionally plagioclase twinning. There are occasional quartz phenocrysts, both anhedral and euhedral, ranging in size from 0.3 to 1 mm and phenocrysts of biotite and uralite after augite have been observed in some sections. The ground mass consists of altered felspar and quartz. The total rock composition is approximately 75 % sericitized felspar, 10 % - 25 % quartz, and the balance as biotite and iron oxide.

3.2. Structure

The main ore zone strikes east-west and is exposed at the surface over a length of 55 m with a width of 9 m. It is contained to the north and south by a series of near vertical en echelon shears which step to the north. To the west the ore cuts at the granite contact and plunges east following the granite contact in depth. The mineralization has been traced by drilling to a depth of 40 m and terminates 6 m above the granite. The eastern limit has not been determined, but appears to be nearly vertical.

A tongue of low grade ore extends down hill from the main ore zone as the result of leaching and reprecipitation of uranium by groundwater circulating in the closely jointed volcanics.

Within the main ore zone, the ore occurs as elongate lenses up to 9 m long, 0.6 m wide and 5 m deep. The lenses usually strike east-west following the main direction of shearing and dip north at 45° - 70°. However, flat north dipping clay filled shears often contain patches of ore, and a small rich shoot was found in a north-south shear at 25 m depth 36 m south of the main ore zone.

3.3. Mineralization

The main ore lenses consist of a central core of remnant pitchblende showing veinlet and colloform textures, surrounded by massive yellow uranium ochres which replace both pitchblende and adjacent wall rock. These lenses pinch out into quartz veins up to 150 mm wide and 1 m long, generally showing comb structure with films of yellow uranium minerals throughout and yellow prismatic crystals in drusy cavities.

Outside the main ore lenses, secondary dispersion of uranium minerals along joints in the country rock is limited to the top 10 m below the surface.

Although pitchblende is the primary ore mineral, the bulk of the ore consists of the uranyl silicate minerals sklodowskite, boltwoodite and betauranophane formed by supergene oxidation of pitchblende under tropical conditions (McAndrew (10)). Minor amounts of the phosphates saleeite, torbernite and autunite are also present.

The ore contains virtually no thorium or rare earths. However free gold (electrum) is present, with values of up to 62.2 g/t gold recorded, and silver values are similar. The gold and silver values increase with uranium content. Small quantities of galena, copper carbonates and manganese oxides are associated within the ore, but it is essentially free of sulphide minerals.

4. ORIGIN

Morgan (11) suggested that the mineralization was deposited by hydrothermal solutions emanating from the adjacent granite intrusive. However, subsequent U-Pb dating by Hills et al. (12) on pitchblende from the Pandanus Creek Mine and the Cobar II prospect in the Seigal Volcanics 20 km to the north indicated that mineralization at both localities was emplaced about 850 Ma ago. Webb (4) dated the youngest granite intruding the mine host rocks at 1773 ± Ma, so the intrusive granites of the Nicholson Granite Complex as a direct hydrothermal source were precluded.

Any theory of origin must explain how pitchblende was emplaced at the same time in both the Cliffdale Volcanics at the mine site and in formations unconformably overlying the Cliffdale Volcanics and granites as at the Cobar II prospect. In each case the mineralization is deposited in pre-existing structures in volcanics.

The writers believe that the most probable source of the uranium were the basement rocks forming the Murphy Tectonic Ridge. Following deposition of the overlying Middle Proterozoic sediments, major north-west faults developed which extended into the basement rocks, and older north-east faults bounding the ridge were reactivated. Hydrothermal solutions generated at depth during these tectonic movements ascended along the major fault planes, causing extensive silicification, and migrated to more distal minor structures where pitchblende was precipitated preferentially in the volcanics which presented more favourable chemical environments than the adjacent sediments.

The textures and composition of the primary ore at Pandanus Creek have characteristics of an epithermal deposit, suggesting precipitation at a temperature of less than 200°C at a depth of approximately 1000 m which is consistent with the probable thickness of overlying rocks existing at the time of emplacement.

The mineralization was selectively precipitated as open space fillings in sheared quartzites developed within the contact aureole of a granite intrusion in preference to the surrounding tightly jointed volcanics. The relatively impervious granite stock apparently formed a barrier to further lateral migration of the mineralizing fluids westwards and thus precipitation of pitchblende was localized adjacent to the contact.

The adjacent unconformity with overlying sandstone does not appear to have been a major controlling factor in the formation of the deposit. The ore postdates the unconformity and the top of the deposit has been removed by erosion, so it is possible that the mineralization did extend into overlying formations.

The overlying sandstone protected the mineralization within the volcanics from weathering and erosion until post Mesozoic time. Remobilization has been limited to the immediate vicinity of the original ore emplacement.

REFERENCES

(1) ROBERTS, H.G., RHODES, J.M., YATES, K.R., Calvert Hills, N.T., 4 Mile Geological Series, Explan. Notes Bur. Miner. Resourc. Geol. Geophys. Austr. (1963) 7-11.

(2) GRIMES, K.G., SWEET, I.P., Westmoreland, Queensland 1:250000 Geological Series, Explan. Notes Bur. Miner. Resourc. Geol. Geophys. Austr. (1979) 8-11.

(3) GARDENER, C.M., Precambrian geology of the Westmoreland region, Northern Australia, Part III: Nicholson Granite Complex and Murphy Metamorphics, Report 1978/32, Bur. Miner. Resourc. Geol. Geophys. Austr. (1978) unpublished.

(4) WEBB, A.W., Carpentaria age determination project report AN 2/1/0 - 2850/75 AMDEL, Adelaide (1975) unpublished.

(5) WEBB, A.W., Report AN 2/1/0 - 1814/73 AMDEL, Adelaide (1973) unpublished.

(6) DUNN, P.R., PLUMB, K.A., ROBERTS, H.G., A proposal for time-stratigraphic sub-division of the Australian Precambrian, J. Geol. Soc. Austr. 13 (1966) 593-608.

(7) NEWTON, H.J., McGRATH, M.G., The occurrence of uranium in the Milestone Authority to Prospect, Wollogorang District, N.T., in: Stillwell Anniversary Volume, Australasian Inst. Min. Metall., Melbourne (1958) 177-185.

(8) HILLS, J.H., THAKUR, V.K., Westmoreland Uranium Deposits, in: C.L. Knight (editor), Econ. Geol. of Australia and Papua New Guinea - 1. Metals, Monograph Series 5, Australasian Inst. Min. Metall., Melbourne 1 (1975) 343-347.

(9) DODSON, R.G., PRITCHARD, C.E., Uranium in the Pine Creek Geosyncline, in: C.L. Knight (editor), Econ. Geol. of Australia and Papua New Guinea - 1. Metals, Monograph Series 5, Australasian Inst. Min. Metall., Melbourne 1 (1975) 281-284.

(10) McANDREW, J., Sklodowskite from Cobar No. 2 Prospect, Northern Territory, in: Stillwell Anniversary Volume, Australasian Inst. Min. Metall., Melbourne 1 (1958) 169-175.

(11) MORGAN, B.D., Uranium ore deposits of Pandanus Creek, in: J. McAndrew (editor), Geology of Australian Ore Deposits, 8th Commonwealth Mining and Metallurgical Congress, Melbourne 1 (1965) 210-211.

(12) HILLS, J.H., RICHARDS, J.R., The age of uranium mineralization in Northern Australia, Search 3 (1972) 382-385.

STRUCTURE RELATED URANIUM MINERALIZATION IN THE WESTMORELAND DISTRICT, QUEENSLAND, AUSTRALIA

W.E. Schindlmayr, B. Beerbaum

Urangesellschaft Australia Pty. Ltd.

Melbourne

Australia

Abstract

STRUCTURE RELATED URANIUM MINERALIZATION IN THE WESTMORELAND DISTRICT, QUEENSLAND, AUSTRALIA

The Westmoreland Uranium District straddles the boundary between Queensland and the Northern Territory of Australia some 100 km south of the coastline.

Middle Proterozoic conglomerate/sandstones and a basic volcanic sequence of the McArthur River Basin unconformably overly Lower Proterozoic metamorphics and acid volcanics, both intruded by high level granites, which are exposed in an EW trending uplift. Basic dikes, thought to be feeders to the multiple basic extrusions were emplaced mainly along the NE trending structures dissecting the sandstone sequence.

Uranium mineralization in the district frequently occurs as vertical or subvertical, discontinuous lenses or sheets adjacent to or within these dike filled structures. The primary minerals are uraninite and protobrannerite. Gold may occur coincidental to uranium. Uraninite is the last replacive mineral phase, following cementation and argillic alteration of the host rocks and the introduction of chlorite/hematite.

The primary origin of the uranium remains open due to lack of conclusive evidence for introduction of the uranium into the system either as detrital component or by exhalative volcanogenic activity or by hydrothermal remobilization from deep seated sources. It is postulated that a heat flow event at about 820 Ma generated and maintained convection flow cells within permeable host rocks and that uranium introduced to circulating oxygenated formation waters by any one or more of the above processes was precipitated against physico-chemical barriers such as basic dikes or basaltic flows due to the abundant supply of divalid iron as reductant.

1. INTRODUCTION

The Westmoreland Uranium District is located some 100 km south of the Gulf of Carpentaria straddling the border between Queensland and the Northern Territory of Australia and some 385 km NNE of the mining city of Mt. Isa.

This paper will deal in detail only with uranium occurrences within Queensland which in prior publications have often been referred to as the Red Tree Prospect or deposit. Other deposits of the district are described elsewhere in this volume (Morgan et al. (1)).

Mineralization was first indicated by an airborne survey of the Bureau of Mineral Resources in 1956 and found the same year to occur as secondary mineralization in quartzitic sandstones of Carpentarian age. A case history of exploration efforts from 1956 through 1979 was presented by Fuchs and Schindlmayr (2).

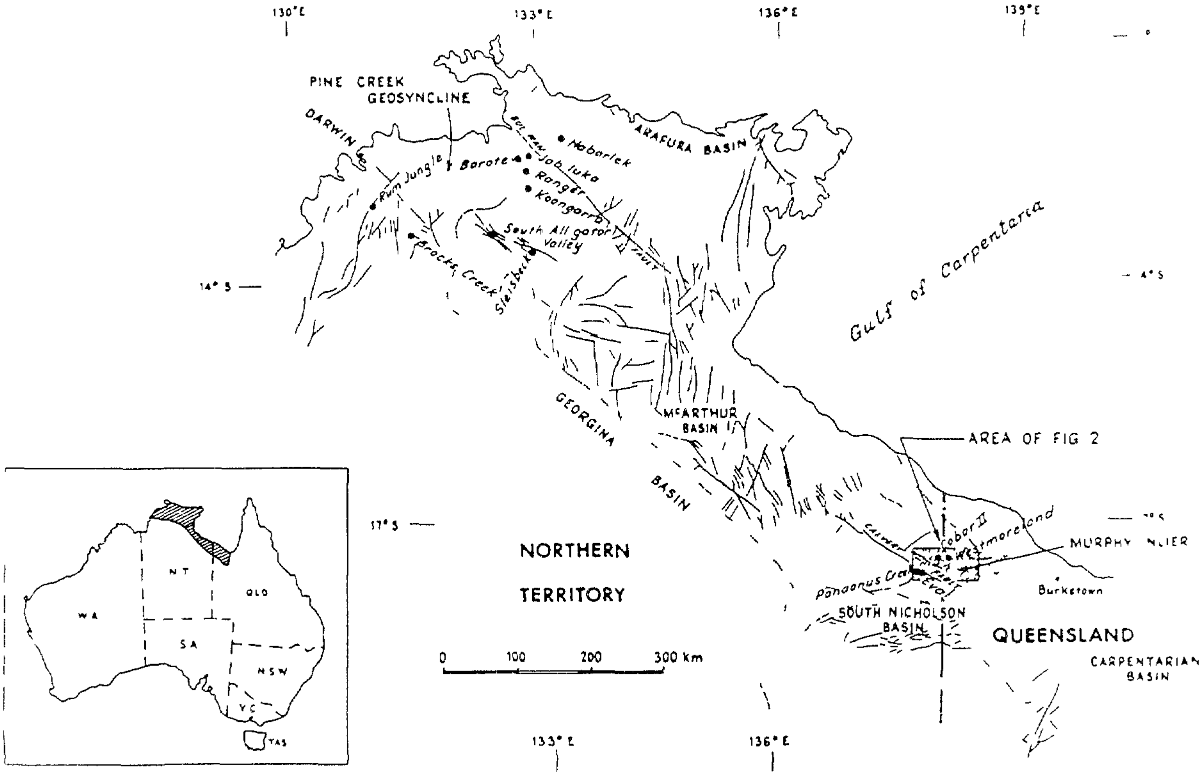

FIG. 1. Location of Uranium Deposits and Fracture Pattern of Northern Australia (after Hills et al. (16)).

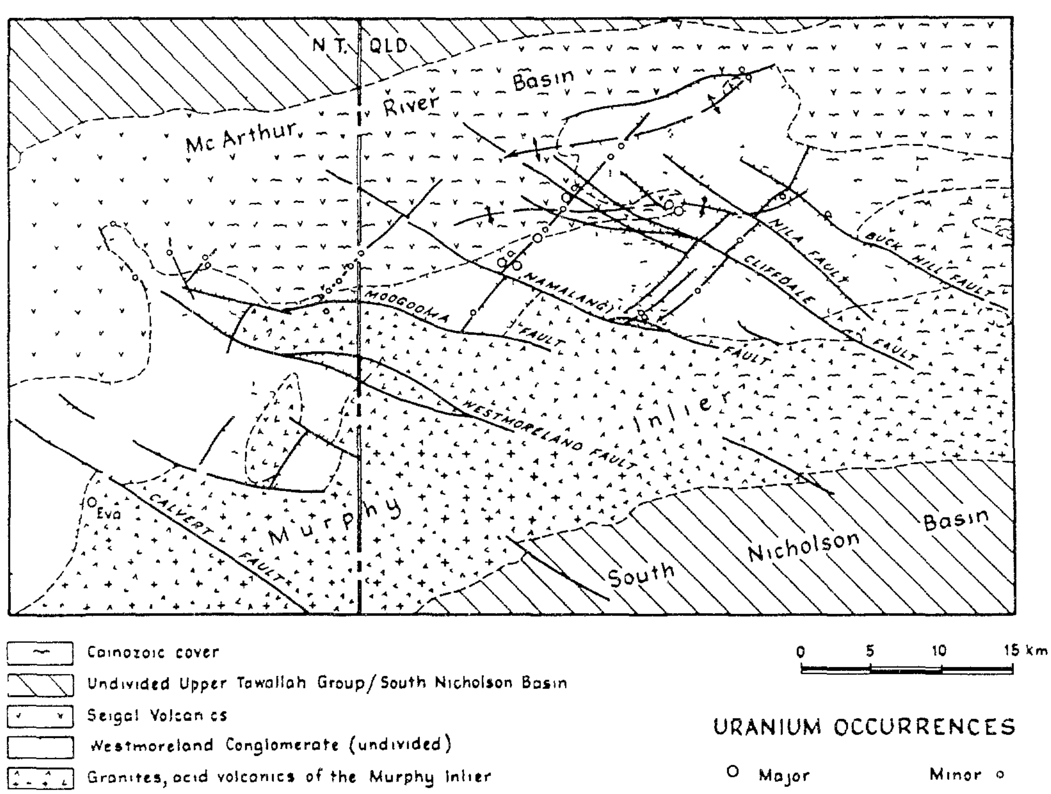

FIG. 2. Simplified Geology and Uranium Occurrences

2. REGIONAL GEOLOGY

2.1. Tectonic setting

The Westmoreland Uranium District straddles the boundary between two major Proterozoic tectonic units: to the N and NW the Carpentarian McArthur River Basin and to the S and SE the Carpentarian Lawn Hill Platform and the overlying South Nicholson Basin of Carpentarian and Adelaidian Age (Fig. 1). The Boundary Zone is a belt of Lower Proterozoic to Carpentarian 'basement' rocks that constitute the Murphy Tectonic Ridge, which during Middle and Upper Proterozoic formed a topographic barrier between the two depositional areas. That part of the Murphy Tectonic Ridge, which is presently exposed in an ENE trending window of some 150 x 25 km, is called the Murphy Inlier. A thin veneer of Cretaceous and Cainozoic rocks masks the Proterozoic to the east (Carpentarian Basin) and west (Northern Territory Shelf).

The McArthur River Basin is a largely undeformed basin extending some 600 km NW, to where the Lower Proterozoic 'basement' at its western margin hosts the uranium deposits of the East Alligator and South Alligator River Uranium Fields.

The Middle Proterozoic sequence has been generally folded into ENE trending synclines and anticlines parallel to the trend of the Murphy Ridge itself.

A pattern of NE trending structures (Fig. 2) represent zones of weakness in the basement that were repeatedly used as feeder slots for the extrusion of thick basic to acid volcanic sequences that overly the basal clastic sediments. This is evidenced by basic to intermediate dike fillings in numerous localities. Only minor vertical displacement occurred along these structures commencing during the close of sedimentation of the basal clastics.

These NE trending structures are predominant in controlling mineralization within the Westmoreland area (Fig. 2).

A regional pattern of WNW to NW trending faults dissects the Murphy Ridge and McArthur River Basin sediments alike, always associated with substantial horizontal displacement and in places with significant vertical throw. The most persistant of these faults, the Calvert Hill Fault, runs for some 180 km with a horizontal slip of up to 7 km and vertical throw up to 750 m. The trend continues to and is evident again in the East Alligator River Region (e.g. Bullman Fault, Fig. 1).

Within the Westmoreland area, this trend is well represented (Fig. 2) by (from NE to SW) the Buck Hill Fault, Nila Fault, Cliffdale Faults North and South Branches, Namalangi Fault, Moogooma Fault and Westmoreland Fault. Whilst only horizontal displacement (N-block west) of 250 - 400 m with little or no vertical throw has effected the blocks N of Namalangi Fault, the block south of it has suffered selective block tilting with resulting compressional folding along N-trending axis (Moogooma Dome) and was down-dragged against Cliffdale Volcanics along the Moogooma Fault, causing steepening of dips and partial subpression of the stratigraphic sequence.

These faults affect all Proterozoic units and displace mineralization and therefore postdate at least with latest rejuvenating movements the emplacement of mineralization.

In the area described in more detail, dips are generally low (3° - 10°) towards the keel of the Longpocket Syncline (Fig. 3).

2.2. Stratigraphy

The stratigraphic units outcropping in the general Westmoreland Area were first summarized by Carter (3) and Roberts et al. (4). The stratigraphy was since revised several times, the most recent revisions being by Sweet et al. (5), Mitchell (6), Gardener (7), Plumb (8), Sweet et al. (9), Sweet (10).

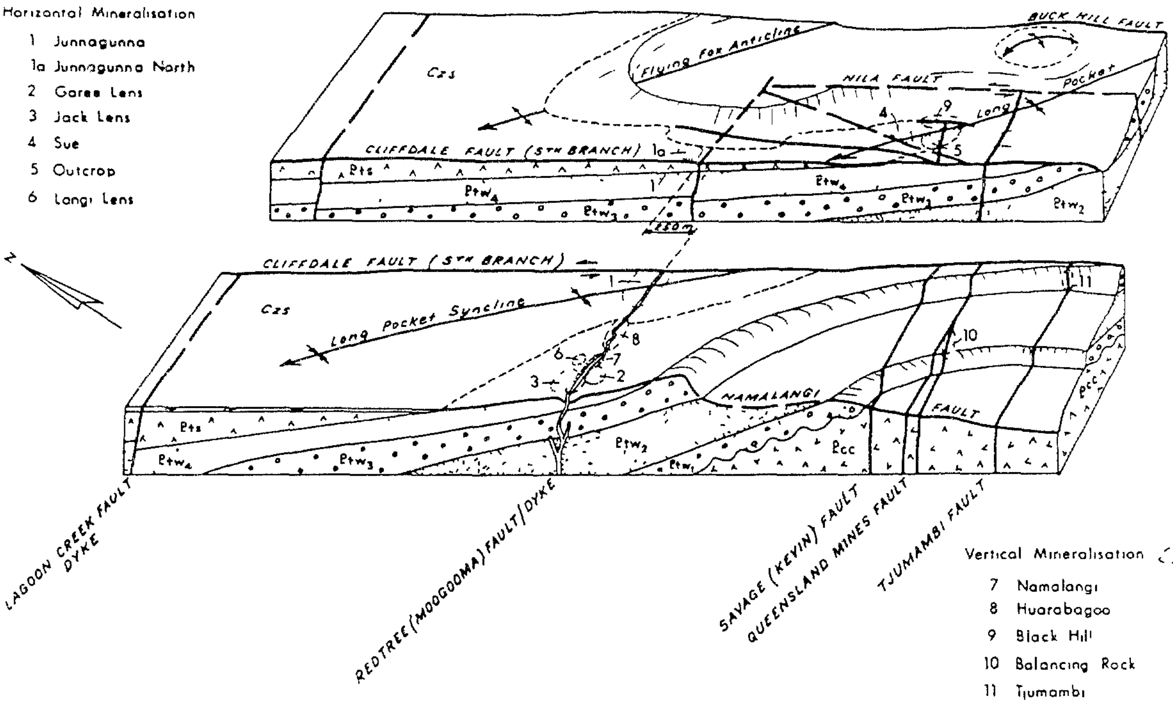

FIG. 3. Simplified block diagrams/sections showing relationship of mineralization to NE structural trend.

2.2.1. Murphy inlier sequence

The oldest rocks, exposed only in the western half of the Inlier are the Murphy Metamorphics. They were described by Roberts et al. (4) as geosynclinal peletic quartzofeldspathic metasediments and metavolcanics and consist mainly of quartz-albite-biotite chlorite schist and quartz-albite-muscovite gneisses in lower amphibolite facies of regional metamorphism. Subordinate graphitic and cherty units are known to occur. They are generally correlated to the Lower Proterozoic sequence of the Pine Creek Geosyncline (Fig. 1), although detailed correlations remain obscured.

Unconformably overlying the Lower Proterozoic basement relief and not effected by regional metamorphism are the Cliffdale Volcanics sequence of acid volcanics of variable thickness comprising predominantly massive layers of ignimbrites and rhyolites with rhyodacites and minor pyroclastics accounting for the balance. A detailed subdivision of this volcanic pile into 5 units is described by Mitchell (6).

Individual flows can be followed over distances up to 60 km. Younger units appear progressively removed towards the east by uplift and erosion prior to the McArthur River sequence (2.2.2.).

Age datings from the upper part of the Cliffdale Volcanics have yielded a Rb-Sr isochron age of 1770 ± 20 Ma (Sweet et al. (9)), which correlates them well to the Edith River Volcanics of the South Alligator Valley Uranium District (Fig. 1) of the Pine Creek Geosyncline (1760 Ma).

The Nicholson Granite Complex clearly intruded Murphy Metamorphics and on latest work, comprises of a series of related intrusions (emplaced at successively higher levels with time) which are largely consanguinious with Cliffdale acid volcanic extrusions. Gardener (7) describes at least 8 intrusive phases yielding Rb/Sr-isochron ages ranging from 1860 ± 103, 1843 ± 83, 1773 ± 24 to 1751 ± 67 Ma.

The younger phases correlate well with those of early Carpentarian intrusives of the Pine Creek Geosyncline (Nabarlek Granite: 1760 Ma, Tin Camp Granite, Yeuralba Granite: 1730 - 1780 Ma) and represent high level granites which are anomalous in tin and uranium.

Whilst it was previously thought (Roberts et al. (4)) that Cliffdale Volcanics were extruded into an eroded surface of Nicholson Granite, it is now believed from recent age datings and mapping (Gardener (7), Sweet (10)) that all of the Cliffdale Volcanics were intruded by the Nicholson Granite Complex at some stage.

Swarms of rhyolitic dikes occur in Cliffdale Volcanics and Granite intrusions and are thought to have preceded late stage intrusions.

Basic dikes dissecting Cliffdale Volcanics are regarded as feeder dikes for the extrusion of Seigal Volcanics and/or other basic volcanics higher up in the McArthur River Basin Sequence.

2.2.2. Basal McArthur River Basin Sequence (Tawallah Group)

After a period of gentle uplifting of the Murphy Ridge so as to create a physical barrier to subsequent sedimentation, which separated the McArthur River and the South Nicholson Basin, and of removal by erosion of the upper units of the Cliffdale Volcanics in the east (Middle Proterozoic Unconformity) deposition of a basal clastic sequence (the Westmoreland Conglomerate) in a terrestrial environment and shedding from a predominantly eastern and northeastern source area was initiated by periodic rapid uplifting of that source area. This source area is not presently known The clastic sequence attains thickness of over 1000 m near the ridge and up to 1700 m in local graben structures created by movements along NW trending faults (e.g. Calvert Fault) and thins out around basement reliefs and towards the crest of the Murphy Ridge.

In the immediate Westmoreland area this clastic sequence is overlain with apparent conformity by a sequence of 1600 m plus of basic lavas (Seigal Volcanics) with numerous interbeds of siltstone and sandstone, followed by near shore marine/lagoonal stromatolithic dolomites, sandstones and siltstones (McDermott Formation), quartz sandstones (Sly Creek Sandstone), siltstones (Aquarium Formation) and again basalts and trachytes of the Settlement Creek and Gold Creek Volcanics.

Cretaceous Mullaman Formation is locally preserved as valley-fill and plateau cover. The Tertiary is evidenced by substantial peneplanations, laterite development and surface silicification.

Only the lower two members of the Tawallah Group are of interest for this paper and are described in more detail below.

(i) The Westmoreland Conglomerate consists of quartz sandstone, orthoquartzites, conglomeratic sandstones and conglomerates and was, generally, deposited in a high-energy fluviatile to estuarine environment from a source area to the east. Clasts comprise mainly of acid volcanics, vein quartz and ortho-quartzites with subordinate Murphy Metamorphics. Compared to the lithologies exposed in the Murphy Inlier today, the near total absence of granite clasts is conspicuous; rare, thin layers of siltstone or shale may indicate temporary interruptions of the high-energy sedimentation due to breaks in the uplifting of the source area or near structures active during sedimentation.

SW of the Calvert Fault the sequence can only be subdivided into two units, whereas to the NE of the Calvert Fault including the Westmoreland Uranium District, four units are well recognized, numbered Ptw_{1-4} respectively.

The basal lenticular conglomerates/cobble beds (Ptw_1) overly Cliffdale Volcanics with pronounced unconformity filling relief depression in the erosional surface. Around inselbergs of Cliffdale Volcanics, the basal conglomerate is seen to thin out or even pinch out against these local highs. This is followed by resistant (cliff forming) quartz sandstones and orthoquartzites. Clasts comprise of ignimbrite, rhyolite and dark-grey or purple sandstone/orthoquartzite of yet unknown origin. Ptw_1 thins from 240 m in the east to 60 m or less near the Northern Territory border.

Ptw_2 is a unit of thick beds of medium grained to pebbly sandstone, conspicuous by large scale trough cross bedding. It probably represents deposition in a deltaic environment. It ranges in thickness from 300 - 500 m and rests conformably on Ptw_1 as part of the same cycle. Its top is marked by the onset of another cycle of high-energy fluviatile deposition of Ptw_3 and locally, by strong angular unconformity (Moogooma Dome Area).

Ptw_3 is prominent by its conglomeratic sandstone and prominent cliff forming lenticular conglomerates/cobble conglomerates near its top. Clasts of Cliffdale Volcanics abound. A thin layer of shale/siltstone indicative of a temporary marine ingression is locally developed at the top of this member.

Ptw_4, which in the context of this paper is the most important unit, comprises of fine to coarse grained orthoquartzite. Pebbles of mainly vein quartz and orthoquartzite and to a lesser extent acid volcanics are scattered throughout and several horizons of pebbles beds or even conglomerate layers occur towards the top, which act as marker beds for at least some of the area in an otherwise rather variable sequence. The thickness of Ptw_4 in the keel of Longpocket Syncline ranges from less than 60 m in the east to more than 120 m near the border.

Acid volcanic shards are increasing in the matrix toward the top of the unit in certain areas; together with the occasional thin tuff bands, this is an indication of eruptive volcanic activity commencing during the late stage of the deposition of Westmoreland Conglomerate, which locally contributed pyroclastic material into sandstone derived from distal sources. The Ptw_4 was probably laid down in a predominantly estuarine environment with the occasional recurrance of higher energy deposition of deltaic or fluviatile conditions.

(ii) The Ptw_4 unit is, on a regional scale, conformably overlain by the Seigal Volcanics, a thick pile of basic shallow water lava extrusions with frequent, short ingressions of clastic sedimentation between flows. Generally, a layer of siltstone (0 - 6 m thick) marks the onset of intensive volcanic activity, followed by a multitude of individual flows of massive or amygdaloidal basalts, trachytes and minor acid variations (rarely exceeding 20 m thickness).

Whilst the topographic relief of the Seigal Volcanics in the Northern Territory can be quite rugged, in Queensland the volcanics are generally peneplained and covered by a thin veneer of Tertiary laterites and Cainozoic sands and soils. Outcrops are seen only where silicification has occurred along faults.

Acid to intermediate precursors of the Seigal Volcanics are found around extrusive centres as single or multiple sills/dikes intruded into the upper portions of the Ptw_4-unit with 'wet' contacts. One such extrusive centre is located in the eastern Longpocket Valley. There, the sills/dikes appear to be a controlling factor for the precipitation of uranium mineralization.

The prominent NE-trending structures (Fig. 2) are frequently found to be filled with volcanic dikes (basaltic, andesitic, trachytic and rarely acid extrusive phases). To a limited degree, this also holds for EW trending structures.

The chemical composition of the dike material is not inconsistent with that of the directly overlying Seigal Volcanics, and it is assumed that the structures were utilized repeatedly as feeders for the extrusion of basalt flows.

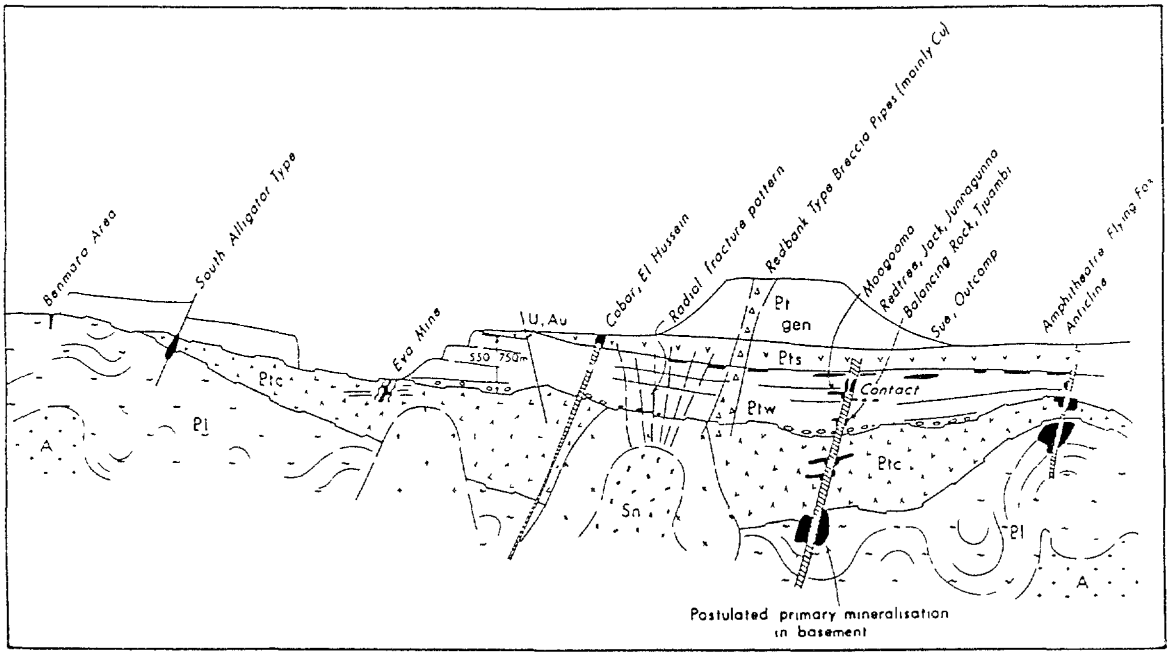

FIG. 4. Westmoreland Area, schematic model of mineralization

2.3. Mineralization

Uranium prospects had been found since the fifties in the Murphy Inlier and onlapping McArthur River Basin Sequence in numerous localities and stratigraphic levels ranging from prospects in the Murphy Metamorphics and in the Cliffdale Volcanics or some high level granites to those in all units of the Westmoreland Conglomerate and in the overlying Seigal Volcanics (Fig. 4). Most of these occurrences were originally described by Brooks (11), and Lord (12). Predominantly these occurrences are located in or closely associated with either quartz-filled regional faults, dike-filled structures dissecting the Tawallah Group sediments/volcanics or with shear zones within a variety of lithologies. Uranium was mined only from the Eva Mine (Morgan (13)), which is described in more detail elsewhere in this Volume (Morgan et al. (1)). Geological resources of economic significance are confined to date to the Ptw_4 unit of the Westmoreland Conglomerate (Hills et al. (14)).

Mineralization of copper is associated with shear zones in granites of the Murphy Inlier and with volcanic breccia pipes (Red Bank) related to the Gold Creek Volcanics. Tin and tungsten occurrences are known from quartz veins and greisens related to late, high-level intrusives.

3. WESTMORELAND (RED TREE) URANIUM OCCURRENCES

Within Queensland, mineralization of uranium was located in all units of the Westmoreland Congomerate and at the base of the Seigal Volcanics. With the exception of heavy mineral horizons in Ptw_3, almost all occurrences are spatially related to either:

- NE trending structures with proven or suspected dike filling,

- or volcanic sills,
- or EW trending structures with volcanic dike filling,
- or quartz breccias of NW trending regional faults,
- and/or the proximity to the contact between uppermost Ptw_4 and the overlying Seigal Volcanics.

Fig. 2 and 3 show the minor and major occurrences. Over 90 % of all resources located to date are contained in the upper half of Ptw_4 in the vicinity of the features listed above.

3.1. Geometry and distribution of major uranium occurrences

Uranium mineralization of economic significance occurs in two general configurations which may be coexistent (Fig. 5).

3.1.1. 'Vertical type' mineralization

Lensoid, tubular or irregular bodies of 'higher' grade uranium mineralization in sandstone, which are sub-parallel to, adjacent to or even transgressing into basic dikes, where these dissect the Ptw_4 unit (Fig. 5). Mineralization may occur on both sides of the dikes but is generally stronger and more compact on one side. Mineralization frequently terminates several metres above the top of Ptw_3, but sparse deeper drilling did encounter the occasional mineralization within Ptw_3 at the dike or within the dike. Statistically, the best mineralization with grades sometimes exceeding 1 % U_3O_8 occurs at levels along the dike between 45 and 60 m below the Seigal Volcanics where these are preserved (A in Fig. 5), or at a level between 10 and 50 m below surface, where the sandstone was exposed to surface weathering, with an apparent development of a secondary horizontal dispersion wing into the dike and away from it (B in Fig. 5).

Deflections in the dip of the dike are frequently seen to be associated with compact and good grade mineralization at the foot-wall side (C in Fig. 5).

Vertical type mineralization of significance has been intersected along the Red Tree Dike System from the Jack Lens to Junnagunna over a strike length of 8.5 km. Whilst generally of higher grade than the horizontal wing, definition of geological resources proves to be difficult due to the rather discontinuous and erratic nature of high grade mineralization within an envelope of semicontinuous and near-predictable low grade mineralization of 300 - 500 ppm U_3O_8.

Minor mineralization of the 'vertical type' was found associated with other north-east trending faults (from west to east: Lagoon Creek Fault, Queensland Mines Fault and Tjuambi Faults and with the east-west trending Black Hill Dike System (Fig. 3)).

3.1.2. 'Horizontal type' mineralization

Blanket type, tabular or lensoid bodies of mineralization sub-parallel to or adjoining the contact between Ptw_4 and either the overlying Seigal Volcanics (D) or intermediate sills intruded into the upper Ptw_4 (E in Fig. 5). Significant horizontal mineralization may extend as much as 600 m away from the dike,

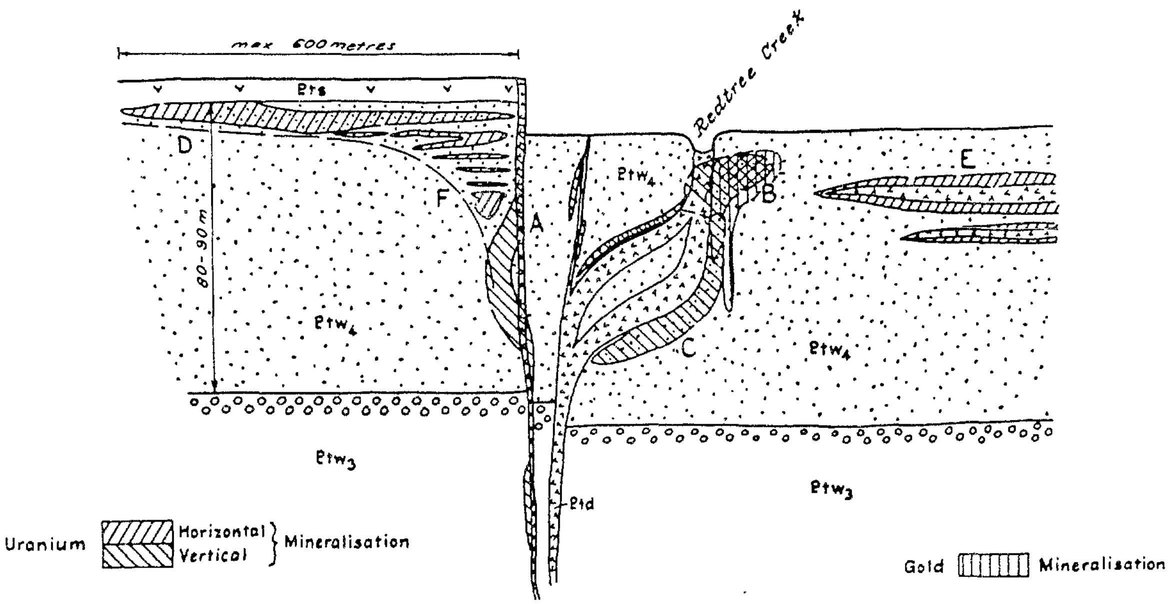

FIG. 5. Westmoreland Area, schematic diagram of types and geometry of uranium and gold mineralization.

but has to date not been found remote from dike structures. Horizontal mineralization in the immediate vicinity of the dikes generally tends to split up into thinner layers/discontinuous horizontal lenses stacked above each other over a thicker interval creating the impression of a gradual change from horizontal to vertical type mineralization in an asymptotic curve (F in Fig. 5).

Horizontal type mineralization forms by far the majority of geological resources outlined to date in six different bodies.

3.2. Host rock to vertical type mineralization

The gross of vertical type mineralization is emplaced within the sandstones of the Ptw_4 unit adjacent to the dike-filled, NE-trending structures and in xenoliths or blocks of sandstone enclosed by bifurcating dike systems. To a lesser extent mineralization occurs within the basic dikes.

3.2.1. Ptw_4 - petrography

Virtually all of Ptw_4 can be classified as orthoquartzite of fine to coarse grain size, with pebbles of vein quartz and Cliffdale Volcanics scattered throughout and with local development of layers/lenses of quartzose grits, conglomeratic orthoquartzites or conglomerates. The sequence is highly variable horizontally and vertically and, with the exception of levels containing conglomerate/conglomeratic sandstones or pebble layers or, in the case of the Upper Longpocket Valley near the Red Hill Fault of shale interbeds, drill hole correlation is difficult even over short distance.

Quartz grains are generally well rounded, but maybe corroded by replacive minerals. All rocks contain small amounts of lithic material including felsite (probably Cliffdale Volcanics), metaquartzites and vein quartz. Feldspar was probably present, but has been replaced by clay minerals. Quartz and above lithic components, by their textural relationship point to a distal source. In contrast to that, vitric and acid to intermediate tuffs in the sandstone matrix, increasing to tuffaceous sandstones or locally even sandy tuff lenses towards the upper part of Ptw_4 indicate the onset of the Seigal Volcanics event with local eruptive centres shedding pyroclastic components into otherwise mature sandstone. Carbonaceous matter may have been present in the sandstone.

The quartz framework is always cemented by secondary quartz overgrowth that is in optical continuity with the quartz grains. Both framework grains and cement are appreciably stressed.

Detrital heavy minerals are relatively scarce and mostly scattered, rarely forming distinct layers. Tourmaline, zircon, xenotime, leucoxene and monazite are seen. Gold may be present as detrital component.

Post-lithification alteration and deposition of younger, replacive minerals are a regional feature of the host rock. The mechanism was one of low-temperature hydrothermal/metasomatic emplacement of mainly illite-sericite with incipient replacement of the quartz cement and of certain framework grains (e.g. feldspar). Other replacive mineral phases include kaolinite-illite, pro(Fe-) chlorite, hematite, siderite and rare apatite.

The sandstone lithologies show little or no thermal effects at the contact to the basic intrusive dikes, indicating low temperature conditions of dike emplacement.

3.2.2. Dike rock petrography

Dikes have virtually always suffered severe argillic alteration to the extent that their classification is based only on relict textural features and the nature of alteration minerals.

There are at least two distinct types of dike rocks which may represent separate extrusive phases of material derived from a related source. Clear affinities exist to the chemistry of overlying Seigal Volcanics:

(i) dolerite - basalt group

(ii) microsyenite group

They are of similar fine grain size, but the basaltic phase is amygdaloidal, sometimes banded, with amygdales containing quartz, hematite, K-feldspar and chlorite.

Feldspars are replaced by aggregates of sericite, quartz and dusty brown opaques.

Mafic and interstitial minerals are replaced by aggregates of chlorites (Mg-chlorites) and dusty opaques. Silicification is rare and associated with brecciation. Opaque minerals include leucoxene formed from primary magnetite/ ilmenite, and hematite deriving from alteration of ferromagnesian minerals.

3.3. Mineralization

Ore minerals represent several phases of epigenetic, low temperature hydrothermal processes of ore emplacement at a stage well post-dating diagenesis, tectonic stress and a regional low temperature argillic alteration process. Uranium and gold mineralization coexists in places and are the youngest mineral phases.

3.3.1. Uranium minerals

Minerals of economic interest are dominated by uranium oxides with subordinate protobrannerite and secondary uranium minerals of the phosphate, vanadate, silicate, arsenate and sulphate groups, in descending order of importance. A list of uranium minerals identified in the Westmoreland area is presented in Table I.

TABLE I. URANIUM MINERALS PRESENT IN THE WESTMORELAND AREA

I. BASEMENT	
METAMICT ILMENITE - DAVIDITE - BRANNERITE MINERALS	
II. OVERLYING SEDIMENTS & VOLCANICS	
OXIDES:	
URANINITE *	UO_2
PITCHBLENDE	
GUMMITE	
BRANNERITE *	(U, Ce, Y, Ca) $(Fe, Ti)_2 \cdot O_6$
VANDENDRIESSCHEITE	$PbO \cdot 7UO_3 \cdot 12H_2O$
PHOSPHATES:	
TORBERNITE *	$Cu\ (UO_2)_2 \cdot (PO_4)_2 \cdot 8\text{-}12H_2O$
METATORBERNITE *	$Cu\ (UO_2)_2 \cdot (PO_4)_2 \cdot 8H_2O$
RENARDITE	$Pb\ (UO_2)_4 \cdot (PO_4)_2\ (OH)_4 \cdot 7H_2O$
PHOSPHOURANYLITE	$Ca\ (UO_2)_4 \cdot (PO_4)_2\ (OH)_2 \cdot 6H_2O$
AUTUNITE *	$Ca\ (UO_2)_3 \cdot (PO_4)_2 \cdot 10\text{-}12H_2O$
PARSONITE	$Pb_2\ UO_2 \cdot (PO_4)_2 \cdot 2H_2O$
SALEEITE	$Mg\ (UO)_2 \cdot (PO_4)_2 \cdot 10H_2O$
VANADATES:	
CARNOTITE *	$K_2\ (UO_2)_2\ (VO_4) \cdot 3H_2O$
FRANCEVILLEITE	$(Ba, Pb)\ (UO_2)_2 \cdot (VO_4)_2 \cdot 5H_2O$
SILICATES:	
SKLODOWSKITE	$Mg\ (UO_2)_2\ Si_2O_6\ (OH)_2 \cdot 5H_2O$
COFFINITE	$U\ (SiO_4)_{1-x}\ (OH)_{4x}$
SODDYITE	$(UO_2)_2\ SiO_4 \cdot 2H_2O$
ARSENIDES:	
METAZEUNERITE	$Cu\ (UO_2)_2\ (AsO_4)_2 \cdot 8H_2O$
URANOSPINITE	$Ca\ (UO_2)_2\ (AsO_4)_2 \cdot 10H_2O$
NOVACEKITE	$Mg\ (UO_2)_2\ (AsO_4)_2 \cdot 12H_2O$
SULPHATES:	
ZIPPEITE	$K_4\ (UO_2)_6 \cdot (SO_4)_3 \cdot (OH)_{10} \cdot 4H_2O$

* MAJOR MINERALS

NOTE: THORIUM IS ONLY PRESENT IN ALTERATION PRODUCTS OF DETRITAL TH-MINERALS IN HEAVY MINERAL LAYERS. MINERALS ARE THOROGUMMITE AND FLORENCITE.

Whilst mineralization in some horizontal orebodies that were open to surface oxidation (Jack Lens, Langi Lens, upper parts of Garee Lens and Outcamp) is preserved exclusively or predominantly as grain coating and interstitial filling of the host rock with secondary uranium minerals together with hematite, chlorite and sericite, the deeper parts of oxidized orebodies (Garee Lens, Outcamp) and all horizontal orebodies preserved under volcanics cover (Junnagunna, Sue, Outcamp) and almost all vertical type mineralization is present as uranium oxides.

3.3.2. Sandstone hosted uranium mineralization (vertical type)

Uraninite is the main ore mineral occurring either as idiomorphic grains up to 0.05 mm or as very fine-grained, soft, sooty, 'pitchblende'-like material.

It occurs disseminated throughout the matrix or in small veins exhibiting colloform or dendritic textures, mostly intimately spatially associated with one or all of sericite aggregates, chlorite or hematite. It also occurs without other replacive minerals in microfractures within the framework grains.

There is no lithological factor apparent which might explain that uranium was emplaced here and not elsewhere. Only a broad, erratic relationship exists between uranium and an increase of younger, introduced minerals (in the mineralized host rock) but no close connection between species/quantity of other replacive minerals and the amount of uranium mineralization is seen.

The textural relationship between uraninite and other minerals clearly indicates that the uraninite is independent of all other minerals and that it is most likely the youngest mineral present in these rocks (with the possible exception of some gold). Where there appears to be a textural association between pitchblende and another mineral, this is because the introduced minerals are all generally confined to the cement and matrix remnants (i.e. they replaced the cement and matrix) and, being more permeable than the original quartz cement, they provide access to the rocks.

Intensity of uranium mineralization varies from a regional sandstone background of 4 - 6 ppm to values in excess of 1 % U_3O_8 but averages between 0.15 and 0.30 % U_3O_8. It is generally in equilibrium with its daughter products and conforms with the natural $U_{238/235}$ ratio.

3.3.3. Dike hosted 'vertical type' uranium mineralization

Within the dike rocks, uranium occurs either as uraninite or as protobrannerite.

Uraninite is present either as porous coke-like patches (to 01. mm) with colloform texture or as clots of uraninite forming thin contorted seams of high grade generally aligned with fractures or parallel to banding indicated by amygdales. Uraninite also frequently occurs in the core of amygdales with crazing pattern.

Again, there is no close relationship between the pervasive argillic-sericitic alteration of the dike rocks and the amount of uranium mineralization present, nor is there a definite relationship of uraninite to any or all of the other introduced replacive minerals.

Proto-brannerite is present diffusely scattered throughout in varying amounts and grain sizes within the clouds of leucoxene/sphene which derived from the leucoxination of primary magnetite/ilmenite.

The term proto-brannerite is used here to indicate that the mineral has formed in situ by introduction of uranium to the titanomagnetite-ilmenite after the deuteric alteration of the dike material. Proto-brannerite accounts for only about 10 % of economic grade mineralization within the dike.

3.3.4. Gold mineralization in sandstone and dike

Gold values of economic significance are reported from various localities in the general Westmoreland area (e.g. Eva Mine, Morgan et al. (1)) to occur associated with uranium mineralization, and this was confirmed by drill core analysis for portions of the Junnagunna horizontal mineralization as well as for vertical type mineralization in portions of Huarabagoo (Fig. 5). Values reach 80 g Au/t, but are generally more about 0.2 - 7 g Au/t.

There appears to be a loose spatial relationship between uranium and gold mineralization to the extent, that high grade uranium intersections in or in the vicinity of the dike frequently carry high gold values, but high uranium is also known to occur without appreciable gold and vice versa.

In the sandstones, gold is frequently found as irregular to subspherical grains of about 10 µ within framework grains (in particular felsite grains), associated with gangue, mainly sideritic carbonates but also quartz and sericite, and as inclusions in uraninite and 'pitchblende'. It also occurs as irregular, dendritic and/or rounded free masses up to 2 mm (from Heavy Mineral Concentrate Studies of Bulk Stream Sediment Samples).

In a sample from the Lagoon Creek Fault near the border gold as droplets of 2 - 3 µ was seen to occur in the central portions or cores of concentric radiating 'pitchblende' masses, mostly within pitchblende, but also in shells of chalcopyrite.

In dike rock gold occurs in close association with 'pitchblende' as blebs, as irregular and dentritic particles and as films with average grains sized 3 - 6 µ. They are embedded in, and intergrown with pitchblende, rarely with galena.

Results of testing the Westmoreland Conglomerate for placer-type gold mineralization were ambivalent, but data seem to be pointing more to a spatial relationship of geochemical Au-anomalism with either NE-trending structures with dike filling and associated U-occurrences, or with EW trending late stage shears or swarms of shears with quartz filling or quartz breccias.

3.3.5. *Other minerals*

Other ore minerals include pyrite, marcasite and chalcopyrite, radiogenic and other galena, sphalerite and Co-Ni-sulfarsenides; bismuth and bismuthinite occur in minor amounts near gold within dikes or are associated with pyrite in areas of sandstone hosted U/Au mineralization. Samples from the dump of an explanatory shaft in the Jack Lens contained significant amounts of chalcocite as intergrown with digenite and covellite within the sericitic matrix/cement, suggestive of a Copperbelt type mineralization. Thorium and Rare Earth minerals are absent from the ore.

3.4. Origin of mineralization

On present state of knowlege, the origin of the uranium remains open. There is no evidence of detrital uraninite within the sandstone sequence, and only few sightings of detrital davidite, monazite, thorite have been made. Detrital zircon is present throughout.

The felsic components of the orthoquartzites contain devitrified rhyolites and pyroclastics. To date, it is not known whether devitrification has taken place prior to deposition or in situ. The uranium background of the underlying Cliffdale Volcanics is elevated as is that of some of the consanguineous high level granites. Investigations of the thermoluminescence characteristics of Ptw_4 samples by Hochmann et al. (15) tends to favour this synsedimentary uranium introduction.

The pyroclastic influx during the late Ptw_4 sedimentation points to volcanic eruptive activity. It is conceivable that this would have been accompanied by exhalative, subaquatic action delivering heavy metal bearing solutions into the immature sediment.

All three of the above possible sources have to be seen against the overwhelming evidence, that uranium was emplaced into its present location well after consolidation and tectonism of the host rocks by later low temperature, low pressure processes. Determination of the U-Pb age of radiogenic galena from Huarabagoo (Hill et al. (16)) and other localities in the Westmoreland district (Eva Mine, Cobar II) provided an age for original introduction of mineralization at 820 Ma followed by an episode at about 430 Ma during which new uranium may have been introduced. These values closely resemble data obtained from some of the uranium occurrences in the Pine Creek Basin.

In contrast, the youngest intrusive activity was dated at 1770 ± 24 Ma and the Seigal Volcanics are tentatively dated 1680 Ma by correlation to volcanics in the Mt. Isa area (Sweet et al. (9)) but are probably somewhat older on the basis of recent dating of 1680 Ma of the McArthur River Tuffs higher up in the McArthur Basin sequence (verbal communication, N.T. Geol. Survey). This would place the deposition of the Westmoreland Conglomerate somewhere between say 1750 and 1700 Ma. A detrital nature of U-introduction, therefore seems improbable.

Alternatively, the uranium may have been introduced into the system by ascending hydrothermal solutions, which used the pre-existing shears and alteration zones as preferred channelways. Uranium mineralization adjacent to dike structure in the lower Ptw-sequence (Balancing Rock Occurrence, Moogooma Dome) tends to support that assumption.

It is conceivable that U-bearing solutions have derived by thermal remobilization from older uranium deposits of the East Alligator River type at depth. Near-surface mineralization would then represent upward leakage and redeposition of uranium from postulated high-grade primary uranium concentrations within the 'basement' (Fig. 4) which were mobilized during yet undefined events about 820 Ma with a possible repetition around 430 Ma.

3.5. Model of the emplacement

Evidence shows the uranium to be the youngest or one of the youngest mineral phases to be introduced into the system after:

- cementation of quartz sandstone with secondary quartz growth;
- a tectonic event causing stress to framework grains and cement alike;
- a regional event introducing replacive sericite, illite, chlorite and hematite;
- emplacement and subsequent argillic alteration of dikes related to the Seigal Volcanics.

Evidence also shows, that uranium emplacement is not only related to vertical structures, which could have acted as passage ways for ascending fluids, but also to horizontal geological boundaries such as basic sills and the overlying Seigal Volcanics.

Irrespective of whether uranium was introduced to ground waters by either ascending hydrothermal fluids or by the release of uranium into the ground water by devitrification of metastasis of volcano-clastic sandstone components or by leaching of U-bearing heavy minerals within the sandstone or by exhalative supply of heavy metals, it is argued, that oxigenated ground water carrying uranyl-complexes circulated within the more permeable layers (least cemented or with highest degree of replacive alteration or micro fracturirg), and that uranium was precipitated against geochemical barriers of reducing character and/or against permeability barriers. Hochmann et al. (15) describes this process in more detail. The basic dikes, sills and basic lavas then overlying all of the Westmoreland Conglomerate would have acted as such geo-chemical barriers by supplying divalent iron as reducing agent to precipitate uranium out of solution within a limited distance from the source of reductants. In addition, the dike structure and the overlying volcanics would have constituted a physical barrier to groundwater circulation resulting in a longer reaction period at this geochemical interface.

It is postulated that a rejuvenation of the vertical structure as channelways for ascending hydrothermal fluids and/or heat flow ascending upwards along the structures at about 820 Ma was responsible and sufficient to generate convection flow cells within reasonably permeable units of the Westmoreland Conglomerate sequence proximal to the structure, and to maintain them for such a time as to allow uranium accumulation by progressive precipitation against physicochemical barriers to occur. The mechanics of such a flow cell could be similar to those described by Fehn et al. (17).

A secondary remobilization and redepositioning of uranium and gold with preferential high-grade concentration some 10 - 35 m below surface is seen in areas, where the upper Ptw_4 was subjected to surface oxidation processes about the water table. Oxidation of primary uranium minerals has occurred in host rocks exposed above the water table.

ACKNOWLEDGEMENTS

The consent of the partners in the Westmoreland Joint Venture, Queensland Mines Ltd. and IOL Petroleum Ltd., to the publications of this paper is gratefully acknowledged.

The authors wish to thank all of Urangesellschaft's and the partners' geologists that have contributed over the years to the growing wealth of information on the project and, in particular, Rod Evans and Bruce Penny for their initiative and enthusiasm as Project Manager, and Walter Fander of Central Mineralogical Services for his petrographic and mineralogic contributions.

REFERENCES

(1) MORGAN, B.D., CAMPI, D., Pandanus Creek Uranium Mine, Northern Territory, Australia (1985) this volume.

(2) FUCHS, H., SCHINDLMAYR, W.E., The Westmoreland Uranium Deposit, Queensland, Australia, in: Uranium Exploration Case Histories, IAEA Vienna (1981) 59-73.

(3) CARTER, E.K., Westmoreland, Queensland - 4 Mile Geological Series, Bur. Miner. Resourc., Australia, Explanatory Notes SE (1959) 54-55.

(4) ROBERTS, H.G., RHODES, J.M., YATES, K.R., Calvert Hills, Northern Territory 1:250000 Geological Series, Bur. Miner. Resourc., Australia, Explanatory Notes SE (1963) 53-58.

(5) SWEET, I.P., SLATER, P.J., Precambrian Geology of the Westmoreland Region, Northern Australia, Part I: Regional Setting and Cover Rocks, Bur. Miner. Resourc., Australia, Record 1975/88 (1975) unpublished.

(6) MITCHELL, J.E., Precambrian Geology of the Westmoreland Region, Northern Australia, Part II: The Cliffdale Volcanics, Bur. Miner. Resourc., Australia, Record 1976/34 (1976) unpublished.

(7) GARDENER, C.M., Precambrian Geology of the Westmoreland Region, Northern Australia, Part III, The Nicholson Granite Complex and Murphy Metamorphics, Bur. Miner. Resourc., Australia, Record 1978/32 (1978) unpublished.

(8) PLUMB, K A., DEPRICK, G.M., WILSON, I.H., Precambrian Geology of the McArthur River - Mount Isa Region, Northern Australia, in: R.A. Henderson and P.J. Stephenson (editors), The Geology and Geophysics of Northeastern Australia, Geol. Sec. Australia, Queensland Division, Brisbane (1980) 8 pp.

(9) SWEET, I.P., MOCK, C.M., MITCHELL, C.E., 1:100000 Geological Map Commentary Seigal, Northern Territory and Hedley's Creek, Queensland Sheet Area, Bur. Miner. Resourc. Geol. and Geophys., Australia (1981) 32 pp.

(10) SWEET, I.P., Definitions of new stratigraphic units in the Seigal and Hedley's Creek 1:100000 Sheet Areas, Northern Territory and Queensland, Bur. Miner. Resourc., Australia, Report 225 (1981) 17 pp.

(11) BROOKS, J.H., The Uranium Deposits of Northwestern Queensland, Geol. Survey of Queensland, Publication 297 (1960) 50 pp.

(12) LORD, J.H., Report on an inspection of uranium discoveries in the Calvert Hills area, Northern Territory, Bur. Miner. Resourc., Australia, Rec. 1956/115 (1956) unpublished.

(13) MORGAN, P.D., Uranium Ore Deposit of Pandanus Creek, in: J. McAndrew (editor), Geology of Australian Ore Deposits, 8th Commonwealth Mining and Metallurgy Congress, Melbourne 1 (1965) 210-211.

(14) HILLS, J.H., THAKUR, V.K., Westmoreland Uranium Deposits, in: C.L. Knight (editor), Econ Geol. of Australia and Papua New Guinea - 1 Metals, Monograph Series 5, Australasian Inst. Min. Metall., Melbourne 1 (1975) 343-347.

(15) HOCHMANN, M.B.M., YPMA, P.J.M., Theroluminescence applied to Uranium Exploration and Genesis of the Westmoreland Uranium Deposits - Implications for the Northern Territory, to be presented to the Austr. Inst. Min. Metall. Conference, Darwin, Aug. 1984, in preparation.

(16) HILLS, J.H., RICHARDS, J.R., The Age of Uranium Mineralization in Northern Australia, Search, 3 N° 10 (1972) 382-385.

(17) FEHN, U., CATHLES, L.M., HOLLAND, H.D., Hydrothermal Convection and Uranium Deposits in Abnormally Radioactive Plutons, Econ. Geol. 73 (1978) 1556-1566.

MT. PAINTER URANIUM DEPOSITS

I. P. Youles
Oilmin N.L.
Adelaide
Australia

Abstract

MT. PAINTER URANIUM DEPOSITS

The Mt. Gee, Armchair, Streitberg Ridge and Radium Ridge primary uranium deposits consist of uraninite, pyrite, chalcopyrite, molybdenite, monazite, fluorite and barite in a matrix of chlorite and hematite, which infilled and replaced, as layers, a potash rich (10 % K_2O), partly sericitized, granitic breccia in the Radium Ridge Beds (interpreted about 700 Ma). Minor amounts of sandstone, siltstone, diamictite and arkose also occur. Uranium content averages 0.1 % along with Cu 0.05 %, Mo 0.03 %, Co 0.035 % and Ce group 0.5 %. Isotopic data indicate a magmatic origin and fluid inclusions show temperatures of 300°C - 400°C with aqueous solutions of low salinity.

The Hodgekinson deposit consists of uraninite with silica, pyrite, minor arsenopyrite and trace sulphides in brecciated, foliated, granitic rocks, which were silicified or kaolinized and sericitized; repetitive brecciation with infillings of uraninite, pyrite and chalcedony occurred, the latest being a secondary enrichment through downward leaching.

Early mine workings are in permeable zones, usually faults, in or adjacent to primary deposits; torbernite and autunite were deposited in voids by groundwaters of probable Tertiary age.

1. INTRODUCTION

The Mt. Painter uranium deposits are scattered over an area of about 80 km² within the Mt. Painter Precambrian Inlier (Fig. 1). Its climate is semi-arid with an average rainfall of less than 25 cm per annum. Knife-edged ridges rise 50 - 100 m from usually dry creek beds of a youthful drainage system. Intense exploration for uranium and radium occurred from 1910 to 1917, 1923 to 1937, 1945 to 1950 and from 1967 to 1972. Coats et al. (1) included a detailed study of all data on the area, except that from the late 1960's, in their investigations of the regional geology and mineralization of the whole of the Mt. Painter Province. Dickinson et al. (2) and Stillwell et al. (3) reported on all previous uranium investigations and Youles (4) reported on the late 1960's exploration by the current tenement holders, The Oilmin Group. In addition, Major (5), (6), Youles (7), (8) and Lambert et al. (9) report on various aspects of the uranium mineralization associated with granite breccias, mostly from scientific investigations carried out by the South Australian Department of Mines and Energy in the 1970's.

2. REGIONAL GEOLOGICAL SETTING

The Mt. Painter inlier is in the north eastern portion of the Adelaide Geosyncline (Fig. 1). It consists mainly of metasedimentary and metavolcanic crystalline rocks of the Radium Creek Metamorphics (unknown age) intruded by Middle

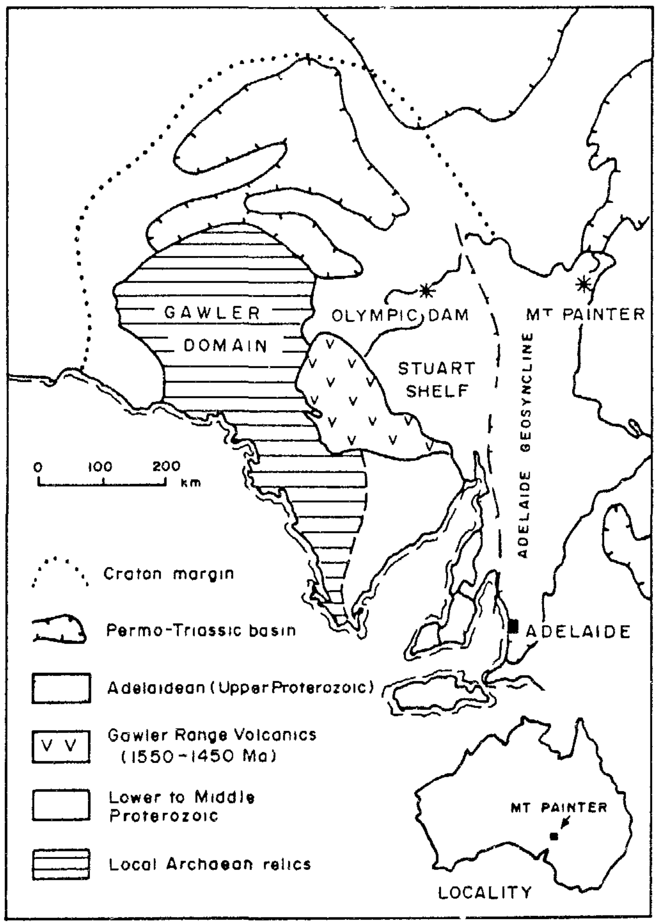

FIG. 1. Geological map southern part of South Australia showing main lithological and tectonic features and location of Mt. Painter deposits (Roberts et al. (12)).

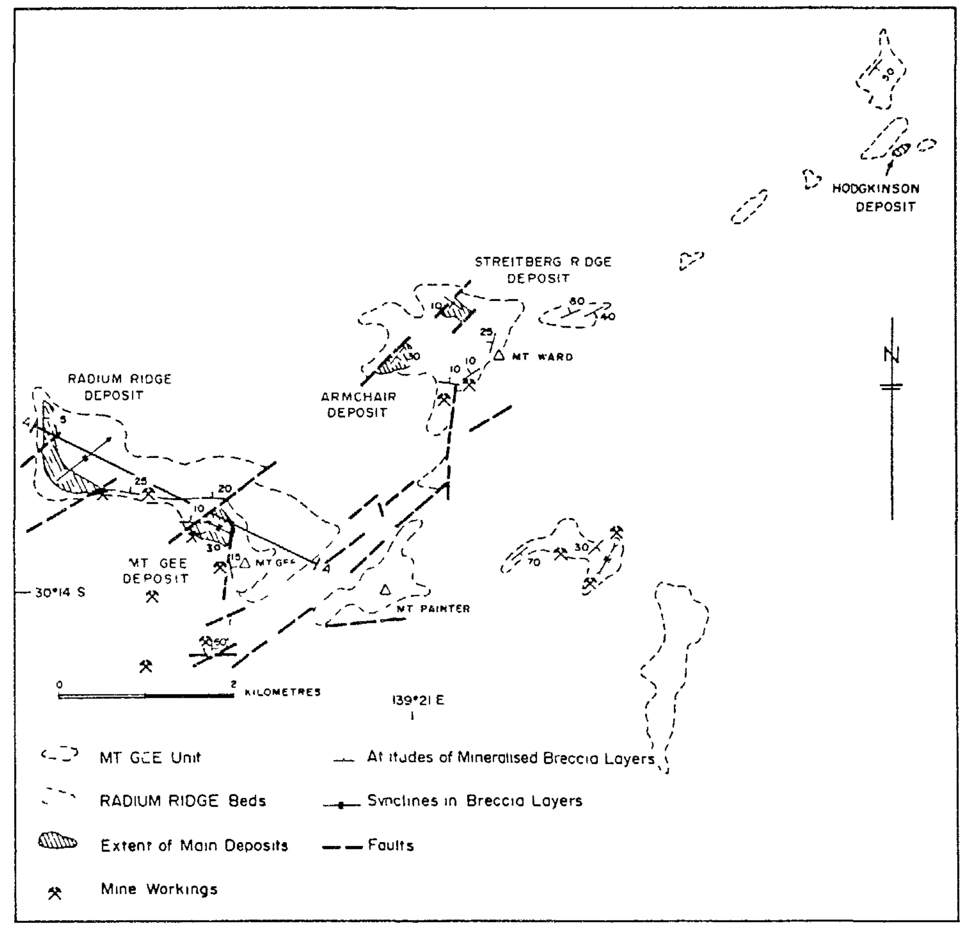

FIG. 2. Distribution of main uranium deposits - Mt. Painter area (after mapping by South Australian Department of Mines and Energy, Drexel (13) and Youles (4)).

Proterozoic granites (1500 - 1600 Ma); flanking the inlier with regional unconformity are Upper Proterozoic sediments and volcanics. Outliers of interpreted Upper Proterozoic (700 Ma) granite breccias and clastic sediments called the Radium Ridge Beds occur within the southern portion of the inlier and host the major uranium deposits (Fig. 2).

The crystalline basement rocks and sediments have been folded about mainly north-easterly trending axes and faulted in dominantly north-easterly and northerly directions. The latest period of strong deformation was the Palaeozoic Delamerian orogeny with intrusion of granodiorites and pegmatites (460 - 370 Ma).

Mesozoic and Cainozoic sediments cover eastern parts of the inlier and host the Beverly sedimentary uranium deposit (Haynes (10)) 20 km east of Mt. Painter.

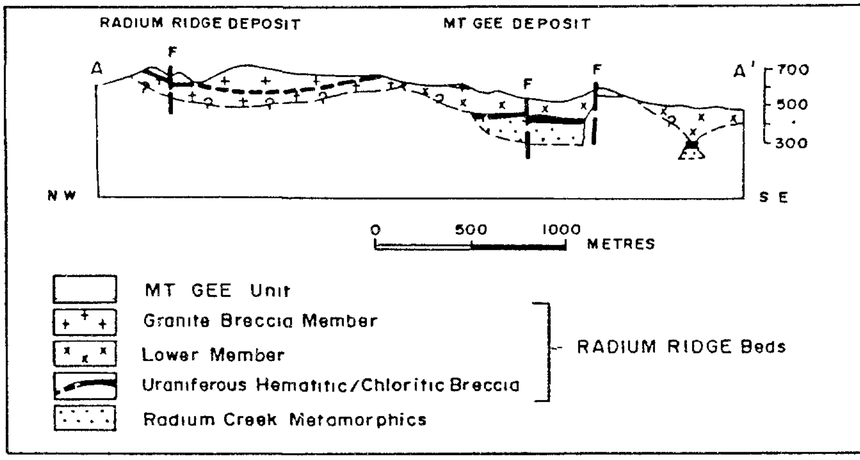

FIG. 3. Section along A-A', fig. 2, from drill-hole data (after Youles (7)).

3. URANIUM DEPOSITS

3.1. Primary strata-bound type

Primary strata-bound uranium mineralization occurs in four separate layered deposits totalling some 8 million tonnes of grade 0.06 % to 0.1 % U_3O_8. In addition, Dickinson et al. (2) estimated that the East Painter deposit consists of about 10 million tonnes at 0.015 % U_3O_8. These deposits replace moderate to high matrix granite breccia layers within the dominantly low matrix granite breccia sequence of the interpreted Sturtian Radium Ridge Beds (Table I). This sequence is overlain unconformably by the Mt. Gee Unit (Table I) which are also interpreted as Sturtian (Major (6)), (Fig. 2 and 3).

3.1.1. Radium Ridge Beds

Within the Radium Ridge Beds in the Mt. Gee area, a lower member consists of polymict breccia, arkose, diamictite (equated to Sturtian tillite), siltstone and sandstone; at its base is an uraniferous hematitic granite layer which hosts the Mt. Gee deposit. Overlying the lower member is a sequence of granite breccia and arkose, with minor sandstone and siltstone lenses; the granite clasts in the breccia are mainly potash rich ($\pm$ 10 % K_2O). Within this sequence, there is also a uraniferous hematitic chloritic granite breccia layer which hosts the Armchair,

TABLE I. MT. PAINTER LITHOLOGIES (AFTER YOULES (4), MAJOR (5), (6)).

ROCK UNIT	THICKNESS	LITHOLOGY
MOUNT GEE UNIT (AGE UNKNOWN)	50 M +	IRREGULAR, EXTRUSIVE, BANDED TO RHYTHMICALLY LAYERED SILICA (AS QUARTZ OR CHALCEDONY) AND IRON (AS HEMATITE OR JASPER), MINOR FLUORITE, ZEOLITES, CALCITE, MONAZITE, TRACE URANIUM. ALSO IN DIKES AND BRECCIA PIPE WITH LOW TEMPERATURE ALTERATION ZONES (MONTMORILLONITE, CHLORITE TO OCHEROUS HEMATITE).
	UNCONFORMITY	
RADIUM RIDGE BEDS (INTERPRETED UPPER PROTEROZOIC)	600 M +	GRANITE (K-FELSPAR) BRECCIA MINOR ARKOSE, SANDSTONE AND SILTSTONE. HIGH MATRIX MINERALIZED GRANITE BRECCIA LENSES. (STREITBERG RIDGE, ARMCHAIR AND RADIUM RIDGE DEPOSITS).
LOWER MEMBER	250 M +	POLYMICT AND GRANITE BRECCIAS, DIAMICTITE, ARKOSE, MINOR SANDSTONES AND SILTSTONES. HIGH MATRIX MINERALIZED GRANITE BRECCIA LENSES MORE FREQUENT TOWARDS BASE. (MOUNT GEE DEPOSIT AT BASE).
	UNCONFORMITY	
MOUNT PAINTER COMPLEX (GRANITES, MIDDLE PROTEROZOIC, MIDDLE PALAEOZOIC)		GRANITE, GNEISS, SCHIST, QUARTZITE, RARE PEGMATITE.

TABLE II. STRATA-BOUND MINERALIZATION, PRINCIPAL FEATURES (SUMMARIZED FROM MAJOR (6), YOULES (7)).

MAJOR HOST ROCK:	GRANITE (ALKALI-K) BRECCIA
MINOR ROCK TYPES:	ARKOSE, DIAMICTITE, SANDSTONE, SILTSTONE, POLYMICT BRECCIA
MINERALIZATION:	URANINITE, TRACE BRANNERITE
	MINOR MOLYBDENITE, CHALCOPYRITE, BORNITE, COVELLITE, CHALOCITE, TRACE GOLD, SILVER.
	PYRITE MONAZITE, TRACE BASTNAESITE, ZENOTIME
	HEMATITE, CHLORITE, SERICITE, FLUORITE, BARITE
	TRACE RUTILE, SPHENE, APATITE, MAGNETITE, CARBONATE, GALENA, SPHALERITE, ZIRCON, ILMENITE

TYPE:	DISSEMINATE, STRATIFORM HYDROTHERMAL, SIMILAR AGE TO HOST BRECCIAS; YOUNGER HYDROTHERMAL ALTERATION IN PART. UNMETAMORPHOSED
ATTITUDE:	GENERAL DIPS RANGE UP TO 45° - FAULTED AND FOLDED (SYNCLINES ONLY REMAIN)
FORMAL NAME.	RADIUM RIDGE BEDS UMBERATANA GROUP, UPPER PROTEROZOIC

Streitberg Ridge and Radium Ridge deposits. Both mineralized layers grade laterally to breccia layers which consist of mainly unsorted, angular fragments, from 1 mm to at least 60 cm across, set in a matrix of much finer angular fragments of the same components; the percentage of matrix ranges from almost nil to 75. Granite and granitic gneiss predominate, but schist, quartzite, carbonate rocks and siltstone have also been recorded.

3.1.1.1. Uranium mineralization

All of the primary uranium deposits are disseminated replacements of breccia layers. Table II summarizes the principal features, Table III the modal mineralogy and Table IV the geochemical data.

TABLE III. MINERAL COMPOSITION - MT. PAINTER DEPOSITS

	ARMCHAIR %	STREITBERG RIDGE %		HODGKINSON %
QUARTZ	5 - 30	10 - 35		30 - 45
K-FELSPAR	10 - 50	0 - 35		10 - 30
CHLORITE	20 - 60	30 - 70		NIL
HEMATITE	15 - 40	5 - 40	PRYRITE	1 - 3
SERICITE	5 - 20	(PRESENT) MUSCOVITE AND/OR SERICITE		1 - 20
MONAZITE	1 - 3	1 - 3		< 1
RUTILE/SPHENE	TRACE	1		1 - 2
FLUORITE	TRACE	0 - 15		NIL
SIDERITE	TRACE	TRACE CALCITE AND DOLOMITE		NIL

NO DATA AVAILABLE FOR MOUNT GEE AND RADIUM RIDGE DEPOSITS, BUT HEMATITE TO CHLORITE RATIO INCREASES AT MOUNT GEE AND DECREASES AT RADIUM RIDGE.

Most mineralized breccias have clasts derived from a quartz-microcline granitic rock associated with specular hematite; much of this hematite is derived from, or has replaced, earlier magnetite. These breccias have a matrix of, or are cemented by, authigenic chlorite or ochreous hematite which replaced chlorite, and quartz; most of the microcline is chloritized. Uranium, as uraninite (0.2 mm to 0.4 mm), occurs in the hematitic chloritic matrix, together with the other minerals given in Table II. Fluorite, hematite and pyrite form grains up to 5 mm; the other minerals are generally fine-grained. In general, the uranium and sulphide contents increase as the primary hematite to chlorite ratio increases.

Studies of fluid inclusions in quartz and monazite from the uraniferous breccias indicate temperatures of homogenization of mostly 300°C - 400°C with a few earlier and later inclusions indicating 150°C - 300°C and that the inclusions contain aqueous solutions of low salinity.

The thickness of the mineralized breccias ranges from 1 m to at least 70 m; layering is generally not apparent in the fresh rock, but is accentuated by weathering at most exposures. In the weathered zone, which generally extends to 25 m, chlorite has been altered to hematite and goethite and uraninite to secondary minerals; secondary pitchblende has been identified in the primary zone. At all prospects the exposures are massive, layered hematitic breccias and have a radioactivity three to ten times background.

TABLE IV. COMPOSITION OF MINERALIZATION - MT. PAINTER DEPOSITS (AFTER YOULES (8)).

	MOUNT GEE	STREITBERG	ARMCHAIR	RADIUM RIDGE
PPM				
U_3O_8	1000	950	900	620
Au	0.01	< 0.01	<0.01	<0.01
Ag	2.0	1.5	1	1.5
La	4200	2000	600	220
Ce	6000	3000	1500	700
Nd	800	600	300	150
Cu	800	300	300	150
Pb	200	150	80	35
Zn	300	400	250	350
Ni	5	20	10	12
Co	100	600	400	200
Mo	200	400	400	100
As	50	50	50	50
Bi	3	3	1	21
Sn	10	4	6	20
Cd	20	3	3	3
Y	600	250	40	180
BaO	330	280	280	10000
MnO	1500	6000	4000	3000
%				
Fe	22.2 • (ACID SOLUBLE)			
P_2O_5	0.29 •			

INCREASING CONCENTRATION OF ORE METALS

COMPOSITE BULK SAMPLES FROM RANDOM DRILL HOLES, ANALYSED BY AUSTRALIAN MINERAL DEVELOPMENT LABORATORIES, ADELAIDE, SOUTH AUSTRALIA

PART OF MOUNT GEE DEPOSIT LATER ALTERED BY MOUNT GEE UNIT (TABLE II)

• ANALYSES FROM ONE DRILL HOLE

3.1.1.2. Isotopic studies

Isotopic studies (Lambert et al. (9)) show that $d^{34}S$ values for 38 specimen of pyrite from breccias mostly range from - 2.8 % to + 3.5 % (average + 1.6 %, standard deviation 1.2 %) with two samples close to - 8 %. Lambert et al. (9) concluded that the pyrite was probably precipitated from reducing fluids containing magmatic S. Three barite samples have $d^{34}S$ values close to + 16 % and Lambert et al. (9) suggested that this could be magmatic or groundwater S or remobilized from barite.

25 calcite samples have $d^{13}C$ values of + 22.3 % to - 4.2 % and $d^{18}O$ values of - 4.0 % to + 23.1 % with an inverse relationship between the two. Lambert et al. (9) implied that some CO_2 was from a $d^{13}C$ depleted source such as graphite or methane and some mixing of magmatic or metamorphic fluids with meteoric waters occurred.

3.1.1.3. Age dating

Uranium-lead isotopic analyses of monazite associated with the uranium mineralization were interpreted to give a 440 $\pm$ 50 Ma age for the monazite (Pidgeon (11)). In a re-interpretation of that data (Fig. 4) a primary age of

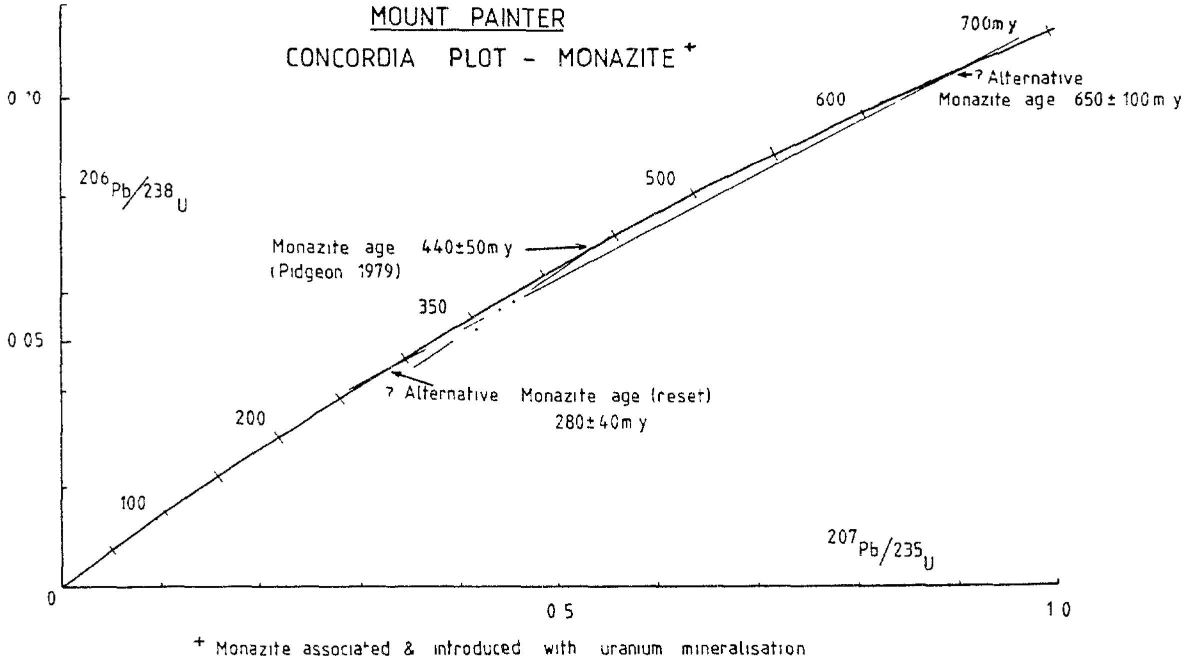

FIG. 4. Uranium-lead age dating of monazite from Armchair and Streitberg Ridge deposits (after Pidgeon (11)).

650 ± 100 Ma (i.e. Sturtian) is also possible with a reset age of 280 ± 40 Ma, (from cooling after late Palaeozoic Delamerian orogeny and intrustions).

3.1.2. Mt. Gee Beds

Intruding and unconformably overlying the Radium Ridge Beds are the siliceous and ferruginous rocks of the Mt. Gee Unit. These consist mainly of massive and layered quartz-specular hematite rocks intruded by vughy white quartz and 'nail-hole' quartz (Stillwell et al. (3)); hematitic siltstones, chalcedony, agate and jasper are present also. One small breccia pipe cemented by these Mt. Gee type rocks occurs 0.5 km ESE of Mt. Gee (A.H. White, pers. comm.).

Petrological studies indicate that the silica-iron rocks formed in a subaqueous environment and consist of reworked material, which was derived from a chemical (hydrothermal) precipitate and then cemented by later quartz. Homogenization temperature of mostly 100°C - 200°C with a few very late stage at up to 450°C were obtained from fluid inclusions in quartz and fluorite from the Mt. Gee unit. Minor minerals observed are fluorite, monazite, magnetite, pyrite, chalcopyrite and laumontite. This mineral assemblage is somewhat similar to that of the uraniferous breccias in the Radium Ridge Beds.

In the vicinity of Mt. Gee, the Mt. Gee uranium deposit in part underwent low temperature hydrothermal alteration. Chlorite became ochreous hematite and the uranium, molybdenum and cobalt contents reduced; the country rocks were kaolinized and montmorillonite introduced. This alteration was particularly widespread below and east of Mt. Gee, such that uranium intersections in drilling averaged less than 0.05 % U_3O_8.

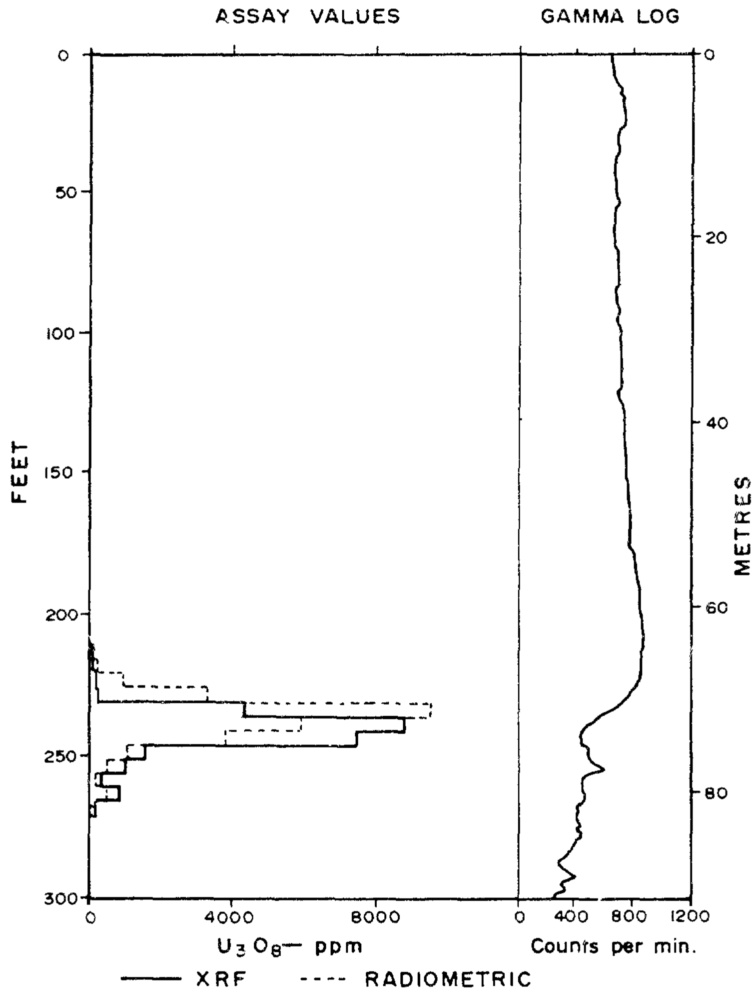

FIG. 5. Assays and gamma log, drillhole No. 21, Hodgkinson Deposit, showing downward leaching of uranium and effect of radon emanations.

3.2. Primary and secondary vein-type

3.2.1. Hodgkinson deposit

The Hodgkinson deposit (Fig. 2) differs from the bedded breccia deposits. It is smaller (250,000 t), has a higher grade (0.25 % U_3O_8), occurs in a foliated, brecciated and re-brecciated granitic rock, and chlorite and hematite are notably absent (Table II). Breccia veins (2 - 25 cm wide) and small exposures of breccia, similar to those of the Radium Ridge Beds, occur adjacent to the prospect. Much of the surrounding granitic gneisses of the Radium Creek Metamorphics have a uranium content of around 50 ppm.

Primary mineralization followed brecciation of the host rock and consisted of silica, pyrite, minor arsenopyrite and uraninite (5 - 15 microns), and trace amounts of sphalerite, greenockite, chalcopyrite and molybdenite. The uraninite was deposited mostly along the cleavage planes and fractures in altered microcline crystals. The granitic host rocks were silicified or kaolinized and sericitized. These mineralized rocks were subsequently brecciated and uraninite, pyrite and chalcedony were introduced as an infilling; after re-brecciation, iron-rich chalcedony, which contained some pyrite and a dispersed gummite-like mineral, were introduced, partially filling the cavities formed.

In section, the uraniferous zone is an inverted cone, with its top at 65 m to 100 m below the surface. In the upper zone, there is strong radioactivity with low to moderate uranium content and this grades downwards into a zone having weaker radioactivity but higher uranium content (Fig. 5). Above the cone, the mineralized host rock is ferruginous, has been extensively leached and contains small lenses of secondary uranium minerals. High surface radioactivity was detected only along the fault bounded northern side of a small hill which is parallel to and vertically above mineralization (Youles (4)).

In the middle of the deposit, flows of radon gas and air were detected at surface emanating from drillholes which penetrated the mineralization at about 70 m below surface. The radon gas rapidly coated walls of drill holes with its decay product Bi^{214}, such that readings on down-hole gamma logs were about 800 counts per minute for most of the run, but dropped to about 400 counts in the ore zone (Fig. 5).

As groundwaters at the deposit contain around 3000 ppb U_3O_8, groundwaters over an area of 4 km^2, underlain by granitic gneisses around the deposit were sampled in 19 boreholes. The results gave a range of 130 ppb to 6800 ppb U_3O_8, with an average of 1730 ppb U_3O_8. Similar groundwaters have probably supplied much of the uranium to the Beverley sedimentary uranium deposit, 15 km east and down drainage from the Hodgkinson deposit.

3.3. Secondary vein-type

Within this category are all the old mine workings as described by Blisset (in Coats et al. (1)). The majority are in or adjacent to the strata-bound uranium deposits (Fig. 2), in permeable zones, usually faults, in which groundwaters deposited autunite and torbernite (Coats et al. (1)). These deposits are small and high grade and total reserves were estimated at 500 tonnes at 0.33 % U_3O_8 (Dickinson et al. (2)).

A notable exception are the workings (Painter No. 1 & 2), (Dickinson et al. (2)) midway between the Radium Ridge and Mt. Gee deposits (Fig. 2), which are in and adjacent to two quartz-hematite-monazite-fergusonite exposures (Stillwell et al. (3)). However, close drilling at this locality failed to intersect the rock at depth. It is concluded that the mineralized rocks are either very localized pods and associated with the $\pm$ 400 Ma granites, or large clasts within the Radium Ridge Beds.

4. GENESIS

4.1. Strata-bound mineralization

In a recent discussion (Youles (8)) the strata-bound uranium deposits at Mt. Painter are shown to be very similar to the strata-bound mineralization at Olympic Dam (Roberts et al. (12)) in type, geochemistry, mineralogy and host rock. In addition to the vast differences in scale and intensity, the main geological variation is that molybdenum at Mt. Painter substitutes for copper and gold at Olympic Dam (cf. porphyry-type deposits).

Based on the extensive research reported by Roberts et al. (12) the Radium Ridge beds were formed by rapid erosion and deposition with little transport in a high-energy arid environment; earth movements continued throughout. At the onset of deposition (Lower Member, Radium Ridge Beds), clasts were derived mostly from the local basement (Radium Creek Metamorphics). The environment was partly sub-aqueous, as evidenced by the water-laid sediment; there were also occasional marine incursions, which deposited interbeds of a diamictite identical in clast types and matrix to the Sturtian diamictite of the Adelaide Geosyncline. With time, marine incursions ceased, the environment became almost totally sub-aerial and the clasts were derived from a microcline granite; it is probable that this alkali granite resulted from K-metasomatism prior to brecciation.

Lambert et al. (9) purport to show that the granite breccias and mineralization at Mt. Painter resulted from ascent of granitic magmas to shallow crustal levels and list a number of features which indicate to them that the breccias are not sedimentary. They refer to:

- the 'restricted development' of the breccias (areal extent at least km²); this is consistent with a sedimentary unit being preserved in synclines (Fig. 2 and 3);

- the occasional 'gradational and irregular boundaries'; these are consistent with mineralization of rocks deposited in a sub-aerial environment of high energy erosion and deposition (by analogy with Olympic Dam) (Roberts et al. (12));

- the extensions to 'considerable depths', being 600 m; this is quite logical for a gently folded sedimentary unit such as the Radium Ridge Beds;

- 'cross-cutting relationships'; these only occur peripheral to the Radium Ridge Beds and are associated with the younger Mt. Gee unit; none of the four main layered uranium deposits exhibit cross-cutting features;

- the 'fine-scale matrix-mineral veining' in some clasts; this is consistent with fine cracks being developed during erosion, transport and deposition in a high energy arid environment and subsequently mineralized.

From the foregoing, it is quite apparent that the granite breccias and mineralization of the Radium Ridge Beds are part of a folded sedimentary sequence mineralized about the same time as deposition (Major (5)).

During deposition of the Radium Ridge Beds, pulses of hydrothermal solutions rich in iron, uranium, molybdenum, cobalt and rare earths were added and replaced the breccias; isotopic data indicate a magmatic source and some mixing with meteoric waters and support the sedimentary hydrothermal interpretation.

Following erosion of the Radium Ridge Beds, low temperature hydrothermal activity ensued, depositing silica-iron rocks of the Mt. Gee unit at surface and as dikes and pipes, and altering in part the Radium Ridge Beds and basement. This may be a late stage fumarolic activity after the main uranium mineralization or a much younger event. The somewhat similar mineral assemblage to that of the strata-bound uranium mineralization led Lambert et al. (9) to equate all hematitic breccias as time equivalents of the Mt. Gee unit despite field evidence of a dike and a pipe of Mt. Gee unit rocktypes cutting the Radium Ridge Beds and an unconformity between them. In addition, rocks of the Mt. Gee unit have more than 50 % silica, almost no uranium nor chlorite and 200°C lower fluid inclusion homogenization temperatures. This difference was also noted by Blisset (in Coats et al. (1), page 214).

The invariable dominant microcline granitic clasts associated with the mineralization, even in the Lower Member of Radium Ridge Beds, which is generally polymict, suggests a volcanic component. However, no positive volcanic features have been observed. The unusual element association and consequent mineral assemblage of the uraniferous breccias and the possible late stage fumarolic rocks coupled with the K-feldspar granite clasts suggest that the mineralization resulted from continental peralkaline igneous activity.

During the Lower Palaeozoic Delamerian orogeny, the Radium Ridge Beds and Mt. Gee unit were gently folded, with axes trending NE and NW and faulted dominantly NE with lesser N. Presently, through erosion, the two units occur as remnants in synclines.

4.2. Primary vein-type

At the Hodgkinson deposit, the primary hydrothermal mineralization was introduced into and partly replaced brecciated granitic rock; however, the ages of these events are unknown. A Palaeozoic age is favoured for the primary uranium based on the marked difference to the interpreted Upper Proterozoic Sturtian strata-bound mineralization.

The conical shape of the deposit and the disequilibrium of the uranium suggest that primary grade was enriched by uranium leached from the oxidized zone and redeposited as sooty uraninite at lower levels in a reducing environment. This secondary enrichment probably commenced in the Tertiary and is continuing today, as shown by the very high uranium content in groundwater and disequilibrium of the uranium.

4.3. Secondary vein-type

As described in detail by Blisset (in Coats et al. (1)), the concentrations of secondary uranium minerals occurred during a Tertiary deep weathering period; recent lowering of the water table since Pleistocene times has led to further oxidation, in which torbernite and autunite in part decomposed to uranophane, gummite and uraniferous ochres.

ACKNOWLEDGEMENTS

The mineralogical and petrological information is from unpublished reports prepared for South Australian Department of Mines and Energy (S.A.D.M.E.) by S. Whitehead, R. Cooper and B. Stevenson (Australian Mineral Development Laboratories (AMDEL), Adelaide) and for the Oilmin Group by R. Davey and S. Whitehead (AMDEL) and H.W. Fander (Central Mineralogical Services, Adelaide). The fluid inclusion data is from unpublished reports prepared for S.A.D.M.E. by B. Collins (AMDEL). The author is extremely grateful to the Director-General of the S.A.D.M.E. for the use of data generated under departmental scientific projects on the Mt. Painter area. The author is also grateful for the many geological discussions with former colleagues at S.A.D.M.E., in particular R.B. Major and J.F. Drexel, and for the drafting of text figures by I. Blicans (Into Drafting Geological Services, Adelaide).

This paper is published by permission of the Oilmin Group.

REFERENCES

(1) COATS, R.P., BLISSET, A.H., Regional and Economic Geology of the Mt. Painter Province, S. Aust. Geol. Surv., Bull. 43 (1971).

(2) DICKINSON, S.B., WADE, M.L., WEBB, B.P., Geology of the East Painter Uranium Deposits, in: S.B. Dickinson et al. (editors), Uranium Deposits in South Australia, S. Aust. Geol. Surv., Bull. 30 (1954) 84-93.

(3) STILLWELL, F.L., EDWARDS, A.B., Uranium minerals from Mt. Painter, in: S.B. Dickinson et al. (editors), Uranium Deposits in South Australia, S. Aust. Geol. Surv., Bull. 30 (1954) 94-114.

(4) YOULES, I.P., Mount Painter Uranium Deposit, in: C.L. Knight (editor), Economic Geology of Australia and Papua New Guinea - 1 Metals, Monograph Series 5, Australasian Inst. Min. Metall. (1975) 505-508.

(5) MAJOR, R.B., The uranium-bearing Radium Ridge Beds, Mt. Painter, South Australia, Int. Geol. Cong. 25, Sydney, Abstracts 1, Sec. 4 (1975) 175 pp.

(6) MAJOR, R.B., The uranium-bearing Radium Ridge Beds and the Mount Gee Beds, Mt. Painter Area, South Australia, S. Aust. Dept. Mines Ener., Summary Rep. (1978) unpublished.

(7) YOULES, I.P., Comparison of Olympic Dam Copper-Uranium Deposit and Mount Painter Uranium Deposits, S. Aust. Mines Ener., Rep. BK 78/85 (1978) unpublished.

(8) YOULES, I.P., Comparison of Olympic Dam and Mt. Painter deposits, as discussion of ref. (12) in: Econ. Geol. (in press).

(9) LAMBERT, J.B., DREXEL, J.F., DONNELLY, T.B., KNUTSON, J., Origin of Breccias in the Mt. Painter Area, South Australia, Geol. Soc. Aust. 29 (1982) 115-125.

(10) HAYNES, R.W., [illegible]erley Sedimentary Uranium Orebody, Frome Embayment, South Australia, in: C.L. Knight (editor), Economic Geology of Australia and Papua New Guinea, 1 Metals, Monograph Series 5, Australasian Inst. Min. Metall. (1975) 808-813.

(11) PIDGEON, R.T., Reports U-Pb Age of Monazite Samples 930, 931 & 932, S. Aust. Mines. Ener. File DM 601/74 (1979) unpublished.

(12) ROBERTS, D.E., HUDSON, G.R.T., The Olympic Dam Copper-Uranium-Gold Deposit, Roxby Downs, South Australia, Econ. Geol. 78 (1983) 799-822.

(13) DREXEL, J.F., Geology of a portion of the southern Mt. Painter Inlier, S. Aust. Mines. Ener. Rep. BK. 80/120 (1980) unpublished.

PETROGRAPHIC-GEOCHEMICAL CHARACTERISTICS AND GENESIS OF AN ALBITIZED URANIFEROUS GRANITE IN NORTHERN CAMEROON, AFRICA

M. Oesterlen
Urangesellschaft mbH
Frankfurt am Main

U. Vetter
Bundesanstalt fur Geowissenschaften und Rohstoffe
Hannover

Federal Republic of Germany

Abstract

PETROGRAPHIC-GEOCHEMICAL CHARACTERISTICS AND GENESIS OF AN ALBITIZED URANIFEROUS GRANITE IN NORTHERN CAMEROON, AFRICA

A petrographic and geochemical investigation of an albite-uraninite paragenesis associated with the Panafrican Kitongo granite was made. Several distinct mineralization phases were identified.

Partial melting of a granodioritic source rock produced a restite-bearing I-type monzogranite in the magmatic stage. The granite ascended synorogenically in tectonic structures and intruded volcanosedimentary rocks of upper amphibolite facies, which occur in the granite as xenoliths. Residual late-magmatic melts enriched in K or Na were formed locally.

In the post-magmatic stage, the granite was first affected by two phases of pneumatolytic to hydrothermal metasomatism: a first albitization led to the replacement of plagioclase by albite, the alteration of hornblende to Na-Ca amphibole, and the formation of a Zr-Ce-La mineralization. In the second albitization phase, the potassium feldspar component of the alkali feldspar and the quartz was replaced by albite, proceeding in steps until replacement was complete. Additional Zr, Ce, and La were introduced again, but remobilization of these elements also occurred. Riebeckite and aegirine were formed and partly altered. The hydrothermal phase of uraninite mineralization followed and then two late-hydrothermal phases: a quartz-epidote-carbonate paragenesis and an economically insignificant sulfide mineralization. The post-magmatic events are restricted to a region of jointed and sheared granite along the Kitongo fault zone.

A comparison with other albite-uranium occurrences shows that in contrast to the Kitongo occurrence, which is in an I-type granite, most of the deposits of this type are in S- and A-type granites. This explains differences between the Kitongo occurrence and the others, e.g. different uranium phases and a lack of enrichment of Sn, W, F, Li, Nb, Ta, and Y.

1. INTRODUCTION

In 1981, a technical cooperation project in northern Cameroon was agreed upon between the Federal Republic of Cameroon and the Federal Republic of Germany, following a project proposal by Gehnes and Thoste (1). This research is based on field work by Oesterlen (2) and interpretation of thin sections and chemical analysis of surface samples collected up to the middle of 1983. Since then, a

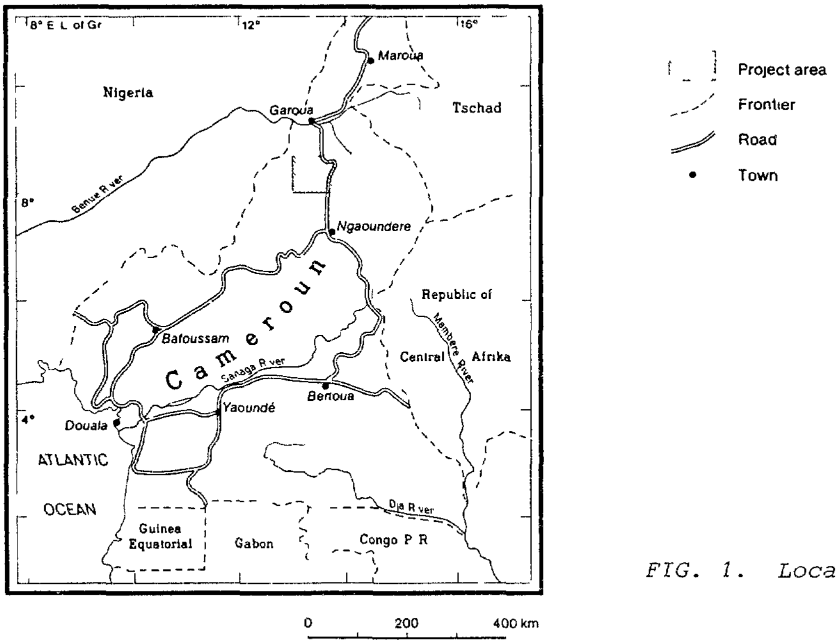

FIG. 1. Location of the project area

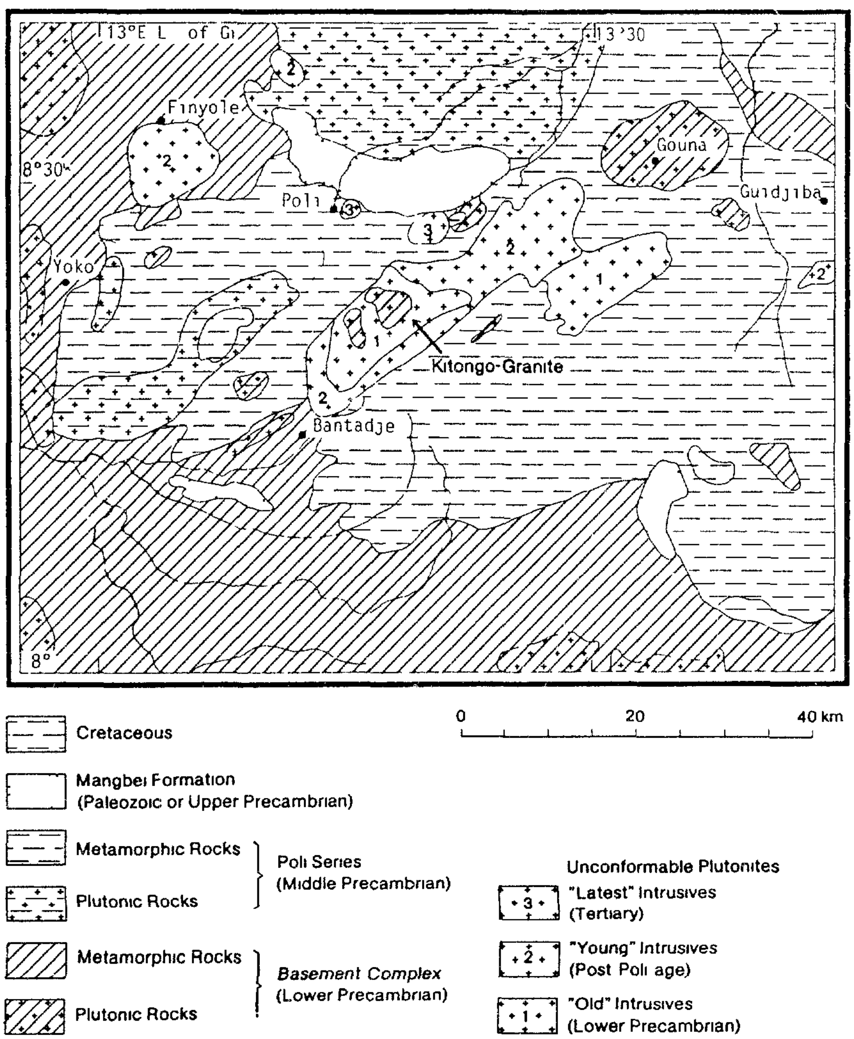

FIG. 2. Geological sketch map of the project area, simplified (after Koch (3)).

TABLE I. STRATIGRAPHY OF THE PROJECT AREA, SIMPLIFIED (AFTER KOCH (3)).

STRATIGRAPHY		LITHOLOGY	
TERTIARY		BASALTIC PLUGS IGNEOUS RING COMPLEXES	'LATEST' INTRUSIONS
CRETACEOUS		SHALES SANDSTONES CONGLOMERATES	
PALAEOZOIC ?	MANGBEI SERIES	ARCOSIC SANDSTONES CONGLOMERATES	
		ACID AND INTERMEDIATE VOLCANIC LAVA	'YOUNG' INTRUSIONS
PRECAMBRIAN	POLI SERIES (PC A-B ?)	GABBRO AND GRANODIORITE	
		QUARTZITES META-VOLCANITES SCHISTS GNEISSES	'OLD' INTRUSIONS
	BASEMENT COMPLEX (PC C-D ?)	GRANITE, GRANODIORITE, DIORITE AND SYENITE	
		MIGMATITES QUARTZITES AMPHIBOLITES MICASCHISTS GNEISSES	

drilling program has been carried out in the project area, the evaluation of which will yield further results. This will be the subject of a future paper.

The Kitongo Granite, named after the nearest village, is about 10 km southeast of the town of Poli in the Benue district of Cameroon (Fig. 1). The granite rises from the surrounding plain (ca. 500 m above m.s.l.) to elevations of more than 2,000 m. It is bounded on the northwest by a very long cliff 100 - 300 m high.

The rocks of the study area are predominantly of Precambrian age (Fig. 2). The basement complex, consisting of magmatic and metamorphic rock units, is characterized by high-grade metamorphism or partial to complete anatexis. The general strike is N to NE with a steep dip. The basement is overlain by the rocks of the Poli series (mainly metavolcanites and subordinate intrusive rocks), probably of the Kibaran orogeny (1800 - 1200 Ma). They are distinguished from the basement primarily by a lower grade of metamorphism, their tectonic style, and their strong foliation. Their strike is predominantly E to NE. The Precambrian Poli schists are overlain in turn by the Palaeozoic or Mesozoic Mangbei series. The youngest stratigraphic units are the clastic rocks of the Cretaceous in the Benue basin and Tertiary ring complexes and basalts (Table I).

Several discordant granite intrusions of various ages occur in and around the working area (Fig. 2): the 'old intrusions' of the lower to Middle Precambrian, the 'young intrusions' of Panafrican age, and the 'latest intrusions' of the Tertiary (Koch (3)). The Kitongo Granite has not yet been dated. Field observations suggest that it belongs to the 'young intrusions', although Koch (3) classified it as 'old intrusion'.

The oldest prominent regional structural element is the NE strike of the trough containing the Poli series. This direction was dominant during the Panafrican Orogeny, which is expressed primarily by fracturing and shearing movement, in addition to the magmatic activity, and played an important role also for the Kitongo Granite. The Panafrican tectonic structures were overprinted by the fracture tectonic structures of the Cretaceous which were formed in connection with the break-up of the Gondwana craton and the formation of the Benue Graben; the NE trend was reactivated, as demonstrated by the Benue Graben and the Kitongo fault zone (Fig. 2).

The Precambrian stratigraphy is not yet entirely understood. Rb/Sr age determinations (whole-rock and mineral ages) have yielded only Panafrican ages (550 ± 100 Ma) for rocks of different origin (Poli series, basement gneiss, and granites from Gouna, Gode and Nyore). But several samples taken from the central part of the mobile belt yielded ages greater than 2500 Ma (Precambrian D). Therefore, it seems reasonable that most of the mobile belt belongs to the older Precambrian, but that the original age was overprinted by the Panafrican event (Bessoles and Trompette (4)).

2. GEOLOGY OF THE KITONGO GRANITE AND ITS COUNTRY ROCK

The predominant rock type is a light grey, medium grained hornblende-biotite granite containing porphyritic alkali feldspar and a pronounced parallel texture throughout the rock (gneissose granite). Broad veins of fine grained leucocratic microgranite cut through the granite at many places (Oesterlen (2)).

A typical feature of the granite is the elongated xenoliths orientated in the same direction as the parallel fabric of the rock with the length of their long axis ranging from several mm to several dm. They occur throughout the granite but are more frequent and extraordinarily large at the contact with the country rock (Fig. 3). Petrographically, the xenoliths are predominantly medium grey, fine

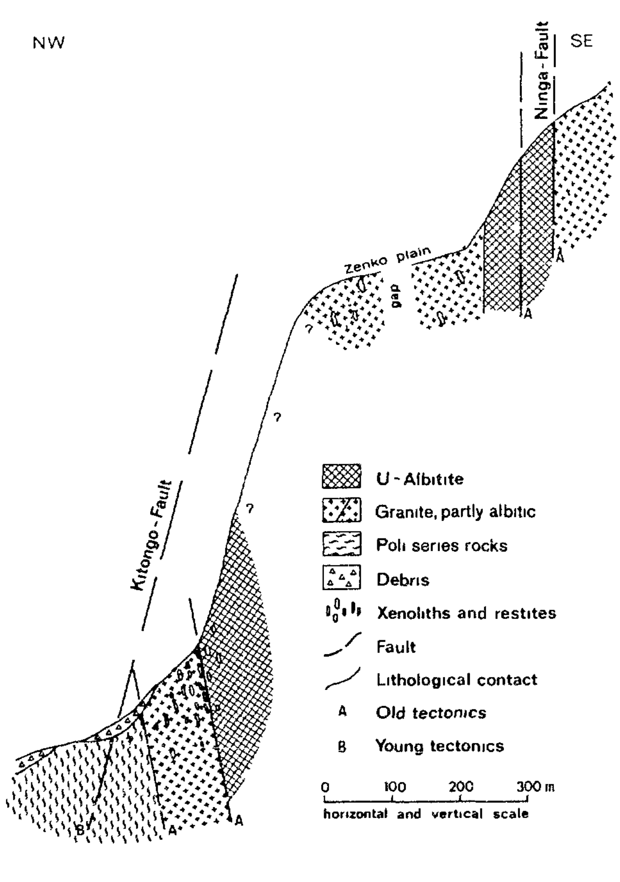

FIG. 3. Geological cross section of the Kitongo Cliff (Oesterlen (2)).

grained hornblende- and biotite-bearing quartz diorite without orientation. The margins of the xenoliths often contain porphyroblastic alkali feldspar, but the contact to the granite is always sharp.

Rock with a composition very similar to that of some of the xenoliths also occurs outside the granite: on the northwest flank in small isolated outcrops within the Poli series and on the southeast flank, where they are apparently the country rocks of the intrusive granite, but in a coarser grained facies (Fig. 4). The relationship between the diorite rock and the Poli rocks could not be clarified due to the poor outcrop situation, but several inclusions of Poli rocks found in the diorites indicate the older intrusive origin of the diorite.

Pink albitite, 500 m long and ca. 100 m thick, occurs on the northwest margin of the granite along the Kitongo fault (Fig. 4). The northeast end of this rock is bounded by the transverse Ninga fault, stretching along it several 100 m to the southeast. The albitite, in general, is hornblende-bearing and quartz-poor to quartz-free. The hornblende crystals have the same orientation as the granite. Surface samples of the albitite typically show small irregular cavities.

The Poli series is the host rock along the northwest flank of the Kitongo Granite (Fig. 4). The contact is covered by large blocks at the foot of the Kitongo cliff. The Poli series consists mainly of dark-grey, basic metavolcanics (metalava and meta-tuffite) and subordinate, light-grey, clastic and carbonatic metasediments: gneisses, sericitic quartzites, and calc-silicates. Regional metamorphism has reached the amphibolite facies. Diopside, hornblende, Ca-rich plagioclase and almandine, diagnostic for the metamorphic stage according to Winkler (5), were identified. P. Müller (personal communication) recognized sillimanite and andalusite. These results are in contrast to Koch (3), who classified the metamorphism of the Poli series as being 'weak'.

Poli series rocks are also found as inclusions in the contact zone between the Kitongo Granite and the Poli series, as well as xenoliths in quartz diorite in the area of the Poli rocks. Contact metamorphic features at the contact of the Poli rocks with the granite were not observed. The differences in the p-T conditions were obviously not strong enough.

The tectonic processes are manifested in the granite in several ways. The already mentioned NE trend (ca. 55°) appears in the fabric and in the margin of the granite (Fig. 2). This is evidence that the granite is a structure-controlled, synorogenic intrusion of the Panafrican Orogeny. The regional foliation of the Poli series follows the same direction. The previously existing lineament along which the melt ascended is represented by the northwest edge of the granite. The margin, which is up to 50 m thick and enriched in inclusions, demonstrates the intrusive character of the granite (Read (6)). The contact to the southeast, however, is represented by a transition zone up to 2 km wide, characterized by very large, boulder-sized inclusions. These conditions indicate the roof of the pluton rather than a lateral contact (Fig. 4).

The 'old' tectonic structure of the Panafrican Orogeny naturally predominates in the Kitongo Granite. Typical elements of granite structure are present, e.g. joints and faults formed along the Q, S, L, and D planes (Fig. 5). The EW-trending D structures, in parts present as wide shear zones, in addition to the Q and L structures, were significant for the post-magmatic events.

The 'young' structures of the Lower Cretaceous are less obvious. Their trend is nearly the same as that of the 'old' ones, but the stress field has been rotated 90° (Fig. 5). The main trend of the granite, the ca. 55° direction of the S plane, was reactivated as the Q plane. The 'young' Kitongo fault was produced by normal faulting. Further elements are a bimodal shear system with subhorizontal movement in the 5° and 135° directions. On the basis of gravimetric measurements, Louis (7) identified two NE-running lineaments in Central Africa, which have been followed from Cameroon to northern Sudan. The Kitongo fault coincides with the southern part of this lineament and is apparently part of it. Louis considers these elements expressions of the Congo craton plate boundary, a hypothesis to which the authors agree.

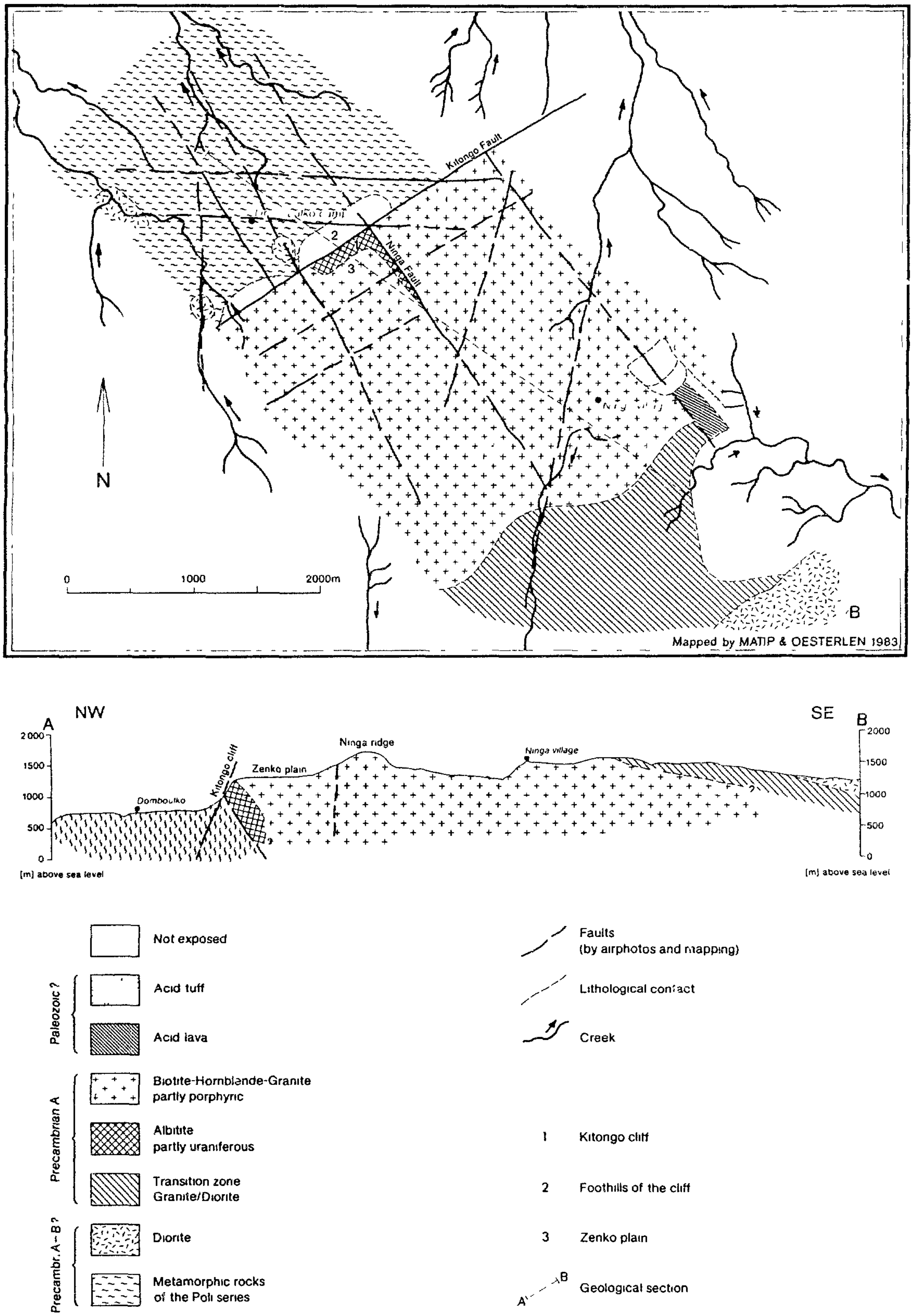

FIG. 4. Geological sketch map of the Kitongo area (Oesterlen (2)).

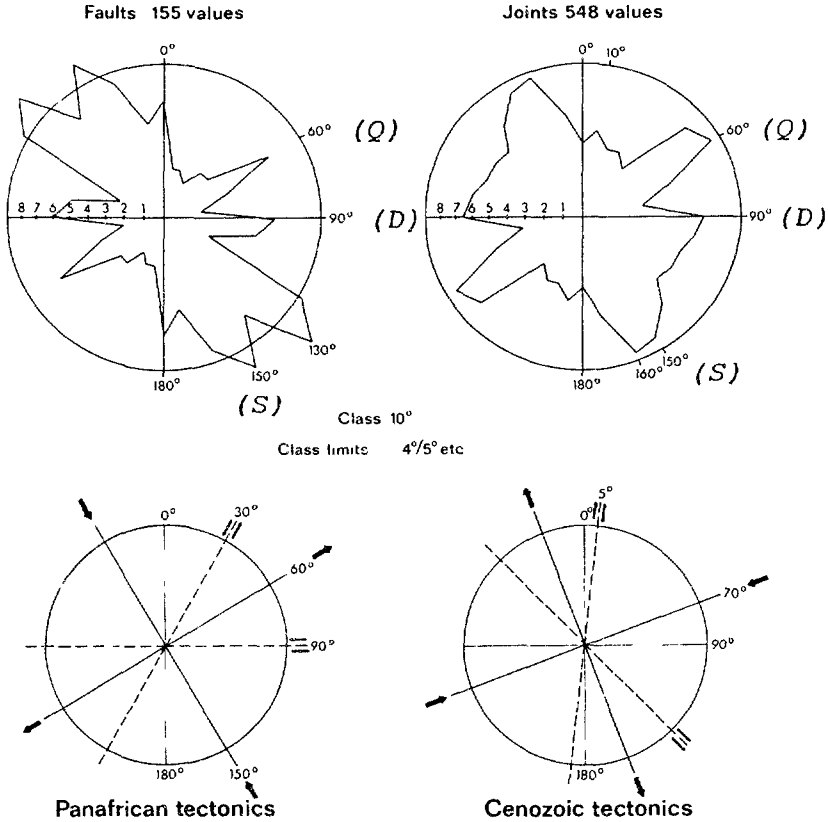

FIG. 5. Rose diagrams of faults and joints, Kitongo Granite, and strain-stress diagrams (Oesterlen (2)).

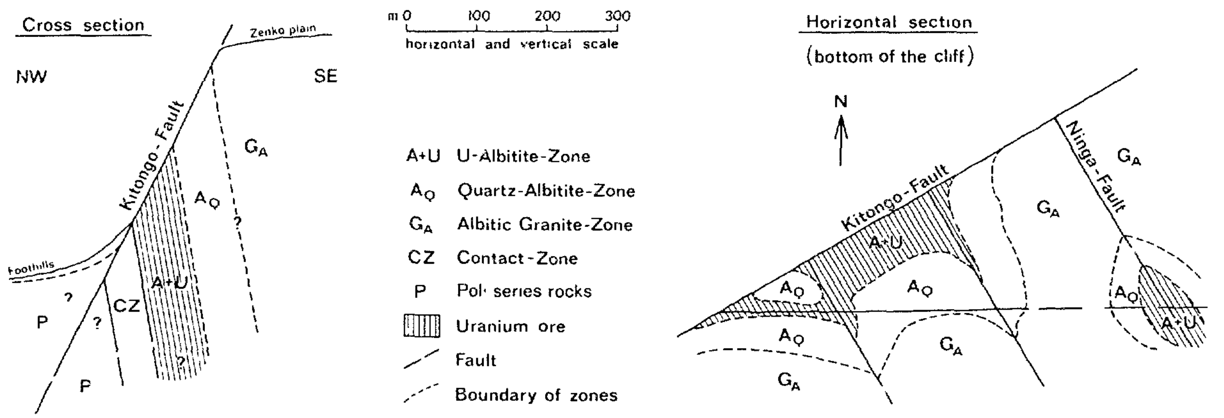

FIG. 6. Geological model of the Kitongo albite-uraninite mineralization (Oesterlen (2)).

3. URANIUM MINERALIZATION OF THE KITONGO GRANITE

The uranium mineralization occurs along the Kitongo and Ninga faults on the northwest margin of the intrusive (Fig. 4). The ore is mainly of the disseminated type. The cataclastic type associated with the shear zones also has a considerable thickness. The vein type, however, is subordinate; the veinlets are very thin (< 1 cm) and rare (Oesterlen (2)).

The primary uranium mineral is uraninite (Müller and Weiser (8)). It is found between albite crystals as very small grains together with magnetite or hematite, frequently on the margins of mafic minerals. Secondary minerals are uranophane or beta-uranophane.

The uranium mineralization is spatially associated with the albitic lithofacies and the Panafrican structural elements. The Kitongo fault and the Q, L, and D structures of the granite obviously played an important role in the genesis of the mineralization (Fig. 6). The fault structures of the Cretaceous are younger than the uranium mineralization.

4. PETROGRAPHY OF THE ROCK UNITS

Petrographic studies of the Kitongo samples were made by Fritsche (9), Fritsche and von Pechmann (10), and Müller and Weiser (8). The results in this paper are based on a reexamination of all available thin sections.

4.1. Gneissose hornblende-biotite granite

The coarse grained alkali feldspar (25 - 40 vol%) is xenomorphic to hypidiomorphic (porphyroblasts) and shows strong perthitic exsolution (spindle, vein and patchy perthite up to 40 % albite). Sometimes it has albitic margins that optically have the same orientation as the perthitic albite. The plagioclase (25 - 35 %) is medium grained and xenomorphic or hypdiomorphic. The grains are polysynthetically twinned, show weak zonation, and sometimes are altered to sericite. The medium sized quartz grains (20 - 35 %) have undulatory extinction and show interlocking growth. Green hornblende (5 - 10 %) and biotite (5 - 10 %) are the mafic minerals. They emphasize the gneissose structure of the granite. Accessory minerals are magnetite, hematite, sphene, apatite, epidote, and zircon.

Most of the samples show evidence of a syn- to post-crystalline tectonic event. This seems to increase with decreasing distance from the Kitongo fault. It is indicated by bent plagioclase twinned laminations, orientated undulatory extinction of quartz, sometimes by ruptured feldspar and quartz grains, and sometimes even by mylonitization of thin (up to several mm wide) zones, especially in quartz crystals.

A special variety of the granite is the potassium-feldspar granite found only in the immediate vicinity of the Kitongo fault, and the albitite. Because of its restricted occurrence, it is not yet fully clarified whether it was formed by post-magmatic microclinization or local late-magmatic residual differentiation. On the one hand, the samples contain albitic or albitized plagioclase; on the other hand, the coarse grained perthitic alkali feldspar lacks younger growth rims (porphyroblastesis) and the primary content of mafic minerals (e.g. biotite and hornblende) is considered low. Arguments for local, K-rich, residual differentiation have the greater weight.

4.2. Albitite

Albite is, by far, the most frequent mineral (60 - 95 %). Without a doubt, the albite is a replacement mineral, having in many cases the shape of the replaced mineral. In thin sections, it could be seen that the albitization occurred in two stages:

(i) The first stage is characterized by the replacement of the anorthite component of the plagioclase. The transformation took place, in general, within the primary crystal, easy to recognize in the preservation of the bent twinned lamination. Only in zones of extreme shearing is the bent and ruptured plagioclase recrystallized to mosaic albite as early as in this stage. Biotite is almost completely altered in this first stage and the common hornblende is replaced by Na-Ca hornblende (optical data indicated a barkevikitic amphibole, but microprobe analysis by P. Müller of the BGR shows a hastingsite composition). In some samples, however, Ca-free amphibole (riebeckite), in addition to the Na-Ca hornblende, is found in this stage as rim alteration, progressive growth, or new formation. A second generation of zircon and magnetite is found in fissures and at grain boundaries. This stage is confirmed in the potassium granite samples. Within the albitization front, the first stage is overprinted by the second.

The phenomemon of complete albitization of the plagioclase in alkali-rich granites has been described by Soviet authors. According to their reports, several Soviet albite uranium occurrences have reached only this stage.

Mica-rich gneiss included as xenoliths of the country rocks in the granite demonstrates the direct transformation on grain rims of biotite to riebeckitic alkali hornblende.

(ii) The second stage of the albitization began on a broad front along fault zones. First, the potassium feldspar parts of the perthites were completely replaced (quartz albitite), followed by the stepwise replacement of quartz until it also was completely replaced (quartz-free albitite). Tectonic events also took place during this stage. The submicroscopic cloudiness of replaced K-feldspar remained in weakly deformed rocks. With increasing tectonic stress, the primary plagioclase recrystallized as mosaic albite. This albite migrated from grain boundaries to the albitized perthites and recrystallized there in the form of chess-board albite. The cloudiness of the feldspar is irregular. In the last part of this stage an albitite was formed whose leucocratic phase consists exclusively of mosaic albite.

Na-Ca hornblende can still be identified in some samples, but it is replaced to a large extent by Ca-free, fibrous riebeckite (Na-hornblende). Sometimes new aegirine appears in small amounts in addition to riebeckite. But the hornblende minerals are frequently already disintegrated to partly opaque mineral aggregates, probably by strongly oxidizing solutions rich in carbonate. These aggregates consist of carbonate (siderite?), limonite, magnetite, ilmenite, and hydrobiotite.

4.3. Diorite xenoliths

The main mineral is hypidiomorphic to idiomorphic plagioclase (>50 %) with zonation. The grains of alkali feldspar (0 - 15 %) are considerably smaller and xenomorphic, apart from the porphyroblasts on the xenolith rims. Quartz (5 - 10 %) occurs in the interstices. The mafic minerals are green hornblende (5 - 15 %) and biotite (maximal 12 %). Accessory minerals are mainly idiomorphic titanite (maximal 5 %), opaques, and zircon. Needle-like apatite is found in leucocratic and mafic phases. Some diorite xenoliths have been albitized. Beginning at fractures, mosaic albite replaces feldspar, partially or completely. Common hornblende has been transformed to Na-Ca hornblende or riebeckite. Most of the biotite has been altered (2 %).

Petrographic criteria support the identification of the xenoliths as restite (White and Chappell (11), see also chapter 6).

The quartz diorite and quartz monzodiorite cropping out in the foreland of the granite have a petrography similar to that described above and, thus, will not be described further. They can, however, be distinguished by several characteristics: the plagioclase and alkali feldspar are mostly altered to sericite and the biotite is completely chloritized. In addition, these rocks sometimes show a weak, parallel fabric and contain inclusions that are probably of the Poli series.

4.4. Poli series

The modal composition varies considerably. The meta-volcanites are represented mainly by gneisses, the meta-sedimentary rocks by sericite quartzites or quartzite schists.

(i) The gneiss consists mainly of fine grained xenomorphic alkali feldspar (25 %), plagioclase (25 %), and quartz (25 %). The feldspar is sometimes altered completely to sericite and recognizable only in relicts. Quartz has undulatory extinction. Biotite (5 - 20 %, beige to brown pleochroism) and green hornblende (0 - 15 %) emphasize the rock texture. Accessory minerals are opaques, epidote, rutile, and leucoxene. The texture is intersertal.

Amphibolite gneiss is rare and consists mainly of green hornblende (>50 %). It forms idiomorphic laths or xenomorphic poikilitic crystals. The feldspar (20 %) is corroded and altered to sericite. The quartz content is low (15 %). Biotite (5 %) is chloritized. Accessory minerals are opaques, epidote, and leucoxene.

(ii) The sericite quartzite and sericite-quartzite schist consist of 50 - 90 % quartz and 10 - 40 % muscovite or biotite. The quartz grains have intersertal texture and undulatory extinction. The mica is in the form of parallel oriented platelets. The feldspar content is low (0 - 15 %) and increases with increasing biotite content. Sericite occurs along grain boundaries. The fabric is fine grained and shows subparallel orientation.

The Poli rocks occur along the Kitongo fault zone also as inclusions in granite and albitite. The albitization formed replacement features already described above.

4.5. Classification using the Streckeisen diagram

When the modal compositions of the rocks described above are plotted in a Streckeisen diagram (Streckeisen (12)), the Kitongo Granite falls into the field for monzogranite and syenogranite (Fig. 7). The albitite plots mainly in the fields for alkali-feldspar syenite and quartz alkali-feldspar syenite, a very few in the field for alkali-feldspar granite. The close relationship between the granite and the albitite is demonstrated by one albitite sample which plots in the syenogranite field. The diorite samples plot in the fields for quartz monzodiorite and quartz diorite, but the albitized diorite samples plot in the quartz alkali-feldspar syenite field.

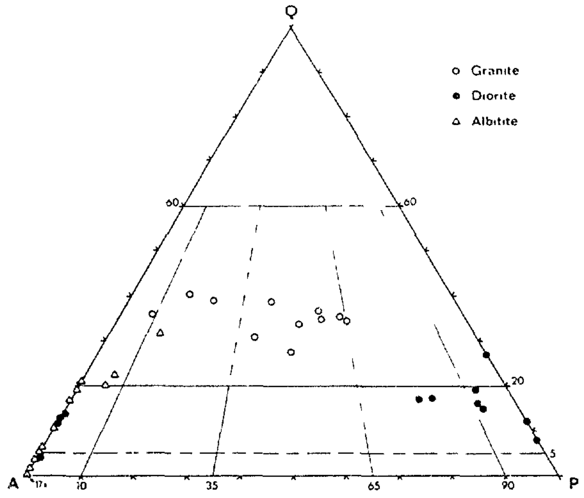

FIG. 7. Modal classification of the Kitongo granitoid rocks (after Streckeisen (12)).

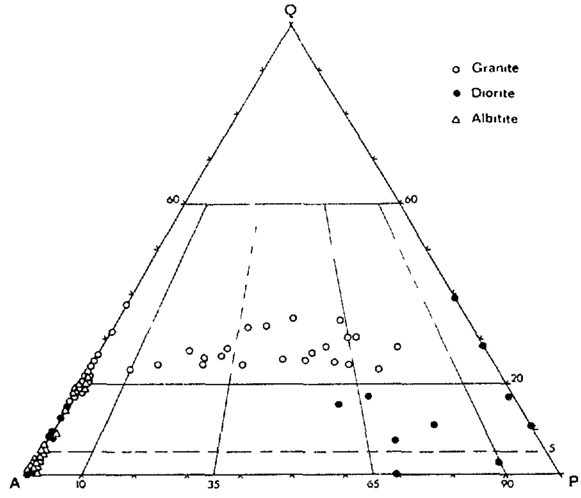

FIG. 8. Normative classification (after Streckeisen (12), calculations after P. Müller (13)).

5. GEOCHEMISTRY OF THE ROCKS

The investigations are based on the chemical analysis of 141 rock samples for 11 major and 26 trace elements. Computerized programs by P. Müller (13) and Kottrup and Rehder (14) were used for the interpretation of the data in terms of petrochemistry, geochemistry, and economic geology.

5.1. General Description

The chemical composition of the rock types described above in terms of their lithology is given in Table II as the mean values of 11 major and 15 trace elements.

The normative values of the main rock constituents, calculated using the 'Pseudo-Rittmann Norm' of Müller (13) and plotted in a QAP tertiary diagram, have a distribution similar to that of the modal composition (Fig. 8). Most of the granite samples plot in the monzogranite field. They extend, however, through the syenogranite into the alkali-feldspar granite and quartz alkali-feldspar syenite fields, where the microcline granites, nearly free of Ca, are clustered. On the other side, the granites extend to the granodiorite field. The albitites, also without plagioclase, naturally plot within the alkali-feldspar syenite field, the quartziferous albitites within the quartz alkali-feldspar syenite and alkali-feldspar granite fields. The albitized diorite restites plot together with the albitites in the quartz alkali-feldspar syenite field, the non-albitized diorites in the quartz monzodiorite and quartz diorite fields, in full agreement with the modal composition.

The composition of the alkali feldspar is shown as a function of quartz in a Qu-Ab-Or ternary diagram using the CIPW values (Fig. 9). The Kitongo Granite is characterized by an Ab/Or ratio of 60:40, the microcline granites by higher Or values. The non-albitized diorites have an Ab/Or ratio of 70:30, the albitized diorites plot in a separate cluster with a ratio of 90:10. The albitites plot along the Ab-Qu edge of the triangle in a quartz-poor and a quartz-free cluster.

The different rock types are similarly classified when the CIPW values are plotted in an An-Ab-Or ternary diagram subdivided according to Hietanen (15) (Fig. 10). The microcline granites and the normal granites plot in the granite

TABLE II. MEAN OF MAJOR AND TRACE ELEMENTS OF THE ROCK UNITS (IN WT %).

	NORMAL GRANITE 25 SAMPLES	K-GRANITE 15 SAMPLES	QUARTZ-ALBITITE 23 SAMPLES	PURE ALBITITE 33 SAMPLES	DIORITE-RESTITE 6 SAMPLES	ALBITE-RESTITE 7 SAMPLES	FORELAND DIORITE 4 SAMPLES	META-VOLCANITES POLI 8 SAMPLES	META-SEDIMENTS POLI 4 SAMPLES
SiO_2	69.60	71.29	69.80	63.91	57.91	60.84	54.32	58.46	72.64
TiO_2	0.45	0.23	0.30	0.41	1.29	0.98	1.58	1.32	0.22
Al_2O_3	14.39	14.13	15.59	17.76	15.76	16.51	16.23	15.98	14.67
Fe_2O_3	3.32	2.68	3.02	4.05	7.11	6.53	8.48	8.78	3.59
MnO	0.06	0.05	0.05	0.08	0.12	0.16	0.13	0.15	0.02
MgO	0.86	0.03	0.07	0.28	3.68	1.60	3.82	3.04	0.23
CaO	1.88	0.34	0.35	0.92	6.05	2.84	5.92	4.91	0.16
Na_2O	4.56	4.64	8.90	10.09	4.40	6.86	3.76	3.56	1.17
K_2O	3.21	5.35	0.21	0.21	1.84	1.57	2.05	1.73	4.56
P_2O_5	0.12	0.02	0.09	0.22	0.35	0.26	0.38	0.22	0.03
SO_3	0.15	0.16	0.16	0.13	0.17	0.11	0.23	0.17	0.19
Ba	637	128	81	157	436	728	636	409	554
Ce	92	244	317	344	101	102	94	83	110
Cr	22	15	12	10	138	24	250	49	14
Cu	13	10	19	19	60	45	47	33	63
F	664	310	398	406	1129	874	710	386	182
La	41	113	139	176	46	53	45	41	47
Ni	17	8	7	6	53	18	107	42	7
Pb	19	15	80	147	16	21	48	42	79
Rb	71	58	11	16	59	40	16	10	12
Sr	372	37	53	157	644	260	581	334	53
Th	11	13	16	17	12	5	11	7	11
U	5	8	905	1257	3	63	3	2	6
V	41	7	12	19	143	93	190	168	19
Y	44	24	58	101	30	90	30	42	133
Zr	276	574	618	737	227	282	182	180	505

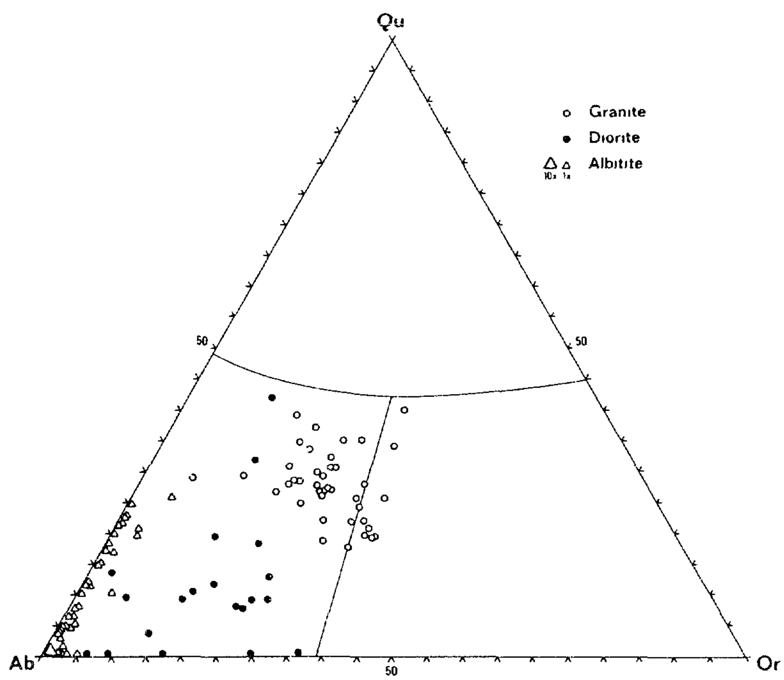

FIG. 9. CIPW-normative Qu-Ab-Or ternary diagram (cotectic line at pH_2O = 2,000 bars, after Winkler (5)).

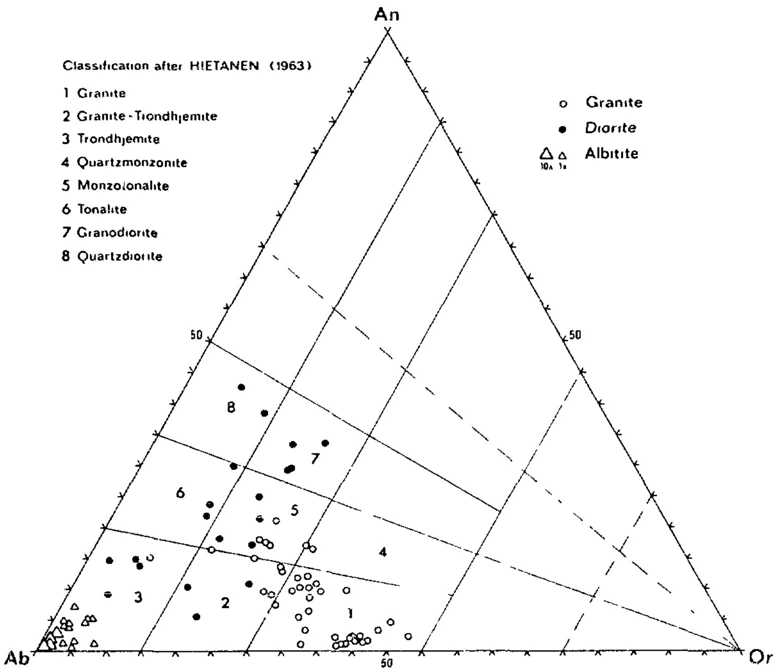

FIG. 10. CIPW-normative classification using the An-Ab-Or triangle diagram (after Hietanen (15)).

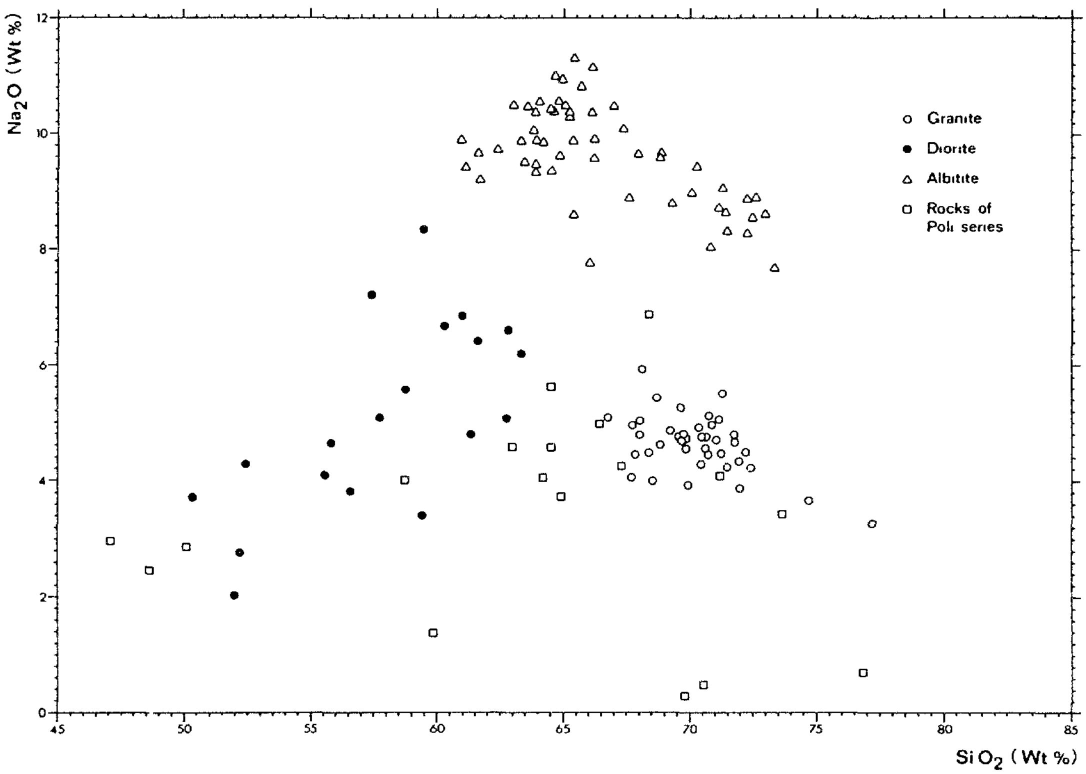

FIG. 11. Variation diagram SiO_2-Na_2O.

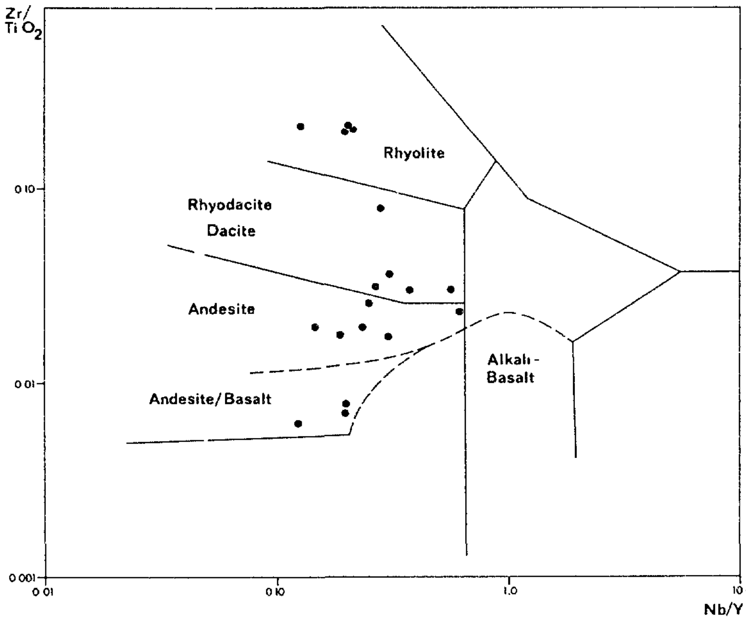

FIG. 12. Discrimination diagram Nb/Y - Zr/TiO_2 of Poli series rocks (after Floyd and Winchester (17)).

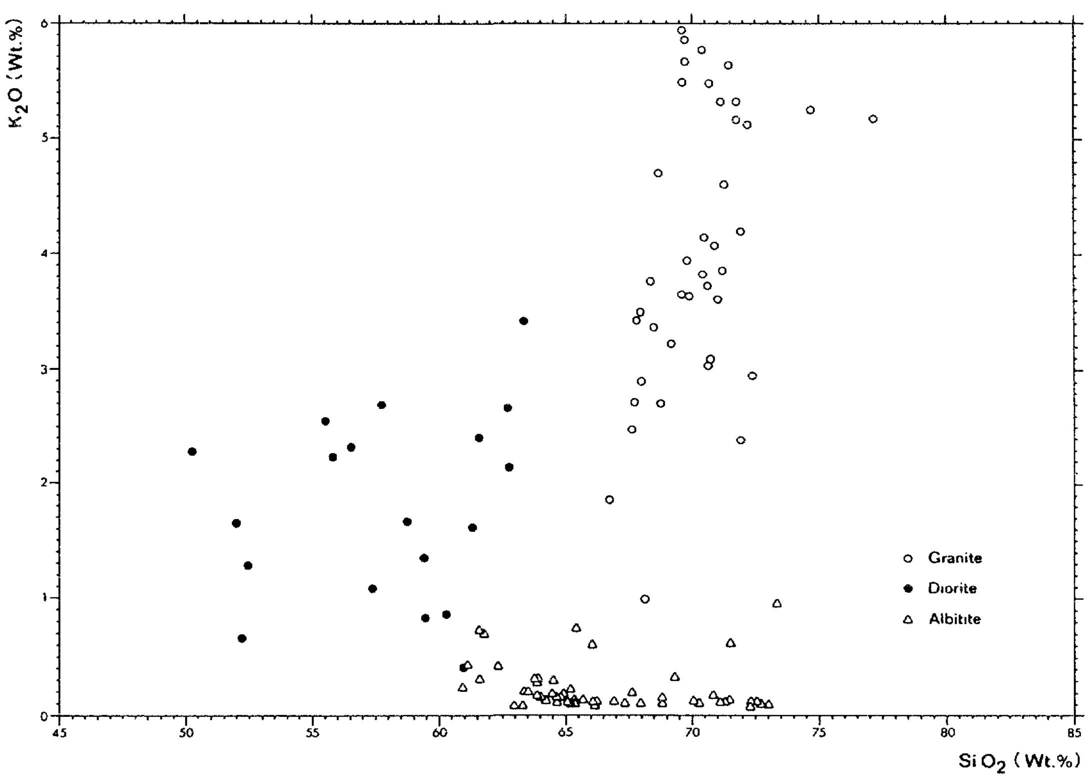

FIG. 13. Variation diagram SiO_2-K_2O.

field but as separate groups. The former are not in the potassium granite field due to their elevated Na values. The plagioclase of the diorite restites have a Ab/An ratio of 60:40. The albitized diorites plot next to the albitites in the trondhjemite field.

The classification scheme of Shand (16) is subdivided into Al-rich 'peraluminous' rocks, alkali-rich 'peralkaline' rocks, and an intermediate group of 'meta-aluminous' rocks on the basis of the molar ratios of Al_2O_3, Na_2O , K_2O, and CaO. Some of the hornblende-biotite granites and the potassium granites are meta-aluminous ($K_2O + Na_2O < Al_2O_3$), some are peraluminous ($K_2O + Na_2O + CaO < Al_2O_3$). The diorites are meta-aluminous. It becomes obvious that all of the magmatic rocks belong to the calc-alkali suite.

The Harker diagram of the major elements SiO_2 and Na_2O (Fig. 11) shows very clearly the individual rock units. The granite cluster is distinctly separated from the albitites by their Na_2O content. The albitite field contains the quartz albitites, with elevated SiO_2 values, and the quartz-free albitites. The diorite group has a greater scatter and is distributed in the non-albitized and albitized subgroups. The rocks of the Poli series are divided into three clusters: intermediate metavolcanites, between the diorite and granite groups; the basic metavolcanites, to the left of the diorites; and the metasedimentary rocks, distinguished by high SiO_2 and low Na_2O values. This diagram shows very clearly the geochemically similar compositions of the Poli metavolcanites and the diorites, which also corresponds to a similar mineralogical composition.

For a further subclassification of the volcanites of the Poli series, the immobile elements Ti, Nb, Y, and Zr were plotted according to Floyd and Winchester (17) (Fig. 12). The diagram shows the same three clusters as the Harker diagram. Most of the samples are dacites and andesites. The few basic samples plot as subalkaline basalts. The metasedimentary rocks plot in the rhyolite field due to their high SiO_2 content.

5.2. Magmatic formations

5.2.1. Monzogranite and Na phase

The SiO_2-Na_2O correlation diagram shows a wide variation in Na_2O (3.8 - 5.9 %) for the granite cluster (Fig. 11). This is due to the presence of two different types of granite which are closely related to one another via intermediate compositions. Some of the normal granite which was classified petrographically as monzogranite, plots as a weakly albitized syenogranite (Fig. 8). As described in chapter 4, this granite has albite rims around the alkali feldspar and the green hornblende is partly transformed to Ca-Na hornblende. The occurrence of Na granite found locally throughout the normal granite and the lack of a replacement fabric indicate late magmatic autometasomatism during the crystallization of the magma. Equilibrium between the melt and the Na-rich late differentiate was attained.

5.2.2. K phase

The potassium granite, described in chapter 4, plots separately from the normal granites in the SiO_2-K_2O and SiO_2-Na_2O Harker diagrams (Fig. 11 and 13). The K_2O and SiO_2 contents are higher, the values for CaO, MgO, Al_2O_3, and TiO_2, as well as the trace elements Ba, Nb, Y, Li, and V are lower. But the transition to the normal granites is gradual.

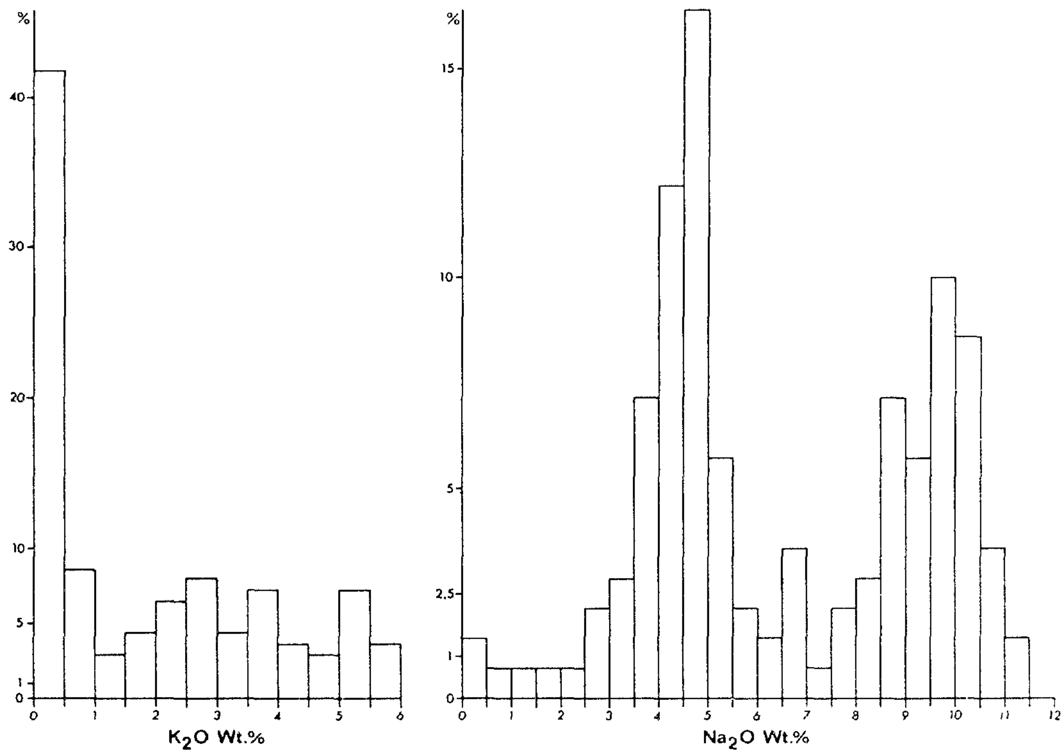

FIG. 14. Frequency distribution of the elements K_2O and Na_2O (141 samples: granite, albitite, diorite, Poli rocks).

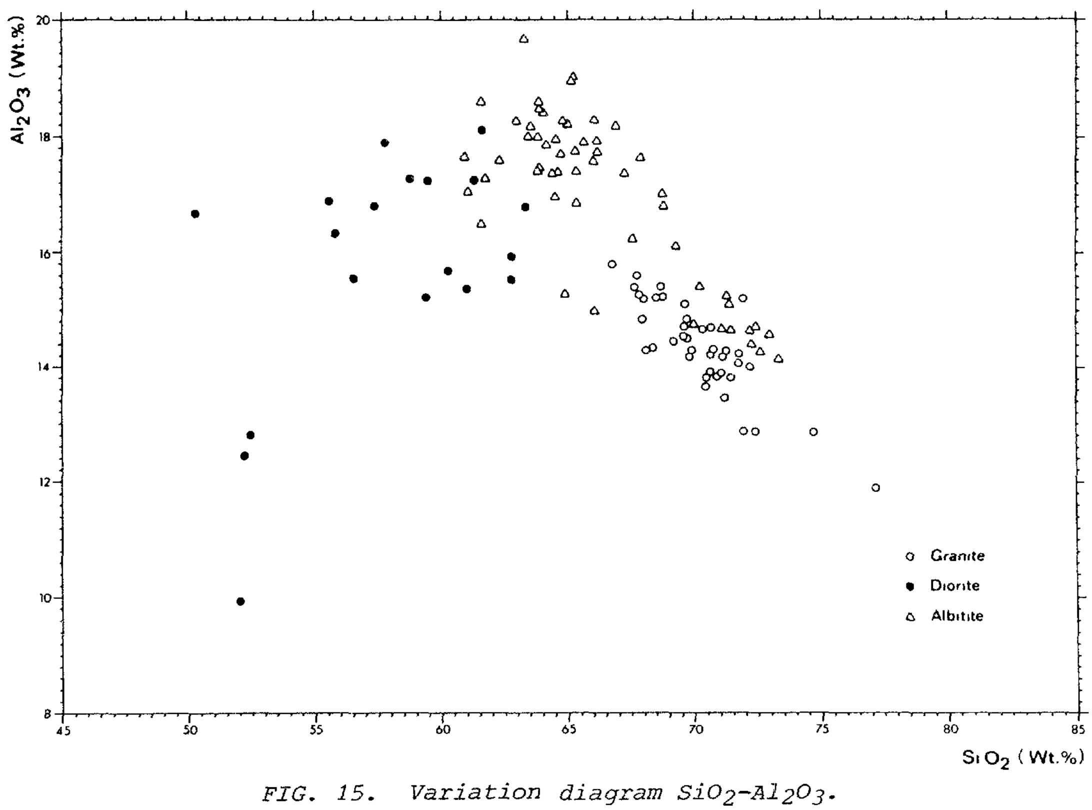

FIG. 15. Variation diagram SiO_2-Al_2O_3.

The occurrence of the potassium granite along the Kitongo fault in direct contact not only with albitites, but also with normal granite further to the northeast, as well as petrographic arguments, indiciate a late magmatic origin. Potassium-feldspatization of this kind is described in the Soviet literature (Abou-Zied and Kerns (18)).

The potassium granite very probably covered a larger area originally and has undergone post-magmatic albitization. Only those areas have remained that were beyond the metasomatic front.

The frequency distribution of the K_2O in the histogram in Fig. 14 shows four maxima:

(i) The main maximum has the lowest K values and corresponds to the albitites;

(ii) the next maximum has 2 - 3 % K_2O and corresponds to the diorites and the rocks of the Poli series;

(iii) the third maximum (3.5 - 4 %) corresponds to the normal granite;

(iv) and the fourth one corresponds to the potassium granite.

5.3. Post-magmatic formations

5.3.1. Na phases

The Na phases produced a partial or complete albitization of the rocks. This albitization differs from that of the late-magmatic Na phase not only in terms of petrographic criteria, but also with respect to the resulting significantly higher Na_2O content, as can be seen in the SiO_2-Al_2O_3 correlation diagram (Fig. 15). These higher Na_2O contents are due to the much more active solutions of this Na phase. In this and other correlation diagrams, all three of the replacement reactions of the palaeosome described in chapter 4 can be recognized:

(i) The replacment of plagioclase by albite is indicated by a very slight increase in SiO_2 and Na_2O and simultaneous decrease in CaO (Fig. 15 and 16).

(ii) The replacement of alkali feldspar is indicated by an increase in Na_2O and a decrease in K_2O with constant SiO_2 and Al_2O_3 (Fig. 17 and 18).

(iii) The replacement of quartz is indicated by a decrease in SiO_2 with simultaneous increase in Na_2O and Al_2O_3 (Fig. 11 and 15).

Further geochemical indication of the replacement of feldspar is the decrease in trace elements Sr (which substitutes Ca in plagioclase) and Ba and Rb (which are bound in the potassium feldspars).

The correlation diagrams also show that the potassium granite, some of the diorite restites, and the inclusions of country rock in the northwest contact zone were albitized in addition to the biotite-hornblende granite (Fig. 11). This can also be seen in the frequency distribution of Na_2O (Fig. 14): the main maximum is formed by the granites and diorites; the bimodal maximum with the high Na_2O values corresponds to the quartziferous and quartz-free albitites; the third maximum (6.5 - 7 % Na_2O) corresponds to the albitized diorite restites; the fourth one, with the very low Na_2O values, corresponds to the metasediments of the Poli series.

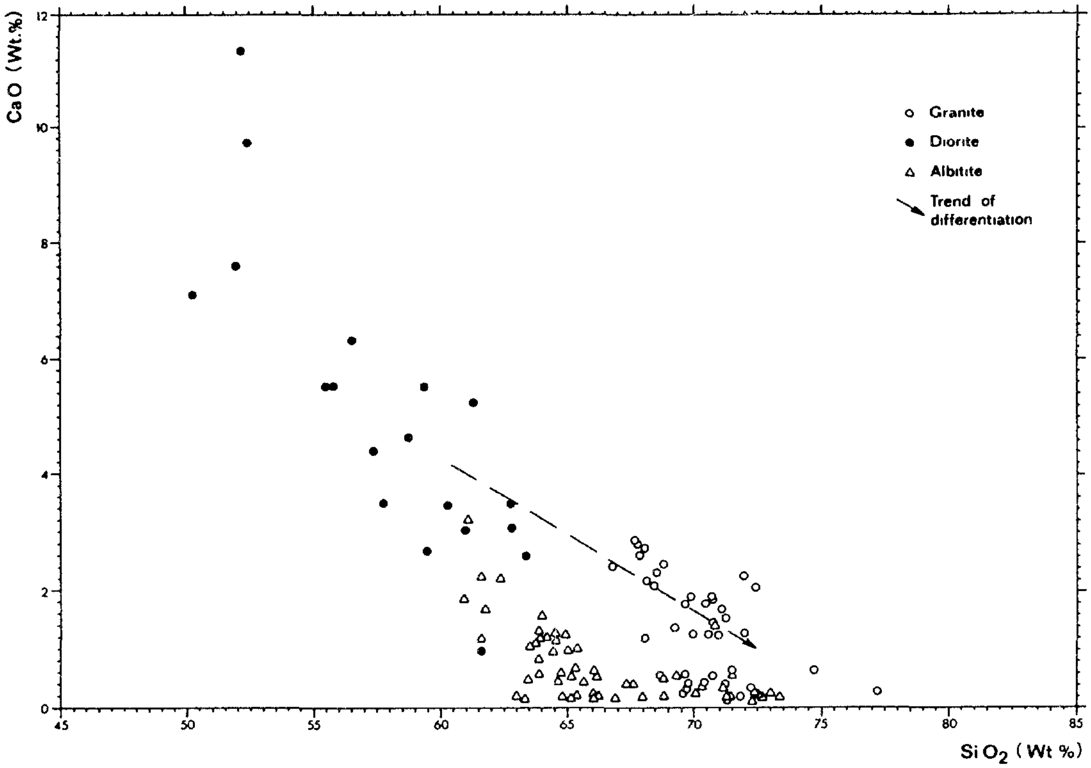

FIG. 16. Variation diagram SiO_2-CaO

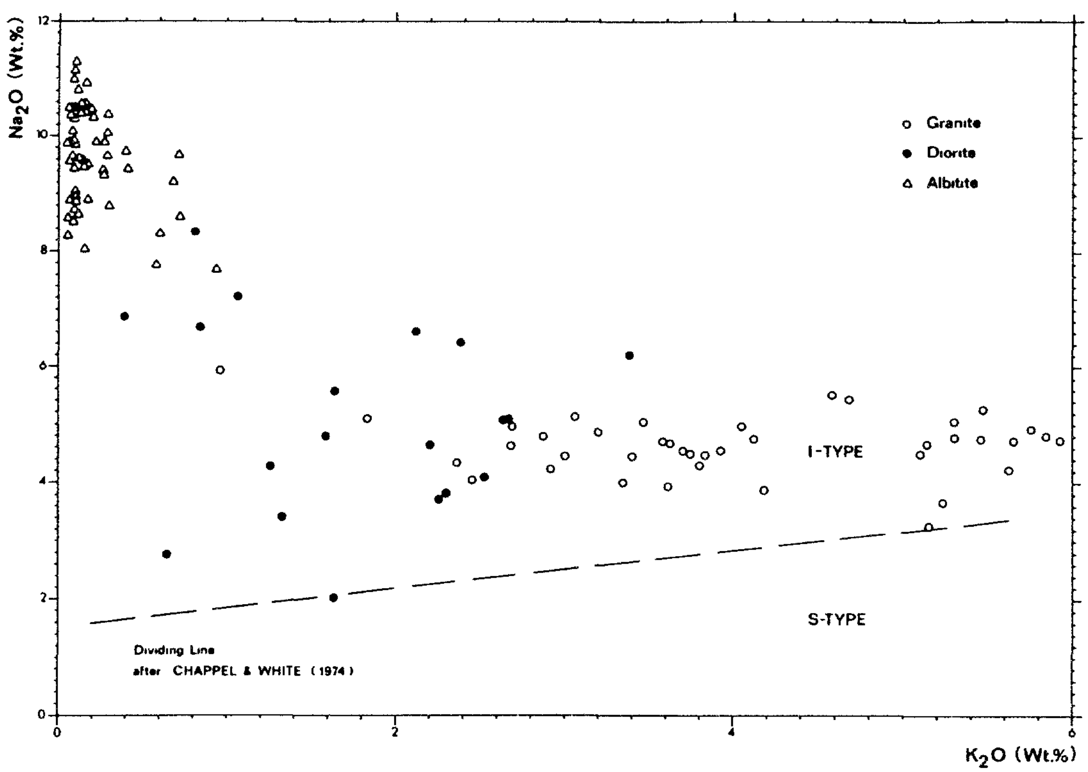

FIG. 17. Variation diagram K_2O-Na_2O (dividing line after Chappel and White (31)).

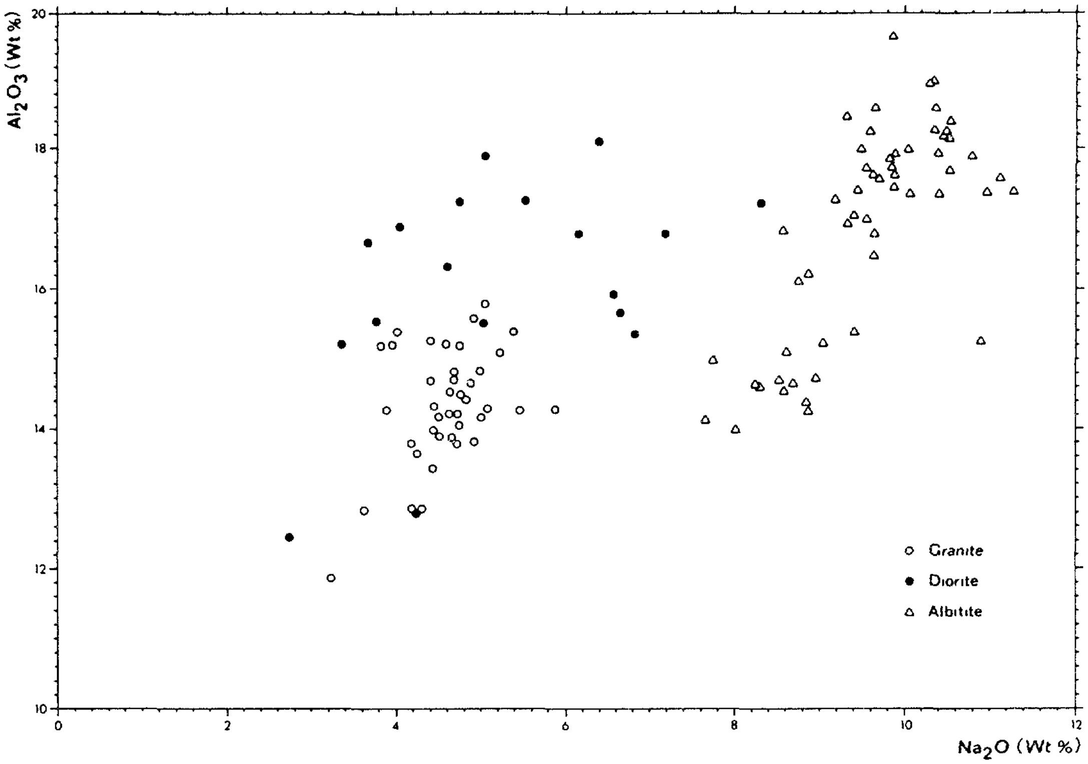

FIG. 18. Variation diagram Na_2O-Al_2O_3.

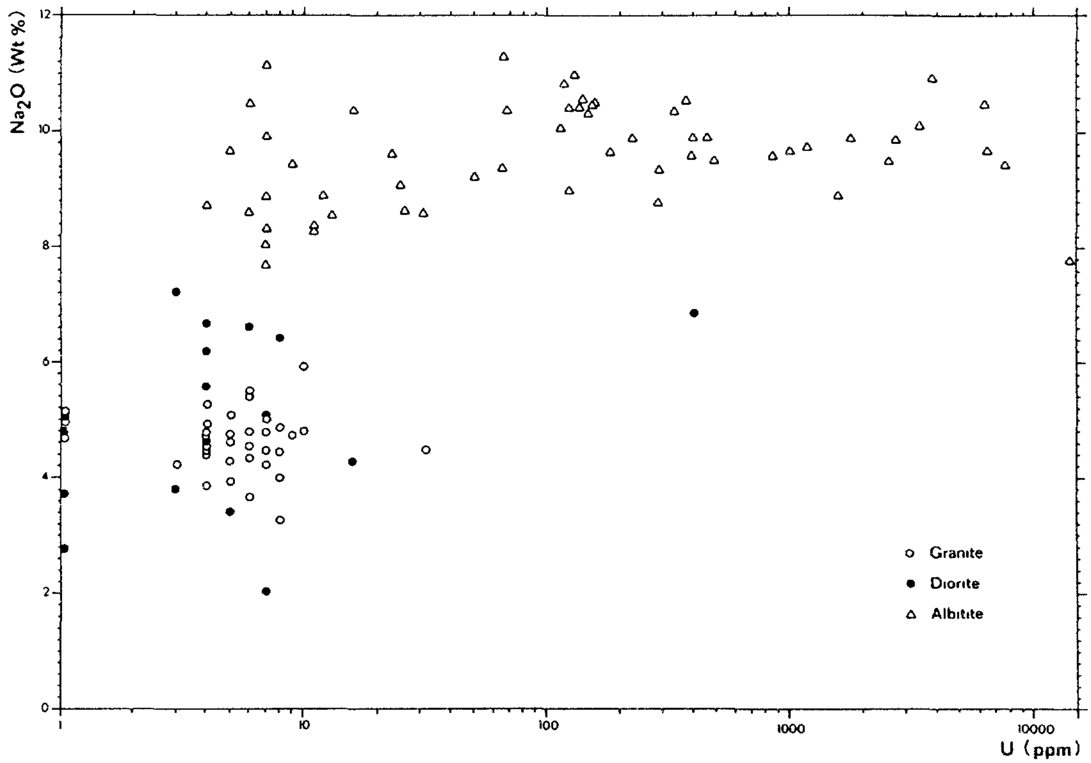

FIG. 19. Variation diagram U-Na_2O

The distribution of the albitites along the tectonized zones of the 'old' Kitongo and Ninga faults (Fig. 4) demonstrates the dependence of the albitization on the tectonic structures formed during the orogeny. The ascent of the hydrothermal Na phases did not occur until after the crystallization of the magma, as shown by the replacement fabric, but it did occur before the uranium phase.

5.3.2. Uranium phase

In contrast to the synchronous occurrence of the Na and the uranium phases described in many publications, the U mineralization of the Kitongo Granite occurred in a separate phase. It can be seen in the U-Na_2O diagram shown in Fig. 19 that the two elements do not correlate, i.e. the U concentration does not increase with increasing Na_2O, which nearly reaches the theoretical saturation limit of pure albite (11.8 wt%). A few of the albitite samples had no elevated U content; on the other hand, one granite and two diorite samples contained uranium without being albitized. This is in agreement with the observation under the microscope that the uraninite grains occur either at the rims of albite crystals or in very thin fissures associated with a new generation of quartz and apatite (disseminated and cataclastic ore types).

The correlation of U with Pb is linear and positive, which is due to the fact that radiogenic lead is an end product of the radioactive decay of uranium. Moreover, small amounts of thorium were introduced with the uranium and is probably incorporated in the uraninite lattice.

5.3.3. Zr-Ce-La phase

The Ce-La and Ce-Zr correlation diagrams (Fig. 20 and 21) show that there is a positive linear relationship between these three trace elements. The ratio of their average concentrations is about Zr/Ce/La = 5:2:1. There is no correlation with either uranium or K_2O. But it can be seen in the Ce-Na_2O diagram (Fig. 22) that all three trace elements are significantly enriched in the potassium granites and highly enriched in most of the albitites; in some of the albitites there is no enrichment of these elements relative to normal granite. This normal granite, together with the diorite, is characterized by average concentrations of Zr = 250 ppm, Ce = 100 ppm, and La = 50 ppm (after Wedepohl (19).

Numerous grains of secondary zircon associated with magnetite and ilmenite were observed under the microscope in certain rock samples. Zircon can contain considerable amounts of Ce and La in addition to zirconium (Görz (20)) and is therefore considered to be a mineral phase of the paragenesis of these elements. According to Bowden (21), alkali hornblende, a constituent of the albitites, is also able to incorporate Zr and REE. Another explanation is that in addition to zircon, secondary apatite and subordinate amounts of unidentified monazite are present, which could be responsible for the high enrichments of Ce and La.

The chronological classification of this phase is not so evident. Observations under the microscope and geochemical data indicate the following interpretation: the first hydrothermal Na phase, which replaced the plagioclase, introduced the elements Zr, Ce, and La. The resulting geochemical paragenesis is preserved only in the potassium granite at the edge of the albitite zone. The second introduction of Zr, Ce and La probably occurred with the second Na phase, followed by a remobilization of all three elements. Thus, local enrichments or depletions occurred, as indicated, for example, by the albitites without elevated Zr, Ce, and La values.

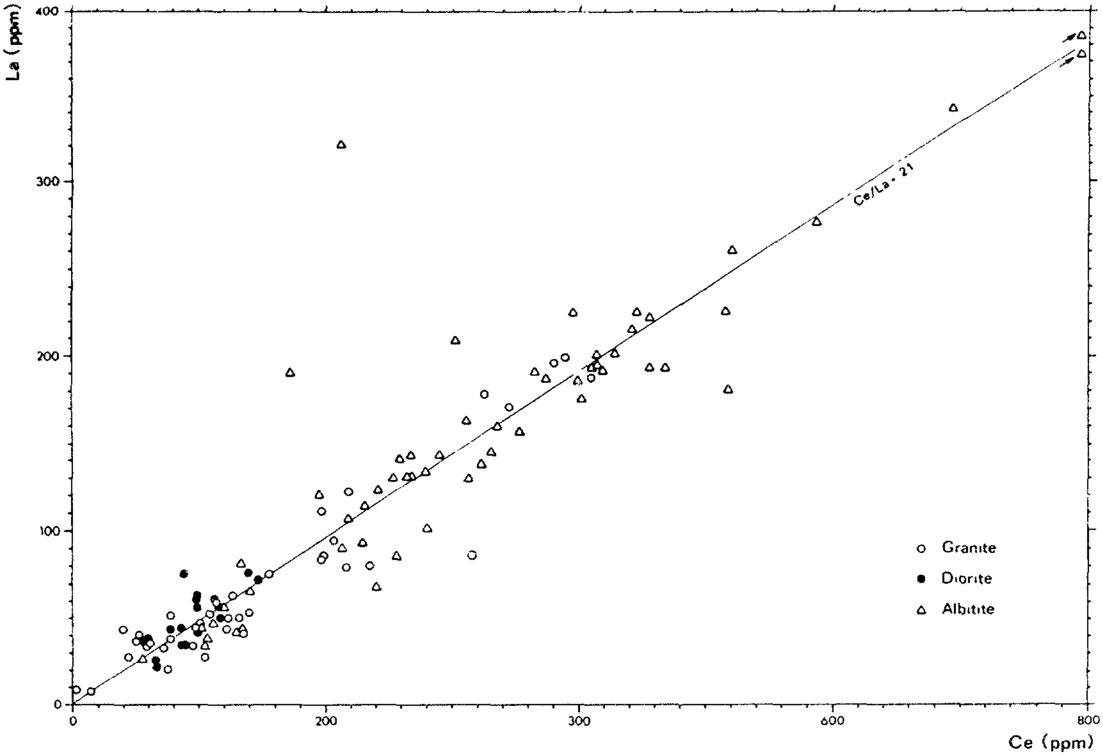

FIG. 20. Variation diagram Ce-La

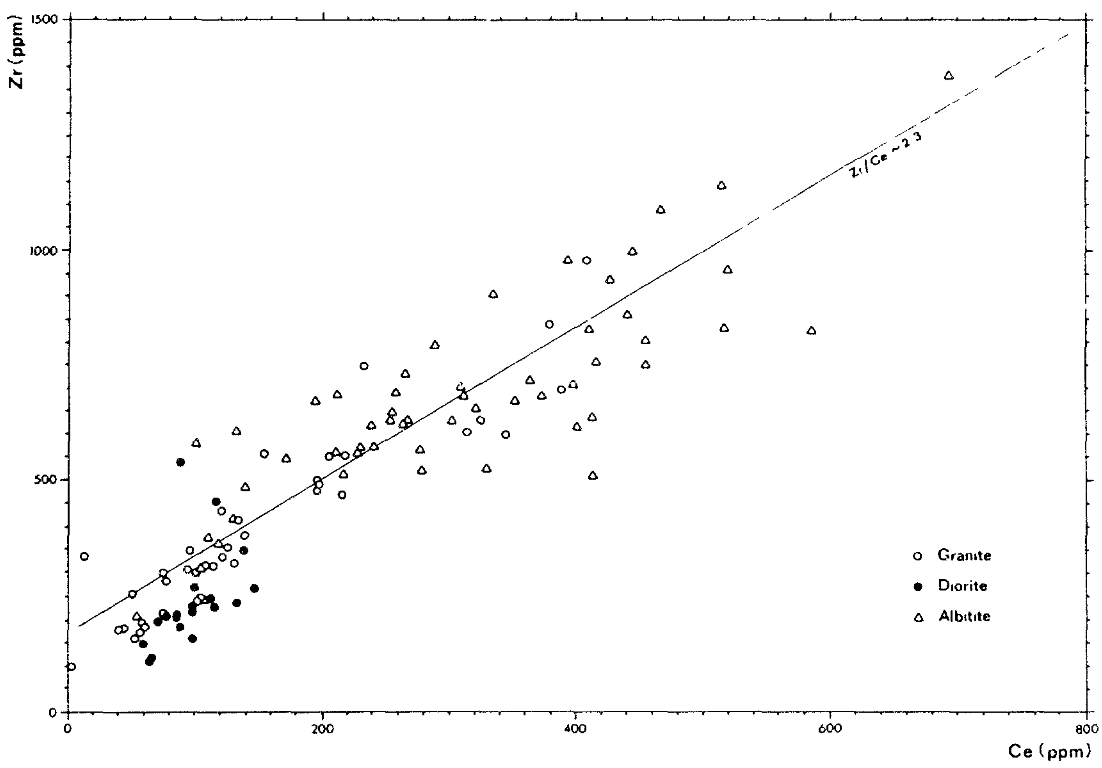

FIG. 21. Variation diagram Ce-Zr

Ce- and La-bearing uranium minerals, e.g. chevkinite, nenadkevite, davidite, and pyrochlore, are often described in the literature on albite-uranium occurrences. This kind of uranium phase does not occur in the albitite of the Kitongo Granite. Nevertheless, these mineral phases demonstrate that Zr, Ce, and La can remain in solution by forming complexes until the last hydrothermal phase (Wedepohl (19)). This is confirmed by Bowden (21) who writes that alkaline magma can concentrate considerable amounts of Zr, Ce, and La in the hydrothermal phase.

5.3.4. Further hydrothermal events

The uraninite mineralization was not the last event in the hydrothermal history of the Kitongo Granite. Under the microscope, two further mineral parageneses were identified in fine fissures in albitites. The first is carbonate (calcite), epidote, clear albite, and quartz. The second phase is an economically unimportant sulfide mineralization consisting of galena, sphalerite, pyrite, chalcopyrite, covellite, and bornite. These sulfides apparently occur only in the cataclastic type of uranium ore, where they occur as individual grains in fissures. Both parageneses belong to the epi-thermal vein filling of the hydrothermal system. It is suggested that the sulfide ore originated by remobilization of disseminated sulfide in the Poli metavolcanites (Müller and Weiser (8)).

5.4. Summary of the evidence for metasomatic albitization

The most important arguments for the formation of albitite by metasomatism are summarized in the following:

(i) Geological evidence

- ° The albitization is not restricted to the Kitongo Granite, but also occurred in other rock types: the quartz diorite and quartz monzonite restites and the inclusions of Poli country rock at the NW contact, as far as these are within the metasomatic front.
- ° The albitization proceeded from tectonic structures and thus is found either in cm-thick zones along joints in the granite or in strongly tectonized fault zones more than 100 m thick, i.e. the Kitongo fault.
- ° The multi-phase Na metasomatism, corresponding to several replacement stages, can be recognized in the field as quartziferous or quartz-free albitite.

(ii) Petrographic evidence

- ° The three replacement stages identified under the microscope which correspond to two separate albitization phases;
- ° the replacement fabric of the albitites, and
- ° the preservation of primary structural features, although the rocks have been almost completely transformed.

(iii) Geochemical evidence

- ° The separate stages of replacement are recognizable in correlation diagrams for various element pairs.

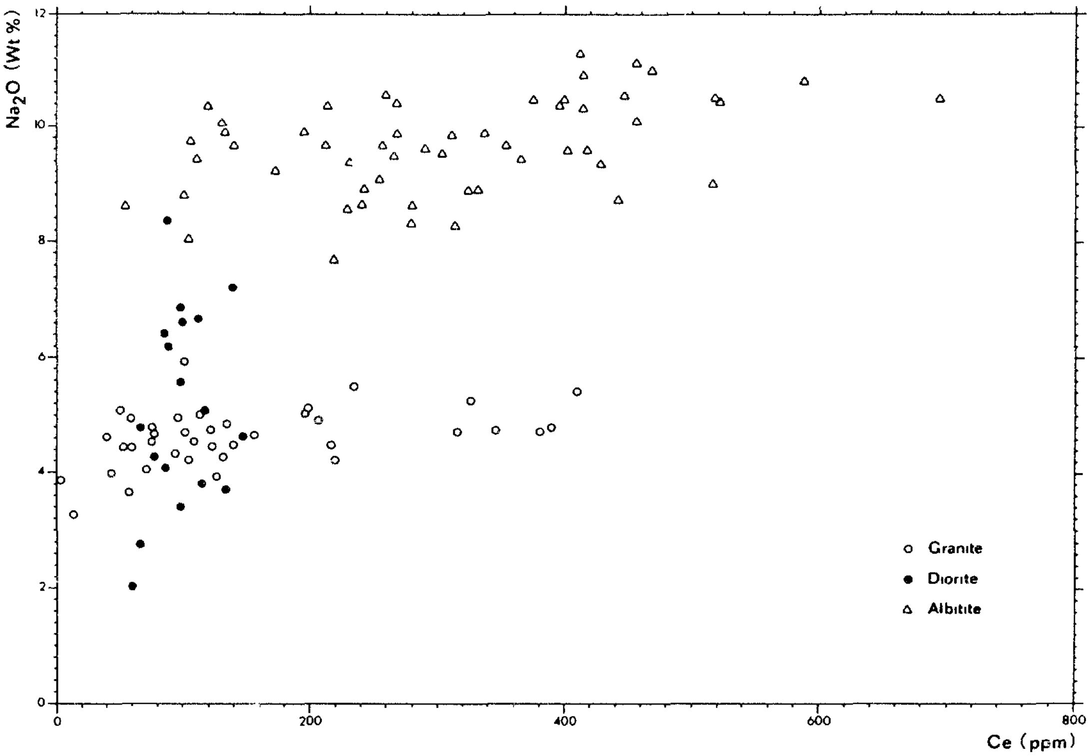

FIG. 22. Variation diagram Ce-Na_2O

° Immobile trace elements of the palaeosome (Ti, Nb, and Ta) remained unchanged during the metasomatism.

(iv) Literature

The pneumatolytic and hydrothermal Na metasomatism of granitoid rocks has been described for several decades in the literature (Gilluly (22), Palivcova (23), and others). Albitization associated with uranium mineralization has been known in the western hemisphere for only about ten years (Leroy (24), (25), Cuney (26), Ballhorn et al. (27), and Oesterlen (2)). But albitite-uranium occurrences have been described on numerous occasions in the Soviet literature for the last twenty years, for example Kazanskiy et al. (28), Voskresenskaya (29), Kashdan (30) and Abou-Zied and Kerns (18).

5.5. Material balance of the metasomatism

Using the computer program 'Pattern Net' (Kottrup and Rehder (14)), elements in the granite samples characteristic for metasomatism were compared with those of the albitites (Fig. 23 and 24). The ranges of element concentrations are represented either in linear or logarithmic manner by the length of the radials, with the lowest value at the center and the maximum at the margin. One line around the diagram represents one sample.

The elements enriched in the albitite relative to the granite are shown in Fig. 23. The weakly albitized potassium granites are noticeable in the granite diagram as a separate group with elevated Zr, La, and Ce and depleted Y. In the

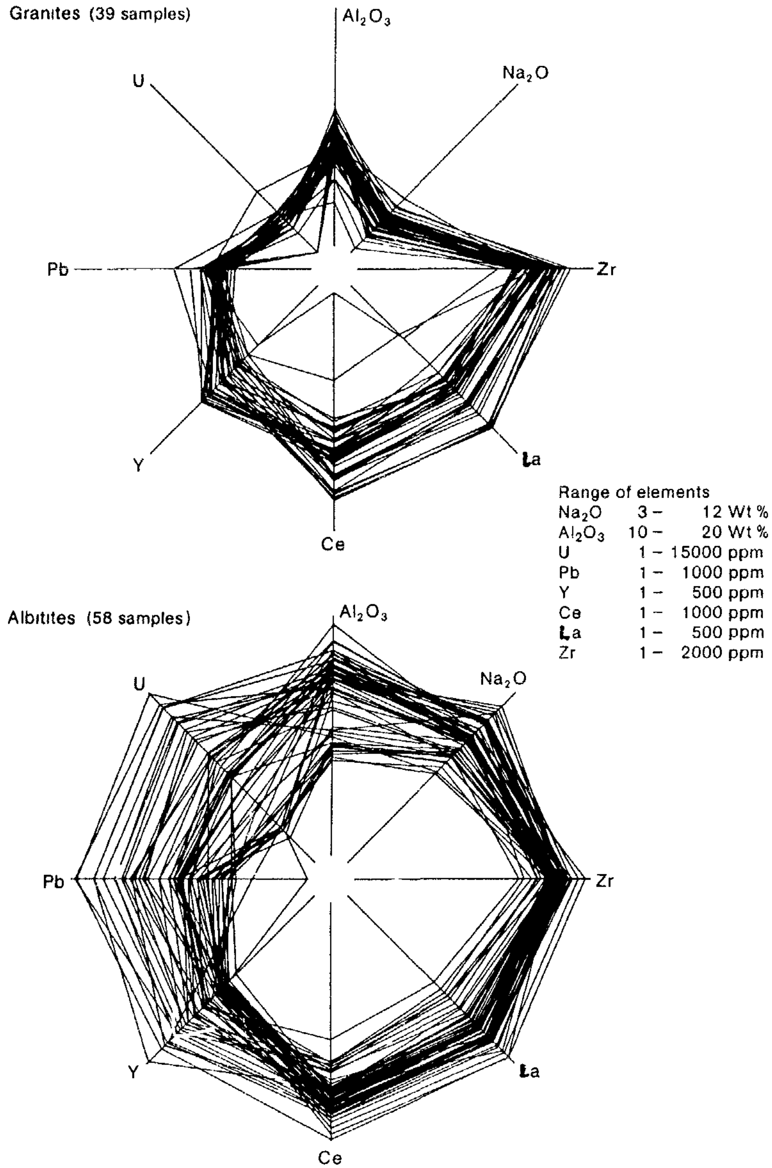

FIG. 23. Material balance of metasomatism – added elements.

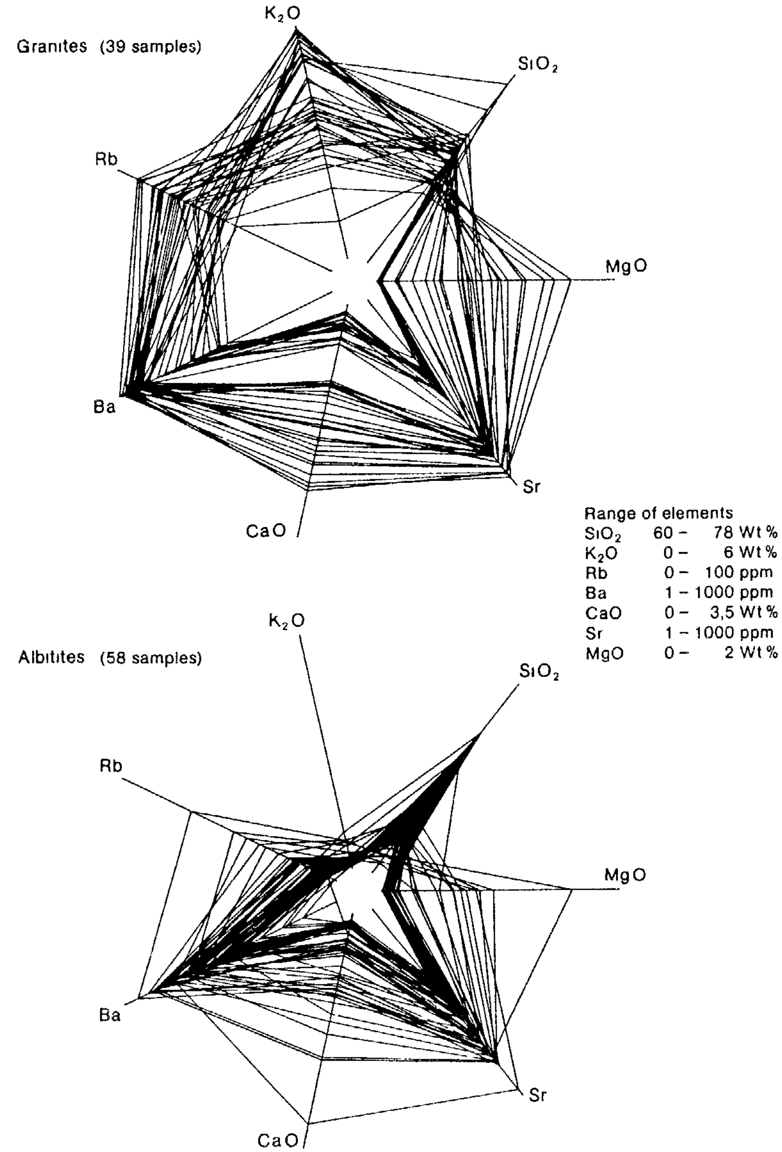

FIG. 24. Material balance of metasomatism – removed elements.

albitite diagram there is also a group of samples characterized by a low Y value, which probably represents completely albitized potassium granite.

The elements depleted in the granite during albitization are shown in Fig. 24. The potassium granite group stands out distinctly in the granite diagram due to the high K_2O values and low SiO_2, Sr, CaO, and Ba. The second albitization phase altered not only rocks with extremely low MgO values, but also rocks with normal MgO values, without significantly changing the MgO content.

6. GENESIS OF THE KITONGO GRANITE

One of the significant results of studies of the petrology of granite about ten years ago was the recognition that most granites must have been formed by partial anatexis (Winkler (5), Chappell and White (31). Sedimentary sequences, crustal magmatic rocks, and rocks of the upper mantle have been considered primary source rocks. Chappell and White (31) have distinguished two principal types of granites: S-type and I-type. The S-type was formed from sedimentary rocks, the I-type from various magmatites. The geochemical, mineralogical, and petrological differences between the two types are derived from differences in the source rocks. Due to their sedimentary origin, S-type granites are depleted in CaO and Na_2O and enriched in Al_2O_3. These element concentration changes do not occur in granites from magmatic source rocks, i.e. I-type. Granites formed by partial melting consist of a molten part and 'restites', i.e. relict mineral paragenesis and/or relict individual crystals (White and Chappell (11)).

The Kitongo Granite has undergone significant changes in major element concentrations through late magmatic events, as described above. In spite of this, it was possible to come to the definite conclusion that the Kitongo Granite has petrographic and geochemical I-type characteristics.

(i) Geochemical evidence

The monzogranite has relatively high concentrations of Na_2O (mean 4.6 %) and CaO (mean 1.9 %) and an average concentration of Al_2O_3 (mean 14.4 %). The molar ratio of $Al_2O_3/(Na_2O+K_2O+CaO)$ is <1.1, as described by Chappell and White (31) for I-type. This is also supported by the correlation of K_2O and Na_2O (Fig. 17). All of the granite and diorite samples plotted in the field typical for I-type granites according to Chappel and White (31).

(ii) Mineralogical evidence

The Ca content of the Kitongo Granite led to the formation of hornblende and titanite, which together with biotite are typical mafic minerals for the I-type. The dioritic restite inclusions support the hypothesis of I-type genesis. They also contain the typical minerals hornblende, biotite, and titanite; they are more basic than the granitic rocks and are very uniform in their mineralogy. The unoriented granitic fabric also indicates a magmatic source rock (Fig. 15 and 16). This is in contrast to the xenoliths of the S-type granites, which have a heterogeneous mineralogical composition and chemical composition (White et al. (32)).

(iii) Petrological evidence

With only a few exceptions, the rocks of the Kitongo Granite and of the restites have CIPW normative values for corundum of <1 wt%, typical for the I-type. Characteristic for the S-type are elevated normative corundum values, due to an excess of Al_2O_3. The Qu-Ab-Or ternary diagram of normative values also provides evidence for the genetic type (Fig. 9). The points for the samples of Kitongo Granite and the restites are all on the feldspar side of the cotectic line, typical for the I-type according to White et al. (32).

(iv) The magmatic source rock

Anatexis of the source rocks produces, depending on the degree of melting, either minimum melts consisting of Na_2O, K_2O, SiO_2, and Al_2O_3 (White and Chappell (11)) or non-minimum melts, in which the minerals of CaO, MgO, FeO, and TiO_2 are melted, too. The Kitongo Granite is a non-minimum melt formed at relatively high temperatures. This is demonstrated by the proportion of the mafic minerals pyroxene, hornblende, and biotite that are present, as well as by the Na-rich alkali feldspar and the relatively low SiO_2 (ca. 70 wt%). Thus, the magmatic source rock had to have a composition between the restites and the new partial melt. A granodioritic composition is suggested for the composition of the magmatic source rock of the Kitongo Granite.

7. GENESIS OF THE ALBITE-URANINITE MINERALIZATION

7.1. Formation of the residual fluid magmatic phase

The intrusion of the Kitongo Granite came to a standstill in the rocks of the Poli series at a relatively deep level in the crust. These rocks had already been metamorphosed to the upper amphibolite facies and therefore reveal no contact metamorphism. The roof of the intrusion crops out at present.

The melt began crystallization at the contact resulting in the formation of a residual melt enriched in volatile components. The melt became slightly enriched in Na_2O in the roof zone; a residual melt rich in potassium locally formed K-feldspar-rich granite in the contact zone. This could happen only in a stable, pressure-resistant roof zone ('pressure-quenched carapace', Plimer (33)). With continuing crystallization, a volatile phase developed which was enriched in the elements Na, U, Zr, Ce, La, Fe, and Al. The elements Ce, La, Zr, U, and Fe probably formed alkaline complexes with sodium hydrogen carbonate, carbonate, and hydroxide, and possibly sodium phosphates and chloride also. Uranium was present in an oxidation state of +6 due to the elevated Eh values. Under these conditions it is highly soluble in strongly alkaline solutions, forming uranyl complexes (Krauskopf (34)). Thorium is unable to form complexes under these conditions; thus, a fractionation of thorium and uranium occurred.

7.2. Pneumatolytic to hydrothermal processes

Hydrothermal processes were initiated by renewed fracturing of the intrusion at the contact caused by increasing internal hydrostatic pressure during the gradual cooling of the melt and renewed orogenetic movement. The fluid phase migrated into the fault-controlled zones of minimum pressure and impregnated the entire tectonized area. The decomposition of the alkaline complexes and the two-stage albitization resulted from the step-wise reduction of pressure, each phase followed by the formation of a new, chemically different, cooler hydrothermal fluid phase, probably with a new pH, too. The elements Zr, Ce, and La precipitated forming zircon, magnetite and secondary apatite (and possibly monazite). It is likely that these elements were remobilized by the changing physical and chemical conditions. The aqueous alkaline solutions must have had a temperature of 350 - 400°C at a pressure of 0.7 - 1.0 kbar according to fluid inclusion studies by Leroy (24).

Uraninite then precipitated as a separate phase, but probably still in the katathermal range. The fact that uraninite crystallized and not, for example, davidite, a Ce-bearing uranium iron titanite, indicates that the REE and zirconium had already precipitated. The uraniferous solutions migrated in nearly the same channels as the previous solutions, but the precipitation of the uraninite was now aided by the better porosity, i.e. permeability, of the albitite with respect to the granite (Abou-Zied and Kerns (18)) and by the newly formed alkali-hornblende and magnetite, which served as crystallization nuclei for the uraninite. With further cooling, small amounts of carbonate, epidote, and quartz precipitated in fissures, as well as the sulfides.

The 'telescoping' of the different mineral phases, from katathermal-stage albite to the uraninite, and finally to the sulfides of the epithermal stage, is explained by a closed hydrostatic system in which the residual melt, source of the solutions, continually drew back further and further towards depth.

The uranium is to be considered a component of the magmatic system and was probably mobilized by leaching of uraniferous silicates such as zircon, titanite, hornblende, and biotite of the granodioritic source rock. Its enrichment was a result of fractional crystallization and differentiation of the melt during the intrusion and crystallization (Dybek (35)). Deuteric alteration of the Kitongo Granite can be excluded as source of the uranium (Cuney (26)).

7.3. Further characteristics of the albite-uraninite mineralization

A comparison of the Kitongo albite-uraninite mineralization with other occurrences in the literature (mainly Soviet) reveals the following common characteristics:

° The uranium mineralization has a hydrothermal, metasomatic origin.

° The uranium mineralization is associated genetically and spatially with Na metasomatism of a granitic pluton.

° The albite-uraninite mineralization occurs in pre-existing lineaments that can be followed for long distances. These lineaments are intracratonic or at the margins of a craton.

° The mineralization was formed at considerable depth.

° The mineralization was formed as part of a multi-step process.

Differences from the occurrences described in the literature is the occurrence of the Na metasomatism in several stages and formation of the uranium mineralization in a separate stage after the albitization. Another significant result is the occurrence of the Kitongo uranium mineralization in an I-type granite. The plutons in the literature are not classified genetically, but the chemical and mineral composition and metallogenesis described for these occurrences permit, in general, the assignment to either S- or A-type granites (Collins et al. (36)). The Kitongo occurrence demonstrates that hydrothermal to metasomatic albite-uranium mineralization can also develop in I-type granites.

Lastly, the unusual continuity of the chemical composition of the magmatic rocks in the study area should be mentioned: Rocks with a high Na content have remained predominant from the Precambrian Kitongo Granite to the Palaeozoic volcanites and the syenites of the Tertiary ring-complexes. The reason for this may probably be found in the geotectonic location of the region, which also finds expression in the repeated reactivation of the NE-striking lineament. In any case, the present study makes it clear that the albite-uranium occurrence did not originate from descending migration of solutions.

ACKNOWLEDGEMENTS

The authors wish to thank Dr. M. Kürsten and Dr. W. Stahl of the BGR and Dr. W. Spross and Dr. H. Fuchs of Urangesellschaft for permission to carry out this work in the BGR. Thanks are due G. Kottrup and S. Rehder for their friendly aid and advice in applying the MAX program, as well as Dr. H. Raschka, J. Lodziak, D. Requard, and Dr. H. Gundlach for the XRF and chemical analyses. We also thank Dr. A. Müller for his support of this work and Dr. P. Müller for discussions of petrographic problems and a critical review of the manuscript. Dres. V. Thoste and R. Fritsche provided valuable advice. The authors wish to express their recognition of the good cooperation with the Ministry of Mines and Energy in Yaounde/Cameroon, and in the field with geologist O. Matip.

Permission to publish this paper has been granted by the Ministry of Mines and Energy of the Federal Republic of Cameroon and the Federal Institute for Geosciences and Natural Resources (BGR) of the Federal Republic of Germany.

REFERENCES

(1) GEHNES, P., THOSTE, V., Uranprospektion in Nord-Kamerun, Projektprüfungskommission, unpublished report, BGR, Hannover (1981)

(2) OESTERLEN, M., Uranium Exploration in Poli, Northern Cameroon, unpublished report, Urangesellschaft, Frankfurt (1983) 67 pp.

(3) KOCH, P., Notice explicative sur la feuille Garoua-Oest, Direction des Mines du Cameroun, Paris (1959)

(4) BESSOLES, B., TROMPETTE, R., La chaine panafricaine 'zone mobile d'Afrique centrale (partie Sud) et zone mobile Soudaniase', Mém. BRGM 92 (1980) 396 pp.

(5) WINKLER, H.G.F., Die Genese der metamorphen Gesteine, Springer, Berlin, Heidelberg, New York (1967) 237 pp.

(6) READ, H.H., The Granite Controversy, Murby, London (1955) 430 pp.

(7) LOUIS, P., Contribution gêophysique â la connaissance gêologique du bassin du lac Tschad, Off. Recherche Scientif. Techn. Outre-Mer, Mem. 42 Paris (1970) 311 pp.

(8) MÜLLER, P., WEISER, T., Untersuchungen an Proben der Uranvererzung Goblê, Nord-Kamerun, unpublished report, BGR, Hannover (1982) 15 pp.

(9) FRITSCHE, R., Mineralogical Report 82-39, unpublished report, UEB, Bonn (1982) 15 pp.

(10) FRITSCHE, R., von PECHMANN, E., Mineralogical Reports 83-31 and 83-32, unpublished reports, UEB, Bonn (1983) 39 pp., 5 pp.

(11) WHITE, A.J.R., CHAPPELL, B.W., Ultrametamorphism and Granitoid Genesis, Tectonophysics 43 (1977) 7-22.

(12) STRECKEISEN, A., To Each Plutonic Rock Its Proper Name, Earth Sci. Rev. 12 (1976) 1-33.

(13) MULLER, P., Von der CIPW-Norm ausgehende Berechnung von Mineralbestanden magmatischer Gesteine in Analogie zu der Modalzusammensetzung plutonischer und vulkanischer Gesteine, Geol. Jb. 55 (1982) 3-41.

(14) KOTTRUP, G., REHDER, S., Multivariate Analysis for Exploration, unpublished report, BGR, Hannover (1983)

(15) HIETANEN, A., Idaho Batholith near Pearce and Bungalow, Clearwater County, Idaho, USA, U.S. Geol. Surv. paper 344-D (1963) 35-42.

(16) SHAND, S.J., Eruptive Rocks, Wiley, New York (1951)

(17) FLOYD, P.A., WINCHESTER, J.A., Identification and Discrimination of Altered and Metamorphosed Volcanic Rocks Using Immobile Elements, Chem. Geol. 21 (1978) 291-306.

(18) ABOU-ZIED, S., KERNS, G., Albitized Uranium Deposits, Six Articles Translated from the Russian Literature, U.S. Department of Energy, Grand Junction, Colorado (1980)

(19) WEDEPOHL, K.H., Handbook of Geochemistry, Springer, Berlin, Heidelberg, New York (1978)

(20) GÖRZ, H., Microprobe Studies of Inclusions in Zircons and Compilation of Minor and Trace Elements in Zircons from the Literature, Chem. der Erde 33 (1974) 326-327.

(21) BOWDEN, P., Zirconium in Younger Granites of Northern Nigeria, Geochim. Cosmochim. Acta 30 (1966) 985-993.

(22) GILLULY, J., Replacement Origin of the Albite Granite Near Sparta, Oregon, U.S. Geol. Surv. Prof. Paper 175-C (1933) 65-81.

(23) PALIVCOVA, M., Igneous-looking Metasomatic Hydrothermal Albitites, Acta Musei Nationalis Pragae, XXIII B 5 (1967) 125-148.

(24) LEROY, J., Les episyénites non minéralisées dans le massif de granite à deux micas de Saint-Sylvestre (Limousin, France): Equilibres entre minéraux et solutions, Thèse 3ème cycle, Univ. Nancy I (1971) 87 pp.

(25) LEROY, J., The Margnac and Famay uranium deposits of the La Cranzille district (Western Massif Central, France): Geologic and Fluid Inclusions Studies, Econ. Geol. 73 (1978) 1611-1634.

(26) CUNEY, M., Geologic Environment, Mineralogy and Fluid Inclusions of the Bois Noirs Limouzat Uranium Vein, Forez, France, Econ. Geol. 73 (1978) 1567-1610.

(27) BALLHORN, R.K., THAKUR, V.K., FONTE, J.E.C., SUCKAU, V., Geology of the Espinharas Uranium Deposit, Brazil, IAEA-AG 162/27 Vienna (1981) 521-533.

(28) KAZANSKIY, V.I., LAVEROV, N.P., TUGARINOV, A.I. Sources of ore material in endogenic uranium deposits, Int. Geol. Rev. 19 (1977) 283-294.

(29) VOSKRESENSKAYA, M.N., Sodic Metasomatism as Feature of Tectonomagmatic Activation in Precambrian Formation, Int. Geol. Rev. 18 (1976) 935-939.

(30) KASHDAN, A.B. Die Formationszugehorigkeit der wirtschaftlichen Typen von Uranlagerstatten, Zt. angew. Geol. 24 (1978) 472-476.

(31) CHAPPELL, B.W., WHITE, A.J.R., Two Contrasting Granite Types, Pacific Geol. 8 (1974) 173-174.

(32) WHITE, A.J.R., WILLIAMS, J.S., CHAPPELL, B.W., Geology of the Berridale 1:100000, sheet 8625, Geol. Surv. New South Wales, Dept. Mines (1977) 138 pp.

(33) PLIMER, I.R., The Geology of Tin and Tungsten Deposits, Course Handbook, Inst. Mineral. Petrol., Univ. Leoben, Austria (1983) 212 pp.

(34) KRAUSKOPF, K.B., Introduction to Geochemistry, McGraw Hill, New York (1967) 721 pp.

(35) DYBEK, J., Zur Geochemie und Lagerstättenkunde des Urans, Clausthaler H. Lagerstättenkunde Geochem. 1, Berlin (1962) 163 pp.

(36) COLLINS, W.J., BEAMS, S.D., WHITE, A.J.R., CHAPPELL, B.W., Nature and Origin of A-Type Granite with Particular Reference to Southeastern Australia, Contrib. Miner. Petrol. 80 (1982) 189-200.

URANIUM-BEARING SILICEOUS VEINS IN YOUNGER GRANITES, EASTERN DESERT, EGYPT

H.A. Hussein, M.A. Hassan, M.A. El-Tahir, A. Abou-Deif
Nuclear Materials Corporation
Cairo
Egypt

Abstract

URANIUM-BEARING SILICEOUS VEINS IN YOUNGER GRANITES, EASTERN DESERT, EGYPT

The post-tectonic younger granites of Egypt represent the magmatic activity marking the end of the cratonization process of the Pan-African Orogeny. Several of these plutons are hosts of rare metal mineralization in the Eastern Desert of Egypt. Two of them, namely El-Erediya and El-Missikat plutons, are hosts of siliceous vein-type uranium mineralization. In both occurrences, the mineralization is structurally controlled by faults and their feather joints which are associated with NE to ENE shear zones. Widespread silicification, and to a lesser extent kaolinization and sericitization, as well as other alterations accompany the uranium mineralization. Uranium is concentrated in the centre of the mineralized faults and fractures together with jasper (in El-Erediya) or black silica and to a lesser extent jasper (in El-Missikat). Pitchblende is the primary mineral which suffered intensive oxidation and probably leaching relics protected by silica. This resulted in a spotty distribution of uranium and radioactivity in the oxidation zone. Present data suggest an origin by hydrothermal fluids derived, most probably, from the younger granite magma. Uranium was derived from the magma itself, or from another deep source. Contributions from the granitic plutons by leaching through circulation of meteoric waters cannot be ruled out at the present state of knowledge.

1. INTRODUCTION

The granitic rocks in Egypt are broadly classified into two main groups: older syn- to late tectonic granites referred to as grey granites and younger or post tectonic granites, referred to as pink granites (El-Ramly et al. (1), Akaad et al. (2), El-Ramly (3), Sabet (4), El-Gaby (5), Akaad et al. (6)). Recently, Hussein et al. (7) added a third group of alkaline granites which was previously identified with the younger granites.

The younger granite plutons are intruded into country rocks of cratonized oceanic material (metamorphosed sediments, volcanics and ophiolitic melanges) as well as older batholithic syn-tectonic granitoids, calc-alkaline volcanics and molasse sediments. Their age range is about 600 - 570 Ma (Hashad (8)) and they represent the magmatic activity in the Egyptian basement.

The most characteriscic features of the younger granites in the central Eastern Desert are (El-Ramly et al. (1), Akaad et al. (2), El-Ramly (3), Sabet (4), Sabet et al. (9), Akaad et al. (6), Greenberg (10), Hussein et al. (7), and Stern et al. (11)):

(i) They form relatively small bodies with circular or oval outlines; average outcrop area of individual plutons is about 40 km².

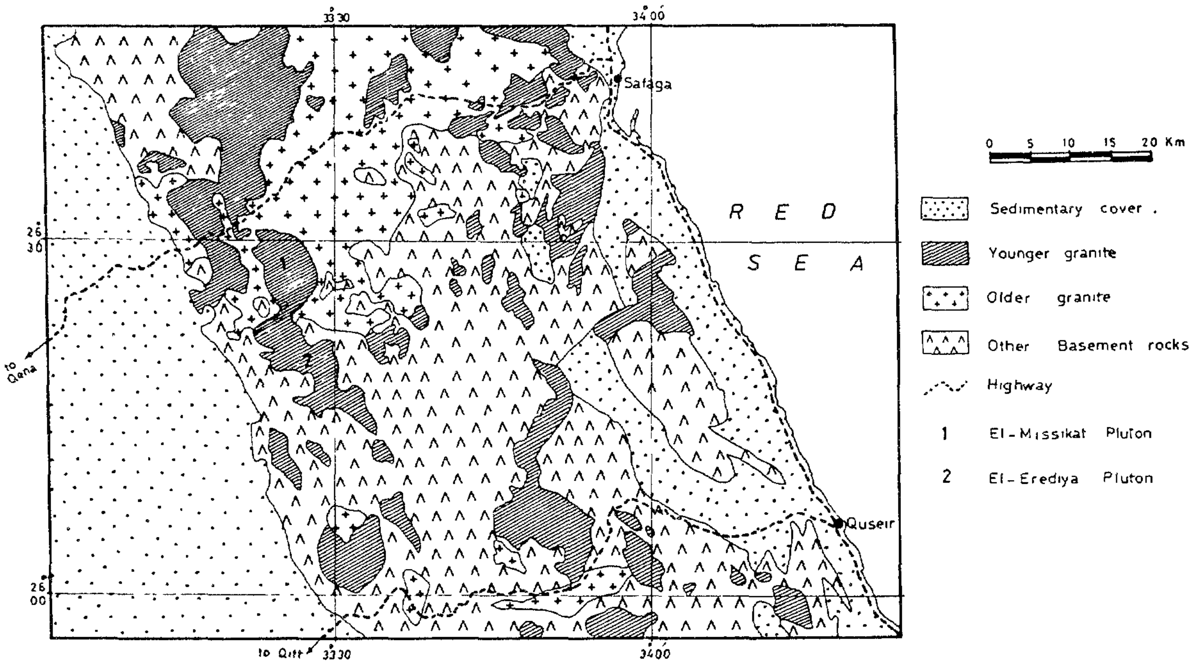

FIG. 1. Location of El-Erediya and El-Missikat plutons, Eastern Desert, Egypt

(ii) They are mostly leucocratic, most often of pink to red colour. They show considerable uniformity in composition and mineralogy within plutons. Most plutons consist almost entirely of quartz, K-feldspar and sodic plagioclase. The more mafic bodies contain moderate amounts of biotite and hornblende.

(iii) The plutons are epizonal, unfoliated and have sharp contacts with all surrounding rock types. They are devoid of pegmatites, but contain quartz veins.

(iv) They are mostly peraluminous to slightly peralkaline, rich in LIL elements, but not as rich as similar post tectonic plutons from other areas. They typically have low $^{87}Sr/^{86}Sr$ ratios (0.701 - 0.7025) and are neither associated with mafic differentiates nor with other diverse rock types found in many post-tectonic alkali granite provinces.

(v) Their chemical composition is characterized by 70 - 75 % SiO_2, 4 - 5 % K_2O and $K_2O/Na_2O \sim 1$.

(vi) They can be considered products of partial melting of cratonized material in the lower crust with some additions from the mantle, or by anatexis in the upper mantle.

Many of these younger granite plutons are affected by post magmatic deuteric and hydrothermal alterations associated in many places by rare metal mineralizations (Hunting (12), Bugrov et al. (13), Hussein (14), Sabet et al. (15)). An aeroradiometric survey in the central Eastern Desert discovered in various younger granite plutons between Qena-Safaga and Qift-Quseir highways (Fig. 1) several significant radiometric anomalies (Ammar (16)). Ground follow-up of these anomalies indicate that two of them are related to siliceous uranium-bearing veins in the peripheral parts of two of the younger granite plutons. These plutons are El-Erediya pluton (El-Kassas (17)) and El-Missikat pluton (Bakhit (18)). Surface and subsurface studies were carried out on these two occurrences (El-Tahir (19), Abu Deif (20)). The present paper describes these two occurrences as examples of vein-type uranium deposits in granitic rocks.

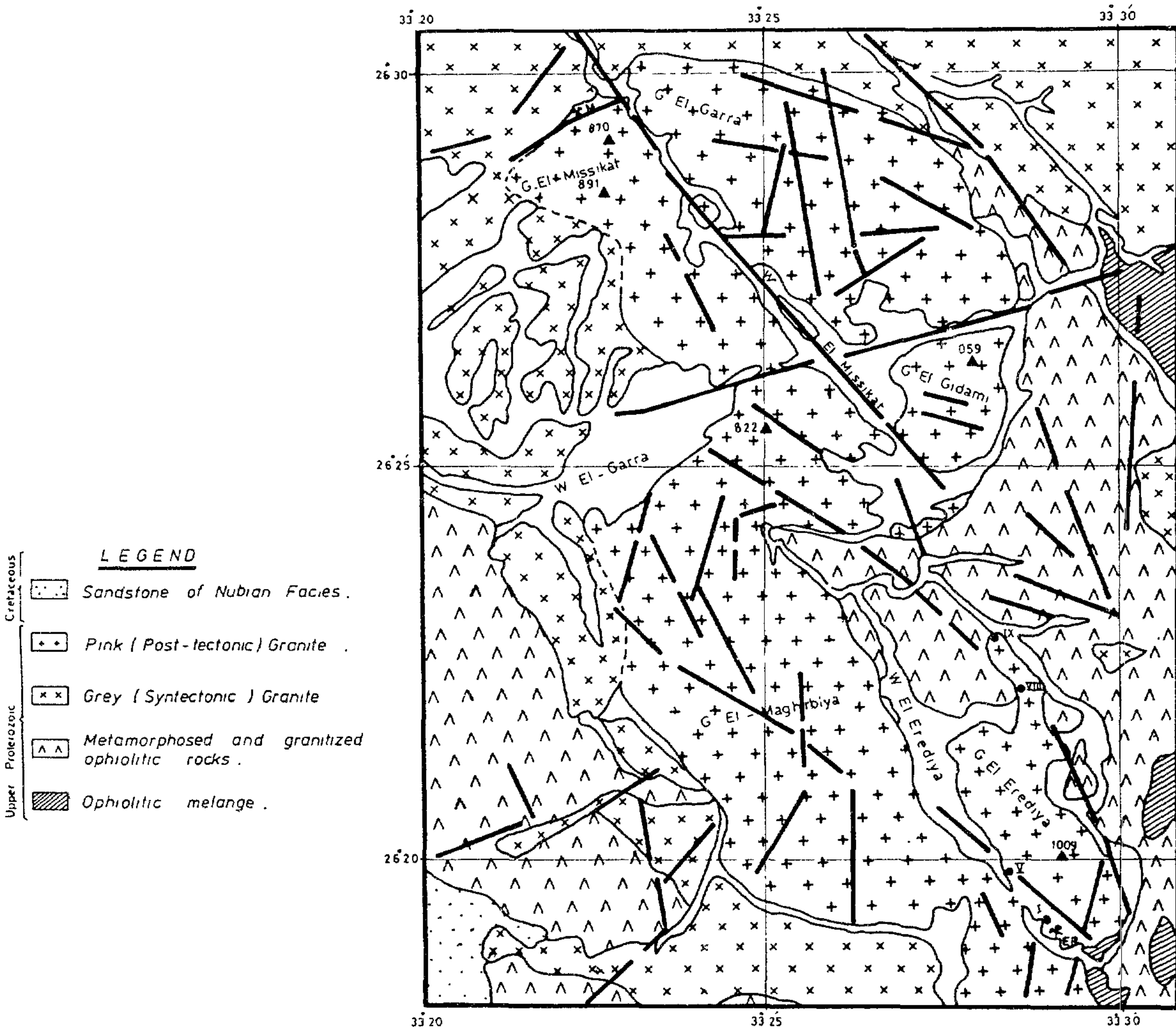

FIG. 2. Geologic map of El-Erediya / El-Missikat area.

2. GEOLOGIC SETTING OF EL-EREDIYA AND EL-MISSIKAT AREAS

Fig. 2 is a geologic map of the area including both El-Erediya and El-Missikat plutons. El-Erediya pluton is roughly elongated in shape and composed of two masses: Gebel El-Maghrabiya and Gebel El-Erediya. El-Erediya uranium occurrence is located in the southern part of El-Erediya granite, close to its contact with the country rocks. El-Missikat is circular in shape and is dissected by two major NW and ENE faults into four separate bodies. El-Missikat uranium occurrence is located on the northwestern slopes of Gebel El-Missikat, very close to the contact of the pluton.

2.1. El-Erediya area

Gebel El-Erediya is an oval shaped pink granite elongated in NW-SE direction with a length of 6.5 km and width of 2.5 km. Its contacts with the country rocks are mostly sharp and distinct. The granite is dissected by dikes and veins of aplites, porphyries, pegmatite and jasper as well as few basaltic dikes. It

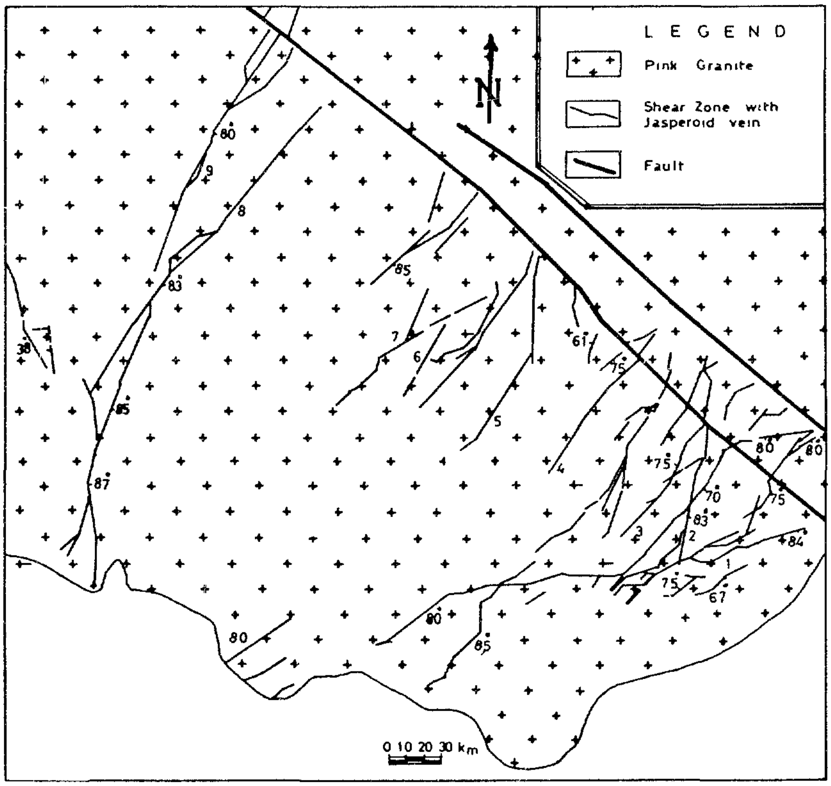

FIG. 3. Silicified shear zones of El-Erediya uranium occurrence.

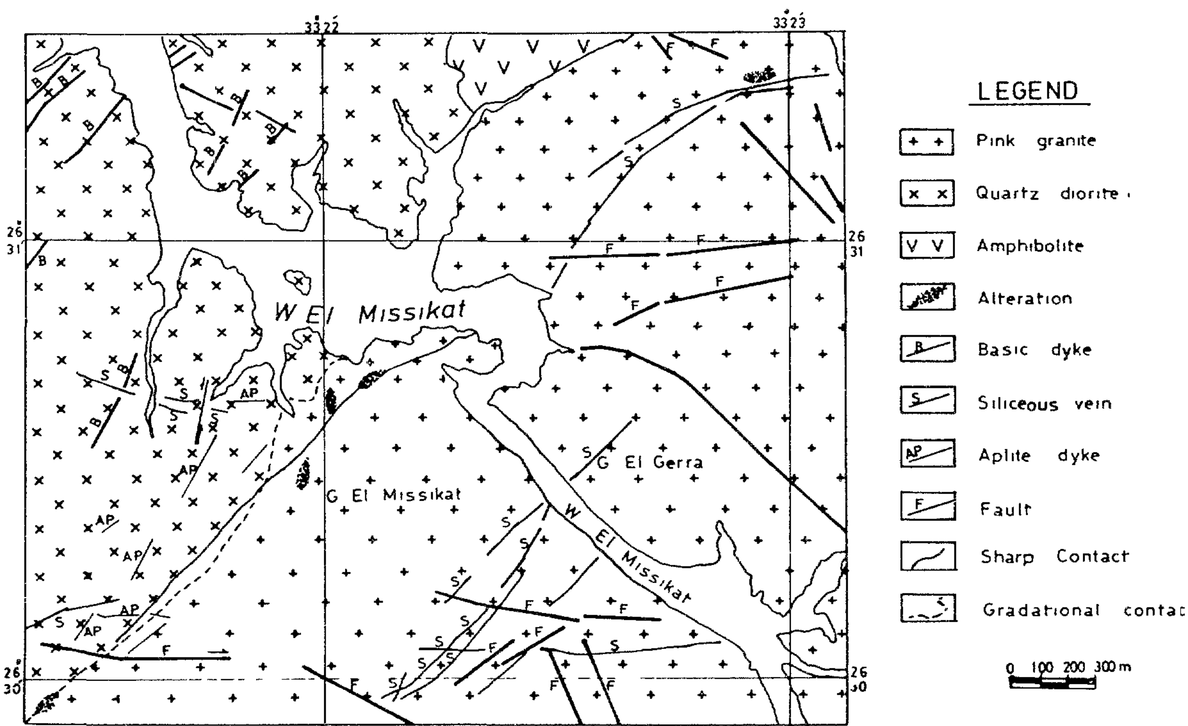

FIG. 4. Geologic map of the northern part of Gebel El-Missikat.

is bound from the northeast and southwest by two NW faults, and dissected by several others.

The granite of El-Erediya is essentially composed of alkali feldspars, quartz and plagioclase, with very subordinate amounts of biotite, sphene, apatite, zircon and opaque minerals. Hydrothermal alterations are common in the form of silicification, kaolinization as well as subordinate sericitization and argillic alteration. Jasper is commonly developed as fracture fillings, associated by hematitization and limonitization. The granite around the jasper veins is highly silicified with a deep reddish colour due to impregnation of the feldspars by hematite dust. This effect dies out gradually away from the veins which occur mostly along faults and fractures and which are branching out from them into the centre of shear zones. Jasper is the ultimate product of silicification of the granite in which the minerals are progressively replaced by jasper. The silicified granite zone is surrounded by a zone of kaolinized granite, which grades outwards into the fresh granite. Hematitization, limonitization and manganese stainings are common, without a regular pattern.

El-Erediya granite has a background radioactivity ranging between 35 - 50 μR/hr. High radioactivity was recorded in the extreme southern part of a mineralized shear zone (No. 8 in Fig. 3), (El-Kassas (17)) which carry disseminated pitchblende and secondary uranium minerals, mainly uranophane with subordinate β-uranophane, soddyite and renardite (Attawiya (21)). Detailed survey of the area around this shear zone showed the occurrence of several others which are very similar in all aspects except radioactivity and uranium content (Fig. 3).

2.2. El-Missikat area

The pink granite of Gebel El-Missikat is medium to coarse grained and composed of potash feldspars (mainly perthite), quartz, sodic plagioclase and subordinate biotite. Iron oxides occur as clots of hematite and limonite. Silicification, sericitization and kaolinization are common. The pink granite has a gradational contact with the grey granite. Within the contact zone (several tens of metres) it contains abundant mafic minerals and encloses dark, rounded to oval shaped xenoliths as well as pegmatite lenses ranging in size from few cm to about 3 m, some of which contain magnetite.

Across the northwestern slope of Gebel El-Missikat, an ENE trending shear zone is located. It extends southwestwards within the older granite and northeastwards in Gebel El-Garra (Fig. 4).

This shear zone is defined by an intricate system of siliceous veins which have a general ENE trend. In several places, the shear zone is defined by two veins of ENE trend which seem to fill segments of 2 parallel faults with a horizontal component of displacement. In such places, feather fractures are developed at low angles to the main veins. These feather fractures are also filled by siliceous veinlets. The granite between the siliceous veins is highly brecciated, silicified and altered. Besides widespread silicification, sericitization and kaolinization are also common, with a less regular zoning pattern than in El-Erediya. Other siliceous veins also occur in several parts of Gebel El-Missikat and Gebel El-Garra, some with radiometric anomalies. Visible uranium minerals were recorded in this shear zone.

3. El-EREDIYA URANIUM OCCURRENCE

The outcrops of the shear zone in El-Erediya occurrence are mostly in the form of linear segments of a general north eastward trend (Fig. 3). They are vertical to very steeply dipping southeast. Their structural details are given in

TABLE I. FREQUENCY DISTRIBUTION AND MAIN DIRECTIONAL TRENDS OF LINEAR SEGMENTS OF THE SHEAR ZONES AND THEIR LENGTH PROPORTIONS, MEASURED ON THE SURFACE OF EL-EREDIYA OCCURRENCE.

TREND	FREQUENCY		LENGTH PROPORTION		DIRECTION AND AMOUNT OF DIP
	NO.	%	LENGTH M	%	
N-S	12	12.6	326	12.1	MOSTLY DIPPING TO E (VERY STEEPLY), OCCASIONALLY TO W (VERY STEEPLY)
NNE-SSW	25	26.3	790	29.3	NEARLY EQUALLY DIPPING TO ESE (VERY STEEPLY), OR TO WNW (STEEPLY)
NE-SW	36	37.9	963	35.7	MOSTLY DIPPING VERY STEEPLY SE TO VERTICAL, OCCASIONALLY DIPPING NW (VERY STEEPLY)
ENE-WSW	16	16.8	492	18.2	MOSTLY DIPPING N (STEEPLY), OCCASIONALLY NNW
E-W	3	3.2	52	1.9	MOSTLY DIPPING N (STEEPLY), OCCASIONALLY TO S (VERY STEEPLY)
NNW-SSW	3	3.2	77	2.8	VERTICAL TO STEEPLY WSW
TOTAL	95.0	100.0	2,700	100.0	

TABLE II. FREQUENCY DISTRIBUTION OF THE STRUCTURAL FEATURES IN THE MAIN DIRECTIONAL SETS, EL-EREDIYA.

SET NO.	TREND	FRACTURES WITH JASPER		FRACTURES WITH MN & FE OXIDES		FRACTURES WITH APLITES		BARREN FRACTURES		FAULTS		TOTAL	
		NO.	%	NO.	%	NO.	%	NO.	%	NO.	%	NO.	%
1	N-S	23	13.4	12	10.0	5	33.3	14	18.7	7	16.7	61	14.4
2	NNE-SSW	46	26.7	24	20.0	1	6.7	11	14.7	9	21.4	91	21.4
3	NE-SW	72	41.8	53	44.2	-	-	24	32.0	17	40.5	166	39.2
4	ENE-WSW	23	13.4	21	17.5	-	-	10	13.3	2	4.8	56	13.2
5	E-W	6	3.5	3	2.5	-	-	4	5.3	3	7.1	16	3.8
6	NNW-SSE	2	1.2	-	-	4	26.7	1	1.3	-	-	7	1.7
7	NW-SE	-	-	6	5.0	5	33.3	8	10.7	4	9.5	[illegible]	5.4
8	WNW-ESE	-	-	1	0.8	-	-	3	4.0	-	-	4	0.9
TOTAL		172	100.0	120	100.0	15	100.0	75	100.0	42	100.0	424	100.0

Table I and Fig. 5a. The jasperoid veins within the shear zone vary in thickness between 2 and 20 cm and are filling mostly parallel fractures in the centre of the zones. Where they intersect, the thickness increases up to 50 cm. Table II and Fig. 5b-f show structural features at subsurface.

Systematic measurements of gamma radioactivity were carried out on the granite and the shear zones in the subsurface using GM counter model GMT-3T (Table III). From these radiometric data, a threshold value for anomalous radioactivity was found to be 80 cps, below which all values are considered background fluctuations. Spot anomalies, ranging between 80 and 130 cps, were located in the shear zones mainly along faults and fractures occupied by jasperoid veins. The highly radioactive parts are restricted to shear zone No. 2, where 7 highly radioactive sections were located. Three of these sections (No. IV, V, and VI, Table IV) are connected with massive and disseminated pitchblende as well as secondary minerals, mainly uranophane. The total extent of these three sections is 38 m along the central part of the shear zone.

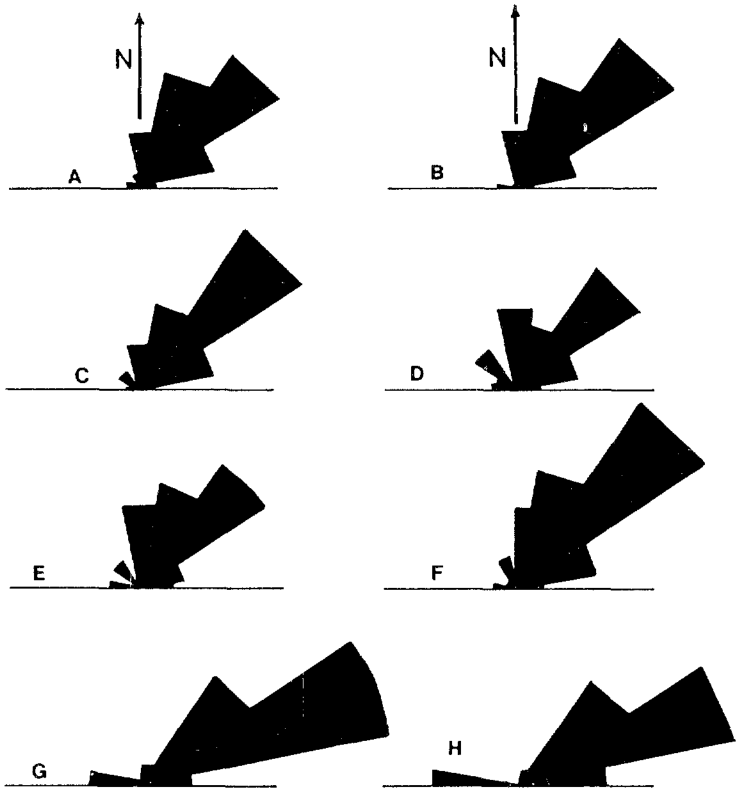

FIG. 5. Rose diagrams of the structural features of El-Erediya (a-f) and El-Missikat (g, h) uranium occurrences. a) 95 segments of silicified shear zones in the outcrop; b) 172 fractures by jasper at subsurface; c) 120 fractures with stainings of manganese and iron oxides at subsurface; d) 75 barren fractures at subsurface; e) 42 faults; f) all structural elements at subsurface (424 elements); g) 33 main siliceous veins within the shear zone at surface; h) 229 fractures filled with silica at subsurface.

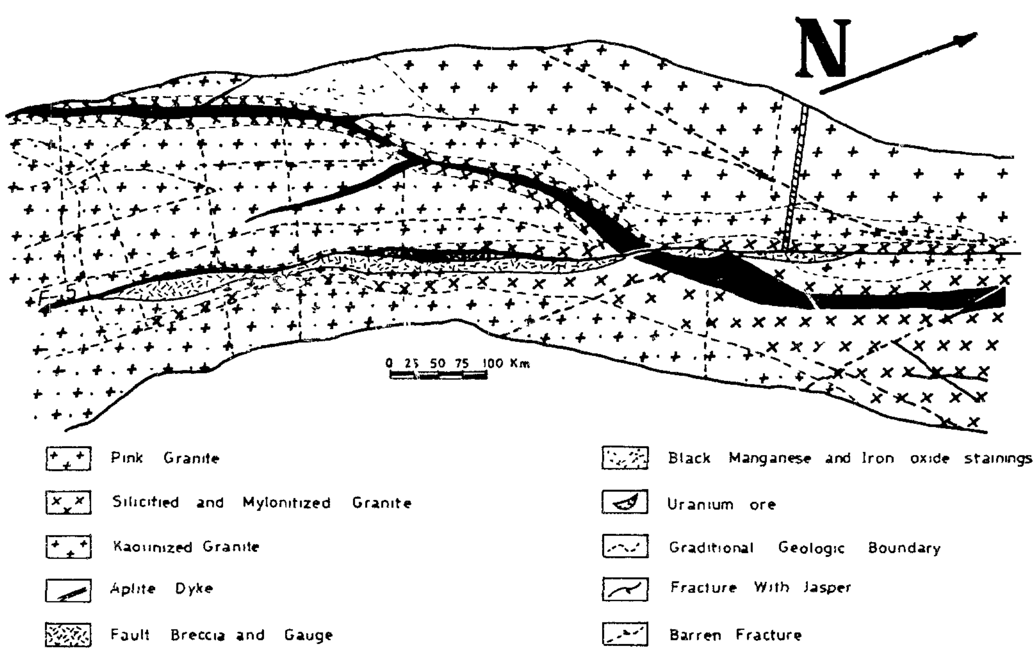

FIG. 6. Subsurface geologic map of the mineralized section no. IV of shear zone no. 2, El-Erediya uranium occurrence.

TABLE III. RESULTS OF GAMMA RADIOACTIVITY MEASUREMENTS ON THE ROOF OF UNDERGROUND TUNNELS ALONG EL-EREDIYA SHEAR ZONES.

NUMBER OF SHEAR ZONES	STATISTICAL PARAMETERS		
	RANGE CPS	ARITHMETIC MEANS CPS	STANDARD DEVIATION CPS
MAIN ADIT	35 - 120	45.0	9.69
SHEAR ZONE 1 DRIFT I	35 - 80	47.48	6.96
SHEAR ZONE 2 DRIFT II + III	40 - 3000	70.53	112.57
SHEAR ZONE 3 DRIFT IV + V	35 - 90	44.00	9.44
SHEAR ZONE 4 DRIFT VII	40 - 95	51.7	10.2
SHEAR ZONE 5 DRIFT IX	40 - 80	52.3	9.15
SHEAR ZONE 6 DRIFT XI	40 - 120	49.02	6.66
SHEAR ZONE 7 DRIFT VI	40 - 80	47.54	6.52
SHEAR ZONE 8 DRIFT VIII + XIII	40 - 130	56.60	8.92
SHEAR ZONE 9 DRIFT X	40 - 120	49.4	8.28

TABLE IV. RESULTS OF GAMMA RADIOACTIVITY OF THE THREE MINERALIZED SECTIONS OF SHEAR ZONES NO. 2, MEASURED ON THE ROOF OF DRIFT II AND III OF EL-EREDIYA EXPLORATORY MINE.

RADIOACTIVITY / MEASURED ON	RADIOACTIVITY IN CPS USING INSTRUMENT G.M.T. 3T								
	ANOMALY NO. IV			ANOMALY NO. V			ANOMALY NO. VI		
	RANGE	$\bar{x}$	S	RANGE	$\bar{x}$	2	RANGE	$\bar{x}$	S
ALL THE ROOF OF THE MINERALIZED SECTION	40-3000	117.0	249.4	40-1300	85.65	121.4	40-450	76.29	41.80
FRACTURES FILLED BY JASPER (MINERALIZED FRACTURES)	70-3000	242.3	540.14	60-1300	168.54	282.24	70-450	128.77	60.36
SILICIFIED AND MYLONITIZED GRANITE	40- 200	77.0	39.4	40- 200	65.8	27.0	40-140	67.5	25.00
KAOLINZED GRANITE	40- 85	65.0	10.7	40- 85	54.88	9.6	40-85	58.37	10.63

3.1. Mineralized section No. IV

In this section, the mineralization occurs at the hanging wall of a jasperoid vein occupying the main fault at the centre of the shear zone with clear alteration zoning (Fig. 6). It occurs in the form of a thin band of yellow secondary uranium minerals which extends for about 2 m, with a thickness between 2 and 4 m. The jasperoid vein occupies a fault zone (F-5) at the centre of the shear zone. The thickness of jasper ranges between 2 and 10 m. The fault strikes generally N40°E - S40°W and dips steeply (70° - 85°) SE. This fault is open in many parts along its extension, and these openings are filled by breccia and fault gauge 2 - 20 m in width, and 1 - 4 m in length.

Besides the well displayed alteration zoning, there are red hematitization, some yellow limonitization and black manganese and iron oxide stainings. Hematitization is closely connected to the parts around the mineralization. Limonitization is very abundant and occurs as yellow patches and stainings on some fracture and joint planes.

Another jasperoid vein 5 - 15 cm thick, with many branches, passes through the mapped area (Fig. 6) with a general trend of N50°E - S50°W and dip of 80°SE. It is intersected by the mineralized fault at the central part of the mapped area. There is no brecciation and no uranium mineralization associated with this jasperoid vein.

3.2. Mineralized section No. V

This section is located few metres to the west of section No. IV and is connected with the same fault No. 5 (Fig. 7). The jasperoid vein is thin and varies from 2 to 5 cm in thickness. The same zoning of alteration also occurs here.

Secondary uranium minerals occur disseminated in fault gauge and mixed with the argillic alteration products in the fault zone. Very closely spaced fractures and microfractures form a network branching from the main fault. Secondary uranium minerals occur within these microfractures but also as disseminations in the country rock.

3.3. Mineralized section No. VI

This section is located about 22 m west of section V (Fig. 8). Primary and secondary uranium minerals were encountered in this section. They are closely connected with fractures and faults occupied by jasper. The same zoning of alteration occurs here. However, the kaolinized granite is sheared in some parts. The mineralized fault (F-7, Fig. 8) trends in N60°E - S60°W and dips 80° to SE. It deviates to N50°E - S50°W at the eastern side. At the central part of this section many fractures branch from the main fault with an average angle of 30°, forming a net work, with lensoidal bodies of fault breccia. In this part a lens of massive pitchblende enveloped by a thin layer of secondary uranium minerals was encountered. This lens extended along F-7 for about 4 m. Its maximum thickness was 30 cm, which thinned out on both sides to a thin film at the jasperoid vein. The lens was located at nearly middistance between the roof and floor of the excavation and extended vertically for an average distance of 40 cm. The pitchblende was protected between two sets of jasperoid veins filling fault No. 7 and its branches. Furthermore, secondary uranium minerals occur at the westernmost part, filling microfractures deviated from the main fault at the centre of the shear zone.

The data presented here for the three mineralized sections of shear zone No. 2 show that

(i) the uranium mineralization is spotty and disconnected. It is restricted to jasperoid veins along ENE faults or to gauges of these faults.

(ii) Alteration zoning is consistent.

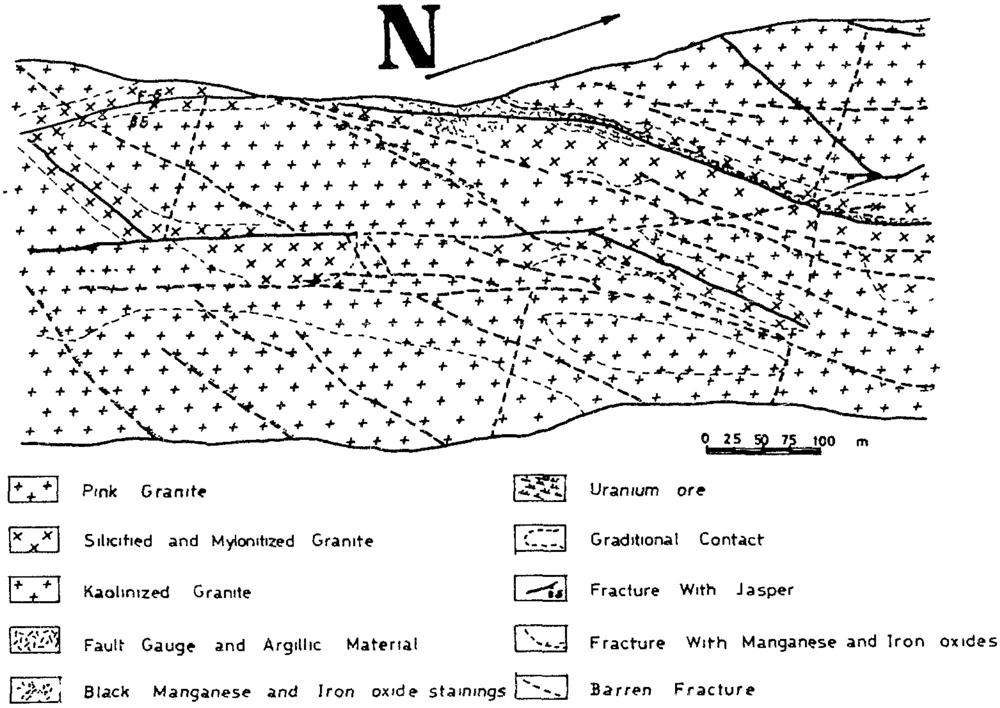

FIG. 7. Subsurface geologic map of the mineralized section no. V of shear zone no. 2, El-Erediya uranium occurrence.

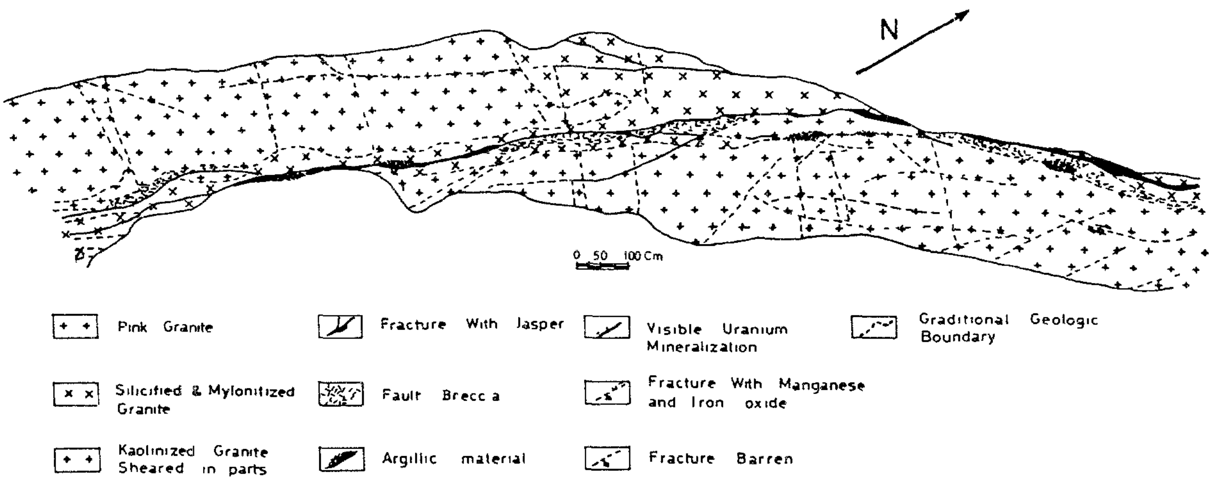

FIG. 8. Subsurface geologic map of the mineralized section no. VI of shear zone no. 2, El-Erediya uranium occurrence.

(iii) The radioactive halo around the mineralization is very narrow.

(iv) The primary mineral is pitchblende which is highly oxidized to secondary minerals, except where jacketed by silica.

(v) Jasper veins were produced in more than one generation, mineralization is associated with the latest one.

4. EL-MISSIKAT URANIUM OCCURRENCE

From surface and subsurface observations, it was found that uranium minerals as well as high radioactivity are associated with the siliceous veins within and branching from the shear zone. These veins are irregular in shape and variable in thickness from few cm to about 3 m. They are always surrounded by a zone of silicified granite up to 5 m thick.

These types of siliceous material filling the veins can be distinguished into three types, namely light-coloured silica, black silica and jasperized silica. The light-coloured silica is micro- to cryptocrystalline while the latter two types are cryptocrystalline to amorphous. The light-coloured silica displays various colours such as white, grey and pale brown. It is non-radioactive and not associated with uranium minerals. The black coloured silica shows the maximum radioactivity and is the main host of the uranium minerals. The jasperized silica has a deep to rose colour, shows moderate radioactivity and also contains concentrations of uranium minerals, but to a lesser extent than the black silica. Brecciation is very common in which both black and jasperized silica contain subangular fragments of the light-coloured silica. Also, the jasperized silica is brecciated and invaded by straight and sinous veinlets of jasperized silica. This, as well as cross cutting relations of veinlets of the three types of silica shows that they represent three main generations of silica introduction separated by periods of brecciation. The earliest generation was the light-coloured silica, followed by the black silica and then finally by jasperized silica. Vugs are also common within the brecciated parts of the veins.

33 main siliceous veins within the shear zone on the surface were measured and their trends are presented in Fig. 5g. Within the investigated part of the shear zone in subsurface, 229 veins and veinlets of silica were measured and their trends are presented in Fig. 5h. Northerly trending faults cut and displace the mineralized shear zones in several places. Some of them have weak alteration zones, but all are non-radioactive and non-mineralized.

At surface, all radiometric anomalies in the shear zone are connected with black silica and to a lesser extent to jasperized silica. Most of these anomalies are spotty and disconnected, extending only for few centimetres. However, within a section of about 500 m in the middle of the shear zone, the anomalies are intense and extend for variable distances up to about 5 m along the shear zone. The anomalies in this section are associated with well developed parts of the siliceous veins. Visible secondary uranium minerals (mainly uranophane) are disseminated within these anomalies. Few channel samples across the shear zone within this anomalous section assay up to about 5,000 ppm U.

On the other hand, several radiometric anomalies were also recorded within the mineralized section of the shear zone at subsurface. Some of the anomalies are associated with visible secondary uranium minerals disseminated in altered rocks which occur as lensoidal masses, elongated mostly in the direction of the shear zone. These masses may be correlated with those at surface (Fig. 9).

The secondary uranium minerals occur as thin films or bundles of acicular needles, as well as fine clots along microfractures, and coating cavities and vugs. Very fine grains of pitchblende were also recorded in some black and jasperized silica samples. Small amounts of pyrite, chalcopyrite, galena, sphalerite and molybdenite are present in association with the uranium minerals. Fluorite is consistently accompanying the uranium minerals. It occurs as discrete well formed cubes up to 3 mm across or as aggregates of very minute crystals lining cavities, vugs and fractures. It displays various colours such as pink, green, yellow, purple, blue, violet and colourless.

The chemical composition of 12 selected channel samples from the mineralized section of the shear zone at surface are given in Table V (Attawiya (22)). This shows that the main chemical constituent of the veins is silica. Al_2O_3, CaO, Na_2O and K_2O constitute together less than 4 % of the rock and are present mostly in form of minor amounts of feldspar and its alteration products of clay minerals,

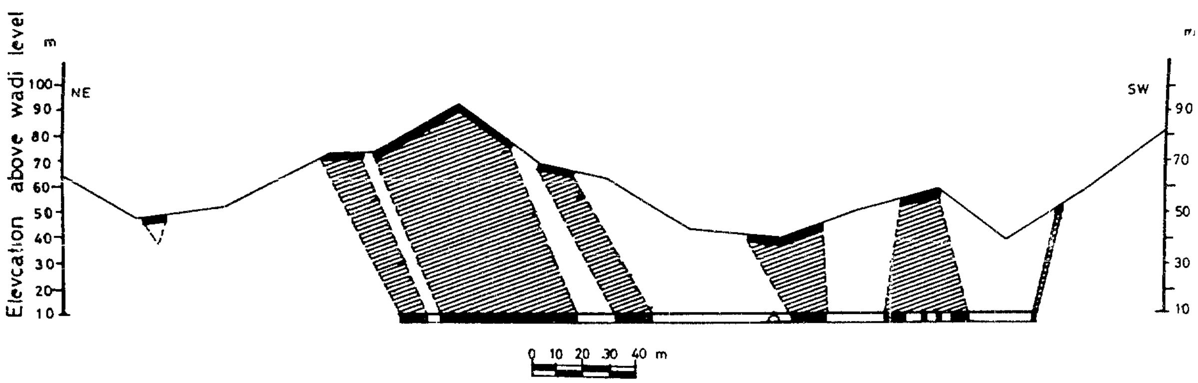

FIG. 9. Projection of explored surface and subsurface of El-Missikat uraniferous shear zone.

TABLE V. RANGE AND AVERAGE OF MAJOR AND TRACE ELEMENTS IN 12 CHANNEL SAMPLES OF THE MINERALIZED SECTION OF EL-MISSIKAT SHEAR ZONE COMPARED WITH A FRESH GRANITE SAMPLE (IN %).

	CHANNEL SAMPLES		FRESH GRANITE
	RANGE	AVERAGE	
SiO_2	91.10 - 96.49	93.87	74.05
TiO_2	0.04 - 0.34	0.15	0.06
Al_2O_3	0.77 - 4.85	2.81	13.75
Fe_2O_3	0.67 - 2.20	1.02	1.03
FeO	0.07 - 0.28	0.18	0.44
MnO	0.01 - 0.07	0.02	0.04
MgO	0.07 - 0.35	0.15	0.34
CaO	0.23 - 0.93	0.36	0.63
Na_2O	0.03 - 0.07	0.04	4.41
K_2O	0.10 - 0.78	0.45	4.04
P_2O_5	0.01 - 0.02	0.01	0.19
H_2O+	0.11 - 0.33	0.27	0.33
H_2O-	0.04 - 0.33	0.22	0.08

as well as fluorite (for CaO). Attawiya (22) noted a strong negative correlation between U and Th in these samples. He explained this as a probable result of oxidation and leaching of uranium.

The data presented here for El-Missikat uraniferous shear zone indicate that

(i) the concentration of uranium minerals is restricted to the black silica and to a lesser extent to the jasperized silica in veinlets trending ENE within the shear zone;

(ii) the uranium minerals are spotty and disconnected but there may be a correspondence between surface and underground concentrations of uranium minerals indicating probably the vertical extent of the mineralized part, a case not encountered in El-Erediya;

(iii) silica was introduced along fractures in three generations; uranium is associated with the later two.

(iv) the primary mineral is pitchblende in disseminated form which is highly oxidized and associated with base metal sulfides.

5. ORIGIN OF THE URANIUM MINERALIZATION AT EL-EREDIYA AND EL-MISSIKAT OCCURRENCES

Mineralogical, petrographical and geochemical studies on these two occurrences are still scarce, so only inferences can be made at the present state of knowledge concerning their origin. The field studies presented here indicate the similarity of both occurrences which suggest a common or similar mode or origin. Both are an example of the simple pitchblende vein deposits referred to by Gangloff (23). They are closely associated with and restricted to the younger granite itself. So it is reasonable to suppose that the mineralization is related to the granite. Thus, three aspects of the origin of El-Erediya and El-Missikat uranium occurrences will be discussed here: the source of the granite, the source of the mineralizing fluids and the source of the uranium.

According to Greenberg (10), Hussein et al. (7) and Stern et al. (11) the El-Erediya and El-Missikat granites originated from partial melting of subcrustal material of oceanic character with possible additions from the mantle.

Greenberg (10) showed that El-Erediya and El-Missikat plutons have been affected by widespread deuteric and hydrothermal alterations. This soaking is a common phenomenon in the younger granites of Egypt (Bugrov et al. (13), Hussein (14), Sabet et al. (15)). The uranium-bearing fluids could have been derived from the same magma that formed the granite itself, most probably at a late stage of the magmatic activity. However, other sources of mineralizing and alteration fluids cannot be excluded at present. For example, Simpson et al. (24) showed that uranium concentrations in some granites of the British Isles were formed by circulation of meteoric waters in convection cells created by diapiric intrusions of granitic magma into high levels of the crust. These convection cells leach out metals in descending currents and redeposit them in the roof and peripheral parts of the granitic plutons. A similar model may be proposed for El-Erediya and El-Missikat uranium occurrences. Widespread hydrothermal alteration with associated mineralizations were reported by Habib (25) around some younger granite plutons in the Eastern Desert. The wide occurrence of siliceous and jasperoid veins in El-Erediya and El-Missikat plutons (Fig. 3, 4), although barren, is significant in this respect.

Two possible sources can be considered for uranium. It can be released from the granite itself by dissolution of accessory uranium-bearing minerals and then be redeposited in shear zones by percolating fluids (Attawiya (22)). This was shown in the case of Tertiary granites of south England by Simpson et al. (24). On the other hand, Rogers et al. (26) showed that there is a mechanism, though poorly understood, by which uranium is released from the mantle into liquid and fluid phases. It is possible that uranium may be released from the mantle not only into magmas but directly into volatile phases. A third theoretically possible source is leaching of uranium from metasediments and acidic metavolcanics of the country and roof rocks.

6. CONCLUSIONS

El-Erediya and El-Missikat uranium occurrences occur in two younger granite plutons in the central Eastern Desert of Egypt. These younger granites were produced by the magmatic activity marking the end of the Pan African Orogeny and the beginning of an orogenic activity in the Egyptian basement. The two uranium occurrences represent a case of simple pitchblende siliceous vein-type deposits. The deposition of uranium minerals is structurally controlled by northeasterly fractures within the granite and hosted in cryptocrystalline to amorphous jasperoid and black silica, which was introduced in more than one generation due to repeated rejuvenation of structures. Associated alterations are silicification, kaolinization and sericitization which are zonally arranged around the veins. Widespread hematitization and manganese and iron oxide stainings are imposed on altered and fresh rocks. The primary mineral is pitchblende which occurs in the form of fine disseminations in the silica, as thin films or streaks along fractures or as lensoidal masses between intersecting fractures. It has been strongly oxidized and probably also intensely leached, resulting into highly spotty distribution of radioactivity and uranium along shear zones. The secondary minerals are mainly uranophane, beta-uranophane, soddyite and renardite. Subordinate amounts of sulfides as well as fluorite are the main associates of the mineralization. The present data suggest that the mineralizing fluids have their source in the granitic magma itself with possible contributions from meteoric waters. Uranium was leached out from the accessory U-bearing minerals, with possible addition from the mantle carried up by the hydrothermal fluids.

It is notable that high radiometric anomalies associated with signs of uranium mineralization widely occur in the Egyptian younger granites in many areas from the far south to the far north in the Eastern Desert. This indicates the great potential of these granites as host for uranium deposits.

ACKNOWLEDGEMENTS

The authors express their thanks to Prof. Dr. Abdallah A. Abdel-Monem who kindly reviewed and criticized the manuscript.

REFERENCES

(1) EL-RAMLY, M.F., AKAAD, M.K., The basement complex in the central Eastern Desert of Egypt between latitudes 24°30' and 25°40'N, Geol. Surv. Egypt, paper no. 8 (1960) 24 pp.

(2) AKAAD, M.K., EL-RAMLY, M.F., Geological history and classification of the basement rocks of the central Eastern Desert of Egypt, Geol. Surv. Egypt, paper no. 9 (1960) 24 pp.

(3) EL-RAMLY, M.F., A new geological map for the basement rocks in the Eastern and south Western Deserts of Egypt, scale 1:1,000000, Annals Geol. Surv. Egypt, 2 (1972) 1-18.

(4) SABET, A.H., On the stratigraphy of the Egyptian basement rocks, Annals Geol. Surv, Egypt, 2 (1972) 79-102.

(5) EL-GABY, S., Petrochemistry and geochemistry of some granites from Egypt, N. Nb. Miner. Abh. 124 (1975) 147-189.

(6) AKAAD, A.K., NOWEIR, A.M., Geology and lithostratigraphy of the Arabian Desert orogenic belt of Egypt between latitudes 25°35' and 26°30'N, IAG (Jeddah), Bull. 3, V. 4 (1980) 127-135.

(7) HUSSEIN, A.A., ALI, M.M., EL-RAMLY, M.F., A proposed new classification of the granites of Egypt, J. Volc. Geoth. Res. 14 (1982) 187-198.

(8) HASHAD, A.H., Present status of geochronological data on the Egyptian basement complex, IAG (Jeddah), Bull. 3, V. 4 (1980) 31-46.

(9) SABET, A.H., BESSONENKO, V., BYKOV, B.A., The intrusive complexes of the central Eastern Desert of Egypt, Annals Geol. Surv. Egypt, 6 (1976) 53-73.

(10) GREENBERG, J.K., Characteristics and origin of Egyptian Younger Granites, Geol. Soc. Am., Bull. 92 (1981) 749-840.

(11) STERN, R.J., GOTTFRIED, D., HEDGE, C.E., Late Precambrian rifting and crustal evolution in the north Eastern Desert of Egypt, Geology, vol. 12 (1984) 168-172.

(12) HUNTING, Assessment of the mineral potential of the Asswan Region, U.A.R. Photogeological Survey, Hunting Geology and Geophysics Ltd. (1967).

(13) BUGROV, V.A., ABOU EL GADAEL, A., SOLIMAN, M.M., Rare metallic albitites as a new type of ore mineralization in Egypt, Annals Geol. Surv. Egypt, 3 (1973) 185-206.

(14) HUSSEIN, A.A.A., Results of mineral exploration program in South Eastern Desert of Egypt, Annals. Geol. Surv. Egypt, 3 (1973) 109-124.

(15) SABET, A.H., CHABANENCO, V., TSOGOEV, V., Tin-tungsten and rare metal mineralization in central Eastern Desert of Egypt, Annals. Geol. Surv. Egypt, 3 (1973) 75-86.

(16) AMMAR, A.A., Application of Aerial Radiometry to the Geology of Wadi El Gidami Area, Eastern Desert, Ph.D. Thesis, Fac. of Science, Cairo University (1973) 424 pp.

(17) EL-KASSAS, I.A., Radioactivity and geology of Wadi Atalla area, Eastern Desert of Egypt, Ph.D. Thesis, Ain Shams University, Cairo (1974) 502 pp.

(18) BAKHIT, F.S., Geology and radioactive mineralization of Gebel El-Missikat area, Eastern Desert, Egypt, Ph.D. Thesis, Ain Shams University, Cairo (1978) 280 pp.

(19) EL-TAHIR, M.A., Radioactivity and mineralization of granitic rocks of El-Erediya occurrence and its comparison to El-Missikat - Rea El-Garra occurrence, Eastern Desert, Egypt, Ph.D. Thesis, Al Azhar University, Cairo (1984) (in preparation).

(20) ABOU DEIF, A., Uranium mineralization along Qena-Safaga Road, M.Sc. Thesis, Al Azhar University, Cairo (1984) (in preparation).

(21) ATTAWIYA, M.Y., Mineralogical study of El-Erediya-1 uranium occurrence, Eastern Desert, Egypt, Arab. Jour. Nucl. Sc. Techn. no. 2, 16 (1983) 221-234.

(22) ATTAWIYA, M.Y., On the geochemistry and genesis of the uranium mineralization of El-Missikat area, Egypt, Annals Geol. Surv. Egypt (1984) (in press).

(23) GANGLOFF, A., Notes sommaires sur la gêologie des principaux districts uranifêres etudiês par le CEA, in: Uranium exploration geology, IAEA Vienna (1970) 77-105.

(24) SIMPSON, R.A., BROWN, G.C., PLANT, J., OSTLE, D., Uranium mineralization and granitic magmatism in the British Isles, Phil. Trans. R. Soc. London, 291 A (1979) 385-412.

(25) HABIB, M.E., Landsat Invest. of Mineralized granites in the area bet. Geb. El-Urf and El-Erediya due West of Safaga, Egypt, Proc. 8th Inter. Symp. Bordue University (1982)

(26) ROGERS, J.W., RAGLAND, P.C., NISHIMORI, R.K., GREENBERG, J.K., HAUCK, S.V., Varieties of granitic uranium deposits and favourable exploration areas in the Eastern United States, Econ. Geol. 73 (1978) 1539-1555.

GEOLOGY AND ORIGIN OF THE SCHWARTZWALDER URANIUM DEPOSIT, FRONT RANGE, COLORADO, USA

A. R. Wallace
U.S. Geological Survey
Denver, Colorado
United States of America

Abstract

GEOLOGY AND ORIGIN OF THE SCHWARTZWALDER URANIUM DEPOSIT, FRONT RANGE, COLORADO, USA

The Schwartzwalder uranium deposit in Colorado was formed from evolved connate fluids which leached all the vein mineral components from the host metamorphic terrane. The metamorphic rocks were deposited in a Proterozoic submarine environment with associated volcanic activity. Uranium mineralization occurred 69.3 $\pm$ 1.2 Ma ago during incipient uplift of the crystalline block of the Front Range. Carbonate-rich fluids produced successive carbonate-sericite and hematite-adularia alteration assemblages in the wall rocks around fractures in the metamorphic rocks. Three stages of subsequent vein mineralization generated massive pitchblende veins with carbonate, sulfide, and adularia gangue. Breccia dikes composed of remobilized fault gouge and ore were emplaced both before and after pitchblende deposition.

The alteration and vein assemblages were produced during repeated major movement along faults in the basement. Fault movement across a narrow zone of brittle rock in the metamorphic sequence provided a permeable conduit along which the hydrothermal fluids ascended. Episodic brecciation dramatically reduced the large confining pressure and induced CO_2 evolution. This process simultaneously increased the pH, decreased the $f(O_2)$ and $f(CO_2)$, and led to the alteration of the wall rocks and the subsequent deposition of adularia, carbonates, and pitchblende in the veins. Reduced and intermediate sulfur species in solution reduced the uranium carried in solution.

Geologic evidence and carbon, sulfur, oxygen, and lead isotopic data require that the components for the vein minerals were derived almost entirely from the metamorphic terrane, and that sedimentary and magmatic sources were volumetrically insignificant at best. The fluids were probably originally of meteoric derivation and resided in deep fracture zones for much of the Mesozoic.

1. INTRODUCTION

The Schwartzwalder uranium deposit, in the Front Range near Denver, Colorado (Fig. 1), is the largest known vein-type uranium deposit in the United States. It is one of more than twenty such deposits that form an elongate belt along the eastern part of the range front. The deposit was discovered in 1949 and, during nearly continuous production since that time, has produced more than 17 million pounds of U_3O_8.

The geology of the deposit has been described by a number of workers during the course of its development, and many other workers have speculated on the origin of the deposit. This report summarizes the results of recent studies, described in greater detail in Wallace et al. (1), Ludwig et al. (2), and Wallace et al. (3), that demonstrate a connate-hydrothermal origin for the deposit.

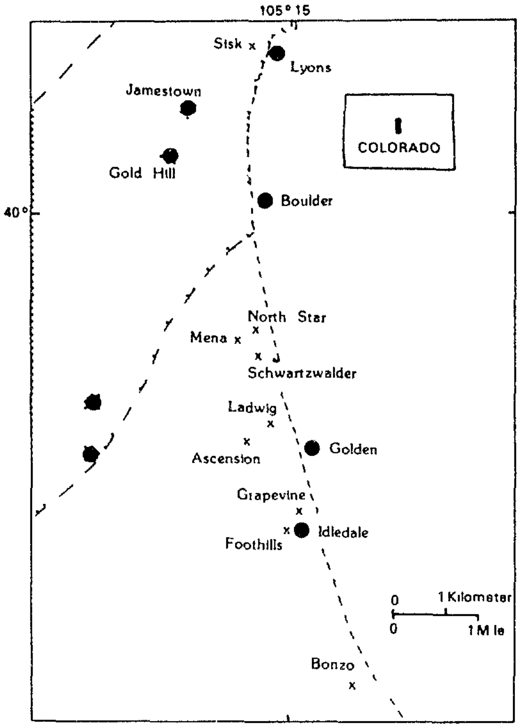

FIG. 1. Location of the Schwartzwalder uranium mine and other uranium mines in the east-central Front Range, Colorado, USA. Stippled area shows the Colorado mineral belt.

2. REGIONAL GEOLOGIC SETTING

The Front Range is composed of Proterozoic metamorphic and igneous rocks which were locally intruded by small stocks of Late Cretaceous to Tertiary age. The protoliths for the metamorphic rocks include sedimentary and volcanic rocks which were deposited in a volcanic arc-backarc basin approximately 1,800 Ma ago (Hills et al. (4)). Several episodes of dynamothermal metamorphism, accompanied by the intrusion of batholiths, transformed the rocks into an amphibolite-grade assemblage of schists and gneisses.

Phanerozoic sedimentation covered the basement with a thick section of sediments, although uplift of the basement during Pennsylvanian and Late Cretaceous orogenesis episodically stripped off the sedimentary cover. Sedimentary rocks of Pennsylvanian to Holocene age, including the basal arkosic Upper Pennsylvanian and Lower Permian Fountain Formation, unconformably flank the exposed basement. Exposure of the basement after Pennsylvanian uplift permitted the formation of a regolith in the crystalline rocks prior to the deposition of the Fountain Formation.

Episodic Proterozoic deformation folded and fractured the crystalline rocks. Brittle deformation created a laterally extensive set of northwest-trending faults which were subsequently reactivated during basement uplift in the Pennsylvanian and the Laramide (Late Cretaceous-Early Tertiary) orogenies. Laramide uplift also generated steep reverse faults along the flanks of the range.

3. GEOLOGY OF THE DEPOSIT

A Proterozoic sequence of hornblende gneiss and mica schist, separated by a relatively thin transition zone of garnet-biotite gneiss and quartzite, hosts the uranium veins of the Schwartzwalder deposit. The hornblende gneiss unit in-

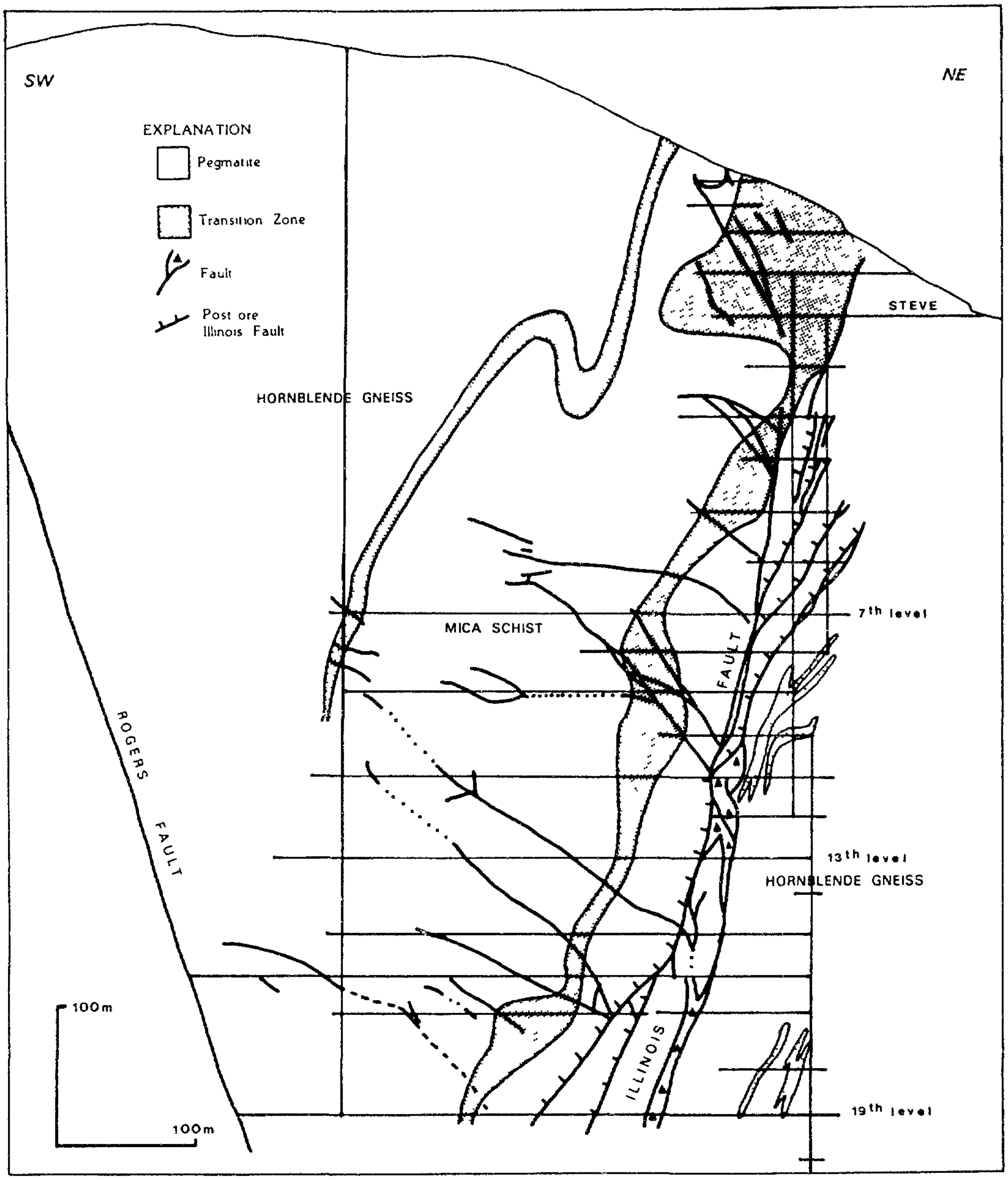

FIG. 2. Cross section of the Schwartzwalder uranium deposit, showing mine workings and geology. From Wallace et al. (1).

cludes layers of amphibolite and calc-silicate gneiss. The hornblende gneiss grades stratigraphically upward into a thin layer of clean quartzite, which is locally intercalated with a micaceous lithology. The garnet-biotite gneiss is massive and contains more than twenty weight percent iron; local facies contain several volume percent pyrite, pyrrhotite, and other sulfides. The mica schist, which is a regionally extensive unit, is predominantly a foliated quartz-mica schist, but it also contains layers of quartzite, conglomerate, iron-formation, and amphibolite. Pegmatite and aplite dikes cut the metamorphic sequence.

The metamorphic rocks were folded during Proterozoic deformation into a steeply plunging synform; as a result, the metamorphic layering is nearly vertical throughout the deposit. Subsequent brittle deformation generated a steeply dipping, northwest-trending fault system which cut and deformed the synform at the crest of the folded transition zone; pegmatites were locally intruded into the faults.

Phanerozoic orogenesis reactivated the faults during Pennsylvanian and Laramide times; the latter episode produced the open structures in which the ore was deposited. The fracture system at the deposit includes three major sets of faults:

(i) the northwest-trending Rogers fault, which consists of two parallel segments,

(ii) the Illinois fault, a steeply dipping cymoid fracture, that formed between the two segments of the Rogers fault, and

(iii) concave-downward tension fractures on the hanging wall of the Illinois fault (Fig. 2). Subseqent, perhaps mid-Tertiary, movement generated a post-ore Illinois fault which is subparallel to its predecessor and which truncated the earlier Illinois fault and tension fractures.

Fault movement in the relatively brittle and texturally homogeneous rocks, especially the garnet-biotite gneiss and quartzite, generated relatively permeable conduits filled with poorly sorted breccia. In contrast, movement in the mica schist produced gouge-filled and impermeable fault zones, and movement in the lithologically and texturally heterogenous hornblende gneiss unit produced variably open and sealed conduits. Therefore, the combination of the steep dips of the layering and cross-cutting Illinois and Rogers faults with the brittle behaviour of the rocks of the transition zone (contrasted with the more ductile enclosing units) produced a deep conduit that concentrated the ascending hydrothermal fluids in a relatively narrow zone.

The uranium ores of the Schwartzwalder deposit are confined entirely to the fractures related to the three fault systems. The post-ore Illinois fault, although devoid of ore, contains carbonate and sulfide gangue minerals that are of supergene origin (Wallace et al. (3)). Hydrothermal fluids altered the wall rocks prior to vein mineralization, and repeated fault movement throughout mineralization continually reopened the veins and modified existing textures.

4. HYDROTHERMAL ALTERATION

Two successive episodes of hydrothermal alteration preceded vein mineralization. Early alteration imposed a carbonate-sericite assemblage on the rocks and was followed by a major episode of fault movement and brecciation. Subsequent, but demonstrably still pre-ore, alteration created a much narrower hematite-adularia assemblage only in the pre-existing alteration assemblage.

The carbonate-sericite alteration pseudomorphically replaces the mafic minerals in the metamorphic rocks; only minor sericite replaces the metamorphic feldspars, and quartz remains unaltered. As a result, the more mafic rocks, such as the hornblende and garnet-biotite gneisses, are more thoroughly altered than the quartzite. The mica schist, due to the gouge formed during fault movement, was impermeable and consequently is not altered. Calculated chemical gains and losses during this period of alteration show that SiO_2 and S were removed and CO_2 introduced into all the rocks. Potassium was selectively enriched in the low-potassium hornblende gneiss, and calcium was similarly enriched in the calcium-poor garnet-biotite gneiss. The concentrations of iron and magnesium remained relatively constant during alteration. Microprobe analyses corroborate this relation and demonstrate that the compositions of the secondary carbonates mimic the Fe-Mg composition of the original mafic minerals.

The hematite-adularia assemblage, which forms a relatively thin alteration zone adjacent to the veins, was generated at the expense of the carbonate-sericite assemblage. Hematite replaces the iron-bearing carbonates and is also disseminated in the metamorphic feldspars; it does not replace metamorphic ferromagnesian minerals. Adularia variably replaces the metamorphic feldspars and the hydrothermal sericite. Because of its lack of alumina, the quartzite was not subject to adularia alteration, but locally a chalcedony-hematite assemblage replaces the quartzite. Chemical analyses of rocks in the hematite-adularia zones show a general increase in SiO_2 and K_2O and a decrease in Al_2O_3, CO_2, MgO, CaO, and Na_2O, although equal volume replacement could not be demonstrated for this episode of alteration.

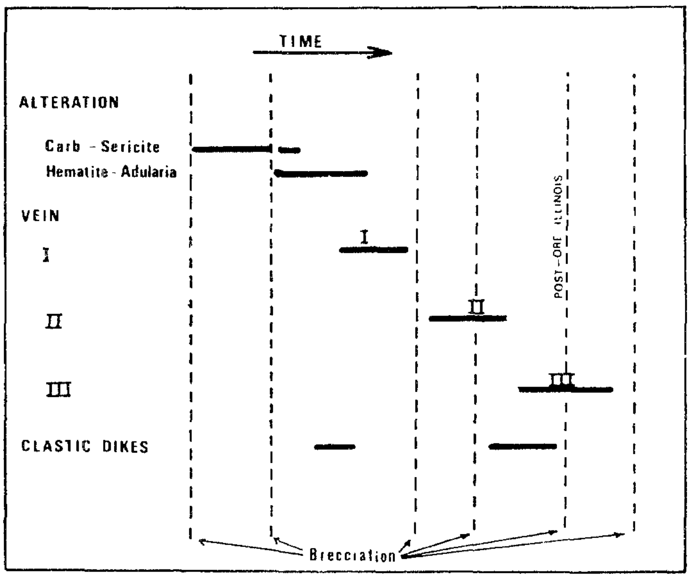

FIG. 3. Paragenetic diagram of the major episodes of alteration, vein mineralization, and emplacement of breccia dikes. Also shown are the major periods of fault movement and related brecciation.

5. VEIN MINERALIZATION

Deposition of uranium and related gangue minerals in the active fault systems occurred during three stages of vein mineralization and two episodes of breccia dike injection (Fig. 3). Mineralization took place 69.3 $\pm$ 1.2 Ma age, concurrent with incipient Laramide uplift of the Front Range (Ludwig et al. (2)). Vein mineralization followed the hematite-adularia stage of alteration and an intervening major episode of fault-related brecciation.

Stage I minerals are sparse, but they indicate at least one pre-pitchblende episode of mineralization. Fragments of pyrite, galena, chalcopyrite, and sphalerite are ubiquitous in all veins; their absence from the enclosing wall rocks precludes local derivation from those rocks.

Stage II mineralization, which included three substages, produced all the pitchblende and most of the gangue minerals in the veins. The first two substages (Stage IIa and IIb) deposited uranium minerals and were separated by a major episode of brecciation; the third substage (IIc) produced a carbonate-sulfide gangue in depositional continuity with IIb. Pitchblende, ankerite/dolomite, adularia, coffinite, and an unnamed Fe-Mo-As sulfide dominated Stages IIa and IIb; carbonates, adularia, and various base-metal sulfides and sulfosalts compose the mineralogy of Stage IIc. Early minerals are extremely fine grained and are intimately mixed with rock fragments and flour. Minerals of Stages IIb and IIc are progressively coarser grained, and rock fragments are less common.

The simple mineralogy of Stage III includes calcite, pyrite, and minor marcasite, all of which are coarse grained. Textures are extremely variable and indicate low-energy deposition with periodic episodes of violent brecciation and fluidized fragment transport. This assemblage is prevalent in the Illinois fault and fills fractures that are demonstrably older than the post-ore Illinois fault.

Breccia dikes composed of rock flour and small fragments of altered rock were emplaced in the veins both prior to and after pitchblende deposition; all dikes are indurated by fine-grained adularia and carbonate. Multiple injections took place during both episodes of dike emplacement. Significant quantities of ore fragments were incorporated into the dikes that formed after ore deposition, although subsequent dikes are devoid of any such fragments.

The veins change downward between the 15th and the 17th level (Fig. 2) from wide zones of mineable ore to narrow, pitchblende-free structures. At lower levels the faults are filled with post-ore breccia dikes, which become increasingly less abundant at higher levels. Ores are present at somewhat greater depths due to downward displacement of several of the tension faults during movement along the post-ore Illinois fault.

6. GEOCHEMISTRY OF ALTERATION AND VEIN MINERALIZATION

6.1. Alteration

On the basis of reconstruction of the depth of mineralization and on stable isotope fractionation and mineral stabilities, the pressure and temperature during alteration were approximately 1,000 bars and greater than 200°C, respectively. Pseudomorphic alteration of amphibole to carbonate and sericite requires an $f(CO_2)$ of at least 1.0 bar, whereas similar alteration of biotite demands an $f(CO_2)$ near 1 kbar at 225°C. The formation of sericite under these conditions requires a maximum pH of 5.65 if K^+ is 0.1 molar. In contrast, the formation of hematite from iron-bearing carbonates and its precipitation in feldspars suggest an increase in pH and a decrease in either the $f(CO_2)$ or increase $f(CO_2)$. Similarly, presuming relatively constant K^+, the subsequent formation of adularia and destruction of sericite demonstrate an increase in pH.

Although the fracture system was initially relatively open, allowing the ubiquitous carbonate-sericite assemblage to form, the wide alteration halo and the presence of sericite suggest that the rocks buffered the fluids and that fluid flow was sufficiently slow to permit water-rock interaction. However, the two stages of alteration were separated by a major episode of brecciation which undoubtedly increased the rate of fluid flow, decreased the water-rock interaction, and thereby favoured the formation of adularia. Also, considering the exceptionally large $f(CO_2)$, major brecciation would have drastically reduced the confining pressure and induced CO_2 effervescence, an increase in pH, and a decrease in $f(O_2)$. Therefore, large-scale brecciation and channel dilation served to produce the observed change from the carbonate-sericite assemblage, which formed at a relatively low pH and very large $f(CO_2)$, to the hematite-adularia assemblage, which was produced under conditions of increasing pH and decreasing $f(CO_2)$.

6.2. Vein mineralization

On the basis of fluid inclusions filling temperatures and on stable isotope fractionation pairs, the temperatures during vein mineralization decreased from above 225°C during Stage I to 86° - 190°C in Stage IIc. Mineral stabilities indicate that the shift from alteration into early vein mineralization took place in response to a decrease in $f(O_2)$ and a concomitant increase in pH. The dominant sulfur species were HSO_4^- and SO_4^{-2}, with a trend approaching the sulfide-sulfate boundary. The major carbon species in solution was H_2CO_3; the concentration of methane was insignificant.

By Stage IIc the fluids had cooled to at least 190°C and probably lower. The coexistence of adularia, chalcopyrite, and pyrite required a pH equal to or greater than 6. Carbonates were still the dominant carbon species, and the fluid chemistry had approached and perhaps entered the sulfide-dominant field.

Pitchblende was deposited between Stages I and IIc. As deduced from the environments of those stages, pitchblende deposition occurred during increasing pH and decreasing $f(O_2)$; both H_2CO_3 and HCO_3^- were abundant, and the sulfate-dominated fluid was approaching the sulfide-dominant field. Under such conditions, uranium was likely carried in a uranyl carbonate complex, and other minerals, such as iron, molybdenum, and arsenic, may have been carried in carbonate and (or) chloride complexes.

The destruction of the uranyl carbonate complex prior to pitchblende deposition was most likely the product of CO_2 evolution during major episodes of fault movement. CO_2 evolution from the fluid would have also produced a pH increase, thereby favouring the deposition of adularia and, during slightly earlier alteration, hematite, and would have induced the observed decrease in the $f(O_2)$ during vein mineralization. The fluid did not boil, however, as a dilute solution with a confining pressure of at least 300 bars (the hydrostatic minimum) should not boil (Haas (5)).

Pitchblende was precipitated from solution by intermediate and reduced sulfur species in solution. Organic matter is not present in the veins, and hematite formed significantly earlier than pitchblende; neither, therefore, was a mechanism for uranium reduction and precipitation. As noted previously, the trend in fluid chemistry approached and perhaps surpassed the sulfide-sulfate boundary at intermediate pH's, a region of stability for intermediate sulfur species. These and (or) progressively more stable sulfide species were able to reduce uranium to form pitchblende; sulfide deposition with pitchblende indicates that reduced and intermediate sulfur species were also precipitated in significant amounts. In addition, decreases in temperature, $f(O_2)$, and pressure and increases in pH led to the precipitation of metal sulfides from various carbonate and chloride complexes. Therefore, pressure release due to brecciation conceivably induced the deposition, either directly or indirectly, of all the observed vein minerals.

7. STABLE ISOTOPES

The stable isotopic compositions of host rock, alteration, and vein minerals were determined by Wallace et al. (3). The oxygen isotope values for alteration and vein minerals from Stages I and II demonstrate that the fluid $\delta^{18}O$ values for the fluids were between 4.6 and 9.7 per mil. The $\delta^{18}O$ values of late Stage IIc and Stage III carbonates show that the fluid composition decreased from -2.5 to -0.6 per mil in Stage IIc to between -9.5 and -2.5 per mil in Stage III. The data from the earlier stages are compatible with either a magmatic source or equilibration of water with metamorphic rocks in a rock-dominant system. The progressively lighter values in the later stages demonstrates progressive mixing of the heavier water with water of probably meteoric origin.

Carbon isotopic values show that the alteration-Stage I-Stage II carbonates were precipitated from a fluid with a $\delta^{13}C$ of approximately -3.6 per mil; values for Stage IIc and III reflect a fluid composition of -4.9 per mil. Although these values eliminate reduced carbon as a source, they permit both metamorphic carbonate and magmatic carbon as possible sources.

The sulfur isotopic compositions of the sulfide minerals in the veins reflect the progressive change from a sulfate-dominated field towards a sulfide-dominated field. Stage I sulfides precipitated from a fluid with a $\delta^{34}S$ of about 0.0 per mil, and their values are consequently very light. Sulfides precipitated during Stage II, near the sulfide-dominant field and with a similar $\delta^{34}S$, have values between -17.1 and 1.6 per mil. Stage III sulfides, which, based upon the oxygen isotope data, were probably deposited from sulfate-dominant meteoric water, have extremely light values that indicate that the fluid $\delta^{34}S$ remained at about 0.0 per mil. These data are consistent with magmatic, sedimentary, and metamorphic sulfur sources.

8. SOURCE OF VEIN COMPONENTS

As defined by the geologic and isotopic data, possible sources for the fluids and dissolved mineral components include the arkosic Pennsylvanian and Permian Fountain Formation, which overlay the basement at the time of mineralization; an unrecognized Laramide intrusive; or the Proterozoic crystalline rocks. However, all evidence collected by Wallace et al. (1) , Ludwig et al. (2), and Wallace et al. (3) demonstrates that the metamorphic host rock terrane was the source for both the fluids and the vein-filling components of the deposits.

Ludwig et al. (2) demonstrated that the uranium and lead in the deposit were derived from a 1,730 $\pm$ 120 Ma old source. The Fountain Formation was derived from the Proterozoic basement, and is therefore a possible source rock. However, the Schwartzwalder-type deposits are found only in the metamorphic terrane of the Front Range, whereas the Fountain Formation, at the time of mineralization, blanketed both igneous and metamorphic basement terranes, and the controlling basement faults extend through both terranes. Therefore, descending fluids carrying metals from the overlying sedimentary rocks were unlikely sources for the mineral components.

The oxygen, sulfur, and carbon isotopic data readily permit a magmatic source for those components, but the uranium and lead data preclude a Laramide magmatic source for those two elements. Magmatic fluids could have leached the uranium and lead from the Proterozoic rocks, but these fluids would have concurrently been contaminated with Proterozoic oxygen, sulfur, and carbon during water-rock interaction. Furthermore, carbonate-adularia veins related to the uranium deposits are restricted to the metamorphic terrane, whereas the known Laramide plutons, of which none are known near the deposits, are not similarly restricted. Therefore, magmatic carbon is not a likely source for the vein carbonates.

All the geologic and isotopic data are consistent with a Proterozoic metamorphic source. The fluid compositions of carbon, oxygen, and sulfur were derived from interaction with the metamorphic host rocks, and the uranium and lead data require a source whose age is identical to that of the metamorphic rocks. The water may have been present in two reservoirs: the deep northwest-trending fault zones which were exposed during Pennsylvanian uplift and along which meteoric water likely circulated, and (or) the regolith in the metamorphic rocks immediately beneath the Fountain Formation. At the time of incipient Laramide uplift, these reservoirs were charged with isotopically evolved connate water that had relatively large concentrations of metals and carbonate. Fault movement created conduits of locally high permeability with relatively low fluid potential, thereby inducing migration of the fluids into these zones. As uplift continued, meteoric and less-evolved fluids were drawn into the system at the source areas, producing the observed decrease in the $\delta^{18}O$ of the hydrothermal fluids. Stage III mineralization represents deposition from fluid of predominantly meteoric origin.

The geologic and isotopic evidence at the uranium deposits in the Front Range indicates that the hornblende gneiss units were probably the major sources for uranium, lead, carbonate, and metals. Geologic and isotopic data indicate that the host and nearby metamorphic rocks represent a metamorphosed sequence of submarine sedimentary and volcanic rocks with associated iron-formation and disseminated sulfides (Wallace et al. (1); Wallace et al. (3)). Uranium is associated with Proterozoic stratiform massive sulfide deposits in Colorado (Sheridan et al. (6)), as well as with exhalative environments elsewhere in North America. Therefore, the geologic association of the Laramide vein deposits with volcanogenic host rocks coincides favorably with the requirement that the mineral components were derived from the metamorphic terrane.

9. CONCLUSIONS

The evidence from Wallace et al. (1), Ludwig et al. (2), and Wallace et al. (3) provide the basis for developing an exploration model for Schwartzwalder-type uranium deposits. The essential ingredients include the following:

(i) The source of the mineral components, and the rock in which the water, regardless of its primary origin, resided, was a submarine sedimentary and volcanic sequence. The uranium deposited with these units was not necessarily abundant, based upon the data of Ludwig et al. (2), nor was it preconcentrated during subsequent metamorphic events; and,

(ii) The structural setting served as a fluid reservoir and subsequently provided conduits for fluid migration to the site of deposition. In the Front Range, the structurally complex margin of the rising basement block provided the necessary features that were not present or were less developed in the core of the block. Furthermore, the structural development at the Schwartzwalder deposit was not repeated to such a great extent anywhere else along the emerging range front, a factor that limited the size of the other uranium deposits in the area (Wallace et al. (1)).

Other factors, such as abundant carbonate for transporting uranium and large confining pressures which were periodically and drastically reduced during fault movement, were clearly important in the development of the Schwartzwalder deposit. However, these influences cannot be evaluated until the proper host rock and structural setting are defined during an exploration program.

ACKNOWLEDGEMENTS

This paper summarizes the results of a cooperative study by Joseph F. Whelan, Kenneth R. Ludwig, and me, all of the U.S. Geological Survey, and by Richard C. Karlson of Cotter Corporation. The contributions of my colleagues to the study and the cooperation of Cotter Corporation have been invaluable during the course of the project. This paper benefitted from thorough reviews by Connie Nutt and Gary Landis.

REFERENCES

(1) WALLACE, A.R., KARLSON, R.C., The Schwartzwalder uranium deposit, I, Geology and structural controls on mineralization, Econ. Geol. (in press).

(2) LUDWIG, K.R., WALLACE, A.R., SIMMONS, K.R., The Schwartzwalder uranium deposit, II, Age of uranium mineralization and Pb-isotope constraints on genesis, Econ. Geol. (in press).

(3) WALLACE, A.R., WHELAN, J.F., The Schwartzwalder uranium deposit, III, Alteration, vein mineralization, light stable isotopes, and genesis of the deposit, Econ. Geol. (in press).

(4) HILLS, F.A., HOUSTON, R. S., Early Proterozoic tectonics of the central Rocky Mountains, North America, Contributions to Geology, University of Wyoming, 17 (1979) 89-106.

(5) HAAS, J.L., Jr., The effect of salinity on the maximum thermal gradient of a hydrothermal system at hydrostatic pressure, Econ. Geol. 66 (1971) 940-946.

(6) SHERIDAN, D.M., RAYMOND, W.H., Preliminary data on some Precambrian deposits of zinc-copper-lead sulfides and zinc spinel (gahnite) in Colorado, U.S. Geol. Survey Open-File Report 77-607 (1977) 27 pp.

GEOLOGY AND GENESIS OF URANIUM DEPOSITS AT THE PITCH MINE, SAGUACHE COUNTY, COLORADO

J. T. Nash
U.S. Geological Survey
Denver, Colorado
United States of America

Abstract

GEOLOGY AND GENESIS OF URANIUM DEPOSITS AT THE PITCH MINE, SAGUACHE COUNTY, COLORADO

Uranium ore in the Pitch Mine, Saguache County, Colorado, occurs mainly along the Chester fault zone, in fault slices that make up the footwall of the Chester upthrust. The ore occurs in the Mississippian Leadville Dolomite, in sandstone, siltstone, and carbonaceous shale of the Pennsylvanian Belden Formation, and in Precambrian granitic rocks and schist. About half of the ore is in the dolomite; and the uranium-mineralized zones are generally thicker, more uniform, and of higher grade in dolomite. The physical reason for this concentration in dolomite is that the dolomite is brecciated: it is the only rock type that is pervasively brecciated in the fault zone. The chemical reason for the concentration in the dolomite is probably the presence of sulfide ion as a reductant: pitchblende and coffinite seem to have been co-precipitated with FeS_2 (as pyrite and marcasite).

Chemical analyses of 116 rock and ore samples demonstrate that ore-bearing dolomites are significantly enriched in FeO, K_2O, S, Mo, Cu, and Ni. Some statistical tests suggest that SiO_2, Al_2O_3, Ba, Sr, Pb, Zn, and V are also enriched with uranium. The strong association of uranium with sulfur, iron, and molybdenum is most important geochemically. Petrologic studies reveal only minor alteration of dolomite adjacent to pitchblende and coffinite. The dark carbonate rocks are not bleached, but minor amounts of very fine grained silica were precipitated along with pitchblende, coffinite, and FeS_2. The geochemistry and the association of pitchblende with marcasite and pyrite suggest that uranium was deposited by aqueous sulfide derived from metastable sulfur compounds, such as thiosulfate, or by biogenic processes.

The Leadville Dolomite is the most important host for uranium in the Pitch Mine, but other units contain important uranium resources where fractured along the Chester fault zone. Brittle character is a prime requirement for favourable host rocks. Chemical properties of host rocks are also important; favourable hosts contain pre-ore sulfide minerals and organic matter. The juxtaposition by faulting of blocks of brecciated Leadville Dolomite and organic-sulfide-rich shale and fine sandstone of the Belden formation may have provided the required combination of structural permeability and a source of reductant.

The Laramide age of Chester fault is a maximum age for the uranium deposits. The most likely time of formation is the Oligocene, when volcanic rocks covered the fault zone, because alteration of volcanic rocks was probably the source of uranium and of silica that formed jasperoid bodies in the fault zone.

Observed and interpreted features at the Pitch deposit suggest a model of ore formation that has wide application around the world. Key factors are:
- a wide zone of brecciation in brittle rocks, as is commonly produced by upthrusts;
- a reductant provided by reactive pre-ore sulfide minerals or organic material and sulfate-reducing bacteria;
- a viable source of uranium, such as altered volcanic rocks.

Pitch mine-type deposits may contain 2000 - 30000 t U_3O_8 with mixed high and low grades.

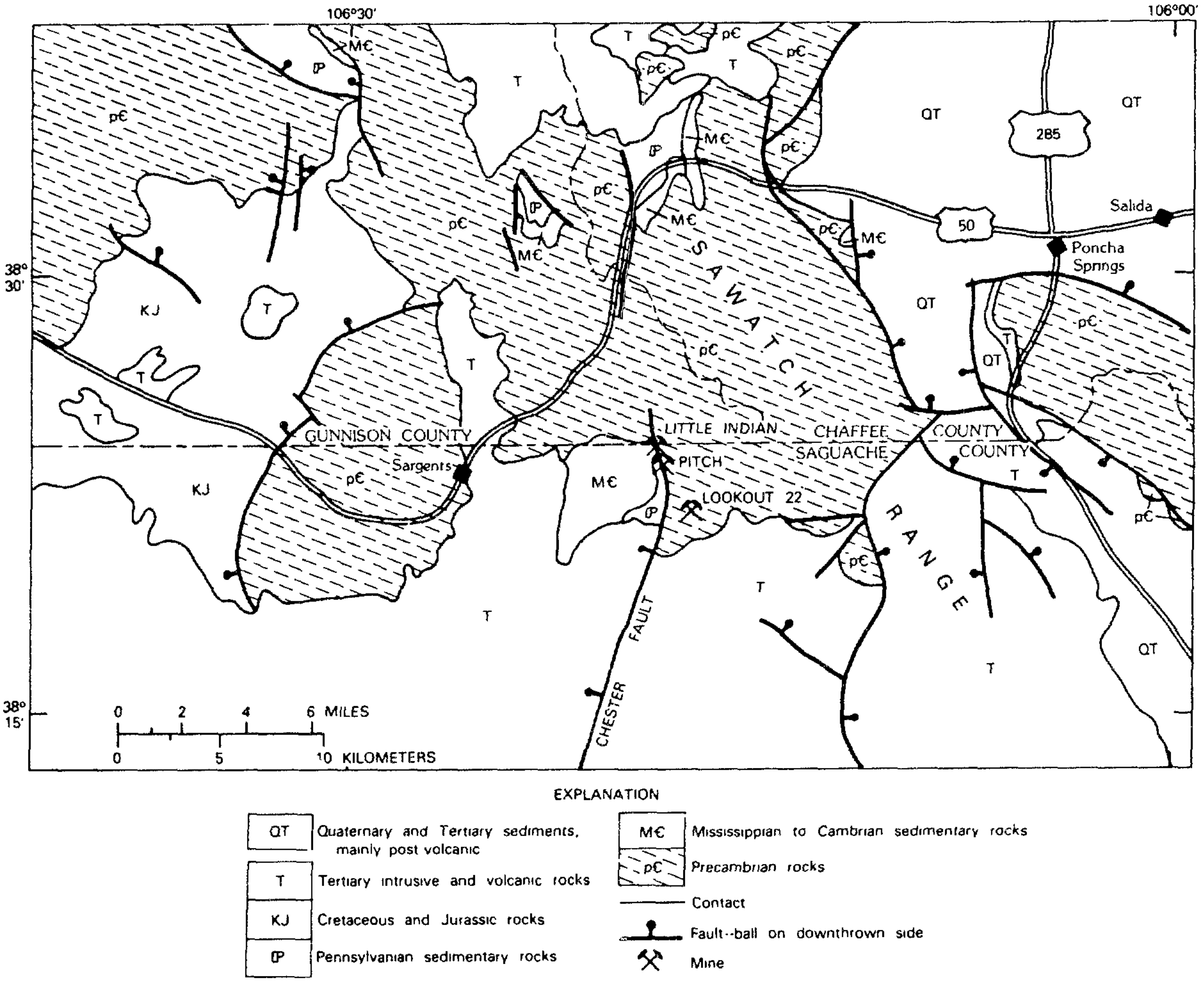

FIG. 1. Generalized geologic map and location of the Pitch Mine, Colorado (after Tweto et al. (19)).

1. INTRODUCTION

The Pitch Mine is in Saguache County, Colorado, about 60 km east of Gunnison (Fig. 1).

The Pitch deposit (formerly known as the Pinnacle) and several other uranium prospects were located in 1955. Mining began in 1959 with the opening of two adits, and ceased in 1962 when the contract with U.S. Atomic Energy Commission expired. About 90,700 t of ore averaging 0.50 % U_3O_8 (454,000 kg U_3O_8) was mined and another 45,400 kg U_3O_8 was recovered by solution mining (Ward (1)). In 1972, Homestake Mining Company acquired the property and began to reevaluate the mine area for additional reserves amenable to open-pit mining, because the previous history of the mine had demonstrated that fault offsets of ore and unstable wallrocks made underground mining costly.

In the period 1972 to 1977, Homestake Mining Company documented a reserve minable by open-pit methods of 1.9 million tonnes of ore at an average grade of 0.17 % U_3O_8 (3,245,000 kg U_3O_8) (Ward (1)). Rather than seek high-grade 'vein-type' ore, Homestake explored for more dispersed ore. Success came in 1973 when the company recognized a 'new' type of ore in brecciated dolomite of the Mississippian Leadville Dolomite. The dolomite was found to be complexly faulted bet-

TABLE I. SIMPLIFIED STRATIGRAPHIC COLUMN IN THE PITCH MINE AREA (AFTER OLSON (6))

OLIGOCENE (?)	QUARTZ LATITE TUFF	SANDY TUFF, 0 - 20 M THICK
	UNCONFORMITY	
PENNSYLVANIAN	BELDEN FORMATION	CONTAINS THREE UNITS: LOWER WHITE SANDSTONE AND BLACK SHALE (40 - 90 M THICK); MIDDLE BLUE-GRAY LIMESTONE WITH RED SHALE AND FINE-GRAINED SANDSTONE (30 - 60 M THICK); AND UPPER GREEN AND BROWN SANDSTONE AND GRAY SHALE (200 M OR MORE THICK)
	UNCONFORMITY	
MISSISSIPPIAN	LEADVILLE DOLOMITE	DARK-BLUE-GRAY TO BROWNISH-GRAY DOLOMITE AND MINOR LIMESTONE; CONTAINS CALCITE AND CHALCEDONY VEINLETS AND LOCAL BLACK CHERT ZONES; ABOUT 130 M THICK
DEVONIAN	PARTING QUARTZITE	VARICOLOURED SHALE AND QUARTZITE; ABOUT 3 - 6 M THICK
	UNCONFORMITY	
ORDOVICIAN	FREMONT DOLOMITE	BLUE-GRAY LIMESTONE AND DOLOMITE; ABOUT 55 M THICK
ORDOVICIAN	HARDING QUARTZITE	WHITE QUARTZITE, COMMONLY LIMONITE-STAINED, AND SOME BLACK SHALE; ABOUT 10 - 12 M THICK
	UNCONFORMITY	
ORDOVICIAN	MANITOU DOLOMITE	LIGHT-PINKISH-GRAY DOLOMITE, 75 - 90 M THICK
CAMBRIAN	SAWATCH QUARTZITE	VITREOUS QUARTZITE; LESS THAN 1 M THICK
	UNCONFORMITY	
EARLY PROTEROZOIC (?) ROCKS		MICA SCHIST, GNEISS, AND AMPHIBOLITE, INTRUDED BY GRANITIC ROCKS

ween slices of sandstone, siltstone, and shale of the Pennsylvanian Belden Formation. Much of the ore mined in 1959 - 1961 also was probably in Leadville Dolomite, but was not recognized as such (J.M. Ward, Homestake Mining Co., oral communication, 1979). Homestake has mined the deposit at a rate of about 600 t per day from an open pit that ultimately will be about 1500 m long and have an average depth of 120 m, but mining ceased in February 1984.

2. GEOLOGIC SETTING

Rocks ranging in age from Precambrian to Oligocene (?) are known in the Pitch Mine area (Table I). Precambrian rocks are chiefly pegmatitic granite, hornblende-biotite schist, hornblende gneiss, and pegmatite. A hematitic regolith was developed on the Precambrian rocks prior to the Cambrian. About 600 m of Paleozoic rocks were deposited above the Precambrian. The lower part of the Paleozoic section, predominantly dolomite, contains units of quartzite, which are useful stratigraphic markers between the similar-appearing dolomites. The Mississippian Leadville Dolomite, the youngest dolomite unit, is the darkest dolomite in the area, and generally is massive with faint laminations. The Leadville is predominantly dolomicrite in the mine area. The dolomite probably formed through early diagenesis of sediments (Nash (2)). The top of the Leadville Dolomite is locally limonitic, the result of a karst that was developed

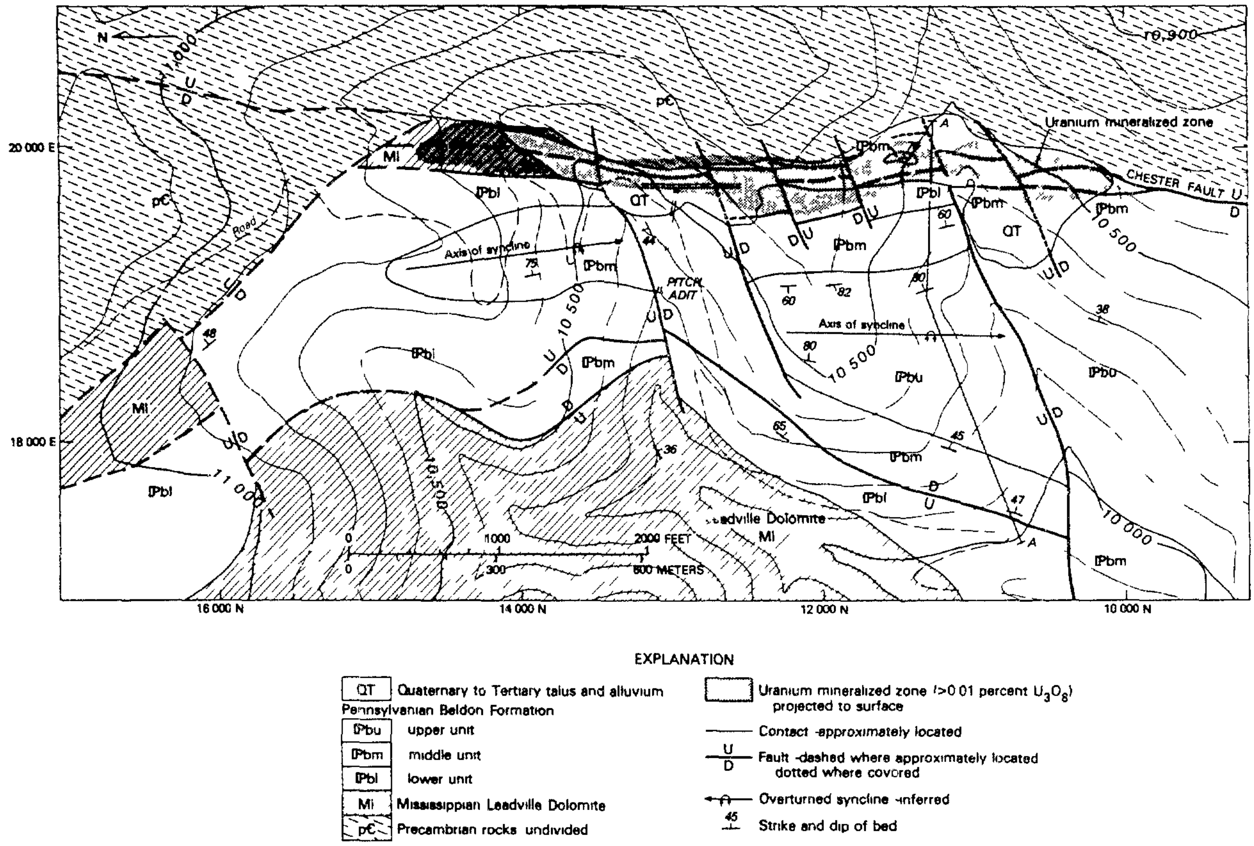

FIG. 2. Geologic map of the Pitch Mine area. Cross section A-A' is shown in Fig. 3. Geology in places adapted from Olson (6) and from J.M. Ward (Homestake Mining Co., unpublished data 1972-1980). Base generalized from 1:2400 map of Homestake Mining Co., grid is mine coordinate system used by Homestake Mining Co.. Elevation contours in feet.

prior to deposition of the Pennsylvanian Belden Formation. The Belden Formation comprises diverse rock types, including coarse kaolinitic sandstone, green, clay-rich, fine sandstone, black and red shale, and gray and black limestone and minor dolomite. Abrupt facies changes within the Belden are common over lateral distances of 300 m. A few erosional remnants of Oligocene (?) quartz latite flows are preserved a kilometer north of the Pitch Mine at a higher elevation. About 6 km south of the mine, more than 300 m of Tertiary andesitic volcanics of the San Juan volcanic field cover Paleozoic rocks.

The major structural feature in the mine area is the Chester fault, which dips east about 70°, strikes nearly due north, and places Precambrian rocks above and west of Paleozoic rocks (Fig. 2 and 3). Net reverse movement along numerous faults is more than 600 m. The fault zone is about 100 m wide in the mine area (Fig. 2). Paleozoic rocks immediately west of the Chester fault are folded into a south-plunging syncline whose east limb is probably overturned under the fault zone (Fig. 3). Farther west, the Paleozoic rocks have a low dip and are gently warped in broad folds. East-trending faults cut the Chester fault zone and form rotated blocks. The Chester fault is of Laramide age; Cretaceous rocks about 20 km to the west are displaced by similar reverse faults. Oligocene (?) volcanic rocks show small displacement, probably from reactivation along the Chester fault.

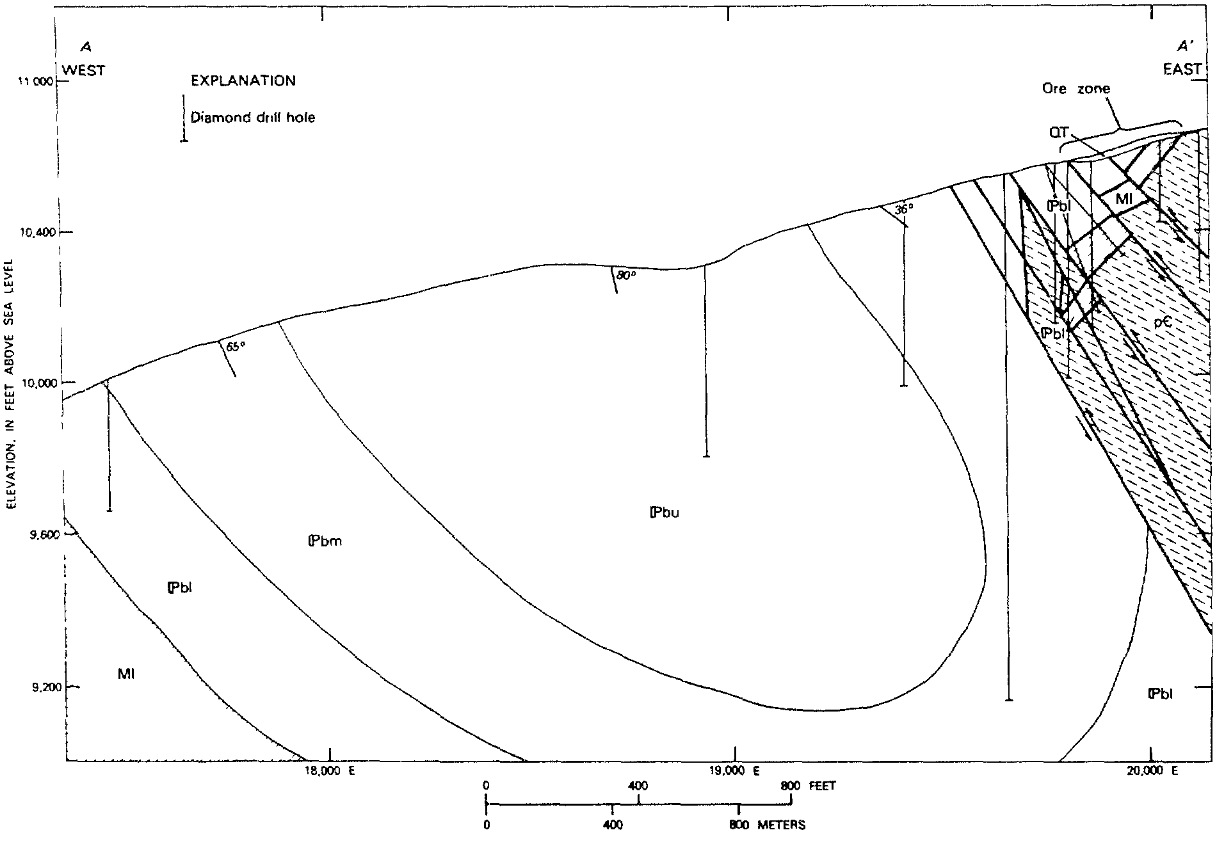

FIG. 3. Cross section of the Pitch Mine area. Line of section shown on Fig. 2. Structure shown in the ore zone is highly simplified. Symbols explained on Fig. 2.

3. URANIUM DEPOSITS

Uranium at the Pitch Mine occurs as oxidized and reduced uranium minerals in dark-gray dolomite of the Leadville Dolomite and in sandstone, black shale, and coaly shale of the Belden Formation. The majority of reserves, notably those having grades in excess of 0.10 % U_3O_8, are in brecciated dolomite. The Belden Formation hosts a relatively large volume of low-grade mineralization, and Precambrian granitic rocks contain local pockets of uranium where fractured. Oxidation occurs to depth of about 100 m along some fracture zones; in the oxidized zones radioactivity greatly exceeds equivalent uranium content. Production from the mine was about 500,000 kg U_3O_8 from 1959 to 1962 (Ward (1)).

The Pitch deposit is the largest in an area of about 50 km² known as the Marshall Pass district. Five other types of uranium deposits occur in this area:

(i) Precambrian biotite schist hosts vein deposits 2 km east of the Pitch Mine. The pitchblende and hexavalent uranium minerals are locally very rich and probably reflect, at least in part, supergene enrichment (Malan (3), Gross (4)).

(ii) Precambrian pegmatite contains veinlets of pitchblende near the Pitch Mine (Ward (1)).

(iii) Ordovician quartzite is fractured along the Chester fault zone 2 km north of the Pitch Mine at the Little Indian Mine, where about 29,500 kg U_3O_8 was mined. Known uranium minerals are hexavalent, but a bed containing organic pellets and carbonaceous debris in the quartzite is regionally radioactive.

(iv) Cretaceous black shales are radioactive in many places about 6 km west of the Pitch Mine and first attracted prospectors to the area.

(v) Eocene (?) carbonaceous regolith contained small but high-grade concentrations of uranium ore that yielded about 1800 kg U_3O_8 from several small deposits 2 - 11 km east of the Pitch Mine (Gross (4)). The regolith is developed in Precambrian rocks and in places is overlain by Tertiary volcanic rocks (Malan (3)); the deposits were mined so quickly that no geologic features were recorded.

The ages and genetic relations of these varioûs types of ore deposits are unresolved problems. Most observers suspect they share a common source, and they may share some formative processes as well.

4. STRUCTURAL CONTROL OF ORE

The most important control on ore at the Pitch deposit is fracturing of brittle rocks along the Chester fault. A review of the literature (Nash (5)) indicated that the structural features here are similar to those at other Rocky Mountain upthrusts, many of which have been explored for petroleum, and can be explained by experimental deformation behaviour. The Chester fault generally dips 60° - 70° to the east, but the highest level of exposure, 1 km north of the Pitch Mine, seems to have flatter dip near 45°. Similarly, other Rocky Mountain upthrusts are characterized by concave downward fault surfaces, and low dip at high structural levels. Paleozoic sedimentary rocks in the footwall of the Chester fault are folded into a probable overturned syncline (Fig. 2 and 3). Some faults west of the upthrust are mapped as thrusts (Olson (6)) and may be splits from the main Chester fault. The Chester fault creates a zone of brecciation about 100 m wide at the Pitch Mine, and the brecciation is particularly intense in the Leadville Dolomite. Maximum fracturing occurs where the fault plane intersects brittle beds at angles near 70°.

The Chester fault zone displays many of the features described in other upthrusts (e.g., Berg (7)) which recently have been explained as products of forced folding and faulting (Stearns (8)). Geologic features (Stearns (8)) and laboratory experiments (Friedman et al. (9)) indicate the importance of pressure, ductility, stratigraphic layering, and degree of attachment to the basement. The basement acts as a massive ram that induces ('forces') folding, faulting, or both in overlying sedimentary rocks. The sedimentary cover at the Pitch Mine is described as 'attached, brittle sections' (Stearns (8)), a circumstance that results in many local faults and fractures because the brittle rocks are attached to the uplifting Precambrian block and cannot slip along it. For uranium and other ore deposits, the importance of this style of deformation is that it generates a large volume of brecciated rock, which is favourable for ore deposition (Nash (5)).

5. PETROLOGY OF ORES AND ALTERATION

Uranium minerals in Pitch Mine ores are inconspicuous, despite ore grades locally in excess of one percent. Primary ores are dark gray to black but do not look much different from other dark dolomite breccias. Uranium, chiefly as pitchblende, and iron sulfides fill the matrix of breccias. Macroscopic and microscopic studies reveal no alteration selvage in dolomite next to uranium minerals. The matrix is a dark mixture of comminuted dolomite, some fine silica, pitchblende, pyrite, and marcasite. Unbroken dolomite contains sparse uranium minerals. Microscopic study of dolomite breccia ore reveals a relatively simple assemblage of pitchblende, coffinite, pyrite, marcasite, and minor quartz. Veinlets of pitchblende and coffinite more than 1 mm wide are rarely seen. About half of the black uranium minerals have low reflectivity under oil immersion and reflected light, and some have reddish internal reflections; these observations suggest that coffinite is an important uranium mineral, but its abundance and age relative to pitchblende could not be determined with confidence. FeS_2 is both isotropic (pyrite) and anisotropic (marcasite). With high magnification under oil immersion and reflected light, the marcasite is slightly paler yellow than pyrite and tends to form rectangular grains. In most samples marcasite equals pyrite in abundance. Marcasite of similar habit is abundant at the Midnite Mine, Washington (Ludwig et al. (10)), and in many sandstone-type uranium deposits (Goldhaber et al. (11)).

The matrix of most breccias contains fine-grained dark material. Some of this material is fragments of Belden Formation black shale in poly-lithic breccias, but most is simply a fine-grained mixture of dolomite, pitchblende and coffinite, and iron sulfides. Analyses of dolomite breccias indicate organic carbon contents in the range of 0.1 - 0.7 %, which suggests that part of the dark colour may be from organic material, but iron sulfides and uranium minerals are thought to be the predominant source of the colour.

Dolomites in the ore zone and in breccias along the Chester fault show no recrystallization effects that can be related to ore or fracturing. Many are dolomicrites with grain size less than 10 microns, and dolomite in the matrix is also typically finely crystalline (less than 16 microns) and generally is finer than the dolomite in the breccia fragments. Texture of dolomite is uniform within fragments but differs between fragments in the same thin section, indicating that there was no post-fault recrystallization. Even the edges of dolomite breccia fragments show no bleaching or recrystallization adjacent to pitchblende in the matrix.

Three types of alteration are observed in the Leadville Dolomite:

(i) Oxidation, in places accompanied by leaching of carbonate minerals;

(ii) Subtle silicification by addition of thin films of silica in fractures;

(iii) Pervasive silicification to produce jasperoid.

The first two alterations are part of ore processes, and the last is not directly related to ore but may reflect processes operating in source rocks.

Oxidation has penetrated to depths of more than 100 m along faults, and some breccia zones are pervasively oxidized to depths of about 60 m. Two extreme cases of a continuum are most easily described. Extreme oxidation and acid alteration at shallow levels has created porous, cellular rocks in which carbonate is removed, and the rock is a lacey silica boxwork encrusted by limonite. The altered rock is essentially a gossan. It trends to be highly radioactive but is deficient in uranium. This type of disequilibrium indicates either leaching of uranium in the past million years or localization of radium by sulfate (Phair et al. (12)). The other type of oxidation is massive or brecciated dolomite that has an ocher colour imparted by hydrous iron oxides. The ocher dolomite is slightly softer than the unoxidized equivalent, but X-ray diffraction and petrographic studies show essentially no difference in major minerals. Pyrite was destroyed and replaced in situ by iron oxides that retain the cubic form, and other iron oxides permeated grains and cracks to produce a pronounced stain. Chemical analyses indicate many of these rocks have several percent of iron more than equivalent unoxidized dolomites. Uranium content of most ocher dolomites is only 50 - 200 ppm but probably was higher before oxidation. This oxidative alteration was produced by sulfuric acid generated by oxidation of sulfide minerals.

Subtle silicification of dolomite is best observed on newly exposed rocks in the Pitch open pit. Very thin films of quartz, sufficiently crystalline to sparkle in sunlight, coat breccia fragments in the ore zone. These quartz films, possibly obscured by mud and dust, were not detected while logging drill core and are not visible in most thin sections. Many samples of ore contain more silica than barren equivalents. This alteration seems to be related to ore in zones of pitchblende and sulfide minerals, but the outer limits are not known.

Pervasively silicified Leadville Dolomite occurs at many locations along the Chester fault north of the mine. This rock is best termed jasperoid (Lovering (13)); it is dark gray to reddish black, very fine grained massive chalcedonic quartz with streaks and patches of red iron oxides; it has no vuggy crystals and few carbonate minerals; and its content of SiO_2 is generally more than 90 %. In a few places a replacement interface with dolomite was observed, but in most places a replacement of dolomite is inferred from nearby outcrops of unaltered dolomite. The jasperoid is mildly radioactive in some outcrops. It commonly has a breccia texture of uncertain origin. The breccia was recemented into a strong rock that breaks across the breccia fragments. Individual fragments tend to have slightly different colours, and the matrix tends to be darker owing to its higher content of iron oxides. I believe the rock formed by silicification of a brecciated dolomite because the breccia is healed and is restricted to the Chester fault zone. This silicification is possibly related to alteration of overlying Oligocene (?) tuffs.

6. GEOCHEMISTRY OF ORE

Chemical analyses for major and minor elements in 116 samples of unaltered, altered, and ore-bearing rock from the mine area demonstrate some subtle but significant changes during ore formation. The complete data and statistical analyses can be found elsewhere (Nash (2)); a summary of the data is in Table II. Correlation and factor analyses of 33 chemical variables demonstrate a strong association of total S, FeO, Pb, and Mo with uranium. Other associations (significant at 95 % confidence level) with uranium include Al, Fe_2O_3, K, Mn, Cl, Ba, Sr, Zn, Mg, Cu, and Ni. Relations of uranium with organic carbon were examined in detail and determined to be random. The strong correlation of uranium with sulfur and chalcophile elements confirms the petrographic observations of uranium minerals with sulfides. Statistical tests on three subsets defined by uranium content ($<$500 ppm, 500 - 5000 ppm, $>$5000 ppm) demonstrate progressive enrichment in FeO, K, S, Mo, Cu, and Ni relative to the next lower grade subset.

Oxidized ocher dolomites in the ore zone, typically with uranium content less than 200 ppm, are enriched in Si, Al, Fe_2O_3, K, Ba, Sr, Pb, Zn, Cu, Ni, and V relative to unaltered dolomite samples. The enriched elements are mostly those of the ore suite, which is interpreted to mean that these dolomites once contained as much uranium as the present ore. The gossan-type oxidized dolomites are significantly enriched in Fe_2O_3, Zn, Mo, and Hg relative to ocher dolomite and to unaltered dolomite, suggesting that this suite of elements can be used to evaluate surface showings of dolomite-hosted uranium ore.

7. WHY IS THE LEADVILLE DOLOMITE IMPORTANT?

The fact that most of the reserves at the Pitch Mine occur in the Leadville Dolomite raises questions about the role of this unit as a host rock. The importance of this unit is underscored by two other facts:

TABLE II. STATISTICAL SUMMARY OF CHEMICAL DATA PITCH MINE

CONSTITUENT	MINIMUM	MAXIMUM	GEOMETRIC MEAN	GEOMETRIC DEVIATION	NUMBER
		MAJOR OXIDES (%)			
SiO_2	0.20	97.7	12.26	3.58	116
Al_2O_3	0.03	13.7	1.03	3.78	116
Fe_2O_3	0.02	46.4	0.80	3.64	116
FeO	0.00	4.1	0.23	3.00	116
MgO	0.07	21.0	6.18	4.39	116
CaO	0.15	53.1	19.47	3.07	116
Na_2O	0.00	0.31	0.033	2.35	113
K_2O	0.00	3.40	0.25	3.67	115
H_2O^+	0.10	9.10	0.64	2.22	116
H_2O^-	0.01	5.50	0.36	0.64	116
TiO	0.00	0.78	0.069	2.96	116
P_2O_5	0.00	0.63	0.037	2.42	116
MnO	0.00	0.31	0.062	2.11	116
CO_2	0.00	48.2	22.70	4.52	116
F	0.00	0.21	0.030	1.99	116
S	0.01	7.92	0.12	4.86	116
C ORGANIC	0.00	4.20	0.18	3.38	116
C CARBONATE	0.00	13.07	7.32	2.79	116
		MINOR ELEMENTS (PPM)			
[illegible]	8.91	550.0	29.8	17.4	116
Ba	20.0	2100.0	101.4	2.28	116
Sr	10.0	620.0	92.0	2.84	116
Pb	0.0	220.0	9.67	3.42	101
Zn	5.0	2600.0	33.2	4.50	101
Mo	0.5	88.0	1.38	4.91	101
Hg	0.05	2.6	0.022	5.58	101
U	0.18	33500.0	75.3	16.7	116
Cr	0.5	70.0	11.0	2.60	57
Cu	0.8	70.0	3.02	2.72	57
Ni	0.8	300.0	8.18	3.03	57
V	0.5	70.0	10.9	2.17	57
Zr	2.3	300.0	28.1	3.11	57
		MINERAL CONTENT, BY X-RAY DIFFRACTION (%) *			
DOLOMITE	0.0	100	49	22	116
CALCITE	0.0	100	22	26	116
QUARTZ	0.0	100	24	22	116
CLAY	0.0	30	2	6	116
HEMATITE	0.0	40	0.3	4	116

*RELIABLE ONLY TO ± 10%

(i) Most of the high-grade ore at the Pitch Mine is in dolomite, and

(ii) no other significant uranium deposit in the United States occurs in dolomite.

I cannot definitively answer this question, but offer the following speculation.

The Leadville Dolomite is a favoured host primarily because of its brittle character and structural setting, as described earlier. The uniformity of the dolomite, which has no shale interbeds and a very fine grain size, may have made the Leadville section especially susceptible to the pervasive fracturing and brecciation needed to prepare the ground for emplacement of an economic volume of uranium minerals.

The Leadville Dolomite is clearly not the only brittle potential host rock. The Little Indian deposit occurs in quartzite, and partly in dolomite where these rocks are fractured along the Chester fault. From the pattern of drilling between the Pitch and Little Indian deposits, I infer that other uranium zones occur in Paleozoic dolomites along the Chester fault. Precambrian granitic rocks also host veins of uranium where fractured. My conclusion from these general observations is that several types of rocks can host uranium if they fail by brittle fracture.

Fractured rock alone obviously does not make an ore deposit: chemical factors also must be conducive to ore deposition. The chemical data show a strong association between sulfur, iron, and uranium in the Pitch deposit. The Leadville Dolomite may have been enriched in iron and sulfur as FeS_2 during diagenesis. I favour the concept (Nash (2)) that FeS_2 and organic carbon were enriched in the Leadville during tidal-flat sedimentation and early diagenesis. This FeS_2 and organic carbon then would be available to play a direct or indirect role in chemically localizing uranium in the Leadville after it was fractured and uranium was introduced.

The cycle of sulfur in the Leadville Dolomite may have been similar to that proposed for sulfur in some sandstone-type deposits (Granger et al. (14), Goldhaber et al. (15), Reynolds et al. (16)). The association of uranium with marcasite seems to be a key feature. Experimental, isotopic, and paragenetic data on marcasite strongly support the hypothesis of formation from metastable sulfur oxyanions such as thiosulfate (Granger et al. (14), Goldhaber et al. (15)). An important property of these sulfur oxyanions is that they spontaneously break down (disproportionate) into sulfide and sulfate ions; sulfide ion so generated is an excellent reductant and also would be present to form FeS_2. It is postulated that pre-ore sulfides in the Leadville Dolomite and Belden Formation were oxidized in the near-surface environment, creating thiosulfate or similar ions that moved down the hydraulic gradient of the Chester fault zone, where they broke down and caused reduction of uranyl ions. Additional reduction could have been caused by bacterial sulfate reduction.

The low uranium content of most pyritic Belden sandstones is not easily explained. Low permeability caused by high clay content may explain why some localities are barren. Other localities adjacent to faults and ore-grade dolomite breccia are especially puzzling. One possible explanation is that the pyrite in these sandstones was nonreactive under reducing conditions and thus did not provide sulfur oxyanions capable of reducing uranium: partial oxidation of pyrite creates reactive sulfur species capable of reducing uranium (Granger et al. (14)).

8. SUMMARY: GENETIC MODEL

Information presented in this paper is consistent with, but does not prove, a near-surface genesis for the Pitch uranium deposits shortly after the Oligocene (?) volcanism.

8.1. Ground preparation

Preparation for ore emplacement began with sedimentation and diagenesis which created brittle rocks, some containing diagenetic pyrite, and was furthered by brecciation along the Chester fault in Laramide time. Structural permeability provided by the zones of brecciation is a key ore control.

8.2. Uranium source

Quartz latite welded tuff of Oligocene (?) age, containing pumice and glass, was deposited above the Chester fault zone. This unit was part of a volcanic sequence that was probably several hundred meters thick; thin relicts are exposed between the Pitch and Little Indian Mines (Olson (6)). These tuffs would have been highly reactive shortly after deposition and would have undergone reactions similar to those described by Zielinski (17)). This alteration of volcanic rocks is believed to be the source of the silica that formed the jasperoid along the Chester fault zone in brecciated carbonate rocks below the volcanic rocks. Within 10 km of the Pitch Mine, volcanic rocks are more radioactive today than other rocks, such as Precambrian granite, and the two freshest volcanic samples contain an average of 10.5 ppm U and 35.2 ppm Th. The most radioactive volcanic unit is a high-potassium dacite (64.6 % SiO_2). The quartz latite possibly contained even more uranium than the dacite prior to alteration.

8.3. Paleohydrology

In the Oligocene (?) the Pitch Mine area was beneath a volcanic trough and about 600 m above a paleovalley (Olson (6)). Some lakes probably existed at times and were filled by tuff. Ground water in the Pitch Mine probably flowed southward along the Chester fault zone toward the paleovalley, beneath a cover of volcanic tuff. Volcanism in the area probably heated the ground water, possibly to 50° - 100° C. At a depth of a few hundred meters, in a permeable fault zone, the ground water probably was oxygenated or partially oxygenated. Conditions would have been excellent for uranium transport.

8.4. Uranium deposition

Laterally or downward moving fluids carrying U, Mo, Si, and possibly sulfur oxyanions (Reynolds et al. (16)) deposited uranium and silica upon reaching structural traps that contained reductants. Reduction could have been caused by reduced sulfur species produced by bacteriogenic processes or by inorganic reactions. Silica is not responsive to reduction but can be precipitated in response to cooling (Holland et al. (18)). Temperatures, presumably were below 100°C at the postulated shallow level.

REFERENCES

(1) WARD, J.M., History and geology of Homestake's Pitch project, Saguache County, Colorado (abs.), American Institute of Mining, Metallurgical and Petroleum Engineers, Program of the 107th annual meeting, Denver, Colorado, February 26 - March 2 (1978).

(2) NASH, J.T., Geology, petrology, and chemistry of the Leadville Dolomite, Host for uranium at the Pitch Mine, Saguache County, Colorado, U.S. Geol. Survey Open-File Report 79-1566 (1979) 51 pp.

(3) MALAN, R.C., Geology and uranium deposits of the Marshall Pass District, Gunnison, Saguache, and Chaffee Counties, Colorado, Denver, National Western Mining Conference, Colorado Mining Association (1959) 1-20.

(4) GROSS, E.B., A unique occurrence of uranium minerals, Marshall Pass, Saguache County, Colorado, Am. Mineralogist 50 (1965) 909-923.

(5) NASH, J.T., Supergene uranium deposits in brecciated zones of Laramide upthrusts-concepts and applications, U.S. Geol. Survey Open-File Report 80-385 (1980) 36 pp.

(6) OLSON, J.C., Geologic and structural maps and sections of the Marshall Pass Mining District, Saguache, Gunnison, and Chaffee Counties, Colorado, U.S. Geol. Survey Miscellaneous Investigations Map I-1425, scale 1:24000 (1983).

(7) BERG, R.R., Mountain flank thrusting in Rocky Mountain foreland, Wyoming and Colorado, Am. Assoc. of Petroleum Geologists Bull. 46 (1962) 2019-2032.

(8) STEARNS, D.W., Faulting and forced folding in the Rocky Mountains foreland, in: V. Matthews, III. (editor), Folding associated with basement block faulting in the Western United States, Geol. Soc. Am., Mem. 151 (1978) 1-38.

(9) FRIEDMAN, M., et al., Experimental folding of rocks under confining pressure, Part III - Faulted drape folds in multilithologic layered specimens, Geol. Soc. Am., Bull. 78 (1976) 1049-1066.

(10) LUDWIG, K.R., NASH, J.T., NAESER, C.W., U-Pb isotope systematics and age of uranium mineralization, Midnite Mine, Washington, Econ. Geol. 76 (1981) 89-110.

(11) GOLDHABER, M.B., REYNOLDS, R.L., Origin of marcasite and implications regarding the genesis of roll-type uranium deposits, U.S. Geol. Survey Open-File Report 79-1696 (2979) 40 pp.

(12) PHAIR, G., LEVINE, H., Notes on the differential leaching of uranium, radium, and lead from pitchblende in H_2SO_4 solutions, Econ. Geol. 48 (1954) 358-369.

(13) LOVERING, T.G., Jasperoid in the United States - its characteristics, origin, and economic significance, U.S. Geol. Survey Professional Paper 710 (1972) 164 pp.

(14) GRANGER, H.C., WARREN, C.G., Unstable sulfur compounds and the origin of roll-type uranium deposits, Econ. Geol. (1969) 160-171.

(15) GOLDHABER, M.B., REYNOLDS, R.L., RYE, R.O., Origin of a south Texas roll-type uranium deposit, II. Sulfide petrology and sulfur isotope studies, Econ. Geol. 73 (1978) 1690-1705.

(16) REYNOLDS, R.L., GOLDHABER, M.B., CARPENTER, D.S., Biogenic and non-biogenic ore-forming processes in the South Texas uranium district, Evidence from the Panna Maria deposit, Econ. Geol. 77 (1982) 541-556.

(17) ZIELINSKI, R.A., Experimental leaching of volcanic glass: implications for evaluation of glassy volcanic rocks as sources of uranium, in: P.C. Goodell and A.C. Waters (editors), Uranium in Volcanic and Volcaniclastic Rocks, Am. Assoc. of Petroleum Geologists, Studies in Geology 13 (1981) 1-11.

(18) HOLLAND, H.D., MALININ, S.D., The solubility and occurrence of non-ore minerals, in: H.L. Barnes (editor), Geochemistry of hydrothermal ore deposits, 2nd edition, John Wiley and Sons (1979) 461-508.

(19) TWETO, OGDEN, STEVEN, T.A., HAIL, W.J., Jr., MOENCH, R.H., Preliminary geologic map of the Montrose 1° x 2° Quadrangle, Southwestern Colorado, U.S. Geol. Survey Map MF-761, scale 1:250000 (1976).

URANIUM VEINS IN PORTUGAL

I. R. Basham
British Geological Survey
Edinburgh
Scotland

J. M. Matos Dias
Empresa Nacional de Urano
Urgeiriça
Portugal

Abstract

URANIUM VEINS IN PORTUGAL

Vein-type uranium deposits in Portugal demonstrate a broad temporal and physical spectrum from intragranitic hydrothermal jasper-type veins formed at moderately high temperatures, through lower temperature quartz veins and peribatholithic disseminated mineralization of 'Iberian-type', to undoubted supergene enrichments in surface-related planar traps such as weathered basic dikes. All appear to be in close spatial relationship to 'fertile' Hercynian granites in which uraninite of low thorium content is the main contributor to the enriched uranium levels. The availability of this large source of labile uranium, a pervasive fracture network and a series of tectonic and intrusive events which could generate hydrothermal circulation, allow several alternative genetic models for the mineralization. It now appears that the classic hydrothermal pitchblende veins within the granite are most likely of late-Hercynian age. Many of the mineralogical and depositional characteristics of the lower temperature 'Iberian-type' deposits suggest a temporal continuity to this mineralization but, as yet, no supporting age data are available. It is conceded, therefore, that a considerable time-gap could occur between the two episodes, with the peribatholithic mineralization resulting from later rejuvenation of the hydrothermal convective system.

1. INTRODUCTION

The principal known deposits of uranium in Portugal fall into the general category of vein-type, and include classic hydrothermal veins in relatively large open structures, networks of microveinlets in 'Iberian-type' disseminated deposits and supergene enrichments in planar structural or lithological traps. All lie within the central Iberian geotectonic zone and are closely related spatially to structurally high positions in the Hercynian granitic batholiths.

The history of uranium mining in Portugal began with the discovery of pitchblende vein mineralization at Urgeiriça in 1912. This deposit was exploited for radium until 1940 and for uranium after 1951. In common with most of the larger hydrothermal vein deposits subsequently discovered in the Beiras Region, the ore at Urgeiriça is now worked out, mining having ceased at around 500 metres depth, but exploitation continues by in situ acid leaching. Total production in Portugal up to the end of 1982 was 2,536 t U. Current production has swung from the high-grade vein-type deposits to lower grade surface-related and 'Iberian-type' deposits, the latter offering the best potential for future developments. Current estimated resources of over 11,000 t U occur mainly in this type of deposit. In this paper, discussion of the characteristics of the mineralization will be based on the following general scheme

(i) Hydrothermal, polymetallic pitchblende veins in open structures with jasper or ferruginous white quartz gangue.

(ii) Hydrothermal veins with banded milky white and smokey quartz gangue.

(iii) Pitchblende-fluorite veinlets in episyenites.

(iv) Dominantly hexavalent uranium minerals in quartz veins, tectonic breccias and basic dykes.

(v) 'Iberian-type' disseminated deposits.

The main geological features of central Portugal and localities referred to in the text are given in Fig. 1.

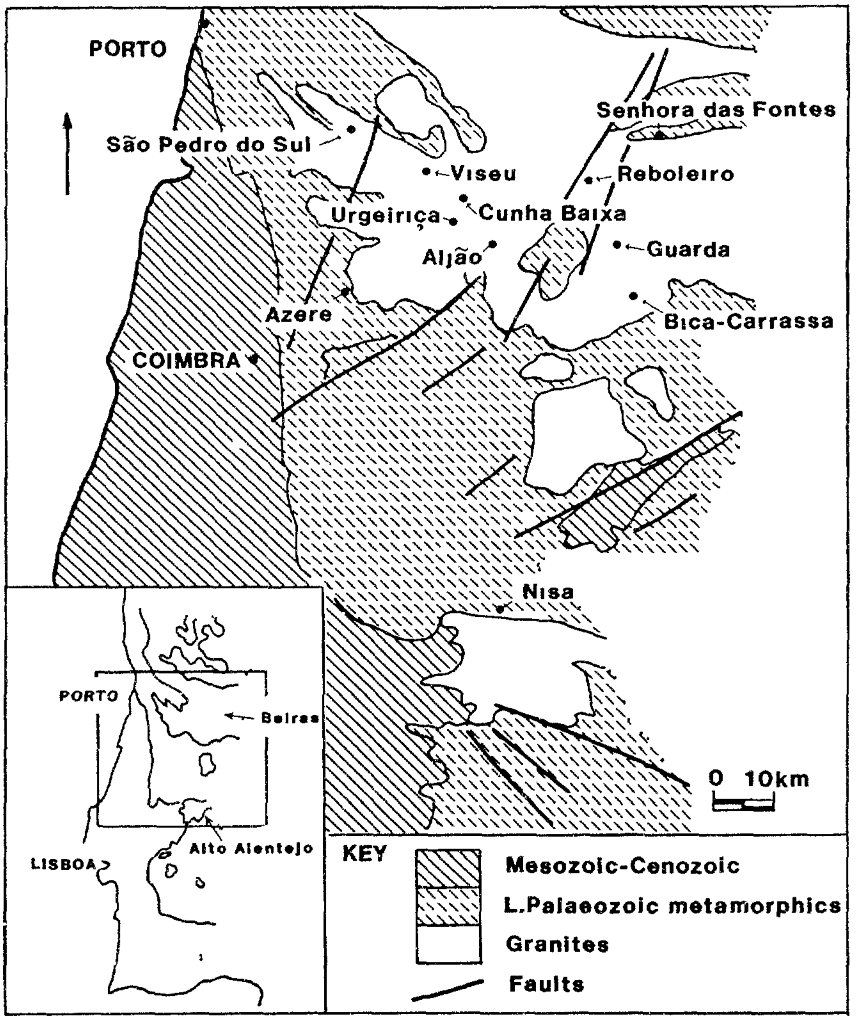

FIG. 1. Simplified geological map of central Portugal showing principal locations referred to in the text.

2. HYDROTHERMAL VEINS IN OPEN STRUCTURES

2.1. Geological framework

Virtually all known uranium-bearing hydrothermal veins occur within the youngest members of the series of Hercynian granites intruded into the pre-Ordovician schist-greywacke complex of central Portugal. These intragranitic veins predominate in the Viseu-Guarda area of the Beiras Region but some types occur to a lesser extent in the Alto-Alentejo Region.

In the Beiras Region the host rocks are uranium-enriched, medium- to coarse-grained porphyritic calc-alkaline (biotite) granites. Numerous pegmatites and aplites and xenoliths or roofs pendant of metasediments indicate emplacement at a structurally high level and enrichment in Li and B is shown in the presence of frequent tourmaline. These so-called 'younger', post-tectonic granites cut across the predominant NW-SE regional trend of the metasediments in which well-marked contact metamorphic aureoles up to 2 km wide are formed. Mendes (1) dated these granites at 280 ± 10 Ma and distinguished them from 'older' foliated two-mica monzonitic granites which were emplaced syntectonically at 298 ± 10 Ma. More recently, Pinto (2) has sub-divided the plutons in the Aveiro and Viseu districts as follows:

- Oldest Variscan granites 379 ± 12 Ma
- Pre-Older Variscan granites 322 ± 15 Ma
- Older Variscan granites 308 ± 10 Ma
- Younger Variscan granites 290 ± 11 Ma
- Newer Variscan granites 280 ± 10 Ma

In general, the older granites are lacking in uranium deposits although some indications have been found in the Oldest and Pre-Older granites and surrounding metasediments in the Pinhel area.

The region is pervaded by networks of late-Hercynian fractures. A conjugate NNW-SSW to ENE-WSW and NNW-SSE to NW-SE system dominates, with a later set of N-S faults and fractures also important. The structural planes are often marked by quartz veins, barren or mineralized. Basic dikes (olivine dolerites and lamprophyres), intruded during the interval 235 - 205 Ma are mostly controlled by 'en echelon' transverse NNE-SSW faults, probably marking the onset of continental breakup (Portugal Ferreira et al. (3)).

2.2. Jasper or ferruginous white quartz veins

2.2.1. Ore controls

The distribution and general characteristics of the veins in the Beiras Region have been discussed in detail by Cameron (4). Further geochemical and mineralogical study of three of these deposits by Pagel (5) indicates that mineralization appears to be concentrated in irregularly distributed zones in the granites where uranium and thorium contents are somewhat higher than regional background levels of 8 ppm U and 10 ppm Th. Mineralization occurs as siliceous-pyrite-galena-pitchblende-type veins in steeply inclined, often brecciated and faulted structures following the dominant late-Hercynian fracture network. The general north-easterly trend appears to be favoured, as in the well-known deposits of Urgeiriça and Bendada districts.

2.2.2. Mineral paragenesis and wall-rock alteration

Although regional variations occur, the paragenesis is characteristically simple:

- Quartz-colourless
- Jasper or ferruginous quartz (with brecciation)
- Pyrite, sphalerite, galena, fluorite
- Quartz-colourless, microcrystalline
- Pitchblende-botryoidal
- Pyrite, chalcopyrite
- Pitchblende-microbotryoidal, colourless quartz
- Pyrite, carbonates, coffinite

In addition to Cu and Zn, weaker but significant levels of As, Mo, Co, Ni, V and Mn are found in some deposits e.g. Urgeiriça and Bica (Pagel (5)). Jasper or reddened quartz is characteristic of the mineralized zones which attain widths of 4 - 5 metres in places, but carbonate, formed late in the paragenesis, is more typical of unmineralized sections of the vein structures.

Sericitic and hematitic wall rock alteration is well-developed, with the width of hematitized zones correlating directly with the uranium content of the lodes (Cameron (4)) and thereby providing a valuable prospecting criterion. Pagel (5), in a detailed study of selected profiles across alteration and mineralized zones from Urgeiriça and Bica-Carrassa, has derived important new evidence for the hydrothermal origin of the veins. Pitchblende occurs between two generations of quartz. The presence of hematite inclusions in the earlier of these, correlating with hematitic wall rock alteration, suggests that the original fluids preceding mineralization were oxidizing. Unfortunately, fluid inclusion data from quartz were difficult to obtain but a consideration of mineralogical and fluid-inclusion data from sericitized zones, and of fluid-inclusion data from vein fluorite and sphalerite, indicates formation involving aqueous hydrothermal fluids at 200 - 250°C. These fluids appear different in physicochemical character to the fluids associated with late-magmatic (deuteric) activity within the granites. Pagel (6) further concludes that pitchblende mineralization resulted from the circulation of hot, hydrothermal fluids in the granite. As these were originally oxidizing, they were possibly of meteoric origin, heated in a geothermal gradient perhaps related to deeper magmatism evidenced by the intrusion of the dolerite-lamprophyre dikes.

2.2.3. Age and origin of the mineralization

The age and origin of the intragranitic veins of Portugal have been a subject of controversy for many years with the bias of opinion favouring a Tertiary age, based mainly on acceptance of the host-structures as Alpine. The recent work of Pagel (5), together with general mineralogical considerations, strongly support a hydrothermal origin. Pagel's results further eliminate hydrothermal activity related to the pegmatitic phase of granite magmatism (as previously proposed by Cotelo Neiva in 1944 (7)). The late-Hercynian fault and fracture systems exploited by the mineralizing fluids were rejuvenated during the Alpine orogeny and hydrothermal fluids would almost certainly have passed through any open structures at that time. Indeed, contemporary thermal spring activity throughout the region follows the same fractures. However, chemical ages based on electron microprobe analyses of pitchblende (Basham et al. (8), Pagel (5)) further minero-chemical data by Cathelineau et al. (9), and a single isotopic pitchblende age of 190 Ma (Darnley (10)) all point to a much earlier age. Current isotopic determinations being made in France (Pagel, personal communication) do, in fact, support an age approaching the late-Hercynian. The connection, first proposed by Cerveira in 1958 (11), between hydrothermal mineralizing fluids and the magmatism giving rise to the basic dikes may be apposite.

Cameron (4) proposed the intensely developed alteration zones of the granites themselves to be the source of uranium for the mineralization. Basham et al. (8) and Pagel (5), have identified low-thorian, magmatic accessory uraninite as the main location of uranium in the granites. This would be readily leached by oxidizing hydrothermal fluids and the low tenor of other metals in the veins could well reflect a granitic source. Cameron (4) calculated the volume of sericitic alteration zones to be more than adequate to account for the uranium in the veins, given only a small proportion of the total uranium content of the granite mobilized. However, although strong evidence exists of uranium mobility in these zones (Pagel (5), Basham et al. (8)), insufficient data on relative uranium contents and locations have been obtained to support such a material balance at this stage.

3. BANDED WHITE AND SMOKY QUARTZ VEINS

While jasper and reddened quartz veins appear to be predominant in the Urgeiriça and Bendada districts of the Beiras Region, white quartz or banded milky white and smoky quartz gangue is more common in the Reboleiro and Guarda districts (Cameron (4)) and is the only type found in the Alto Alentejo Region. Ore controls and mineral paragenesis are similar to the jasper-type deposits but pitchblende tends to be microbotryoidal or 'sooty' and the associated ore minerals of a more restricted suite with pyrite often the only sulphide present. Wall rock alteration is generally developed to a lesser degree.

These features have led Cameron (4) to suggest that these veins were formed at lower temperatures than the jasper-type. There is little further evidence but Pagel (6) concluded this to be the case for the veins at Cunha Baixa. Here, both sets of conjugate NE and WNW trending fractures are mineralized, with basic d kes following the same structures in places. Further reference to this locality is made later (Section 6.3).

4. EPISYENITES

A restricted zone of episyenite occurs within an 'older' foliated monzonite in the Beiras Region at Aljao. Typified by leaching of quartz and development of a cataclastic equigranular fabric with a 7 % porosity, the rock bears a close similarity to those found in Hercynian granites in France (Portugal Ferreira et al. (12)). Small veinlets of pitchblende associated with fluorite occur mainly in the transition zone to unaltered monzonite but the mineralization within the episyenite itself is mainly disseminated autunite formed by supergene remobilization. Portugal Ferreira et al. (12) suggest that the primary ore was deposited from low-temperature hydrothermal fluids introduced along shear zones, possibly related to the intrusion of the regional basic dikes.

5. QUARTZ VEINS, GRANITE BRECCIAS AND BASIC DIKES

5.1. Geological framework and ore controls

Numerous quartz veins and breccia zones occur throughout both the Beiras and Alto Alentejo Regions, closely controlled by the late-Hercynian fracture systems. Mineralization is almost invariably composed of secondary uranium minerals, mainly autunite and torbernite but with lesser, sporadic amounts of others - chiefly hydrated phosphates of Ba, Ca, Mg and rarely, Pb. Mineralization dies out with depth, sometimes with pitchblende or 'sooty', poorly crystalline or amorphus uranium oxide occurring below the surface oxidation zone.

Basic dikes are common in the Beiras Region, following the regional fracture system and sometimes occupying the same fractures as quartz veins. Mineralization is restricted to highly weathered surface zones, occurring as autunite and/or torbernite or high adsorbed levels associated with hydrated oxide weathering products. Grades of up to 0.2 % U_3O_8 are attained to depths of up to 60 m and the deposits are worked as small, selective open-pit operations.

5.2. Origin of mineralization

Surface alteration processes are active to depths of at least 15 m in much of Portugal and redistribution of uranium within the weathering zone obscures any primary features of mineralization. The present regolith represents prolonged weathering throughout the Tertiary period and supergene enrichment of uranium could well explain the high levels accumulated in the traps presented by ferruginous quartz or granite breccias and deeply weathered basic dikes. However, it is also possible that these structures allowed the passage of hydrothermal fluids during Alpine tectonic movements, as discussed earlier. Indeed, a continuum seems to be presented from undoubted supergene enrichments, through intermediate pitchblende-sulphide quartz veins, such as found at Cunha Baixa, to the accepted hydrothermal lodes of the Beiras.

6. 'IBERIAN-TYPE' DISSEMINATED DEPOSITS

6.1. Geological framework

A comprehensive account of the distribution and characteristics of this mineralization, as known in 1966, was given by Limpo de Faria (13). The occurrences are almost invariably found within the contact metamorphic aureoles around 'younger' Hercynian granites intruding the regionally metamorphosed pre-Ordovician 'schisto-greywacke complex'. Indeed, mineralization occurs only in the aureoles of uranium-enriched granites which also contain intragranitic vein-type deposits and has not been found in association with barren granites (such as pre-Ordovician and Mesozoic plutons) intruding lithologically similar metasediments. A close genetic link with the 'fertile' granites is thus indicated and formation by direct remobilization and concentration of syngenetic uranium from the sediments seems less likely.

The main deposits known at present are in the contact zone to the north of the Nisa-Castelo de Vide granite in Alto Alentejo and at Azere in the Beiras Region. Also in the Beiras, a mineralized roof pendant or schist enclave occurs immediately over the previously mentioned vein-type deposits within the granite at Cunha Baixa. A related type of deposit occurs very close to a faulted contact with Pre-Older granite at Senhora das Fontes (Pinhel), and an important new discovery has been made recently by the Direçcao-Geral de Geologia e Minas of Portugal at Horta da Vilariça in Trâs-os-Montes.

The principal areas of interest economically at present are Nisa and Azere. Here, the host metasediments comprise a series of low-grade phyllites, impure quartzites and greywackes, isoclynally folded to give a steeply dipping regional bedding-schistosity which strikes roughly parallel to granite contact. Quartz veins follow the late-Hercynian fracture system and some major ones extend from within the granite into the country rocks (N-S trend at Nisa, NE-SW trend at Azere). At Azere, an apparently conjugate, extensive set of quartz veins occurs parallel to the axial planes of the regional isoclynes. These are barren of primary mineralization. Hornfels zones occur sporadically, close to contacts, and the phyllitic metasediments within the aureoles show recrystallized textures and the common development of cordierite 'spots'.

6.2. Ore controls and mineral paragenesis

6.2.1. Nisa

Pilar (14) described the mineralization in some detail. Secondary minerals, mainly autunite with variable amounts of other phosphates, coat fractures, shear planes or opened planes of schistosity, and impregnate weathered schist fragments, within the 15 m or so of weathering zone. Below about 17 m depth, pitchblende, associated with clear quartz, pyrite and chalcopyrite form an infill to narrow (1 - 2 mm), subvertical fracture-breccias in metasediments. These cross-cut the schistosity roughly normal to the granite contact. Chalcopyrite occurs intergrown with the pitchblende or cutting it in later microveinlets.

6.2.2. Azere

Recent work by the authors and geologists at ENU has shown similar associations to Nisa. At surface, an extensive zone of radiometric anomalies runs more or less parallel to the granite contact mainly within the aureole. Although less pervasive than at Nisa, possibly due to the lower degree of weathering in more rugged topography, mineralization again occurs as secondary minerals near surface. Highest concentrations are found in highly shattered zones associated with axial planes of isoclynal folds, or in zones of intense brecciation in fold limbs along junctions between phyllites and more competent psammitic beds. In contrast to Nisa, a high proportion of the uranium is present in close association (? adsorbed) with secondary iron oxides/hydroxides. Recent drilling has intersected pitchblende microveinlets and networks below about 60 m. These shear and breccia veins cross-cut the thermal metamorphic fabric of the host phyllites and are of hydrothermal character, with ubiquitous pyrite and frequent chlorite and quartz. Tourmaline is also present in places.

6.2.3. Senhora das Fontes (Pinhel)

According to Barros (15) a well-defined zone of mineralization about 190 m in length and extending to a depth of 120 m, occurs very close and parallel to the steeply dipping (? faulted) granite contact. The ore minerals follow distinct fractures in quartz-mica schists and comprise autunite and saleeite in the upper 40 m and pitchblende, pyrite, chalcopyrite and manganese oxides at depth.

6.2.4. Horta da Vilariça (Trás-os-Montes)

Here the granite-schist contact trends WNW and the deposit is located about 1.5 km east of the important Vilariça graben. Although the mineralization seems similar to that at Azere and Nisa, pegmatitic apophyses in the schisto-greywacke complex show high contents of uranium (up to 1000 ppm). Preliminary studies have recognized uraninite as a major location of this uranium.

6.3. Age and origin of the mineralization

Pilar (14) and Barros (15) concluded that the paragenesis and mode of emplacement of the 'primary' mineralization at Nisa and Senhora das Fontes indicate a low-temperature hydrothermal origin from fluid movement related to Alpine tectonism. The secondary minerals in the oxidized zone were considered to result from supergene redistribution of the primary ore.

Recent lithogeochemical and mineralogical studies at Azere and Nisa by the authors have shown the uranium content of unweathered host metasediments to lie within the range for average shales (1 - 13 ppm) and no evidence has been found of syn-sedimentary enrichment in any part of the associated sequences. Fission-track study has revealed minor redistribution and concentration of uranium in both regional and contact thermal metamorphism. Segregation of uranium into quartz veinlets during regional metamorphism and into cordierite 'spots' or recrystallized chlorite-rich bands within the contact aureoles has been found. However, these appear to be local effects which do not alter the whole-rock uranium content radically and are not thought to have effected pre-ore concentration. Possible metasomatic movement during granite emplacement has also been investigated geochemically but no positive correlation between uranium and any other element has been found. Along with the mineralogical data and vein-relationships mentioned above, this evidence is taken to support a post-intrusion, hydrothermal origin for the pitchblende mineralization. Supergene remobilization and concentration into structural or chemical traps has produced the disseminated deposits of secondary minerals in the upper 15 - 40 m of the weathering zone.

Further evidence is afforded at Cunha Baixa where disseminated autunite coats fractures or impregnates argillic or ferruginous altered schist fragments in the near-surface zones of a metasedimentary enclave or roof pendent. Below about 100 m the schists are less altered and shattered, and mineralization, at times including pitchblende, follows more clearly defined vein-like systems (Limpo de Faria (13)). It is not unreasonable to relate these structures to the larger, vein-structures within the granite below, where microbotryoidal pitchblende, pyrite and manganese oxides are thought to represent low-temperature hydrothermal mineralization (Pagel (6)).

Previous writers (Limpo de Faria (13), Pilar (14)) have considered the primary 'Iberian-type' mineralization in Portugal to be either contemporaneous with, or later than the intragranitic veins. Assuming the latter to be Upper Cretaceous to Eocene, based mainly on isotopic pitchblende ages of 60 - 100 Ma (Stieff et al. (16), Horne (17)), a Tertiary age for the former seemed most likely. As it now appears certain that the jasper-type deposits are much older, as discussed above, the time-span over which the 'Iberian-type' could be interpreted to have formed is much wider. Isotopic determinations of pitchblende ages from mineralization at Azere are currently being made.

7. DISCUSSION

7.1. The granites as sources of uranium

Recent mineralogical studies of the accessory mineral suites in the 'younger' uranium-enriched granites by Basham et al. (8) and Pagel (5) have shown these to comprise monazite, zircon, apatite, xenotime (rarely) and low-thorian uraninite. Together with submicroscopic, intergranular uranium ? oxide, the last-named accounts for 50 - 70 % of the whole-rock value of 8 - 20 ppm and thus represents a considerable source of readily leached uranium. This is characteristic of the uranium - 'fertile' granites throughout the Hercynian chain of Europe (France, southwest England, Germany) and in contrast to the uranium-enriched but 'infertile' hornblendic granites of the Hercynian (Pagel (18)) and the Caledonian (Basham et al. (19)). These are characterized by the more stable suite of high-thorian uraninite, thorite, sphene, allanite and zircon. Although few data are available for other granites in Portugal, the uranium- and thorium-enriched Sao Pedro do Sul granite of the Beiras Region is noteworthy in the absence of known mineralization and an accessory suite dominated by thorian uraninite (Basham et al. (20)). Analysis of present-day stream waters draining this granite (Dekkers et al. (21)) shows low concentrations of uranium, indicating a low level of contemporary leaching. In contrast, the streams draining the 'fertile' Nisa granite contain appreciable levels of mobile uranium.

Several models have been proposed relating different mineralizing processes to labile low-thorian uraninite in the 'fertile' Hercynian granites (e.g. Cuney (22) for Bois Noir, France; Ball et al. (23) for southwest England). In Portugal a wide range of conditions of leaching, transport, deposition and concentration could all generate uranium deposits from the common source of uraninite in the 'fertile' granites.

7.2. The mineralization

The foregoing accounts of vein-type uranium deposits in Portugal demonstrate a broad temporal and physical spectrum from hydrothermal jasper-type veins formed at relatively high temperatures, through lower-temperature quartz veins and peribatholithic 'Iberian-type' mineralization, to undoubted supergene enrichments in surface-related traps. The availability of a large source of uranium in accessory uraninite, a pervasive fracture-network and several events (e.g. basic magmatism, Alpine tectonism) which would renew hydrothermal circulation through these open spaces, give rise to a number of alternative mechanisms and timing for these mineralizations. Many of the earlier models have been constrained by reliance on age determinations suggesting an Upper Cretaceous-Eocene age for the earliest of these, the jasper-type intragranitic veins. Current research indicates a much earlier age, probably late-Hercynian. Although it is perhaps premature to speculate until the actual data from reliable isotopic measurements on pitchblende from these deposits, and the 'Iberian-type', are available, it now seems possible that the accepted hydrothermal mineralizations may be closely linked genetically. Late Hercynian tectonic stresses were released in the relatively rigid, crystalline granites by development of large-scale, linear fractures and shear zones which sometimes extend into the metasediments. However, in the latter, the development of fracture systems is more closely controlled by the regional tectonic structures, principally the direction of major-fold axial planes and boundaries between competent and less-rigid beds. Within the narrow contact metamorphic zone surrounding the plutons, the hornfelsic and other recrystallized textures of the phyllitic rocks give rise to a more isotopic behaviour to stress-release with development of networks of microfractures and breccias.

If the uranium-bearing, oxidizing fluids which deposited uranium and minor amounts of other metals in large, open structures within the granites were to move outwards and upwards by convective action, on passing into the contact metamorphic zone the strongly reducing environment of the pyritiferous phyllites would cause further deposition of uranium in the microfracture network. It might be expected that by this time the fluids would be of somewhat lower temperature and possibly depleted in other elements. However, addition of uranium by solution from the granite would have been possible. In addition to accounting for the paragenetic, mineralogical and depositional characteristics of the 'Iberian-type' deposits, this model could also account for the lower-temperature quartz vein mineralization formed in larger fractures at the periphery of the granite masses.

Finally, although the above model implies temporal continuity from deposition of the jasper-type veins to the 'Iberian-type', it is acknowledged that a considerable time-gap could occur, allowing rejuvenation of the hydrothermal convective system at a later period. It is hoped that isotopic age determinations will resolve this problem.

ACKNOWLEDGEMENTS

One of the authors (IRB) gratefully acknowledges the hospitality afforded by ENU for work in Portugal, carried out in connection with a research contract under the Uranium Exploration Programme of the Commission of the European Communities. The paper is published with the approval of the Director of the Empresa Nacional de Urânio, Portugal and the Director, British Geological Survey.

REFERENCES

(1) MENDES, F., Contribution a l'etude geochronologique par la methode au strontium des formations cristallines du Portugal, Bol. Mus. Lab. Min. Geol. Fac. Cienc. Univ. Lisboa 11 (1968) 3-157.

(2) PINTO, M.C.S., Geochemistry and geochronology of granitic rocks from the Aveiro and Viseu districts (northern Portugal). Thesis, University of Leeds (1979) 196 pp.

(3) PORTUGAL FERREIRA, M., REGENCIO MACEDO, C., Actividade magmatica durante o Mesozoico: I - Achega para a datacao K - Ar de rochas filonianas basicas intrusivas na zona Centro Iberica (Portugal), Mem. Not. Mus. Lab. Geol. Univ. Coimbra 87 (1979) 29-49.

(4) CAMERON, J., Mineralogical aspects and origin of the uranium in the vein deposits of Portugal, in: Vein-type and Similar Uranium Deposits in Rocks Younger than Proterozoic, IAEA Vienna (1982) 349-371.

(5) PAGEL, M., Granites et gisements d'uranium du Portugal, typologie, alterations et mineralisations, in: Vein-type and Similar Uranium Deposits in Rocks Younger than Proterozoic, IAEA Vienna (1982) 323-347.

(6) PAGEL, M., Facteurs de distribution et de concentration de l'uranium et du thorium dans quelques granites de la chaine hercynienne d'Europe, Thesis, Institut National Polytechnique de Lorraine (1981).

(7) COTELO NEIVA, J.M., Epocas de metalogenia de diferenciaçao magmatica em Portugal, Publ. Mus. Lab. Min. Geol. Fac. Cienc. Univ. Porto (1944).

(8) BASHAM, I.R., BOWLES, J.F.W., ATKIN, D., BLAND, D.J., Mineralogy of uranium distribution in samples of unaltered and sericitized granite from Urgeiriça, Portugal, in relation to mineralization processes, in: Vein-type and Similar Uranium Deposits in Rocks Younger than Proterozoic, IAEA Vienna (1982) 299-309.

(9) CATHELINEAU, M., CUNEY, M., LEROY, J., LHOTE, F., NGUYEN TRUNG, C., PAGEL, M., POTY, B., Caracteres mineralogiques des pechblendes de la province hercynienne d'Europe, Comparisons avec les oxydes d'uranium du proterozoique de differents gisements d'Amerique du Nord, d'Afrique et d'Australie, in: Vein-type and Similar Uranium Deposits in Rocks Younger than Proterozoic, IAEA Vienna (1982) 159-177.

(10) DARNLEY, A.G., Pitchblende from Carrasca, Portugal, Geol. Survey Great Britain, Atom. Energy Div., Age Determination Rep. No. 17 (1961) 5 pp.

(11) CERVEIRA, A., Notas sobre as pecheblendas francesas de portuguesas, Bol. Soc. Geol. Portugal 12 (1956) 129 pp.

(12) PORTUGAL FERREIRA, M., MATOS DIAS, J.M., Uranium mineralization and episyenites. A case study in Portugal, in: Vein-type and Similar Uranium Deposits in Rocks Younger than Proterozoic, IAEA Vienna (1982) 311-321.

(13) LIMPO DE FARIA, F., Gites d'uranium portugais dans des formations metasedimentaires, Com. Serv. Geol. Portugal 50 (1966) 9-50.

(14) PILAR, L., Condiçoes de formaçao do jazigo uranifero de Niza, Com. Serv. Geol. Portugal 50 (1966) 51-83.

(15) BARROS, R.F., O jazigo da Senhora das Fontes, Com. Serv. Geol. Portugal 50 (1966) 110-129.

(16) STIEFF, L.R., STERN, T.W., Age study of uraninites from the Urgeiriça and Lenteiro mines, Portugal, J.E.N. Technical Paper n° 27 (1960) 11-17.

(17) HORNE, J.E.T., Age of pitchblende from Lenteiros, Reboleiro, Portugal, J.E.N. Technical Paper n° 27 (1960) 7-10.

(18) PAGEL, M., The mineralogy and geochemistry of uranium, thorium and rare earth elements in two radioactive granites of the Vosges, France, Mineralog. Mag. 339 (1981) 149-161.

(19) BASHAM, I.R., BALL, T.K., BEDDOE-STEPHENS, B., MICHIE, U.McL., Uranium-bearing accessory minerals and granite fertility: II Studies of granites from the British Isles, in: Uranium Exploration Methods, OECD/IAEA Paris (1982) 385-413.

(20) BASHAM, I.R., VAIRINHO, M.M.B., BOWLES, J.F.W., Uranium-bearing accessory minerals in the Sao Pedro do Sul Granite, Portugal, in: Vein-type and Similar Uranium Deposits in Rocks Younger than Proterozoic, IAEA Vienna (1982) 279-298.

(21) DEKKERS, M.J., VRIEND, S.P., VAN DIEST, Ph., VAN DER WEIJDEN, C.H., OOSTEROM, M.G., Geochemical controls of transport and deposition of uranium from solution, Case study - Sao Pedro do Sul, Portugal, Summary Rep. State Univ. Utrecht (1983) 54 pp.

(22) CUNEY, M., Geologic environment, mineralogy, and fluid inclusions of the Bois Noirs - Limouzat uranium vein, Forez, France, Econ. Geol. 73 (1978) 1467-1610.

(23) BALL, T.K., BASHAM, I.R., MICHIE, U.McL., Uraniferous vein occurrences of south-west England - Paragenesis and genesis, in: Vein-type and Similar Uranium Deposits in Rocks Younger than Proterozoic, IAEA Vienna (1982) 113-158.

SOBRE EL ORIGEN DE LOS YACIMIENTOS FILONIANOS DE URANIO EN ROCAS METASEDIMENTARIAS: EL CASO DE MINA FE, SALAMANCA (ESPAÑA)

A. Arribas
Universidad de Salamanca
Salamanca
España

Abstract – Resumen

ORIGIN OF URANIUM VEIN DEPOSITS IN METASEDIMENTARY ROCKS: FE MINE, SALAMANCA (SPAIN)

The numerous U deposits occurring in the schist-graywacke complex (CEG) of the Iberian Peninsula, characterized by the mineral association carbonates, pitchblende (coffinite), adularia and Fe sulphides, have both a considerable economic importance and a high metallogenic interest as their origin has not been convincingly explained yet. In fact, since 1959, these mineralizations have been successively attributed to the concentration of U in fractured and brecciated zones of the schists due to one of these processes:

- magmatic, by transportation of U in hydrothermal fluids related to the evolution and emplacement of the Hercynian granites;
- supergenic, by the release of U from the Hercynian granites during the weathering and erosion processes which gave place to the Pliocene peneplan;
- segregation, by leaching of U from plutonic rocks under the effects of late- and/or post-Hercynian tectonic movements;
- diffusion, by concentration of U from fertile metasediments by thermal diffusion or hydrothermal flow.

In this paper, taking into account field and laboratory studies carried out recently in the FE mine, so far the most important Spanish U deposit of this kind, the above mentioned hypotheses are discussed and the main metallogenic features of the orebody are given. Among these, the most significant are: the high geochemical U content, 30 to 200 ppm, of the CEG carbonaceous slates prevalent in the area; the nature and alteration processes, chloritization and hematitization of the host rocks; the radiometric age of the pitchblende 37 to 57 Ma; the low temperature mineral association; the peculiar gravitational textures of the ore minerals; the temperature and salinity of the fluid inclusions of the carbonates, ranging from 230°C to less than 70°C, and from 0 to 25 % NaCl equiv. respectively; and the shallow tectonic activity giving place to the hydraulic fracturing and fault breccias controlling the ore deposition. Finally, the FE orebody is compared with similar U deposits in Spain and elsewhere, and the origin of the mineralization is attributed to seismic pumping of U contained in the CEG carbonaceous slates.

According to this model, the strains developed in the Hercynian basement around shear zones resulting from the Alpine tectonic activity, during Lower to Middle Tertiary times, would have given rise to episodic remobilizations of the U by hydrothermal fluids.

Consequently, when the dilatant zones collapsed, these U-bearing solutions, geothermal in character, were expelled towards the surface depositing the U and accompanying minerals in fractures and breccias associated to the wrench faults.

SOBRE EL ORIGEN DE LOS YACIMIENTOS FILONIANOS DE URANIO EN ROCAS METASEDIMENTARIAS: EL CASO DE MINA FE, SALAMANCA (ESPAÑA)

Las numerosas mineralizaciones de uranio existentes en el complejo esquisto grauvâquico (CEG) de la Peninsula Ibêrica, pertenecientes a la paragênesis carbonatos, pechblenda (coffinita), adularia y sulfuros de Fe, tienen, además de una considerable importancia econômica, un gran interês metalogênico, ya que su origen no ha podido ser explicado todavía de forma convincente. Así, desde 1959, estas mineralizaciones se han venido atribuyendo sucesivamente a una deposición del U en zonas fracturadas y brechificadas del basamento hercînico como consecuencia de uno de estos procesos:

- magmâticos, por transporte del U en fluidos hidrotermales relacionados con la evolución y emplazamiento de los granitos hercînicos;
- supergênicos, por liberación del U de los granitos durante los procesos de meteorización y erosión que dieron lugar a la penillanura pliocena;
- de segregación, por lixiviación del U de las rocas plutônicas como consecuencia de movimientos tectônicos tardihercínicos y/o alpinos;
- de difusión, por redistribución del U contenido en los metasedimentos fêrtiles del CEG por difusión têrmica o flujo hidrotermal.

En este trabajo, basândose en los estudios de campo y laboratorio llevados a cabo últimamente en mina Fê, la más importante de las que existen en España de esta clase, se discuten las hipôtesis anteriores y se exponen los principales caracteres metalogênicos del yacimiento. Entre êstos, los mâs significativos son: el alto contenido geoquîmico en U, de 30 a 200 ppm, de las pizarras ampelíticas, que son predominantes en la zona; la naturaleza y los procesos de alteración, cloritización y hematización, de las rocas encajantes; la paragênesis de baja temperatura; las peculiares texturas geopetales de los minerales filonianos tardíos; la edad radiomêtrica de la pechblenda, 37 a 57 Ma; el rango de temperatura y salinidad de las inclusiones fluidas de los carbonatos de la ganga, variable entre 230° y menos de 70°C y 0 y 25 % equiv. NaCl respectivamente; y el carâcter superficial de los procesos tectônicos que dieron lugar a la fracturación hidraûlica y a las brechas que contienen la mineralización. Finalmente, se compara êsta con la de otros yacimientos españoles y extranjeros, y se atribuye su origen a una reconcentración del U de las filitas ampelíticas como consecuencia del bombeo sísmico provocado en los materiales del CEG por los contragolpes de la orogenia alpina.

De acuerdo con esta idea, las tensiones tangenciales que se desarrollaron en el basamento hercînico durante la primera mitad del Terciario habrîan dado lugar a episôdicas removilizaciones del U de los metasedimentos fêrtiles, el cual, al producirse el colapso de las zonas de dilatación, habría sido expulsado hacia la superficie por los fluidos hidrotermales de carácter geotêrmico que depositaron el U y los minerales acompañantes en las brechas y fracturas asociadas con las fallas de desgarre.

1. INTRODUCCION

Las numerosas mineralizaciones filonianas de uranio existentes en el Complejo esquisto-grauvâquico (CEG) de la Penînsula Ibêrica - entre ellas, las de Saelices, Alameda de Gardôn, Villar de la Yegua y Villavieja de Yeltes, en la provincia de Salamanca; Ceclavîn, Acehuche y Albalá, en la de Câceres; D. Benito, en la de Badajoz; y Nisa, Azere y Nª Sª das Fontes, en Portugal - tienen, además de una considerable importancia econômica, un gran interês metalogênico.

Asî, desde 1959, en que se encontraron los primeros indicios con minerales primarios de uranio, los yacimientos de las pizarras de Salamanca se han venido atribuyendo a alguno de estos procesos:

- magmáticos: por depósito del uranio a partir de fluidos hidrotermales relacionados con el emplazamiento de los granitos hercínicos (Arribas (1), (2), (3));
- supergénicos: por lixiviación del uranio lábil de los granitos durante los procesos de meteorización y erosíon asociados con el desarrollo de la penillanura pliocena, y concentración per descensum de aquel elemento en zonas fracturadas del basamento hercínico (Fernandez Polo (4), Matos Dias (5));
- de segregación: por liberación del uranio de las rocas plutónicas como consecuencia de los procesos tectónicos tardihercínicos o alpinos, y deposición de dicho elemento en zonas fracturadas de los esquistos (Arribas (6));
- de difusión: por lixiviación y concentración del uranio de los metasedimentos fértiles del CEG, especialmente las pizarras ampelíticas, en zonas fracturadas y brechificadas de los esquistos. La movilización y el transporte del uranio se habrían efectuado por difusión térmica o flujo hidrotermal, y en este último caso, en corrientes de convección generadas por los procesos tectónicos post-Paleozóicos (Arribas (7)).

Ultimamente, los estudios de laboratorio y las observaciones realizadas sobre el terreno han proporcionado nuevos datos sobre la metalogenia de este singular tipo de yacimiento, de los cuales, el de mina Fé, situado en las proximidades de Saelices, en la provincia de Salamanca, sigue siendo el ejemplo más importante y representativo.

En este trabajo se resumen los conocimientos actuales y los estudios en curso para establecer un modelo metalogénico que permita explicar el origen de estas mineralizaciones, las cuales, por no alcanzar a veces la superficie, presentan todavía, al tiempo que un gran potencial uranífero, dificultades para su prospección.

2. GEOLOGIA Y MINERALOGIA DEL YACIMIENTO

Las mineralizaciones de uranio de mina Fé (Fig. 1) se encuentran en metasedimentos del CEG formados por una serie alternante de lutitas y areniscas de grano fino, con abundante materia carbonosa y ocasionalmente carácter turbidítico, en la que predominan las ritmitas con estratificación y laminación paralela.

En ocasiones, las rocas epimetamórficas - sericitoesquistos, cloritoesquistos y cuarcitas - muestran todavía estructuras claramente sedimentarias, tales como rizaduras de oleaje, laminación cruzada y ocasionalmente avolutada, marcas de corriente, sedimentación graduada, acanaladuras, y surcos. Además, intercalados en la serie hay también gravas, conglomerados y rocas calco-silicatadas, especialmente anfibolitas cuarcíferas y granatíferas (Arribas et al. (8)), Martín-Izard y Arribas (9)), lo que indica que estas rocas se depositaron en una plataforma continental abierta, o en un mar epicontinental, en el que predominaban los procesos de sedimentación y decantación, en aguas turbias y generalmente por debajo del nivel de base del oleaje, de materiales predominantemente siliciclásticos.

Estas condiciones de deposición quedan reflejadas en el estudio geoquímico realizado sobre cerca de 1000 muestras representativas de las diferentes litologías del CEG de la zona de Ciudad Rodrígo, en la que se encuentran la mayor parte de las mineralizaciones españolas de esta clase (Arribas et al. (9), (10)). De acuerdo con él (Fig. 1), las cuarcitas, conglomerados, esquistos y rocas calco-silicatadas tienen menos de 15 ppm U, mientras que el 15 % de las filitas ampelíticas, que constituyen por si solas el 40 % de la serie estratigráfica, tienen siempre más de 30 ppm U, y muchas veces hasta 200 ppm.

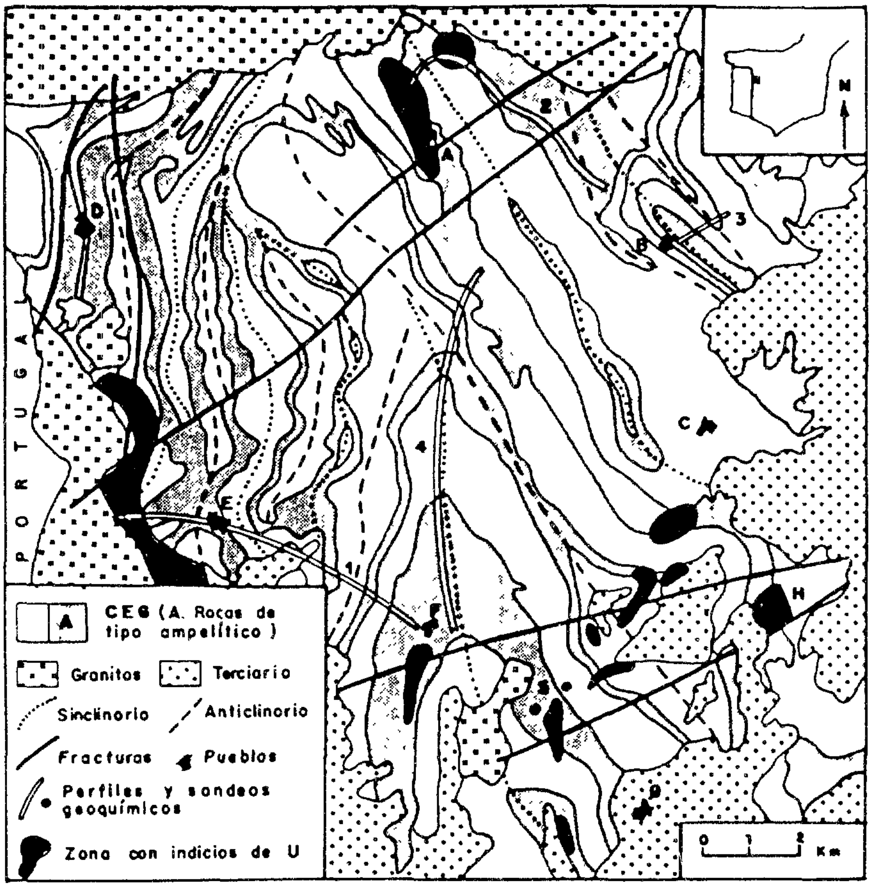

FIG. 1. Distribución de las pizarras ampelíticas (A) en el complejo esquisto-grauváquico (CEG) que forma el borde septentrional de la cuenca terciaria situada al NW de Ciudad Rodrígo (Salamanca). Localidades: A. Villar de la Yegua; B. Castillejo; C. Saelices; D. Aldea del Obispo; E. Alameda de Gardón; F. Gallegos de Argañán; G. Carpio de Azaba; H. Mina Fé. Desmuestros geoquímicos: 1. Alameda; 2. Villar; 3. Castillejo; 4. Gallegos; 5. Sondeos Carpio (según Arribas et al. (8), modificado).

Las rocas del CEG fueron afectadas por dos fases tectónicas hercínicas principales (Fig. 2) que produjeron una esquistosidad de flujo y otra de crenulación (Arribas et al. (11)). Por otra parte, los sistemas de fractura más importantes, localizados preferentemente en las charnelas de los pliegues de primera y segunda fase (Coma (12)), siguieron actuando en épocas posteriores, lo que dió lugar a la formación de brechas (Fig. 3) y fracturas de tensión que sirvieron de conducto a los fluidos mineralizadores.

El yacimiento de Fé, a diferencia de lo que ocurre con la mayoría de las mineralizaciones de esta clase, que generalmente se encuentran en o muy cerca del contacto con las rocas ígneas, se halla a 3 y 5 km de distancia, respectivamente, de los granitos de Gallegos de Argañán y Bañobárez. Por otro lado, un sondeo de 400 m, efectuado en el centro del yacimiento, ni ha llegado al granito ni ha atravesado rocas afectadas por metamorfismo de contacto.

Los minerales de uranio se encuentran en brechas de falla (Fig. 4 y 5) y filoncillos cuya potencia varía de unos milímetros a varios decímetros, correspondiendo los últimos al relleno de fisuras satélites de las fallas que fueron originadas probablemente por fracturación hidraúlica. Ocasionalmente, los filoncillos, al igual que las brechas, coinciden con reaperturas de la esquistosidad o de filones de cuarzo de edad hercínica; siendo de destacar que algunas de las minerali-

FIG. 2. Fé 1. Las brechas y fracturas mineralizadas coinciden generalmente con las charnelas de los pliegues de la 1ª y 2ª fase tectónicas.

FIG. 3. Fé 1, banco 639. Los minerales primarios de U se encuentran solamente en fracturas y estructuras abiertas de las brechas, una de las cuales se ve en la fotografía.

zaciones fueron cubiertas ya por los sedimentos del Terciario inferior que se depositaron sobre el bloque tectónico situado al N de la fosa de Ciudad Rodrigo (Fig. 6).

La paragénesis es de tipo hidrotermal (Fig. 7) y corresponde a la asociación carbonatos-adularia-pechblenda (coffinita)-sulfuros de hierro (Arribas (13), (6) y (7)). Estos minerales (Fig. 8 - 13) van acompañados por pequeñas cantidades de galena, esfalerita, calcopirita y jaspe, éste generalmente hematítico, y trazas de fluorita y hematites (Fig. 13); además, una limitada pero intensa cloritización se desarrolló sobre las rocas encajantes. Los carbonatos, muy abundantes por debajo de la zona de oxidación (Fig. 9 - 10), corresponden a calcita, dolomita y ankerita, ésta última con abundante Mn. Los sulfuros de Fe son pirita y marcasita (Fig. 12). Los minerales supergénicos consisten en gummitas, iantinita, uranotilo alfa, autunita, fosfuranilita, kasolita, renardita, sabugalita, saleíta, johannita, zippeita y uranopilita.

Salvo la adularia, que se depositó únicamente durante la primera etapa del proceso mineralizador, por lo que está frecuentemente cloritizada (Fig. 13), los carbonatos, sulfuros de hierro y minerales primarios de uranio lo hicieron repetidas veces a lo largo de dicho proceso (Fig. 9 - 11). Este tuvo, pues, un carácter intermitente, y de acuerdo con los resultados obtenidos en el estudio de las inclusiones fluidas de los carbonatos de la ganga (Mangas y Arribas (13)), las soluciones hidrotermales, fuertemente cloruradas, se caracterizaron, en general, por un progresivo aumento de la salinidad y descenso de la temperatura de homogeneización; siendo de destacar que los minerales depositados durante las últimas fases de la venida hidrotermal se formaron ya, según indican su composición y textura, a temperatura mucho más baja y en condiciones subsuperficiales (Fig. 8).

En general, las inclusiones fluidas son primarias, acuosas y bifásicas, con relaciones volumétricas V_{gas}/V_{total} que varían del 1 % al 5 %. Las temperaturas

FIG. 4. Fe 3. Aunque las zonas brechificadas pueden tener varios metros de potencia, los minerales de U se hallan normalmente en fracturas que solo miden de unos mm a varios cm de anchura.

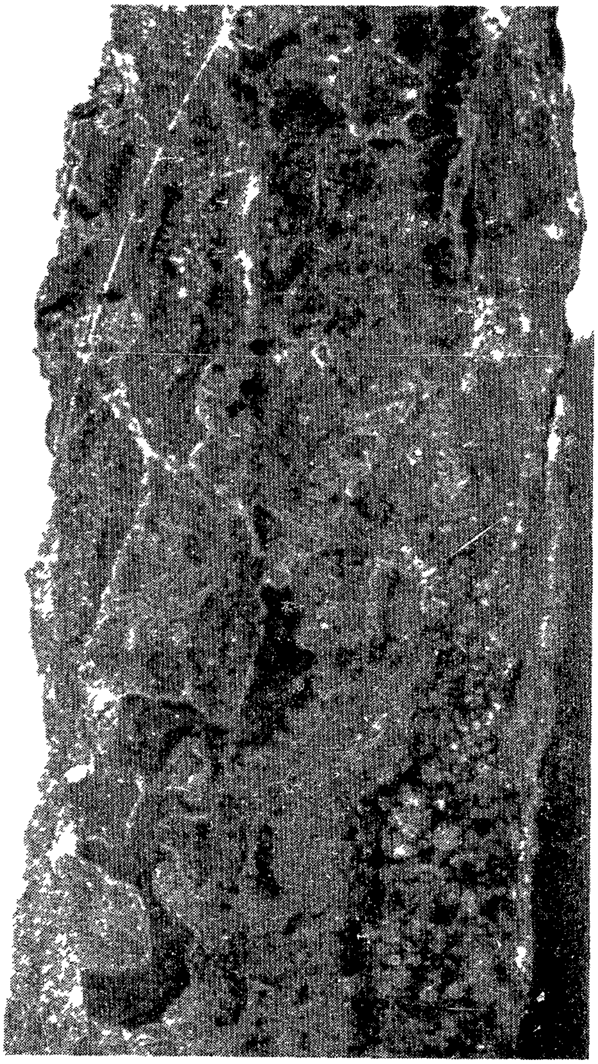

FIG. 5. Las tres generaciones de carbonatos filonianos: los primeros, bien cristalizados, son amarillentos y ricos en Fe; los intermedios, crustiformes, son rosaceos y ricos en Mn; y los ultimos, finamente laminados, se depositaron, por gravedad y a baja temperatura, en los huecos de los anteriores.

de fusión del hielo oscilan entre 0° y -25.5°C, presentando algunas inclusiones temperaturas eutécticas inferiores a -21°C, y solidificación del hielo e hidratos, lo que indica la presencia de iones, tales como Ca^{++}, Mg^{++}, K^{+}, CO_3^{--} y HCO_3^{-}, junto con el Cl^{-} y Na^{+}, que son los dominantes. Las temperaturas de homogeneización varían entre 60° y 230°C, con dos máximos a 80° y 100°C, habiendo confirmado los análisis con la microsonda Raman la ausencia de CO_2, CH_4, N_2 y SO_2 en la fase vapor, y de SO_4^{--} en la fase líquida.

Los significativos cambios de los parámetros físicos y químicos de las soluciones mineralizadoras en el tiempo y espacio confirman la existencia de ambientes subsuperficiales, donde habrían tenido lugar fenómenos de mezcla entre aguas de diferente composición, connatas y vadosas. Las condiciones de atrapamiento de los

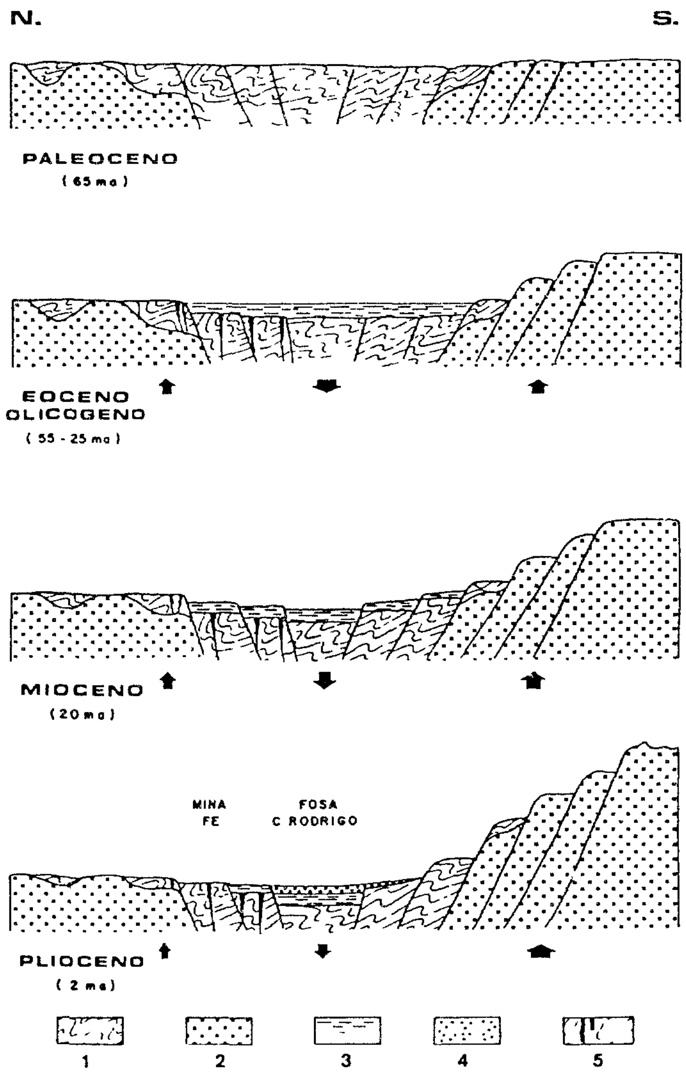

FIG. 6. Relación entre las mineralizaciones de uranio y la evolución tectónica del basamento hercínico de la cuenca de Ciudad Rodrigo durante el Terciario (1. complejo esquisto-grauváquico (CEG); 2. granitoides; 3. Terciario; 4. Pliocuaternario; 5. Brechas uraniferas).

fluidos corresponden a temperaturas decrecientes a partir de 230°C y presiones bajas, aunque suficientes para que no se haya producido ebullición.

La textura bandeada de los minerales que constituyen la parte más importante del relleno filoniano y el cemento de las brechas confirma también el carácter intermitente de la mineralización, la cual está formada por minerales bien cristalizados, caso de la adularia y los carbonatos (Fig. 14, 15), o agregados coloidales, caso de los sulfuros de hierro y los óxidos y silicatos de uranio (Fig. 16, 17). Por el contrario, durante las etapas tardías, los minerales filonianos, excepto la adularia, que se depositaron rítmicamente y a baja temperatura en los huecos que quedaban entre los minerales formados anteriormente (Fig. 5), y entre las brechas y los hastiales (Fig. 8), dieron lugar a sedimentos varvados, finamente laminados (Fig. 10), que presentan texturas geopetales, tales como estratifi-

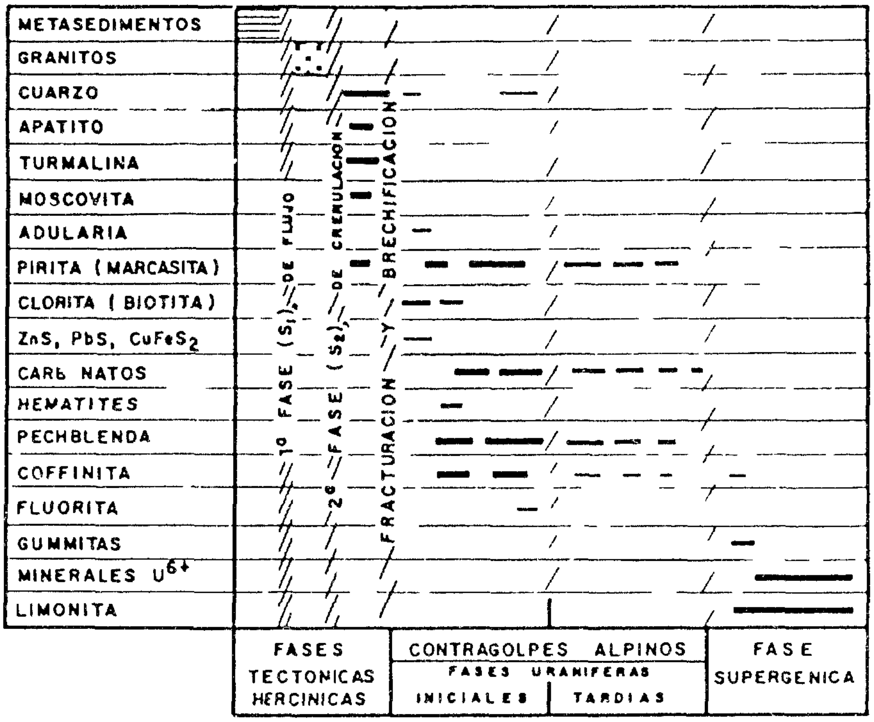

FIG. 7. Microtectonica y sucesión metalogenica en mina Fe.

FIG. 8. Fé 3. Brecha de un cuarzo filoniano hercínico relleno por carbonatos de dos venidas sucesivas: arriba, cristales de ankerita fibroso-radiada depositados a más de 200°C; en el centro, sedimento formado por carbonatos rojos (hematites), grises (pirita) y blanco (calcita pura), depositados, a menos de 70°C y en condiciones casi superficiales, sobre la pechblenda (negro) que se ve en la parte inferior de la fotografía.

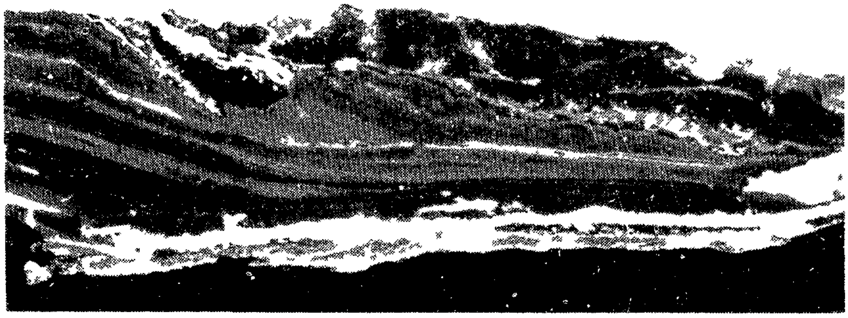

FIG. 9. Fé 3 (1/2 x). La laminación cruzada, de bajo ángulo, que forman los carbonatos, pirita y pechblenda tardíos, revela la intensa actividad cinemática de los fluidos.

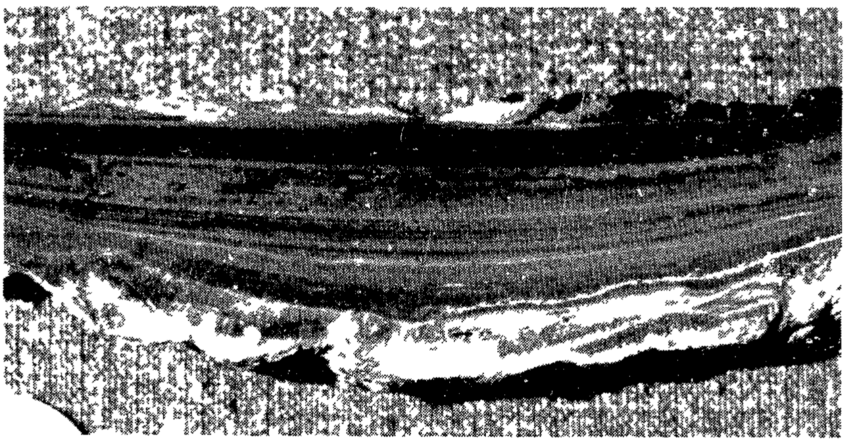

FIG. 10. Fé 3 (1/2 x). Los minerales tardíos se depositaron en los huecos de las brechas como sedimentos finamente laminados.

FIG. 11. Fé 3. Seccion pulida, 100 x NC. Texturas geopetales en un depósito finamente laminado de pechblenda (gris claro) y ankerita (gris obscuro) sobre marcasita (blanco).

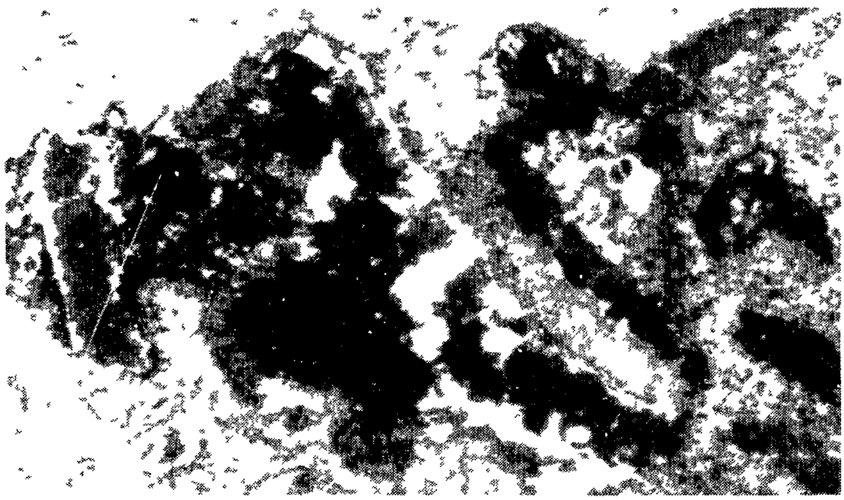

FIG. 12. Fé 1. Sección transparente, 60 x LN. La adularia, reemplazada aquí por clorita fuertemente hematizada, se depositó únicamente durante las fases iniciales de la mineralización.

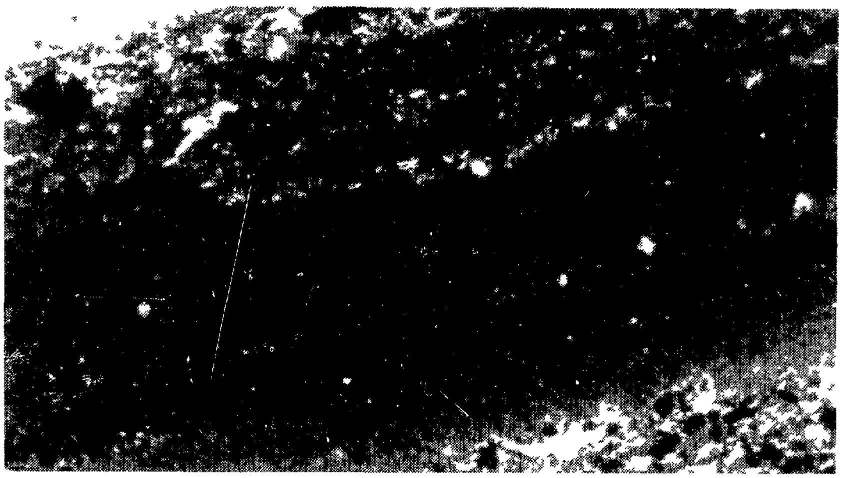

FIG. 13. Fé 3. Sección transparente, 40 x LN. La sedimentación graduada de los carbonatos, sulfuros de Fe, y la pechblenda y coffinita demuestran que, durante las etapas tardías, el depósito de estos minerales se efectuó principalmente por gravedad.

cación graduada (Fig. 11), laminación cruzada de bajo ángulo (Fig. 9, 10) y figuras de carga (Fig. 11, 12).

Estos sedimentos están constituídos, unas veces, por agregados coloidales de carbonatos, pechblenda, coffinita y sulfuros de hierro (Fig. 18), y otras, por fragmentos clásticos de estos mismos minerales y de los que formaban las rocas de caja más o menos cloritizadas y hematizadas. Estos fragmentos fueron arrancados de las propias estructuras filonianas y arrastrados por el agua altamente salina que circuló por las brechas y fracturas durante las últimas etapas del proceso mineralizador (Fig. 19). Por otra parte, la existencia de huecos, ocupados parcial o totalmente por minerales coloidales, principalmente carbonatos, que se depositaron por gravedad y a muy baja temperatura en ambientes casi superficiales, dando lugar a texturas geopetales, permite determinar la posición que tenían aquellas estructuras cuando se depositó en ellas la mineralización (Fig. 5).

Finalmente, cabe destacar que las primeras determinaciones geocronológicas efectuadas en una pechblenda de mina Fé, banco 639, m. 140, por el método U/Pb y Pb/Pb (Tabla I), corresponden a una edad comprendida entre 37 y 57 Ma. Esto hace coincidir el emplazamiento de la mineralización con la primera mitad del Terciario, es decir, con los momentos en que actuaban sobre el basamento hercínico los contragolpes alpinos que iban a dar lugar a la fosa tectónica de Ciudad Rodrígo, y con la edad de 58 Ma - obtenida por el método K/Ar - de la alunita de las areniscas silíceas que forman la base del Terciario en la cuenca del Duero (Blanco et al. (14)), y con las que se inició precisamente la sedimentación alpina en dicha fosa.

FIG. 14. Fé 1, banco 639. SEM, 100 x. Adularıa rodeada por pechblenda con fisuras de retracción. Nótese la abundancia de fragmentos clásticos en los óxidos de U.

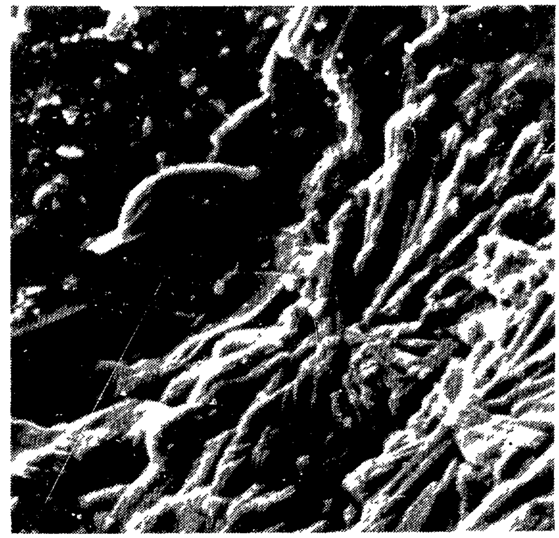

FIG. 15. La preparación de la Fig. 11 vista con el SEM, 350 x. Aspecto fibroso-radiado de los carbonatos tardíos que crecen sobre los esferulitos de pechblenda y coffınita.

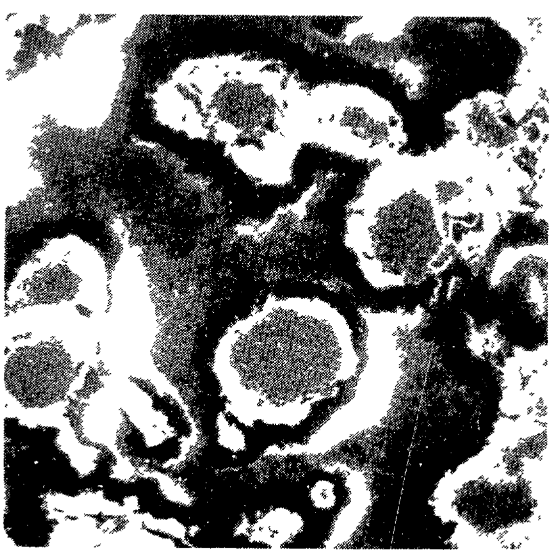

FIG. 16. Otro campo de la muestra de la figura 14, SEM, 2500 x. Textura vacuolar del gel formado por sulfuros de Fe y óxidos de U. La pirita (gris obscuro) aparece rodeada sucesivamente por pechblenda y coffinita (gris claro). Los carbonatos (negro) ocupan los huecos de los anteriores.

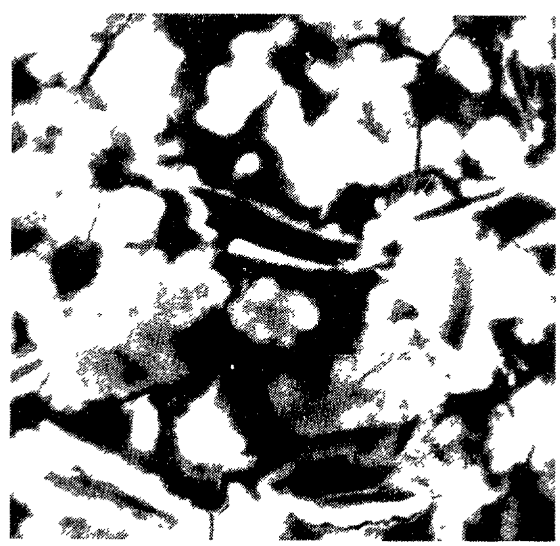

FIG. 17. La muestra de la Fig. 11 vista con el SEM x 600. Fragmentos clásticos de micas y pechblenda rodeados por pechblenda, coffinita y calcita.

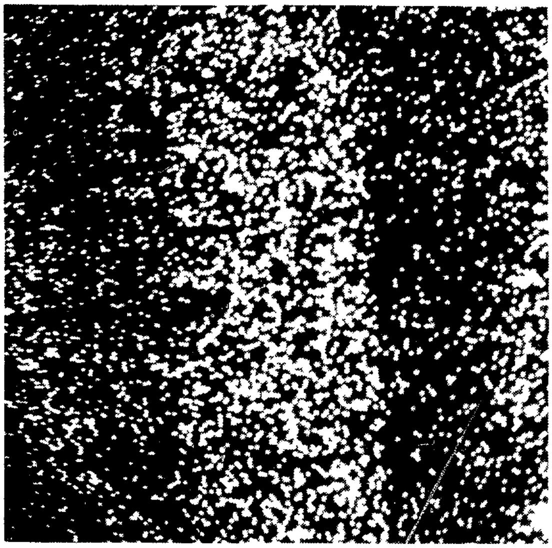

FIG. 18. La muestra de la Fig. 13 vista con el SEM x 200. Microsedimentos formados por pechblenda y carbonatos.

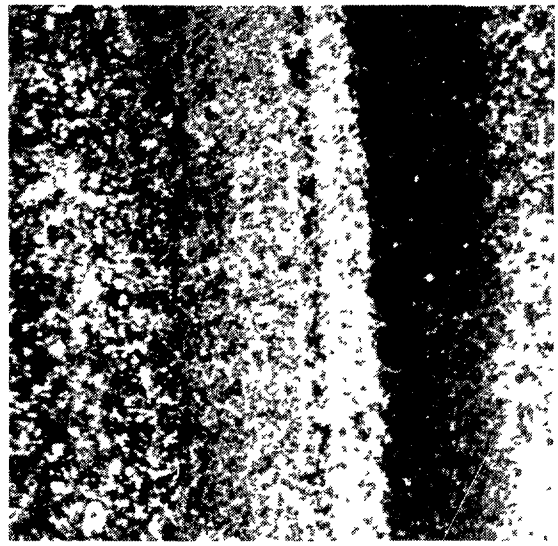

FIG. 19. Distribución del U en la figura anterior.

TABLA I. EDADES APARENTES Y RELACIONES ISOTÓPICAS DE UNA MUESTRA DE PECHBLENDA DE MINA FÉ, SAELICES (SALAMANCA).

	$^{206}Pb/^{238}U$	$^{207}Pb/^{235}U$	$^{207}Pb/^{206}U$
RELACIONES	0.0057772	0.037570	0 047165
ERRORES	0.74 %	0.76 %	0.175 %
EDADES	37.13 MA	37.45 MA	57.65 MA

CONCENTRACIONES EN LA PECHBLENDA

PB TOTAL	11,305.8 PPM
PB COMUN	34.0 PPM
U	24.45 %

COMPOSICIÓN ISOTÓPICA DE LA GALENA DE MINA FÉ

$^{206}Pb/^{207}U$	18.975	± 0.12 %
$^{206}Pb/^{208}U$	68.724	
$^{206}Pb/^{204}U$	2,652.6	± 0.60 %
$^{207}Pb/^{204}U$	138.79	± 0.56 %
$^{208}Pb/^{204}U$	38.598	

ANALISTA KEN LUDWIG, USGS, DENVER (EEUU)

3. LOS PROCESOS GENETICOS

Con los datos que se tienen hasta ahora, se pueden establecer las siguientes conclusiones metalogênicas:

- Los minerales primarios de uranio de mina Fé no tienen origen magmático en sentido estricto, ya que algunas de las estructuras filonianas no son características de este tipo de yacimientos. Además, la mineralización está muy alejada del granito, y su edad es claramente posterior a la del emplazamiento de las rocas plutónicas hercínicas.
- El origen supergénico, per descensum, durante el Plioceno, debe ser igualmente descartado, ya que algunas mineralizaciones primarias, e incluso secundarias, están fosilizadas por los sedimentos del Terciario. Además, la presencia de ciertos minerales, p.e., la adularia y clorita, y las temperaturas de homogeneización de las inclusiones fluidas de los carbonatos de la ganga indican condiciones físico-químicas de deposición que no pueden ser atribuídas a procesos supergénicos.
- Una segregación del uranio de las rocas plutónicas fértiles como consecuencia de procesos de albitización, moscovitización y deformación análogos a los que parecen haber dado lugar a algunos yacimientos de uranio en los granitos hercínicos europeos, seguida de la concentración de este elemento en zonas tectonizadas de los esquistos, debe ser igualmente descartada, ya que en las proximidades de mina Fé no hay rocas intrusivas y la edad de la pechblenda es muy posterior a las de las mineralizaciones intragraníticas.

Por todo éllo, en tanto se terminan las nuevas dataciones geocronológicas que se están efectuando en el Laboratorio Geoquímica Isotópica de la Universidad de Montpellier para confirmar la edad de los minerales primarios, y se concluyen los análisis isotópicos del O^{18}, C^{13} y S^{34} de los silicatos, carbonatos y sulfuros filonianos, y el estudio de las inclusiones fluidas de los carbonatos de la ganga, que permitan conocer la naturaleza de los fluidos mineralizadores y determinar su papel en la génesis del yacimiento, el origen de la mineralización se atribuye aquí a una removilización y transporte del uranio contenido en los metasedimentos fértiles del complejo esquisto-grauváquico, especialmente en las pizarras ampelíticas, y a su posterior deposición, a partir de un complejo uranil-carbonatado, en zonas fracturadas y brechificadas de los esquistos.

En este trabajo, teniendo en cuenta, además de otros factores a los que se alude más adelante, la única edad conocida de la pechblenda, se propone que la movilización del uranio pudo tener lugar bajo los efectos de la actividad tectónica que, durante el Terciario inferior, se desarrolló sobre el basamento hercínico como consecuencia de los contragolpes de la orogenia alpina. En estas condiciones, las tensiones creadas por dicho proceso orogénico habrían dado lugar a una distensión y microfisuración de las rocas en la parte superior de la corteza y, con éllo, a la movilización de una considerable cantidad de fluidos que habrían sido expulsados hacia la superficie por las fracturas y brechas asociadas con las zonas de cizalla.

Por lo que se refiere al mecanismo que pudo provocar el transporte y deposición del uranio y de los otros elementos que le acompañan en la paragénesis, especialmente Mg, Ca, K, Fe, Mn, C y S, que dieron lugar a la formación de clorita, adularia, carbonatos y sulfuros de Fe, existen dos posibilidades: la difusión térmica y el flujo hidrotermal. La primera, invocada ya por Arribas (7) para explicar el origen de estos yacimientos, se habría producido, según las ideas de Laffite (15), Schipulin (16) y Costeseque et al. (17), por migración iónica y sin apenas renovación de los fluidos. En cuanto a la segunda, el flujo se habría generado por un aumento del gradiente geotérmico como consecuencia de los procesos tectónicos.

En el momento actual y dado que las texturas filonianas indican una intensa actividad cinemática de los fluidos, la hipótesis más verosímil parece ser la segunda. En este caso, el movimiento de las soluciones hidrotermales se habría producido en una sola dirección, o bien formando corrientes de convección que, en sucesivas venidas, habrían dado lugar a la cloritización de las rocas encajantes y al depósito de la adularia, calcita y los sulfuros de hierro que constituyen la ganga principal de las mineralizaciones con pechblenda. Minerales, por cierto, que, como se indica más adelante, son característicos también de los productos de alteración que se forman hoy en algunos campos geotérmicos.

4. EL ORIGEN POR BOMBEO SISMICO

El mecanismo de movilización y transporte del uranio que se sugiere aquí para explicar la génesis del yacimiento de Fé coincide, en líneas generales, con el proceso de bombeo sísmico (seismic pumping) que Sibson et al. (18) propusieron para explicar el origen y carácter intermitente de algunos fluidos hidrotermales.

De acuerdo con esta idea, la difusión de los fluidos en la parte superior de la corteza puede ser atribuida, entre otras causas, a los procesos de dilatación que preceden al desencadenamiento de los terremotos poco profundos. En estos casos (Fig. 20), antes de que se produzca un seísmo por rotura y desplazamiento do una zona de cizalla, las rocas situadas alrededor del foco sísmico se dilatan bajo la acción de los esfuerzos tectónicos tangenciales, lo que da lugar al desarrollo de microfisuras y fracturas de tensión normales al eje menor del elipsoide de deformación ($\delta 3$). En estas condiciones, al disminuir la presión de los fluidos intergranulares en la zona de dilatación, y a medida que aumentan el coeficiente de fricción y, con él, la resistencia a la rotura, se dirigen hacia aquella zona los fluidos de las rocas adyacentes. Más tarde, al llenarse las fisuras con los fluidos emigrados, aumenta de nuevo la presión intersticial y disminuye la resistencia de la roca. Es entonces, al ser superado el coeficiente de fricción por los esfuerzos tangenciales, cuando se produce el colapso de la zona de cizalla, se desencadena el seísmo, y se comprime bruscamente la zona de dilatación, con lo que los fluidos son expulsados hacia la superficie a través de las brechas y fallas de desgarre.

La cantidad de agua que se puede liberar por este mecanismo es considerable, ya que Tsuneishi y Nakamura (19) han calculado que la serie de terremotos de Matsushiro - originada por movimientos de cizalla producidos alrededor de una falla de desgarre, y cuya energía fue equivalente a la de un solo seísmo de magnitud M 6.3 - dió lugar, en un año, a la expulsión de 10^7 m^3 de una solución hidrotermal rica en Na, Ca y Cl, y saturada en CO_2.

En este sentido, dadas las importantes zonas de fractura que afectan al CEG al N y O de Ciudad Rodrígo - de las cuales, dos, la que pasa por Saelices y Gallegos de Argañán, y cruza la Mina Fé, y la que atraviesa el zócalo entre Barquilla y Alameda, tienen más de 10 y 15 km de longitud respectivamente -, los procesos de bombeo sísmico generados por los contragolpes alpinos podrían haber dado lugar a una amplia movilización de los fluidos del basamento hercínico y a su desplazamiento, bien fuera a impulsos o formando corrientes de convección más o menos continuas, hacia las fracturas y brechas en las que finalmente se depositaron el uranio y los elementos acompañantes. Es decir, que habrían sido los elementos químicos extraídos de las propias rocas encajantes los que habrían dado lugar a los minerales y gangas que constituyen el yacimiento de Fé.

En apoyo de esta hipótesis, se deben tener en cuenta los siguientes hechos:

- La paragénesis de mina Fé está formada por minerales depositados en fracturas y brechas semejantes a las que existen en algunas zonas sísmicas actuales relacionadas con importantes fallas y zonas de cizalla.

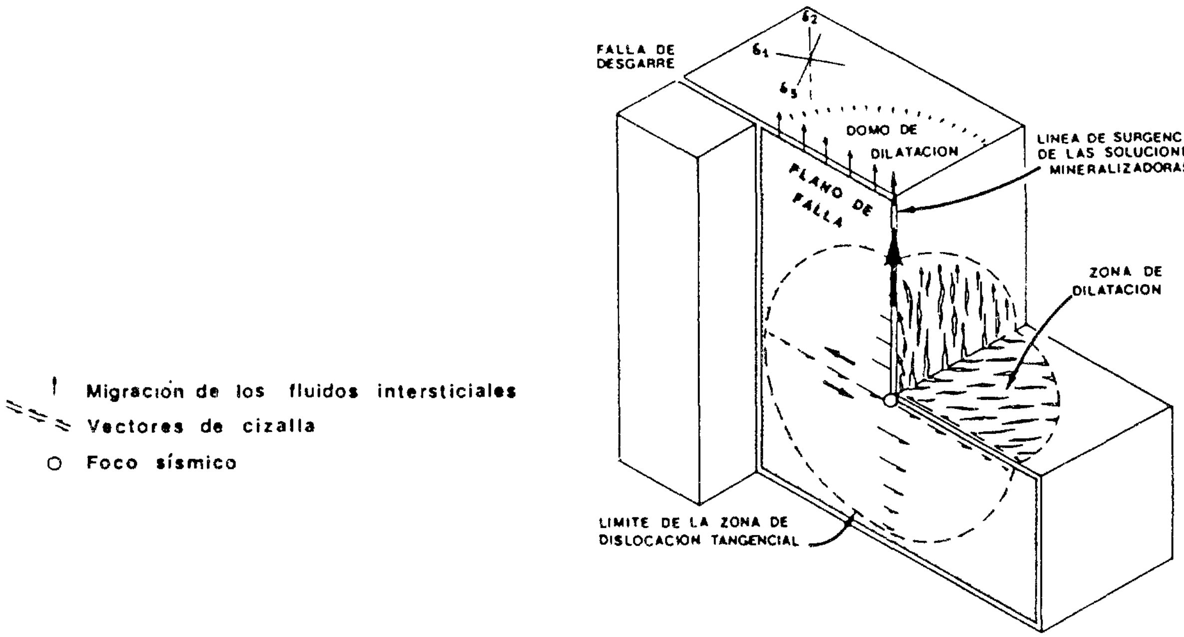

FIG. 20. En el modelo por bombeo sísmico (Sibson et al. (18)), la expulsión de los fluidos concentrados en la zona de dilatación producida por una deformación tangencial se efectúa a través de la falla de desgarre originada por colapso de la zona de cizalla.

- La mineralización fue originada por fluidos hidrotermales de carácter intermitente, salinidad creciente y temperatura cada vez más baja; hasta el punto de que, durante las fases finales del proceso genético, se formaron sedimentos finamente laminados cuyos materiales se depositaron a partir de aguas subsuperficiales de baja temperatura. Estos sedimentos, que frecuentemente tienen aspecto varvado, están constituídos a veces por fragmentos clásticos de los minerales que rellenaron previamente las mismas estructuras filonianas.

- La edad de la mineralización, entre 37 y 57 Ma, corresponde a la fase orogénica pirenaica, y coincide por tanto con la de los contragolpes alpinos que dieron lugar al desarrollo de importantes brechas y zonas de fractura en el zócalo hercínico.

- El estudio geoquímico de la serie estratigráfica, realizado según perfiles transversales a los anticlinorios de Alameda y Gallegos de Argañan, y a los sinclinorios de Villar de la Yegua y Castillejo (Arribas et al. (8) y (10)), y otro de las filitas ampelíticas de mina Fé, indican que más del 15 % de estas rocas, que constituyen a su vez el 40 % de la serie estratigráfica, contiene más de 30 ppm de U, lo que represente un enorme stock metal, con valores que llegan a 200 ppm.

- La asociación adularia-carbonatos-sulfuros de hierro, que acompaña a los minerales de uranio, y la cloritización sufrida por las rocas encajantes son análogas a las que se están produciendo en algunos campos geotérmicos actuales.

En los apartados siguientes se aportan datos que vienen a confirmar las observaciones anteriores y sirven de respaldo al modelo metalogénico que se propone en este trabajo.

5. LOS FLUIDOS DE LOS CAMPOS GEOTERMICOS ACTUALES

Un dato de particular interés se refiere a la composición de los fluidos del campo geotérmico Cesano, concretamente los del Pozo 1, situado 20 km al NNW de Roma, y a las alteraciones que éllos están originado en las rocas encajantes.

El sondeo tiene 1435 m de profundidad y atraviesa una secuencia de rocas piroclásticas, de composición leucítica, que contiene intercalaciones de sedimentos lacustres, y que está depositada, a partir de los 1370 m, sobre rocas carbonatadas, cenozoicas, de tipo flysch. En este pozo hay dos acuíferos: uno, no confinado, en las volcanitas, y otro, confinado, en la serie sedimentaria subyacente (Baldi et al. (20)).

TABLA II. COMPOSICIÓN MEDIA DEL AGUA PRODUCIDA POR EL SONDEO CESANO 1, EN PPM (SEGÚN CALAMAI ET AL. (21)).

pH	8.50	Co	0.02
Ca	106.00	Ni	0.02
Mg	17.00	Hg	0.001
Na	78,930.00	U	0.04
K	48,350.00	Ba	0.10
NH_4	87.00	Sr	0.05
Fe	0.70	Mn	0.10
Li	380.00	HCO_3	5,850.00
Rb	450.00	SO_4	163,290.00
Cs	80.00	H_3BO_3	15,160.00
As	8.30	Cl	42,850.00
Cu	0.012	F	100.00
Zn	0.04	SiO_2	132.00
Pb	0.01	TSD	356,000.00

El sondeo produce unas 250 t/h de agua caliente y otras 50 t de vapor con una presión de 12 a 16 kg/cm²g. La temperatura en el fondo del pozo, antes del flashing, cuando aún no se ha alcanzado el equilibrio térmico, es de 210°C, si bien la del acuífero sobrepasa probablemente los 300°C. El agua de este sondeo, una de las soluciones naturales más concentradas que se conocen en el mundo (Calamai et al. (21)), contiene 356,000 ppm de sales disueltas, especialmente sulfatos de K y Na (Tabla II), lo que es lógico dada la naturaleza alcalino-potásica de las rocas volcánicas encajantes. Por otra parte, hay que destacar el alto contenido en SO_4, HCO_3, H_3BO_3 y Cs; el normal en Ca y Mg, lo que se debe a que una parte importante de estos elementos se sustrae con los carbonatos y la clorita para formar parte de los filoncillos y zonas alteradas de las rocas encajantes; el bajo en Fe, Mn, As, SiO_2 y metales pesados; y la ausencia de H_2S, lo que revela el carácter no reductor de la solución.

Por lo que se refiere a los gases, su principal componente es el CO_2, el cual constituye del 96 al 98 % en volúmen. El resto está formado por metano, N y H_2S; siendo de destacar que los gases, a diferencia del agua no confinada, que se mueve libremente por las rocas piroclásticas, se encuentran exclusivamente en el acuífero inferior, confinado en la serie sedimentaria, y sólo ocasionalmente puede escapar hasta el acuífero situado en las volcanitas.

Actualmente, el pozo Cesano 1 está siendo afectado por una intensa alteración hidrotermal (Enzo Locardi, comunicación personal) que es especialmente intensa a partir de los 611 m. Esta alteración, que se desarrolla tanto sobre las rocas piroclásticas como sobre la serie carbonatada subyacente, está dando lugar a la formación de nuevos minerales que reemplazan a las rocas encajantes o rellenan sus huecos y fisuras. Entre estos minerales se encuentran: sulfatos (yeso, anhidrita, georgyta, glauberita, thenardita y cesanita), silicatos (stilbita, celadonita, adularia y moscovita), carbonatos (calcita, dolomita y ankerita), apatito, hematites y pirita; siendo de destacar que la asociación carbonatos-adularia-anhidrita-pirita es la más frecuente y aumenta con la profundidad.

En cualquier caso, las semejanzas entre los minerales que se están formando en el campo geotérmico Cesano 1 y los que acompañan a la pechblenda en los yacimientos de los esquistos del CEG son evidentes, y no sólo por lo que se refiere a las mineralizaciones de mina Fé, sino también a las de otros yacimientos análogos que existen en la provincia de Salamanca (Arribas et al. (8)).

6. SEISMOS ACTUALES ASOCIADOS CON CIZALLAS

Las fracturas y brechas con las que están asociadas las mineralizaciones uraníferas de las pizarras del O. de Salamanca podrían haber sido concecuencia de fenómenos sísmicos análogos a algunos de los que se producen actualmente. Este es, por ejemplo, el caso de las fallas normales e inversas originadas en la región de El Asnam por el terremoto que, en 1980, sacudió a Argelia, y que permitió observar, por vez primera en el Mediterráneo occidental, la falla inversa causante del seísmo (Hatzfeld y Philip (22)).

La traza de esta falla, que tiene dirección N 40°E, buzamiento NW 50°, y un salto total que llega a ser de 6 m, se puede seguir sobre el terreno a lo largo de casi 40 km, estando situado el foco sísmico a unos 8 km de profundidad. Hacia el N, es decir, en el bloque levantado, la falla está acompañada por otras normales, más o menos oblícuas a élla, que dan lugar a deslizamientos importantes del terreno según esfuerzos tensionales cuya dirección varía de E-W a N-S.

En el caso de El Asnam, la zona activa definida por la sismicidad se extiende sobre una distancia bastante mayor que la indicada por la falla en superficie, lo que demuestra que esta estructura es mucho más importante en profundidad. Además, la orientación y distribución de la actividad sísmica demuestran que el plano de falla es prácticamente vertical en el tramo SW y subhorizontal en el tramo medio, y que se ramifica según un complicado haz de fracturas en el tramo NE.

Como se ve, estas características son muy semejantes a las que presentan algunos de los sistemas de fractura que afectan a los esquistos de Salamanca. Por éllo, no resulta difícil admitir que las fallas y brechas existentes en la zona de mina Fé representan la parte profunda, en niveles que no estaban muy alejados de la superficie, de las dislocaciones causadas en el basamiento hercínico por los esfuerzos de compresión y distensión originados por los contragolpes alpinos.

7. EL CALOR DE DEFORMACION EN LAS ZONAS DE CIZALLA

Un problema importante para explicar el origen de los yacimientos de uranio de las pizarras de Salamanca es determinar la fuente de calor que pudo contribuir a poner en movimiento los fluidos que transportaron el uranio.

En este sentido, si se admite que el desencadenamiento del proceso pudo ser debido a un bombeo sísmico o a cualquier otro mecanismo tectónico, el gradiente térmico podría haber sido originado por la propia deformación y de forma análoga a como parece ocurrir en las zonas de cizalla continentales (Brun y Cobbold (23)).

Así, los efectos de la transformación de la energía mecánica en térmica - un fenómeno físico bien conocido en mecánica de fluídos tanto desde el punto de vista teórico como experimental - han sido estudiados en las dislocaciones tangenciales que se producen no solo en las zonas de cizalla sino también en la base de los mantos de corrimiento y el borde de los diapiros. En todos estos casos se admite que las deformaciones mecánicas pueden dar lugar a elevaciones de temperatura de varios cientos de grados; y aunque estos gradientes deberían ser detectados geológicamente, Brun y Cobbold (23) justifican la falta de pruebas porque, en su opinión, el ablandamiento térmico que se produce en las zonas de cizalla hace que la mayor parte de la deformación se concentre en segmentos muy definidos. Además, tal y como sugieren Fleitout y Froidevaux (24), el aumento de temperatura y la acumulación de tensiones en la zona deformada disminuyen y se equilibran con el tiempo a medida que aumentan el volúmen de la anomalía térmica y la anchura de la zona dislocada; siendo evidente, en cualquier caso, que el calor producido por la deformación en la zona de cizalla puede ser tan importante como para llegar a fundir las rocas afectadas.

Por lo que se refiere a las numerosas e importantes fracturas que atraviesan a los esquistos de Salamanca, y aunque aquéllas no se pueden comparar exactamente con las cizallas que, a niveles mucho mas profundos, afectaron a dichos materiales a finales del Paleozoico, es evidente que éstas estructuras podrían ser el resultado de dislocaciones tangenciales producidas en el zócalo hercínico por la orogenia alpina. Si éllo fuera así, el calor originado por estas tensiones desde finales del Cretácico a mediados del Terciario se habría disipado por medio de los fluidos expulsados hacia la superficie a través de las fracturas y brechas originadas por los contragolpes alpinos, y una vez que se amortiguaban los seismos provocados por el colapso de las zonas de dilatación.

En estas condiciones, las sucesivas venidas hidrotermales originadas por bombeo sísmico habrían continuado transportando y depositando los elementos extraídos de las rocas encajantes en tanto la temperatura alcanzaba un estado de equilibrio.

8. YACIMIENTOS DE URANIO CON CARBONATOS, ADULARIA Y SULFUROS DE HIERRO

Aparte del yacimiento de Midnite, en el estado de Washington (Ludwig et al. (25)), cuyas características geológicas y mineralógicas son, salvo por lo que se refiere a la edad de los granitos y rocas metamórficas encajantes, muy parecidas a las de los yacimientos en pizarras de la Península Ibérica, hay que destacar la existencia, también en los EE.UU., de otras mineralizaciones uraníferas, cuyas afinidades con las españoles, especialmente las de Fé, son notables. Se trata del grupo de yacimientos situado sobre el flanco centro-oriental de Front Range, en Colorado, entre 5 y 10 km al NW de Golden, y concretamente de las minas Ludwig, Mena, Ascensión y Schwartzwalder (Wallace (26)); siendo esta última no solo el mayor yacimiento de uranio de tipo filoniano que se conoce en los EE.UU. sino también uno de los más profundos, ya que la mineralización ha sido reconocida hasta 800 m de profundidad.

Por lo que se refiere a Midnite (Nash (27)), las mineralizaciones de uranio se encuentran en una serie metasedimentaria del Proterozoico que está formada por filitas grafitosas y piritosas y rocas calcosilicatadas, atravesada por una cuarzo-monzonita porfídica que se emplazó hace 75 Ma, durante el Cretácico. El aspecto morfológico de la mineralización es muy parecido al de las venillas de mina Fé, pero hasta ahora no ha sido citada la presencia de brechas, aunque sí de numerosas fallas. La mineralización, de características microscópicas análogas a la de los esquistos de Salamanca, está formada principalmente por pechblenda, coffinita, pirita y marcasita, las cuales van acompañadas por cantidades variables de esfalerita, calcopirita y galena (Ludwig et al. (25)). La hisingerita, un silicato de hierro hidratado, rico en Ca, que a veces forma filoncillos casi puros en las rocas estériles, constituye la única ganga de las venillas con pechblenda y coffinita, en las cuales apenas hay cuarzo y carbonatos. Esta última característica, junto con la ausencia de adularia, constituye la principal diferencia con las mineralizaciones de la Península Ibérica, con las que, por lo demás, tienen un parecido extraordinario.

En cuanto al origen de Midnite, de los tres posibles propuestos inicialmente por Nash (27) - singenético, hidrotermal y supergénico - este autor ha pasado a sugerir un modelo metalogénico parecido al que se propone en este trabajo para las mineralizaciones de la Península Ibérica; es decir, un proceso de reconcentración del uranio de las rocas encajantes, precámbrias, por aguas meteóricas descendentes que se calentaron en profundidad, y que habría tenido lugar durante una fase erosiva que se desarrolló hace 51 Ma. Sin embargo, en el caso de Midnite, Nash (27) piensa que el uranio de las rocas metamórficas no es singenético, sino que fué introducido en éllas, desde las rocas plutónicas, por procesos hidrotermales de baja temperatura.

Por el contrario, a diferencia de lo que ocurre en Midnite, la paragénesis y situación geotectónica de los yacimientos de Colorado son muy parecidas a las de mina Fé, ya que el uranio se halla en zonas de fractura y brechas de falla, de dirección predominante NW-SE, que pueden tener varias decenas de metros de anchura y hasta 60 km de longitud. Estas estructuras intersectan, hacia el NW, rocas predominantemente graníticas, y hacia el SE, materiales metasedimentarios y metavolcánicos formados por gneises y micacitas, frecuentemente grafitosos y piritosos, cuarcitas, y rocas calcosilicatadas. En las rocas graníticas, el cemento de las brechas, afectadas por hasta cinco etapas cataclásticas, es una mezcla de cuarzo y hematites de grano fino. En cambio. en las rocas metamórficas, el cemento está formado esencialmente por carbonatos y adularia, mientras que los fragmentos de las brechas, que son las portadoras de los minerales de uranio y han sido afectadas también por varias etapas de rotura, muestran los efectos de una hematización y cloritización de variable intensidad. Además, en la zona de transición entre las rocas graníticas y las metasedimentarias, las brechas de matríz silícea fueron brechificadas y cementadas de nuevo por carbonatos y adularia, lo que no ocurre con las brechas carbonatadas de los terrenos metamórficos, en las que no hubo nunca una silicificación previa.

En la mina Schwartzwalder, la mineralización se depositó en tres etapas (Rich (28)): la primera está formada por adularia, pechblenda, jordisita y una sustancia hidrocarburada; la segunda, por ankerita, pirita, marcasita y pequeñas cantidades de calcopirita, esfalerita, galena y barita; y la tercera, por calcita y pirita. Las inclusiones fluidas de la ankerita homogenizan a 140°C, y las de la calcita entre 75° y 165°C. En este yacimiento, aunque Rich propuso un origen descendente por lixiviación del uranio contenido en los granitos meteorizados y erosionados, y/o en las arcosas paleozóicas, la mayor parte de los autores se inclina por un origen ascendente de tipo hidrotermal.

9. CONCLUSIONES

Las mineralizaciones filonianas de U existentes en las pizarras del Macizo Hespérico, entre ellas, las del complejo esquisto-grauváquico de la provincia de Salamanca, se han atribuido a procesos magmáticos (per ascensum), supergénicos (per descensum), y de segregación del U a partir de los granitos o metasedimentos fértiles que intruyen o están intercalados, respectivamente, en los esquistos del basamento.

En este trabajo, el origen de estas mineralizaciones, y concretamente las de mina Fé, se explica por una lixiviación del U contenido en la materia carbonosa de las pizarras ampelíticas y por su deposición en zonas fracturadas y brechificadas de los esquistos; procesos éstos que habrían tenido lugar, durante el Terciario, como consecuencia del bombeo sísmico provocado en el zócalo hercínico por los contragolpes alpinos. Este modelo metalogénico se apoya en los siguientes hechos y observaciones:

- La abundancia y alto contenido geoquímico en U de las filitas ampelíticas existentes en las zonas donde se encuentran los yacimientos, ya que el 15 % de aquellas rocas tiene más de 30 ppm de U - algunas hasta 200 ppm - y el 50 % de este U es lábil, es decir, fácilmente lixiviable.

- La edad de la pechblenda, entre 37 y 57 Ma, correspondiente al Terciario inferior, lo que hace coincidir el emplazamiento de la mineralización con los procesos orogénicos alpinos, y concretamente con las fases tectónicas que mayor repercusión tuvieron en el basamento.

- La localización de los minerales primarios de U en fracturas y brechas de falla originadas por deformaciones tangenciales, subsuperficiales, debidas a fenómenos sísmicos análogos a algunos de los que se producen en la actualidad.

- La fosilización de algunas mineralizaciones primarias, e incluso secundarias, por sedimentos del Terciario atribuidos al Oligoceno.

- La intensa, aunque limitada, cloritización y hematización de las rocas encajantes, y la paragénesis (carbonatos, adularia y sulfuros de Fe), de temperatura media a baja, que acompaña a los minerales primarios de U (pechblenda y coffinita). Estas alteraciones y la asociación mineral son, salvo por lo que se refiere a la presencia de minerales de U, análogas a las que tienen lugar en algunos campos geotérmicos actuales.

- La existencia en el CEG de niveles carbonatados y calcosilicatados capaces de producir los fluidos ricos en $CO^{--}{}_2$ y Mg^{++} que pudieron transportar el U como complejo uranil-carbonatado, y que dieron lugar a la cloritización de las rocas de caja y a la formación de los carbonatos de la ganga.

- La temperatura y salinidad de las inclusiones fluidas de estos carbonatos, especialmente de los que se depositaron durante las fases precoz y principal de la mineralización, cuyos valores varían entre 230° y 70°C, y 0 y 25 % equiv. NaCl respectivamente.

- La peculiar textura de los minerales filonianos tardíos, los cuales se depositaron en huecos de las brechas y fracturas, en ambientes subsuperficiales, formando microsedimentos finamente laminados y con texturas geopetales, tales como estratificación graduada, laminación cruzada y figuras de carga.

Todos estos factores parecen demostrar que, en efecto, las mineralizaciones de Salamanca, y concretamente las de mina Fé, se deben a una lixiviación del U de las pizarras fértiles, especialmente las ampelíticas, como consecuencia del bombeo sísmico provocado en las rocas del zócalo por los procesos tectónicos alpinos a principios del Terciario (Fig. 6). El U, en forma de complejo uranil-carbonatado, y los otros elementos que forman los minerales de las paragénesis procederían entonces de las propias rocas encajantes, y habrían sido transportados y redepositados en las fracturas y brechas de falla por fluidos hidrotermales, de carácter geotérmico, que fueron expulsados hacia la superficie al producirse el colapso de las zonas de cizalla.

Una dificultad existe, sin embargo, para aceptar plenamente esta hipótesis: el hecho de que el grado de consolidación de los materiales del CEG, y concretamente el de maduración de la materia orgánica con la que va asociado el uranio, tenía que estar lo suficientemente avanzado en el Terciario como para impedir una fácil lixiviación de aquel elemento, incluso por fluidos hidrotermales.

Por ello, el origen de estas mineralizaciones se explicaría mejor admitiendo que el U se pudo concentrar previamente - p.e. durante la orogenia hercínica, cuando los sedimentos del CEG no habrían sufrido aún los efectos del metamorfismo regional - en determinados horizontes o estructuras de las pizarras ampelíticas, y que posteriormente, bajo los efectos de la tectónica alpina y por los mecanismos propuestos en este trabajo, pudo ser removilizado y depositado en las fracturas y brechas de falla donde se encuentra en la actualidad.

En este caso, el hecho de que la mayoría de las mineralizaciones de esta clase se sitúen en o cerca del contacto con los granitos - la mina Fé es la principal excepción - se podría atribuir al distinto comportamiento mecánico que, ante los esfuerzos tectónicos, presentan las pizarras y las rocas plutónicas. Ello habría dado lugar a que las grandes fracturas que atraviesan a ambos tipos de roca respondieran de distinta forma al paso de los fluidos que lixiviaron las pizarras, cuya circulación habría estado condicionada por la forma de los cuerpos graníticos a lo largo de cuyos bordes se encuentran normalmente estes mineralizaciones.

En consecuencia, desde un punto de vista práctico, dadas las analogías que presentan las mineralizaciones de Salamanca con otras de parecidas características mineralógicas y tectónicas existentes dentro y fuera de la Península Ibérica - p.e. las de Nisa, en Portugal, y Midnite y Schwartzwalder, en los EE.UU. - sería interesante comprobar si el modelo metalogénico que se propone en este trabajo es válido para otros yacimientos, en cuyo caso podría ser aplicado para la prospección y exploración de este singular tipo de mineralizaciones uraníferas.

AGRADECIMIENTOS

El autor desea expresar su agradecimiento a Ken Ludwig (Branch of Isotope Geology, U.S. Geological Survey, Denver, EE.UU.) por el análisis isotópico que ha permitido datar la pechblenda de mina Fé, y a ENUSA por las facilidades y el permiso dado para realizar este estudio.

REFERENCIAS

(1) ARRIBAS, A., Mineralogy of the Spanish uraniferous deposits, XXII Int. Geol. Congr., Copenhague 15 (1960) 98-108.

(2) ARRIBAS, A., Mineralogía y metalogenia de los yacimientos españoles de uranio: las pizarras uraníferas de la provincia de Salamanca, Est. Geol. 18 (1962) 155-172.

(3) ARRIBAS, A., Las pizarras uraníferas de la provincia de Salamanca, Est. Geol. 1 (1970) 7-45.

(4) FERNANDEZ POLO, J.A., Génesis de los yacimientos uraníferos en metasedimentos de Salamanca (España), Col. Luso-Hisp-Francés de Miner. Uraníf. Metasedim., JEN, Madrid (1965) 45 pp.

(5) MATOS DIAS, J.M., SOARES DE ANDRADE, A.A., Uranium deposits in Portugal, Uran. Exp. Geol. IAEA, Vienna (1970) 129-252.

(6) ARRIBAS, A., Caracteres geológicos de los yacimientos españoles de uranio, Stud. Geol. 9 (1975) 7-63.

(7) ARRIBAS, A., Sobre el origen de las mineralizaciones españolas de uranio en rocas metasedimentarias, Libro Jubilar J.M. Rios, Geología de España, Tomo II IGME (1980) (en prensa).

(8) ARRIBAS, A., MARTIN-IZARD, A., MONTES, J., Las mineralizaciones de uranio de la zona de Alameda de Gardón y su posición en el contexto geotectónico de las pizarras del Oeste de la provincia de Salamanca, VIII Reun. Geol. Oest. Penins., Stud. Geol. (1983) (en prensa).

(9) MARTIN-IZARD, A., ARRIBAS, A., Relaciones entre la estratigrafía y las mineralizaciones uraníferas del complejo esquisto-grauváquico en el Oeste de la provincia de Salamanca, I. Congr. Esp. Geol., Segovia, Tomo II (1984) 577-587.

(10) ARRIBAS, A., MARTIN-IZARD, A., MONTES, J., Distribución geoquímica del uranio en los metasedimentos del C.X.G. del Oeste de la provincia de Salamanca, VII Congr. Int. Min. Met., Barcelona I (1984) 353-357.

(11) ARRIBAS, A., GARCIA-LUIS, A., JIMENEZ, E., MARTIN-IZARD, A., Estudio geológico del área del proyecto Quercus, Instituto de Geología Aplicada, Universidad de Salamanca (1980) 125 pp.

(12) COMA, F., Litología, tectónica y mineralización del yacimiento Fé, Saelices el Chico (Salamanca), VIII Reun. Geol. Oest. Penin., Stud. Geol. (1983) (en prensa).

(13) MANGAS, J., ARRIBAS, A., Características físico-químicas de los fluidos asociados con las mineralizaciones de uranio de mina Fé (Salamanca), VII Congr. Int. Min. Met. Barcelona I (1984) 435-451.

(14) BLANCO, J.A., CORROCHANO, A., MONTIGNY, R., THUIZAT, R., Sur l'age du début de la sédimentation dans le basin tertiaire du Duero (Espagne), Attribution ou Paléocene par datation isotopique des alunites de l'unité inférieure. C.R. Acad. Sc. Paris 195, 2 (1982) 259-262.

(15) LAFFITE, P., Introduction a l'étude des roches métamorphiques et des gites métallifères, Masson, Paris (1957) 249-263.

(16) SCHIPULIN, D.K., On thermodiffusion of components during the formation of stratabound sulfide ore deposits, Soc. Mining Geol. Japan (IMA-IAGOD meeting 1970) 3 (1971) 274-276.

(17) COSTESEQUE, P., DANDURAND, J.L., FORTUNE, J.P., SCHOTT, J., TOLLON, F., On three factors essential to the formation of ore deposits, Geochemical preconcentration, fracturation and thermal gradient, Prob. of Ore Dep. (IAGOD Symp. 74), Varna 2 (1974) 269-278.

(18) SIBSON, R.H., McM.MOORE, J., RANKIN, A.H., Seismic pumping. A hydrothermal fluid transport mechanism, Jour. Geol. Soc. 131 (1975) 653-659.

(19) TSUNEISHI, Y., NAKAMURA, K., Faulting associated with the Matsushiro swarm earthquakes, Bull. Earthq. Res. Inst. Tokyo Univ. 48 (1970) 29-51.

(20) BALDI, P., CAMELI, G.M., LOCARDI, E., MOUTON, J., SCANDELLARI, F., Geology and Geophysics of the Cesano Geothermal Field, 2nd U.N. Symp. Dev. Use Geoth. Res., Lawr. Berk. Lab., Univ. California (1975) 871-881.

(21) CALAMAI, A., CATALDI, R., DALL'AGLIO, M., FERRERA, G.C., Preliminary report on the Cesano hot brine deposit, 2nd U.N. Symp. Dev. Use Geoth. Res., Lawr. Berk. Lab., Univ. California (1975) 305-313.

(22) HATZFELD, D., PHILIP, H., Il y a un an, El Asnam, La Recherche 127 (1981) 1284-1287.

(23) BRUN, J.P., COBBOLD, P.R., Strain heating and thermal softening in continental shear zones: a review, Journ. of Struct. Geol. 2 1/2 (1980) 149-158.

(24) FLEITOUT, L., FROIDEVAUX, C., Thermal and mechanical evolution of shear zones, Journ. of Struct. Geol. 2, 1/2 (1980) 159-164.

(25) LUDWIG, K.R., NASH, J.T., NAESER, C.W., U-Pb isotope systematic and age of uranium mineralization, Midnite mine, Washington, Econ. Geol. 76 (1981) 89-110.

(26) WALLACE, A.R., Structural and mineralogical characteristics and distribution of carbonate-dominated fault breccias associated with uranium deposits, Front Range, Colorado, Econ. Geol. 77 (1982) 1945-1950.

(27) NASH, J.T., Geology of the Midnite Uranium Mine Area, Washington, maps, description and interpretation, Open-File Reports 77.592 (1977) 39 pp.

(28) RICH, R.A., Genetic implications of preliminary mineralogic, paragenetic and fluid inclusion data for the Schwartzwalder Uranium Mine, Colorado (USA), IAEA, Lisbon meeting on uranium in granites (1979) 20 pp.

URANIUM DEPOSITS SPATIALLY RELATED TO GRANITES IN THE FRENCH PART OF THE HERCYNIAN OROGEN

B. Poty[1], J. Leroy[1,2], M. Cathelineau[1], M. Cuney[1,3], M. Friedrich[1], M. Lespinasse[1,4], L. Turpin[1,5]

[1]CREGU
Vandoeuvre-les-Nancy

[2]E.N.S.G.
Nancy

[3]C.R.P.G.
Vandoeuvre-les-Nancy

[4]E.N.S.M.I.M.
Nancy

[5]C.E.A.-I.R.D.I.-C.E.N.
Gif-sur-Yvette

France

Abstract

URANIUM DEPOSITS SPATIALLY RELATED TO GRANITES IN THE FRENCH PART OF THE HERCYNIAN OROGEN

During the last ten years, a number of research projects have been conducted on the French part of the Hercynian orogen especially on the vein-type uranium deposits. This paper is a review of the new concepts worked out on this type of uranium occurrences.

Sources for uranium mobilization and metallogenic stages appear to be more diversified and complex than suggested in previous models. In particular, an intermediate stage of uranium concentration, structurally controlled, occurring at a late magmatic stage and related to uranium enriched fine grained intrusions has been discovered in the Saint-Sylvestre and Bois Noirs granites. Uranium metallogenesis for vein-type deposits appears now to occur during four main periods: Middle Palaeozoic, Early Permian, Jurassic, and Alpine to the present day. The physicochemical conditions of 'episyenites' formation and uranium deposition have been largely revised by additional mineralogical and fluid inclusion studies, and by the development of stable and radiogenic isotope measurements. Origin of the fluids related to 'episyenitization' and uranium mineralizations has been outlined. All these studies have considerably reinforced the hydrothermal genetic model for the Hercynian vein-type uranium mineralizations.

1. INTRODUCTION - URANIUM METALLOGENESIS IN THE EUROPEAN PART OF THE HERCYNIAN OROGEN

The Hercynian orogen represents an important U, Sn, W metallogenic province which extends from Erzgebirge to Portugal through Black Forest, Vosges, the crystalline massifs of the Alps, Massif Central, Vendée, Brittany, Cornwall, and Spain in Europe (Fig. 1), and from New Hampshire to New Brunswick in North America. This uranium province is characterized by the scarcity of Precambrian basement and the absence of Archaean, unlike most other metallogenic uranium provinces in the world, and by the close spatial relationship between uranium vein de-

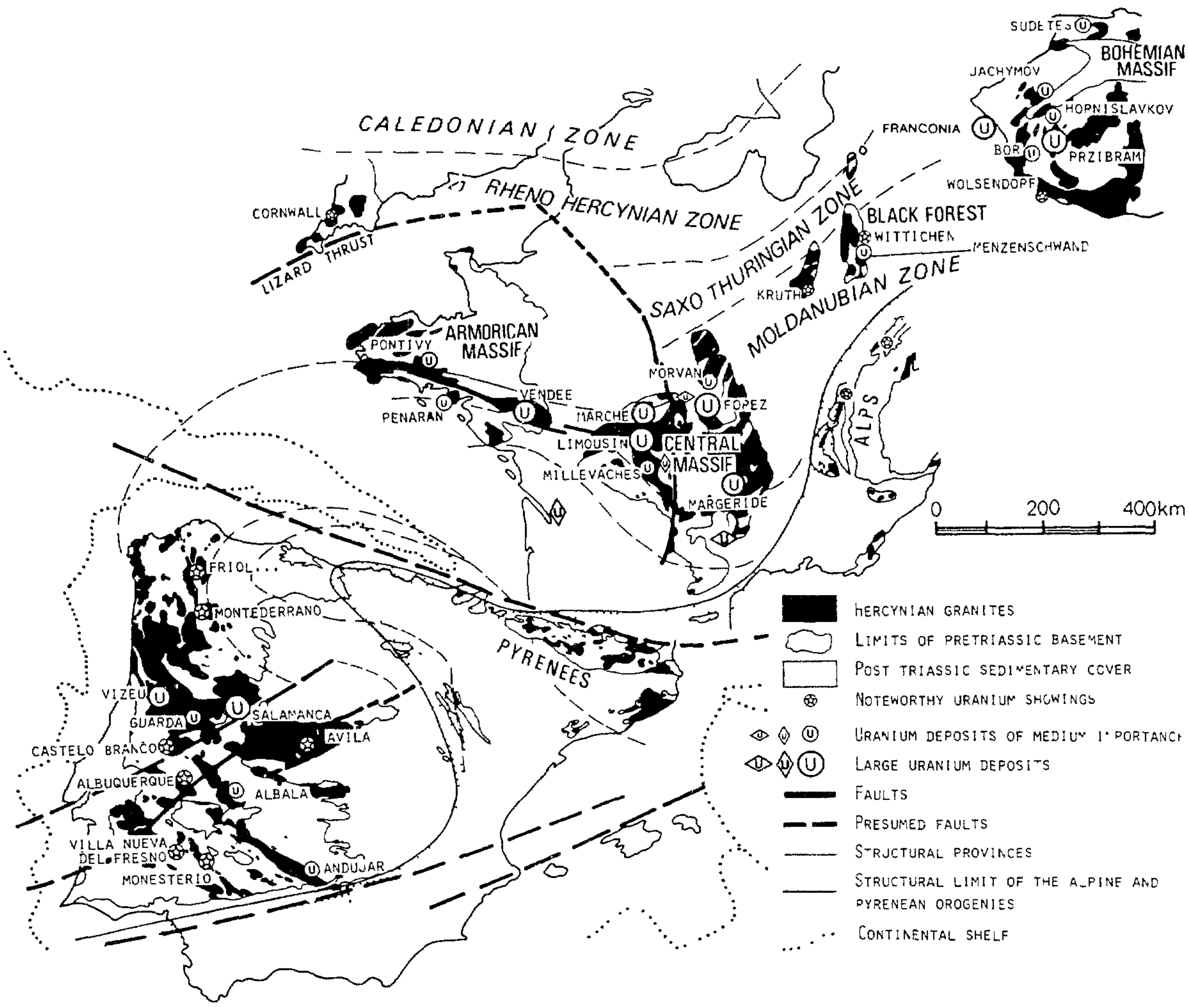

FIG. 1. Location of uranium vein deposits in the Central European part of the Hercynian orogen. Structural reconstitution after Matte (112).
○ - Palaeozoic deposits; ◇ Permian deposits; ◊ Tertiary deposits.

posits and uraninite-bearing peraluminous leucogranites emplaced during carboniferous time (300 - 330 Ma). The U, Sn, W province of southeastern China has close similarities with the Hercynian one, but is of Jurassic age (Yenshan).

Uranium vein deposits are located either within granitic bodies (Fanay, Margnac in Massif Central) or in metamorphic septas (Metairie Neuve in southern Brittany), or at the contact between the granite and surrounding metamorphic rocks (Le Chardon in Vendêe), or in the metamorphic rocks in the vicinity of the granite (Penaran in southern Brittany, Le Retail in Vendêe, Franconia, Jachymov in Bohemia, Fê in western Spain) (Peinador Fernandes et al. (1)).

In France, most of these deposits have given U-Pb isotopic ages between 260 and 280 Ma (Kosztolanyi (2), Leroy and Holliger (3) and work in progress in Forez and Vendêe). However, recent results have demonstrated and emphasized the importance of older ages for several intrametamorphic deposits (Devillers and Menes (4), Cathelineau (5), (6) and Cathelineau and Holliger, in prep.).

Within the alpine orogen, several uranium concentrations have been described (Poncerry (7), Labhart and Rybach (8)) in the Hercynian crystalline massifs. Most of these uranium concentrations result from a Hercynian metallogenic event with minor alpine reworking (Negga (9), Holliger and Negga, in prep.).

Sedimentary uranium deposits are located either in Permian (Lodêve in SE Massif Central) or Tertiary (Coutras in Aquitaine Basin) molassic basins at the margins of the Hercynian chain. The main uranium source for these deposits is also considered to be the Hercynian peraluminous leucogranites.

During the past ten years, a number of research projects have been conducted on vein-type deposits in France. These projects renewed considerably the metallogenic concepts on these occurrences.

2. MORPHOLOGY OF THE URANIUM OCCURRENCES

Two morphologic types of uranium occurrences can be distinguished. Occurrences of the vein-type are located within either granites or the surrounding metamorphic units. Occurrences of the disseminated type have always been found within the granitic massifs.

2.1. Vein-type occurrences

Structural studies were carried out on all these vein-type deposits. Besides the data of the mining geologists (unpublished reports), there are those of Lilliê (10) on the Mortagne district and Cathelineau (11) on the Penaran deposit (South Brittany), Marquaire and Moreau (12), Moreau and Ranchin (13), Fraipont (14) on the Saint-Sylvestre district (Limousin) Sirna (15) on the Grandrieu district (Margeride).

As for any vein-type mineralization, the existence of mechanical discontinuities within a homogeneous granitic massif is one of the most important factors for the opening of veins and ore precipitation. In the case of uranium mineralizations, chemical effects can be added to the mechanical ones. This structural control of mineralizations can be illustrated on the Chardon and Fanay mines.

The Chardon deposit (Fig. 2) is located at the contact between the Mortagne two-mica granite and metamorphic series which are compressed between the granite towards the south and the Pallet gabbro towards the north. The structural relationships between the metamorphic units and the granite are those of a ductile

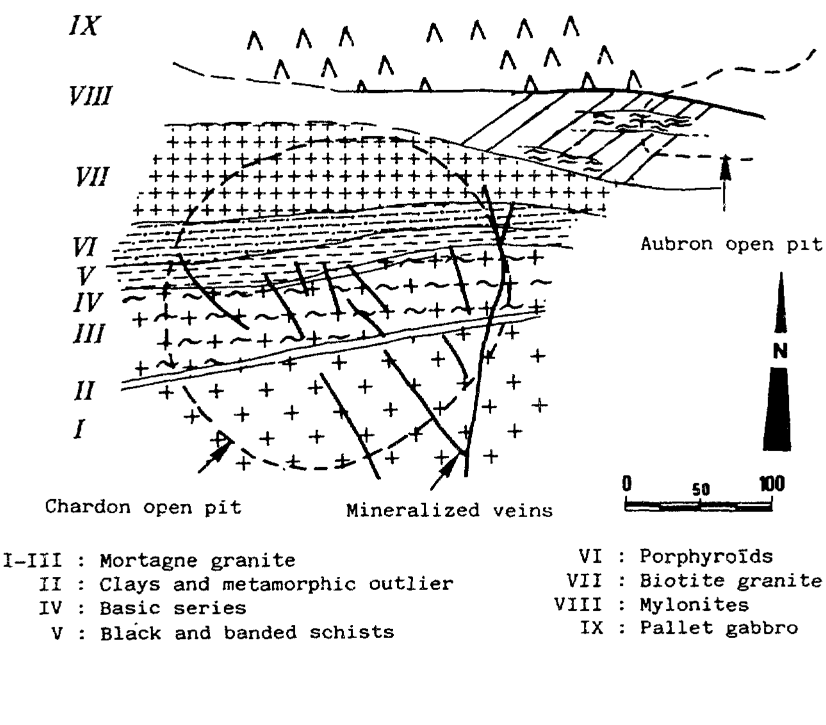

FIG. 2. Northern contact of the Mortagne Massif in the Chardon mine (Vendée) (Cathelineau (5)).

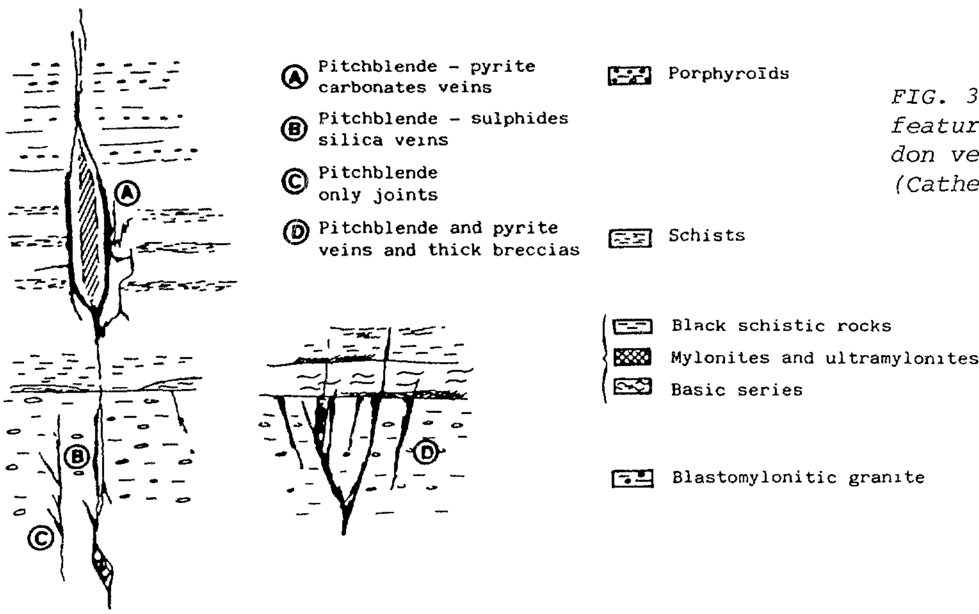

FIG. 3a. Structural features of the Chardon veins (Vendée) (Cathelineau (5)).

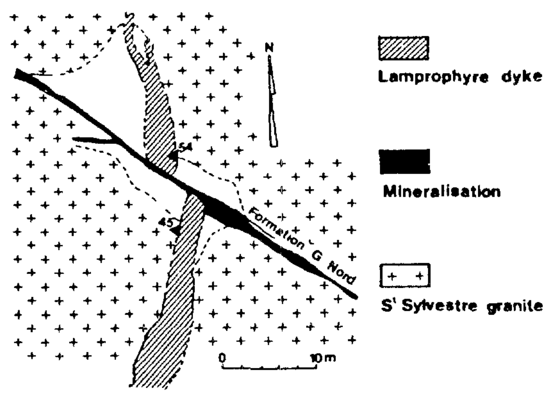

FIG. 3b. Relation between two-mica granite-lamprophyric dike and pitchblende vein (Fanay mine, Limousin, northern G formation) (doc. Cogema, in Leroy (18)).

zone and result from east-west dextral shearing and north-south compression. Towards the contact, progressive blasto-mylonitization of the granite is observed. The mineralization occurs as veins which cut both granite and all the metamorphic units. Mineralized veins and breccias are spread near the contact with the mafic rocks, one of the metamorphic units, although they become narrower in the basic rocks (Fig. 3a).

Similarly, uranium veins in the Fanay mine crosscut north-northeast trending lamprophyric dikes. Veins are often larger near the intersection with the dikes, and frequently end within them (Fig. 3b). Sarcia and Sarcia (16) indicated a strong correlation between the increase in size of the veins, their original thickness and the pitchblende content.

The influence of mafic units and more generally of ductile units is first mechanical. Ductile units create anisotropy in homogeneous environments, whereas competent units open preferentially near contacts with more ductile units. Furthermore, the lack of open faulting in ductile units makes them acting like mechanical screens for fluid flows. In contact with mafic rocks, chemical effects can be added. This point will be emphasized later.

2.2. Disseminated-type occurrences

Part of the deposits located within granitic massifs are associated with strongly altered granites, in the French terminology called 'episyenites'. These rocks play an important role as reservoir for several types of ore (U but also, Sn, W, Au, ...).

2.2.1. Definition

Episyenitic zones are described in most of the granites of the Hercynian orogen. They occur as irregular pipes in relation with faults (Fraipont (14), Lespinasse (17), Fig. 4). Any type of rocks may be affected, and numerous occurrences are barren. Common features concerning their mineralogy and genetic conditions can be observed in many episyenites. These similarities are independent of the location and nature of host rock lithology (Leroy (18), (19), Martin (20), Michel (21), Alabosi (22), Cathelineau (23)).

First stage of formation is the dissolution of magmatic quartz. The removal of quartz minerals leaves vugs whose volume and shape are identical to the previous quartz boundaries when no later tectonic disturbance occurs. This alteration transforms granites into vuggy feldspathic assemblages which constitute good reservoir rocks for later alteration or mineralizations.

Dequartzification leads to mineralogical compositions somewhat similar to that of a syenite; this explains the word 'episyenite' commonly used in the French literature.

2.2.2. Mineral associations

According to the nature of the fluids, and to the stability fields of other granitic minerals during or after quartz dissolution, the resulting mineralogy may largely differ:

(i) In the Limousin and Marche area, as in the Pontivy district, all the granitic minerals are either dissolved, transformed or chemically reequilibrated. Quartz is dissolved; feldspars, mainly plagioclases, are partially altered to phengites. These micas are richer in Si, K, Fe and poorer in Al, Na, Ti than granitic muscovites (Leroy and Cathelineau (24), Alabosi (22), Leroy (19)). In contact with secondary micas, orthoclase is Na depleted and K enriched. White micas generated from biotites are similar to those generated from feldspars, but contain small crystals of hematite which indicate oxidizing conditions. Granitic muscovites are reequilibrated with the new chemical conditions and their chemical composition becomes similar to that of secondary micas.

(ii) In Margeride, quartz leaching may be the only consequence of alteration and the result is thus a vuggy rock of a roughly syenitic composition. Alkali metasomatism is frequently associated with quartz dissolution. Different types of vug fillings (Cathelineau (25), (23)) and alteration assemblages of relic minerals of the granite may be observed:

° phengite, chlorite, albite in the Margeride biotite granite, in Les Pierres Plantées

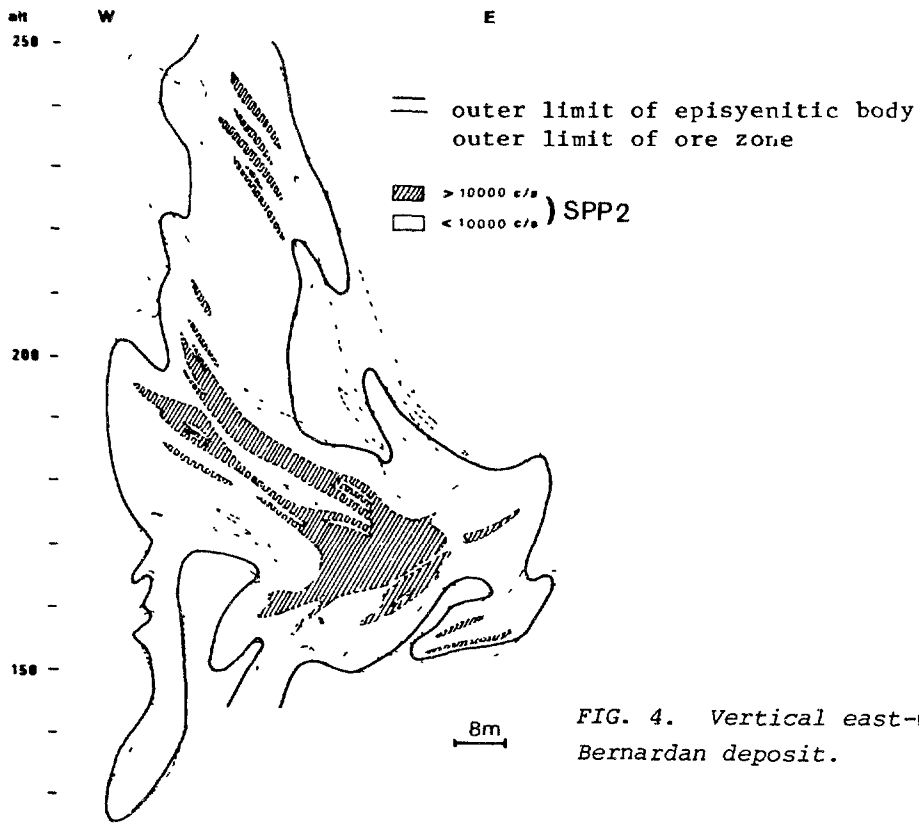

FIG. 4. Vertical east-west cross-section, Bernardan deposit.

- ° adularia, dolomite, pyrite, anatase in the biotite granite and vaugnerites in Les Pierres Plantées
- ° adularia, albite, in the leucogranite in Les Pierres Plantées, Le Villeret and Le Cellier
- ° adularia, in some altered leucogranites of the Grandrieu Massif.

2.2.3. Geochemistry

This alteration systematically corresponds to a loss of SiO_2. The behaviour of other major elements is very variable. In Les Pierres Plantées, Margeride (Cathelineau (25)), Le Bernardan; Marche (Leroy (19)), Prat Mérien, Ty Gallen and Poulprio, Pontivy (Alabosi (22)), K is strongly enriched and Na is depleted. On the contrary, in the Hyverneresse deposit, Millevaches (Martin (20)), K content remains constant. In all the deposits, Rb content increases in connection with intensity of the muscovitization of plagioclases. This alteration is important in deposits from La Marche, Pontivy and Saint-Sylvestre massifs, and weak in the deposit of Millevaches. Thorium and REE contents are not disturbed. This means that monazite remains stable or metastable during this alteration.

2.2.4. Alteration zoning

Around the dequartzified and white mica enriched granite (episyenite s.s.), no macroscopic alteration can be observed. This contact between granite and episyenite was considered as the limit of the hydrothermal phenomena (Leroy (18)).

In fact new mineralogical and geochemical data on Le Bernardan deposit (Leroy and Cathelineau (24), Leroy (19)) and on the Pontivy deposits (Alabosi (22)) indicate that the granite surrounding the episyenitic bodies is richer in phengite. This corresponds to a slight K and Rb increase. Around a central core with no quartz and with mica enrichment, a phengite-rich zone exists. The thickness of this zone is correlated to the density of micro-fractures in the rocks (permeability) and to the volume of the episyenitic bodies (intensity of the hydrothermal alteration). It can vary from some metres to 30 - 40 m.

2.2.5. Physico-chemical characteristics and genetic model for episyenitization

Fluid inclusion studies indicate that the leaching solutions were aqueous with a rather low salt content, 4 - 15 wt% equiv. NaCl in the Margnac and Fanay deposits (Leroy (18)), 0 - 7 wt% equiv. NaCl in the Hyverneresse deposit (Martin (20)), and 2 - 6 wt% equiv. NaCl in Le Bernardan deposit (Leroy (19), Lespinasse (17)). Fluid inclusion studies led to similar temperatures in all these deposits (300°C - 380°C). From H and O isotopic studies (Turpin (26)), these solutions are considered to be of meteoric origin.

Episyenites are the result of a hydrothermal alteration of rocks by meteoric waters in relation with active fracturation. A local increase of the heat flow related to mantle uplift at the end of the Hercynian orogeny as indicated by magmatic activity (lamprophyric and microgranitic dikes) generated convective circulations similar to those described in present day geothermal systems.

Uranium mineralizations occur in all deposits during later events; datings in progress show a time gap of 20 - 30 Ma between the formation of episyenites and the first concentration of economic mineralization (Respaut (27), Turpin and Leroy in prep.).

3. MAIN FRENCH URANIFEROUS DISTRICTS RELATED TO GRANITES

3.1. Massif Armoricain

In the Massif Armoricain, most of the deposits are spatially associated with leucogranites and fault systems related to major Hercynian shearing zones, especially the South Armoricain one ('zone broyée sud-armoricaine or Z.B.S.A.). These zones represent earlier boundary limits between Hercynian tectonic microplates (Cogné (28), Autran and Cogné (29)). They consist of Cambro-Silurian series and are characterized by a complex tectono-metamorphic evolution which began during Devonian times. In these areas of increased heat flow and of crustal thinning, partial fusion of the basement occurred, and provided sources of magma for numerous syntectonic intrusions. Hyperaluminous granitic magmatism is the most widespread and the most important with respect to metallogenesis (Renard (30)). Leucogranite ages range from 300 to 350 Ma (Rb-Sr whole rock isochron: Sonet (31), Peucat et al. (32), Guineberteau (33)).

3.1.1. Pontivy-Rostrenen Massif (Brittany)

The Pontivy-Rostrenen Massif is located in the southern part of Brittany in relation with the Z.B.S.A. (Fig. 1). Several types of peraluminous granites compose this complex massif (Fig. 5, Marcoux (34), (35), Alabosi (22)).

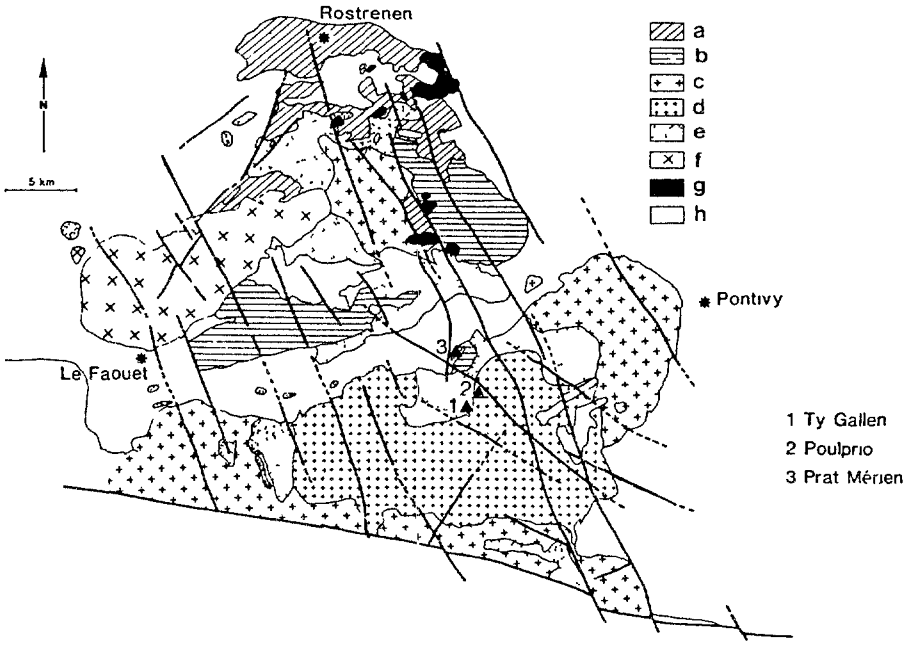

FIG. 5. Localization of the Ty Gallen, Poulprio and Prat Mérien deposits in the Pontivy Massif (Marcoux (34)). Biotite (a) and muscovite (b) Rostrenen granite; coarse (c) medium (d) and fine (e) Pontivy granite; Langonnet granite (f); granodiorite (g); metamorphic rocks (h).

Uraniferous deposits and occurrences are mainly located in the southern part of the Pontivy granites. They form a SW-NE, 4 km wide band near the contact with metamorphic formations. Several types of deposits are distinguished and described in Germain et al. (36) and Marcoux (34): brecciated veins within the granites, disseminations in episyenitic lenses, precipitations in contact with metamorphic enclaves.

Detailed studies have been carried out by Alabosi (22) on three small deposits (Ty Gallen, Poulprio, Prat Mérien). These deposits are related to N 140 - 160°E elongated episyenites. Episyenites and mineralizations are similar to those of the Saint-Sylvestre area (Massif Central).

3.1.2. Deposits in Vendée and southern Brittany

3.1.2.1. Geologic setting of the deposits

Uranium deposits are located along the contact zones between leucogranites and their surrounding metamorphic and/or magmatic rocks. Deposits within granitic massifs or in the metamorphic units are less frequent and not more than one to two kilometres away from the contact zone (Fig. 6).

(i) Intragranitic deposits: Commanderie deposit (COM), (Gerstner (37), Cathelineau (11), (38)) - The Commanderie deposit is the only strictly intragranitic deposit of the Mortagne Massif. It is located in a muscovite biotite leucogranite (Renard (30)). Numerous features allow its comparison with other intragranitic deposits of the French Massif Central (Cuney (39), Leroy (18)).

(ii) Contact deposits: Chardon (CHA) and Ecarpière (ECA) deposits (Tayeb (40), Cathelineau (5), (41), Cathelineau and Leroy (42)) - The Char-

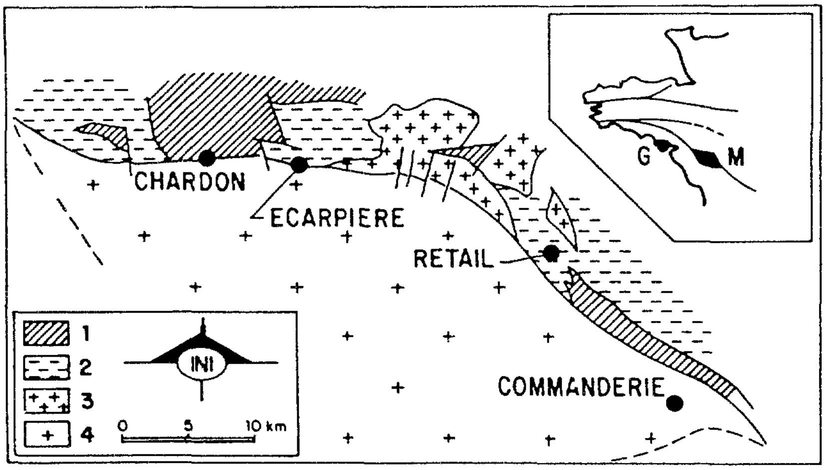

FIG. 6. Geological setting of uranium deposits in western France. G and M: Guérande and Mortagne leucogranite. 1. sillimanite - cordierite gneiss; 2. basic series; 3. biotite granites; 4. Mortagne leucogranite (Cathelineau (6)).

don deposit is located in the northeastern part of the Mortagne Massif at the contact between a two-mica porphyritic granite and metamorphic series (Lasnier and Marchand (43), Dumas and Leblanc (44), Fig. 2). The metamorphic series consist of three main units:

° amphibolites, some of which are gabbros with a granulite facies mineral association,

° low-grade schists with chemical characteristics, typical for shales (Cathelineau (45)),

° a highly deformed quartzfeldspathic unit (blastomylonite), the origin of which has not yet been fully established.

The Ecarpière deposit has a similar location, a few kilometres to the east, at the contact zone between the Mortagne granite and mylonites of various origins (mainly sheared granodiorites). In both deposits, the structural relationship between the metamorphic series and the granite is that of a ductile zone resulting from an east-west dextral shearing and a north-south compression caused by the overthrusting of the granitic block (Cathelineau (45)). The mineralization occurs in tension joints, conjugate shear joints and extension joints related to the last activity of the Z.B.S.A. (Lillié (10), Cathelineau (5), (11)). These veins crosscut all metamorphic units without offsets.

(iii) Intra metamorphic deposits: Retail (RET) and Penaran (PNR), (Cathelineau (5), (11)) - The Retail deposit (Ruhlmann et al. (46), Cathelineau (5)) is located in a thin complex zone, bordering on the northeastern part of the Mortagne Massif. This fringe zone is composed of various units: relics of granulitic facies rocks, medium to high grade gneisses and basic intrusions. These series present polymetamorphic characters: medium to high grade events affect aluminous series and previous granulitic units (retrograde metamorphism of coronitic gabbros and cordierite-sillimanite anatexites); then subsequent stages of retrograde metamorphism occur through general amphibolitization and low grade stages. The uranium deposits (Penaran, Metairie Neuve) of the Guérande peninsula (southern Brittany) are, as in Vendée, located near an hyperaluminous granite (Ouddou (47)). Structural studies show that ore has precipitated in an open fault network, located in a metamorphic unit ('porphyroids'), a few hundred metres north of the granite (Cathelineau (11)). Metamorphic series consist of graphitic quartzites, micaschists and blastomylonitic units (Valois (48)).

3.1.2.2. Mineral associations

A general paragenetic sequence is proposed and summarized from a number of already published detailed descriptions. Seven main stages have been defined from the vein opening to the late remobilization of already deposited ores (Table I) (Cathelineau (25), (49), (23)).

TABLE I. MAIN HYDROTHERMAL STAGES OBSERVED IN URANIUM DEPOSITS OF VENDEE AND SOUTHERN BRITTANY. TEMPERATURES OF DEPOSITION ARE ESTIMATED FROM FLUID INCLUSION DATA, AGES FROM U-PB GEOCHRONOLOGICAL STUDIES (SEE REFERENCES IN TEXT) (IN: CATHELINEAU (6)).

	STAGE	PHYLLOSILICATES	IRON MINERALS	T°C	AGE (MA)
I		PHENGITE (COM)	HEMATITE	200 - 400	
II	QUARTZ Q1 (RARE)	ILLITE (PNR) M.L. ILL./SM.	PYRITE HEMATITE	300 - 420 200 - 350	
III	PITCHBLENDE I	M.L. ILL./SM.	PYRITE	300 - 420 200 - 350	A) 340 B) 280 - 260
IV A)	QUARTZ PITCHBLENDE II	M.L. ILL./SM. + SM	HEMATITE GOETHITE	150 - 250	280 - 230
IV B)	AXIAL FILLING		COMPLEX RECURRENCES	90 - 150	
V	COFFINITE (FLUORITE-ADULARIA)	K. CA SMECTITE	MARCASITE		
VI	LATE REMOBILIZATIONS U^{4+} MINERALS SUPERGENE U^{6+} MINERALS	KAOLINITE	PYRITE MELNIKOVITE HYDROXIDES	0 - 100	180 70 0

Important differences have been observed in the mineralogy of the main stages of uranium deposition (stage III) or axial filling of the veins (stage IV), following the host rock lithology. A clear zoning of paragenetic sequence is observed from the intragranitic to the metamorphic deposits. This zoning is similar to the zoning observed in the Hercynian orogen of western Europe from the inner to the outer part (Geffroy (50), Cathelineau (5)).

(i) Intragranitic deposits (Si-K-Fe-Al) show very simple mineral associations consisting of iron minerals, silica and phyllosilicates.

(ii) Contact deposits: intragranitic deposits close to the contact (Si-Fe-S-F) show recurrences of pyrite, quartz, microcrystalline silica and fluorite in some cases (ECA); typical simultaneous growth of pitchblende with pyrite or silica are observed; when veins cross the contact between granite and metamorphic units, carbonates become dominant and are associated with more than one sulfide (pyrite, marcasite, chalcopyrite and/or galena) and clays (intrametamorphic part of the deposit).

(iii) Intrametamorphic deposits exhibit complex paragenetic sequences:

° in the Penaran deposit (Fe-S-Ni-Co-As-Pb-Zn-Cu), the subsequence is observed following the pitchblende deposition marcasite/pyrite + arsenopyrite/Ni-Co rich pyrites/galena/chalcopyrite + sphalerite/bornite + covellite;

° in the Retail deposit (Se-Bi-Cd-Cu-Pb/S-As-Fe), during pitchblende deposition, the paragenetic sequence is bismuthinite - Bi-selenides/greenockite + clausthalite/chalcopyrite + clausthalite. A sulfide stage (löllingite-galena-pyrite-melnikovite) follows the selenide stage. Covellite-bornite-umangite-klockmannite-digenite-tennanite/chalcocite-wittichenite are deposited in a later stage.
The main conclusions regarding the detailed physico-chemical studies of solid and fluid phases related to the main mineralizing stage (III) led to the distinction between two fundamental groups of deposits (Cathelineau (6)):

(iv) Intrametamorphic deposits, characterized by

° complex paragenesis: three main associations (Fe-Cu-Zn-Pb/As-Ni-Co/Cd-Pb-Bi-Se) indicate significant reactions between ore fluids and metamorphic environments on a wide scale;

° high temperatures of formation (close to 400°C) which explain the cubic habit of uranium oxides in the Penaran deposit;

° small interactions between fluids and host rocks in the vicinity of mineralized veins;

° formation ages older than all other dated occurrences known in Europe (Leutwein (51), Kosztolanyi (2)). These ages are estimated to be older than 340 Ma (Devillers and Menes (4), Holliger and Cathelineau in prep.).

(v) Intragranitic and contact deposits, where

° mineral associations are much simpler,

° fluid temperatures range from 150 to 300°C,

° geochronological studies (Kosztolanyi (2), Holliger ard Cathelineau in prep.) show that intragranitic and contact deposits are formed during the same metallogenic event. This important stage is dated 260 - 280 Ma,

° deposition of uranium is mainly influenced by external parameters: hydraulic fracturing, observed in nearly almost all deposits, which can lead to a decrease in gas fugacity (CO_2, F, ...) or reactions between fluid and host rock, as demonstrated in the Chardon and Ecarpière deposits. These reactions follow classical models involving carbonate (Naumov (52), Sokolova and Acheyev (53), Cathelineau and Leroy (42)) or fluorite (Cathelineau (41)) deposition.

3.2. Massif Central

The Massif Central is the most important part of the Hercynian orogen in France, and the richest uranium deposits known in this country are located and mined there. These deposits are mainly hosted in two-mica granites (Fig. 1).

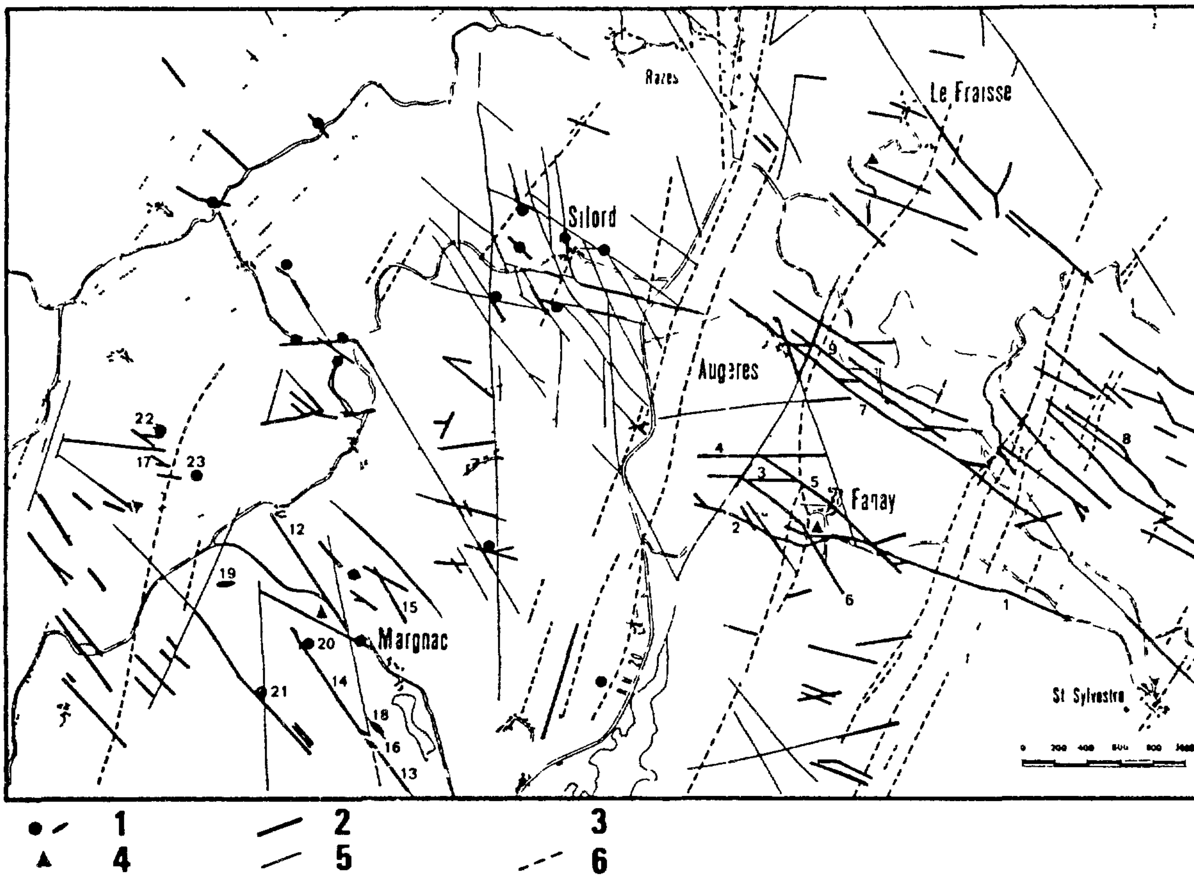

FIG. 7. The faulting system in Margnac and Fanay deposits (Moreau and Ranchin (13)). 1. episyenitic body; 2. ore vein; 3. microgranite vein; 4. mine shaft; 5. barren fault; 6. lamprophyric dike.

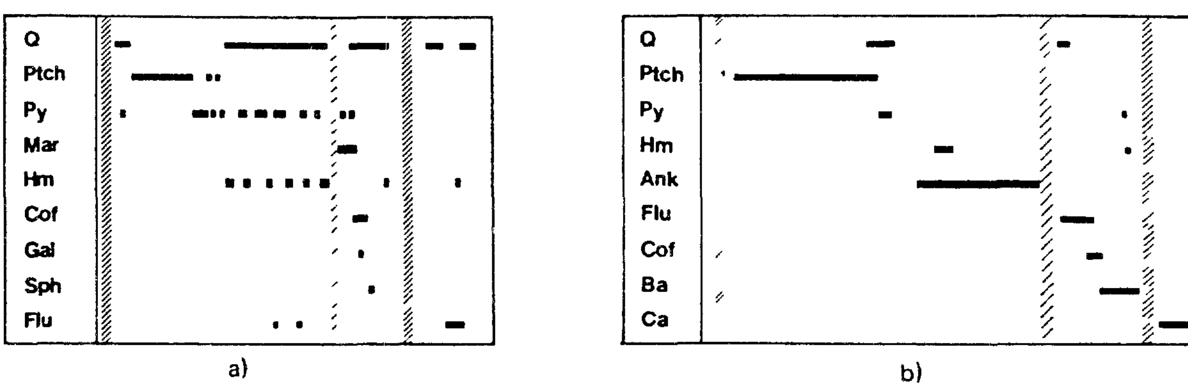

FIG. 8. Paragenetic sequences observed in Fanay, Margnac I veins (a) and Margnac IV veins (b); q - quartz, Ptch - pitchblende, Py - pyrite, Mar - marcasite, Hm - hematite, Cof - coffinite, Gal - galena, Sph - sphalerite, Flu - fluorite, Ank - ankerite, Ba - barite, Ca - calcite (Leroy (18)).

3.2.1. La Crouzille district (Saint-Sylvestre Massif)

The La Crouzille uraniferous district, mined by Cogema, is presently the main intragranitic district. The host rocks are the Saint-Sylvestre granites (Ranchin (54), Friedrich (55), Cuney et al. (56)) and the mineralizations (pitchblende, coffinite, supergene autunite and black minerals) occur in veins or are disseminated in episyenitic pipes. When the episyenitization process is related to east-west and north-northeast directions, the circulation of uraniferous solutions and the pitchblende precipitation are guided by north-west structures (Fig. 7).

A large amount of data has been published on this district and its geological setting by Geffroy and Sarcia (57), (58), Sarcia and Sarcia (59), (16), Marquaire and Moreau (12), Barbier (60), Geffroy (50), Leroy (61), Moreau and Ranchin (13), Poty et al. (62), Leroy and Sonet (63), Moreau (64), and Leroy (18).

3.2.1.1. Paragenetic sequence

Mineralogical studies indicate that the paragenetic sequences are essentially the same for both types of mineralizations (Fig. 8).

The first stage of deposition corresponds to the 'pitchblende-pyrite' stage. Following a discrete hyaline quartz deposition, pitchblende precipitates with pyrite. Simultaneous growth features between both minerals are observed. They are followed without brecciation by a microcrystalline hematitic quartz. This quartz phase contains pyrite and hematite. Hematitization immediately follows the crystallization of pyrite during precipitation of quartz. In some veins, ankerite and hematite are observed in place of hematitic quartz.

Subsequent to an episode of brecciation, hyaline quartz precipitates with iron sulfides (marcasite, pyrite). During this second stage, pitchblende is transformed into coffinite which mainly occurs as concretions on prismatic secondary quartz. Banded violet fluorite, pink barite and white calcite end the paragenetic sequence.

3.2.1.2. Wall rock transformations during mineralization stages

Wall rock alteration is not very important in volume, but may in part explain the chemical composition of pitchblende and its precipitation (Leroy (18), Cathelineau and Leroy (42), Cathelineau et al. (65), Leroy and Holliger (3)). In granitic and episyenitic host rocks, pitchblende precipitation is accompanied by a general phengitization of all minerals. In contact with lamprophyric dikes, a similar evolution is observed. If carbonates are present in the fresh rocks, they are dissolved at the proximity of pitchblende veins. Chemically, in both types of host rocks, this first stage corresponds to a K metasomatism, which appears to be one of the main characteristics of 'Hercynian' intragranitic deposits (Cathelineau (25)). This enrichment is accompanied by Si and Na losses in granitic environments and by Na, Ca and Mg leaching in mafic rocks. The chemical composition of pitchblende reflects these chemical migrations (Cathelineau et al. (65), Leroy and Holliger (3)). After hematitization of wall rocks at the end of this first stage (microcrystalline quartz), white micas are no longer stable and montmorillonite precipitates during coffinite stage. Some adularia is locally observed with clay minerals.

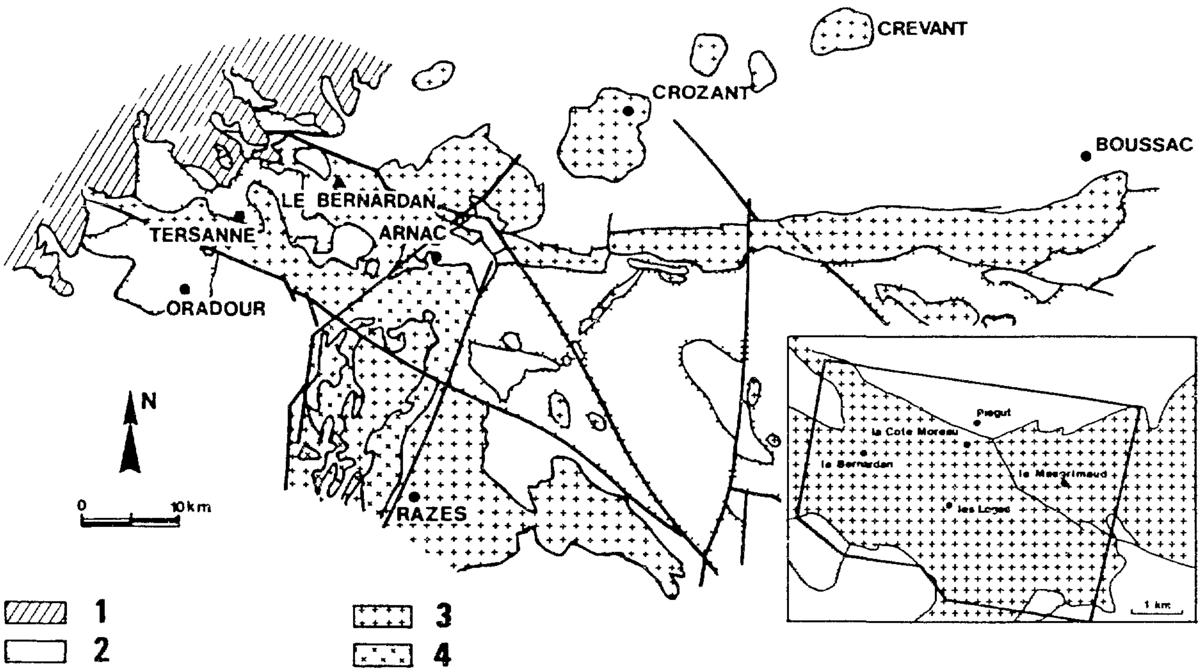

FIG. 9. Localization of Le Bernardan deposit in the western part of the Marche granite (northern Limousin, in Leroy (19)). 1. sedimentary rocks, 2. biotite granite; 3. biotite-muscovite granite; 4. structured sillimanite granite.

3.2.1.3. Fluid inclusion and isotope studies

Fluid inclusion studies indicate that pitchblende is deposited from CO_2-rich solutions at temperatures of 340 - 350°C. N_2, H_2S and traces of hydrocarbons have been observed in these fluid inclusions with a Raman microprobe. From isotopic studies ($\delta^{13}C$ = -17,6 ‰), a mantellic origin cannot be supported for this CO_2 (Turpin (26)). Another important result are the high values of $\delta^{18}O$ (+8 to +15‰) and δD (-45 to -30 ‰) of metal-bearing fluids (Fig. 9), which probably means that formation (or metamorphic) waters were involved in the geothermal systems during ore deposition stages. Boiling features are observed in CO_2-bearing fluid inclusions. This fact has led Leroy and Poty (66) and Leroy (18) to invoke a transport of uranium as uranyl-carbonate complexes and a precipitation of pitchblende after the destruction of the complexes during this boiling and/or a reaction with mafic minerals. Following this first stage, the CO_2 content of fluids decreases and the solutions are purely aqueous. Temperature regularly decreases from 350°C (pitchblende) to 140°C (coffinite) and to less than 100°C (calcite).

U-Pb studies carried out on pitchblende from Margnac and Fanay veins give an age of 275 Ma (Leroy and Holliger (3)). During the transformation of pitchblende into coffinite, very rare crystals of galena precipitate within the coffinite. Using these crystals, a 5 Ma time interval is suggested between pitchblende precipitation and its alteration into coffinite.

3.2.2. La Marche deposits

The Bernardan deposit is the main uranium mine in the Marche Occidentale peraluminous granite of the Dong Trieu Mining Company (Fig. 10). Other smaller deposits are known in this area: Les Loges, Mas Grimaud, Côte Moreau, all located in

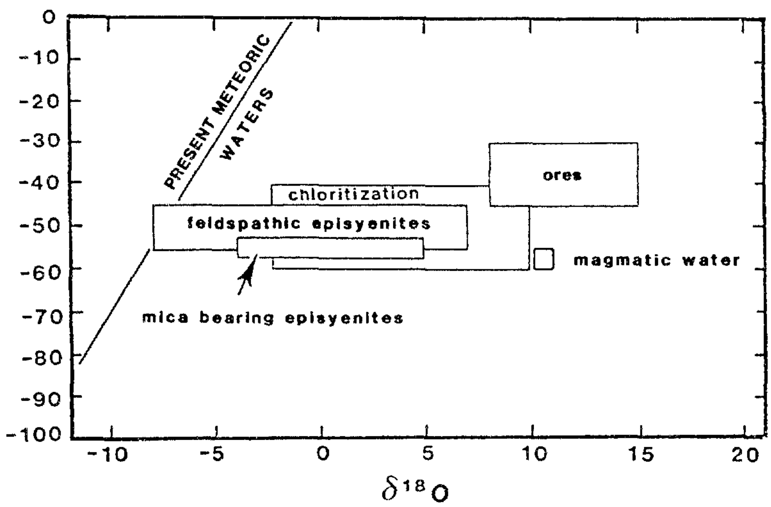

FIG. 10. $\delta^{18}O/\delta D$ diagram applied to altered facies and ores of the Saint Sylvestre Massif (Turpin (26)).

the granite, and Piegut in the Aigurande gneisses, north of the granite. All intragranitic deposits belong to the 'disseminated-type'. The uraniferous mineralization is located in episyenitic columns similar to those of the Margnac deposit.

3.2.2.1. La Marche Occidentale granites

The Marche Occidentale is a complex granitic massif located in the western part of a roughly EW granitic belt. It is limited to the north by a main mylonitic zone ('dislocation de la Marche'). Its southern and eastern limits are also structurally controlled. Two main types of granites compose this massif (Ranchin (54), La Roche et al. (67)): biotite granites, assimilated to the Guêret granite, intruded by two-mica granites. All known deposits are located within these two-mica granites.

3.2.2.2. Structural studies (Lespinasse (17))

The early structure of the Marche Occidentale granite is controlled by the 'dislocation de la Marche'. It is a nearly vertical thick mylonitic zone, oriented either N 90°E (regional direction) or, in its central part, N 120°E. The associated ductile deformation (orthogneissification of the granite) appears to be mainly a sinistral shearing in its N 90°E part, and mainly a flattening in its N 120°E part (Lespinasse and Pecher (68)).

The late Hercynian deformation is more brittle and marked by a complex set of extensional and slicken-side faults. An analysis of the striated fault-planes shows that the late Hercynian fracturation is the result of the superposition of at least three different stress fields; the main stress σ_1 has successively been orientated N 20°E, N 150°E, N 80°E. It appears that the N 20°E direction of compression, the only one coherent with the ductile deformation, corresponds to the earlier tensor; it is followed by the N 150°E direction and finally by the N 80°E one. In the Bernardan deposit, the principal episyenitic bodies are structurally controlled by N 20°E and, less clearly, by N 150°E faults Percolation of the hydrothermal fluids occurred through a dense set of above oriented fractures at all scales. Part of the percolating fluids have been preserved in numerous healed microcracks, which now appear as thin trails of fluid inclusions. These trails are observed in the quartz fillings of some of the mesoscopic fractures, but also form a dense set in all the preserved quartz crystals of the bulk granite around the episyenites. Trails of fluid inclusions are preferentially oriented conformably along the main direction of stress (N 20°E) which is the direction of the episyenitic column section (Lespinasse and Pecher (69)). Thanks to the above chronology, it is possible to follow the variations of temperature with time (Pecher et al. (70)).

3.2.2.3. Uraniferous mineralizations and modifications of the host rock

Most uraniferous minerals are disseminated in the episyenitic columns. Locally carbonates are relatively abundant. Pitchblende is the primary uraniferous mineral. Coffinite is due to a hydrothermal alteration of the primary uranium oxide and never occurs during supergene processes. Fluorite and barite are deposited during the coffinite phase, accompanied by clay minerals and adularia. Present studies indicate that these clay minerals are K-Ca montmorillonite with adularia within the episyenitic and mineralized bodies, whereas smectites and kaolinite are observed outside them. This second zoning is superimposed to the first one (episyenitic alteration) and corresponds to the end of the geothermal system (Leroy (18), (19)).

The nature of present uraniferous supergene minerals depends on the redox conditions of the ground-water table, autunite in the oxidizing upper levels, sooty pitchblende in the reducing lower ones. Ningyoîte (U^{IV} phosphate) is locally known between these two zones.

3.2.3. Millevaches Massif (Hyverneresse deposit)

The Millevaches complex is made up by several types of granites (Stussi (71), Monier (72)). Some uranium deposits are known in this massif. To the present day, the best studied one is the Hyverneresse deposit, which is located close to the north-east tectonic border of the massif within a coarse grained two-mica granite. A fine grained granite in veins is also observed in the open pit. Its relations with the coarse grained granite indicate that this latter one was not completely crystallized during the intrusion of the fine grained granite.

The uraniferous mineralization is disseminated in episyenitic bodies (Martin (20)) and controlled by N 130°E faults. Pitchblende with pyrite is the primary mineralization. This first stage also corresponds to an increase of the white mica alteration of the host rocks. Coffinite with sulfides (pyrite, marcasite, galena) is the second uraniferous mineral. Clay minerals (montmorillonite) and, locally, Fe dolomite are observed. From fluid inclusion studies, uraniferous solutions are CO_2-rich and their temperature is close to 350°C.

3.2.4. Uranium deposits of the northeastern part of the Massif Central (Montagne Bourbonnaise)

3.2.4.1. Geologic setting

In the northeastern part of the Massif Central, only one large uranium deposit has been discovered: the Bois Noirs Limouzat uranium vein (B.N.L.) (Fig. 11). Several minor deposits have also been mined such as Lachaux and St. Priest (B.N.2). This area is a granitic horst faulted by N 165° deep faults and limited to the west and to the east by Oligocene grabens.

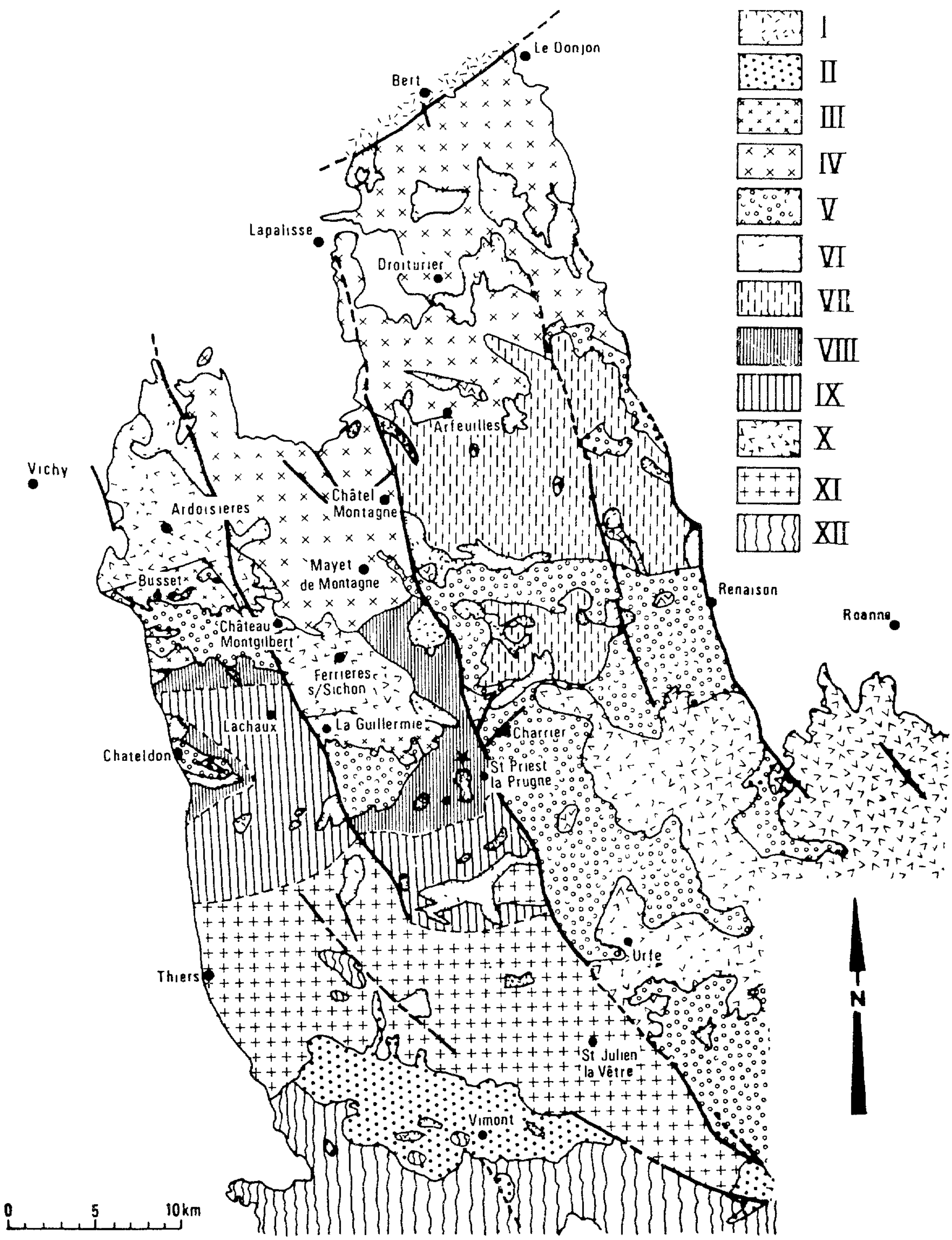

FIG. 11. Geological map of the Montagne Bourbonnaise, simplified from Kurtbas (73). I. Permian sedimentary rocks; II. Vimont two-mica granite; III. Busset and La Guillermie granites; IV. Mayet-Arfeuilles-Droiturier granites; V. porphyritic microgranite cover; VI. fine grained granites; VII. Madeleine granite; VIII. northern facies of the Lachaux-Bois Noirs granite; IX. central facies of the Lachaux-Bois Noirs granite; X. Devonian and Visean sedimentary rocks; XI. St. Julien-la-Vêtre southern Bois Noirs granite; XII. metamorphic basement. The star locates the Bois Noirs-Limouzat deposit.

Three main granitic units of different ages are distinguished (Kurtbas (73)):

(i) Pre-Visean: St. Julien la Vêtre granite in the south,

(ii) Visean: Lachaux, Bois Noirs, Madeleine (Bois Noirs sensu lato) granites in the centre dated by Rb/Sr whole rock isochron at 347 Ma (Vialette (74)),

(iii) Post-Visean: Mayet, Arfeuilles, Droiturier granites in the north.

Lamprophyric dikes and several generations of microgranites are intruded up to 270 Ma.

The earliest structures are of E-W directions. They are the global orientation of contacts between the different petrologic units, of the fold axis of Visean sediments occurring as a small basin in this area, and of the foliation acquired during magmatic and ductile stages in the Bois Noirs granite. An early generation of microgranites is syntectonically injected along these E-W structures in the northern porphyritic facies of the Bois Noirs granite. This direction is also that of the primary pitchblende-iron sulfides ore. Thus, these E-W structures were already active during the intrusion of the Bois Noirs granite (347 Ma) and were reactivated several times up to the deposition of the primary uranium ore (Holliger and Cuney in prep.).

N 135° - 165°E structures belong to an associated and nearly vertical tectonic system generated by a N 25°E compression. This system divides the whole Montagne Bourbonnaise in lense-shaped blocks along which uranium occurrences and the BNL deposit are located. Before Stephanian these faults acted essentially as shear zones, whereas they were related to a vertical displacement during alpine orogeny. N 40° - 60°E structures are mostly represented by the Bert-Blanzy Stephano-Permian graben which does not present any clear influence regarding uranium mineralizations in the granites.

3.2.4.2. Host rocks

The two main economic uranium deposits (Lachaux and essentially BNL) were located in the northern facies of the Bois Noirs granite (s.l.). This granite is slightly peraluminous and shows geochemical and mineralogical affinities with subalcaline granites (Pagel and Leterrier (75)): high K (4.3 - 4.1 %), Th (37 - 33 ppm), U (7 - 11 ppm) and REE contents, occurrence of titanite, allanite and uranothorite in the less differentiated facies. Mineralogical similarities with peraluminous granites are also present: moderate development of muscovite, local occurrence of cordierite and appearance of monazite and xenotime in the more differentiated facies.

This granite is intruded by typical fine grained peraluminous muscovite-bearing granites, the proportion of which increases with depth as observed in deep drill holes (-500 m) in the BNL mine. These fine grained granites are much richer in uranium (10 - 30 ppm) mostly expressed as uraninite of low thorium content easily leachable by hydrothermal processes. They are frequently injected along E-W structures.

In the northern facies of this granite, where all deposits and most uranium occurrences are located, the mean uranium content of fresh granite is only 7 ppm, mainly located in refractory uranothorite. Uraninite is not very abundant and appears to crystallize mostly in fractures at a subsolidus stage contrary to what is observed in the fine grained granites (Le (76), Cuney (39)) and generally in peraluminous granites (Pagel (77), Friedrich and Cuney (78), Friedrich (55)). The ThO_2 content of these uraninites is very variable (2 - 15 wt%) unlike what is observed in peraluminous (ThO_2 = 2 wt%, Friedrich (55)), or subalcaline granitoids (ThO_2 = 10 - 15 wt%, Pagel (79)). This is interpreted as a polygenic origin: uraninite of high thorium content crystallizes at the magmatic stage in equilibrium with uranothorite, whereas uraninite of low thorium content crystallizes in shear zones in fluids expelled from the fine grained granites. This model is similar to the one proposed by Friedrich (55) for the Saint-Sylvestre Massif, but at Saint-Sylvestre coarse and fine grained granites are both strongly peraluminous.

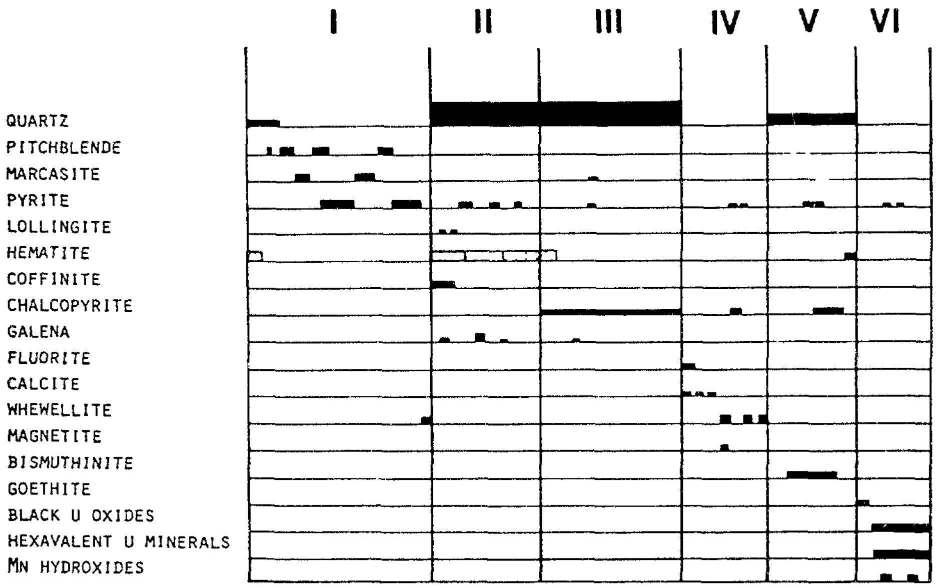

FIG. 12. Paragenetic sequence of the Bois Noirs deposit (Cuney (39)).

3.2.4.3. Uranium mineralizations of the Bois Noirs-Limouzat deposit

Six stages of mineral deposition have been recognized in the BNL deposit (Cuney (39), Fig. 12). During the first stage, only observed in E-W structures, euhedral quartz (Q_1), pitchblende, marcasite and As-rich pyrite are deposited. Pitchblende mainly occurs on the pyramides of Q_1 and between marcasite and pyrite growths. It also appears on the growth zones of Q_1 and pyrite. The subsequent stages of mineral deposition do not bring any new uranium supply to the veins. However, two main stages of remobilization have been observed. During stage II, part of the pitchblende is altered into coffinite, together with an important hematitization.

During alpine orogeny and up to the present time, the Montagne Bourbonnaise uplift leads to the meteoric alteration of uranium ore. A 'per descensum' redeposition occurs in the N 135° - 165°E fault system as sooty pitchblende and hexavalent uranium minerals (mostly torbernite and urancphane). About half of the uranium reserves is located in these structures.

From fluid inclusion data it appears that the metal-bearing solutions were aqueous fluids of low salinity (0.34 wt% equiv. NaCl) containing about 1 mole % CO_2. Uranium was transported mainly in the form of uranyl-monocarbonate ($UO_2(CO_3)^{\circ}$) with a significant amount of H_2S. The fluid pressure dropped from lithostatic to hydrostatic regime in breccia zones, leading to a decrease in CO_2 and carbonate ions concentration in the solutions. In the breccia zone the surface available for fluid rock interaction increased considerably. Part of the remaining dissolved CO_2 reacted with plagioclase to form calcium carbonates. These successive decreases of CO_2 activity led to the unstability of uranyl-carbonate complexes, and the liberated uranyl ions were available for reduction by the reduced sulfur species present in the solution.

U-Pb isotopic determinations indicate a lower Permian age (270 Ma) for the primary uranium ore, whereas hexavalent uranium minerals (Holliger and Cuney, in prep.) are due to a recent to present reworking.

3.2.4.4. Lachaux deposits

The Lachaux deposits have been described by Poughon and Moreau (80). Some primary pitchblende-sulfide ore has been locally preserved in E-W structures. However, most of the known ore is related to a recent reworking (probably of alpine age) in the exclusive form of parsonsite (U-Pb phosphate).

3.2.5. Margeride deposits

The Pierres Plantées, Cellier and Villeret deposits (Cariou (81)) are located in the Grandrieu leucogranite (southeastern part of the French Massif Central). As many laccolites, dikes and veins of peraluminous granites in this area, the Grandrieu leucogranites (Stussi (82)) are intrusive in the large Margeride biotite (Couturié (83)). Isotopic ages obtained on these leucogranites range from 293 to 305 Ma (Couturié (83), Respaut (27)). The Pierres Plantées and Villeret deposits are spatially associated with episyenites (Cathelineau (23)). The first alteration process (hydrothermal quartz leaching) occurred thirty million years after granite crystallization (Respaut (27)).

Several stages of alteration and uranium deposition are defined. In each metallogenic event, new mineralization and alteration parageneses are superimposed on the previous ones (Fig. 13) as follows.

(i) Pitchblende stage: pitchblende-dolomite (sulfides) veins occur in the deep levels of the Pierres Plantées mine.

(ii) Coffinite stage: alteration of pitchblende into coffinite induces a complete loss of the initial geochronological information. This mineral is dated at 197 $\pm$ 4 Ma (Respaut (27)). This age may be related to distensive movements associated to the opening of the Atlantic Ocean; this hypothesis was already proposed by Bonhomme (84), Baubron et al. (85) and Lancelot et al. (86) for other deposits.

(iii) Above uranium mineralizations are locally leached and redeposited along roll fronts, through oxidation-reduction processes (Cathelineau (38)). Two types of roll fronts are distinguished:

° iron dominant roll front involving the following sequence: oxidized zone with hematite; goethite + calcite + pitchblende; reduced zone with pyrite;

° manganese dominant roll front characterized by the sequence: manganite-coffinite-goethite-reduced zone. These stages are more recent and estimated at 90 Ma (Respaut (27)).

All these alterations have transported the early metal concentrations into strongly altered granite and explain the complex pattern of the present day mineralization.

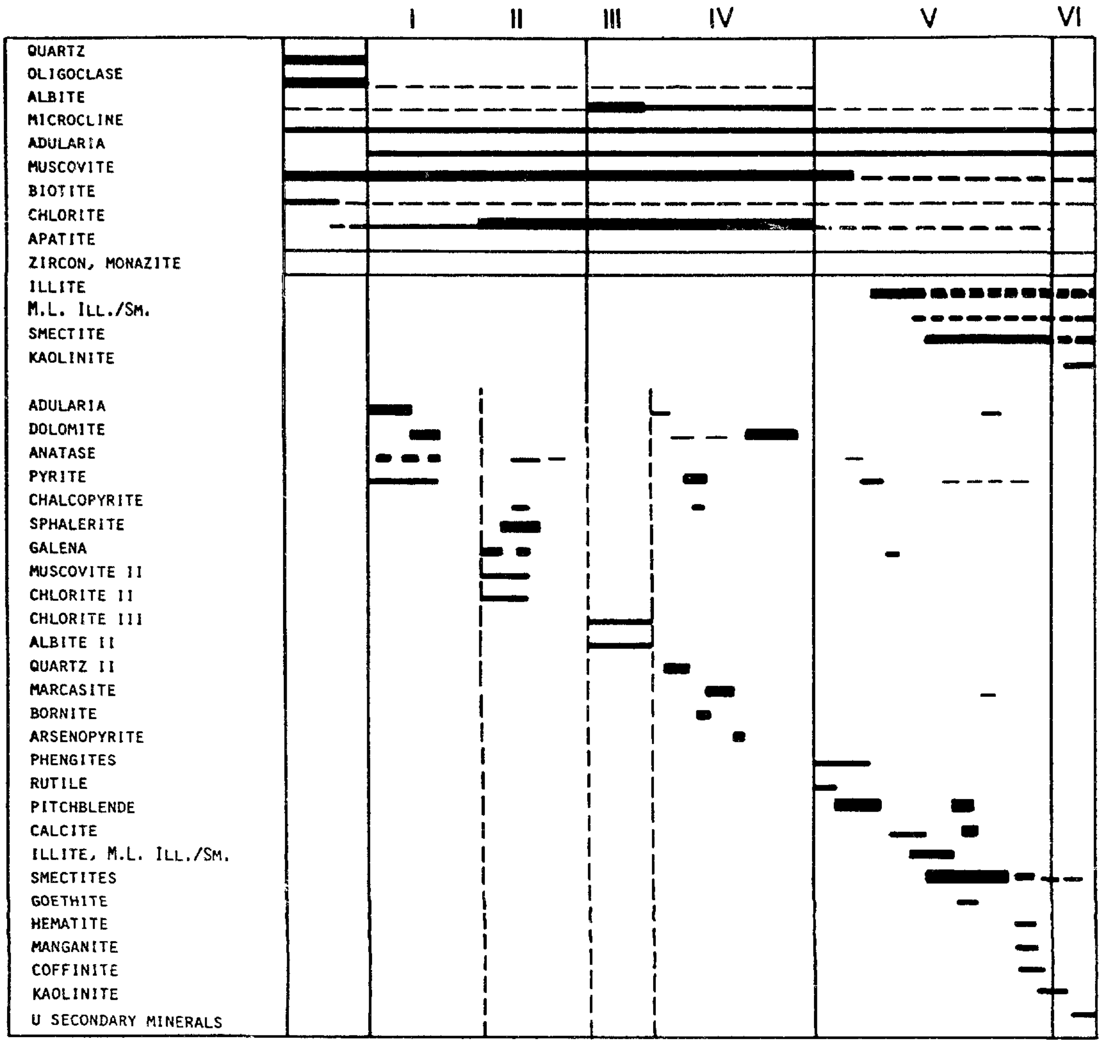

FIG. 13. Paragenetic sequence in the Pierres Plantées deposit (Cathelineau (23)). The upper part of the diagram shows changes in granite mineralogy and the lower part shows mineralogy of veins and fillings.

4. CONCLUSIONS

4.1. Previous genetic models

Several genetic models have been successively proposed for the uranium deposits of the French part of the Hercynian orogen. During the fifties, a hydrothermal origin for most vein-type deposits in the world was favoured from the works of Lindgren (87) and Schneiderhöhn (88). Geffroy and Sarcia (89) proposed such a model for the French uranium vein-type deposits. However, Roubault and Coppens (90), (91) already observed that uranium could be leached out from the granites near surface to form autunite. They suggested that uranium vein-type deposits may not have exclusively a deep hydrothermal origin, but may result from an 'in situ' concentration process by remobilization of dispersed uranium from adjacent enclosing rocks (lateral secretion). However, they did not clearly specify whether uranium mobilization was a supergene or a hydrothermal process.

Bigotte (92) proposed that uranium veins were originated from the remobilization of stratiform uranium concentrations through phreatic waters. Moreau et al. (93) were more specific about this model. They suggested that uranium vein deposits resulted from supergene weathering of uranium-rich granites or sediments due to the percolation of oxidizing meteoric fluids under a tropical climate prevailing during Permian time. For these authors, such a model could explain the rapid decrease of uranium mineralization with depth, the bulb shape of the ore zone and the occurrence of hematite. This model was adopted and extended by numerous authors: Matos Dias and Soares de Andrade (94) for Portugal, Langford (95) for vein deposits of the Northern Territory in Australia and in (96) for deposits in North America such as Beaverlodge, Knipping (97) for the Rabbit Lake deposit and Barbier (98) in France. Magne et al. (99) demonstrated experimentally that bacteria can leach uranium from granites. They suggested that the Limousin deposits may result from such a mechanism. Thus until 1974 the supergene model for uranium vein deposits was widely accepted all over the world.

New constraints on the genesis of uranium mineralizations were brought forward by fluid inclusion studies (Leroy and Poty (66), Poty et al. (62)) associated with paragenetic mineral studies (Cuney (100), (39), Moreau (64), Leroy (18)). For these authors, the primary uranium mineralization is the result of a hydrothermal leaching of uraninite from enclosing granites. Pressure, temperature and composition of hydrothermal fluids were decisive arguments for presenting the new hypothesis. It was shown that pitchblende is not deposited simultaneously with hematite but in rather reducing conditions together with iron sulfides. A recent supergene remobilization which may represent nearly half of the uranium content of some uranium deposits (such as the BNL deposit) leads to the bulb shape of most near surface mineralizations. But the progress of mining in the different uranium districts shows presently that uranium mineralization is almost everywhere observed below 350 m depth.

4.2. Uranium sources

4.2.1. The peraluminous granites

The high uranium average content (10-20 ppm) of peraluminous granites in the form of uraninite was pointed out as the major uranium source for uranium occurrences (Barbier et al. (101), Barbier and Ranchin (102), Ranchin (54), Renard (30), Le (76), Moreau (64) and others). Extensive pervasive leaching of disseminated uraninites appears to be the most plausible mobilization process. Up to recent studies, uraninite crystallization and distribution were attributed to late magmatic and hydrothermal processes. Recent work (Cuney et al. (103), Ball and Basham (104), Pagel (77), (79)) emphasized that uraninite clearly belongs to the magmatic paragenesis. Friedrich and Cuney (78), Friedrich (55), Cuney et al. (105) show in the Saint-Sylvestre granitic complex that uraninite presents two types of distribution. A first one is homogeneously distributed in a rock sample and its abundance is correlated to magmatic differentiation processes. A second one is distributed along shear zones, developed at a magmatic stage, and crystallizes from fluids expelled from uranium-rich fine grained granite bodies. These granites are simultaneously emplaced with the enclosing coarse grained facies along shear zones which are active at a magmatic stage (magmatic faulting) (Mollier and Bouchez (106), Mollier (107)).

The geographical location of uranium mineralizations deposited in brittle fractures fit the location of the primary enriched zones (preconcentrations) at different scales. In some of the districts of Saint-Sylvestre (Friedrich (55)) and in the BNL deposit the overlap in direction and location between magmatic and brittle structures is fairly good (metric to hectometric).

The fine grained granite intrusions in the Bois Noirs and Saint-Sylvestre complexes represent specialized magmas enriched in incompatible elements (U, Li, F, Sn ...). The uraninite 'preconcentration' (up to 50 or locally 100 ppm) enhances considerably the available uranium potential of the source. The qualitiy of the overlap between magmatic and brittle structures may increase the efficiency of uranium mobilization.

4.2.2. Other sources

New geochronological data (Devillers and Menes (4), Cathelineau and Holliger in prep.) have led to the discovery of ages close to or older than 340 Ma for intrametamorphic deposits (Penaran and Métairie Neuve in southern Brittany and Retail in Vendée). These deposits are older than the adjacent granites. Thus, other uranium sources than granites must be searched for in the enclosing metamorphic rocks, such as black shales and acid volcanics (Cathelineau (5)).

In Vendée most of the deposits are located at the contact between granites and metamorphic rocks in large mylonitic zones. Mylonitization of either metamorphic rocks or granites may favour uranium leaching by hydrothermal solutions.

4.3. General paragenetic sequence

A general paragenetic sequence for French intragranitic deposits is given by Geffroy (50). The recent studies leave this sequence practically unchanged if we except minor additions.

In all deposits, pitchblende is the primary uraniferous mineral. Only rare quartz is observed before pitchblende in small amounts and usually begins the sequence. When Fe-minerals precipitate with pitchblende, they are iron sulfides (pyrite and marcasite). Hematite and other ferric minerals always occur after pitchblende. This fact means that reduction and precipitation of uranium is not coupled with an oxidation of ferrous iron. During this first stage, a general K-metasomatism occurs in the wall rocks or in the host rocks. At least, whatever their temperature is, fluids belong to the C-H-O system.

The second uranium stage corresponds to the formation of coffinite from pitchblende in hydrothermal conditions (130°C - 150°C). Fe-minerals are once again sulfides. This rather high sulfur fugacity also explains the precipitation of lead, released from pitchblende, as galena. During this stage, quartz precipitates and the adularia-montmorillonite association often replaced the muscovites.

Carbonates, barite, fluorite are known in all deposits. Their abundance and their position in the paragenetic sequence vary.

The third and last uranium stage corresponds to recent to present supergene reworkings which led to hexavalent uranium minerals (phosphate, silicate ...) in the oxidized levels of the ground-water table, and tetravalent uranium in the reduced levels. Coffinite is never observed with such supergene processes in granitic environments.

4.4. Genetic models

At least four stages of activity are distinguished by U-Pb isotopic studies carried out on uranium deposits spatially related to French Hercynian granites: 340 Ma and older, 260 - 280 Ma, 190 - 170 Ma and 0 Ma.

4.4.1. Middle Palaeozoic mineralizations

A 340 Ma age is actually known in three deposits from southern Brittany and Vendée, Penaran, Métairie Neuve and Le Retail. Older ages are also found in Le Retail deposit. These deposits show complex paragenetic sequences. They are all located in metamorphic units - this explains their complex mineralogy (As, Se, Bi, Pb, minerals) - close to peraluminous granites whose age is not enough accurately known.

These isotopic studies (U-Pb) oblige to consider a new period of formation of uraniferous occurrences. With such an age they can be related to circulations of hot fluids in metamorphic units at the end of the Middle Devonian regional metamorphism, during magmatic activity or both. All these deposits are close to granites, but are separated from them by a main shear zone. Thus, the present spatial relationships with granites are not primary and cannot be used as a reference to investigate them in metamorphic units.

4.4.2. Lower Permian mineralizations

Lower Permian is the main period for uranium mineralization. Deposits of this age are known in all the Hercynian orogen. They are all located within peraluminous granites. Some veins can escape from the granite into the surrounding metamorphic units. Detailed mineralogical, geochemical and fluid inclusion studies have been carried out on numerous deposits and indicate a rather similar history.

At the end of Hercynian orogeny (290 - 300 Ma), a general mantle uplift took place, associated with a rather important magmatic activity (lamprophyric dikes, microgranites, granites). In places, the heat flow was higher, faulting was more important, deep convective circulations of meteoric waters occurred. This process led to the local episyenitization of granites, probably at the beginning of the hydrothermal activity. The mixture of 'heavy' fluids of diagenetic or metamorphic origin, rich in C and S compounds (CO_2, hydrocarbons, H_2S), with these hot meteoric waters is an important character of pitchblende deposition. Uranium was transported as hexavalent U complexes and precipitated as pitchblende either in veins related to active fracturing or disseminated in vuggy episyenites. Boiling of the fluids through pressure drop, and/or reactions with mafic host rocks such as lamprophyric dikes, are some of the mechanisms suggested for the precipitation of pitchblende.

Early hydrothermal transformation of pitchblende into coffinite occurred during the lowering of isotherms. Mineral and chemical modifications of the host rocks took place during all these stages.

This hydrothermal activity occurred during 20 - 30 Ma which is a much longer duration than what is actually known for present geothermal systems. But the heat source and the scale of these phenomena are completely different since similar magmatic and hydrothermal activities with the same age are known from west to east of the French part of the Hercynian orogen.

4.4.3. Jurassic mineralizations and/or remobilizations

Jurassic hydrothermal activity is described in the north and in the southeast of the French Massif Central in various deposits (Baubron et al. (108), Bonhomme (84), Bonhomme et al. (109), Joseph et al. (110), George (111)). For Bonhomme (84), this age corresponds to the distensive tectonics related to the opening of the Atlantic Ocean and of the Tethys.

In uranium vein-type deposits spatially related to granites, this Jurassic activity is known from U-Pb isotopic dating. It corresponds either to a local remobilization of the primary mineralization in some veins (La Crouzille, NW of Massif Central, Leroy and Holliger (3)) or, may be, to a new mineralizing phase (Margeride, SE of the Massif Central, Respaut (27)). For the Margeride deposits, it is presently not possible to demonstrate whether this age is related to the primary mineralization or to a secondary remobilization. Mineralogical observations in progress tend to indicate that a complete remobilization of an earlier mineralization could occur during this Jurassic hydrothermal activity.

4.4.4. Present remobilizations

The latest events known in all these deposits correspond to recent (some million years) supergene remobilizations. Present features, observed in the deposits, partly result from these supergene processes and are mainly controlled by redox mechanisms. Hexavalent uranium minerals are present in the oxidized levels, whereas tetravalent secondary minerals occur in the deeper reduced levels. Uranium leaching in the upper part of mineralized bodies results in an enrichment at depth. These features were the basis of the 'per descensum' hypothesis which formerly prevailed for all French uranium deposits spatially related to granites.

ACKNOWLEDGEMENTS

This paper is a summary of results accumulated during three decades by the French Atomic Energy Commission, further on by Centre de Recherches Radiogéologiques, and during those last years at Centre de Recherches sur la Géologie de l'Uranium (CREGU). Thus, it has been possible thanks to the financial support of the French Atomic Energy Commission, Compagnie Générale des Matières Nucléaires, Total Compagnie Minière, Compagnie Minière Dong Trieu, Compagnie Française de Mokta, and Société Nationale Elf Aquitaine.

We thank the geologists of these companies for their cooperation in field and mines, for providing the necessary documents as well as for their criticism in the course of the different studies. C. Bizard discussed particularly the manuscript.

REFERENCES

(1) PEINARDOR FERNANDES, A., JAMET, P., LE CAIGNEC, R., MOREAU, M., SERRANO, J.R., ZIEGLER, V., Gisements d'uranium dans les schistes péribatholitiques (type ibérique) et dans les leucogranites (type Limousin) (Portugal, Espagne, France), livret guide d'excursion, Sci. de la Terre, Nancy XXIII (1979) 47 pp.

(2) KOSZTOLANYI, Ch., Géochronologie des gisements uranifères français par la méthode uranium plomb, Influence du déséquilibre radioactif sur les résultats, unpublished thesis, Univ. Nancy I (1971) 279 pp.

(3) LEROY, J., HOLLIGER, P., Mineralogical, chemical and isotopic (U-Pb method) studies of Hercynian uraniferous mineralizations (Margnac and Fanay mines, Limousin, France), Chemical Geology 45 (1984) 121-134.

(4) DEVILLERS, C., MENES, J., Ages de la minéralisation uranifère de Penaran, Technical Paper, CEA-DRA/SAECNI 76 (1977) 383-150.

(5) CATHELINEAU, M., Les gisements d'uranium liês spatialement aux leucogranites sud-armoricains et à leur encaissant métamorphique, Sci. de la Terre, Mem., Fr. 42 (1981a) 475 pp.

(6) CATHELINEAU, M., Uranium veins in western France, Mineralogy and geochemistry of uranium deposition, in: Proceedings of ICAM 84 Congress, Los Angeles, TMS AIME (1984) 1083-1094.

(7) PONCERRY, E., Contribution à l'étude gêologique des granitoides de Vallorcine, Beaufort, Lauzière, de leur encaissant et des minéralisations uranifères associées (Alpes françaises), unpublished thesis, Univ. Grenoble (1981) 316 pp.

(8) LABHART, T.P., RYBACH, L., Granite und Uranvererzungen in den Schweizer Alpen, Geol. Rdsch. 63 (1974) 135-147.

(9) NEGGA, H.S., Comportement de l'uranium lors des métamorphismes tardi-hercynien et alpin dans les massifs des Aiguilles Rouges et de Belledonne (Vallorcine, Lauzière), Alpes Occidentales, unpublished thesis, Univ. Nancy I (1984) 420 pp.

(10) LILLIE, F., Analyse tectonique et fracturation des gisements uranifères de Vendée, unpublished thesis, Univ. Strasbourg (1974) 101 pp.

(11) CATHELINEAU, M., Les gisements uranifères de la Presqu'île Guérandaise (Sud-Bretagne), approche structurale et métallogénique, Mineralium Deposita 16 (1981b) 227-240.

(12) MARQUAIRE, C., MOREAU, M., Esquisse gêologique du Nord Limousin et répartition des minéralisations uranifères, Rapport CEA R 3684 (1969) 7-40.

(13) MOREAU, M., RANCHIN, G., Altêrations hydrothermales et contrôles tectoniques dans les gites filoniens d'uranium intragranitiques du Massif Central français, in: Les roches plutoniques dans leurs rapports avec les gites minéraux, Symp. E. Raguin, Paris (1971) 77-100.

(14) FRAIPONT, P. de, Approche multiscalaire de la fracturation du massif granitique de Saint Sylvestre, Télédétection et analyse tectonique appliquées aux gisements d'uranium de la division de la Crouzille (Cogema) Limousin, Massif Central français, unpublished thesis, Univ. Strasbourg (1982) 201 pp.

(15) SIRNA, C., Tectonique cassante des granites de Grandrieu, Margeride. Recherches appliquées aux gisements d'uranium de Langogne (Lozère, Massif Central français), Thèse 3e cycle, Univ. Strasbourg (1980) 111 pp.

(16) SARCIA, J., SARCIA, J.A., Gites et gisements du Limousin, in: Les minerais uranifères français, II. P.U.F. Ed. (1962) 185-292.

(17) LESPINASSE, M., Contexte structural des gisements d'uranium de la Marche Occidentale, Fracturation, circulations fluides, propagation de l'épisyénitisation, Gêol. Géochim. Uranium, Mêm. Nancy 8 (1984) 200 pp.

(18) LEROY, J., The Margnac and Fanay uranium deposits of the La Crouzille district (western Massif Central, France), geologic and fluid inclusion studies, Econ. Geol. 73 (1978) 1611-1634.

(19) LEROY, J., Episyénitisation dans le gisement d'uranium du Bernardan (Marche), Comparaison avec des gisements similaires du Nord Ouest du Massif Central français, Mineralium Deposita 19 (1984) 26-35.

(20) MARTIN, S., Episyênitisation et minéralisation dans le leucogranite d'Hyverneresse (Nord Millevaches, M.C.F.), unpublished thesis, Univ. Clermont II (1981) 222 pp.

(21) MICHEL, J.J., Episyênite et concentrations uranifères associées dans le massif de St. Sulpice-Les-Feuilles (Hte Vienne), unpublished thesis, INPL (1983) 461 pp.

(22) ALABOSI, M. Les altérations hydrothermales associées aux gisements d'uranium de Ty Gallen, Poulprio et Prat Mérien (Massif de Pontivy, Morbihan, France), unpublished thesis, Thèse 3e cycle INPL (1984) 113 pp.

(23) CATHELINEAU, M., Quartz leaching and hydrothermal alkali metasomatism in granites (submitted to Journal of Petrology) (1985)

(24) LEROY, J., CATHELINEAU, M., Les minéraux phylliteux dans les gisements hydrothermaux d'uranium, I: Cristallochimie des micas hérités et néoformês, Bull. Mineral. 105 (1982) 99-109.

(25) CATHELINEAU, M., Potassic alteration in french hydrothermal uranium deposits, Mineralium Deposita 18 (1983a) 89-97.

(26) TURPIN, L., Altêration hydrothermales et caractérisation isotopique (O-H-C) des minéraux et des fluides dans le massif uranifère de St. Sylvestre, Extension à d'autres gisements intragranitiques d'uranium français, Géol. Géochim. Uranium, Mêm. 6, Nancy (1984) 190 pp.

(27) RESPAUT, J.P., Géochronologie et géochimie isotopique U-Pb de la minéralisation uranifère de la mine des Pierres Plantées (Lozère) et de son encaissant: le massif granitique de la Margeride, unpublished thesis, U.S. T.L. Montpellier (1984) 122 pp.

(28) COGNE, J., La chaine hercynienne Ouest-Européenne correspond-elle à une orogène par collision?, in: Coll. Intern. CNRS n° 268 (1977) 113-121.

(29) AUTRAN, A., COGNE, J., La zone interne de l'orogenèse varisque dans l'ouest de la France et sa place dans le développement de la chaine hercynienne, in: Géologie de l'Europe, C6-4, 25th CGI, Paris (1980) 90-111.

(30) RENARD, J.P., Etude pétrographique et géochimique des granites du district uranifère de Vendée, Liaison entre l'évolution minéralogique et le comportement de l'uranium, Sci. de la Terre, Mem. Fr. 30 (1971) 214 pp.

(31) SONET, J., Contribution à l'étude géochronologique du massif de Mortagne (Vendée), C.R. Acad. Sci. Fr. 264 (1967) 225-298.

(32) PEUCAT, J.J., CHARLOT, R., MIFDAL, A., CHANTRAINE, J., AUTRAN, A., Définition géochronologique de la phase bretonne en Bretagne centrale par l'étude Rb-Sr des granites du domaine centre armoricain, Bull. BRGM I (1979) 349-356.

(33) GUINEBERTEAU, B., Le massif granitique de Mortagne sur Sèvre (Vendée), Structure, gravimétrie, mise en place, distribution de U/Th/K, unpublished thesis, Univ. Nantes (1984) 178 pp.

(34) MARCOUX, E., Le district de Pontivy, Sa place dans la métallogénie plombo-zincifère du Massif Armoricain (France), unpublished thesis, Univ. Clermont II (1980) 252 pp.

(35) MARCOUX, E., Le massif de Pontivy (Massif Armoricain, France), une association géographique de trois unités leucogranitiques, C.R. Acad. Sci. Fr. 294 (1982) 1095-1097.

(36) GERMAIN, C., KERVELLA, M., LE BAIL, F., Gisements et indices uranifères de la Bretagne, in: Les minerais uranifères français, III, P.U.F. Ed. Paris (1964) 209-275.

(37) GERSTNER, A., Le gisement de la Commanderie, in: Les gisements uranifères français, II. P.U.F. Ed. Paris (1962) 345-363.

(38) CATHELINEAU, M., Les mécanismes de type 'roll-front' dans les granites, un modèle de remobilisation dans les gisements hydrothermaux d'uranium, C.R. Acad. Sci. Fr. 294 II (1982a) 865-868.

(39) CUNEY, M., Geologic environment, mineralogy, and fluid inclusions of the Bois Noirs Limouzat uranium vein, Forez, France, Econ. Geol. 73 (1978) 1567-1610.

(40) TAYEB, G., Les gisements de l'Ecarpière et du Chardon, in: Les minerais uranifères français, II. P.U.F. Ed. (1962) 368-391.

(41) CATHELINEAU, M., Signification de la fluorine dans les gisements d'uranium de la chaine hercynienne, Bull. BRGM II 4 (1982b) 407-413.

(42) CATHELINEAU, M., LEROY, J., Reactions between uranium veins and their host rocks in Vendée and Limousin (France), Min. Mag. 44 (1981) 417-423.

(43) LASNIER, B., MARCHAND, J., Mise en évidence d'une bande métamorphique et d'une lame gabbroîque métamorphique au niveau de la mine du Chardon (CEA), Doc. inédit. Div. de Vendée (1969) 27 pp.

(44) DUMAS, J., LEBLANC, P., Etude pétrographique du Chardon, Rapport interne Cogema Vendée (1978) 30 pp.

(45) CATHELINEAU, M., Caractérisation minéralogique, géochimique, et structurale de l'encaissant granitique et métamorphique du Chardon (Cogema, Vendée) Bull. BRGM Fr. II 4 (1979) 291-300.

(46) RUHLMANN, F., GILLET, Y., LISSILOUR, J., Une occurrence uranifère à selenium et bismuth dans la ceinture métamorphique du leucogranite de Mortagne sur Sèvres (Vendée), Bull. Mineral. 103 (1980) 245-249.

(47) OUDDOU, D., Le massif de Guérande Le Croisic (Loire Atlantique), Caractérisations géochimiques et minéralogiques de l'évolution magmatique, Implications métallogéniques, unpublished thesis, INPL Nancy (1984) 306 pp.

(48) VALOIS, J.P., Les formations métamorphiques de Penaran (presqu'ile de Guérande, Loire Atlantique) et leur minéralisation uranifère, unpublished thesis, Univ. Nancy (1975) 136 pp.

(49) CATHELINEAU, M., Les minéraux phylliteux dans les gisements hydrothermaux d'uranium. I Distribution et évolution cristallochimique des illites interstratifiés, smectites et chlorites, Bull. Mineral. 103 (1983b) 553-569.

(50) GEFFROY, J., Les gites uranifères dans le Massif Central, in: Géologie, géomorphologie et structure profonde du Massif Central français, Symp. J. Jung (1971) 541-579.

(51) LEUTWEIN, F., Alter und paragenetische Stellung der Pechblende erzgebirgischer Lagerstätten, Geologie 6-8 (1957) 797-805.

(52) NAUMOV, G.B., On the transport of uranium in carbonate hydrothermal solutions, Geokhimiya n° 1 (1959) 6-19.

(53) SOKOLOVA, N.T., ACHEYEV, B.N., Causes of localization of uranium mineralization in contact metamorphism aureoles of granitoids, Géochem. Internat. 9 (1972) 1067-1077.

(54) RANCHIN, G., La géochimie de l'uranium et la différenciation granitique dans la province uranifère du Nord-Limousin, Sci. de la Terre, Mém. Fr. 19 (1971) 394 pp.

(55) FRIEDRICH, M., Le complexe granitique hyperalumineux de St. Sylvestre, Nord Ouest du Massif Central français, Géol. Géochim. Uranium, Mém. Nancy 5 (1984) 361 pp.

(56) CUNEY, M., FRIEDRICH, M., POTY, B., Pétrologie et géochimie des radioéléments dans les granites et dans les leucogranites en particulier, Conséquences génétiques et applications à la prospection, Documents du BRGM 79 (1984) 91-125.

(57) GEFFROY, J., SARCIA, J., Contribution à l'étude des pechblendes françaises, Sci. de la Terre 2 (1954) 1-157.

(58) GEFFROY, J., SARCIA, J., Les minerais noirs, in: Les minerais uranifères français, I. P.U.F. Ed., Paris (1960) 5-86.

(59) SARCIA, J., SARCIA, J.A., Les gites d'uranium du Nord Limousin, Sci. de la Terre, Mém. 4 (1956) 239-306.

(60) BARBIER, J., Zonalités géochimiques et métallogéniques dans le massif de St. Sylvestre (Limousin/France), Mineralium Deposita 5 (1970) 145-156.

(61) LEROY, J., Les épisyénites non minéralisées dans le massif de granite à deux micas de St. Sylvestre (Limousin, France), Equilibres entre minéraux et solutions, unpublished thesis, Univ. Nancy I (1971) 87 pp.

(62) POTY, B., LEROY, J., CUNEY, M., Les inclusions fluides dans les minerais des gisements d'uranium intragranitiques du Limousin et du Forez (Massif Central français), in: Formation of uranium ore deposits, Proc. IAEA, Symp. Athènes (1974) 569-582.

(63) LEROY, J., SONET, J., Contribution à l'étude géochronologique des filons de lamprophyres recoupant le granite à deux micas de St. Sylvestre (Limousin Massif Central français), C.R. Acad. Sci. Fr. 283 (1976) 1477-1480.

(64) MOREAU, M., L'uranium et les granitoïdes: essai d'interprétation, in: Geology, mining and extractive processing of uranium, Symp. I.M.M. London (1977) 83-102.

(65) CATHELINEAU, M., CUNEY, M., LEROY, J., LHOTE, F., NGUYEN TRUNG, C., PAGEL, M., POTY, B., Caractères minéralogiques des pechblendes de la province hercynienne d'Europe, Comparaison avec les oxydes d'uranium du Protérozoïque de différents gisements d'Amérique du Nord, d'Afrique et d'Australie, in: Vein-type and similar uranium deposits in rocks younger than Proterozoic, Proc. IAEA, Symp. Lisbonne 1979 (1982) 159-177.

(66) LEROY, J., POTY, B., Recherches préliminaires sur les fluides associés à la genèse des minéralisations en uranium du Limousin (France), Mineralium Deposita 4 (1969) 395-400.

(67) LA ROCHE, H., de, STUSSI, J.M., CHAURIS, L., Les granites à deux micas hercyniens français, essais de cartographie et de correlations géochimiques appuyés sur une banque de données, implications pétrologiques et métallogéniques, Sci. de la Terre, Fr. XXIV (1980) 5-121.

(68) LESPINASSE, M., PECHER, A., Déformation ductile et rupturelle au voisinage de la faille de la Marche: données sur les orientiations de raccourcissement tardi hercyniennes dans le Nord-Ouest du Massif Central français, C.R. Acad. Sci. Fr. 298 (1984) 17-20.

(69) LESPINASSE, M., PECHER, A., Microfissuration and regional stress field: a study of the preferred orientation of fluid inclusion planes in a granite from the Massif Central, France, (submitted to Journal of Structural Geology (1985)).

(70) PECHER, A., LESPINASSE, M., LEROY, J., Relation between fluid inclusion trails and regional stress field: a tool for fluid chronology, Example of an intragranitic uranium ore deposit, north-west French Massif Central, Lithos (1985) (in press).

(71) STUSSI, J.M., Caractères et zonalités pétrographiques majeurs dans la zone nord orientale leucogranitique du Plateau de Millevaches (Massif Central français), Sci. de la Terre 2 (1977) 103-128.

(72) MONIER, G., Pétrologie des granitoides de Sud Millevaches (MCF), minéralogie, géochimie, géochronologie, unpublished thesis, Clermont Ferrand II (1980) 288 pp.

(73) KURTBAS, K., Les granites de la Montagne Bourbonnaise (Massif Central, France), Leur évolution pétrographique et géochimique, unpublished thesis, Univ. Nancy I (1972) 233 pp.

(74) VIALETTE, Y., Age des granites du Massif Central, Soc. Géol. France Bull. 15 (1973) 260-270.

(75) PAGEL, M., LETERRIER, J., The subalkaline potassic magmatism of the Ballons massif (southern Vosges, France), Shoshonitic affinity, Lithos 13 (1980) 1-10 pp.

(76) LE, V.T., Gêochimie de l'uranium et du thorium dans les granitoîdes et formations associées de la Montagne Bourbonnaise (Massif Central français), unpublished thesis, INPL, Nancy (1975) 372 pp.

(77) PAGEL, M., Facteurs de distribution et de concentration de l'uranium et du thorium dans quelques granites de la chaine hercynienne d'Europe, unpublished thesis, INPL (1981) 566 pp.

(78) FRIEDRICH, M., CUNEY, M., Cristallisation de l'uraninite et polygenisme dans le complexe granitique de St. Jouvent, Brame, St. Sylvestre (Limousin), C.R. Acad. Sci. Fr. 296 (1983) 1249-1252.

(79) PAGEL, M., Successions paragênétiques et teneurs en uranium des minêraux accessoires dans les roches granitiques, guides pour la recherche des granites favorables à la présence de gisements d'uranium, in: Uranium Exploration Methods, Proc. NEA/IAEA Symp. Paris (1982) 445-456.

(80) POUGHON, A., MOREAU, M., Les gisements à parsonsite de Lachaux, Nancy Sci. de la Terre 3 (1955) 1-2, 190-235.

(81) CARIOU, P., Les gites et indices uranifêres des régions médiane et sud du Massif Central francais in: Les minerais uranifêres français, III. P.U.F. Ed., Paris (1964) 1-156.

(82) STUSSI, J.M., Les leucogranites du Massif de la Margeride, Caractêres pétrochimiques, Rapport sur l'action concertêe CRPG-CFMU (1978) 50 pp.

(83) COUTURIE, J.P., Etude pêtrographique, gêochimique et structurale du massif granitique de la Margeride, Ann. Sci. Univ. Clermont-Ferrand 62, 29 (1977) 320 pp.

(84) BONHOMME, M.G., Age triasique et jurassique des argiles associées aux minêralisations filoniennes et des phénomênes diagênêtiques tardifs en Europe de l'ouest, Contexte géodynamique et implications gênêtiques, C.R. Acad. Sci. Fr. 294 (1982) 521-524.

(85) BAUBRON, J.C., DEFAUT, B., DEMANGE, J., MAURY, R.C., Une coulée sous-marine d'âge jurassique moyen dans les Causses: le basalte alcalin des Vignes (M. C.F.), C.R. Acad. Sci. Fr. 287 (1978) 225-227.

(86) LANCELOT, J.R., de, SAINT ANDRE, B., LA BOISSE, H., Systêmatique U-Pb et évolution du gisement d'uranium de Lodêve (France), Mineralium Deposita 19 (1984) 44-53.

(87) LINDGREN, W., Mineral deposits, McGraw Hill Book C. Ed. New York, 4th ed. (1983) 930 pp.

(88) SCHNEIDERHÖHN, H., Erzlagerstätten, Gustav Fischer Verlag Stuttgart, 3rd ed. (1955) 375 pp.

(89) GEFFROY, J., SARCIA, J., La notion de 'gite êpithermal uranifêre' et les problêmes qu'elle pose, Soc. gêol. France Bull. 6 (1958) 173-190.

(90) ROUBAULT, M., COPPENS, R., Sur les relations entre certains gites filoniens d'uranium et la présence d'inclusions radioactives dans les roches encaissantes, C.R. Acad. Sci. Fr. 240 (1955) 214-216.

(91) ROUBAULT, M., COPPENS, R., Observation de déplacements de l'uranium dans les roches cristallines, relations possibles de ce phênomêne avec la genêse de certains gisements, Proc. Int. Conf. Peaceful Uses Atom. Energ. Genêve (1958) 335-337.

(92) BIGOTTE, G., Cycle de l'uranium, International Geological Congress, XXII Session, New Delhi, India, Part V, Genetic problems of ores (1964) 351-358.

(93) MOREAU, M., POUGHON, A., PUYBARAUD, Y., SANSELME, H., L'uranium et les granites, Chronique des Mines et de la Recherche minière 350 (1966) 47-50.

(94) MATOS DIAS, J.J., SOARES de ANDRADE, A.A., Uranium deposits in Portugal, Uranium Exploration Geology, Proc. IAEA Vienna (1970) 129-142.

(95) LANGFORD, F.F., A supergene origin for vein-type uranium ores in the light of Western Australian calcrete-carnotite deposits, Econ. Geol. 69 (1974) 516-526.

(96) LANGFORD, F.F., Superficial origin of North American pitchblende and related uranium deposits, American Association of Petroleum Geol. Bull. 61 (1977) 28-42.

(97) KNIPPING, H.D., The concepts of supergene versus hypogene emplacement of uranium at Rabbit Lake, Saskatchewan, Canada, in: Formation of uranium ore deposits, Symp. Athens, Proc. IAEA (1974) 569-582.

(98) BARBIER, J., Continental weathering as a possible origin of vein-type uranium deposits, Mineralium Deposita 9 (1974) 271-288.

(99) MAGNE, R., BERTHELIN, J.R., DOMMERGUES, Y., Solubilisation et insolubilisation de l'uranium des granites par des bactéries hétérotrophes, in: Formation of uranium ore deposits, Symp. Athens, Proc. IAEA (1974) 86-88.

(100) CUNEY, M., Le gisement uranifère des Bois Noirs - Limouzat (Forez, France), Relations entre minéraux et fluides associés, unpublished thesis, Univ. Nancy I (1974) 174 pp.

(101) BARBIER, J., CARRAT, H.G., RANCHIN, G., Présence d'uraninite en tant que minéral accessoire usuel dans les granites à deux micas uranifères du Limousin et de la Vendée, C.R. Acad. Sci. Fr. 264 (1967) 2436-2439.

(102) BARBIER, J., RANCHIN, G., Zonalité pétrographique et géochimique dans le massif granitique de St. Sylvestre, in: Géologie de l'uranium dans le massif granitique de St. Sylvestre (Limousin/Massif Central français), Rapport CEA R 3684 (1969) 57-113.

(103) CUNEY, M., LEROY, J., PAGEL, M., Comportement de l'uranium et du thorium dans les granites uranifères français, Sci. de la Terre, Série 'Informatique Géologique', Nancy 13 (1979) 55-63.

(104) BALL, T.K., BASHAM, I.R., Radioactive accessory minerals in granites from Southwest England, Proceedings of the USSHER Soc. 44, 3 (1979) 437-448.

(105) CUNEY, M., FRIEDRICH, M., DRIN, N., Traitement par l'analyse statistique de données multivariables sur le complexe de Brame, St. Sylvestre, St. Goussaud (Limousin, France), Différenciation magmatique et polygénisme, Sci. de la Terre, 'Informatique Géologique', Nancy (1985) (in press)

(106) MOLLIER, B., BOUCHEZ, J.L., Structuration magmatique du complexe granitique de Brame, St. Sylvestre, St. Goussaud (Limousin, Massif Central français), C.R. Acad. Sci. Fr. 294 (1982) 1329-1334.

(107) MOLLIER, B., Le granite de Brame, St. Sylvestre, St. Goussaud, Ses structures magmatiques, Une étude de la distribution de l'uranium à l'échelle du grain, Géol. Géochim. Uranium, Mém. Nancy 7 (1984) 148 pp.

(108) BAUBRON, J.C., JEBRAK, M., JOANNES, C., LHEGU, J., TOURAY, J.C., ZISERMAN, A., Nouvelles datations K/Ar sur des filons à quartz et fluorine du Massif Central français, C.R. Acad. Sci. Fr. II 290 (1980) 951-953.

(109) BONHOMME, M.G., BUHMANN, D., BESNUS, Y., Reliability of K/Ar dating of clays and silicifications associated with vein mineralizations in Western Europe, Geol. Rdsch. 72 (1983) 105-117.

(110) JOSEPH, D., LHEGU, J., TOURAY, J.C., Un témoin d'une activité géothermique au Lias dans le Morvan: le filon 'René bis' (La Petite Verrière) Saône et Loire, Bull. BRGM Fr. II 5 (1973) 398-401.

(111) GEORGE, E., Les minéralisations uranifères jurassiques liées spatialement à une discordance hercynienne, Pétrographie, minéralogie et géochimie des gisements du Rouergue (Aveyron, France), Géol. Géochim. Uranium, Mém. Nancy 9 (1984) 221 pp.

(112) MATTE, P., Raccord des segments iberiques d'Europe sud-occidentale, Franz Kossmat Symposium, Nova Acta Leopoldina 224 (1974) 239-262.

THE URANIUM DEPOSIT 'KRUNKELBACH' IN THE SOUTHERN BLACK FOREST, FEDERAL REPUBLIC OF GERMANY

H.W. Bültemann, W.D. Bültemann
Gewerkschaft Brunhilde
Uetze
Federal Republic of Germany

Abstract

THE URANIUM DEPOSIT 'KRUNKELBACH' IN THE SOUTHERN BLACK FOREST, FEDERAL REPUBLIC OF GERMANY

The hydrothermal uranium deposit of the Krunkelbach valley close to the village of Menzenschwand lies in the southern Black Forest of the Federal Republic of Germany. It is still being explored from surface and underground. The deposit is in the contact zone between the Variscan Bärhalde granite - a typical two-mica granite - and the gneiss massif of the Feldberg. The ore veins strike E and NW. The mineralization was localized by a well developed NNW striking fault zone. The main uranium mineral is pitchblende of different generations. A great number of secondary uranium minerals have been recognized. Gangue material consists of various generations of carnelian or jasper, barite and fluorite.

1. REGIONAL GEOLOGICAL SETTING

The Black Forest province of Baden-Württemberg State comprises the eastern half of a broad Mesozoic-Tertiary north-plunging uplift divided from its western counterpart, the French Vogeses, by the Rhine graben. The northern Black Forest province is capped by the undeformed Triassic Buntsandstein which dips gently northeastward. The southern Black Forest exposes a crystalline basement which is a westward extension of the Moldanubian zone of Bohemia, deformed and metamorphosed during the Hercynian orogeny. Rocks range from Precambrian gneisses and gneiss-anatectites, through metamorphosed Upper Devonian and carboniferous sediments to Late Variscan granites and porphyries (Fig. 1, 2).

2. HISTORY AND DEVELOPMENT

Uranium was discovered in the Krunkelbach valley about 2 km NW of Menzenschwand village in the southern Black Forest in 1957. Two students of the University of Freiburg found glacial boulders containing uranium mica and uranopilite in a matrix of quartz-hematite vein material (Metz and Rein (1), Rein (2), Kirchheimer (3)). Gewerkschaft Brunhilde undertook exploration in 1960 which resulted in the discovery of the uranium ore deposit in the western part of the valley in 1962 (Kirchheimer (3), Schauer (4), Bültemann, H.W. (5), (6), (7), (8), Bültemann, W.D. (9), (10)). Systematic physical exploration was begun in 1963 and is continuing. For environmental protection this exploration is conducted underground. The prospect was opened by an adit to a blind shaft from which drifts and crosscuts at several levels were driven. The shaft presently is 249 m deep and excavation is continuing to identify the limits of the ore.

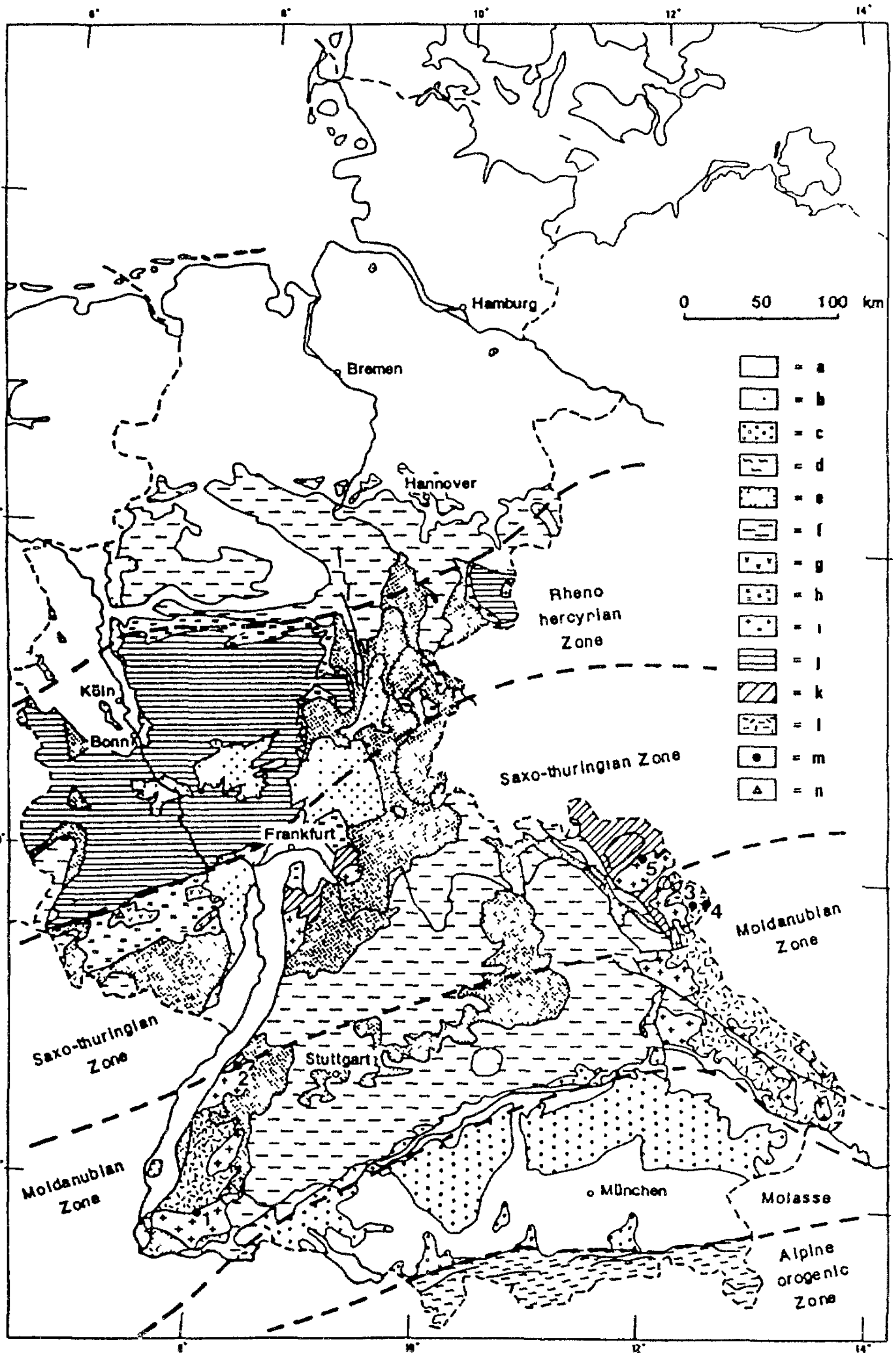

FIG. 1. Uranium occurrences of the Federal Republic of Germany. I. Geology: a) Quaternary, b) Tertiary, c) Alpine molasse (Tertiary), d) Alpine orogenic zone (Mesozoic), e) Mesozoic sandstones, f) Mesozoic, g) Permian volcanics (rhyolite), h) Permo-Carboniferous, i) Variscan granites, j) Rheno-Hercynian zone (Palaeozoic), k) Saxo-Thuringian zone (metamorphic), l) Moldanubian zone (metamorphic), m) uranium occurrences with more than 500 t U-content, n) operating uranium mill. II. Uranium occurrences: 1. Krunkelbach mine, Menzenschwand (Baden-Wurttemberg), 2. Mullenbach mine, Baden-Baden (Baden-Wurttemberg), 3. Höhenstein mine, Mähring-Poppenreuth (Bavaria), 4. Waldel mine, Mähring (Bavaria), 5. Christa mine, Groß-schloppen (Bavaria).

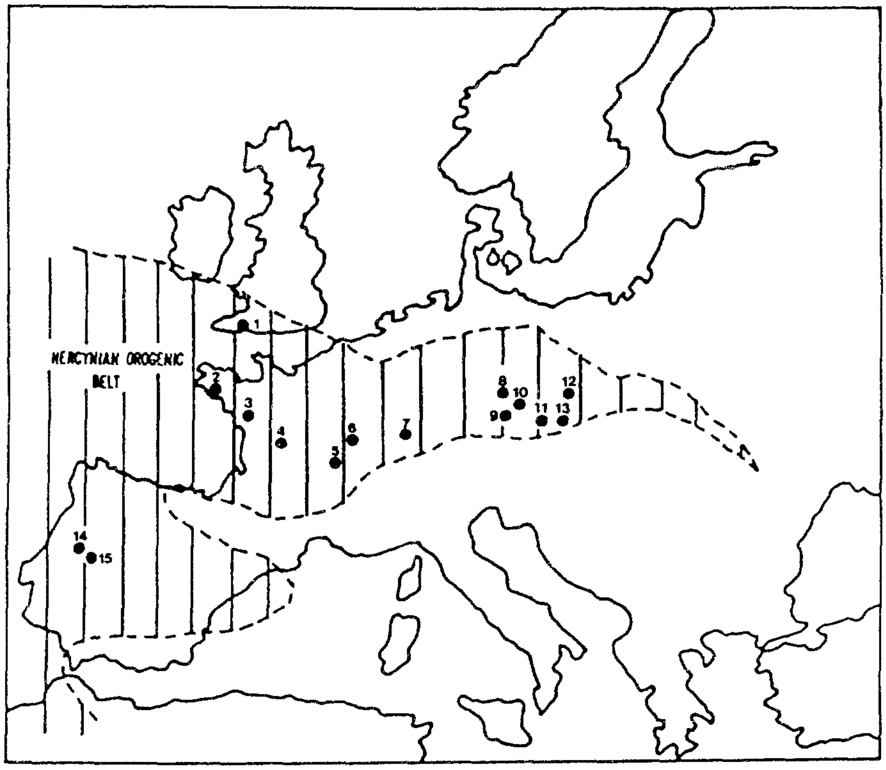

FIG. 2. Hercynian orogenic belt and location of hydrothermal uranium districts in Europe. 1. Cornwall, 2. Bretagne (Kersegalec, Quistiave), 3. Vendée (Commanderie, Le Chardon, La Chapelle Largeau), 4. Limousin (La Crouzille, Margnac, Fanay, Le Brugeaud), 5. Forez (Les Bois Noirs), 6. Morvan (La Faye, Les Brosses), 7. Black Forest (Menzenschwand), 8. Thuringia (Ronneburg), 9. NE Bavaria (Mähring, Poppenreuth, Großschloppen) and W Bohemia (Dylen, Zadni Chodov, Vitkov II), 10. Saxony (Schneeberg, Aue, Johanngeorgenstadt), 11. Central Bohemian Massif (Příbram), 12. Silesia (Schmiedeberg), 13. Labe Lineament region (Rozna, Olsi), 14. Guarda Viseu region (Urgeiriça, Nisa), 15. Salamanca (Ciudad Rodrigo).

A reserve of 1,000 t U_3O_8 in ore averaging 0.7 % U_3O_8 has been proven. For the time being the provincial government of Baden-Württemberg has withheld permission to mine the deposit.

The Krunkelbach uranium deposit is within a Late Hercynian granitic complex which intruded Precambrian gneiss of the Feldberg and Upper Devonian sediments (Fig. 3).

The granitic complex of the southern Black Forest includes the St.Blasien granite, Schluchsee granite, Ursee granite and Bärhalde-Hochfirst-Eisenbach granite. These range in composition from early leucocratic phases, through granodiorite to late acidic deuteric granites. The complex is cut by numerous dikes of granite and quartz porphyry, representing late derivatives of granitization (Fig. 3, 4).

The deposit is in the contact zone between the Bärhalde granite body and enclosing gneisses and anatectites of the Feldberg massif (Fig. 3, 4). The Bärhalde granite, with its eastern companion near Neustadt-Hochfirst-Eisenbach represents the youngest generation of granite in the southern Black Forest. It is a typical deuteric, two-mica granite (Emmermann (11), Barthel and Mehnert (12)).

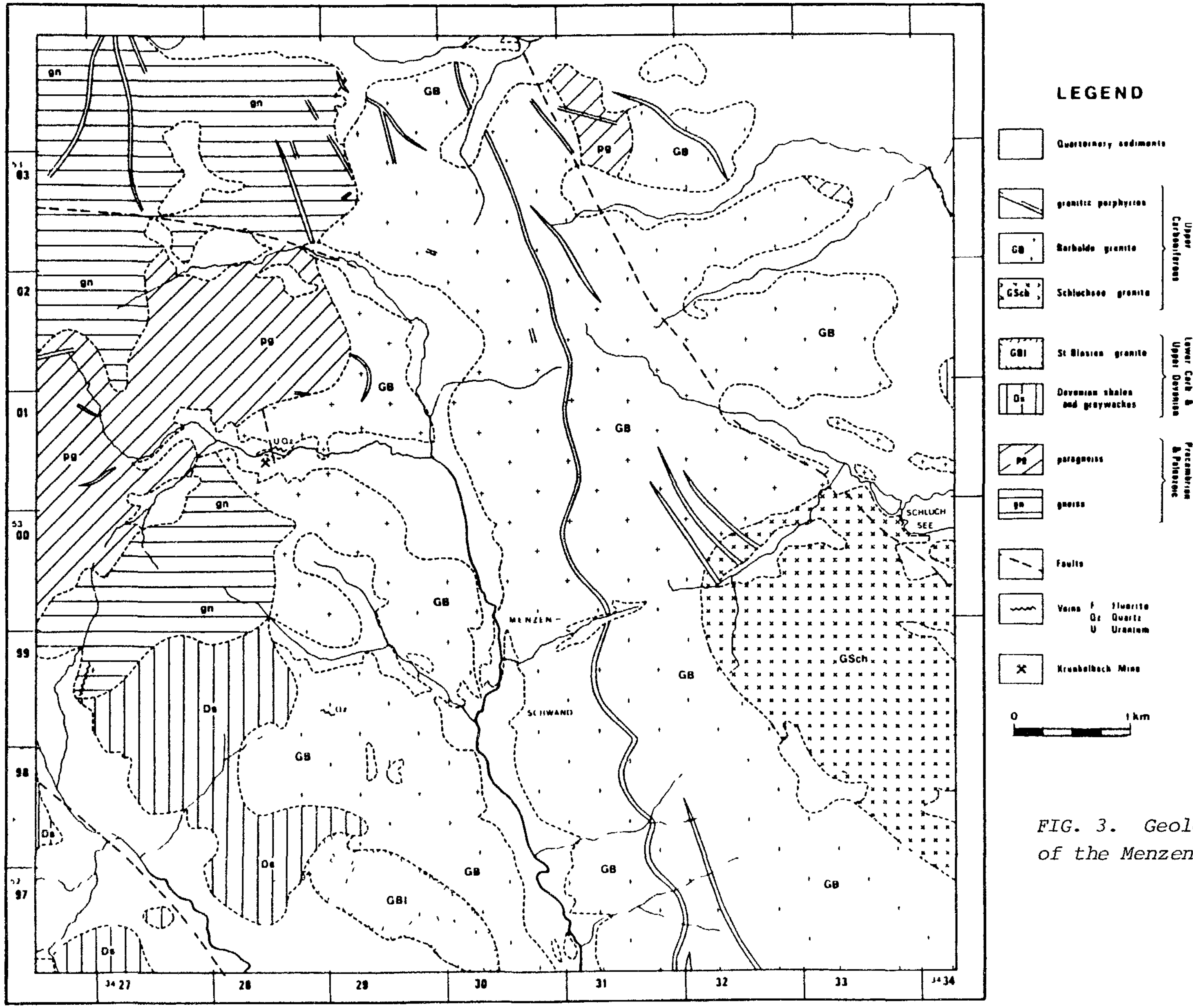

FIG. 3. Geology of the Menzenschwand area

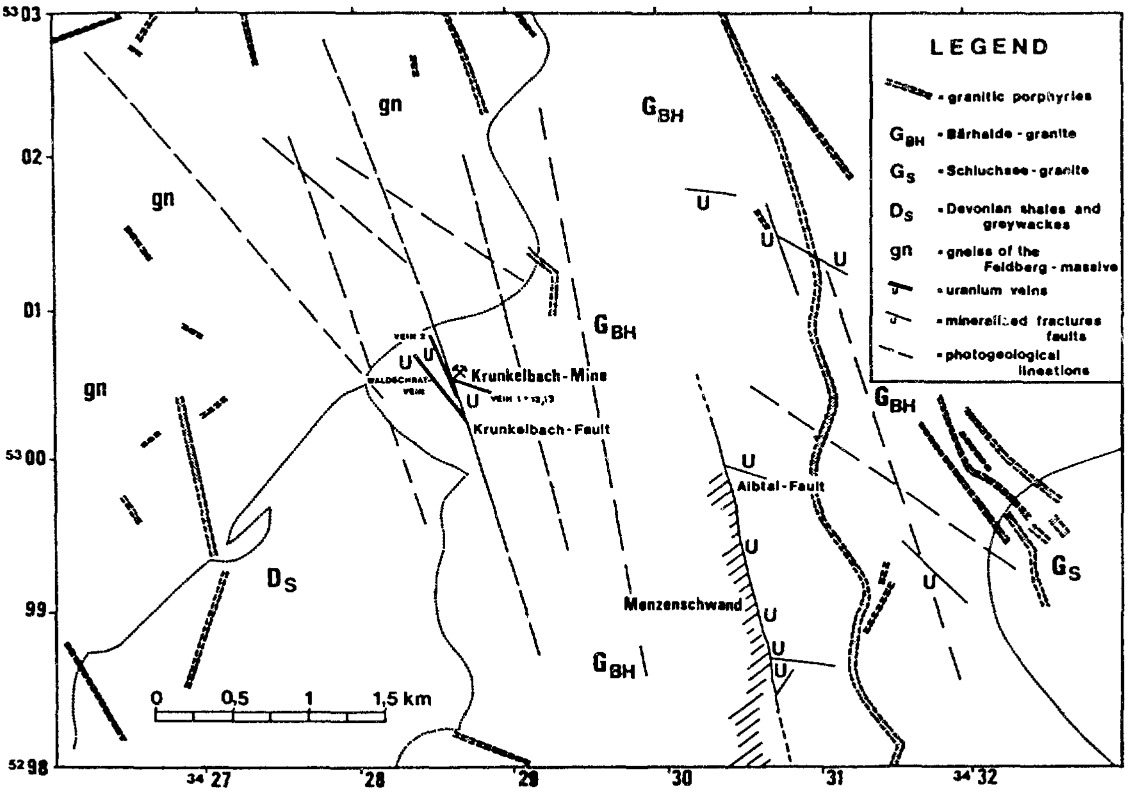

FIG. 4. Structural map of the Krunkelbach deposit and its surroundings including results of aerial photo interpretation and geology.

3. BÄRHALDE GRANITE COMPLEX

The Bärhalde granite crops out in a band 2 - 6 km wide, extending from near the town of St. Blasien, northwestward to the Feldberg massif, comprising an area of about 45 km² cutting the Badenweiler-Lenzkirch zone. Between the gneisses and anatectites of the Feldberg massif is a narrow zone of 'Randgranite' (Metz and Rein (1)) which Altherr (13) designated an 'anatectic complec' border zone between the Feldberg massif and the southern Black Forest matrix gneiss. However, many outcrops of 'Randgranite' exhibit anatectic features with frequent feldspar metablastesis.

In the west and southwest the Bärhalde granite is in direct contact with the Lower Carboniferous St. Blasien granite. In the south it is bound by the slightly older Schluchsee granite which has a 'whole-rock' age of 315 $\pm$ 10 Ma (Emmermann (11), Wendt et al. (14), Wendt (15)), and a mineral age of 325 $\pm$ 3 Ma (Wendt et al. (16)). Age relations between Bärhalde and Schluchsee granites have not been resolved. K/Ar ages of 332 $\pm$ 2 Ma and Rb/Sr ages of 333 $\pm$ 3 Ma were obtained for both granites (Wendt et al. (16)). The latter age is believed more probable. However, field relations suggest that the Bärhalde granite is younger. On the strength of these observations an age of 320 - 325 Ma is assumed here for the Bärhalde granite, which agrees fairly well with the whole-rock age of 307 $\pm$ 4 Ma obtained by Wendt et al. (14), Wendt et al. (16) and Guba (17).

In the southwest the Bärhalde granite intruded Upper Devonian schists and greywackes of the Spießhorn complex. Both, the Bärhalde and Schluchsee granites, are cut by dikes of Permian (?) quartz porphyry. Mapping by Wimmenauer and Schreiner (18) and Bültemann (9) disclosed a great number of these dikes ranging to several tens of metres thick, rather than a porphyry massif as portrayed by Metz

TABLE I. MINERAL COMPOSITION OF THE BÄRHALDE GRANITE (IN VOL%) (AFTER EMMERMANN (11)).

	$\bar{x}$ (55)	VARIATION
PLAGIOCLASE	25.3	17.4 - 29.2
QUARTZ	34.2	28.1 - 45.5
POTASSIUM-FELDSPAR	33.5	24.5 - 38.2
BIOTITE	2.2	1.5 - 7.0
'PALE' MICA	4.8	1.1 - 6.2
AN - CONTENT	3 - 5	0 - 15

TABLE II. CHEMICAL COMPOSITION OF THE BÄRHALDE AND HOCHFIRST-EISENBACH GRANITE (IN WT%, * IN PPM) (AFTER EMMERMANN (11)).

	BÄRHALDE GRANITE		GRANITE OF HOCHFIRST-EISENBACH		URSEE-GRANITE	
	$\bar{x}$ (11)	VARIATION	$\bar{x}$ (6)	VARIATION	$\bar{x}$ (4)	VARIATION
SiO_2	75.45	74.82 - 75.68	75.11	74.72 - 75.32	74.82	74.56 - 75.65
TiO_2	0.07	0.03 - 0.15	0.06	0.04 - 0.07	0.05	0.03 - 0.06
Al_2O_3	13.55	13.26 - 13.78	13.65	13.45 - 13.88	13.84	13.66 - 13.95
Fe_2O_3	1.21	1.02 - 1.35	1.31	1.07 - 1.43	1.35	1.22 - 1.45
MgO	0.17	0.12 - 0.28	0.20	0.15 - 0.23	0.20	0.10 - 0.24
CaO	0.31	0.17 - 0.48	0.36	0.28 - 0.43	0.37	0.32 - 0.40
Na_2O	3.32	3.11 - 3.41	3.17	2.98 - 3.26	2.94	2.69 - 3.15
K_2O	5.01	4.68 - 5.65	5.00	4.72 - 5.34	4.98	4.82 - 5.09
P_2O_5	0.19	0.12 - 0.28	0.26	0.21 - 0.31	0.32	0.29 - 0.34
Zr *	56	30 - 115	50	22 - 81	38	29 - 44
Ba *	293	92 - 853	190	77 - 761	135	90 - 170
Sr *	15	1 - 40	30	8 - 53	28	22 - 34
Rb *	477	330 - 620	559	416 - 674	531	458 - 596

TABLE III. AVERAGE MINERAL COMPOSITION OF THE THREE GRANITES OF THE AREA (IN VOL%) (AFTER EMMERMANN (11)).

	BÄRHALDE GRANITE	SCHLUCHSEE GRANITE	GRANITE OF ST. BLASIEN
PLAGIOCLASE	25.3	26.0	38.1
QUARTZ	34.2	31.6	24.9
POTASSIUM-FELDSPAR	33.5	35.5	24.5
BIOTITE	2.2	6.4	12.5
MUSCOVITE	4.8	0.4	-
AN-CONTENT	3 - 5	15	35
NORM. AB/AN	54.6	6.3	3.5

TABLE IV. AVERAGE MINERAL COMPOSITION OF THE THREE GRANITES OF THE AREA (IN WT%, * IN PPM) (AFTER EMMERMANN (11)).

	BÄRHALDE GRANITE	SCHLUCHSEE GRANITE	GRANITE OF ST. BLASIEN
SiO_2	75.45	71.30	67.45
TiO_2	0.07	0.23	0.55
Al_2O_3	13.55	14.25	15.74
Fe_2O_3	1.21	2.58	3.23
MgO	0.17	0.72	1.43
CaO	0.31	1.05	2 03
Na_2O_3	3.32	3.28	3.42
K_2O	5.01	5.32	4.38
P_2O_5	0.19	0.12	0.25
Zr *	56	167	210
Ba *	293	1079	1180
Sr *	15	85	342
Rb *	477	289	222

and Rein (1) on their geologic-petrologic map of the Schluchsee area, and rather than an eastern phase of the Bärhalde granite as interpreted by Emmermann (11).

The mineralogy of Bärhalde granite samples is shown in Table I. The chemical composition of samples of Bärhalde and Hochfirst-Eisenbach granite are presented in Table II. Tables III and IV compare the average mineral and chemical compositions of the Bärhalde, Schluchsee and St. Blasien granites. The data show significant differences in distribution of major and trace elements. Quartz (silica) increases from the oldest to the youngest granite. The decrease in biotite corresponds with decreases in Ti, Fe, and Mg concentration. The Bärhalde granite is a typical Late Variscan two-mica granite, similar to almost all granites of this age and composition in western Europe. Such granites are well-known for their uranium content and potential. They commonly host uranium deposits.

4. STRUCTURES AND ORE CONTROL

The Krunkelbach area is influenced by three structural trends. The most significant is expressed by the Krunkelbach fault which strikes NNW (155° - 165° azimuth) and dips steeply ENE to vertical. The fault can be traced at least 2.5 km to the NNW as confirmed by underground drifts. Its probable continuation to the SSE is obscured on the surface by valley glacial till. The fault is deep and well developed; it controlled the growth of the orebody (Fig. 5). It was reactivated several times, the last affiliated with the Tertiary formation of the Rheintal graben. Resultant movement was left-lateral with a reverse component. Exact displacement is unknown but the vertical component is estimated as 100 m minimum.

Tertiary formation of the Rheintal graben created numerous similar faults parallel to the graben extending to the Swabian Alb on the east. Intersection of these faults with east trending structures localized the basalts of the Swabian Alb. Two such east trending faults localized uranium mineralization where they intersected the Krunkelbach fault. These are Vein No. 1 and Vein No. 12 (Fig. 4).

4.1. Veins No. 1 and No. 12

Vein No. 1 is the oldest structure cutting the Krunkelbach fault. It strikes 98° - 116° in azimuth. Vein No. 12 strikes 102° - 125° azimuth. Both veins dip steeply NE, but locally overturn to the SW. They are well developed only on the

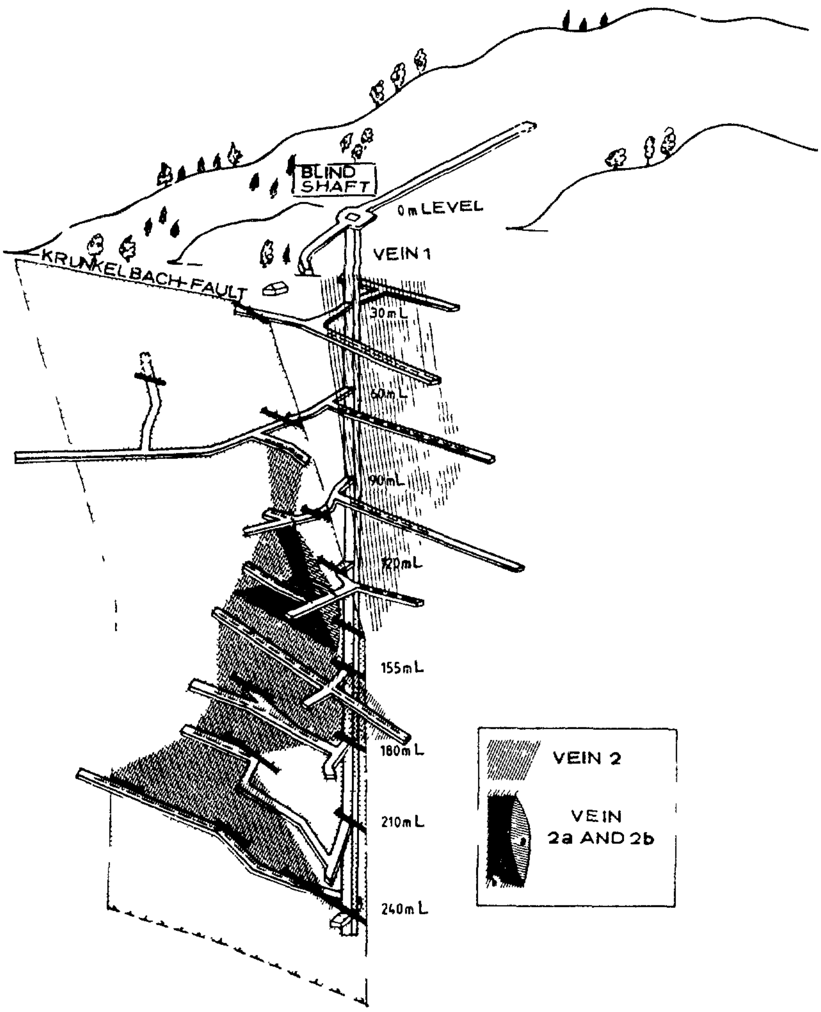

FIG. 5. Krunkelbach mine, Menzenschwand, Black Forest: generalized cross-section of vein and fault system.

east side of the Krunkelbach fault and appear to be cut by the Krunkelbach fault, but offset continuations have not been found. Structural details have suggested offsets exceeding 200 m, but recent investigations suggest displacement of only a few tens of metres.

In both veins, mineralization decreased eastward and died out in depth towards the steeply dipping Krunkelbach fault. Wedging results from slight curvatures in the strike of both veins towards the south and in their dip towards the SW. Wedging of Vein No. 1 just below the 120 m level coincides with steepening of the Krunkelbach fault which becomes vertical between 135 and 242 m. The close relation between the fault and the mineralized veins is proven by the fact that mineralization begins within 10 m E of the fault and decreases eastward away from the fault in both veins. The Krunkelbach fault on this basis is believed to have been the access channel used by uraniferous hydrothermal fluids. Geologic surface mapping and aerial photo interpretation reveal the existence of additional structures east of and parallel to the Krunkelbach fault. Conceivably Veins No. 1 and No. 12 also could be mineralized where they approach these other structures. The Albtal fault in Menzenschwand valley was mapped by Bültemann (9) (Fig. 4) for 2 km of strike length parallel to the Krunkelbach fault. It is anomalously uraniferous at several localities along its outcop, similar to the outcrop of the Krunkelbach fault.

4.2. Vein No. 13

This vein, also known on the east side of the Krunkelbach fault, is exposed on the adit and 30 m levels. It strikes 108° - 125° in azimuth and varies from NE to SW in steep dip. Increases in vein width and uranium content accompany rolls to a SW dip indicating the NE side sank in reference to the SW side. The behaviour of the vein in depth remains unknown.

4.3. Vein system 2 and breccia zone

Vein 2, on the down-thrown western side of the Krunkelbach fault, has an associated breccia zone and is economically significant. The vein and zone have been traced from the surface to the 240 m level (Fig. 4, 5). Near the fault, the vein strikes NNW at 155° - 165° azimuth, parallel to the fault, but with decreasing uranium content.

The breccia zone associated with Vein 2 illustrates selectively stronger shattering and textural deformation of granite on the western side of the Krunkelbach fault. Openings were cemented by younger quartz and chért containing sulfides and hematite, often specularite. The breccia zone usually contains more uranium. Within the breccia zone, Vein 2 exhibits well defined vein structure with a consistent strike and steep ENE dip, implying the vein is later than the breccia. The vein varies from 0.2 to 6 m wide, maximum width coincides with highest uranium grade. The vein and breccia zone apparently were strongly influenced by the Krunkelbach fault even though they were mineralized with uranium only away from the fault. In contrast to veins No. 1 and No. 12 which are well mineralized from the surface downward, Vein 2 and the breccia contain uranium only below the 30 m level. Intensive exploration failed to find ore above. Below the 90 m level, two high grade ore shoots have been identified in Vein 2, separated by low grade intervals. The shoots pitch 50° - 84° NNW where the vein dips ENE. They have horizontal lengths of 20 - 30 m and vertical heights of about 60 m. Vein thickness in the shoots averages about 2.5 m. The sterile interveining portions of the vein exhibit similar horizontal dimensions. Evidence suggests continuation of the series of ore shoots to the NNW, the horizontal distance between shoots increasing as the angle between the fault and vein widens. The dying of each ore shoot seems to be accompanied by the growth of a new shoot farther to the NNW.

The Krunkelbach fault is believed to have exerted significant influence on the mineralization of Vein 2 by reopening parts of the earlier vein to provide new paths for mineralizing fluids. Paragenesis suggests that Vein 2 belongs to the system containing Veins No. 1 and No. 12 east of the fault. If this is true, rotation of the block west of the fault is required, but this has not been demonstrated.

4.4. Waldschrat vein

The Waldschrat is another uraniferous vein in the western block. It has been investigated from the surface to 210 m depth. Drilling on the 210 m level indicated the Waldschrat to be roughly parallel to Vein 2 in strike (135° - 150°) and dip. The vein also has an associated breccia zone. At the surface the Waldschrat appears as a quartz-barite-fluorite vein with weakly anomalous radioactivity. Uranium content increases with depth. Grade also improved considerably along strike on the 60 m level as the vein was followed for 125 m. Horizontal core drilling from the 155 m level also demonstrated higher uranium grade. Additional horizontal drilling from the 210 m level is in progress.

TABLE V. PARAGENESIS OF THE KRUNKELBACH MINE (AFTER BÜLTEMANN (8)).

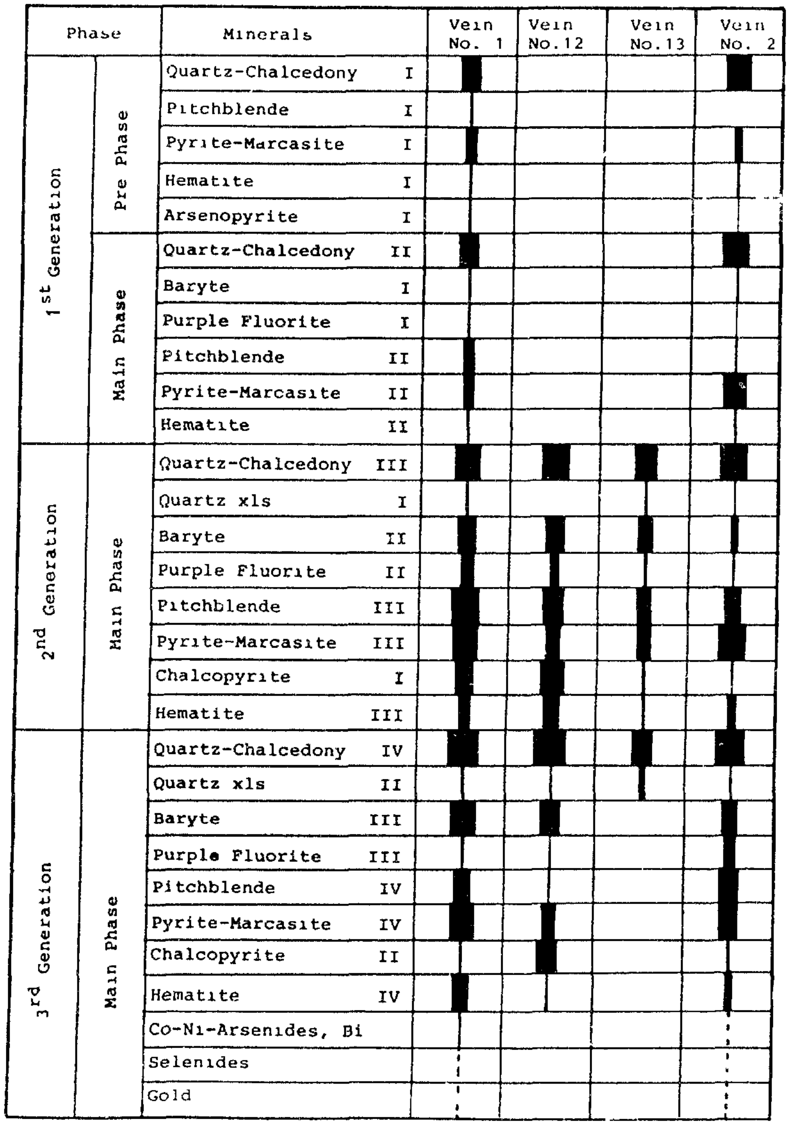

4.5. General vein characteristics

The widths of all veins encountered range from a few cm to 6 m. Grade ranges to a maximum of 8 % U_3O_8. The principal ore mineral is pitchblende; idiomorphic crystals of uraninite are rare. Sooty pitchblende and sometimes well crystallized coffinite are common.

5. MINERALOGY

5.1. Veins No. 1 and No. 12

Both these veins follow old faults which strike generally E. The veins are strongly brecciated locally but otherwise are undeformed. Uranium mineralization products are mostly colloidal pitchblende with its secondary oxidation products.

Coffinite, rarely crystalline, occurs with hematite and abundant pyrite, marcasite and chalcopyrite. Vein No. 12 is richer in sulfides and copper than Vein No. 1. Individual crystals or clusters of arsenopyrite occur in small amounts throughout the deposit. Rarely gold and late selenides (umangite, klockmannite, and clausthalite) are found. Typical minerals of the Bi-Co-Ni association (safflorite, nickelin, löllingite and bismuth) occur sporadically and represent a late stage of mineralization. Gangue consists of quartz (partly smoky), chert (chalcedony), barite, purple fluorite, and carbonates (calcite, dolomite and ankerite). Carbonates usually fill vugs or coat quartz and also are late and rare.

That Vein No. 12 is richer in copper seems unusual because both veins are otherwise similar and close together. One possible explanation is that the Cu-rich solutions were introduced later than uraniferous solutions, when Vein No. 1 already had been selectively largely sealed by earlier mineralization products (Table V).

5.2. Vein No. 13

The mineral assemblage of this vein is very similar to that of Veins No. 1 and No. 12. However, as this vein is far more brecciated, uranium is more irregularly distributed. The uranium content is too low to be economic (Table V). It occurs mainly in lenses or relicts of pitchblende and coffinite with sulfides and barite. The relative age of this vein has not been recognized, but it may be considerably younger than Veins No. 1 and No. 12.

5.3. Waldschrat vein

This vein strikes NW and also is strongly brecciated. Its uranium thus exhibits lenticular distribution similar to Vein No. 13. Grade improves down dip, however. The main uranium minerals are pitchblende, minor uraninite, and coffinite. Chalcopyrite, hematite and minor arsenopyrite are associated in a gangue similar to that of other veins.

5.4. Vein No. 2

This vein is most typical of the brecciated veins. Most likely an existing pyrite-chalcopyrite-quartz-chert-carnelian vein was refractured leaving angular and partially rounded relicts cemented by late quartz-chert-barite-fluorite. Early pyrite fragments are coated with late sooty pitchblende.

Following refracturing, kidney-shaped masses of coarse-grained pitchblende accompanied by pyrite, marcasite, chalcopyrite, minor and arsenopyrite (always euhedral), and trace copper selenide were precipitated in several phases. The pitchblende commonly fills open spaces between large barite crystals which were intensely coloured by radiation damage and finely disseminated hematite. Pitchblende commonly replaces early pyrite, chalcopyrite, barite and chert, but locally the reverse relation illustrates a post-pitchblende assemblage. Cyclic mineralization may be represented.

Chert and carnelian often contain more than 1 % U_3O_8, but the contained uranium is too fine-grained and disseminated to be identified mineralogically under the microscope. Pitchblende and coffinite are most likely. Uraniferous chert is

TABLE VI. URANIUM MINERALS OF THE KRUNKELBACH MINE (BÜLTEMANN (7), (8), FEHR (19))

<u>OXIDES AND HYDROXIDES</u>	
PITCHBLENDE/URANINITE	UO_2
IANTHINITE	$UO_2.5UO_3.10H_2O$
BILLIETITE	$BaU_6O_{19}.11H_2O$
WÖLSENDORFITE	$(Pb, Ca)\ U_2O_7.2H_2O$
SCHOEPITE	$UO_3.2H_2O$
VANDENDRIESSCHEITE	$PbU_7O_{22}.12H_2O$
CURITE	$Pb_2O_5O_{17}.4H_2O$
CLARKEITE	$(Na, Ca, Pb)_2U_2(O, OH)_7$
STUDTITE	$UO_4.4H_2O$
<u>CARBONATES</u>	
RUTHERFORDITE	$UO_2(CO_3)$
JOLIOTITE	$UO_2CO_3.2H_2O$
<u>SULFATES</u>	
ZIPPEITE	$K_4(UO_2)_6(SO_4)_3(OH)_{10}.4H_2O$
URANOPILITE	$(UO_2)_6(SO_4)(OH)_{10}.12H_2O$
JOHANNITE	$Cu(UO_2)_2(SO_4)_2(OH)_2.6H_2O$
<u>TUNGSTATES</u>	
URANOTUNGSTATE *	$(Fe, Ba, Pb)(UO_2)_2(WO_4)(OH)_4.12H_2O$
<u>PHOSPHATES</u>	
TORBERNITE	$Cu(UO_2)_2(PO_4)_2.8\text{-}12H_2O$
META-TORBERNITE	$Cu(UO_2)_2(PO_4)_2.8H_2O$
AUTUNITE	$Ca(UO_2)_2(PO_4)_2.10\text{-}12H_2O$
META-AUTUNITE	$Ca(UO_2)_2(PO_4)_2.2\text{-}6H_2O$
SALEEITE	$Mg(UO_2)_2(PO_4)_2.8H_2O$
URANOCIRCITE	$Ba(UO_2)_2(PO_4)_2.8\text{-}12H_2O$
META-URANOCIRCITE II	$Ba(UO_2)_2(PO_4)_2.6H_2O$
BASSETITE	$Fe^{+2}(UO_2)_2(PO_4)_2.8H_2O$
BERGENITE	$Ba(UO_2)_4(PO_4)_2(OH)_4.8H_2O$
PHOSPHURANYLITE	$Ca(UO_2)_3(PO_4)_2(OH)_2.6H_2O$
<u>ARSENATES</u>	
HEINRICHITE	$Ba(UO_2)_2(AsO_4)_2.10\text{-}12H_2O$
META-HEINRICHITE	$Ba(UO_2)_2(AsO_4)_2.8H_2O$
ZEUNERITE	$Cu(UO_2)_2(AsO_4)_2.10\text{-}16H_2O$
META-ZEUNERITE	$Cu(UO_2)_2(AsO_4)_2.8H_2O$
NOVACEKITE	$Mg(UO_2)_2(AsO_4)_2.12H_2O$
ABERNATHYITE	$K(UO_2)(AsO_4).4H_2O$
AS-URANOSPATHITE	$(HAl)_{05}(UO_2)_2(AsO_4)_2.20H_2O$
KAHLERITE	$Fe^{+2}(UO_2)_2(AsO_4)_2.nH_2O$
ARSENURANYLITE	$Ca(UO_2)_4(AsO_4)_2(OH)_4.6H_2O$
<u>SILICATES</u>	
COFFINITE	$U(SiO_4)_{1-x}(OH)_{4x}$
URANOSILITE	$UO_3.7SiO_2$
SODDYITE	$(UO_2)_2SiO_4.2H_2O$
URANOPHANE	$Ca(UO_2)_2.Si_2O_7(OH).2H_2O$
BETA-URANOPHANE	$Ca(UO_2)_2Si_2O_7(OH)_2.4H_2O$
BA-URANOPHANE	$Ba(UO_2)_2Si_2O_7(OH)_2.nH_2O$
CUPROSKLODOWSKITE	$Cu(UO_2)_2Si_2O_6(OH)_2.6H_2O$
KASOLITE	$Pb(UO_2)SiO_4.H_2O$

* WALENTA (20), (21)

SOME FURTHER, PROBABLY NEW SECONDARY URANIUM MINERALS ARE UNDER INVESTIGATION. THERE ARE K-FE-URANYL-ARSENATES, NI-, CO- AND BI-URANYL-ARSENATES AND URANYL CARBONATES.

THE MOST IMPORTANT URANIUM-FREE SECONDARY MINERALS ARE: MALACHITE, AZURITE, DIGENITE, NEO-DIGENITE, COVELLITE, IDAITE, BROCHANTITE, MIMETESITE, BEUDANTITE, CHLOROTILE, PHARMACOSIDERITE, CHRYSOCOLLA, ETC.

dark grey to nearly black, but uraniferous carnelian remains red. This second generation of pitchblende is commonly fresh in appearance, but close to fault zones it is replaced by pitchblende, sooty pitchblende or even secondary uranium minerals. These secondary uranium minerals occur to depths of 240 m; they consist of uranium micas (uranocircite, heinrichite, torbernite, zeunerite, autunite, phosphuranylite, uranospathite, bergenite, kahlerite, bassetite and K-uranyl-arsenate) and uranium silicates (soddyite and uranophane) (Table VI). Secondary copper minerals and rare selenides occur with sulfides.

Arsenopyrite commonly is idiomorphic. In one case considerable gold was found between pitchblende and secondary uranium minerals. Carbonates (calcite, dolomite, ankerite) are minor.

6. CONCLUSIONS

Detailed microscopy shows four pitchblende generations (Table V). The first probably was Variscan, shortly following the opening of fissures during cooling of the granite. In such partly mylonitized fissures within granite, high-temperature silica gel precipitated as chert/carnelian with finely disseminated pitchblende, pyrite, marcasite, and arsenopyrite. Not much later botryoidal pitchblende with pyrite, marcasite, chalcopyrite, and arsenopyrite formed in the chert matrix. The younger phase may represent volcanism which produced the quartz porphyry dikes.

During the post-Variscan Saxonian deformation (Jurassic-Cretaceous) the quartz-uranium assemblage was remobilized. The new product is characterized by the so-called red iron-barite assemblage which includes abundant sulfides, fluorite, and quartz. Here, massive pitchblende occurs in fragments of coarse-grained red barite and chert, several tens of centimetres in size. The parent hydrothermal solution must have been highly oxidizing. Besides sulfides which are stable at high oxidation potentials, the minerals are exclusively oxides, iron always being trivalent.

A Tertiary remobilization is recognizable by carbonates (calcite, dolomite) selenides, and typical minerals of the Bi-Co-Ni association which formed mainly in vugs.

Finally, post-glacial pitchblende was found coating secondary uranium mica and uranophane (Ramdohr (22)). To this generation also belongs the so-called radium-barite which is strongly radioactive due to the partial replacement of Ba by Ra. Such barite is usually idiomorphic.

It is thought that uranium was extrinsically introduced only during the initial Variscan mineralization. Thereafter this uranium appears to have been partially remobilized, but not significantly redistributed during subsequent mineralizations, without substantial introduction of new extrinsic uranium.

ACKNOWLEDGEMENTS

The representative of Gewerkschaft Brunhilde, Dr.-Ing. Wolfgang Hamma, supported the work summarized in this paper and gave permission for its publication. The authors also wish to thank Dr. John W. Gabelman, Danville, Ca, USA, who kindly read and rewrote the translation and Dipl.-Geol. Jost Haneke, Gewerkschaft Brunhilde, for preparing the drawings.

REFERENCES

(1) METZ, R., REIN, G., Geologisch-petrographische Übersichtskarte des Südschwarzwaldes 1:50,000 (1957).

(2) REIN, G., Ein Pechblendevorkommen bei Menzenschwand im Südschwarzwald, N.Jb.Miner.Abh. 94 (1960) 721-732.

(3) KIRCHHEIMER, F., Die Entdeckungsgeschichte des Uranvorkommens bei Menzenschwand im südlichen Schwarzwald: Der Aufschluß, 10 (1964) 263-266.

(4) SCHAUER, H., Uranerzführende Gänge im Bärhaldegranit (Südschwarzwald), N.Jb.Miner.Mh 6 (1962) 121-124.

(5) BÜLTEMANN, H.W., Uran im Schwarzwald, VDI-Nachrichten 18, Nr. 12 (1964) 1-2.

(6) BÜLTEMANN, H.W., Die Uranvorkommen Ellweiler in Rheinland-Pfalz und Menzenschwand im Schwarzwald, Erzmetall XVIII (1965) 79-83.

(7) BÜLTEMANN, H.W., Das Uranvorkommen im Krunkelbachtal bei Menzenschwand, Lapis 4 (1979) 27-30.

(8) BÜLTEMANN, H.W., Interne Berichte, Uetze (1960-1984) (unpublished).

(9) BÜLTEMANN, W.D., Die Uranlagerstätte 'Krunkelbach' bei Menzenschwand, Hochschwarzwald, und ihr geologisch-lagerstättenkundlicher Rahmen, Z. Dt. geol. Ges. 130 (1979) 597-618.

(10) BÜLTEMANN, W.D., Interne Berichte, Uetze (1973-1984) (unpublished).

(11) EMMERMANN, R., Granitbildung im Verlauf einer Orogenese (Die petrogenetische Entwicklung der Granitserie des Südschwarzwaldes), Habilitationsschrift, Univ. (TH) Karlsruhe (1973) (unpublished).

(12) BARTHEL, F., MEHNERT, K.R., Die Verteilung von Uran und Thorium im Malsburger Granit, N.Jb.Miner., Abh. 114 (1970) 18-47.

(13) ALTHERR, R., Der 'Randgranit' der Zone Badenweiler-Lenzkirch (Südschwarzwald): Ein anatektischer Komplex, Diss. Albert-Ludwig-Univ. Freiburg i.Br. (1975) 106 pp.

(14) WENDT, I., LENZ, H., HÖHNDORF, A., Das Alter des Bärhalde-Granites (Schwarzwald) und der Uranlagerstätte Menzenschwand, Geol. Jb. E2 (1974) 131-143.

(15) WENDT, I., Die geochronologische Interpretation von Rb/Sr-Gesamtgestein- und Mineraldaten in Kombination mit K/Ar-Mineraldaten, Vortrag Frühjahrstagung Dt. Min. Ges., Sektion Geochemie, Bensheim (1972)

(16) WENDT, I., HÖHNDORF, A., BÜLTEMANN, H.W., BÜLTEMANN, W.D., Das Alter der Pechblende der Lagerstätte Menzenschwand, Schwarzwald, Z.dt.Geol.Ges. 130 (1979) 619-626.

(17) GUBA, I., Zur Tektonik der Uranerzgrube 'Krunkelbach', Gewerkschaft Brunhilde, Bericht, Uetze (1977) (unpublished).

(18) WIMMENAUER, W., SCHREINER, A., Geologische Karte von Baden-Württemberg 1:25,000, GLA Baden-Württemberg, Blatt 8114 Feldberg, Erläuterungen Blatt 8114 Feldberg (1981).

(19) FEHR, T., Neue Mineralien 1979-1985, Christian Weise Verlag, München, entnommen, Berichtigungen nach Amer. Mineral. (1985).

(20) WALENTA, K., Uranotungstit, ein neues sekundäres Uranmineral aus dem Schwarzwald, Tschermaks Min. Petr. Mitt. 34 (1985) 25-34.

(21) WALENTA, K., Uranosilit, ein neues Mineral aus der Uranlagerstätte Menzenschwand im südlichen Schwarzwald, N.Jb.Miner. Mh., H.6 (1983) 259-269.

(22) RAMDOHR, P., Eine subrezente Bildung von Uranpecherz aus U^{+6}-Lösungen, Jb. Geol. Landesamt Baden-Württemberg 6 (1963) 539-542.

THE GROßSCHLOPPEN-HEBANZ URANIUM OCCURRENCES - A PROTOTYPE OF MINERALIZED STRUCTURE ZONES CHARACTERIZED BY DESILICIFICATION AND SILICIFICATION

H. G. Dill
Federal Institute for Geosciences and Natural Resources
Hannover

S. G. Kolb
Esso Erz GmbH
Nürnberg
Federal Republic of Germany

Abstract

THE GROßSCHLOPPEN-HEBANZ URANIUM OCCURRENCES - A PROTOTYPE OF MINERALIZED STRUCTURE ZONES CHARACTERIZED BY DESILICIFICATION AND SILICIFICATION

The uranium occurrences at Großschloppen and Hebanz are situated along the northern margin of the Fichtelgebirge close to the Muenchberg Gneiss Massif. They belong to the vein-type uranium metallogenic province of the western edge of the Bohemian Massif. Both occurrences are situated along the contact of the Late Variscan biotite granite/granodiorite 'No. I' (Weißenstadt-Marktleuthen Porphyry Granite) which intruded the Upper Proterozoic to Early Paleozoic metasediments. The country rocks were assimilated to a certain degree along the contact by the granite producing heterogeneous rocks of dioritic to granodioritic composition and igneous texture.

The granite-metasediment contact is crosscut by NNW to NW trending faults some of which are mineralized by uranium oxides, sulfides and selenides. The mineralization controlling structures at Großschloppen and Hebanz are enveloped by alteration zones showing an opposing trend of silica migration.

The Großschloppen structure was pervasively silicified, whereas in Hebanz desilicification resulted in the formation of 'calcitic episyenites'. These alteration centres are succeeded laterally by various stages of argillization (advanced argillization, intermediate argillization, sericitization, propylitization). The alteration processes are supposed to be of Lower Permian age as indicated by the parallel trend of Rotliegend quartz porphyries and the Hebanz structure zone.

At Großschloppen six alteration stages are recognized. They are separated by tectonic hiati and characterized by different quartz modifications and U minerals.

During the first stage the major portion of the uranium was concentrated as spherulitic and layered pitchblende. The uranium oxide was replaced during the later stages by younger quartz, selenides and sulfides along shrinkage cracks and rhythmic banding followed by dolomite, barite, fluorite and calcite. The mineralization belongs to the 'polymetallic U paragenesis' (Dill (1)) (uranium oxides associated with various sulfides, arsenides, selenides and native elements of Fe, Cu, Zn, Pb, Bi, Co, Ni, Au). Specularite is a common Fe-oxide in various stages. The quartz veins are stained by secondary uranium minerals (uranophane, torbernite) along hairline cracks and fractures. The secondary minerals also coat the primary uranium oxides.

Uranophane has been detected at Großschloppen in drillholes down to a depth of 450 m beneath surface, whereas saleeite only occurs within the upper 100 m.

The primary age of the mineralization is Late Permian to Early Triassic. The re-deposition of uranium under oxidizing conditions as well as cementation phenomena indicated by the occurrence of native copper took place during the Miocene and Pliocene peneplenation.

1. INTRODUCTION

The Großschloppen-Hebanz U occurrences are located 225 km E of Frankfurt (Fig. 1) within the Fichtelgebirge Mountains, Bavaria.

A detailed description of the discovery and geologic evaluation of the Großschloppen vein-type uranium deposit was recently published by Moore et al. (2).

In 1976 Esso Erz GmbH initiated a regional uranium exploration programme and on March 8, 1977, Esso succeeded in finding a point-source gamma anomaly in the Großschloppen area. Drilling of the discovery started in September 1977 and underground exploration began in December 1979.

Some remarks as to the secondary U minerals of the Großschloppen occurrence have been given by Dill (3). Age datings were carried out by Carl et al. (4).

2. REGIONAL GEOLOGICAL SETTING

The NW-SE running mineralized structures (Fig. 2) at Großschloppen and Hebanz are situated along the boundary of the Fichtelgebirge and the Muenchberg Gneiss Complex, which is separated from the anchimetamorphosed Paleozoic rocks of the Frankenwald to the NW as well as from the Fichtelgebirge Zone by prominent NE-SW trending fault zones.

Albite-bearing pegmatitic mobilizates (Fig. 1b) are particularly observed along the SE-margin of the gneiss complex and formed during retrogressive metamorphism. Similar Na-rich mobilizates are commonly encountered in the Poppenreuth-Maehring U district (Dill (5)) along the boundary between the Saxothuringian and the Moldanubian zone. The Fichtelgebirge area is characterized by granitic intrusives of Upper Carboniferous age.

By chronological order, two groups of granitic rocks can be distinguished:

(i) Weißenstadt-Marktleuthen Granite: (granite 'No. 1') 310 $\pm$ 14 Ma

(ii) Peripheral Granite, Central Granite, Tin Granite: 288 $\pm$ 4 Ma to 285 $\pm$ 6 Ma (Besang et al. (6)).

The ages of the granite intrusions are considered to be the upper limit of the formation of the Großschloppen-Hebanz uranium occurrences which are controlled by structures cutting the Weißenstadt-Marktleuthen Granite.

The younger granites contain 6 - 7 ppm U, whereas the older granite has an average content of only 4 $\pm$ 1 ppm U (Richter et al. (7)).

Situated between the two granite groups are metasedimentary rocks of Upper Proterozoic to Early Paleozoic age (Stettner (8), (9)). Parts of this sequence may be attributed to those Precambrian rocks which are believed to be the most fertile rock sequence for U preconcentration along the western edge of the Bohemian Massif (Stettner (10), Dill (11)).

The contact zone of the metamorphic rocks and the Weißenstadt-Marktleuthen Granite is characterized by hybrid rocks of granodioritic to dioritic composition.

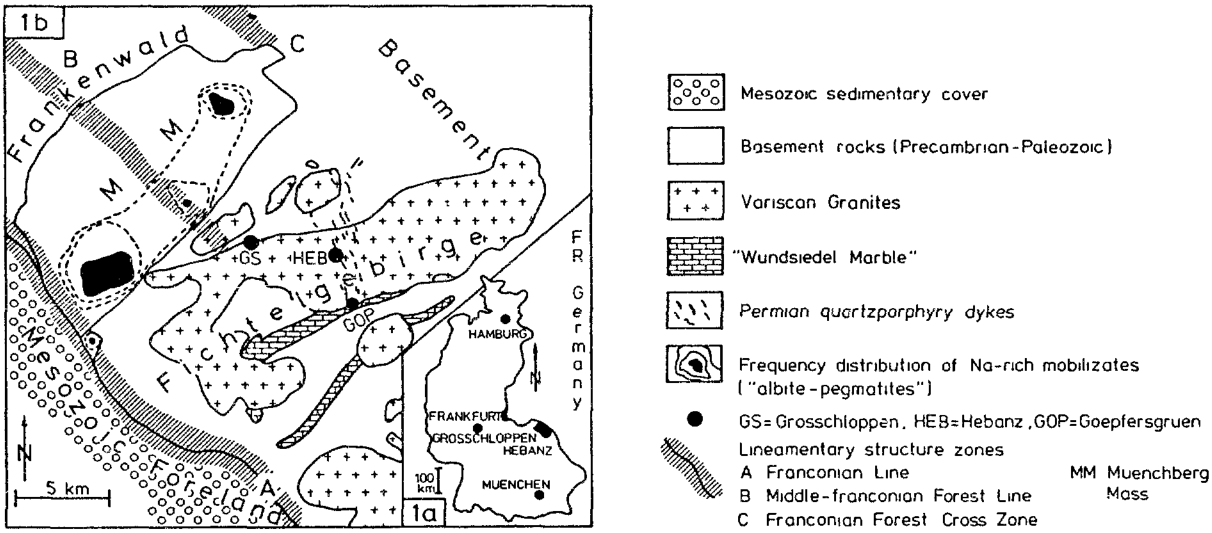

FIG. 1a. Scetch map of Hebanz-Großschloppen exploration sites.

FIG. 1b. Geological setting of Großschloppen-Hebanz uranium exploration sites (geology after Stettner (9), Na pegmatites after Bauberger (24)).

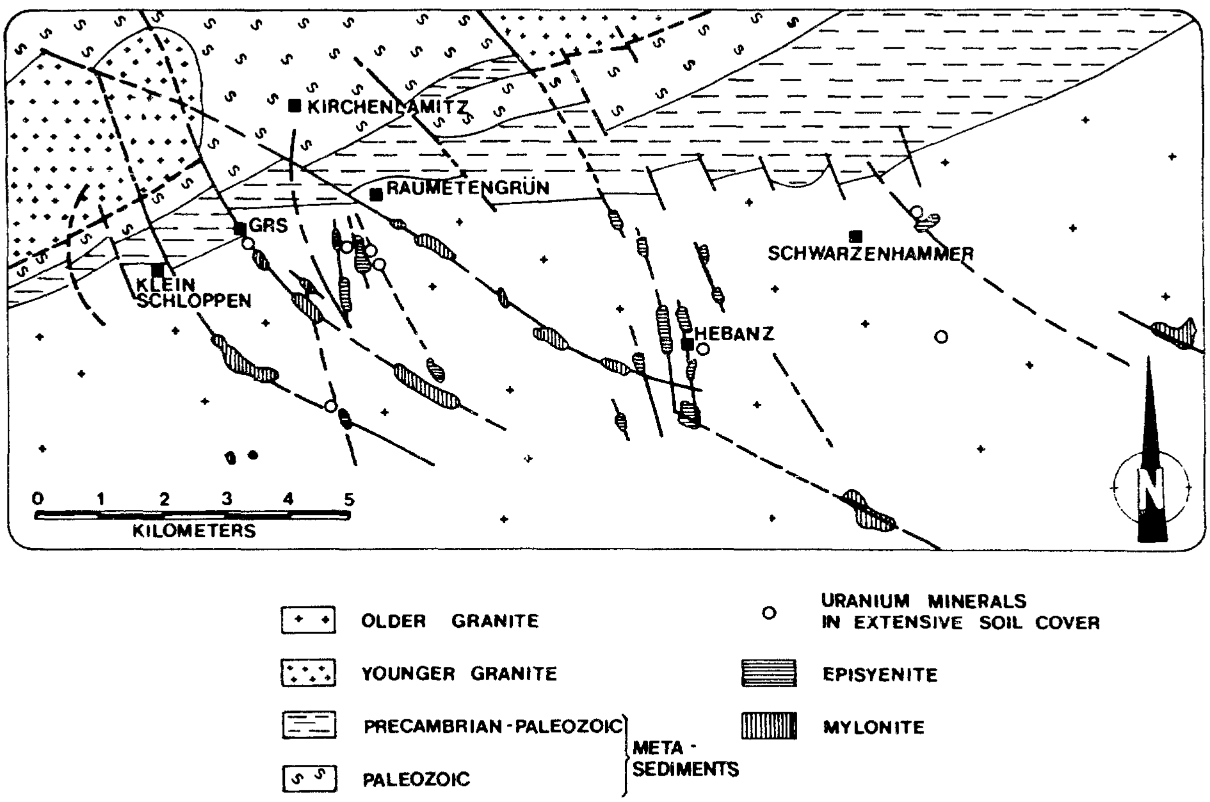

FIG. 2. Geology and structural pattern of the NW edge of the Weissenstadt-Marktleuthen-Porphyry Granite ('Older Granite').

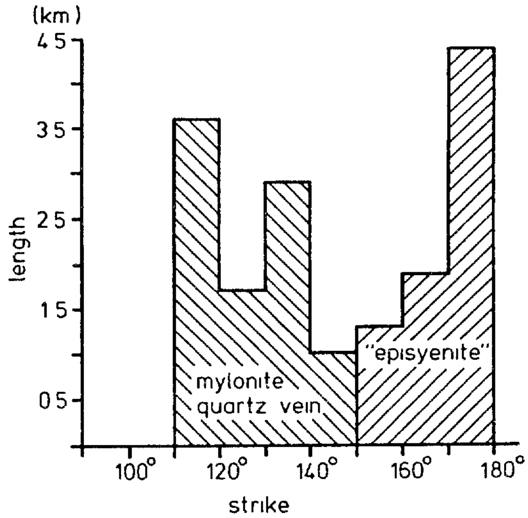

FIG. 3. Strike of alteration zones plotted versus length of structure they are associated with.

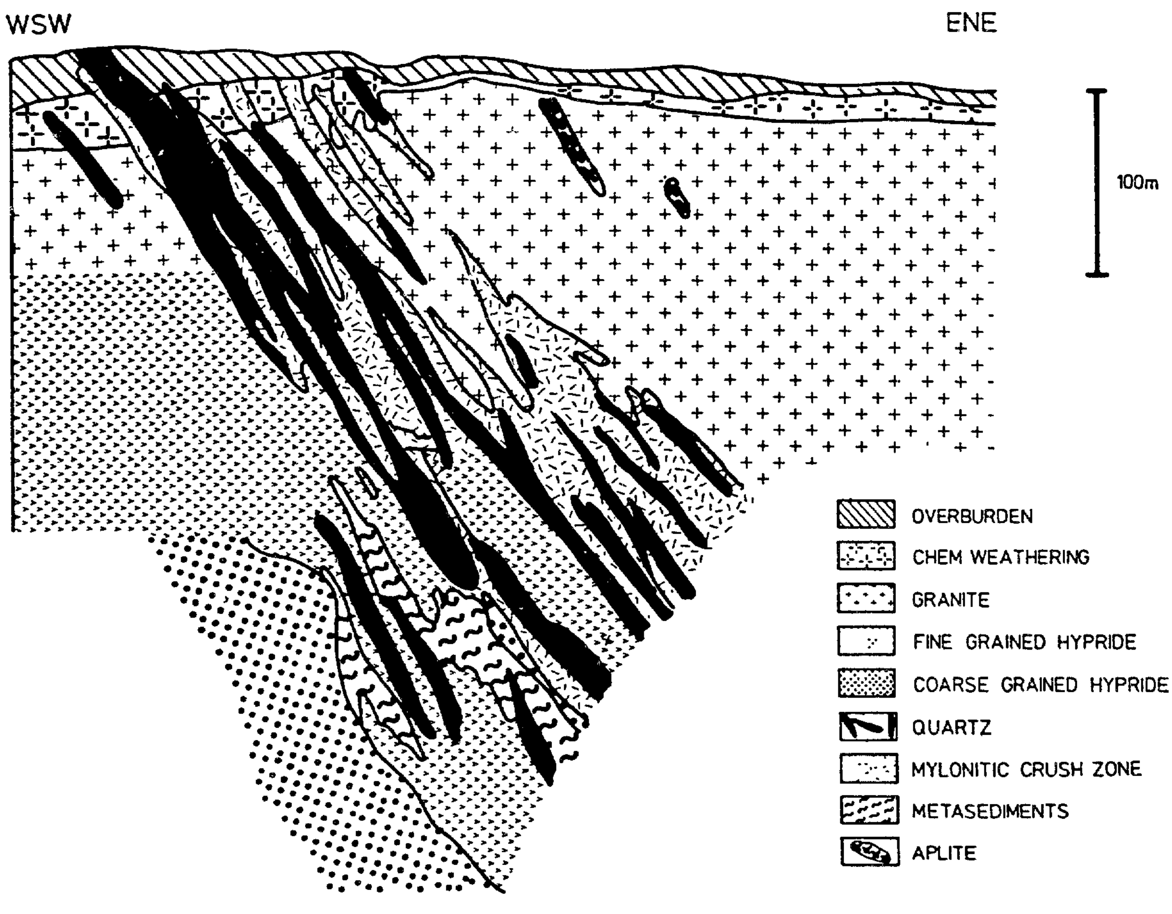

FIG. 4. Section through the Großschloppen uranium quartz vein system.

The youngest Variscan igneous rocks are lamprophyres and quartz porphyries of Upper Carboniferous to Permian age. During Mesozoic times neither evidence for igneous activity nor any ruptural deformation are recognized. Subsequently peneplenation took place during the Late Miocene and the Pliocene. During this period weathering processes caused the formation of kaolinized saprolite and also the formation of secondary U minerals.

The most important 'per descendum' U occurrence adjacent to the Großschloppen-Hebanz U district is the Rudolfstein vein-type mineralization (Lenz et al. (12), Gudden et al. (13)) S of the U occurrence. This mineralization which merely consists of uranium micas and uranophane (Dill (3)) is in contrast to Großschloppen situated within the highly differentiated and U-enriched G_4 ('Tin Granite'). U is supposed to have been removed from the enclosing granitic country rocks and deposited along faults crossing old greisen zones in a reducing environment (Lenz et al. (12)).

3. THE ORE-BEARING STRUCTURES

A set of NW to NNW running faults cuts the northwestern margin of the Weissenstadt-Marktleuthen Granite.

Near Großschloppen and Hebanz U mineralization is observed along these faults accompanied by intensively altered country rocks. Silicification is the principal type of alteration at Großschloppen, in contrast desilicification increased porosity and permeability of the granitic wall rocks at Hebanz (Fig. 2).

Two remarkable maxima are observed when plotting the strike length of the structures versus strike direction. The quartz-veins are prevalently running 110° - 120° and 130° - 140° whereas the episyenites are aligned more or less along NS trending structures (Fig. 3).

The general strike direction of the Großschloppen vein-system is NW-SE dipping 80° NW to 40° NE. Subordinate orientations are N 10° W and E 165° S (Moore et al. (2)). Veins join upward and northward and branch downward and to the S (Fig. 4).

This geometry suggests an oblique shear strain system with right-lateral and dip-slip components of offset (Moore et al. (2)).

The hanging wall of the vein system moved to the S. N-trending fractures represent a conjugate system to the principal shear direction. The NW and NNW to NS directions are also recognized on a regional scale as indicated by the distribution of various alteration types, 'episyenites' and mylonitic quartz veins. Based on studies of the alteration phenomena in the area as well as of the structural setting of the entire Fichtelgebirge (Stettner (9)), a counterclockwise rotation of the main compressional component through time may be concluded.

The desilicification is supposed to be Lower Permian in age. This is indicated by NNW-trending quartz porphyry dikes which run subparallel to the episyenite-bearing structures at Hebanz. These dikes have been important for the formation of the steatite deposit near Goepfersgruen (Stettner (14)).

4. WALL ROCK ALTERATION

4.1. The mineralogy of the alteration zones

The unaltered wall rocks are of granodioritic composition. Microcline, microcline-perthite, brownish biotite, oligoclase and quartz are embedded in a hypidiomorphic texture. The accessory minerals are (in order of their abundance) apatite, zircon, monazite and hematite. Anatase and brookite contemporaneously formed during biotite chloritization. Sericitization has been described to be the principal type of autohydrothermal alteration of the Weißenstadt-Marktleuthen Granite.

Two distinct generations of muscovite are developed within the alteration envelopes. Chlorite is the most abundant phyllosilicate within the various fault-controlled alteration zones of the NE-Bavarian exploration sites (Fig. 5). Four different types of chlorite may be distinguished.

(i) Chlorite Ia resembles closely the green biotite although it yields typical x-ray spacings of 14 Å and 7 Å.

(ii) Chlorite Ib may be interpreted due to its optical properties (light green pelochroism, 2(-)) as a Fe-Mg-chlorite (sensu Saggerson et al. (15)). Pseudomorphs after biotite are still decernible.

(iii) In contrast chlorite II exhibits much higher refractive indices (n greater 1,64) and a more intensive pleochroism. This helminth structured phyllosilicate may be a Fe-rich chlorite. Another phyllosilicate very similar to it was termed 'uranous chlorite' due to its elements Fe, Si, Ca, Al, Ti, Mn determined quantitatively by EMP (Dill 16)) and its characteristic interplanar spacing (14 Å, 7 Å).

(iv) The chlorite III alteration does not have a definite spatial position within the alteration envelopes of the mineralized zone. Chlorite III (2 (-) refractive index lower 1,60, light green pleochroism) is only found along narrow hairline cracks cutting the major alteration zone. It is not accompanied by Ti-oxides and thus indicating its discrete formation different from those of chlorite I and II. No uranium mineralization is related to this stage of chloritization.

Smectite and nontronite occurring in fault gouge along fractures within the vein-quartz and its enclosing alteration haloes are of a probable supergene origin or formed during the youngest stages of mineralization.

Quartz crystallized in various different modifications and generations in the vein-type occurrence. One generation has to be dealt with separately, which is the spherulitic quartz. It formed during later stages of episyenitization (Fig. 5). Comparing the amount of this newly formed quartz with the proportion of wall rocks which were silicified, a direct correlation does not exist. The spherulitic quartz belongs to a distinct younger hydrothermal stage not related to the desilicification.

Quartz and feldspar are replaced by calcite (Fig. 6). In the Falkenberg U prospect and in the Hoehenstein U occurrence (Dill (16)) contrary to this dolomite and in some places siderite, are replacing quartz. Epidote is frequently observed in outer parts of the alteration halo in the more or less unaltered country rocks.

4.2. The Großschloppen quartz vein

Four discrete zones of alteration may clearly be indentified in the wall rocks (Weißenstadt-Marktleuthen Granite) adjacent to the mineralized vein system (Fig. 5, 1-5).

(i) Zone 1 displays fresh biotite and feldspars and is frequently cut by veinlets of epidote-quartz-chlorite. The minerals in the vein-

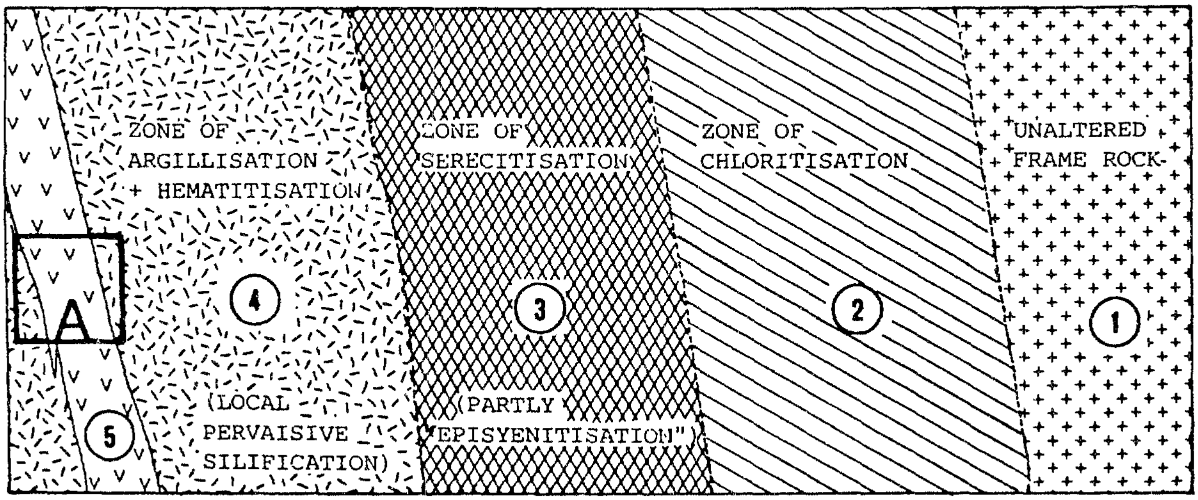

FIG. 5. Alteration zones of Großschloppen U vein-type occurrence. Numbers indicate alteration zones referred to in the text (chapter 4.2 (i) denotes quartz structure s.str.).

lets are neither distinct to any particular mineralizing event nor may they be attributed to the common hydrothermal alteration as described by Müller (17)).
Sericitization has been described to be the principal type of autohydrothermal alteration of the Weißenstadt-Marktleuthen Granite. Epidote chlorite bearing fault gouge is frequently observed in minor faults. Those veinlets are well known from other areas (e.g. Bayerischer Wald; quarries of the Rinchnach Granite) where they are genetically related to prominent linear fault zones as the 'Pfahl' (= 'Great Bavarian Quartz Lode').

(ii) Zone 2 is characterized by intensive chloritization of the granitic wall rocks. Biotite is bleached and altered to green chlorite Ib (also see chapter 4.1.). Along joints chlorite III-deposition took place.

(iii) Zone 3 alteration features resemble those of Zone 2. Frequently minor quartz redeposition took place. Epidote is completely missing in Zone 3, the plagioclases are altered to sericite.

(iv) Zone 4 close to the quartz vein exhibits the most intensive alteration as indicated by the presence of kaolinite and hematite (pinkish quartz and K feldspar).

The zones may be classified according to the proposal of Barnes (18):

Zone 1-2	propylitization
Zone 3	intermediate argillization and sericitization
Zone 4	advanced argillization
Zone 5	quartz vein

4.3. The Hebanz episyenites

Only drill core samples are available to study the Hebanz U occurrence, but these samples give a representative section from the fresh host rock (Weißenstadt-Marktleuthen Granite) through the mineralized episyenites (Fig. 6).

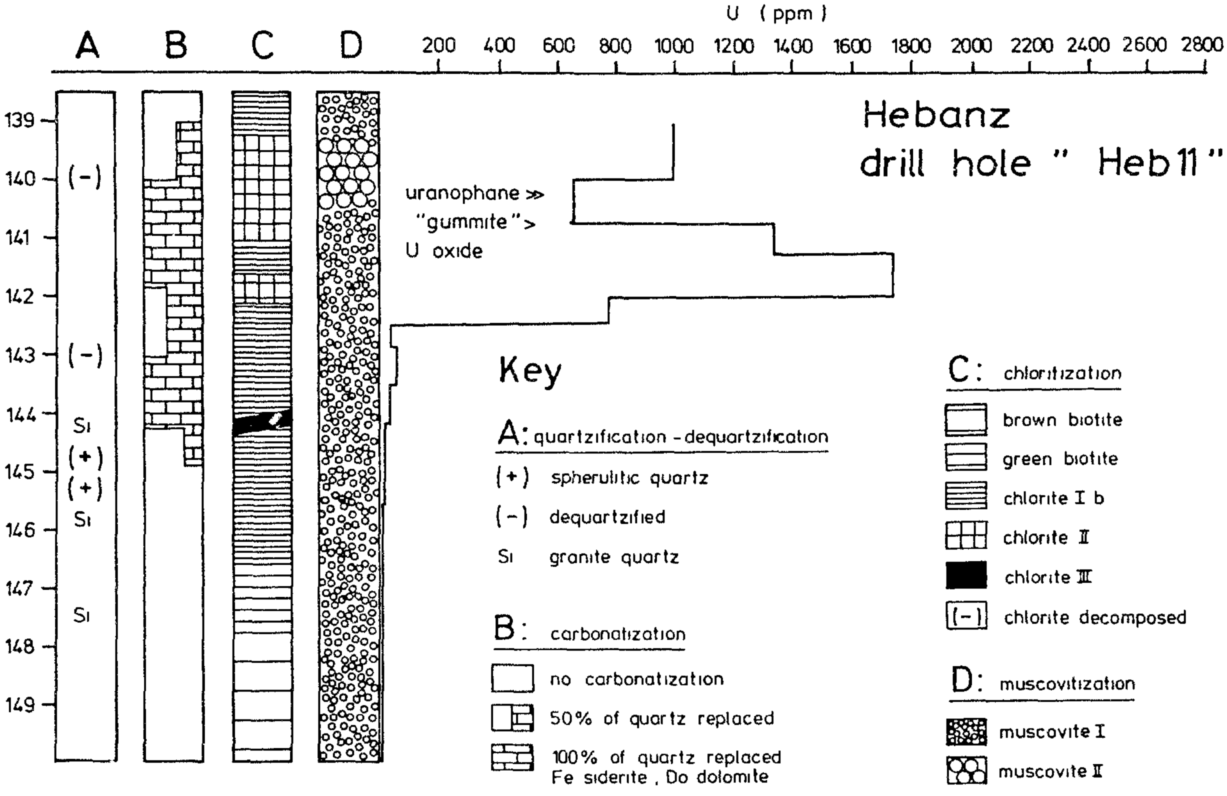

FIG. 6. Alteration zones of Hebanz U-bearing episyenites.

The various alteration zones are numbered according to those described for the Großschloppen quartz vein system (Fig. 5).

- Zone 1 is identical with the autohydrothermally (muscovite I) altered granitic country rocks.

- Zone 2 is characterized by chlorite Ib. Scarcely spherulitic 'star quartz crystals' which point to secondary silicification are recognized.

- Zone 3 represents the ultimate stage of alteration within the Hebanz U occurrence. It is characterized (Fig. 6) by intensive carbonatization and chloritization (Ib/II). Epidote which rarely was encountered in Hebanz was not observed in the same zone in Großschloppen.

4.4. Comparison and discussion of Hebanz and Großschloppen alteration processes

In summary the alteration was not so pervasive in Hebanz as in Großschloppen (see epidote occurrence up to zone 3), where strong acidic conditions are indicated by the presence of kaolinite.

The solution which caused alteration at Hebanz and Großschloppen started marginally from more or less neutral conditions. At Hebanz strong alkaline solutions caused quartz removal along the fault zone and calcite precipitation. At Großschloppen strong acidic conditions caused silicification and kaolinite formation.

The accessory minerals, e.g. zircon (Zr: 199 - 263 ppm), apatite (P_2O_5: 0.32 - 0.40 wtg %) and monazite (Ce: 120 - 140 ppm) are not affected by these

TABLE I. WALLROCKS OF HEBANZ U OCCURRENCE

	MIN	X *	MAX	MIN	X **	MAX
		WTG %			WTG %	
SiO_2	67.18	67.47	67.62	41.58	56.72	64.65
TiO_2	0.51	0.54	0.58	0.50	0.64	0.71
Al_2O_3	14.48	14.61	14.87	13.59	17.42	17.69
Fe_2O_3	1.96	2.42	2.75	2.81	3.95	4.18
MnO	0.03	0.03	0.04	0.04	0.07	0.10
MgO	0.70	0.82	0.88	0.68	0.93	1.15
CaO	1.88	2.29	2.55	2.20	9.30	15.70
Na_2O	2.88	3.02	3.17	2.31	2.69	3.20
K_2O	4.88	4.99	5.09	4.80	6.16	6.54
P_2O_5	0.31	0.32	0.33	0.32	0.38	0.40

CORRELATION COEFFICIENTS: $R > \pm 0.5$
SiO_2 : CaO $R = -0.984$
SiO_2 : U $R = -0.529$

* FRESH GRANITE
** ALTERED GRANITE

percolating solutions. Only between CaO, SiO_2, and U (Table I) correlative relations may be established (U: SiO_2: r = - 0.529, SiO_2: CaO: r = - 0.984).

The solutions alterating the wall rock were derived from deeper parts of the sequence. They are controlled by the Upper Proterozoic country rocks and the Lower Permian igneous activity.

Mg-metasomatism (as it is in the Goepfersgruen steatite deposit) and episyenitization are undoubtedly genetically related. Metacarbonate-bearing horizons of the organogenic subgroup (amphibolites, graphite quartzites, metaphosphorites, calcsilicates, marbles, gneisses) of the Upper Proterozoic 'Varied Group' are assumed to be the source for Mg, Ca and CO_2.

This is also implied by results recently published from the Hoehenstein 80/I drill hole (Richter et al. (19)), where in deeper parts metacarbonates, altered by Mg-metasomatism similar to those from the Goepfersgruen steatite deposit, are overlain by dolomitic episyenites (Dill (7), (16)). This sequence is also observed in the Fichtelgebirge (Fig. 1). Steatitization took place where fault zones crosscut the 'Wunsiedel Marble' of the 'Varied Group' near Goepfersgruen (GOP) and episyenitization was observed along the same structure within the granite (HEB). The depth zonation from Hoehenstein is represented by a lateral zonality in the Fichtelgebirge.

The linkage between source rock and host rock are the Lower Permian dikes intruded along the NNW shear zone (Fig. 1). The age of alteration can, therefore, clearly be established to be Lower Permian.

5. THE GROßSCHLOPPEN HEBANZ U MINERALIZATION

Sulphides and selenides as well as gold (rare amounts) and native Cu accompany the pitchblende at Großschloppen (Fig. 7a)

Based on the criteria published by Dill (1) for the Hoehensteinweg U occurrence this mineral association from Großschloppen may be defined as 'polymetallic U paragenesis'.

Six paragenetic stages have been recognized among which the first stage is the most significant one with respect to uranium concentration.

(i) Stage I: pitchblende (partly with homogeneously distributed galena from the radioactive decay of uranium)

(ii) Stage II: chalcopyrite, klockmanite, umangite, clausthalite, pyrite, guanajuatite (?)

(iii) Stage III: 'nasturane', coffinite

(iv) Stage IV: fluorite, calcite, dolomite, $\pm$ baryte

(v) Stage V: native copper, chalcocite, covellite

(vi) Stage VI: 'gummite', uranophane (at least two generations), torbernite, autunite, saleeite (Fig. 7b).

Hematite is present in all stages, selenides are restricted to the pitchblende mineralization.

The U-oxides form botryoidal layered and spherulitic globules which were infiltrated by sulfides and selenides along shrinkage cracks. Primary uranium minerals and quartz sometimes show such an intimate intergrowth that co-precipitation from colloidal SiO_2-UO_2 solutions may be assumed.

The values of lattice constants do not allow any depth zonation within the exploration gallery (195 m - level: a_o -5423 Å, 140 m - level: a_o -5407 Å and 5443 Å. The values fall into the normal range of pitchblende precipitated out of hydrothermal solutions. Pitchblende was first encountered at the 140 m level within the exploration gallery. Cu-cementation minerals are found from 140 m downwards.

The prevailing UO_2 compound is uranophane. This mineral is recognized even in the deepest drillholes at a depth of 400 m. While the uranophane which occurs in the upper levels of the exploration gallery originated from supergene processes, the uranophane recognized at deeper levels cannot clearly be attributed to either supergene processes or hypogene processes.

Saleeite has been recognized only down to a depth of 100 m and is undoubtedly of supergene origin. This is indicated by the low As-content (100 ppm) which rules out any relation to a reducing environment or to U oxides.

The Hebanz U occurrence exhibits a very monotonous U mineralization consisting only of U oxides and some secondary U minerals. Sulfides are not present.

The mineralization from Hebanz fits well into the class of the 'monotonous U-paragenesis' similar to that of the Falkenberg Granite in the Oberpfalz area.

6. AGE OF MINERALIZATION

The primary U mineralization formed during the youngest stages of the Variscian thermal activity. U/Pb age datings (Carl et al. (4)) yielded a primary intercept of the discordia at 233 $\pm$ 12 Ma and a secondary reshuffling at 6.0 $\pm$ 1.1 Ma. The latter is interpreted to be the true age of the torbernite. Since the torbernite was taken from samples spatially close to pitchblende the first intercept points to the age of formation of the pitchblende.

The isotope data for uranophane clearly indicate two different types. Uranophane I yields t_1 = 268 + 51/-48 Ma and t_2 = 0 - 3.6 Ma and uranophane II t_2 = 0 - 2.0 Ma. Uranophane I is an alteration product of pitchblende whereas uranophane II may be explained by two different modes. It formed either from hydrothermal solutions at the Cretaceous/Pliocene boundary or it has been derived from secondary U-minerals during Late Cretaceous times. However, there is no evidence for hydrothermal activity during Late Cretaceous times.

Like the uranous silicates saleeite formed during Plio-Pleistocene times.

FIG. 7a. Pitchblende with shrinkage cracks formed in brecciated vein quartz, polished section, ppl, scale bar:300 µ, 140 m level

FIG. 7b. Hematized vein quartz with comb-like structures in the central parts with small crystals of saleeite (Großschloppen vein U deposit)

7. METALLOGENETIC CONCEPT

During the Upper Proterozoic within (?) (Behr et al. (20)) and adjacent to the Muenchberg Gneiss Mass sedimentary rocks regarded to be the source for U were deposited in a shallow marine environment (Behr et al. (20)).

Reducing conditions prevailed in the depositional environment of the 'Varied Group' and were most favourable for U-preconcentration. Subsequent deformation and metamorphism disseminated U within the 'fertile' Varied Group (see also for general description Yermolayev (21). NE to NNE trending structure zones (first order structures) governed granitization, diaphtoresis and Na-metasomatism. These structures run parallel to the Muenchberg Gneiss Mass/Fichtelgebirge border zone. Peripherial deformation and late stage movement during the Variscian Orogeny generated NW and NNW trending fault zones. These second order structures control the U-mineralization.

Along the Middle Franconian Forest Line (Dill (22)) to which the Großschloppen structure is also attributed, several hematite occurrences and Cu-Bi-bearing mineralization occurrences (Muenchberg Gneiss Mass, Franconian Forest) are reported.

While the hematite occurrences are frequently found along deep-reaching fault zones together with quartz veins, U mineralization is restricted to areas close to active thermal centres and underlain by favourable source rocks. Episyenitization was influenced by the metacarbonates of the 'Varied Group'. The metacarbonates also caused Mg-metasomatism and steatitization.

The U occurrence may be classified as 'mineralized structure zone' rather than vein-type occurrence. From a structural point of view as well as from the granitic environment the mineralization closely resembles those known from the Mortagne Batholite/Vendée in France (Cathelineau (23)).

ACKNOWLEDGEMENTS

We thank Esso Erz for the permission to publish this study. S.C. Moore supervised the geologic programme carried out underground at Großschloppen. K. Denninger supervised the field team which discovered the Hebanz uranium occurrence and R. Hartmann did the geological evaluation at the Hebanz drill core. Other Esso Erz geologists who contributed to the project's success are C.J. MacLean and N. Neumann.

Chemical data presented in this paper were provided by H. Raschka (Federal Institute for Geosciences and Natural Resources).

The research programme is funded by the Ministry of Technology ('Uranium Concentration Processes and the Formation of Uranium Deposits).

REFERENCES

(1) DILL, H.G., Vein- and Metasedimentary-Hosted Carbonaceous Matter, N. Jb. Miner. Abh. 148 (1983) 1-21.

(2) MOORE, S.C., KOLB, S.G., MACLEAN, C.J., ERICKSON, A.J.,Jr., Geologic Evaluation of the Großschloppen Vein Uranium Deposit, West Germany, Soc. of Min. Eng. of Aime (1983) 1-8.

(3) DILL, H.G., On the formation of the vein-type uranium 'yellow ores' from the Schwarzach Area (NE Bavaria, Germany) and on the behaviour of P, As, V and Se during supergene processes, Geol. Rdsch. 72 (1983) 955-980.

(4) CARL, C., DILL, H.G., Age dating of secondary U minerals from the NE Bavarian basement, Terra Cognita C (1984) 13-14.

(5) DILL, H.G., Plutonic Mobilization, Sodium Metasomatism, Propylitic Wall Rock Alteration and Element Partitioning from the Hoehensteinweg Uranium Occurrence (NE Bavaria, Federal Republic of Germany). Uranium 1 (1983) 139-166.

(6) BESANG, C., HARRE, W., KREUZER, H., LENZ, H., MÜLLER, P., WENDT, J., Radiometrische Datierungen, geochemische und petrographische Untersuchungen der Fichtelgebirgsgranite, Geol. Jb. E (1976) 81-78.

(7) RICHTER, P., STETTNER, G., Geochemische und petrographische Untersuchungen der Fichtelgebirgsgranite, Geol. Bav. 178 (1979) 13-144.

(8) STETTNER, G., Erläuterungen zur Geologischen Karte von Bayern, 1:25,000 Blatt Nr. 5837 Weißenstadt (1964) 194 pp.

(9) STETTNER, G., in: Zitzmann, A., Geologische Übersichtskarte 1:200,000 Sheet CC 6334 Bayreuth (1981).

(10) STETTNER, G., Der Grenzbereich Saxothuringikum/Moldanubische Region im Raum Tischenreuth/Maehring (Oberpfalz) und die Situation des uranführenden Präkambriums. Z. dt. geol. Ges. 130 (1979) 561-574.

(11) DILL, H.G., Neue Ergebnisse zur Mineralogie der primären Uranträger auf den Gruben Hoehensteinweg/Poppenreuth und Waeldel/Maehring in Nordostbayern mit besonderer Berücksichtigung der Uran-, Titan- und Phosphorkohlenstoffverbindungen, Geol. Jb D42 (1980) 3-39.

(12) LENZ, H., WENDT, J., GUDDEN, H., Altersbestimmung an sekundären Uranmineralien aus dem Fichtelgebirge und dem nördlichen Oberpfälzer Wald nach der Pb/U Methode, Geol. Bav. 49 (1962) 124-133.

(13) GUDDEN, H., ECKMANN, N., Die Uranprospektion der Eisenwerkgesellschaft Maximilianshütte in Nordostbayern, Glückauf 106 (1970) 380-387.

(14) STETTNER, G., Die Lagerstätte des Specksteins von Goepfersgruen-Thiersheim im Fichtelgebirge, Geol. Bav. 42 (1959) 1-72.

(15) SAGGERSON, E.P., TURNER, L.M., General Comments on the identification of chlorites in thin sections, Mineralog. Mag. 46 (1982) 469-473.

(16) DILL, H.G., Geologie und Mineralogie des Uranvorkommens am Hoehensteinweg/Poppenreuth (NO-Bayern), Ein Lagerstättenmodell, Geol. Jb. D49 (1982) 3-83.

(17) MÜLLER, G., Die autometamorphe retrograde Umwandlung von Biotiten in Chlorit und Muskovit in sauren Tiefengesteinen, Colum. Mineral. Petr. 13 (1966) 295-365.

(18) BARNES, H.L., Geochemistry of hydrothermal ore deposits (1979) 798 pp.

(19) RICHTER, P., STETTNER, G., Das Präkambrium am Nordrand der Moldanubischen Region im Raum Tirschenreuth/Maehring (NE Bayern) und dessen metallogenetische Aspekte - lithostratographische, petrographische und geochemische Untersuchungen, Geol. Jb. D61 (1983) 23-91.

(20) BEHR, H.J., ENGEL, W., RANKE, W., Muenchberger Gneismasse und Bayerischer Wald - Guide to Excursion No. 2, Microtectonics 80 (1980) 100 pp.

(21) YERMOLAYEV, N.P., Processes of redistribution and extraction of uranium in the progressive metamorphism, Geochem. Int. 8 (1971) 599-609.

(22) DILL, H.G., Zur Geologie und Mineralogie der Schwerspatvorkommen in Nord-Bayern. Mit einem Beitrag zum Strontiumvorkommen bei Stadtsteinach/Frankenwald, Geol. Jb. D61 (1983) 93-145.

(23) CATHELINEAU, M., Les gisements uranifères de la presqu'ile Guerandaise (Sud Bretagne), Approche structurale et metallogenique, Mineralium Deposita 16 (1981) 227-240.

(24) BAUBERGER, W., Über die Albit-Pegmatite, die Muenchberger Gneismasse und ihre Nebengesteine. Geol. Vav. 36 (1957) 5-77.

FAULT-CONTROLLED URANIUM BLACK ORE MINERALIZATION FROM THE WESTERN EDGE OF THE BOHEMIAN MASSIF (NE BAVARIA, FR GERMANY)

H. G. Dill

Federal Institute for Geosciences and Natural Resources

Hannover

Federal Republic of Germany

Abstract

FAULT-CONTROLLED URANIUM BLACK ORE MINERALIZATION FROM THE WESTERN EDGE OF THE BOHEMIAN MASSIF (NE BAVARIA, FR GERMANY)

Structurally controlled epigenetic U black ore mineralizations (U oxides, U titanates, U silicates) are found in the geotectonic units of the Saxothuringian (Frankenwald, Fichtelgebirge) as well as in the Moldanubian (Oberpfaelzer Wald, Bayerischer Wald) of the Variscan orogen. These vein-type occurrences may be classified into three principal types with respect to their structural properties: fault zones with stockwork-like ore shoots, mineralized structure zones, veins s.str.

The relationship between the host and the source rocks is best described by a twofold division. The element content of the Paleozoic vein-type occurrences hosted in black shales is derived from the enclosing wall rocks (host rocks and source rocks are identical), whereas in the rocks of the crystalline basement the 'protore' or the 'low grade concentration' is assumed to have been a metabiolite-bearing horizon of the Upper Proterozoic 'Varied Group' (Bunte Gruppe), from which the elements (U, C, P) were expelled during metamorphism and anatectic mobilization. Concentration and transport took place via convectively circulating fluids. The heat necessary for that circulation is suggested to have been generated by the Late Variscan to Early Alpine igneous rocks (granites, subvolcanoes, dikes) due to results obtained from radioactive age datings.

Hydrothermal wall rock alteration caused the formation of episyenites (quartz is replaced by calcite, dolomite and zeolites). They are in time and space related with silicification phenomena and formation of quartz veins. Furthermore argillation processes (chloritization, sericitization, smectitization, kaolinization) favoured the formation of thick fault gouches. Carbonaceous matter which is of widespread occurrence in some mineralized quartz lodes (e.g. Waeldel/Maehring) has derived similar to uranium from the horizons containing organic matter within the 'Varied Group'. This was confirmed by trace element and isotope geochemistry.

Two characteristic uranium parageneses were determined within the different ore-bearing fractures intersecting the crystalline basement in NW to NNW direction. The so-called 'monotonous uranium paragenesis' is characterized by its simplicity of element composition (U, Si, Fe, Ti) but variable bonding of U (brannerite, 'U leucoxene', neouraninite, pitchblende, 'sooty pitch', coffinite, U-Ti silicates, coffinite). Contrary the 'polymetallic uranium paragenesis' displays a variety of element combinations (U, As, Au, Bi, Co, Ni, Sb, Se, Cu, Fe, Pb, Zn), which is responsible for different sulfides, selenides, arsenides and native elements. Uranium is only observed within pitchblende, its highly oxidized decomposition products, and to a rare extent within coffinite. Selenides are considered to be diagnostic for that mineralization. Judging from the structural properties and from the mineralogy of those vein-type occurrences in NE Bavaria they may act as a transition between the uranium ore deposits known in France and those from Czechoslovakia within the Mid-European U Belt.

1. INTRODUCTION

The most important fault-controlled uranium occurrences in the NE Bavarian basement contain black ore minerals such as uranium oxides, uranium silicates and uranium titanates. The Rudolfstein uranium occurrence hosts uranophane and uranium micas up to the 240 m level (Gudden et al. (1), Dill (2)). Since the occurrences containing secondary minerals ('yellow ore') (Gudden et al. (3)) as well as those with uraninite finely disseminated within pegmatites and granites (e.g. Huehnerkobel Pegmatite, Tin Granite) are only of mineralogical significance, they are not dealt with in this paper in detail. In Table I a subdivision of black ore mineralization with particular reference to their host rock source relationship is presented.

TABLE I: STRUCTURE TYPES OF U MINERALIZATION RELATED TO HOST ROCK/SOURCE ROCK AND GEOTECTONIC SETTING

GEOTECTONIC SETTING	STAGE OF METAMORPHISM	PRINCIPAL TYPE OF ORE MINERALIZATION	SUBTYPE OF ORE MINERALIZATION	AGE OF HOSTROCKS
PERMIAN EMBAYMENT	NON-METAMORPHOSED	1. FAULT ZONES WITH STOCKWORK-LIKE ORE SHOOTS		PALEOZOIC THROUGH UPPER PROTEROZOIC
SAXOTHURINGIAN	VERY LOW GRADE TO LOW GRADE	2. MINERALIZED STRUCTURE ZONES	2.1 QUARTZ LODES 2.2 EPISYENITES 2.2.1 DOLOMITIC 2.2.2 CALCITIC 2.2.3 ZEOLITIC	
MOLDANUBIAN	LOW GRADE TO HIGH GRADE		2.3 FRACTURE ZONES WITH ARGILLIC FAULT GOUGE	UPPER PROTEROZOIC
		3. VEIN S.STR.		

2. REGIONAL GEOLOGICAL SETTING

The NW part of the area under investigation belongs to the Saxothuringian whereas the SE part forms the SW edge of the Moldanubian of the Bohemian Massif within the Central European Variscan Orogen (Fig. 1).

The lithology of the Moldanubian was subdivided (Dudek et al. (4)) into the 'Monotonous Group' (cordierite-bearing gneisses) and into the 'Varied Group' (amphibolites, graphite-bearing metasediments, calcsilicates, marbles, mica schists), both of which were suggested to be Upper Proterozoic in age (Zoubek (5)). North of the Erbendorf Line (Stettner (6)) Early Palaeozoic mica schists, phyllites and quartzites are predominant. Precambrian metamorphic rocks are only exposed in window-like outcrops. The whole basement was intruded by granitic to granodioritic intrusive rocks of Carboniferous age (Besang et al. (7), Köhler et al. (7)).

The NW edge of the studied area comprises slightly metamorphosed Palaeozoic slates, greywackes, limestones, diabases and keratophyres of the Frankenwald. During the Hercynian orogeny, the Muenchberg Gneiss Mass (MGM) was regionally metamorphosed (medium to high grade). This part does not contain ore deposits. After

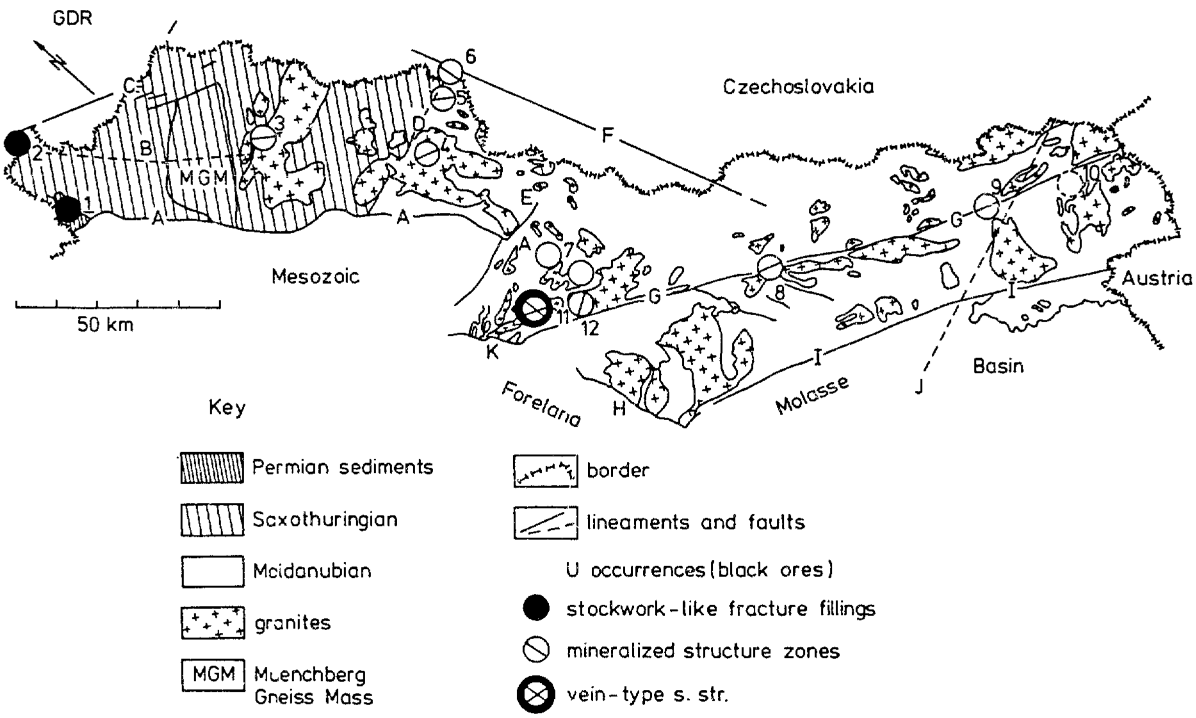

FIG. 1. Scetch map of the U occurrences referred to in this paper. 1: Stockheim, 2: Graefenthal Horst, 3: Großschloppen, 4: Falkenberg Granite, 5: Hoehenstein (+ Griessbach), 6: Waeldel, 7: Schwarzach U occurrences, 8: Altrandsberg, 9: Grafenau, 10: Hauzenberg, 11: Nabburg-Woelsendorf, 12: Altfalter Lineamentary fault zones: A: Franconian Line, B: Middle Franconian Forest Line, C: Franconian Traverse Zone, D: Erbendorf Line, E: Luhe Line, F: Bohemian Pfahl (Great Quartz Lode), G: Bavarian Pfahl (Great Quartz Lode), H: Keilberg Fault, I: Danube Fault, J: Isar Lineament, K: Fensterbach Fault

the Sudetic Movement which was the major tectonic event in that zone, small embayments were filled with clastic sediments of Lower Permian age, containing also tuff intercalations. Apart from small coal seams they merit also special attention on account of their U abundance. Numerous NW to NNW trending faults which originate from the Late Hercynian block tectonic intersect the NE Bavarian Basement. Most of the faults are suggested to have been rejuvenated during Post-Variscan time. Along these structures Fe-, Cu-, Zn-, Ba- and F-bearing vein-type deposits are situated. Only fluorite is mined at present.

3. THE FAULT-CONTROLLED U ORE MINERALIZATION

3.1. Fault zones with stockwork-like ore shoots

These occurrences are restricted to the Palaeozoic rocks of the Frankenwald where two lithological units are considered to be fertile on account of their high U background values, caused by syndiagenetic preconcentration processes:

- Permian coal seams of the Stockheim Rotliegend Trough
- Early Palaeozoic Graptolite Shales from the Graefenthal Horst

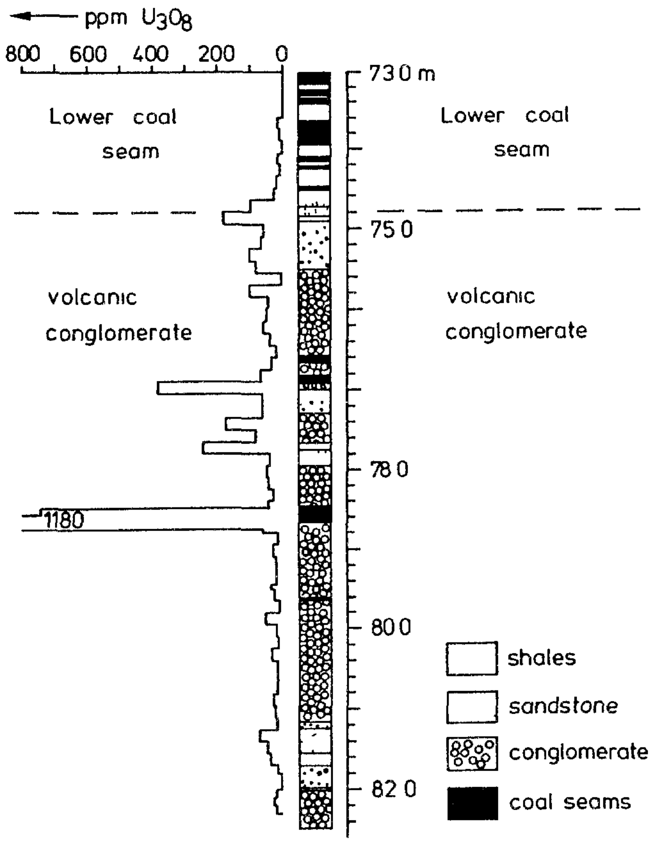

FIG. 2. Drill core section through the Permian coal-bearing volcano-sedimentary sequence mineralized with U - from Dollinger 1983 (9).

3.1.1. The structural controlled uranium ore mineralization from the Stockheim Rotliegend Trough

The Lower Carboniferous greywacke-slate cyclothems of the Teuschnitz Kulm Syncline were unconformably overlain by clastic sediments of the Stockheim Trough. They are truncated by NNW running thrust zones among which the Hasslach Fault is the most prominent, particularly for their uranium mineralization. Fig. 2 displays a drill core section (Dollinger (9)) penetrating the Lower Permian porphyritic layers which were interbedded by thin coal seams. Only where the coal seams are in contact with acid porphyroclastic sediments (U: 60 - 100 ppm, Jacob et al. (10)) the uranium content of the coal beds is also increased. The uranium was syndiagenetically concentrated and was later redistributed along the Hasslach Fault Zone. Those parts of the coal which were affected by a pervasive ruptural deformation were mineralized with pyrite, marcasite, arsenopyrite, chalcopyrite and highly oxidized pitchblende (Dill (11)). The interstices of the coal breccia are partly filled by calcite or by kerogenous matter. Those phenomena may well be compared with those described from Lodève Basin whose environment of deposition is more sapropelitic than at Stockheim. No genetic relation among those U-, Pb-, Zn-, Cu-, Fe-bearing mineralizations from the Stockheim Trough and the enclosing Pb-, Zn-, Cu-, baryte-, ankerite- and hematite-bearing veins of the enclosing rocks of the Teuschnitz Syncline can be established (Dill (11)). No chemical or mineralogical affinity between these veins and their country rocks may be determined, whereas in the Stockheim Trough a remobilization from the enclosing country rocks may be concluded.

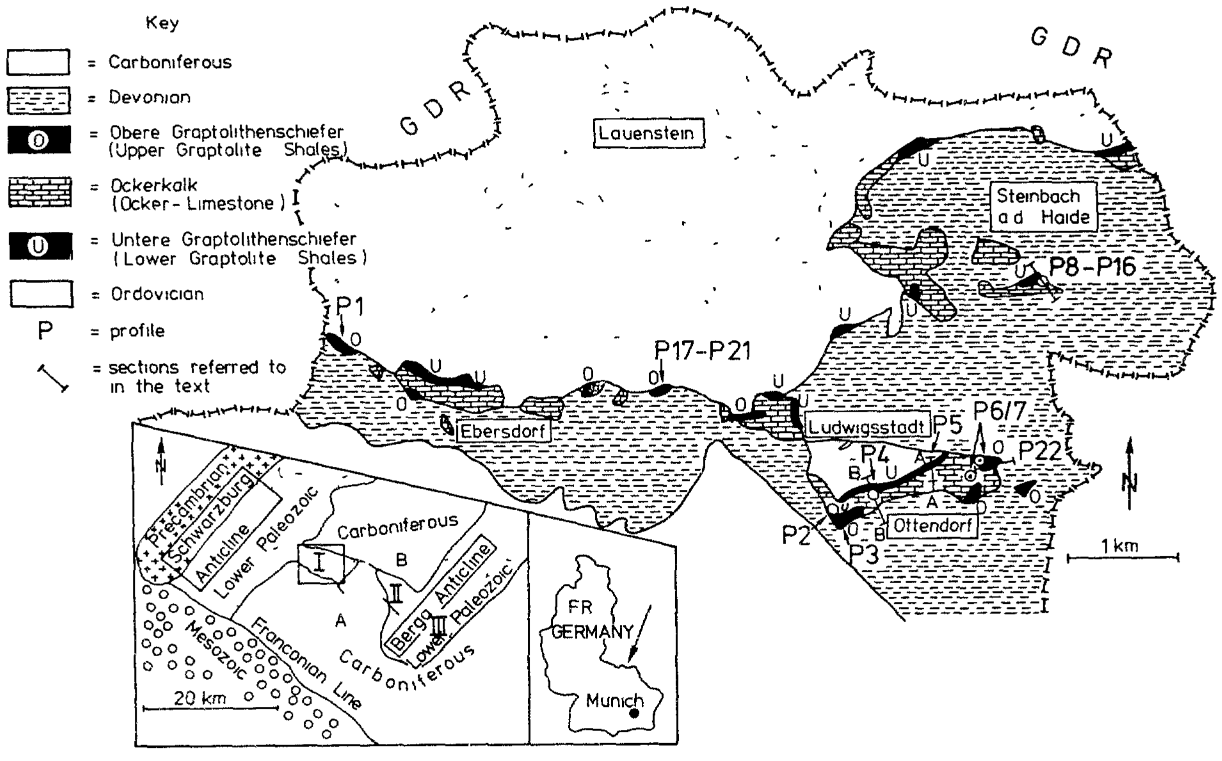

FIG. 3. Geology (Behrens 1965 (12)) of the Graefenthal Horst simplified - from Dill (in prep.).

3.1.2. The structurally controlled uranium ore mineralization of the Silurian and Lower Devonian Graptolite Shales from the Graefenthal Horst

The Graefenthal Horst forms a domelike structure (Fig. 3) (Behrens (12)) containing Ordovician Phycode Beds in its core. Towards the margin Griffelschiefer (Pencil Slates), Lederschiefer (Leather Salte), Silurian to Devonian Slates and Limestones were deposited followed by the pelitic-psammitic beds of the Teuschnitz Kulm Syncline (see also 3.1.1.). The black shales of the Lower Graptolite Shales (U $\bar{x}$ = 40 ppm, Schmid (13)) and the Upper Graptolite Shales (U $\bar{x}$ = 16 ppm) may act as uranium source rock, among which the phosphorite facies has provided the most favourable conditions for syndiagenetic uranium preconcentration (nodular apatite: 131 ppm U_{max}). Due to postdating fracturation, uranium was released and concentrated with ruby sphalerite (Rubinblende), some galena pyrite, chalcopyrite and minor fahlores in these veinlets terminating within the black shales.

The structural evolution was described by Behrens (12). After folding along NE-SW trending fold axis during the Sudetian Movement the SE limb of that anticline was intensively intersected by shear joints (Fig. 4). Uranium concentration is preferently located at the intersections of the NW trending joints with the Graptolite Shales or where lineamentary fault zones cross the Graefenthal Horst. The highest U content (P17 - P21: U_{max} = 4533 ppm; P8 - P16: U_{max} = 430 ppm) (Dollinger (14)) are found close to the intersection of NW-SE normal faults with thrust planes genetically related to the Sudetian Fold Movement.

Microscopic and megascopic studies of the black shales revealed numerous patterns pointing to an in-situ redistribution of elements (e.g. fillings in pressure shadows of pyrite, veinlets terminating within black shales, spherulitic quartz). Pressure solution and subsequent deposition in zones with lower

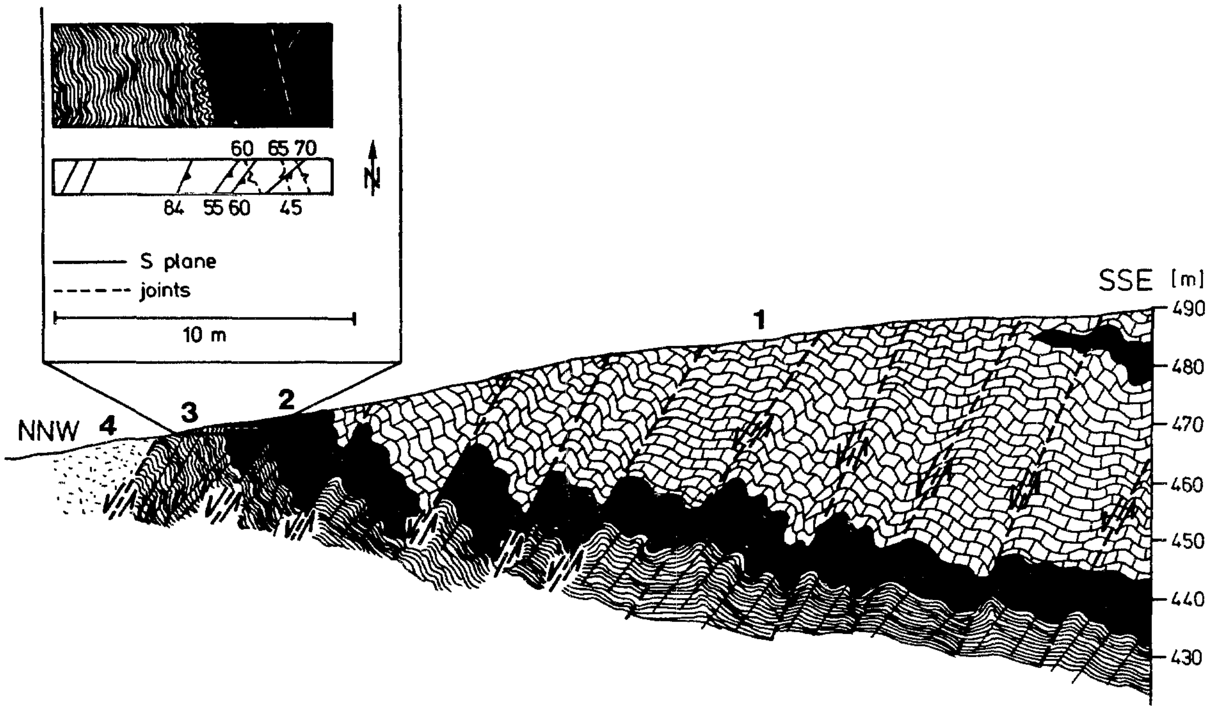

FIG. 4. Profile through the SE limb of Graefenthal Horst near Ottendorf (Fig. 3 B-B). 1: Ockerkalk (Ocker limestone), 2: Black shales of Lower Graptolite Shales, 3: Chert of Lower Graptolite Shales, 4: Ordovician Leather Slate. The profile is based on surface and underground (a) mapping and interpretation of µ-logs from exploration drillings (right hand side).

confining pressure (Ricke rule) plays a major part in the formation of ore mineralization of the Graefenthal Horst. It may also be responsible for the small fault-bound uranium mineralization, although another mobilizing power cannot entirely be neglected when studying this ore mineralization. Along the Thuringian Granite Line (Fig. 3: I Graefenthal Horst, II Lobenstein Horst, III Frankenwald Traverse Zone s.str.) several granite plugs intruded. About 6 km E of the Graefenthal Horst the Weitisberga Pluton (Meinel (15)) was intruded. Ag-rich galena and sphalerite within skarnoid rocks were described by Reh et al. (16). The age of U formation is still ambigous.

3.2. Mineralized structure zones

This type of ore mineralization is not hosted by a distinct well defined stratum rich in uranium. It does not originate from an in-situ redistribution of uranium within one bed, but it is restricted to the 'Varied Group' which has proved to be the source of some other elements (W, Cu, U, C, P) found in Variscan vein-type occurrences (Stettner (6), Dill (17), (18), (19)). Uranium ore mineralization within deep reaching fault zones cutting the rocks of the 'Monotonous Group' are obviously contradicting these assumptions. These lineamentary fault zones mostly associated with some lenses of metabasites or metacarbonates are interpreted to be the trace or a relict of the original source rocks ('Varied Group') which were obliterated by A-subduction (intracratonic) processes (Fig. 5).

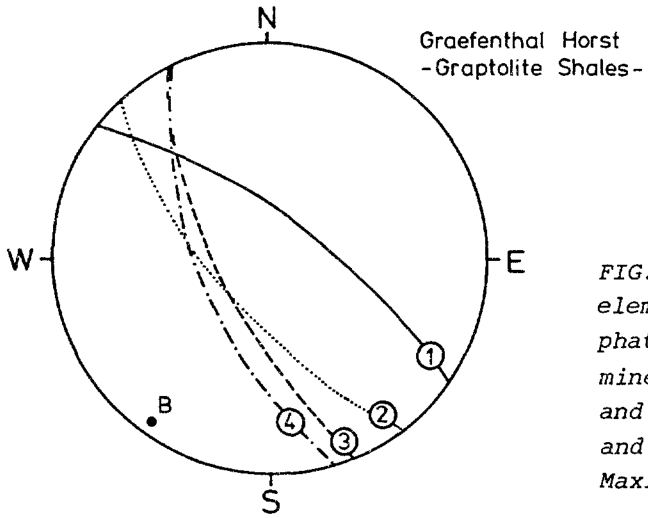

FIG. 5. Summary diagram of structural elements (1: ac girdle, 2: Cu-Ni phosphate-bearing joints, 3: mean of mineralized and non mineralized joints and faults, 4: U-bearing joints and faults, B: B pole of fold axis). Maxima projected on the lower hemisphere.

3.2.1. The Maehring-Poppenreuth-U-district

3.2.1.1. Hoehensteinweg U occurrence

Since this uranium occurrence was described in detail by Bültemann (20), Dill (21), (22), (17), (23), (24), only principal data are added in this paper. The wall rocks consist of biotite mica gneisses ('Varied Group') with conformably intercalated Na-rich granitic mobilizates (Stettner (6), Dill (17)).

Ore mineralization is encountered within steeply dipping NNW to NW striking fracture zones particularly where crossing NW to ENE running granitic mobilizates (Fig. 6). U-bearing fluids penetrated from major faults into wall rocks along foliation. The country rocks are affected by pervasive alteration (sericitization, chloritization, smectitization, to a rare extent kaolinization). Albitization as well as dolomitic episyenitization (Dill (17), (23)) are most common (Tab. II) and are treated in detail in comparison to the other types of episyenitization (e.g. zeolitic, calcitic) in chapter 3.2.2.

The very complex ore mineralization may be subdivided into two major stages, the 'polymetallic' and the 'monotonous U paragenesis' which show remarkable differences regarding mineral association. The typical uranium minerals of the 'monotonous U paragenesis' are brannerite, U-Ti silicates, coffinite, U-leucoxene, 'sooty pitch' and neouraninite (Dill (17)). Pyrite is the only sulfide. The lattice constants of uranium oxides are in the range of a_o: 5428 ($\pm$ 0.002) Å. Contrary to this uranium in the 'polymetallic U paragenesis' is only concentrated in pitchblende (a_o: 5418 - 5436 Å), coffinite, however, was encountered rarely. Pyrite and chalcopyrite are dominating among bismuthinite, nickeliferous pyrite, galena, sphalerite, marcasite, arsenopyrite, Ni-bearing cobaltite, clausthalite, guanajuatite, paraguanajuarite, umangite, native gold and bismuth (Dill (22)). The 'monotonous U paragenesis' is predominantly found in episyenites. Based on radioactive age datings (Carl et al. (25)) the polymetallic (t_1 = 295 $\pm$ 5 Ma, pitchblende), as well as 'monotonous' (t_1 = 336 $\pm$ 17 Ma) U paragenesis are members of the Variscan ore forming cycle, although the brannerite ages cannot be considered very reliable, due to their minute crystals (during preparation wall rock contamination cannot be ruled out). The t_2 ages point to Tertiary and Quaternary redeposition.

3.2.1.2. The Waeldel occurrence

This mineralization (pitchblende, U-leucoxene, coffinite, apatite, Pb-bearing molybdenite, impsonites) is bound to a NS running quartz vein (Guba (26),

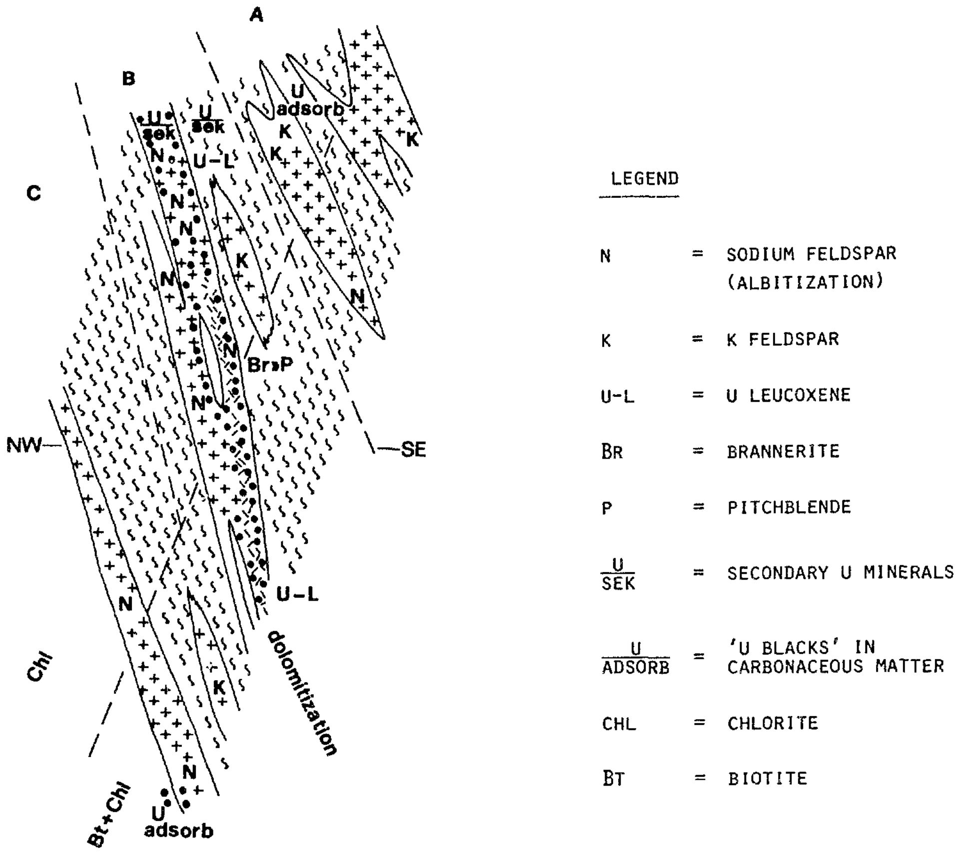

FIG. 6. Typical ore body of Hoehensteinweg U-occurrence subparallel to granite layers conformably intercalated among mica schists (without scale; proprietary), Dill (23).

Dill (27), (28), (29)). It is suggested to belong to the 'monotonous U paragenesis', inspite of the presence of sсme sulfides, e.g. galena which did not originate from lead of the U decay (Dill (28)). The galena (Ag: 12,200 ppm, Bi: 28,900 ppm, Sb: 400 ppm) resembles that from Altrandsberg U occurrence (chapt. 3.2.4.). This katathermal sulfide mineralization appears to be very significant for those quartz lodes at the western edge of the Bohemian Massif (see Fig. 1, F, G).

3.2.1.3. Griesbach U exploration sites

South of Mæhring near Griesbach cordierite K-feldspar biotite sillimanite gneisses with intercalated intermediate to granitic plutonic mobilizates were drilled and an uncommon type of episyenite was found. Quartz mobilizates were replaced by heulandite and stilbite, on account of lower P_{CO2} compared to Hoehenstein. No metacarbonate horizons were mapped in that region, while metacarbonates were penetrated in the deeper lying rock series of Hoehenstein U occurrence (Richter et al. (30)). Zeolites are not considered to be a positive ore guide (U_{max}: 100 ppm).

3.2.2. The Falkenberg-Granite-U-district

The late Carboniferous Falkenberg Granite is the major intrusive body among the plutonic complexes (e.g. Steinwald Granite, Mitterteich Granite, Leuchten-

TABLE II. GEOCHEMISTRY OF FRESH (*) AND ALTERED (**) GRANITIC MOBILIZATES FROM HOEHENSTEINWEG AND FALKENBERG (SEE ALSO FIG. 6) WITH MINIMUM, MAXIMUM AND MEAN VALUES

(A. HOEHENSTEINWEG; B: FALKENBERG)

A.

		MIN	X *	MAX	MIN	X **	MAX
WTG %	SiO_2	54.89	62.53	67.53	49.97	56.24	61.92
	TiO_2	0.06	0.09	0.19	0.07	0.13	0.26
	Al_2O_3	17.69	20.12	23.82	17.75	19.74	21.70
	Fe_2O_3	1.27	2.72	4.16	1.88	1.91	3.57
	MnO	0.02	0.025	0.03	0.03	0.26	0.43
	MgO	0.76	1.63	2.57	1.04	2.48	4.04
	CaO	0.62	0.82	1.38	0.75	2.72	4.71
	Na_2O	4.85	5.78	6.37	4.12	6.67	8.08
	K_2O	2.30	2.87	4.48	2.08	2.64	3.55
	P_2O_5	0.43	0.64	1.12	0.51	0.69	0.84
PPM	Ce	6	17	27	21	23	26
	Y	5	13	19	14	21	33
	Zr	15	22	27	10	39	68

CORRELATION COEFFICIENTS R => ± 0.5
SiO_2 : CaO R = - 0.753
SiO_2 : P_2O_5 R = - 0.566

* = FRESH GRANITE MOBILIZATES
** = ALTERED GRANITE MOBILIZATES

B.

		MIN	X *	MAX	MIN	X **	MAX	LIEBENSTEIN
WTG %	SiO_2	69.28	71.02	73.03	55.33	63.84	69.78	70.17
	TiO_2	0.36	0.42	0.47	0.52	0.60	0.70	0.20
	Al_2O_3	13.34	14.38	15.47	14.44	16.08	19.96	15.50
	Fe_2O_3	2.12	2.39	2.48	1.45	2.93	5.41	1.46
	MnO	0.04	0.05	0.06	0.02	0.08	0.36	0.03
	MgO	0.43	0.46	0.54	0.62	1.33	3.27	0.40
	CaO	0.84	1.02	1.25	0.55	1.87	7.30	0.93
	Na_2O	2.99	3.12	3.29	2.42	2.82	3.18	3.29
	K_2O	3.79	5.67	5.81	5.20	6.57	7.91	6.25
	P_2O_5	0.28	0.31	0.34	0.34	0.38	0.51	0.23
PPM	Ce	90	104	130	66	164	427	53
	Y	12	18	20	17	25	34	11
	Zr	162	187	230	225	253	301	101

CORRELATION COEFFICIENTS R > ± 0.5
SiO_2 : CaO R = - 0.679
SiO_2 : U R = - 0.962
SiO_2 : K_2O R = - 0.930
K_2O : U R = + 0.924
TiO_2 : U R = + 0.635

* = FRESH GRANITE
** = ALTERED GRANITE

berg Granite) in Northern Upper Palatinate. Only in the Falkenberg Granite significant U concentrations were discovered. The host granite is composed of different varieties (granodiorite, granites fine-grained to coarse grained, aplites, pegmatites, dikes). The muscovite cooling ages (314 ± 5 Ma) and biotite cooling ages (303 ± 3 Ma) recomputed by H. Kreuzer (cited Dill (28)) are terminating this fault-bound mineralization versus older ages of formation.

Feather-like ore shoots are observed at the N edge of WNW trending quartz veins (Gudden et al. (3)) in the Falkenberg Granite. Most of these U concentrations are characterized by intensive weathering zones (Haid, Rothenburg, Erkersreuth, Schoenthan, Lengenfeld) which contain autunite, uranophane, torbernite, uranocircite and phospuranylite. They were previously believed to be of hypogene origin (Ernst cited Gudden et al. (3)).

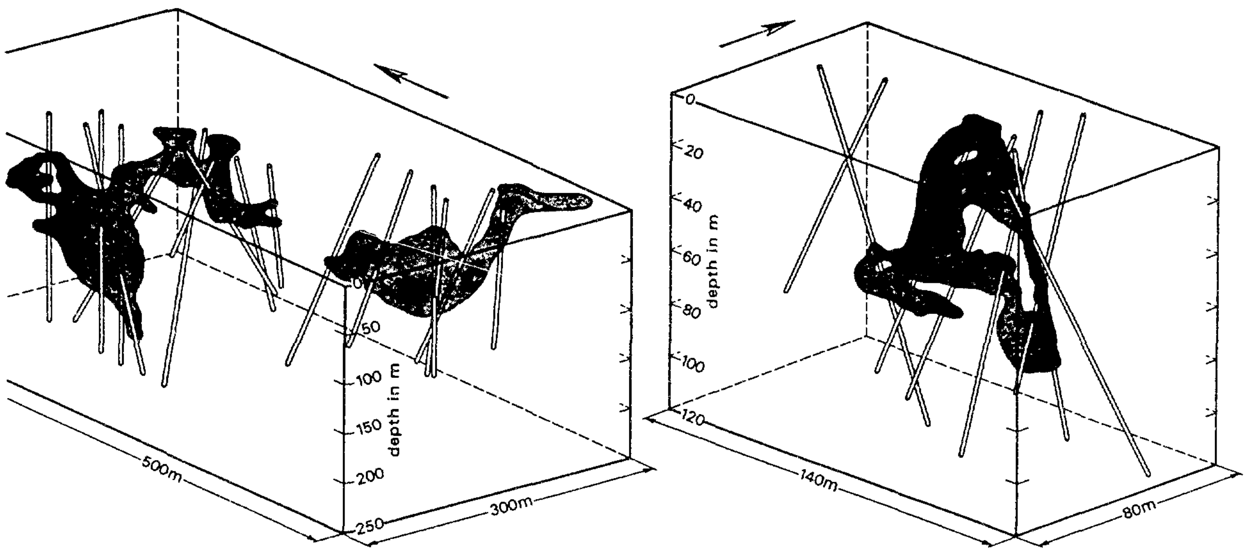

FIG. 7. Ore shoots from Falkenberg U prospect (Gudden et al. (1)) evaluated by drillings drawn in the block diagram.

The only evidence for per ascensum U ore mineralization are badly crystallized U oxides and decomposed U titanates which first were described by Ernst (Strunz (31)). This 'radioactive anatase', a decomposition product of brannerite ('U leucoxene'), clearly points to the affinity of the 'monotonous U paragenesis'. All U mineralizations from the Falkenberg Prospect display very irregularly shaped ore shoots (Fig. 7), (Gudden et al. (1)) and commonly are rimmed by alteration haloes (Table II) composed of sericites, chlorites (three generations), carbonates, secondary quartz and hematite. According to similar types from the Central Massif/France these skeletal granites were named 'episyenites'. By almost total removal of quartz from that rock its composition is shifted from the field of 'granite' into that of 'syenite'. Plagioclases are albitized, chloritized, sericitized, sideritized and calcitized. Biotite is replaced by chlorite and sericite, quartz by carbonate and sericite. Along hairline cracks muscovite (3rd generation), hematite and spherulithic quartz formed. Neither apatite nor zircon or monazite were in any way corroded by these alteration processes, so that an in-situ redistribution can clearly be ruled out. Another mineralogical property of apatites merits special attention. The phosphate crystals are zoned and pigmented by dark matter. These dark inclusions were also found at Hoehenstein (Dill (21)) as well as the Waeldel (Dill (28)), where carbonaceous matter is finely disseminated all over the whole vein. Dollinger (32) described similar phosphates from Hauzenberg Granite which was intruded into metamorphic terrain abundant in organic matter. These properties may shed some light on the 'protore' of that U occurrences. The metabiolite-bearing members of the 'Varied Group' (Dill (18)) are thought to be the most fertile primary environment for preconcentration not only for U but also for W.

The temporal sequence of that alteration is as follows:
muscovite I ⟶ chlorite Ia ⟶ chlorite Ib ⟶ chlorite II ⟶ siderite/calcite ⟶ spherulitic quartz ⟶ chlorite III. Porosity is increased in the carbonate stage. Subsequent processes (e.g. secondary quartz) reduce pore space, so that only prior stages are favourable for ore concentration. In Fig. 8 an outline on different types of episyenitization is presented. In Falkenberg Granite K_2O and SiO_2 are negatively correlated ($r = -0.930$). Quartz was replaced to a large extent by sericite. The less negative correlation between SiO_2 and CaO ($r = -0.679$) is due to the variety of Ca-bearing minerals showing different behaviour during quartz replacement (e.g. siderite, calcite, plagioclase, apatite). The good correlation between K and U ($r = +0.924$) may errone-

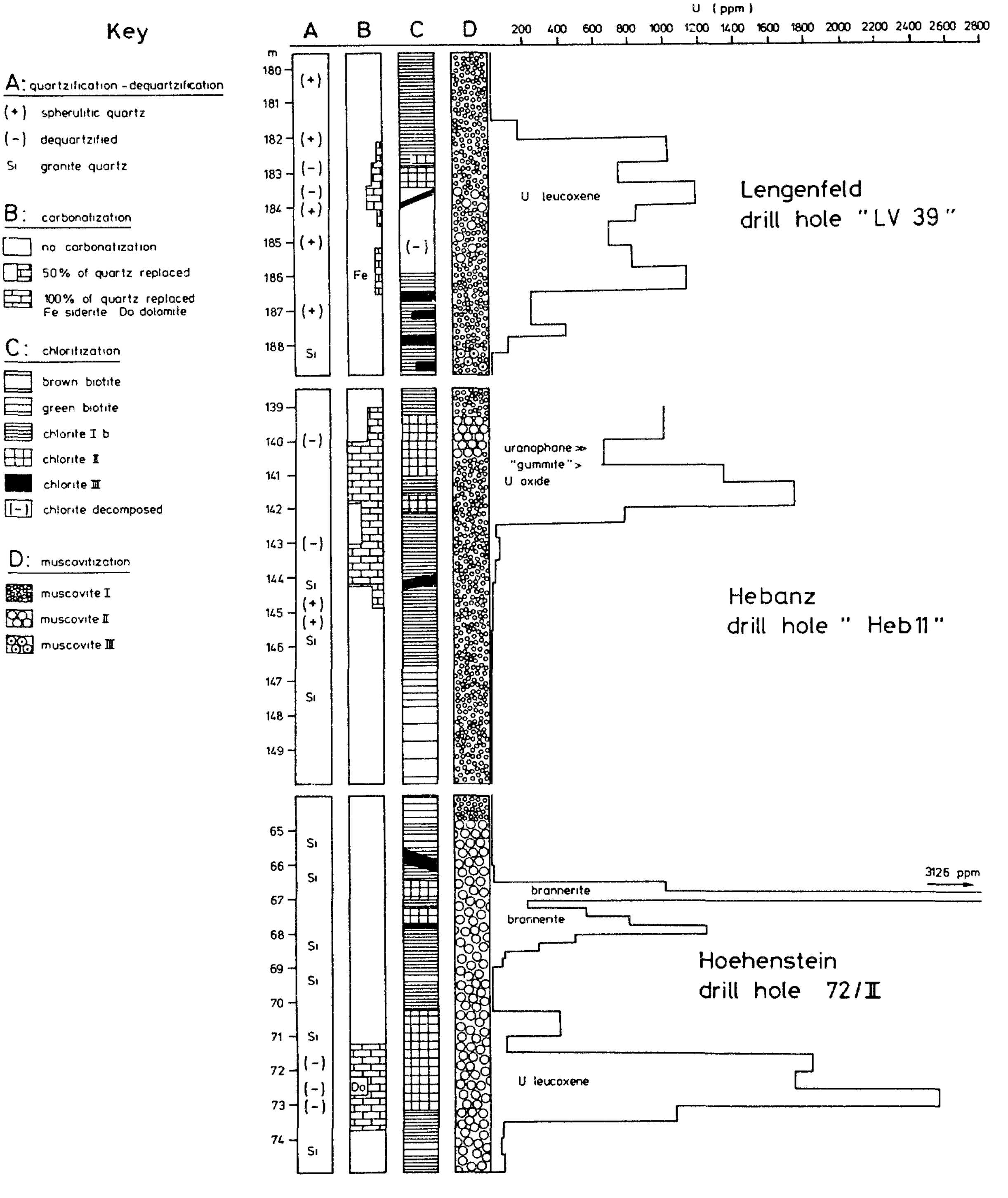

FIG. 8. Drill core section through altered ('episyenites') and U mineralized granites and quartz mobilizates (Lengenfeld/ Falkenberg, Hebanz/Großschloppen, Hoehenstein).

ously lead to the conclusion that there should be a syngenetic relation between uranium mineralization and dequartzification. There is a hiatus between wall rock alteration and U mineralization. Percolating fluids discharged (decrease of pressure) within these vugs and U was trapped like crude oil within porous limestone. This fault-bound wall rock alteration has to be genetically separated from the autohydrothermal post-granitic alteration which is very common in all Variscan granites from NE Bavaria (Dill (1)).

3.2.3. The Schwarzach area

East of the Woelsendorf-Nabburg fluorspar mining district, numerous small U occurrences are aligned along the SE prolongation of the Franconian Line (Fig. 1). The country rocks (biotite-sillimanite-cordierite-gneisses, calcsilicates, orthogneisses and metabasites) are assumed to belong to the Upper Proterozoic 'Monotonous Group' (Stettner (33)). Anatectic pegmatitic and granitic mobilizates formed subparallel to the foliation of the gneisses. After the Variscan regional metamorphism this region was intruded by the older granites (349 + 11 Ma) (Blümel (34)). The terrain was intersected during the Late Variscan Movement by lineamentary fault zones. In the Schwarzach Area U mineralization is located along short termed NW-SE running faults. The only alteration minerals are sericite, chlorite, nontronite, anatase and some calcite. Typical episyenites are missing. The major U minerals (Fürst et al. (35), Dill (22)) are fourmarierite, vandendriesscheite, uranophane, autunite and torbernite. Spheroidic pitchblende is (a_0 = 5415-5, 427 Å) infiltrated by younger sulfides (pyrite, chalcopyrite, chalcocite, marcasite, arsenopyrite, berzelianite, umangite, klockmannite, cuprite and native copper). The mineralization itself as well as the low reflectance of the pitchblende point to low temperature conditions. The age of formation, due to the primary intercept in the concordia plot (Carl et al. (36)) at 361.6 $\pm$ 12.6 Ma (see also age of older granites), is Variscan. The second intercept points to redistribution at the turn Plio-Miocene (6.3 $\pm$ 0.5 Ma) and during Quarternary time. This ore mineralization akin to the 'polymetallic U paragenesis' is called mineralized structure zone. It resembles that mineralization described by Boitsov (37) from the Labe Lineament (CSSR).

The Altfalter U mineralization discovered by Fürst et al. (38) is the 'link' between the 'mineralized structure zones' from the Schwarzach area and the 'vein-type deposits s.str.' from Woelsendorf-Nabburg (chapt. 3.3.). Though lacking any fluorite and baryte it is located along the 'Great Bavarian Quartz Lode (= Pfahl)' within the fluorite mining district. It strikes obliquely (75°/steeply dipping SSE) to the prominent NW-SE running fault zone. The ore mineralogy consisting of spheroidic pitchblende (a_0 = 5444 Å) pyrite, marcasite, chalcocite, digenite and covellite, but devoid of any sulfides typical for that fluorite mining district (e.g. galena, fluorite, baryte, sphalerite) clearly expresses its relationship to that mineralization of the Schwarzach area. Its age of formation is determined to be 205.9 $\pm$ 2.7 Ma (Carl et al. in prep.) and can be interpreted to be the youngest stage of the 'polymetallic U mineralization', which was rejuvenated along the 'Pfahl' within post-Variscan/Alpine time.

3.2.4. Uranium occurrences along the SE branch of the 'Pfahl' (Great Bavarian Quartz Lode)

Only along the 'Pfahl' which runs about 150 km SE-NW through the SE part of the NE Bavarian Crystalline Basement fault-hosted U black ore mineralizations are to be excepted within the Bayerischer Wald. Near Altrandsberg (Bültemann et al. (39)) a U mineralization with U oxides, coffinite and some sulphides was found by drilling. U oxides are very similar to this from Hoehensteinweg described as 'neouraninite (Dill (21)). Besides these U minerals, pyrite, chalcopyrite, galena, sphalerite, native silver, fahl ore, baryte and fluorite were found by Hegemann (40). The last-mentioned sulfides would contradict any classification as 'monotonous U paragenesis', but they have to be considered separately from the real U mineralization (see also Waeldel 3.2.1.2.). The galena shows a weak anisotropy and yields large amounts of Bi (11,000 ppm), Ag (3847 ppm) and some Sb (160 ppm) which are responsible for that anomalous anisotropy. This trace element content is well consistent with the assumption of high temperature of formation (Schroll (41)). The results resemble those from Waeldel U occurrence. Both sulfides are only of mineralogical importance.

During recent exploration work in the southeastern-most branch of the 'Pfahl' near Grafenau and along faults parallel to the 'Pfahl' which cut the Hauzenberg Granite some U mineralizations were discovered. Though being not followed up by further exploration work due to their small size they are of genetic importance. The 'Pfahl' is only mineralized where crossed by some other deep reaching fault zones (see Fig. 1). The ore mineralization shows remarkable differences as to its mineral assemblage. The Grafenau U mineralization consists of sooty pitchblende and U leucoxene (?) with minor sulfides (marcasite, galena, pyrite). The botryoidal pitchblende within the Hauzenberg Granite which is penetrated along shrinkage cracks by sulfides clearly resembles the 'polymetallic U mineralization' while the mineralization near Grafenau which was encountered within biotite gneisses of the tectonized wall rocks of the 'Pfahl' may be accounted to the 'monotonous U paragenesis'.

3.2.5. The Großschloppen-Hebanz-U-district

This is the only U ore mineralization actually of economic importance within the Saxothuringian Zone. It is treated in a special paper (Dill & Kolb, this volume), and will, therefore, only be mentioned for completeness. It is genetically attributed to the 'mineralized structure zone' bearing predominantly the 'polymetallic U paragenesis' and to a lesser degree minerals of the 'monotonous U paragenesis'. Episyenitization plays a major part particularly in the Hebanz Structure.

3.3. The vein-type U occurrences s.str.

In the Woelsendorf-Nabburg fluorite mining district only the Hermine Mine is worked for fluorite. Six veins (Erika, Erna-Anna, Heisser Stein, Johannes-Shaft, Marien-Shaft) in the central area among 50 veins known for fluorite in this 15 km long strip parallel to the 'Pfahl' contained U black ore minerals (Ziehr (42)). The veins predominantly cutting granites of the Naab-Gebirge are mineralized with fluorite, mostly fetid fluorite (= Stinkspat), quartz and baryte. Megascopically galena, sphalerite, hematite, pyrite, some chalcopyrite are discernible. Selenides, arsenides and some native elements (Strunz et al. (43), Seeliger et al. (44)) were only detected by ore microscopy.

Among U minerals pitchblende exceeds coffinite and brannerite is only present to minor quantities. Uraninite was first described to be included by pitchblende (Strunz et al. (43)). It resembles that U mineral from Hoehenstein which was described as 'neouraninite'. The lattice constants of the U oxides from Marien-Shaft are a_o: 5421, 5458, 5478 Å, Johannes-Shaft a_o: 5.05, 5451, 5414 Å and Heisser Stein a_o: 5478 Å; they point to fairly high temperatures of formation.

This is also indicated by the octahedral shape of fluorspar and by the presence of K-feldspar. An old pitchblende mineralization similar to this of Hoehenstein was annealled and rejuvenated during younger mineralizing stages. The ore mineralization points mainly to the 'polymetallic U paragenesis', though traces of the 'monotonous U paragenesis' are recognizable. Alteration processes like those from Hoehensteinweg or Hebanz (Dill et al. (45)) could also be detected. An intensive Mg metasomatism was observed in some parts of Marien-Shaft Vein (pers. comm. Dr. Hannack, Federal Institute). Age determinations (Carl et al. (36)) yielded a primary age of 295 ± 14 Ma. The principle differences between the U mineralization from Nabburg-Wöelsendorf and the mineralized structure zone are the rejuvenation processes as well as repeated mineralizing stages which gave rise to the formation of different U oxides and which lead to more elevated temperatures of formation.

4. SUMMARY AND CONCLUSIONS

(i) Two principle types of U deposits may be distinguished as to their host rock source relationship. Type I is found within organic matter-bearing anchimetamorphosed to low grade regionally metamorphosed Palaeozoic rocks of the Saxothuringian. Type II is typical for medium to low grade regionally metamorphosed rocks and granites of the Saxothuringian and Moldanubian.
In cases of Type I host rock and source rock are identical. On the other hand fault-bound mineralization of Type II is not restricted to a certain fertile bed but to favourable source rock unit ('Varied Group'). The Type II ore mineralizations are closely related in space and time to the Late Variscan igneous rocks. They have been the mobilizing power. No definite thermal activity may be supposed for Type I ore mineralization.

(ii) Three different structure types may be distinguished:
- Fault zone with stockwork-like ore mineralization
- Mineralized structure zones
- Vein-type occurrences s.str.

(iii) Two different types of ore mineralization may be established. The 'polymetallic U paragenesis' (U occurs in single oxides with variable sulfides, arsenides, selenides of Fe, Cu, Zn, Pb, Ni, Co, Bi, and native elements) is assumed to be genetically connected with the granitic activity itself and its post-magmatic phenomena. The 'monotonous U paragenesis' shows a great variability in U bonding (U titanates, U oxides, U-Ti silicates), pyrite is the only sulfide. Though belonging to the Late Variscan thermal activity, it is probably more akin to the rift processes which started during Late Variscan. Triassic to Jurassic redeposition is proved by age datings.

(iv) Episyenitization (calcitic, dolomitic) is to be separated from the autohydrothermal alteration which most of the subsequent granites of the NE Bavarian Basement underwent. It is genetically associated with Mg metasomatism of metacarbonate-bearing horizons underlying the U occurrences as well as with deep reaching fault zones intersecting this basement block.

(v) Plate-boundaries (first order structures) and small faults crossing them (second order structures) are acting as feader channels and as structural traps.

ACKNOWLEDGEMENTS

I am indebted to BP-Gelsenberg, Gewerkschaft Brunhilde, ESSO Erz, Saarberg Interplan Uran and Uranerzbergbau for assistance. I acknowledge the Geological Service of Bavaria (Dr. Gudden, Dr. Schmid) for providing core samples from exploration drillings for this research programme ('Uranium Concentration Processes and the Origin of U Deposits') which was funded by the Federal Ministry of Technology. Chemical analyses presented in this paper were done by Prof. Dr. Gundlach and Dr. Raschka (Federal Institute for Geosciences and Natural Resources), to whom I express my thanks. Dr. Barthel kindly read the manuscript.

REFERENCES

(1) GUDDEN, H., ECKMANN, W., Die Uranprospektion der Eisenwerkgesellschaft Maximilianshütte in Nordostbayern, Glückauf 106 (1970) 380-387.

(2) DILL, H., On the Formation of the Vein-Type Uranium 'Yellow Ores' from the Schwarzach Area (NE Bavaria, Germany) and on the Behaviour of P, As, V and Se during Supergene Processes, Geol. Rdsch. 72 (1983) 955-980.

(3) GUDDEN, H., SCHMID, H., CARDOSO, J., Uran in Bayern, Geol. Surv. of Bavaria (1974) 605 pp.

(4) DUDEK, A., SUK, M., Zur geologischen Entwicklung des Moldanubikums, Ber. geol. Ges. DDR 10 (1965) 147-161.

(5) ZOUBEK, V., Korrelation des präkambrischen Sockels der mittel- und westeuropäischen Varisziden, Z. geol. Wiss. Berlin 7 (1979) 1057-1064.

(6) STETTNER, G., Der Grenzbereich Saxothuringikum-Moldanubische Region im Raum Tirschenreuth-Mähring (Oberpfalz) und die Situation des uranführenden Präkambriums, Z. dt. geol. Ges. 130 (1979) 561-574.

(7) BESANG, C., HARRE, W., KREUZER, H., LENZ, H., MÜLLER, P., WENDT, I., Radiometrische Datierungen, geochemische und petrographische Untersuchungen der Fichtelgebirgsgranite, Geol. Jb. E 8 (1976) 1-78.

(8) KÖHLER, H., MÜLLER-SOHNIUS, D., Ergänzende Rb-Sr-Altersbestimmungen an Mineral- und Gesamtgesteinsproben des Leuchtenberger und Flossenbürger Granits (NE Bayern), N. Jb. Mineral. Mh. 1976 (1976) 354-365.

(9) DOLLINGER, U., Abschlußbericht über die Uranprospektion in der Konzession Kronach-Ludwigsstadt Part. B. UEBG (1974) 8 pp.

(10) JACOB, K.H., JRUSCH, R., GOCK, E., CORDERO ALVAREZ, M., HUGO, P., SCHULTE, N., MEIER zu KÖCKER, GLAESER, B., TAETZ, F., KRUMBEIN, LORENZ, PICKARDT, W., Technische Nutzbarmachung uranhaltiger Kohlen aus dem Stockheimer Rotliegendbecken, TBH, 17 (1983) 1-7.

(11) DILL, H., First occurrences of some uranium minerals and sulfides in the uranium exploration sites of N-Bavaria, N. Jb. Miner. Abh. 147 (1983) 184-190.

(12) BEHRENS, M., Tektonik im nördlichen Fränkischen Schiefergebirge, Ph. Thesis, Univ. Hamburg (1965) 80 pp.

(13) SCHMID, H., Geochemische Prospektion auf Seltene Elemente in paläozoischen Schwarzschiefern des Frankenwaldes, Erzmetall 33 (1980) 540-545.

(14) DOLLINGER, U., Abschlußbericht über die Uranprospektion in der Konzession Kronach, Part. A, UEBG (1973) 38 pp.

(15) MEINEL, G., Petrographische und petrochemische Untersuchungen zum Charakter der synorogenen Metamorphose im ostthüringer Schiefergebirge, Chem. Erde 31 (1972) 2-92.

(16) REH, H., SCHRÖDER, N., Erze, in: HOPPE, W., SEIDEL, G. (eds.), Geologie von Thüringen, 867-897 (1974).

(17) DILL, H., Geologie und Mineralogie des Uranvorkommens am Höhensteinweg bei Poppenreuth (NE Bayern), Ein Lagerstättenmodell, Geol. Jb. D 50 (1982) 3-83.

(18) DILL, H., Vein- and Metasedimentary - Hosted Carbonaceous Matter and Phosphorus from NE Bavaria (FR Germany) and their Implication on Syngenetic and Epigenetic Uranium Concentration, N. Jb. Miner. Abh. 148 (1983) 1-21.

(19) JUNG, R., HÖLL, R., Wolframvorkommen in Nordost-Bayern, Erzmetall 35 (1982) 142-147.

(20) BÜLTEMANN, H.W., Die Uranvorkommen im ostbayerischen Grundgebirge, Raum Mähring, Krs. Tirschenreuth/Oberpfalz, Z. dt. geol. Ges. 130 (1979) 576-596.

(21) DILL, H., Neue Ergebnisse zur Mineralogie der primären Uranträger auf den Gruben Höhensteinweg/Poppenreuth und Wäldel/Mähring in Nordostbayern mit besonderer Berücksichtigung der Uran-Titan- und Phosphor-Kohlenstoffverbindungen, Geol. Jb. D 42 (1980) 3-39.

(22) DILL, H., Zwei selenidführende Uranmineralisationen aus dem ostbayerischen Moldanubikum und ihre mögliche Bedeutung für die Klärung der Lagerstättengenese, Geol. Jb. D 48 (1981) 37-57.

(23) DILL, H., Plutonic Mobilization, Sodium Metasomatism, Propylitic Wall-Rock Alteration and Element Partitioning from Höhensteinweg Uranium Occurrence (Northeast Bavaria, FR Germany), Uranium 1 (1983) 139-166.

(24) CARL, C., DILL, H., Uranium Disequilibria and Modern Redistribution Phenomena in Alteration Zones in the Höhensteinweg Uranium Occurrence, Uranium 1 (1983) 113-125.

(25) CARL, C., DILL, H., KREUZER, H., WENDT, I., U-Pb dating of U ores in NE Bavaria, Terra cognita B 10 (1983) 195-196.

(26) GUBA, J., Geologie, in: Bericht der Gewerkschaft Brunhilde (1980) 34 pp. (unpublished).

(27) DILL, H., Fund einer uranführenden 'Metakieselschieferbrekzie' in der Grube Mähring-Wäldel (Oberpfalz), Z. dt. geol. Ges. 132 (1981) 299-303.

(28) DILL, H., Lagerstättengenetische Untersuchungen im Bereich der Uranerz-Struktur Wäldel/Mähring (NE Bayern), Geol. Rdsch. 72 (1983) 329-352.

(29) DILL, H., WEISER, T., Eine Molybdänsulfid-Impsonit-Mineralisation aus dem Uranvorkommen Wäldel/Mähring (Oberpfalz), N. Jb. Miner. 1981 (1981) 452-458.

(30) RICHTER, P., STETTNER, G., Das Präkambrium am Nordrand der Moldanubischen Region im Raum Tirschenreuth-Mähring (NE Bayern) und dessen metallogenetischen Aspekte; Lithostratigraphische, petrographische und geochemische Untersuchung, Geol. Jb. D 61 (1983) 23-91.

(31) STRUNZ, H., Die Uranfunde in Bayern 1804 - 1962, Nat. Wiss. Ver. Regensburg (1962) 1-92.

(32) DOLLINGER, U., Das Hauzenberger Granitmassiv und seine Umrahmung, Geol. Bav. 58 (1967) 145-168.

(33) STETTNER, G., Grundgebirge, in: Erläuterungen zur Geologischen Karte von Bayern (1981) 168 pp.

(34) BLÜMEL, P., The western margin of the Bohemian Massif in Bavaria, Fortschr. Miner. 61 (1983) 171-195.

(35) FÜRST, M., KRUPP, R., MÜLLER, R., Die photologische Linearanalyse und ihre Anwendung bei der Uranprospektion in der Oberpfalz, Erlanger geol. Abh. 106 (1978) 33 pp.

(36) CARL, C., DILL, H., U/Pb Datierung an Pechblenden aus dem Nabburg-Wölsendorfer Flußspatrevier, Geol. Jb. D 63 (1984) 59-76.

(37) BOITSOV, E.V., Association of pitchblende and selenides in ore of hydrothermal uranium deposits, Atomnaya Energiga 20 (1966) 46-50.

(38) FÜRST, M., BANDELOW, F.K., Strukturelle und szintollometrische Aufnahme im Ostteil des Wölsendorfer Flußspatreviers/Bayern sowie Untersuchungen über eine Pechblendevererzung bei Altfalter, Geol. Rdsch. 71 (1982) 549-577.

(39) BÜLTEMANN, H.W., HOFMANN, R., Uranium occurrences of Bavaria, Germany (with emphasis on the Bavarian Pfahl of the Altrandsberg District), Ore Genesis - The State of the Art (1982) 426-433.

(40) HEGEMANN, F., Die Bildungsweise des Quarzes im Bayerischen Pfahl, Chem. Erde 10 (1936) 521-538.

(41) SCHROLL, E., Analytische Geochemie II (1976) 374 pp.

(42) ZIEHR, H., Die Uranerzparagenese in den Fluoritgängen von Nabburg-Wölsendorf/Ostbayern, Aufschluß 31 (1980) 62-82.

(43) STRUNZ, H., SEELIGER, E., Erzpetrographie der primären Uranmineralien von Wölsendorf - Erste Feststellung von Coffinit in einer Uranlagerstätte Mitteleuropas, N. Jb. Miner. Abh. 94 (1960) 681-719.

(44) SEELIGER, E., STRUNZ, H., Erzpetrographie der Uranmineralien von Wölsendorf, II. Mitteilung: Brannerit, Lermontovit (?), Selen und Selenide, Ni- und Bi-Begleitmineralien etc., N. Jb. Miner. Abh. 103 (1965) 163-178.

(45) DILL, H., KOLB, S., The Großschloppen-Hebanz Uranium Occurrences - A prototype of mineralized structure zones characterized by desilicification and silicification (1985) this volume.

URANIUM DEPOSIT OF JÁCHYMOV, CZECHOSLOVAKIA

J. Komínek
Československý uranový průmysl, koncern
Příbram

T. Veselý
Uranový průzkum, k.p.
Liberec
ČSSR

Abstract

URANIUM DEPOSIT OF JÁCHYMOV, CZECHOSLOVAKIA

The uranium deposit of Jáchymov (Joachimsthal) lies in the Krušne hory Mountains (Erzgebrige), the NW part of the Bohemian Massif. The geology of the area is built up by metamorphic rocks of the Krušne hory complex and by magmatic rocks of the Variscan Karlovy Vary (Karlsbad) Massif.

The uranium ore occurred within NW-NE trending vein systems which can be subdivided into seven individual groups of veins. Most of these veins are carbonate-pitchblende veins, but there are also carbonate-arsenide and quartz-sulfide-bearing veins. The uranium mineralization is concentrated in individual ore lenses or ore pots, which occur mainly where the dip of the veins is not as steep as usual.

Four different types of ore control can be recognized: besides structural and lithological ore control there seems to exist also a close relationship between the mineralization and the morphology of the granite intrusion and the mineralogical composition of the veins.

The Jáchymov uranium deposit is a good example for a hydrothermal vein deposit of the five element types (Ni, Co, Bi, Ag, U).

1. INTRODUCTION

Since the early sixteenth century the ore deposit of Jáchymov has been mined. An extensive system of dewatering tunnels made it already at that time possible to produce ore from a depth of 400 m. The deposit was mined mainly for silver, but there was also some production of Ni and Co ore. The high days of mining, with some interruptions, lasted until the end of the nineteenth century. After the silver was mined out during the nineteenth century, some uranium mining took place, the uranium being used as raw material for paints. At the end of the last century, the mine was closed down but the discovery of radium and its use in medicine led to a short revival of the mine. After the Second World War, the mine was opened again for the production of uranium. Since then, all activities have ceased and the mine was again closed about two decades ago.

2. GEOLOGY OF KRUSNE HORY

2.1. Regional geology

The uranium deposit of Jáchymov is a typical example for a hydrothermal deposit of the Bohemian Massif. Metallogenetically the Krušne hory district belongs to the Saxothuringian zone, which occurs in Czechoslovakia in the NW part of the intensively tectonized zone of the Bohemian Massif (Fig. 1).

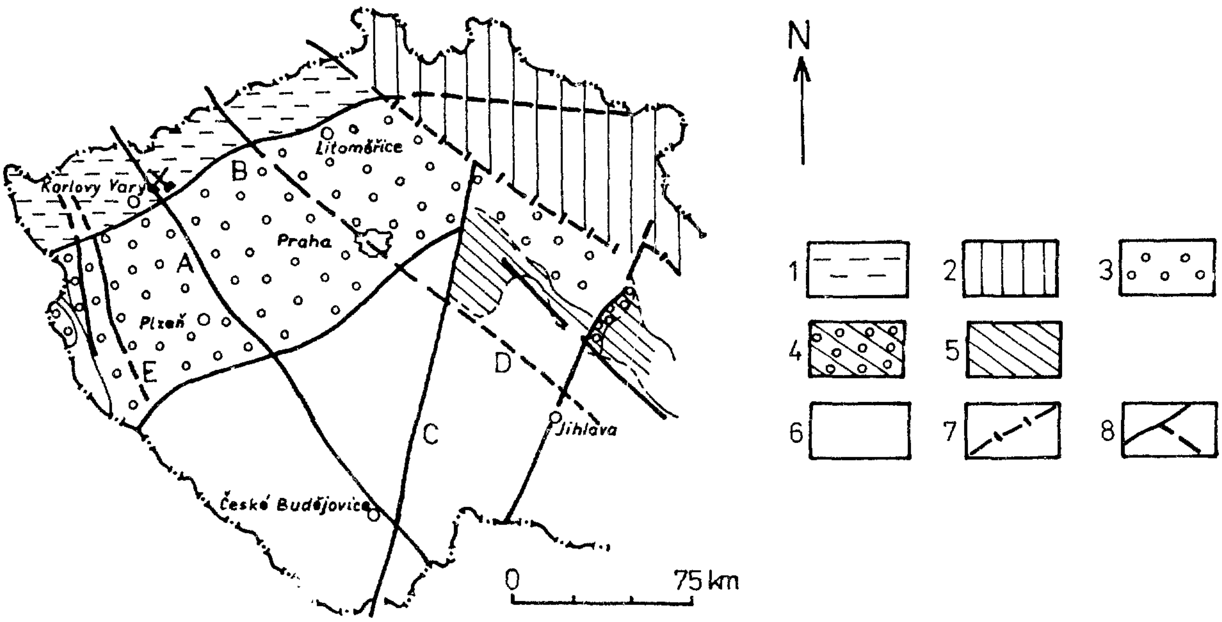

FIG. 1. Western part of the Bohemian Massif (after Mísař et al. (1)); 1. Krušne hory block with the ore deposit of Jáchymov; 2. Lugikum block; 3. Central Bohemian block; 4. Hlinsko zone; 5. Kutná Hora-Svratka zone; 6. Moldanubian; 7. assumed boundary between Lugikum and Central Bohemian block; 8. main fault zones - important for the outlining of the geological boundaries (dashed: assumed); A: Jáchymov fault, B: Litomerice fault, C: Graben zone of Blanice, D: Sazava fault, E: Bohemian Quarzpfahl (giant quartz vein).

Besides the deposit of Jáchymov there are in this area the already mined out uranium vein deposits of Horní Slavkov (Schlaggenwald), the Tertiary stratiform uranium deposits of the Sokolov basins and several small uranium occurrences of different types.

The Krušne hory mining district is situated where two deeply seated fault zones cut each other:

(i) the Jáchymov zone, which has a NW direction, and

(ii) the Krušne hory zone, which runs ENE.

The latter one is parallel to the Litomerice fault further south (Mísař et al. (1)), which is the boundary between the Krušne hory and the Central Bohemian blocks.

The host rocks are mica schists and phyllites of the Lower Palaeozoic and Upper Proterozoic. The granitoid intrusions of the Karlovy Vary Massif have a Late Variscan age. The main structural units of this area are two tectonic blocks, which are separated by the Krušne hory fault zone. The deposit is situated in the northern anticlinal core of the Krušne hory Mountains. The southern block has been down-faulted several hundreds of metres along the Krušne hory fault zone.

The central block lies E of the Jáchymov fault and is characterized by a NE trending fold structure of the Krušne hory anticlinorum. This asymmetric structure shows a gentle dip to NW, but a steep dip to SE. The rocks are phyllites and mica schists belonging to the Prísecnice, Klínovec, Jáchymov and Bozí Dar series. They form several linear asymmetric folds with northerly dipping axial planes (group of authors (1977) (2)).

2.2. Geology of the deposit

The uranium mine area covers almost 45 km² and is situated directly at the crossing of two active, deep seated fault zones. Seven separate vein system groups of different size can be recognized in three different tectonic blocks (Fig. 2).

The main structural elements of the deposit are NW-SE and E-W (or ENE-WSW) trending faults. The most important N-W trending faults are:

- Minor southern fault and central fault, which limit the deposit to the west
- Panorama fault lying in the centre and
- Plavno fault in the east of the deposit

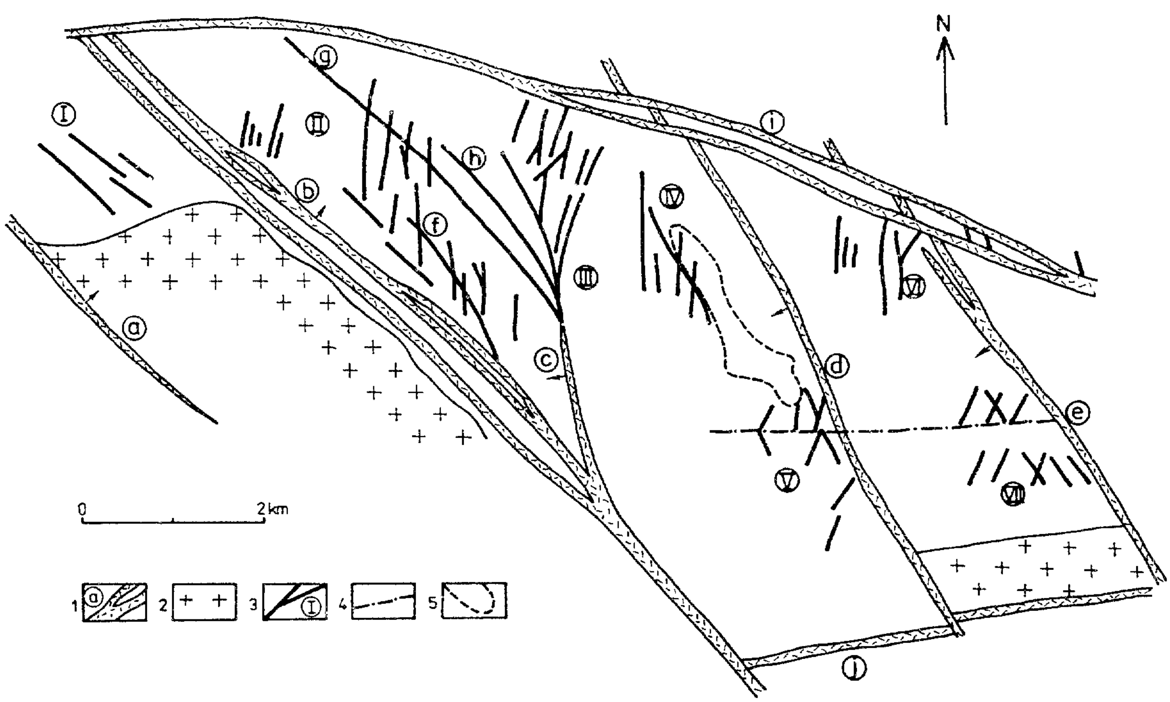

FIG. 2. Schematic map of the fault tectonics of the Jáchymov Camp - projection into the level of the Daniel horizon (630 - 640 m a.s.l.); 1. main fault zones of the deposit: a - minor southern fault, b - central fault, c - midnight fault, d - Panorama fault, e - Plavno fault, f - diagonal fault, g - Arzamasov fault, h - Maria fault, i - northern fault zone, j - Krušne hory fault; 2. granites; 3. vein systems I - VII; 4. Panorama shear zone; 5. boundary of township of Jáchymov.

The strike of these faults varies between 300 and 340°. In the west, the dip is steep (75 - 85°) to E, in the east steep to W. The faults usually are fault zones 20 to 80 m wide, they are filled with clay and mylonitized country rock and usually are filled with quartz and dolomite gangue material. The vertical movement along the fault zones was about 80 to 200 m, the horizontal movement about 100 to 1,000 m. The important E-W (or ENE-WSW) faults are:

° northern fault in the N, and

° Krušne hory fault in the S

Three generations of structures have been identified. The oldest, pre-granitic faults, are characterized by faults along which movements took place in all directions. The faults of the post intrusion phase show downward movements and in the last phase - after the intrusion of the dikes - the NW trending cleavages were opened, preparing the system for small hydrothermal veinlets.

All mentioned faults can be followed up at surface for over tens of kilometres and they also can be recognized underground, except for the Krusne hory fault. In addition, there are numerous less important discontinuous faults and shear zones of different ages, all genetically related to both mentioned fault systems.

The ore deposit is lying within two metamorphic rock units, the Jâchymov series and the Barbara series, which both are members of the mica schist formation (Fig. 3). The total thickness of the mica schists is 900 - 1,000 m. The schists include pyritic and calcsilicate (erlan) horizons, and contain finely disseminated graphitic material. Six different mineral assemblages can be distinguished:

(i) biotite-phlogopite schists

(ii) biotite-sericite schists

(iii) phyllite mica schists

(iv) biotite schists

(v) muscovite and muscovite-biotite schists with amphibole and quartz intercalations

(vi) garnet-muscovite-biotite schists with quartzite and orthogneiss layers

The folding of the area is complex. The Klinove anticlinorum, which comprises the main asymmetric fold system of the mining area, is cut by several cross faults.

The magmatic rocks belong all to the Variscan Karlovy Vary granite Massif. West of the deposit occurs the older porphyritic biotite granodiorite (rock granite), but directly below the ore deposit the younger Erzgebirge-Granit extends. Hydrothermal autometamorphism, a high U/Th ratio and variety of accessory minerals characterize this younger granite.

The hypsometric map of this granite shows very clearly the irregular contact between the granite and the mica schists. The magmatic veins are represented by aplitic granites, aplites, pegmatites, granite-porphyries and lamprophyres. The assumption that each granitic intrusion has its own, individual vein association is most likely correct. The Gebirgs-Granit shows an age of 320 - 340 Ma, the Erzgebirge-Granit of 300 - 310 Ma, and the subvolcanic intrusions and the granite porphyry dikes have an age of 280 - 290 Ma. After the intrusion of the Erzgebirge-Granit, tilting took place along the NW faults. This is well documented by the different depth of the granite contact within different blocks (Fig. 4).

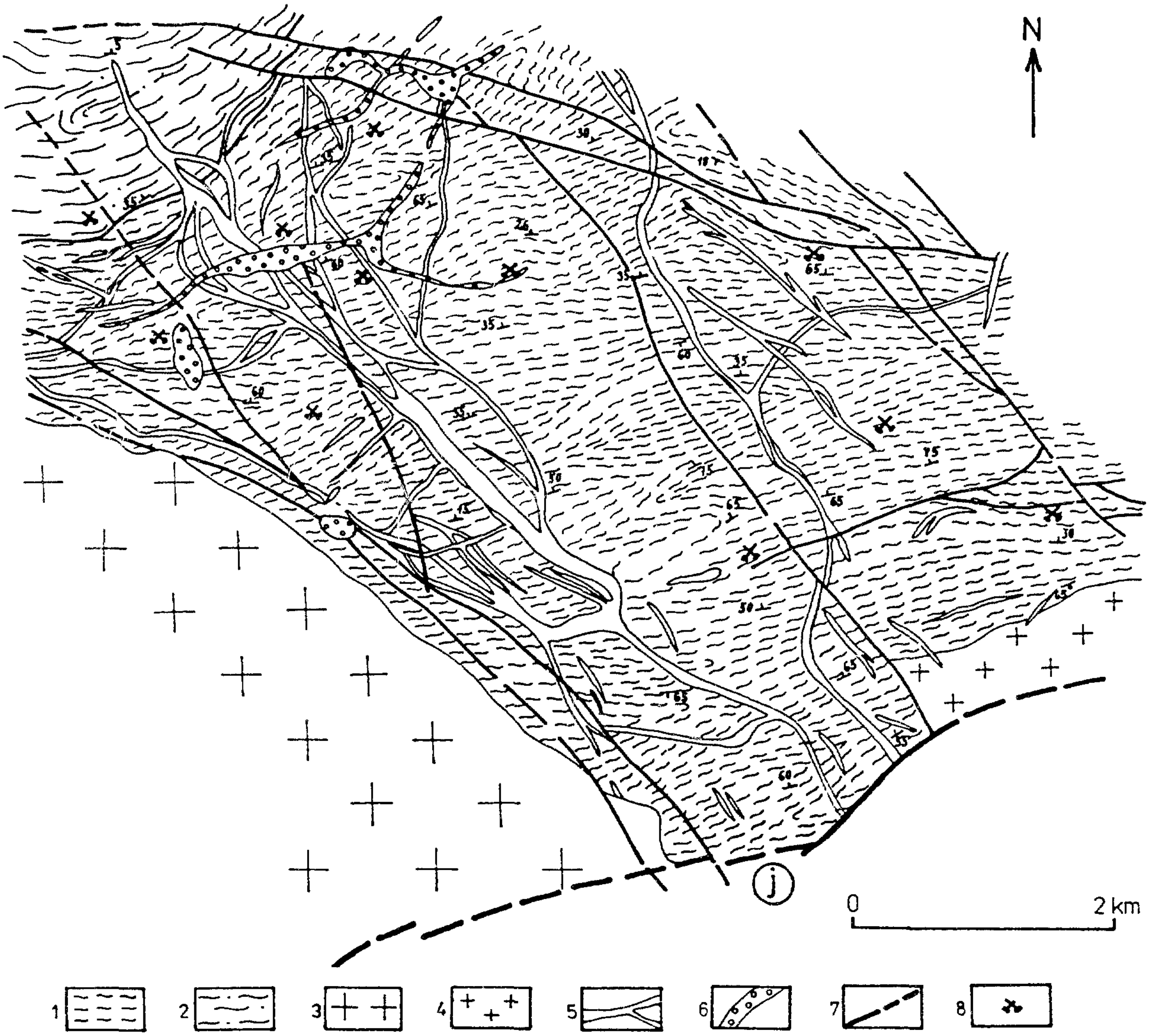

FIG. 3. Schematic geological map of the camp area (group of authors (2)). 1. mica schist series of Jáchymov; 2. Barbara series; 3. Gebirgsgranit; 4. Erzgebirge granite; 5. dikes (granite porphyry, lamprophyre, etc.; 6. basalts and basalt tuffs; 7. main faults (dashed: assumed), j - Krušne hori fault; 8. location of shafts.

The Jâchymov ore deposit is characterized by a U, Ag, Bi, Ni, and Co mineralization. In spite of the fact that these metals occur jointly within individual mineralized veins, the time of precipitation of the different minerals is different.

The mineralized structures recognized underground have been subdivided into two vein systems already 400 years ago:

(i) EW trending veins (so-called dawn veins)

(ii) NW-SE to NE-SW trending veins (so-called midnight veins)

The dip direction of the EW striking axial plane foliation preconditioned the dip of the mineralized veins (dawn veins): in the N of the deposit they have a dip of 60 - 80° to the N, in the S of the deposit they dip with 60 - 80° to the

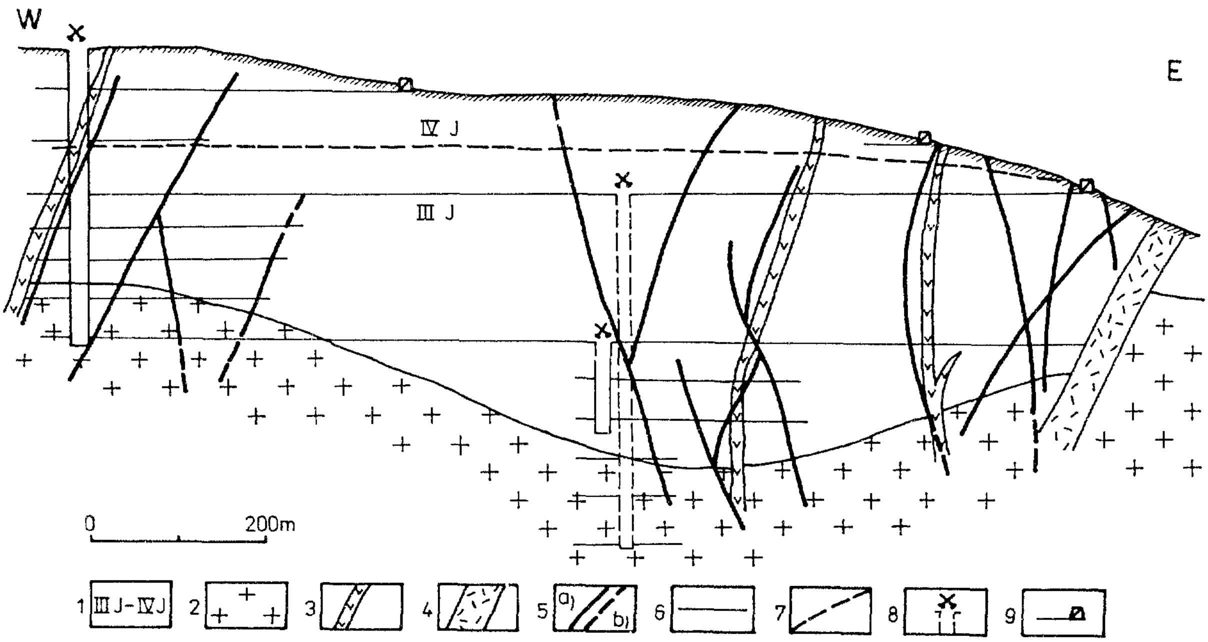

FIG. 4. Schematic cross section through the SW part of the deposit and the Plavno vein system (VII) (after Veselý (3)). 1. the third (biotite-, phlogopite-biotite-albitite schists) and the fourth (muscovite-, muscovite-biotite-, garnet-muscovite- and garnet-muscovite-biotite schists) horizon of the Jáchymov series; 2. Erzgebirge-Granite; 3. lamprophyre; 4. Plavno fault; 5. main structures of the vein system, a - proven, b - assumed; 6. mine levels; 7. boundaries of rock units; 8. shafts; 9. galleries.

S. These veins are younger, have a simple configuration and usually can be followed for a greater distance. They are usually quite wide - about 0.5 m - but contain only some pots with Ag mineralization. They are mostly free of uranium.

The system of the midnight veins, which contain the uranium, are morphologically of a different type. They are irregular open joint systems, have a strike direction of 330° - 20° and dip usually to the W. There is an obvious spacial and genetic relationship between these veins and the NW trending structures. The uranium ore veins are irregularly distributed but concentrate where different joint systems have come together and/or cross each other, and where regional fault zones thin out (Fig. 5) where they cross EW structures (for example vein V and VII) or where faults are cut by down or up thrown blocks (for example vein IV and VI). Only in one single case, no direct relationship between a mineralized vein and a regional fault could be detected.

Some of the veins and vein systems have been explored over a strike length of more than 2.2 km and to a depth of up to 700 m (Veselý (3)).

3. MORPHOLOGY AND MINERALOGY OF THE MINERALIZATION

The development of the ore deposit was a complex and long lasting process during which, in several phases, the following seven different mineral assemblages have been formed:

° garnet-pyroxene with magnetite

° quartz-wolframite-cassiterite

- ° quartz-sulfide
- ° carbonate-pitchblende
- ° carbonate-arsenides
- ° sulfarsenides
- ° quartz-hematite

The first two suites predominate beyond the limit of the Jâchymov U-mines. In the U-mineralized veins, mainly the last five mineral assemblages can be identified. In respect to the uranium-bearing veins two different types, the 'simple' and the 'complex' veins can be differentiated (group of authors (1984) (4)):

(i) The so-called 'simple' veins contain carbonate and pitchblende together with clay and mylonitized host rock material and have a close relationship to structures of a higher order. They have a symmetric shape, are usually 150 - 400 m long, and between 3 and 25 cm wide with exceptions of 50 cm width.
At the contact to the host rock, the veins have discontinuous, comb-like coatings of quartzite-adularia-albite-fluorite aggregates. The centre of the vein is filled with red, coarse crystalline dolomite including relicts of calcite. Pitchblende usually is concentrated at the contact between the comb-like aggregates and the dolomite-forming elongated spherolitic bands of colourful chain-like concentrations either between individual carbonate grains or in the cleavage of carbonates. Coffinite has been found together with comb-like quartz and calcite. The main uranium mineral pitchblende is associated with dolomite 1 and hematite. Dolomite 1 replaces older calcite. Pyrite changes to hematite-forming mineral aggregates together with dolomite, the hematite causing the red colouration.
The carbonate-pitchblende veins formed during two substages: calcite veins with quartz-albite-adularia aggregates together with fluorite, pitchblende 1 and coffinite 1 belong to the older substage, whereas dolomite, hematite and pitchblende 2 precipitated during the later substage. The formation of the important carbonate-pitchblende veins was terminated by the precipitation of smaller amounts of sulfides (galena, sphalerite). Sulfides replaced partly pitchblende and filled cataclastic veinlets.

(ii) Those veins having a more 'complex' nature and a more variable association are characterized by carbonate-pitchblende assemblages and younger minerals associated with carbonate-arsenides and quartz-sulfides. Most of these veins occur within the schistosity and in fractures of a higher order. These veins can be followed for more than 1,000 m and their width varies between 10 and 60 cm. They are often filled with breccias and clay material. In a more complex structural situation, where different veins cut each other, older mineral assemblages also can be recognized. Such veins consist of different generations of quartz and carbonate. The coarse crystalline red dolomite 1 is closely associated with pitchblende, whereas fine grained light coloured dolomite 2, ankerite, and paraankerite include arsenides, baryte, and fluorite. In the younger carbonate-arsenide stage sometimes occur a recrystallized pitchblende 2 and coffinite. It is typical for this type of veins that they also contain Co- and Ni-diarsenides and triarsenides together with native silver, bismuth and arsenic.

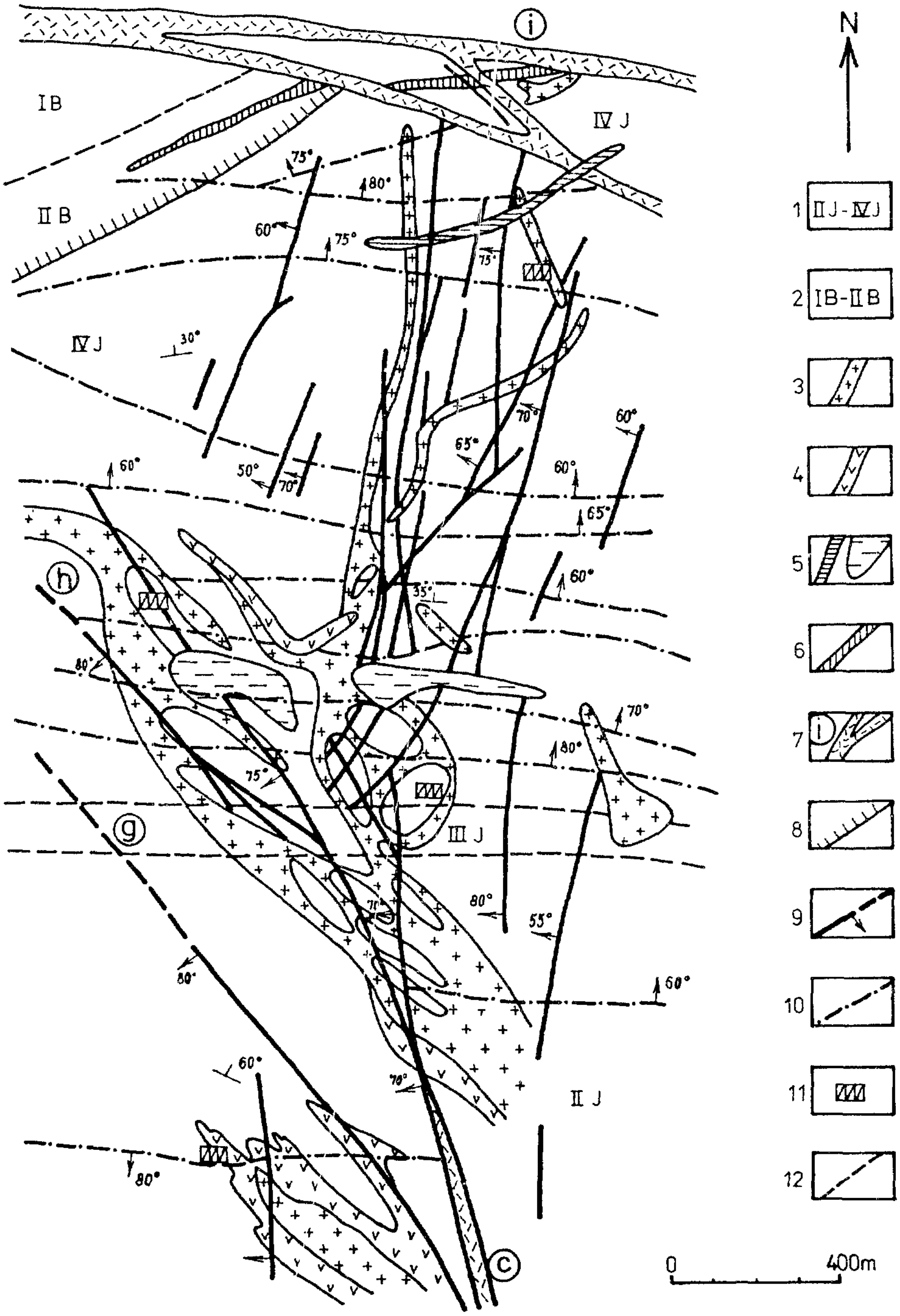

FIG. 5. Schematic geological-structural map of the vein system Rovnost (III), projected into the Daniel level (630 - 640 m a.s.l.) (after Veselý (3)). 1. The second (fine-grained biotite-, sericite-biotite schists and schistose phyllites) to the fourth horizon of the Jáchymov series; 2. the fifth (biotite-, garnet-biotite schists with amphibole layers) and the sixth (muscovite-biotite schists with quartzite and ortho gneiss layers) horizon of the Barbara series; 3. granite porphyry; 4. lamprophyre; 5. basalts and basalt tuffs; 6. ortho gneiss; 7. main faults of the deposit, c - midnight fault, g - Arzamasov fault, h - Maria fault, i - northern fault zone; 8. dislocation fault between the Jáchymov series and the Barbara series; 9. main veins; 10. veins and faults of the EW direction; 11. location of shafts; 12. rock boundaries.

The following vertical zonation can be recognized:

° arsenides and native silver from surface to a depth of 400 m

° arsenides with native bismuth up to 200 - 300 m away from the granite contact

The oldest uranium veins are only preserved in structures of a higher order as these had been closed before younger solutions could affect them. The carbonate-pitchblende veins, which occur in structures of a lower order have a more complex mineralogy as they were repeatedly opened during the mineralizing processes.

In the oxidation zone uranium was depleted and pitchblende changed to secondary uranium minerals. Uranium hydroxides and uranium silicates formed under alcaline conditions, uranium mica, uranium phosphates and arsenates precipitated under acid conditions. The depth of the oxidation zone depends on the weathering profile in well developed shear zones reaching a depth of 300 m.

4. ALTERATION OF THE HOST ROCKS

The pre-ore alteration zones were about 0.5 - 3 m wide. At the footwall this zone usually was wider than at the hanging wall. At the beginning of the metasomatic processes, the dark minerals like pyroxene, hornblende and biotite disintegrated. Ca. Mg, and Fe dissappeared and new minerals like chlorite, pyrite, rutile and phlogopite formed. Calcite is the main mineral at the contact to the veins. The metasomatic processes terminated with an intensive silicification and a depletion of many minerals including calcite, creating a wide zone of quartzification in the metasediments.

The alteration processes connected with the pitchblende mineralization affected only the central parts of the older alteration zones which are usually not more than some cm or tens of cm wide. Pitchblende precipitated together with a recrystallization of albite and adularia in calcite veins, which occur usually in pyritic metasediments. The replacement of pyrite by hematite and the dolomitization of calcite starts in the comb-like quartz crust or within the host rock itself.

5. URANIUM MINERALIZATION

The most important uranium association (carbonate-pitchblende) is irregularly distributed in the various fault and shear zones. Pitchblende, concentrated in elongated lenses, may attain sizes of some metres to several hundreds of metres. Ore lenses larger than 1,000 m² are rare. The width of the lenses varies from a few millimetres to several tens of centimetres. The thickest ore lense occured at the crossing point of the Barbara and Eva II vein.

The ore lenses seem to concentrate mostly in moderately dipping (and also less frequently in horizontal and/or vertical) ore shoots. The richest ore lenses attain a size of up to 100 m x 300 m. In a single vein system occur ore shoots of different size and grade (Fig. 6) and individual ore shoots are separated by steril portions. The ore within complex vein systems has no sharp contact and the width of individual lenses or pots show no relationship to the geometry of the vein, while the distribution and thickness of the ore within simple vein systems are controlled by the geometry of the vein.

The abundance of the ore decreases with increasing distance from the centre of the vein and then the contacts becoming sharper.

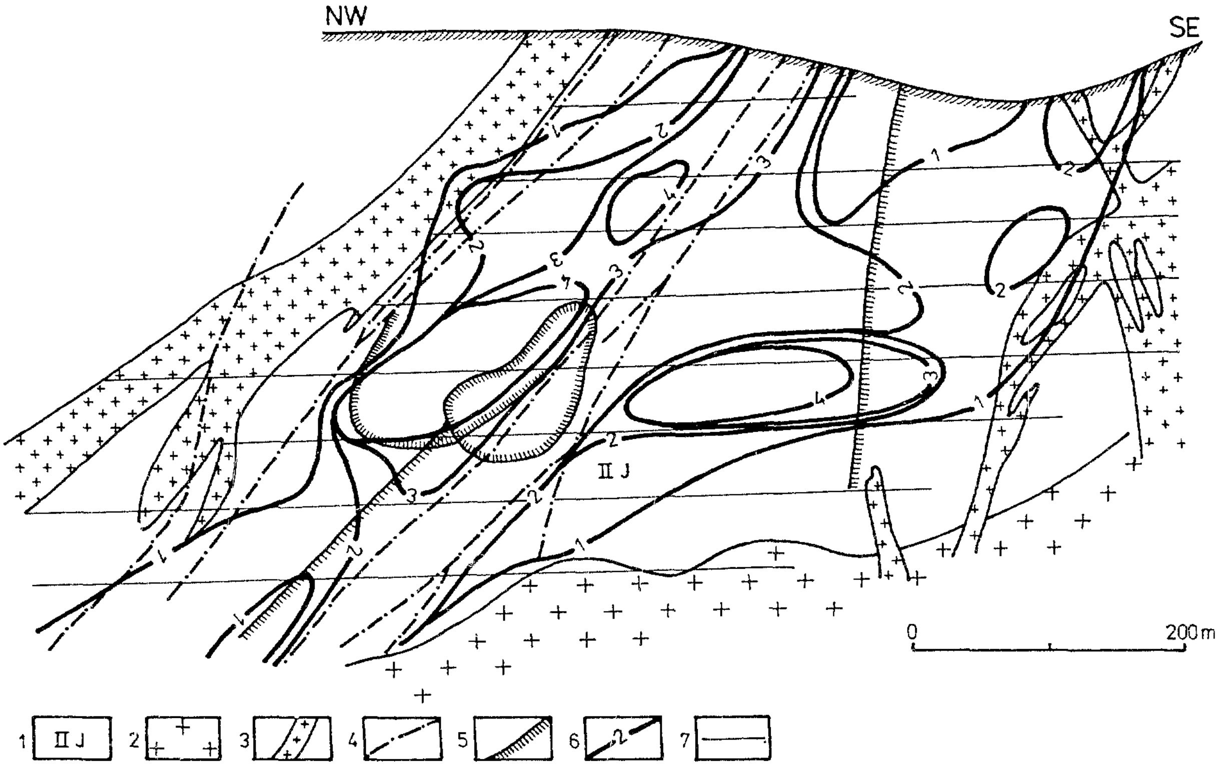

FIG. 6. Schematic cross-section (vertical projection) of the vein A2 of the Abertamy vein system (I) (after Veselý (3)). 1. The second horizon of the Jáchymov series; 2. Erzgebirge-Granit; 3. granite porphyry; 4. veins and faults with EW direction; 5. connecting lines of the splay-veins; 6. isolines of relative ore grades; 7. mine levels.

The uranium mineralization is the result of a medium temperatured hydrothermal process. The age of pitchblende 1 is 270 - 230 Ma, the carbonate-arsenide (and sulfarsenide) mineralization has an age of 150 - 100 Ma.

The age determinations and the geochemical characteristics of the mineralization do not only show a clear spacial but also a genetic relationship with the Erzgebirge-Granit.

6. ORE CONTROL

The uranium mineralization is mainly controlled by the following four factors:

(i) structural control

(ii) lithological control

(iii) control by morphology and distance to the underlying granite and the metasomatism caused by the granite intrusion

(iv) control by mineral composition of the hosting vein

6.1. Structural control

Size and grade of the mineralization within a vein is mainly influenced by a change in width. The richest ore usually occurs where the veins are thickest but it does not necessarily coincide with the geometric centre of the vein. Closer to their margins the mineralization tends to split up into individual veinlets which become more and more barren and filled with younger gangue material.

Another and quite common factor of structural control is the change of the vein's strike or dip direction. Such local changes may increase the ore grade within a vein, yet a more sizeable change tends to influence the larger-scale trend of both ore pots and ore lenses (Fig. 7).

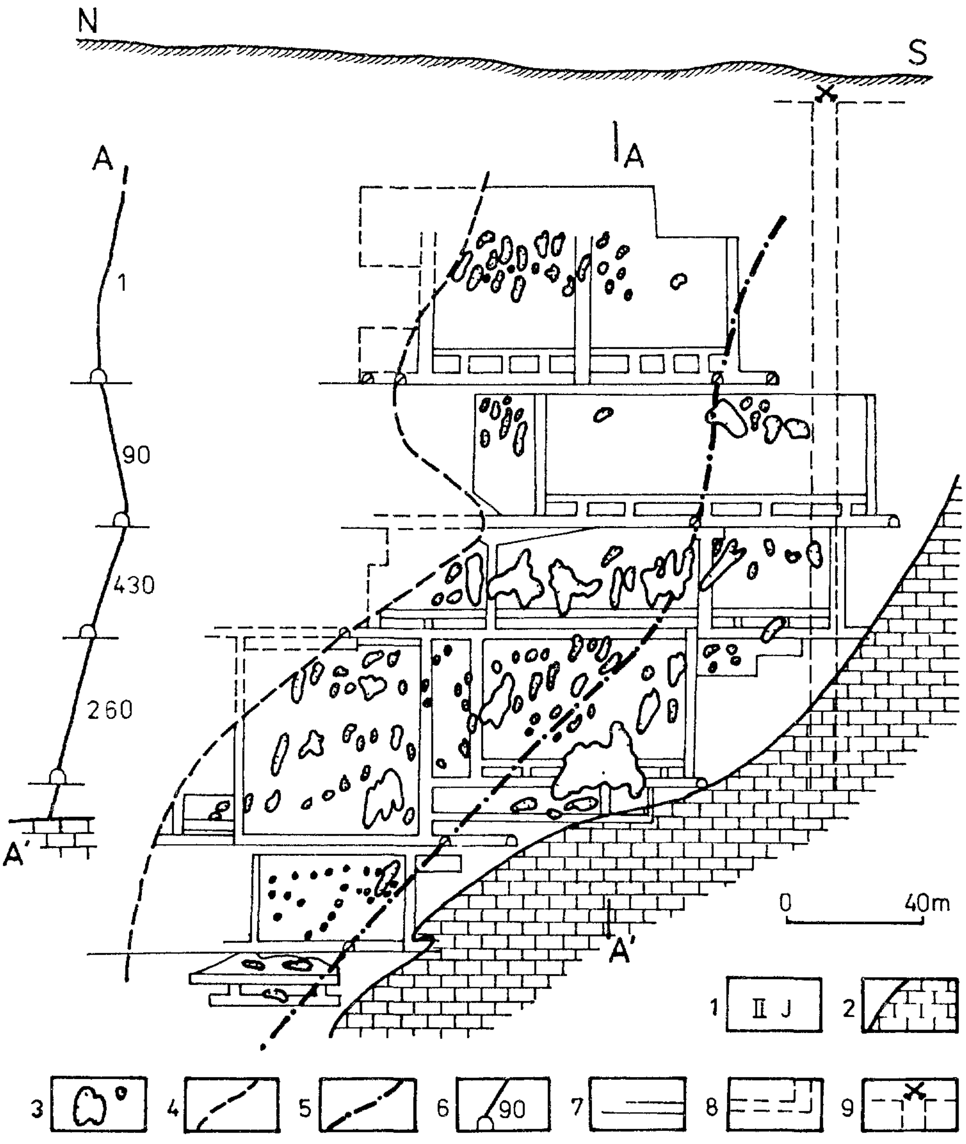

FIG. 7. Schematic cross-section (vertical projection) of the fourth splay vein of the Geschieber vein in the Svornost vein system (IV) (after Veselý (3)). 1. The second horizon of the Jáchymov series; 2. calcsilicates; 3. uranium ore; 4. contact with the Geschieber vein; 5. EW dislocation; 6. relative metal grade values between different levels; 7. mine levels; 8. mine workings beyond the vein; 9. projection of shaft.

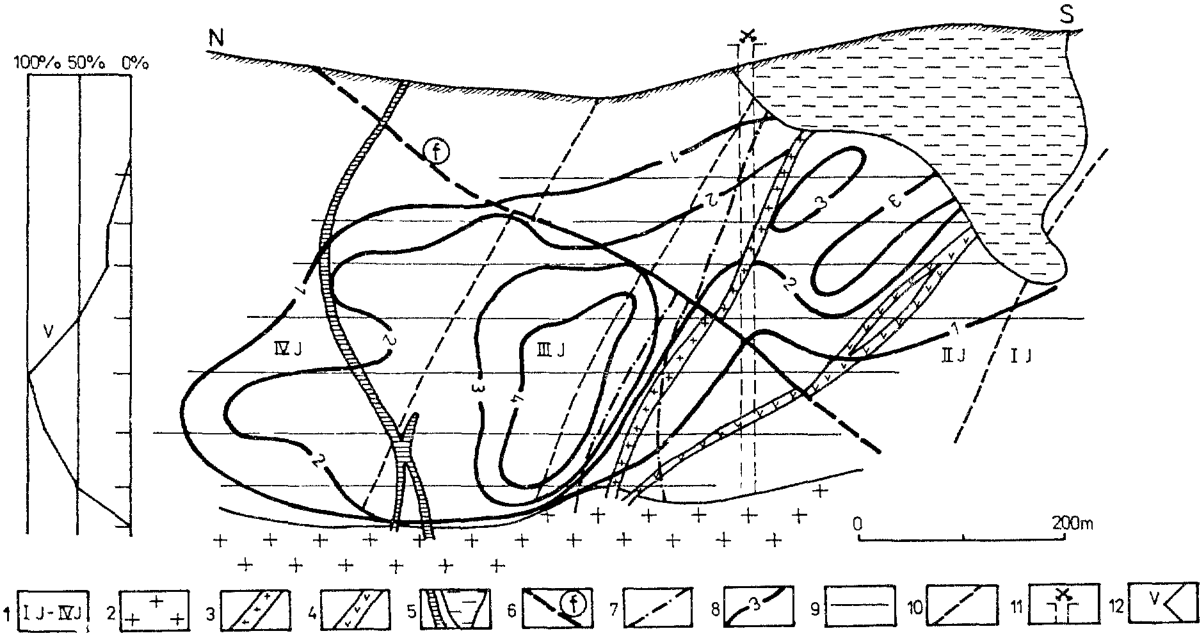

FIG. 8. Schematic cross-section of vein no. 25 of the vein system Barbara-Eva (II) (after Veselý (3)). 1. The first (medium grained, albitized biotite-phlogopite schist) to the fourth horizon of Jáchymov series; 2. Erzgebirge-Granit; 3. granite porphyry; 4. lamprophyre; 5. basalts and basalt tuffs; 6. diagonal faults; 7. veins and faults of the EW directions; 8. isoline of relative ore grades; 9. mine levels; 10. rock boundaries; 11. projection of shaft; 12. curve of vertical metal distribution in relative values.

At crossing points of different structures especially where veins cross EW faults or where different faults join each other lie the richest ore zones. At these locations the ore lenses not only become thicker but also their area increases. Where vein systems split up, especially where one of the splay veins is short (up to 30 m) this short branch is well mineralized. The longer splay, however, is usually not mineralized except at its margins.

The influence of a barrier effect can also be recognized. Especially well developed is this where mineralized veins cut either EW trending dislocation faults or granite porphyry dikes (Fig. 8).

6.2. Lithological control

The rocks surrounding the ore deposits can be subdivided into favourable and unfavourable for the mineralization. Unfavourable units are quartzose mica schists, calcsilicate rocks, granites, granite porphyries, lamprophyres and albitites. Absence of ore in such rocks may be due to their massive texture and their unfavourable chemical composition.

Favourable for the precipitation of uranium are rocks rich in sulfides, Fe-minerals, Ca and Mg carbonates. Especially the positive influence of amphiboles has to be mentioned.

6.3. Control by the spacial distance of the granite

The zone of contact metamorphism surrounding the Karlovy Vary granite Massif is about 20 - 60 m. In areas of depression (of the granite contact), this zone is more narrow, where this contact lies higher, the zone is wider. Recrystallization of the metasediments, formation of new minerals and development of hornfels and massive textures at the direct contact are the main features of this metamorphism.

The granite is surrounded by a U barren zone. In the vein system of Rovnost (III) for example the barren zone above the granite contact is about 120 - 140 m, where the contact is nearly horizontal this zone is 60 - 90 m and close to the depression in the granite this sterile zone is 20 - 25 m. Only in a very few cases the mineralization reaches the granite.

6.4. Control by the mineral composition of the veins

The mineral composition of the veins influences the precipitation of different generations of uranium minerals. Veins filled with red and brown carbonates contain the economically important uranium mineralization characterized by the first pitchblende generation. The less important pitchblende 2 generation occurs only in the younger fine grained and light coloured carbonate veins.

REFERENCES

(1) MÍSAŘ, Z., DUDEK, A., HAVLENA, V., Problémy regionálně-geologisckého clé-neni Českého masivu, Věstník ÚÚG 5, Praha (1983) 305-313.

(2) Group of authors (kolektiv autorů), Krušne hory, západní část 1:50000, soubor oblastních geologických map, ÚÚG, Praha (1977) 40 pp and 9 maps.

(3) VESELÝ, T., Stavba a význam jednotlivých žilných uzlů uranového ložiska Jáchymov, sbor. geol. věd. lož. geol., Praha (1985) (in press).

(4) Group of authors (kolektiv autorů), Československá ložiska uranu, SNTL Praha (1984) 365 pp.

URANIUM DEPOSIT OF PŘÍBRAM, CZECHOSLOVAKIA

R. Petroš, S. Prokeš
Uranové doly k.p.
Příbram

J. Komínek
Československý uranový průmysl, koncern
Příbram
ČSSR

Abstract

URANIUM DEPOSIT OF PŘÍBRAM, CZECHOSLOVAKIA

The uranium deposit of Příbram is the best example for a hydrothermal vein deposit of the Bohemian Massif. It belongs to the Central Bohemian ore district and occurs at the contact between the Central Bohemian granite and weakly metamorphosed sediments of the Upper Proterozoic. The NW-NE trending veins are irregularly distributed. Two types of vein systems can be distinguished: the first is closely associated with NE trending faults, the second type occurs in the continuation of the NW striking structural zone within an anticline of Proterozoic sediments. The mineralization of the veins formed during four phases. The ore deposit represents a classic example of the carbonate-pitchblende ore formation. The main gangue mineral is calcite of different generations, the important ore minerals are pitchblende, anthraxolite and coffinite. Over 50 different secondary minerals have been identified. Main ore control are structural features, whereas lithological ore control can only be recognized on a more regional scale. Besides uranium, the Příbram uranium deposit contains some polymetals and native silver. The age of the mineralization is Late Variscan (270 Ma) and was caused by low temperature solutions. The formation of the deposit is closely connected with the intrusion of Variscan granitoids of the Central Bohemian Pluton.

1. INTRODUCTION

The uranium deposit of Příbram is located SW of Prague in the mining district of Příbram, which is a part of the Central Bohemian ore district. The deposit is the best example for the hydrothermal vein-type deposits of the Bohemian Massif.

In the Příbram district, Ag-, Pb-, and Zn-ore has been mined since medieval times. In the 19th century, pitchblende was first known in this area, and in the vicinity of these classic mines the uranium deposit of Příbram was discovered after the Second World War.

2. GEOLOGY

2.1. Regional geology

In the Central Bohemian ore district, Au, Ag, Pb, Zn, Sb, and U occur in the vicinity of the Central Bohemian Pluton at the boundary between the Teplá-Barran-

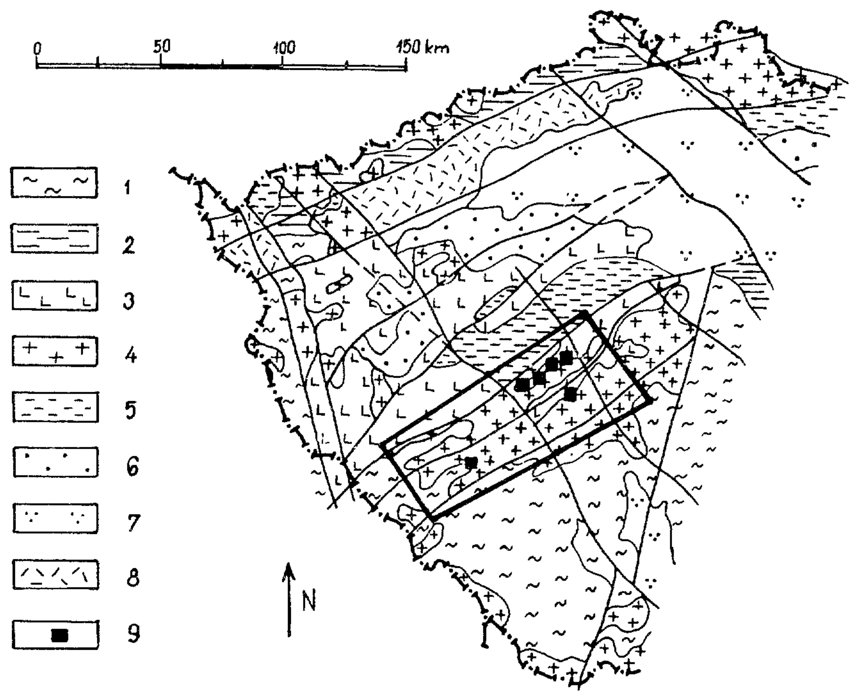

FIG. 1. Schematic geological sketch of the centre of the Bohemian Massif showing the position of the Central Bohemian ore district. 1. Middle Proterozoic (Moldanubian); 2. Upper Proterozoic - Lower Palaeozoic; 3. Upper Proterozoic - Cambrian; 4. granitoid; 5. Lower Palaeozoic; 6. Upper Palaeozoic; 7. Upper Cretaceous; 8. Palaeogene-Neogene; 9. uranium deposits.

dien depression and the Moldanubian block uplands (Fig. 1). The geology of this area is strongly influenced by deep seated structural zones:

- Central Bohemian NE-SW trending fault zone
- NW-SE trending Jáchymov fault zone

The oldest rock formations of the Teplá-Barrandien block lie in the NW part of the area and are of upper Proterozoic age. They are only partly covered by lower Cambrian sediments. The oldest Proterozoic unit is characterized by intercalated horizons of weakly metamorphosed sediments which include spilites, diabase, and amphibolites representing metamorphosed tuffs. In the middle unit occur acid effusive rocks such as quartz porphyries, quartz keratophyres, and also quartzites. The uppermost unit which is usually called the schist unit is composed of metamorphosed flyschoid sediments some showing contact-metamorphic features. Arkoses, arkosic sandstones, conglomerates and shales make up the Cambrian units. All these units have been folded into complex, usually NW trending anticlines and synclines.

The central part of the area is built up by the complex Central Bohemian (granite) Pluton which was intruded along NE-SW fault zones. Different granitoids of variable mineralogical composition, shape and age can be recognized within the pluton. Most of these granitoids have a Variscan age (Bernard and Klomínský (1)).

The eastern and southeastern part of the area consists of gneisses, ortho- and para-amphibolites, and quartzites of the Moldanubian.

The NE and NW trending fault zones belong to the main structural features of the area, which represent the upper parts of deep seated tectonic zones. The Jáchymov fault zone, with its general NW direction, cuts the pluton for over 40 km. The individual faults have a complex shape, are sometimes 100 - 200 m wide and can easily be recognized by their cataclastic features and the hydrothermal alteration zones. In the NW these wide zones split up into 0.5 - 1 m wide individual faults separating undisturbed parts of the granitoids. Not more than 2 - 3 km outside the pluton, the faults wedge out completely and disappear (Fig. 2). The NE-SW faults are well developed and dominate the area's tectonic style. Even the contacts of the intrusions follow this direction. The distribution of the ore deposits within the district is quite irregular.

(i) The Au deposits are in close association with the so-called 'quartz formation' (suite) and occur in the centre of the ore district along fault zones within the down thrown block of metamorphics and granitoids.

(ii) The Ag, Pb, and Zn deposits of the so-called 'polymetallic formation' (suite) are concentrated in the NW part of the district, within the Cambrian which is quite distant from the intrusion. In this area, the NS trending vein zones come close to the important NE faults.

(iii) The uranium ore veins of the 'carbonate-pitchblende formation' (suite) appear in the continuation of the NW trending structures just outside the granite contact, either within upper Proterozoic units (Příbram deposit) or, in the southern part of the area, in the Moldanubian gneiss, and also within the pluton itself. Indications of this mineralization are also found in the shear zones and NW trending veins within coarse grained granitoids. The type of host rock characterizes both the shape and mineralogy of the ore zone.

2.2. Geology of the deposit

A complex geological situation together with an intensive hydrothermal history characterizes the ore district of Příbram, which is 25 km long and about 1 - 2 km wide. In general, however, the ore zones cluster along the granite contact (Fig. 2).

The host rocks are mainly upper Proterozoic schists, which are about 2,000 m thick and can be subdivided into 5 subunits. Above the partly eroded Proterozoic schists, separated by an unconformity, lie polymictic conglomerates, quartz conglomerates, and sandstones of Cambrian age. Both units were folded into a 25 km long anticline (Příbram anticline). Its axial plane dips 30° - 70° SE, the axis plunging up to 30° either to NE or SW (Fig. 2). The SE limb was intruded by granitoid bodies belonging to the Central Bohemian Pluton. The contact zone between the granitoid intrusions and the sediments was cut by many dikes of different composition and directions.

The dislocation faults can be classified by two groups depending on their size and position in respect to the anticline:

° regional longitudinal, diagonal and cross faults

° small longitudinal, diagonal and cross faults

Two important zones, belonging to the regional longitudinal fault type cut off the ore district on the NW. They are 10 and 30 km long and can still be recognized at a depth of 1,5 km without any apparent change, dipping 75° NW. They represent shear zones of up to 50 m width, in which two to three zones of 5 - 20 cm width can be recognized along which movements took place. Repeated movements along these mobile zones resulted in displacements of 300 - 1,200 m vertically and 100 - 200 m horizontally. The regional NW faults belong to the cross faults and they are well developed within the granitoids but wedge out outside the contact zone where the orebodies are situated. The regional diagonal faults are

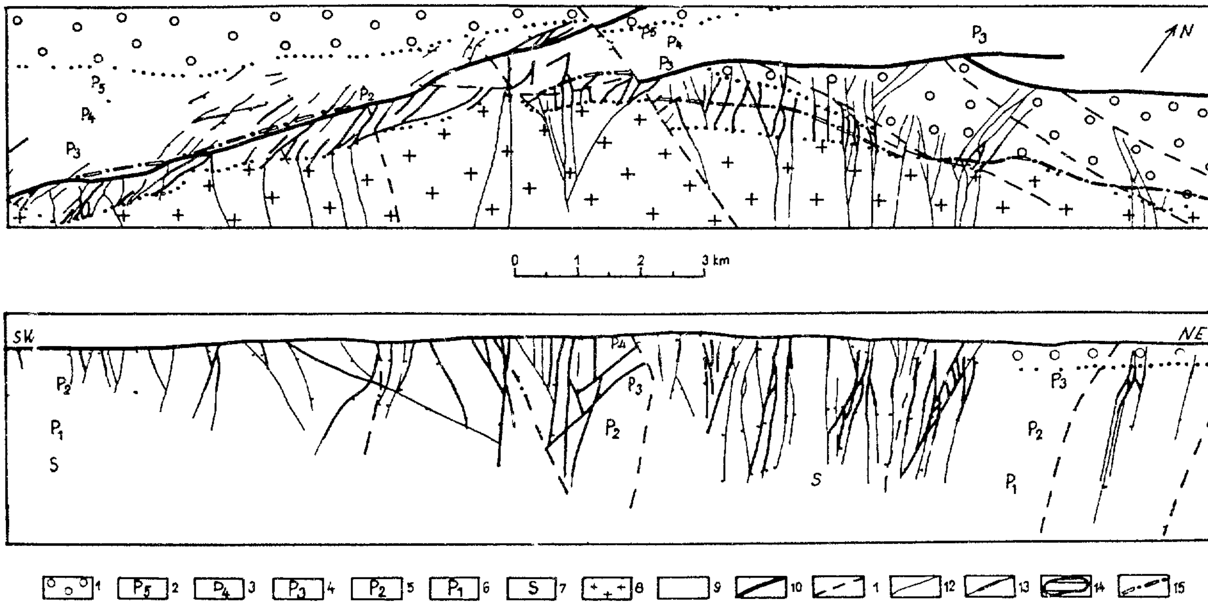

FIG. 2. Geological map and section of the uranium deposit (explanation to FIG. 2, 3, 5). 1. Cambrian sediments, Proterozoic: upper series; 2. sandstones unit P_5; 3. shale siltstone unit P_4; 4. siltstone sandstone unit P_3; 5. conglomerate sandstone unit P_2; 6. siltstone sandstone unit P_1; 7. middle series; 8. granitoid of the Central Bohemian Pluton; 9. rock boundaries; 10. faults of the first order (main faults); 11. mineralized faults; 12. unmineralized faults; 13. faults with uranium ore; 14. orebodies; 15. axis of the Příbram anticline.

found mainly in the centre and in the NE part of the district (Fig. 3). They are 2 - 3 km long and may reach down-dip to a depth of 1,000 m. The main movements along these faults took place before the dikes were intruded. Later movements along these faults were restricted to only a few tens of metres (Petroš (2)).

The smaller faults can be found in the whole district. Three different types can be distinguished:

- mineralized vein structures
- unmineralized vein structures
- dike structures

These faults are tens to hundreds of metres and rarely 1 km long. Movements along these faults were usually small.

Most of the mineralized vein structures have one of the following three directions: 44 % NW-SE, 43 % NS, 13 % NE-SW. The first two, the so-called diagonal and cross veins, cut the foliation whereas the longitudinal ones are parallel to it. Usually, the mineralized veins have a steep dip, except where they are parallel to the foliation (40° - 70°). They have an irregular distribution and may occur in zones or clusters, wherein individual veins are either close to each other or intersect each other.

(1) One group of mineralized veins resulted from the movements along main faults. They follow closely the change of strike and dip of the faults and only rarely branch off these main faults. These veins represent the larger NS and NE-SW faults especially if they join the regional longitudinal faults (Fig. 3). Smaller veinlets of different directions developed during movements along such faults.

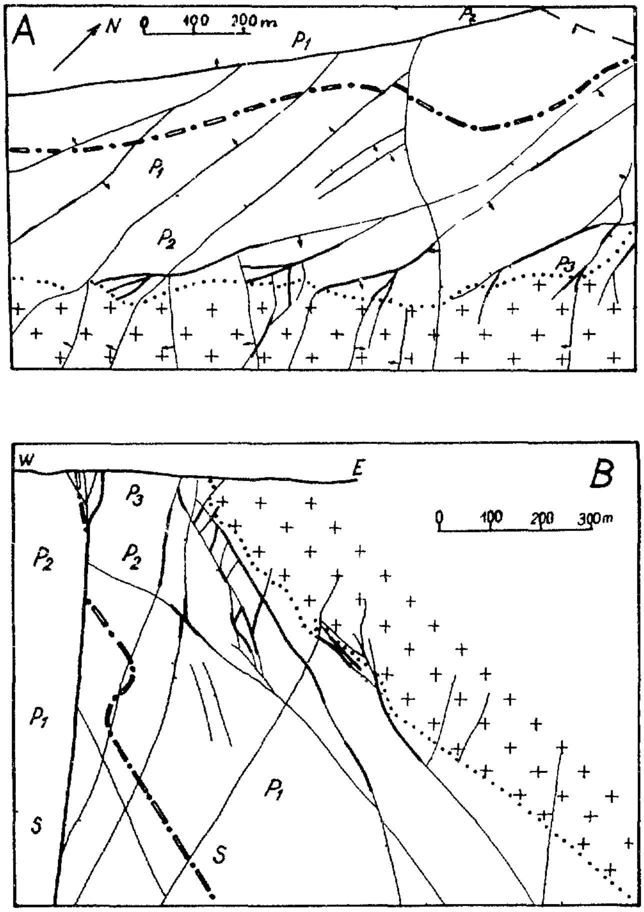

FIG. 3. Geological and structural map (A) and cross-section (B) of a vein associated with longitudinal faults (explanation see Fig. 2).

(ii) There is a second group of veins, which is closely connected with the development of the Příbram anticline in the direct continuation of the structural zone intersecting the pluton. They are best developed in the centre of the anticline, cutting the fold perpendicularly (Fig. 2). As a result of the movements along these faults, small tension vein zones developed in NS direction which were later mineralized.

3. SHAPE AND MINERALOGICAL COMPOSITION OF THE VEINS

The orebodies are complicated systems, which are built up by a series of mineralized cleavages and hydrothermally altered wall rocks. Usually, the width of the mineralization and gangue within the hydrothermally altered breccia zone amounts to about 40 - 50 %. The large veins of more than 500 m length contain gangue material over a width of 5 - 100 cm, and exceptionally up to 12 m; in smaller veins this is less than 50 cm. The shape and size of the ore lenses within a vein depend on local changes in the strike and dip direction of the structures, the type of host rocks, the position of the vein in respect to the anticline contact with the pluton and the orientation of the main faults. The internal structure of the veins shows multiphase movements, and different phases of mineralization and replacements.

4. MINERAL COMPOSITION OF THE VEINS

The mineral association of the veins building up the Příbram uranium ore deposit is a classical example of carbonate-pitchblende ore formation. More than 50 different minerals belonging to different mineralizing phases have been recognized within these veins. The most common mineral is calcite which is of various generations, being classified by the generation groups DK, K1, K2, K3, K4, and K5 (Fig. 4). Calcite usually forms medium to coarse aggregates and vugs. Other important gangue minerals are siderite and dolomite-ankerite. Pitchblende is the most common uranium mineral and is often associated with uranium-anthraxolite. Galena and sphalerite can also be found.

Four different mineral associations of four different mineral phases can be recognized (Komínek and Prokeš (3)):

(i) The siderite-sulfide stage is characterized by siderite, dolomite-ankerite, quartz, galena, sphalerite, and barite, but there are also some chalcopyrite, tetrahedrite, chlorite, and probably also allemontite, skutterudite, löllingite and other minerals.

(ii) At the beginning of the next stage, the calcite stage, the first generation calcite was strongly oxidized during the crystallization of hematite and goethite. Calcite DK and K1 precipitated during this stage accompanied by some sphalerite, galena, chalcopyrite, chlorite, and sometimes native silver.

(iii) During the third stage, the calcite-pitchblende stage, formed the older calcite generation K2 and K3, and then the main uranium ore mineral pitchblende 1 and later K4, the so-called 'ore calcite'. Dolomite, chlorite, and hematite belong also to this stage. Pitchblende occurs as reniform aggregates, fine veinlets as metasomatic pods within calcite DK and K3, and as fine bands along older calcite, or filling older calcite cracks.

(iv) The calcite-sulfide stage is usually represented by younger calcite K5, some uranium-anthraxolite and pyrite. Other more rarely occurring minerals of this stage are: pitchblende 2, coffinite, marcasite, chalcopyrite, tetrahedrite, sphalerite, goethite, montroseite, quartz, chlorite, native silver, pyrargyrite, millerite, nickeline, allemontite, native arsenic, native antimony, safflorite, rammelsbergite, gersdorffite, bornite, chalcocite, palygorskite, pyrrhotine, and others. The existence of all these different minerals can be explained by repeated replacement, dissolution, and recrystallization of older minerals by the younger mineral solutions. Uranium-anthraxolite is a high polymeric bitumen containing pitchblende, coffinite, calcite, and other minerals and forms irregular pods, rounded grains, and veinlets within calcite, and was precipitated directly before or after pitchblende. This uranium complex is always closely associated with pitchblende, which is either cut, surrounded, cemented or metasomatically replaced by the complex.

Coffinite is usually finely disseminated in pitchblende, especially if the latter is associated with uranium-anthraxolite. It occurs as coatings, irregular clusters or as idiomorphic crystals.

Pitchblende 2 occurs as fine spherulitic coatings close to pitchblende 1 and coffinite inclusions and is always together with calcite K5.

A hydrothermal process caused the alteration of the country rocks which always led to the formation of quartz-carbonate-sericite-metasomatites. At the beginning of the mineralization, a sericitization phase prevailed which, after the second stage, was followed by a chloritization phase. During the second stage,

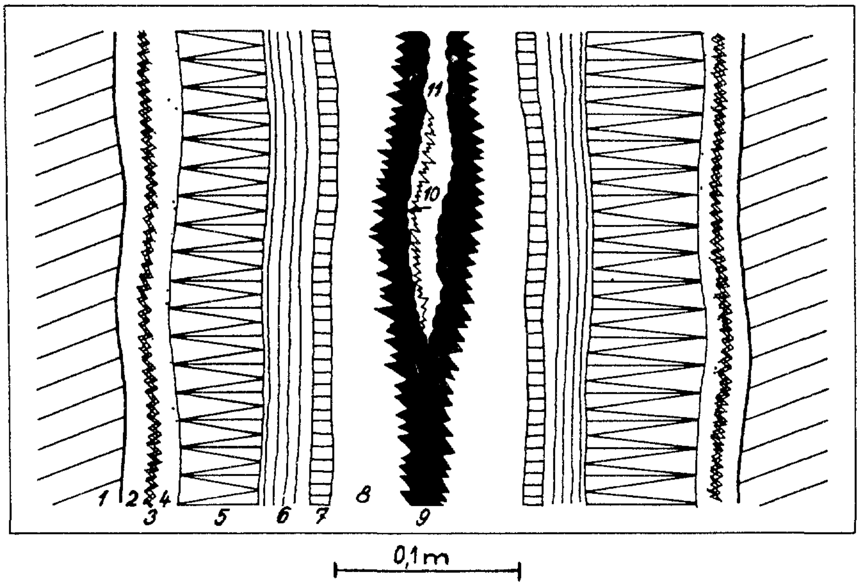

FIG. 4. Schematic section of a hydrothermal vein. 1. host rock; 2. siderite; 3. quartz; 4. ankerite; 5. calcite DK; 6. calcite K1; 7. calcite K2; 8. calcite K3; 9. pitchblende; 10. calcite K4; 11. calcite K5.

hydrohematitization was widespread. The alteration zones in the sediments are usually between 0.1 and 3 m wide, but in cases where different veins come close enough together, the alteration zone can also be of several tens of metres. In the intrusive rocks, the alteration is wider and usually associated with silicification zones.

With respect to the quantitative distribution of the different minerals, four mineralogenetic vein types can be differentiated:

(i) siderite-sulfide veins (usually the minerals of the siderite-sulfide stage),

(ii) calcite-pitchblende veins (only minerals of the three youngest stages),

(iii) mixed veins (minerals of all stages),

(iv) calcite veins (only minerals of the calcite-sulfide stage).

The distribution of the minerals belonging to the different phases is quite different within each of the various vein systems. Veins following diagonal structures or main faults belong to both the siderite-sulfide type and the mixed type. The calcite-pitchblende veins (and sometimes also the mixed veins) occur in NW trending cross faults as well as in structures parallel to the foliation. Some veins with NW-NE direction in the NE part of the deposit belong to the calcite type. In the SW sector of the deposit - away from the intrusive contact - are siderite-sulfide veins and mixed veins, whereas, closer to this contact, calcite-pitchblende veins and mixed veins are more characteristic. In both the central part and the NE part of the deposit, where we find a concentration of the calcite-pitchblende veins, the minerals of the two older phases occur in the centre of the anticline. The minerals of the younger phases, especially the ones of the calcite-pitchblende phase, concentrate mainly along the hinge of the anticline. The relative distribution of the minerals of the two older phases decreases from SW to NE while the minerals of the younger phase increase in this direction. The type of mineral composition changes increasingly from the siderite-sulfide type to the calcite type.

The development of the veins depend on where they also occur to depth. The diagonal veins which are closely connected with the main faults are best developed in the upper part of the deposit, the veins parallel to the foliation in the middle part of the deposit, and the cross veins in the middle and lower part of the deposit. At depth, the thicknesses of the veins decrease. The minerals of the calcite and calcite-pitchblende stages decrease downdip faster than do the others, indicating that the minerals of the youngest and oldest stage are of greater importance.

5. TYPES OF ORE

Three different types of ore can be differentiated in the deposit:

(i) pitchblende ore

(ii) uranium-anthraxolite ore

(iii) sphalerite-galena and silver ores

The main ore types, the pitchblende ore and the uranium-anthraxolite ore, occur in calcite-pitchblende veins and mixed veins. Both types of ore grade into each other. The pitchblende ore seems to occur both inside and directly outside the intrusive contact, whereas the anthraxolite ore occurs farther away from this contact. This well defined zoning depends upon the differing intensity of the anthraxolite development. It's relative content increases in the longitudinal direction from the wing of the deposit to the centre and with increasing depth of the deposit.

The uranium minerals in the veins occur as veinlets, coatings, reniform aggregates, and pods of the size of some mm to tens of cm. Within the veins, the ore lenses show irregular bodies, which are usually grouped in the vertical direction, and include barren zones showing irregular boundaries. The sizes of the individual lenses reach from one to several tens of metres. Most of the veins contain just one mineralized body, but the more extensive vein zones may contain 2 - 15 individual orebodies, separated by barren zones filled with gangue material. The internal structure of individual ore pods is extremely irregular. The mineralized part of a vein may account for 1 - 50 % of the total vein. The size of the orebodies may cover from 1,000 to 100,000 m².

The siderite-sulfide veins and mixed veins sometimes contain sphalerite-galena ore. The economically important veins of this type are usually devoid of uranium.

The rare Ag ore seems to concentrate in the upper part of the orebody, especially in the mixed veins. The main ore minerals are native silver and pyrargyrite, less common are proustite, argentite, etc. This ore formed within the cementation zone by ascending Ag-segregations out of Ag containing galena belonging to the siderite-sulfide veins of the deeper parts of the deposit.

6. ORE CONTROLS

The mineralization of the veins is controlled by lithological, mineralogical, and structural features (Petroš et al. (4)).

(i) Lithological control
This control is caused by the different mechanical properties of the host rock as well as by the chemical characteristics and influence of the hydrothermal solutions. The richest ore zones are in those zones

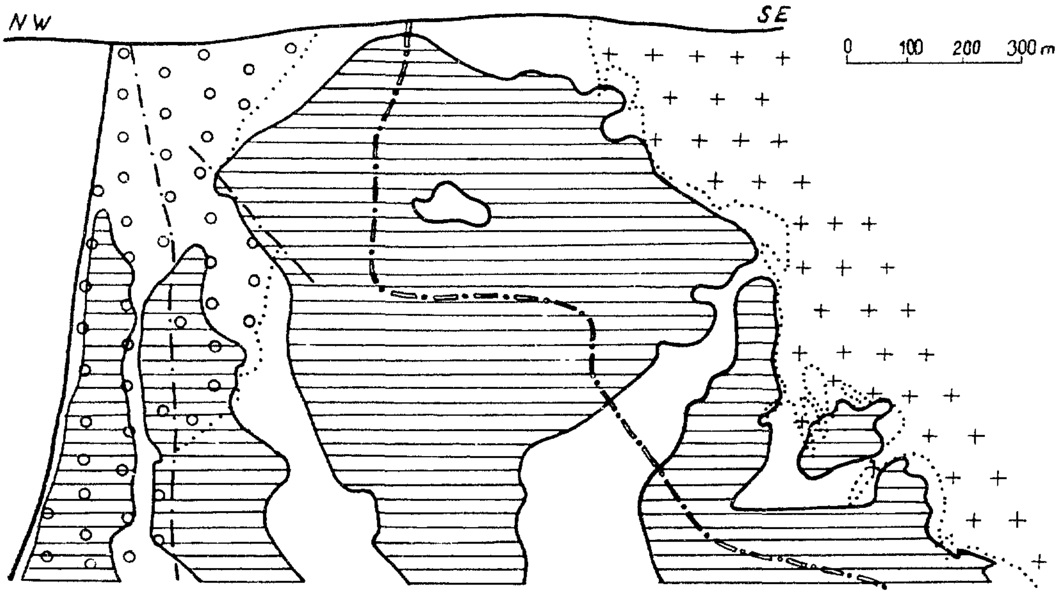

FIG. 5. Vertical projection of an important NW vein (explanation see FIG. 2).

where the rock is most porous and where these rocks have reacted best with the mineralizing solutions. Most of the orebody (98 %) lies in veins within younger Proterozoic rocks, where such conditions were best developed (Petroš (5)). The lithologic influence of the intercalated conglomerate horizon on the veins which parallel the schistosity, and which show high grade ore at the footwall, are also worth to be mentioned. Similar effects have also been recognized at the base of the Cambrian sediments, the contact to the granitoids, and at the footwall of thick dike intrusions.

(ii) Structural control
This controlling factor is the most important one. The development of ore zones depends on the shape of the individual structures, the character of the cleavage system, and the position and dependence of the main structures, i.e. the regional longitudinal faults, the Příbram anticline and the intrusive contact of the granite (Fig. 5). The major part of the ore deposit lies at the centre of the anticline, with its SE limb closest to the granite contact being where the ore veins are best developed. Also the dip of the contact is of importance. Analysing the ore pods and lenses within the veins, a considerable concentration of orebodies can be recognized below the roofing granite contact over a width of 1 km. The various orebodies occur in fault zones of different order (in respect to the main faults). Most of the ore lies in faults of third and higher order, whereas the largest orebodies are in faults of the second order. Such parts of faults and vein systems are most favourable for the formation of ore lenses or ore pods where they show strong bending, where they are splitting up into more faults, or where they intersect other faults or folds, and where they cut the contact of the intrusions under oblique angles. Faults below the granite contacts and below the Cambrian conglomerates also seem more favourable for ore concentration. The best traps for uranium ore however, are where two ore more of the above mentioned features occur together. The development of the mineralized veins becomes poorer with depth, as the splitting up of individual fault zones becomes weaker and the distance between individual veins becomes wider. The amount

and size of mineralized veins increases statistically up to a depth of 500 - 700 m, but decreases again below these levels.

(iii) Mineralogical control
Within the ore deposit, a clear relationship can be recognized between the amount of older calcite K2 and K3 and the uranium mineralization. The correlation coefficient is +0.68. Individual ore lenses and ore pods are always associated with the older calcite, which is an indication for the opening of the system during that time. The precipitation of pitchblende is obviously closely associated with the reducing conditions generated by the older calcite. The formation of the rich uranium ore in areas where the veins are thickest, or where they are disrupted, is caused mainly however, by the CO_2 release of uranium-bearing CO_2 complexes during local pressure releases.

7. FORMATION OF THE URANIUM DEPOSIT

The hydrothermal uranium vein deposits of Příbram have a late Variscan age (270 Ma). The uranium minerals precipitated out of middle to low temperature solutions which contained alkaline-carbonate-uranium complexes. The precipitation of uranium was caused by the degasification and decarbonatization of the solutions. Changes of pH and Eh values were also of importance. The formation of the deposits is closely associated with the Variscan granitoids of the Central Bohemian Pluton. The late phases of this intrusion show very close temporal (ca. 20 Ma), spatial, and geochemical relationships to the ore-forming processes (group of authors, 1984 (6)). It is postulated that the uranium solution originated from within the sediments, and was subsequently enriched during the differentiation of the magma (Vlašímský (7)). The uranium of the granitic rocks was leached again by solutions circulating along NW trending faults (Zikmund (8)). A certain supply of uranium from residual magmatic solutions, indicated by isotopic studies, however, cannot be ruled out (Hladíková et al. (9)). After Škvor (10), also during contact metamorphism some migration of uranium occured within the metasediments.

REFERENCES

(1) BERNARD, J.H., KLOMÍNSKÝ, J., Geochronology of the Variscian plutonism and mineralization in the Bohemian Massif, Vest. Ústř. ůst. geol. 50, Praha (1975) 71-81.

(2) PETROŠ, R., Nástin strukturní geologie příbramského uranového ložiska, in: Hornická Příbram ve vědě a technice, sekce geol., Příbram (1969) 1-17.

(3) KOMÍNEK, J., PROKEŠ, S., Stručná charakteristika minerálního složení žil a rozšíření minerálních komplexů na příbramském uranovém ložisku, in: Hornická Příbram ve vědě a technice, sekce geol., Příbram (1969) 1-31.

(4) PETROŠ, R., KOMÍNEK, J., PROKEŠ, S., Zákonitosti lokalizace uranového zrudnění na ložisku Příbram, in: Hornická Příbram ve vědě a technice, sekce geol, Příbram (1969) 1-15.

(5) PETROŠ, R., Vliv průvodních hornin na vývojmhydrotermálních žil, in: Sbor. vědecké konference VŠB Ostrava, sekce ložiskavá geologie, Ostrava (1980) 86-87.

(6) KOLEKTIV, Československá ložiska uranu, Nakl. technické literatury, Praha (1984) 365 pp.

(7) VLAŠIMSKÝ, P., Geochemie hornin a otázka možných zdrojů hydrotermální mineralizace v příbramské rudní oblasti, Sbor. geol. věd., Lož Geol., Mineral. 24 (1982) 49-89.

(8) ZIKMUND, J., Problém souvislosti metalogeneze a tektoniky ve středočeském plutonu, Sbor. Hornická Příbram ve vědě a technice, sekce geol. lož. nerost. sur., Příbram (1975) 118-133.

(9) HLADÍKOVÁ, J., POŠMOURNÝ, K., ŠMEJKAL, V., Isotopic study of carbon and oxygen of hydrothermal carbonates from Bytíz near Příbram, Čas. pro min. a geol., roč. 18, š. 3 (1973) 245-251.

(10) ŠKVOR, V., Geological aspects of the hydrothermal mineralization in Central Bohemia, Sbor. geol. věd., Geologie č. 31 (1978) 35-43.

CONTRIBUTION TO THE PROBLEMS ON PRE-VARISCAN PRECURSORS OF URANIUM VEIN DEPOSITS IN THE BOHEMIAN MASSIF

J.G. Strnad
Uranerz Exploration and Mining Ltd.
Saskatoon
Saskatchewan, Canada

Motto: '...the metallick and mineral matter which is now found in the perpendicular intervals of the strata; was all of it originally, and at the time of deluge, lodged in the bodies of those strata...' (John Woodward, 1723, possibly 1695)*

Abstract

CONTRIBUTION TO THE PROBLEMS ON PRE-VARISCAN PRECURSORS OF URANIUM VEIN DEPOSITS IN THE BOHEMIAN MASSIF

The regional U background of the pre-Variscan metamorphics yields clarke values or less. Only locally, within the folded and slightly metamorphosed Upper Proterozoic volcano-sedimentary sequences were enhanced U values of Cadomian age localized. Except for the sheared portions of these U-anomalous stratabound bodies, no further enrichment was observed, while their non-anomalous extension in a broader vicinity (at the contact with Variscan granites) encompasses a few small U deposits. Also, the major vein deposits which belong to the Příbram Zone are hosted by their distal (65 km) and broader stratigraphic equivalent, and again, in a series containing only slightly enhanced U values.

Unless the rocks surrounding these deposits are depleted in U, either/or U-anomalous and U-common lithologies could then contribute to the formation of a vein deposit, provided that enrichment processes took place during a subsequent orogeny. Within the broad regional Variscan overprinting, the exclusively effective deposit-generating conditions were fulfilled only at selective sites. These were the broad areas at the intersections of deep-seated structures which, in turn, followed the boundaries of several structural blocks with differing crustal thicknesses and composition, specific thermal regimes, opposing vertical movements and distinct volcanism and magmatism. Three such zones and their two intersections conditioned the development of two principal Variscan U-vein accumulations from the Proterozoic precursors.

1. INTRODUCTION

This study characterizes pre-Variscan uranium precursors and discusses a pattern of a deposit-generating Variscan overprinting at the two principal U zones within the Bohemian Massif.

The updated information has been mostly derived from the publications associated with the International Geological Correlation Program (IGCP) Projects 22 and 91 (Precambrian in younger fold belts and Metallogeny of the Precambrian,

---

* quotation from the third (1723) edition of Woodward's 'An Essay towards a Natural History of the Earth' (according to Horace V. Winchell during the discussion on F. Posepny's presentation of 'The Genesis of Ore Deposits', Chicago, 1893 (31))

respectively) issued by the Institute of Geological Sciences of Charles University and the Geological Survey, Prague. The interpretation of the published observations were assisted by the writer's previous experiences with some aspects of the metallogeny of the Bohemian Massif and by his current assignments oriented towards uranium deposits in other terrains.

2. REGIONAL GEOLOGICAL SETTING

The Bohemian Massif (BM) represents a rhomboidally-shaped block (350 km across) of predominantly metamorphic and granitic rocks, which has emerged through the Meso-Cenozoic cover of central Europe. Its extensions to the N and E are bordered by the ancient East European platform (EEP), (Fig. 1). To the

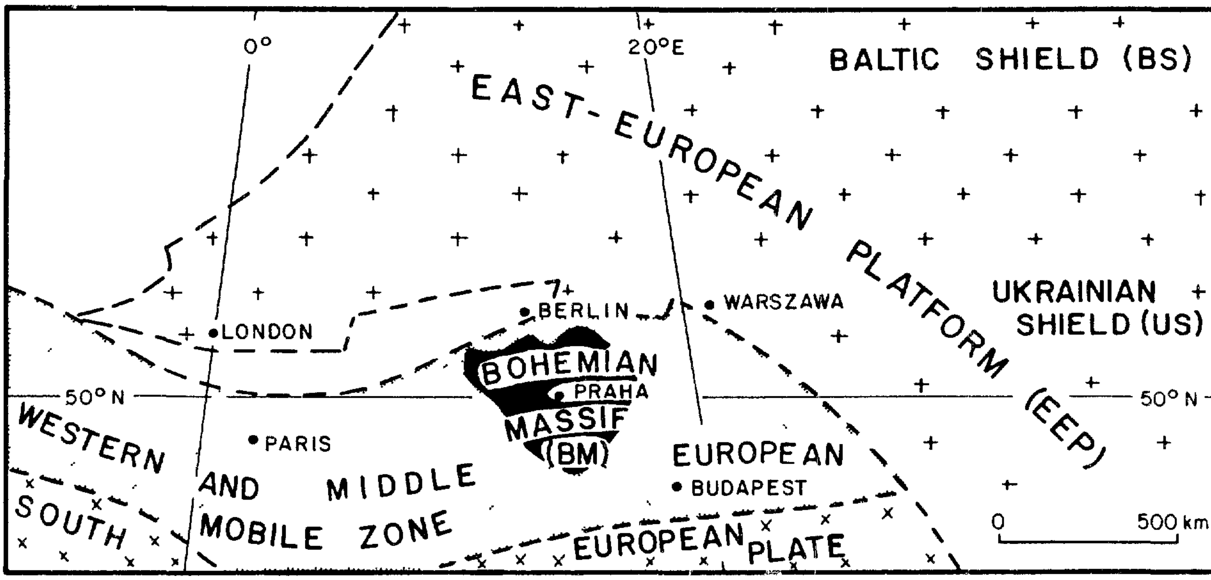

FIG. 1. General geological setting of the Bohemian Massif (simplified from Zeman (11)).

south, beneath the Alps, a contact with the Southern European plate is generally assumed to occur. The BM's orogenic development ended during the Variscan Orogeny with the formation of a pre-Mesozoic craton which shares its principal features with other consolidated basement cores which extend discontinuously further to the W.

Earlier stratigraphic schemes have tended to assign the oldest rocks of the Moldanubicum crystalline complex to Lower Proterozoic or even Archaean ages. In some present concepts (Chaloupsky (1)) two chronostratigraphic Precambrian units are recognized: the Middle Proterozoic Moldanubian (M) and the younger, Brioverian (B). At about 1,000 Ma the Lower B began with the sedimentation of pelite-psammite material together with volcanics. During the Middle B (800 - 700 Ma), another lithologically complex sequence of graphitic schists, crystalline limestones and dolomites was developed. The Upper B consists of flyschoid greywacke, siltstones, and shales which are restricted to narrow basins along the tectonic zones. This sequence includes the so-called Post-Spilitic Group in the Barrandian area. The main Precambrian metamorphic cycle, the Cadomian (Assyntian), has imprinted the principal characteristics of the BM, including its arcuate pattern. Chaloupsky (1) has proposed a synchronous model for the varied sedimentation of the Middle B with the culmination of the metamorphism. Another view suggests that the Cadomian metamorphism is virtually the first one in the major part of the BM and assigns to it a younger, infra-Cambrian period of 600 Ma, and emphasizes that the cycle extended up to 500 Ma, at the onset of the Ordovician. Following the late and terminal episodes of the Cadomian cycle, the transition to the Variscan tectonometamorphic cycle is represented by two Caledonian disturbances (Taconic during the Ordovician and Acadian at the Silurian-Upper Devonian boundary) causing hiatuses and facies changes. During the Variscan cycle, the first orogenic phase (the Early-Bretan) separates Middle and Upper Devonian. The following Bretan phase occurs at the Devonian-Carboniferous boundary causing the main Alpine-style folding and regional metamorphic overprinting of the older units, especially in the centre of the Bohemian Massif. Extensive Variscan plutonism and its paragenetically related processes together with the Meso-Cenozoic re-activation dominate the vein metallogeny of the BM.

3. GEOLOGICAL SETTING OF THE TWO PRINCIPAL URANIUM VEIN-TYPE ZONES

This study focuses on the two principal clusters of the vein-type uranium accumulations in the BM.

3.1. Jáchymov zone

This ancient uranium-producing zone crosses the Saxothuringian block (SB) alongside the NE contact of the Nejdek part of the Karlovy Vary (granitic) Massif (Fig. 2). The U-bearing veins cluster discontinuously within a zone of 40 x 7 km in size (Fig. 3), spreading from the Jáchymov (in German: St. Joachimsthal or Jachimsthal) district on the SE, passing through the Johanngeorgenstadt district and ending on the NW with the Schneeberg-Aue district (the last two being located in the GDR).

The host rock sequence varies from the Upper Proterozoic (?) mesozonal metamorphics to the almost unmetamorphosed Lower Palaeozoic sediments which cover the subjacent hidden part of the Variscan Krusne hory (Erzgebirge) Pluton. The partial fields of the Jachymov district occur above the granitic depressions which occupy different topographic levels beneath the metamorphics (Fig. 3). The deepest depression of the hidden granitic contact lies at sea level, while part of the present metamorphic-hosted surface, coinciding with the pre-Palaeocene peneplain, reaches up to 1,000 m above sea level. Quaternary erosion reduced this maximum vertical thickness so, for example, in the Josef shaft field, the top of the sea level granites were found in mine workings 440 m beneath the surface. The subcropping granitic contact has been systematically drilled with some holes reaching over 1,000 m depth. A complementary picture to the granitic topography has been provided by gravimetry and by reflection seismic methods. The veins in the W-field reach almost to the exocontact of the outcropping granite, while the veins of the distal Plavno field extend up to 5 km away from the same contact. The granites adjust almost concordantly to the foliation of the phyllite series, while in the subjacent steeply-folded mica schist domain the contact cross-cuts the detailed structures of its metamorphic envelope (Sattran (2)). The metamorphics are separated into two lithostratigraphic units: intensively folded mica schists and mica schist gneisses which form (in the centre of the Jachymov district) the Klinovec anticline; and on the N of the district, the superjacent gently folded synform of phyllites. The relationship of both units remains unsolved; it is however accepted that the footwall series might contain the pre-Variscan structural elements, while the phyllite series underwent only the Variscan overprint. The Klinovec anticline extends EW, i.e. oblique to the NE strike which prevails in

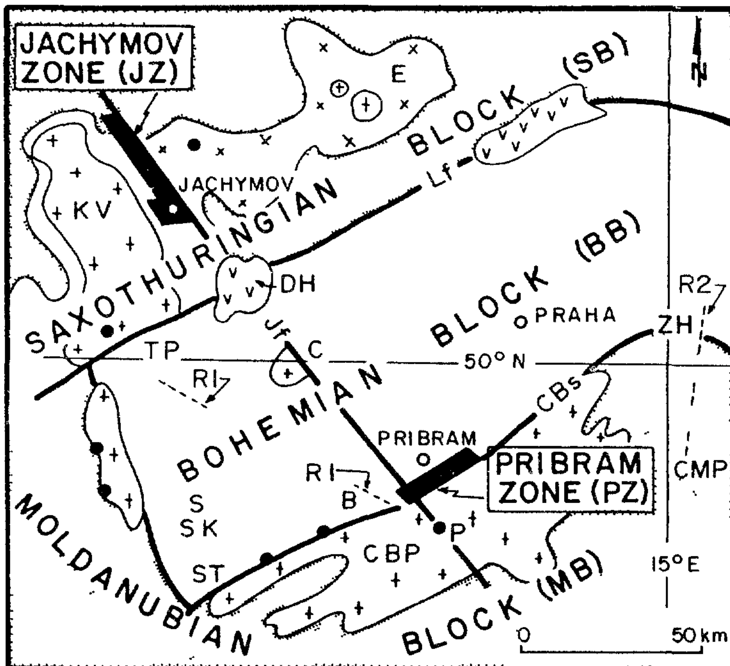

KV, CBP, C, CMP, E, - Karlovy Vary, Central Bohemian, Cista, Central Moldanubian granitic plutons, E - Erzgebirge sub-cropping (-1000 m) granitic pluton, DH - Doupovske Hory Mountains (part of the External Neovolcanic Arc), TP, B, ZH - Tepla Plateau, Barrandian, Zelezne Hory regions, R1, R2 - Region 1 and 2 of the lithogeochemical traverses, ST - uranium protores in the black shales at Struhadlo, S, S, K- uranium protores in the silexites at Stribro, Svojsin and Koksin, P - uranium deposit at Predborice, dots- other small deposits, CBs, Lf, Jf - Central Bohemian suture, Litomerice fault zone, Jachymov fault zone.

Bohemian block (BB) - Ensimatic region with a prolonged subsidence,thinner crust and Proterozoic mafic volcanism, Moldanubian block (MB) and Saxothuringian block (SB) represent emerging ensialic domains with thicker crust and Paleozoic felsic magmatism

FIG. 2. The regional structural setting of the Jáchymov and Příbram U-vein zones within the north-western part of the Bohemian Massif.

the SB. Under the NS-oriented maximal compression, three principal systems of joints were developed: EW, diagonal NE and NW, and the north-striking. Most of the Jachymov ore veins fill the EW and N dilational systems. Uranium has concentrated preferentially within the veins striking N to NNW. The ore shoots within the N veins follow the intersections with EW veins which are steeper than the dip of the strata. The metamorphics of the Jachymov district are cut by extensive EW and NW faults. The NW system was used by both the satellitic granite intrusions and later on the granite porphyry dikes, and was again rejuvenated. All three systems (NW, EW and NNW) also controlled the distribution of Miocene basalts.

3.2. Příbram zone

One hundred and ten km SE of Jachymov extends the NW contact of the Central Bohemian Pluton (Fig. 2). Uranium mineralization and some smaller U deposits occur discontinuously along the major part of this contact. The principal U veins of peribatholitic position, are clustered at the centre of the contact near Pribram (in German: Pribram or Przibram) within a NE-trending zone (18 x 2 km) between Trebsko on the SW and Oboriste on the NE (Fig. 4). Within the Příbram zone (PZ), almost two dozen shafts have been sunk to considerable depths (some 1,200, 1,400 and exceptionally to over 1,800 metres). Drilling, at least in the centre of the zone, explored the host rock to the -1,800 m level. Some uranium-producing veins do not outcrop and were explored and developed from underground workings. (2 - 4 km to the NW, within the separate Brezove Hory and Bohutin districts, are centered the historic and modern-day mining of lead-zinc-silver ores.)

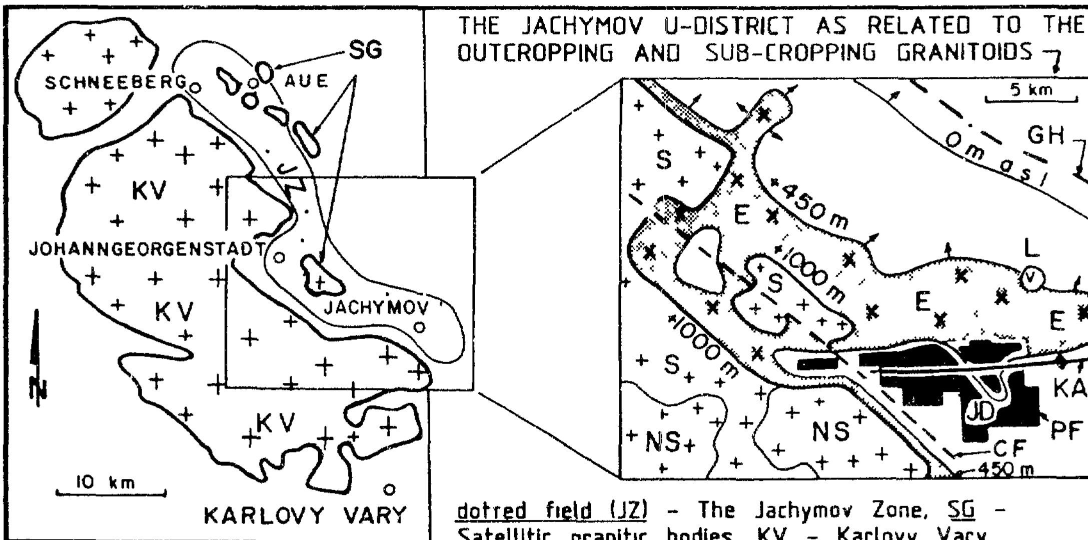

dotted field (JZ) - The Jachymov Zone, SG - Satellitic granitic bodies, KV - Karlovy Vary granitic Massif, S - Sn- Specialized younger granite, NS - Non-specialized older granite, E - Sub-cropping Erzebirge granite above +450 m a s l, GH - Gravity high at Crottendorf, L - Tertiary diatreme at Loucna, KA - Klinovec anticline JD and Black area - The Jachymov district extension, PF - The Plavno shaft field, CF - Central fault.

FIG. 3. The Jáchymov U-vein zone (JZ).

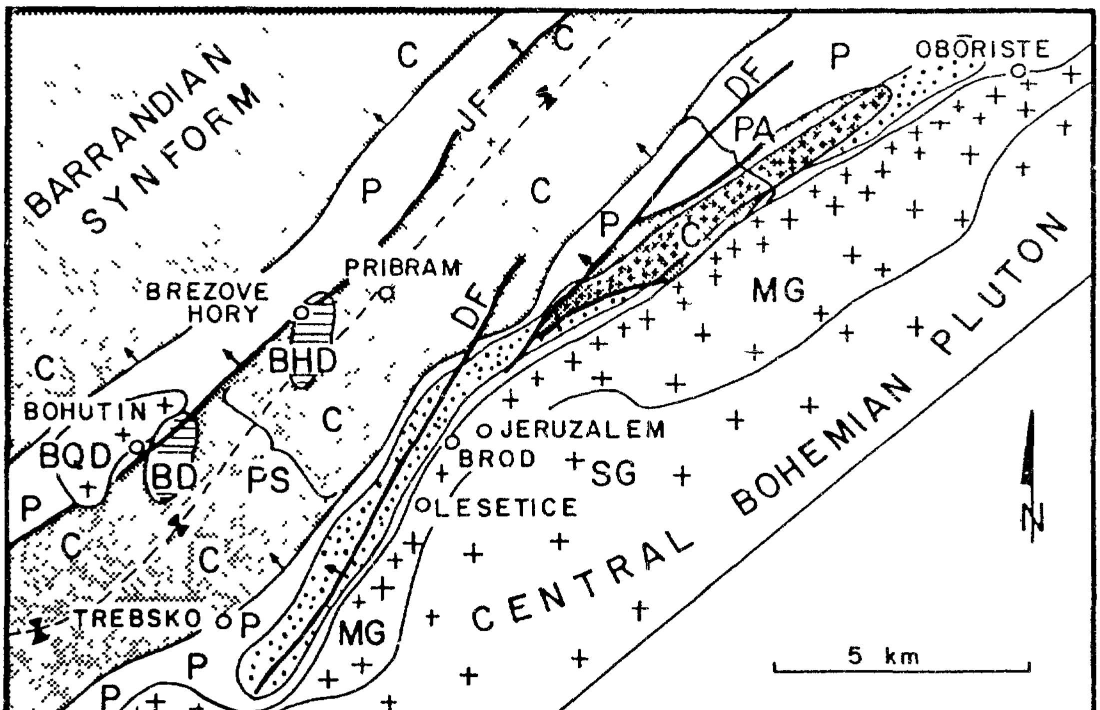

dotted field - The Pribram U-zone, BHD, BD - Brezove Hory and Bohutin Pb-Zn-Ag districts, BQD - Bohutin quartz Diorite; MG, SG - Marginal and Sazava-type of the Central Bohemian Pluton granitolds, PS, PA - The Pribram syncline and the Pribram anticline, P - Proterozoic, C - Cambrian, JF - Jilova porucha fault, DF - Dedovska and Dubenecko-Druhlicka faults.

FIG. 4. The Pribram U-vein zone (PZ).

While the Erzgebirge Pluton has developed mainly as varieties of granodiorites and adamellitic granites, the Central Bohemian Pluton (CBP) includes durbachites (syenites to granodiorites), tonalites (diorites), a moderate portion of felsic rocks and is also strongly differentiated in dike derivates.

The Marginal-type forms a part of the CB Pluton's NW contact and is proximal to the U-producing Pribram zone (PZ). These light-grey coarsely grained equigranular to porphyritic, biotite to hornblende-biotite granodiorites and granites intrude the Proterozoic and Lower Palaeozoic sequences. A polyphased origin has been suggested (Minarik and Pivec (3)) because of the different temperatures found for the microperthites and co-existing plagioclase (500° - 400°C and 1,100° - 800°C respectively). The albite-bearing 'syenitic' rocks have been known in the broader Příbram district since 1932. Further studies and the substantial contribution stressing their hydrothermal origin (Palivcova (4)), and especially the more recent works of Pivec (5), (6) suggested the link of albitization and the ore-forming hydrothermal processes. (Its relationship with the peribatholitic U veins is, however, not apparent.)

The regional Central Bohemian suture (s.l.) beyond its prominent function in controlling the development of the NW margin of the CB Pluton includes also an extremely tectonized peribatholitic domain (Fig. 4). The main tectonic element represents the Jilova porucha (JF) ('clay' fault), striking for a distance of 4 - 5 km parallel with the contact. Although spatially 3 - 5 km away from the axis of the uranium-producing zone (PZ), it controls the extension of Pribram's Pb-Zn-Ag veins in the Brezove Hory and Bohutin districts and dominates the development of the entire peribatholitic terrain, including the PZ. According to a newly introduced Upper Proterozoic stratigraphy (Masek (7)), the JF throws the oldest Blovice Formation of the Kralupy-Zbraslav Group (formerly the Spilitic series) over both the younger Stechovice Group (post-Spilitic series) and the Lower Cambrian. The principal vertical movements along the JF reverse fault predate the emplacement of the pre-Ordovician (Late Cambrian) diabase dikes which may be derived from an epi-Cadomian plutonism. The JF and the diabases are cut by the pre-Variscan quartz-diorite. The presence of pebbles of the contact metamorphosed Lower Cambrian Sadek sandstone in the Lower Devonian Bezdekov conglomerate, suggests that the Bohutin quartz-diorite intruded the Pribram syncline during the Caledonian (Acadian) disturbance at the boundary between the Late Silurian and the Early Devonian (approximately 400 Ma). Such an early (pre-Variscan) plutonism is rarely present (preserved?) within the CBP although it is not unusual in other parts of the BM.

Another prominent en echelon fault tandem, the Dedovska and Dubenecko-Druhlicka (DF), extends within the Pribram anticline parallel to the JF in the closer vicinity (0.3 - 1.2 km) of the CB Pluton contact (Fig. 4). These faults and the inward dipping contact of the CB Pluton control the general location of the U veins in the Pribram zone as defined in this study. While in the Pribram syncline the Pb-Zn veins are hosted by the Cambrian and the situation in the subjacent Upper Proterozoic Stechovice Group remains speculative (Kutina and Telupil (8), Kutina et al. (9)), it is mainly the psammites and shales of the Stechovice Group (and the Cambrian only partly) which host the U veins in the adjacent Pribram anticline. Those mineralized structures, which are either perpendicular or diagonal to the granitic contact, after crossing the contact, are depleted in U within the first ten metres (Hruby and Sorf (10)).

4. PRE-VARISCAN EVOLUTION OF THE HOST LITHOLOGIES

The BM's location in relative proximity to the southern mobile block and western stable plate of the EEP suggests the possibility of some common structural elements. According to Zeman (11), in both the EEP and the western and middle European mobile zone (which includes the BM) are residual sialic blocks which extend within the EW organized Armoricain-Moldanubian zone and its eastern continuation beyond the margin of the EEP. The region was overprinted by NW and NE trending epi-Karelian structures which formed a complex mobile zone with predominantly oceanic and sub-oceanic crust to the W of the EEP. Some authors favour the residual Pentevrian continental blocks to form part of the BM basement while most workers agree that no major magmatism or regional metamorphism took place before 800 Ma.

4.1. A possible source area of the earliest sediments

A certain part of the material contained in some of the BM's metasediments (including those of its oldest area, the Moldanubicum) comes from relatively old sources (2,300 - 2,000 Ma) as interpreted from the U-Pb data on detrital zircons (Grauert et al. (12)). It is possible that the ancient EEP is a source area, however, further observations are needed in order to put Grauert's comment that '...rocks of similar age occur there...' into a more detailed perspective. In both shield areas of the EEP (i.e. the Baltic (BS) and Ukrainian (US)) the time span from 2,300 - 2,000 Ma is governed by the deposition of the Lower Proterozoic Jatulian sediments and also, the interpreted ages are at least 300 Ma younger than the youngest Archaean zircons, and at least 100 Ma older than the earliest zircons of the synorogenic Svecokarelian granites. Rather, it appears that granitoids were developed only locally at the time as indicated by the BM's oldest detrital zircons. Such examples would be the Tavaiarva and Hautovara complexes (2,300 - 2,100 Ma) of the E part (USSR) of the BS; some granitoids (2,200 - 1,800 Ma) from the Saksagan and Krinichan domes and/or other similarly dated ultrametamorphic granitoids studied by Belevcev (13) in the Ukrainian Shield.

The earliest opportunity to generate large amounts of detritus containing Lower Proterozoic zircons was during a period of uplift following the intrusion of the youngest Rapakivi granites (1,550 Ma), prior to the deposition of the Jotnian (1,400 Ma). Although this denudation or, alternatively, the erosion during the older uplift (after the intrusion of the Svecokarelian granites at 1,750 Ma) provided a great supply of detritus, the BM's zircons are also remarkably age monomictic, uncontaminated by younger (Svecokarelian or Rapakivi) zircons. This suggests that the source area was structurally specific with regard to the prevailing styles of both shields.

We have thus indicated that the sialic detritus was at least available in an extraneous source of a modified EEP-type, including its possibly detached portions. If this contributed to the sedimentation in the BM, it might have had an influence on the earliest development of the U-metallogeny. The Middle Proterozoic detritus derived from upper, less metamorphosed, sequences of the EEP might have provided slightly U-enhanced material. Additionally, the erosion in some portions of the source area might have (during the pre-Jotnian) unroofed equivalents of older U-deposits and/or U-enriched lithologies such as

(i) Lower Proterozoic conglomerates (2,300 Ma)

(ii) stratabound mineralization in Jatulian quartzites (2,200 - 2,000 Ma)

(iii) phosphatic horizons regionally associated with Cu-Zn deposits of the Vihanti-type (2,100 - 1,900 Ma)

(iv) albitites in banded iron formation and in ultrametamorphic (granitoid) zones (1,900 - 1,700 Ma)

(v) stratabound mineralization in rhyolitic ignimbrites with associated albitization, as the Duobblon and other types (1,750 Ma)

4.2. Regional background of U values in the Upper Proterozoic

The principal test (Fiala et al. (14)) in the BM focused on the variations of U and Th in pelitic and greywacke-pelitic rocks which underwent various degrees and styles of metamorphism. Two regions (Fig. 2) were studied:

- region 1 covered the transition between the prehnite-pumpellyite facies Upper Proterozoic Barrandian area to the Barrovian kyanite-staurolite zone of the Tepla Plateau (both within the ensimatic Bohemian block), and

- region 2 included the traverse from the Upper Proterozoic chlorite zone of the Zelezne Hory to the cordierite zone adjacent to the Central Moldanubian Pluton (transitional from the ensimatic Bohemian block to the ensialic Moldanubian block).

Fiala's study (14) concluded that the commonly observed trend of decreasing amounts of radioactive elements (U, Th) with increasing metamorphism is not an invariable feature. In the BM this tendency was confirmed only for the Barrovian type while the reverse situation was observed in a periplutonic metamorphic sequence. The original sediments (i.e. low metamorphic grade) of the BM contain ($n = 21$): 2.9 ppm U, 7.0 ppm Th, and 2.0 % K_2O. These values indicate an affinity for the shales of the platform-type rather than to the greywackes of the oceanic crust. However, this average includes two specific lithologies with enhanced U-values: graphitic phyllitic shale from region 2 (3.5 - 6.0 ppm U, averaging 5.7 ppm U), and the greywacke shale from region 1 (1.9 - 7.5 ppm U, averaging 3.8 ppm U). By excluding these two sets containing anomalous U, the rest of the low grade metamorphics (non-greywacke and non-graphitic pelites), here considered the representatives of original pelites, would average only 1.8 ppm U ($n = 13$). This may suggest that the source lithology(ies) was (were) a mixture of rocks of both granitic and oceanic types, or the mixture was developed at the sedimentation site. The relatively low Al_2O_3 (13 %) also shows that the low grade metamorphics tested are semi-pelitic rather than pelitic. The titanium modulus (TiO_2/Al_2O_3) of 0.036 would characterize a source having a dioritic composition (or a mixture of granite with mafics, 0.02 and 0.05 respectively). A participation of the continental crust source against a uniform oceanic source has been earlier suggested for the Upper Proterozoic in the Svojsin area and this would also be in agreement with the above data.

4.3. U protores in the Upper Proterozoic

It is of interest to observe that the only protore U values presently known in the BM exist beyond the SE extension of the proper PZ, where it hosts only small U deposits.

At the SW edge of the Bohemian block, 65 km SE along strike from the PZ, a genetically important U mineralization (or rather a U protore) has been explored (Ordynec et al. (15), Litochleb et al. (16)) at Struhadlo (Fig. 2). Here, within a weakly metamorphosed volcano-sedimentary sequence belonging to the Upper Proterozoic Spilite series (at the exocontact with the amphibole-biotite and biotite granodiorite of the Central Bohemian Pluton) several emanometric anomalies correlating with the black shale horizons were found. The main steeply-dipping graphitic shale sequence also includes a comformable layer of U mineralized tremolitite, possibly of ultramafic origin. The lensoidal U enrichments, at the threshold of 185 Bq/L attain a length of 100 - 200 m, and are 3 - 10 m in width. Trenches, drilling and tunnelling followed up a zone of graphitic and quartzitic pyritiferous shales and tuffites, and outlined several small mineralized lenses. A series of samples traversing one of the lenses (Ordynec et al. (15)) yielded on average 1.40 % C carb., 0.19 % C org., 7.8 % Fe, 530 ppm V, 124 ppm Cu, 56 ppm Ni, 170 ppm Zn, 9 ppm Pb, 2 ppm Th, and 35 ppm U. Richer U samples (64 ppm U) at the centre of the lens were substantially more sulphidic and also slightly richer in graphite and carbonate (3.32 % S, 0.26 % C org., and 2.10 % C carb.), as well as other components similar to the previous set. This would indicate that the additional increase in U is controlled by the carbonate and pyrite veining. In comparison with the average shales, these U protores are more sulphidic, contain four times higher V, double the values of Fe, Cu, and Zn, and are much lower in Th. Of importance is the dating of this 'primary uranium mineralization' (the early protore stage?) as being 700 Ma (Ordynec et al. (15)). This suggests the Late Cadomian event, which is only broadly correlatable with the 647 Ma age (K-Ar) for the interbedded volcanics. Ore concentrate from the same environment yielded a 460 Ma (U-Pb) age which has been interpreted (Ordynec et al. (15)) as a mixture of the Upper Proterozoic (700 Ma) and Late Variscan (256 Ma) material. However, this age also grossly coincides with the Early Caledonian Taconic disturbance and it is only slightly younger than the emplacement of the Příbram diabase dikes.

Similarly enhanced Fe-V-U values were also previously reported from a broadly analogous domain (Fig 2) at Stribro, Svojsin and Koksin (Mrazek and Pouba (17), (18)). Here, the attention was centered on silexites and siliceous stromatolites. These lithologies are associated (Mrazek and Pouba (18)) with the Upper Proterozoic (647 Ma) submarine, alkaline volcanics of the spilite-keratophyre type. The hematite-rich facies contains up to several tens of ppm U. Samples from the Koksin non-carbonaceous silexite and the carbonaceous (0.22 % C org.) siliceous stromatolite yielded 500 - 800 ppm and 1,200 - 1,700 ppm V_2O_3 respectively.

4.4. Uranium content of the host lithologies in the vicinity of the principal U deposits

Except for the above mentioned examples, most of the Upper Proterozoic yields can hardly be considered protores and thus other tests performed around or within the hosts of the U mineralization can be generally expected to provide higher values.

Although within the Jachymov district proper, Babanek (19) presented the first whole rock geochemistry on six different types of metamorphics hosting the U veins a century ago (1884), the recent era of large-scale mining activity has not provided any published lithogeochemical data for this particular field. Undoubtedly of special interest would be systematic data on a lithology which is rather specific not only within the Erzgebirge but also within the JZ - the Jachymov schists (Joachimsthaler Schiefer). This folded and moderately metamorphosed sequence of dark grey to black, often pyritiferous, fine grained, hard, siliceous rocks is known mostly within (and only partly beyond) the range of the Jâchymov veins. The down-dip projection of Sattran's (2) cross-section suggests that it was the very upper portion of the subjacent granite which has consumed a considerable part of the synform containing these particular lithologies.

Within the Pribram zone the oldest (Spilite) Blovice-Tepla series yields an unweighted lithological average of 3.8 ppm U, with a spread of from 2 ppm for the phyllitoids to 5 ppm in the black schists, and 6 ppm in the quartz-keratophyres (Vlasimský (20)). The younger Davle series contains a similar average of 4.1 ppm U, varying from 3 ppm in quartz-keratophyres and their lapilli tuffs to 5 ppm in the Lecice black tuffite shales and 6 ppm in the quartz-porphyries. The youngest (post-Spilitic) Dobris series occurs directly at the contact with the Central Bohemian Pluton and hosts the bulk of the U veins. A lithological mixture of the Dobris series from a distant area indicates 3 ppm U, while an analogous set from the PZ reaches 5 ppm with only subtle variations of different lithologies. Within the PZ alongside its NE extension (i.e. along the granitic contact) no systematic changes of trace elements were observed except perhaps in the Dobris series at the PZ centre (Brod-Jeruzalem field) where one set yields an average U value of 7 ppm. In the opposite direction, both U and Th increase beyond the contact-metamorphic zone. At one site in the Lesetice Mine (Fig. 4), the Dobris series (at 500 - 1,270 m depth) displays 5 ppm U, while the subjacent Davle series (1,270 - 1,850 m depth) shows a lower average of 3 ppm U.

5. STRUCTURAL SPECIFICS OF THE U PRODUCING VARISCAN OVERPRINT

Numerous U accumulations in the Bohemian Massif extend either along or in close proximity with the margin of the ensimatic Bohemian block (BB), which is typified by a prolonged subsidence, thinner crust, and Proterozoic mafic volcanism. Two adjacent blocks, the Moldanubian (MB) on the SE and the Saxothuringian (SB) on NW, represent emerging ensialic regions with thicker crust and Palaeozoic felsic magmatism.

5.1. Regional control

Two NE striking sutures at the borders of the BB, and one NW cross fault zone are the deep-seated structures important in the U metallogeny (Fig. 2). Two major elongated clusters at various locations close to the intersections of these lineaments host the principal U deposits, the Jachymov and the Pribram Zones (JZ, PZ). The JZ extends within the gravity low, granite-hosting SB which displays a high heat flow largely derived from the crust. The PZ occupies the boundary between the regional, moderately-high heat flow of the BB and the gravity-high (!), granite-controlled specific area of the MB which has an extremely low heat flow, generated mostly by the mantle. Both the JZ and PZ are in peribatholitic settings, the first extending above the subjacent granite, while the second is bordered by the inward dipping contact of the outcropping granite.

Both principal U zones (JZ and PZ) exist within or in the proximity of the intersection of the three zones:

(i) Central Bohemian suture (NE)

(ii) Krušne hory (Erzgebirge) zone s.l. (or Litomerice Fault s.s.) (NE)

(iii) Jáchymov Fault (zone) (NW) (Fig. 2)

While the deep-seated character of both NE zones (Variscan orogene-oriented) is commonly accepted, the role of the transversal (NW) Jáchymov Fault needs additional comment. Only short segments of this NW fault can be classified as a 'deep-seated fault hidden beneath the magmatics' (Zeman (21)), other parts having only a supracrustal character. Within the Saxothuringian Block (SB), the Jáchymov Fault (JF) encompasses the following (Fig. 3): the NE edge of the Karlovy Vary Massif and other satellitic granite bodies, a parallel gravity high, and the system of NW fault zones typified by the Central Fault in the Jáchymov district. We do not know the substratum of this segment in sufficient detail. Nonetheless, the following features in my view attest to the specific development in this particular domain of the JF:

(i) The gravity high lineament at Crottendorf (GDR) alone, or combined with the presence of the eclogites in the Klinovec anticline, and

(ii) the hypothetical deep-seated tavite and ijolite equivalents of the Tertiary nephelinites, haynites and haynoporphyries and the author's finding of ilmenite-bearing gabbroid xenoliths in the Tertiary diatreme at Loucna (7 km N of Jáchymov).

Also, the map of Zeman (22) shows the transversal extension of the BB simatic crust beneath the Karlovy Vary (granitic) Massif.

To the SE (Fig. 2) (closer to the boundary of SB and Bohemian Block (BB)), the JF crosses the External Neovolcanic Arc (Strnad (23)) and here triggers the major accumulation of Tertiary volcanics in the Doupovske hory Mountains. Further on, within the NW periphery of the ensimatic BB it transects the Cista-Jesenice-Louny (granitic) Massif and controls the alkali syenite and its associated Mo-(U) mineralization at Cista. With a deep-seated segment, it crosses the Central Bohemian suture (CBS) and demonstrates its (CBS) U-potential by the Pribram U zone. Further to the SE, within Central Bohemian Pluton, it controls the Predborice U deposit (hosted by a block of metamorphosed Palaeozoic sediments).

5.2. Local structural control

Beyond the traditional structural schemes advanced for the JZ and PZ, other specifics could contribute to the formation of the PZ. During the Upper Cambrian, asymmetric folds developed in the peribatholitic domain. The steeper NW limb of the Pribram syncline became overturned and it developed into the large reverse fault (JP) whose minimum vertical movement is 2 km (!). Other antithetically dipping thrusts of Proterozoic over Cambrian can also be interpreted at the proximal granitic contact.

After cessation of the major compressional regime, several pulses of relaxation of elastic strain energy stored within the compresses competent rocks can be postulated. It is obvious that joints would develop within competent lithologies (Cambrian syncline hosting Pb-Zn veins). According to modelling (Kostak and Zeman (24)) other dilatancies may be generated beneath previously compressed competencies as well. The principal episodes in the formation of stratigraphically subjacent pre-U-ore dilatancies were thus supplemented by erosional tapping of the compressed Cambrian anticline during sudden uplifts.

Although it is difficult to extrapolate the uranium available at the time of thrusting, both principal units (Proterozoic and Cambrian) show some enhanced values within the PZ. U gradually increases within the younger Cambrian strata up to 4 ppm. The trend is in part lithologically-controlled. Shales and siltstones contain 5 ppm, while the coarser clastics (sandstone and conglomerates) still yield an enhanced value of 3 - 4 ppm. The reverse faults trapped the cooler intraformational water of the porous Cambrian beneath the warmer and relatively impermeable Proterozoic. Under such tectonic conditions a sizeable reverse thermal gradient (minimum of 60°C) can be postulated to have participated in the circulation of mineralized fluids. Local U contained in the down-faulted lithologies could thus be effectively incorporated into the bulk of available U sources.

6. DISCUSSION

Before discussing the situation in the BM we should emphasize that many metallogenic models require some form of preconcentration of metallic elements, such as for example Strakhov's micro-ore formations (suites). Analogously, the U protore concept is widely accepted in the non-Russian literature as a crucial part of an early development of some types of U accumulations, namely of the unconformity-related deposits as emphasized by Dahlkamp (25).

6.1. Uranium protores in general

Although the protore concept itself apparently matches the modelling of the early stage in the formation of some U deposits, it is very difficult to prove that such protores exist (survive) beyond the non-metamorphosed sequences. A quarter of a century ago, it was known to Page (26) that 'considerable effort has been spent on finding metamorphic equivalents of uraniferous black marine shales' and that 'known graphitic schists have exceedingly low uranium ... mobilized during metamorphism'. Nontheless the excitement triggered by the discovery of the unconformity-type uranium deposit newly induced an unrealistic image of rich U protores (or otherwise 'hot' environment) which ought to surround the U deposits of this type. Later on, it was found (after the discoveries, of course) that Page's observation elegantly survived the thrust of a new genetic type as well.

For example, most updated studies in some critical areas of Lower Proterozoic belts which host sizeable, and in part also extremely rich, unconformity deposits, show that these high metamorphic domains probably may not contain sizeable U-enriched lithologies. Clarke values of U were found in the Wollaston Belt, Saskatchewan, Canada, either regionally (Ray (27)) closer to smaller deposits (Wallis et al. (28)), and also in the immediate vicinity of even giant accumulations such as the Key Lake deposit (Strnad (29), (30)). (Most higher values assigned earlier to protores were consequently recognized as belonging to alteration halos immediately surrounding the deposit.)

These examples show that in some highly metamorphosed terrains, many important deposits occur imprinted on unattractive local and areal U background.

6.2. Uranium protores in the Bohemian Massif

The few data available for moderately to strongly metamorphosed Middle (?) Proterozoic Moldanubian do not allow the estimation of U contribution provided by detritus from continental sources. On the other hand, we may assume with more confidence that these sources were limited during formation of the low-grade metamorphosed Upper Proterozoic Brioverian because (among other reasons) it contains a rounded average of 2 ppm U. This figure allows one to suggest 3 ppm (or less) of U for the BM's regional background, i.e. a value hardly indicative of the region so richly endowed with uranium deposits.

On an areal scale this pattern is not substantially changed even within the Bohemian block, although its low grade metamorphics could be expected to fully preserve the protores. In fact, U anomalous segments were found and assigned the Cadomian age (both observations perhaps being unique in the entire Variscan). However, their frequency and especially their maximally low tens of ppm extending within small lensoid bodies, do not particularly contribute to the bulk average value of these Proterozoic formations.

Relatively detailed studies on the geochemistry (including U) of low-grade metamorphic series hosting U veins in one of two principal U-producing zones (PZ) did produce only an average or only a slightly enhanced U value (two times the clarke value). Thus, again, and this time more importantly, the local environment which hosts the Pribram Zone displays an unattractive U background.

7. CONCLUSION

At least some Variscan principal uranium vein-type accumulations in the Bohemian Massif (BM) are hosted by Upper Proterozoic lithologies with a U low background. Similarly, (and except for small and only slightly U anomalous lensoid bodies) their gross stratigraphic extensions covering broad areas and also the entire BM in bulk display only low U values. In addition, we have observed (beyond the Variscides) analogously U low lithologies surrounding important unconformity-type U deposits.

These examples do differ from a favoured and seemingly simple concept of an association of deposits with a U enhanced environment s.l. The regional background, the occurrences and showings, and finally a sizeable deposit do not always form a sequence consisting of these members continuously developing from the initial lithology and necessarily containing an enhanced U. Perhaps not infrequently all these entities are considerably independent metallogenetical units formed by distinct processes during different episodes, and thus only rarely overlapping each other.

Here, we may add, that also with other metallotects like the specialization of the granites, there are analogous observations featuring generally less, or only a secondarily attractive terrain, if the contents of U would be considered a leading parameter. The Pribram Zone is bordered by a mildly specialized granitic variety and contains less U in comparison with other granitoids of the same pluton, and the Jachymov district occurs at the immediate lateral vicinity of the non-specialized segment of the major granitic pluton.

We have found the protores as of only potential improvement, however, not necessarily as a decisive metallotect if compared with the tectonics s.l. Our examples show the possibility that the non-enriched lithologies could be involved at the beginning of the Variscan overprint. Also, in most cases we cannot judge how anomalous the progenitors were. Thus we have preferred the terms sources or precursors instead of the overly-committed and too specific protores or micro-ores.

Within this seemingly simple appearing tandem, the Proterozoic precursors and Variscan enrichment, at least two phenomena remain problematic. Without further research, we cannot be sure that these assumed sources were unique, or if other more extraneous contributors were involved. Except for the improbability of the lateral-secretion of elements from the immediate wall-rocks (as proposed by Sandberger (cited by Posepny (31)) also for the Pribram (Pb-Zn-Ag) veins one hundred years ago), the position, size and the geometry of the actual source of U as related to the position of the U veins still remain unspecified.

All these uncertainties surrounding the problem of the actual source(s) led me to assume the main precursors in the Proterozoic strata s.l. without going into details, i.e. in a similar way as John Woodward did in his abstractive formulation already three centuries ago.

ACKNOWLEDGEMENTS

This contribution has attempted to analyse most of the recently published observation. The labour of these researchers must be recognized in the first place. The author thanks the managements of Uranerz Exploration and Mining Limited, Saskatoon (Canada), and of Uranerzbergbau GmbH, Bonn (Federal Republic of Germany) for the support provided in this study, and expresses the appreciation to Messrs. R. Orr and R. Loewer for their assistance during the preparation of this paper.

REFERENCES

(1) CHALOUPSKY, J., The Precambrian tectogenesis in the Bohemian Massif, Geol. Rdsch. 67 (1978) 72-90.

(2) SATTRAN, V., The tectonics of the Jachymov ore district (in: Czech, German res.), Sbor. Geol. ved. Geol., G, sv. 10 (1966) 39-81.

(3) MINARIK, L., PIVEC, E., Thermal and crystallization history of the perthites from 'Marginal' type of granitoids of the Central Bohemian pluton (Czechoslovakia), Acta Univ. Carolinae-geol., Slavik vol. no. 3-4 (1977) 319-332.

(4) PALIVCOVA, M., Igneous-looking metasomatic hydrothermal albitites ('syenite of Smolotely', Central Bohemian pluton), Sbor. Nar. Muz. v Praze, 23B, 5 Praha (1967) 125-148.

(5) PIVEC, E., Albitite from Draha near Smolotely (Central Bohemia) (in Czech), Cas. pro min. a geol. 18 (1973) 289-296.

(6) PIVEC, E., New occurrences of albitites from the district of Příbram (in Czech), Cas. pro min. a geol. 20 (1975) 291-298.

(7) MASEK, J., Contribution to the geology of the Proterozoic of the SE limb of the Barrandian basin (in Czech, Engl. res.), in: Z. Pouba edit., Correlation of the Proterozoic and Palaeozoic stratiform deposits, VI, UUG Praha (1981) 14-28.

(8) KUTINA, J., TELUPIL, A., The vertical extent of ore deposition in Pribram, Czechoslovakia, in Z. Pouba and M. Stemprok edit., Problems of hydrothermal ore deposition, Schweizerbartsche Verlag, Stuttgart (1970) 187-193.

(9) KUTINA, J., ADAM, J., PACESOVA, M., On the superabundant content of manganese in Příbram ore veins with respect to wall rock leaching, in: Z. Pouba and M. Stemprok, edit., Problems of hydrothermal ore deposition, Schweizerbartsche Verlag, Stuttgart (1970) 294-298.

(10) HRUBY, J., SORF, F., Some regularities of the localization of uranium mineralization in the metallogenic subprovince of the Bohemian core (in Czech), Geol. pruzkum, Prague 7-8 (1968) 282-283.

(11) ZEMAN, J., Die Krustenentwicklung im voralpinen mobilen Raum südwestl. vom Rand der Osteuropäischen Plattform, Sbor. geol. věd. geol. 35 (1981) 49-73.

(12) GRAUERT, B., HANNY, R., SOPTROJANOVA, G., Age and origin of detrital zircons from the Pre-Permian basement of the Bohemian Massif and the Alps, Contr. Min. and Petrol. 40 (1973) 105-130.

(13) BELEVCEV, YA., N., Geological and physico-chemical conditions of the metamorphogenic ore formation, (in Russian), in: G.A. Glushkova and A.V. Keilman, edit., Metamorphogenic ore formation, Nauka (1977) 5-24.

(14) FIALA, J., VANKOVA, V., KRESL, M., FRANKE, W., Distribution of radioactive elements in three progressively metamorphosed pelite series of the Bohemian Massif, Studia geoph. et geod. 24 (1980) 65-87.

(15) ORDYNEC, G., ZHUKOVA, V.I., HABASKO, J., Pre-Variscan U-mineralization in the Proterozoic of the Bohemian Massif (in Czech, Russian resume), Cas. pro min. a geol. 29 (1984) 69-77.

(16) LITOCHLEB, J., NOVICKA, Z., BURDA, J., Goldmanite from Strudhadla at Klatovy (in Czech), Cas. pro min. a geol. 28 (1983) 103-104.

(17) MRAZEK, P., POUBA, Z., The Fe-V-U formation in the Proterozoic rocks of the Svojsin and Stribro-Plasy volcanic belt (in Czech, English resume), in: Z. Pouba edit., Correlation of the Proterozoic and Palaeozoic stratiform deposits, IV, UUG, Charles Univ. (1976) 53-71.

(18) MRAZEK, P., POUBA, Z., Iron, vanadium and uranium in the Proterozoic rocks of the Bohemian Massif, (in Russian), in: B.M. Shmakin edit., The problems of the geochemistry of endogenous processes, Izd. Nauka, Novosibirsk (1977) 252-260.

(19) BABANEK, F, Über die Erzführung der Joachimsthaler Gänge, Öster. Zeitschr. f. Berg- und Hüttenwesen, Jg. XXXII, No. 1 (1884) 21-24 and 61-62.

(20) VLASIMSKY, P., On the geochemistry of Proterozoic rocks of the Příbram ore district (in Czech), Cas. pro min. a geol. 24 (1979) 113-133.

(21) ZEMAN, J., The characteristics and the dynamics of some deep-seated weakened zones of the Bohemian Massif, (in Czech), Hornická Příbram (1969) 53-76.

(22) ZEMAN, J., The importance of the heterogenity of the crustal development of the Bohemian Massif for the prognostication of the hidden deposits, (in Czech), in: M. Kuzvart edit., Theoretical foundation etc., Charles Univ., Dept. of mineral deposits (1978) 46-50.

(23) STRNAD, J., The connection of one part of the European Neogene volcanism with a kimberlitic magmatism (in Czech, German resume), Cas. pro min. a geol. 7 (1962) 434-442.

(24) KOSTAK, B., ZEMAN, J., Tectonophysical model of deformations in a structure with an elastic competent layer (in Czech, English resume), Cas. pro min. a geol. 27 (1982) 51-61.

(25) DAHLKAMP, F., Geologic appraisal of the Key Lake U-Ni deposits, Northern Saskatchewan, Econ. Geol. 73 (1978) 1430-1450.

(26) PAGE, L.R., The source of uranium in ore deposits, IGC, Report of 21st Session Norden (1960) 149-164.

(27) RAY, G.E., Bedrock geology and geochemistry, Daly Lake (West) area and part of Middle Foster Lake area, Saskatchewan Geol. Survey Rep. 208 (1981) 34 pp.

(28) WALLIS, R.H., SARACOGLU, N., BRUMMER, J.J., GOLIGHTLY, J.P., Geology of the McClean uranium deposits, in: E.M. Cameron edit., Uranium Exploration in Athabasca Basin, Saskatchewan, Canada, Geol. Survey of Canada Paper 82-11 (1983) 71-110.

(29) STRNAD, J., The evolution of Lower Proterozoic epigenetic stratabound uranium deposits (a concept), 26th IGC in Paris, Metallogenesis of uranium, Geoinstitute, Beograd (1981) 99-162.

(30) STRNAD, J., Orientative lithogeochemistry of the Archaean and Aphebian basement in the Key Lake uranium deposit region (Saskatchewan, Canada), Journ. of Geoch. Explor. 19 (1983).

(31) POSEPNY, F., The genesis of ore deposits, Trans. Amer. Inst. Mining Eng. 23 (1894) 197-369.

THE TWO URANIUM DEPOSITS IN THE POLISH PART OF THE SUDETY MOUNTAINS

M. Banaś, K. Mochnacka
University of Mining and Metallurgy
Kraków
Poland

Abstract

THE TWO URANIUM DEPOSITS IN THE POLISH PART OF THE SUDETY MOUNTAINS

Two vein-type polymetallic-uranium deposits are described from the Sudety Mountains, Poland. These are the Kletno deposit and the Kowary deposit.

The Kletno deposit is located in metamorphic rocks, forming the tectonic complex of Śnieżnik Kłodzki. This complex is composed of two units of Precambrian (partly Middle Palaeozoic ?) age: the Stronie supracrustal unit and the infracrustal units of Gierałtów Gneiss and Śnieżnik Gneiss. Also magnetitic skarns, 'quartzites' and erlans are present. The rocks enclosing the Kletno deposit were thrusted over the Stronie schists, along a NNW-SSE striking thrust fault. The ore zone follows the same direction but lies about 100 m away from it. It is located at the contact between the Śnieżnik granitic gneisses above and the marbles below. The ore veins are following either cataclastic quartz zones adjoining magnetite-bearing skarns or nests of black fluorite. The mineralization consists of pitchblende, sooty pitchblende and other secondary U minerals like gummite, fourmarierite, uranophane, metatorbernite and autunite. Magnetite, hematite, pyrite, phyrrhotite, native gold, native silver, sulphides, sulphosalts and selenides of Pb, Zn, Cu, Ag, Bi, Hg, Sb are also present. The ore has six different types of mineral assemblages and parageneses. Alteration processes have been observed in the wall-rocks. Based on microscopic studies of ore minerals the succession of minerals was established.

The polymetallic-uranium mineralization is controlled by two factors: geochemical uranophile environment and intense tectonization causing zones of small fracture type.

The Kowary deposit is located in the southeastern part of the metamorphic cover of the Karkonosze Granite. The host rocks are of Proterozoic (?) or Lower Palaeozoic age. The Kowary deposit was mined for magnetite and uranium ore. The ore bodies were situated in the rock series referred to as 'the ore-bearing formation', which is composed of marbles, erlans and skarns. Usually, this ore-bearing formation is surrounded by gneiss but at places it is in direct contact with a granite. In the west, a main fault cuts this formation. This fault is of particular significance for the uranium mineralization processes.

Two morphologically different types of uranium deposits are distinguished: stockwork deposit and vein deposit. The main ore minerals are pitchblende, accompanied by coffinite, sulphides, sulphosalts, and selenides of As, Co, Ni, Ag, Bi, Cu, Pb, Hg, native Ag, pyrite, and sometimes secondary uranium minerals. Macroscopic and microscopic observations show an alteration of wall-rocks and vein components. The minerals succession was established and four hydrothermal phases can be distinguished.

The deposits described reveal several similarities, but they differ in their relation to magmatism. The mineral assemblages are similar to those occurring in the so-called 'five metals formation deposits', but also some differences were observed. Both deposits seem to be typical hydrothermal mineralizations belonging to the large family of deposits associated with the Variscan orogenesis in Europe.

1. INTRODUCTION

Uranium minerals were described from several localities in Poland, where they formed either deposits or uneconomic occurrences. Hydrothermal deposits are known from the Sudety Mountains. Two representative localities have been described in this paper: the Kletno and the Kowary deposit (Fig. 1), which are worked out now. Both deposits are located in metamorphic rocks belonging to two different structural units of the Sudety Mountains. The Kowary deposit is situated in the Karkonosze-Izera block (Western Sudetes), whereas the Kletno deposit lies within the Ladek-Śnieżnik metamorphic unit (Middle Sudetes). The rock series occurring within the two deposits show close similarities and have often been compared with each other in the literature.

The Sudetes are a part of the Central-European Variscan orogenic belt developed along the northern margin of the Bohemian Massif. They belong to the Sudetic metallogenic region (Osika (1)).

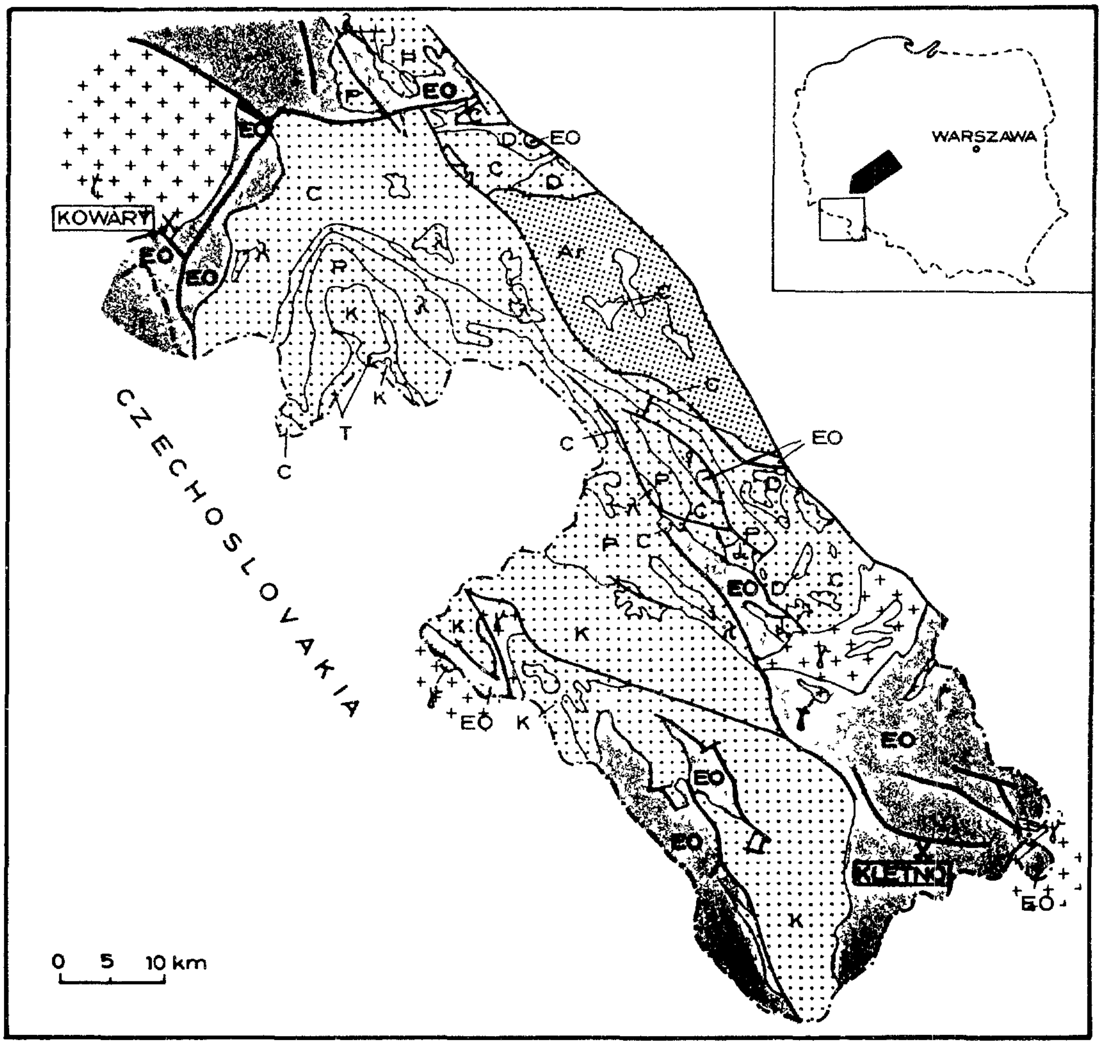

FIG. 1. Geological map of the Sudety Mountains after Sawicki and Teisseyre (26) (simplified). K - Cretaceous, T - Triassic, P - Permian, C - Carboniferous, D - Devonian, EO - Proterozoic, Precambrian, Cambrian, Ordovician, and Silurian, Ar - Archaean, α - old Palaeozoic effusive rocks, λ - volcanic rocks of Upper Carboniferous and Permian, γ - granitoides of Variscan age, φ -gabbro of pre-Variscan age, X - ore deposits described in this paper.

2. KLETNO DEPOSIT

2.1. General geology

The Kletno deposit is located in the Kłodzko District, which is a part of the Middle Sudetes. The area belongs to the tectonic complex of Śnieżnik Kłodzki. The metamorphic rocks of this unit are of Precambrian age (Fig. 2). Two different rock units have been distinguished in this area (Smulikowski (2), Teisseyre (3)):

(i) The Stronie supracrustal unit is built up by mica schists and biotite gneisses with intercalations of graphitic quartzites, quartzites, marbles and amphibolites as well as quartz-microcline-plagioclase schists and leptite gneisses. The rocks are regarded to be of Upper Proterozoic age (Teisseyre (4)).

(ii) The infracrustal unit consists of the Śnieżnik and Gierałtow Gneiss. According to Don (5), the age of these rocks has not yet been finally determined. It is believed, however, that it ranges from Precambrian (?) to Middle Palaeozoic (?). In addition, the deposit contains magnetite-bearing skarns, 'quartzites', calc-silicate hornfelses and the so-called Kletno conglomerates.

The mica schists of the Stronie series are two-mica schists with quartz and chlorite showing evidence of feldspathization. In the eastern zone, at the contact with the Śnieżnik Gneiss, the schists are interbedded with marbles, grading into biotite paragneisses. Compared with the schists, the latter ones show a more advanced feldspathization and a more compact structure. Graphitic varieties of the schists are also present, forming a system of layers up to 2 m thickness. This rock is locally silicified and has a character of graphitic quartzite with dispersed submicroscope graphite in which the carbon content runs up to 5 wt%.

The higher members of the Stronie schists contain interbeds or lenses of marbles up to several dozens of metres. The rock is white, usually thick-bedded, with a fine- or medium-crystalline granoblastic texture. At the contact with schists, the marble contains pyroxenes, garnets, amphiboles, dark micas, phlogopite, plagioclases and epidote. Such a rock is greenish in colour and does not show bedding. It has an aphanitic texture and grades into the so-called erlans or skarnoids, which contain traces of pyrite, pyrrhotite, arsenopyrite and copper sulphides. These rocks presumably owe their origin to the alteration of chemically differentiated marly limestones under conditions of isochemcial metamorphism.

The plagioclase-microcline gneisses occurring in the infracrustal unit are called the Gierałtow and Śnieżnik Gneiss. The former are fine-crystalline, locally migmatitic, showing thin or flaser bedding. They are poor in microcline. The Śnieżnik granitic gneiss is characterized by coarser crystals, a less distinct orientated structure, and above all, by augen textures. Microcline 'eyes' sometimes grow to form megablasts or aggregates of megablasts (Teisseyre (4)).

2.2. Orebody

The host rock of the Kletno deposit strikes NNW-SSE and dips at 30 - 70° to ENE. The Śnieżnik Gneiss series was thrusted over the Stronie schist series along a thrust fault striking NNW-SSE. The thrust zone, up to 3 m thick, contains the 'Kletno conglomerates'. The pebbles are of allochthonous material in relation to the surrounding rocks and are embedded in clay-graphitic cement. The conglomerates are presumably of Upper Carboniferous age (Kasza (6)). The deposit is cut by several faults striking NW-SE and SW-NE. None of these structures are minera-

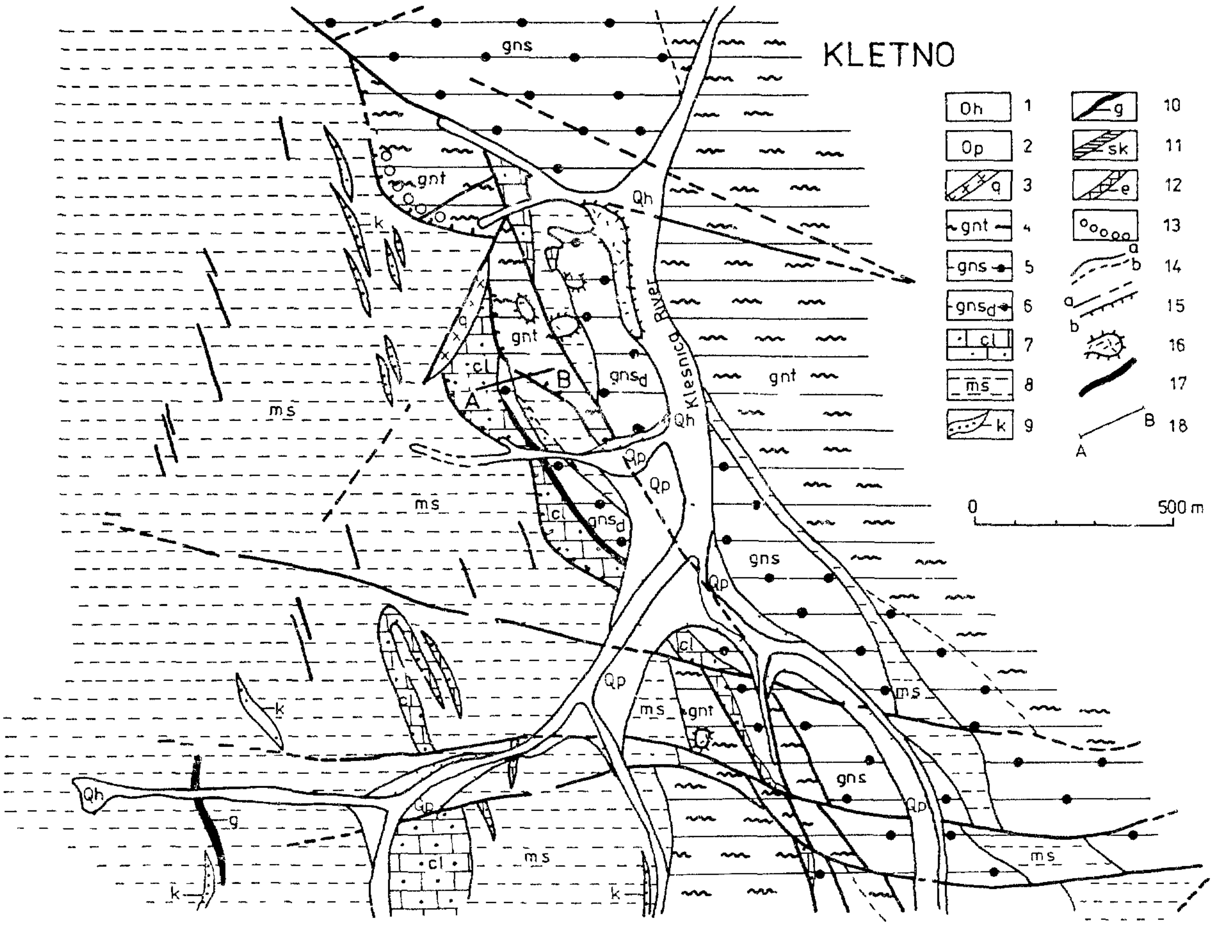

FIG. 2. Detailed geological map of the area of the deposit at Kletno after Don (27). Zone of mineralization and cross-section after Banaś. 1. Holocene alluvium; 2. deposits of Pleistocene terraces; 3. quartz veins ('quartzites' on the cross-section, Fig. 3); 4. transitional and mixed-type gneisses (transition between the Gierałtow and Śnieżnik Gneisses); 5. Śnieżnik Gneiss; 6. fine-augen variety of the Śnieżnik Gneiss (marginal facies); 7. crystalline limestones (marbles); 8. mica schists and paragneisses; 9. light quartzites; 10. graphitic quartzites and schists; 11. skarns (on the cross-section, Fig. 3)· 12. erlans (on the cross-section, Fig. 3); 13. Kletno conglomerates and sandstones; 14. lithological boundaries of distinct (a) and transitional (b) character; 15. faults (a) and thrusts (b); 16. waste dumps; 17. zone of mineralization; 18. line of cross-section A-B (see Fig. 3).

lized. An exception is a thick quartz vein filling a fault zone that penetrates into the gneiss.

The mineralized zone follows the direction of the main overthrust over a length of 500 m, but is about 100 m distant from it (Fig. 2). Exploration work and mining activities have revealed that the zone is located at the contact between the Śnieżnik granitic gneiss above and marbles below (Fig. 3). The ore-bearing sequence comprises from the bottom to the top: marbles, a 2 m thick 'quartzite' zone, magnetite-bearing skarns and gneisses. The thick unit of the so-called 'quartzites' are strongly silicified crystalline limestones which, being subject to a multiphase cataclasis, became the host for either fluorite-quartz veins containing locally barite or for polymetallic orebodies. The skarns are composed of typomorphic minerals, including hornblende, ferrosalite, grossular-andradite, pistacite, and slightly hematitized magnetite. They also contain a fair amount of

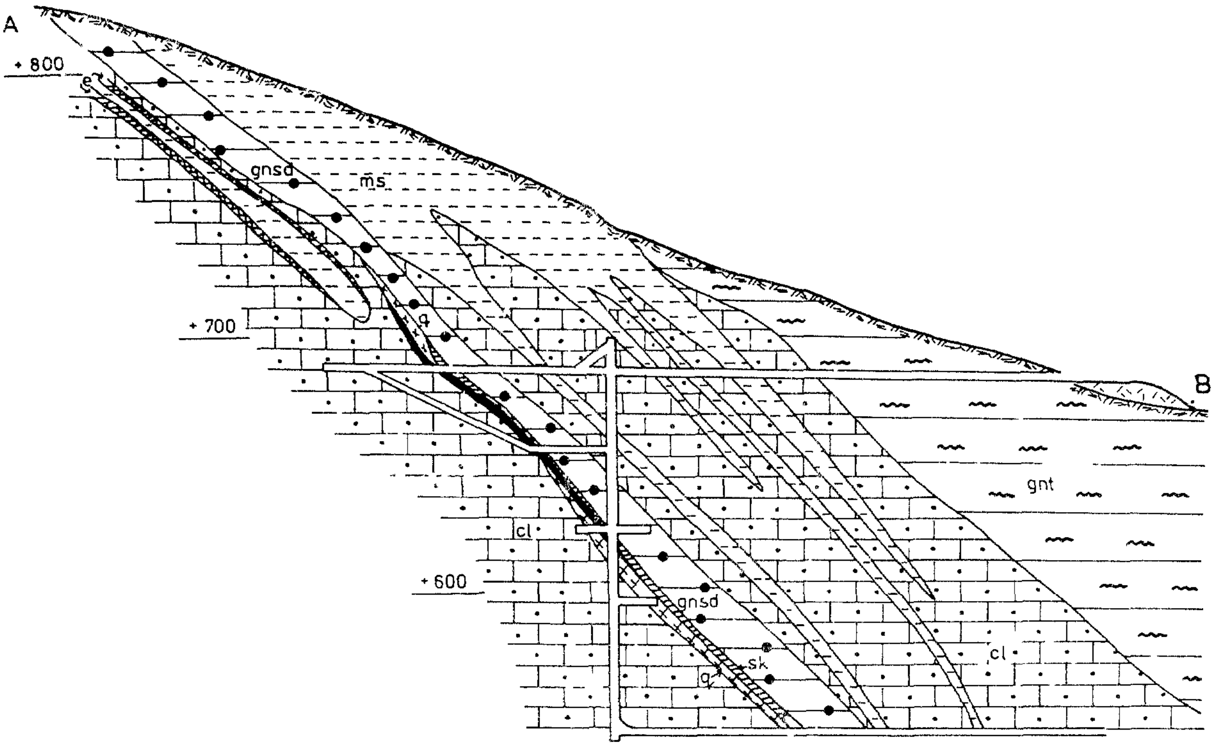

FIG. 3. Geological cross-section A-B through the zone of mineralization at Kletno deposit. Explanations see Fig. 2.

sulphides, pyrite, pyrrhotite, arsenopyrite, chalcopyrite, sphalerite and cosalite as well as calcite-fluorite veinlets and traces of cassiterite. The skarns originated from regionally metamorphosed ferruginous sediments, then were superimposed by contact metamorphism caused by the intrusion of the Śnieżnik granites. Subsequently, the granite was altered to granitic gneisses.

An analysis of the vertical profile of the deposit shows that polymetallic-fluorite mineralization becomes poorer with depth. At a depth of 30 m it grades into quartz and then disappears. Contrary to this, the thickness of the magnetite-bearing skarn body increases downwards, reaching 2.5 m at a depth of 200 m (Banaś (7)).

2.3. Polymetallic uranium mineralization

Fig. 4 shows a typical section through a polymetallic uranium mineralization. Wider ore zones form locally veins grading into pots of up to 40 cm thickness. They are found within cataclastic quartz zones, adjoining magnetite-bea ing skarns, or within pots of black fluorite. Light fluorite is devoid of uranium minerals. As seen in the horizontal level plan (Fig. 5), polymetallic uranium mineralization usually concentrates in fluorite bodies.

Detailed mineralogical studies have revealed the presence of the following ore minerals: magnetite, hematite-specularite, pyrite, pyrrhotite, arsenopyrite, sphalerite, chalcopyrite, bornite, chalcocite, galena, tetrahedrite, cosalite, stromeyerite, miargyrite, wittichenite, cinnabar, clausthalite, umangite, klockmannite, bohdanowiczite, tiemannite, traces of naumannite, eskebornite, native gold and native silver. Minerals within the weathered zone are covellite, malachite, azurite, chrysocolla, anglesite and cerussite, and accessory vein minerals are quartz, barite, fluorite, and calcite.

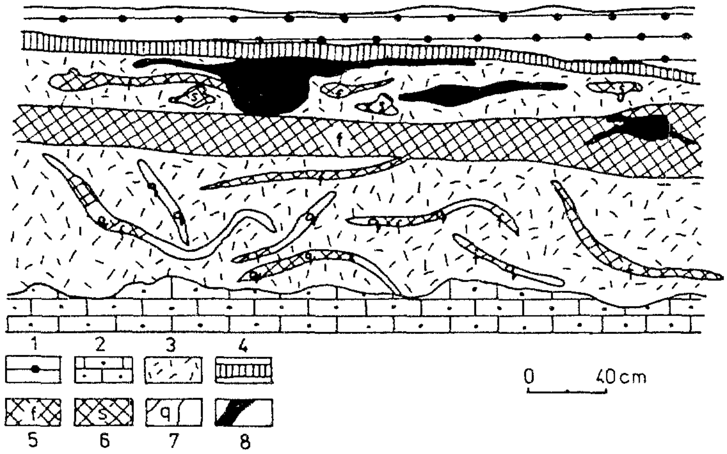

FIG. 4. Sketch illustrating a typical ore-bearing zone at Kletno deposit with the polymetallic-uranium mineralization (wall of an adit). 1. Śnieżnik gneiss; 2. marbles; 3. 'quartzites' originated from the silicification of crystalline limestones; 4. magnetite-bearing skarns; 5. veins of fluorite; 6. pots of sulphides; 7. veins of quartz; 8. veins and pots of polymetallic uranium mineralization.

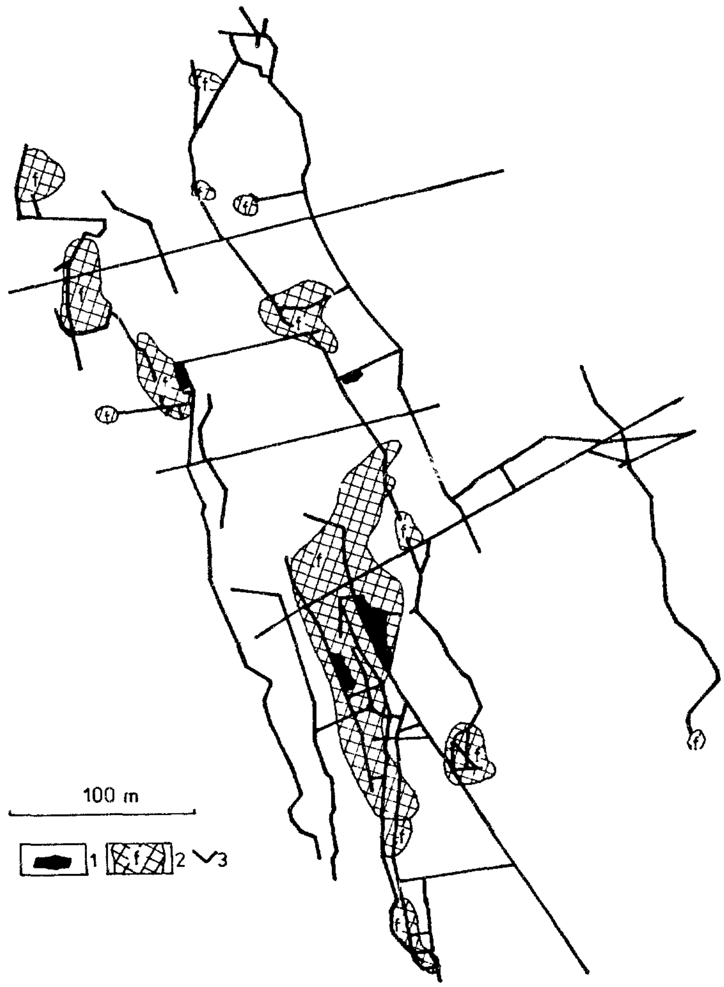

FIG. 5. Level plan of the Kletno mine. 1. aggregates of polymetallic uranium mineralization; 2. pots of fluorite; 3. drifts.

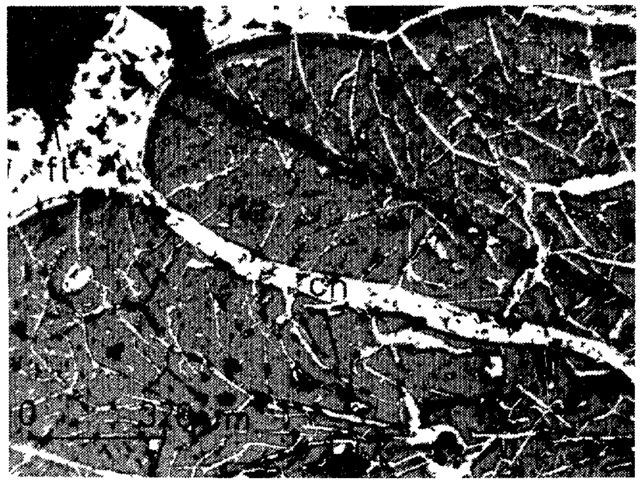

FIG. 6. Flattened aggregates of collomorphic pitchblende (na), surrounded by fluorite (fl) and chalcopyrite (ch). Chalcopyrite also fills the syneresis cracks in pitchblende and replaces it. Reflected light.

Uranium minerals are represented by pitchblende, sooty pitchblende, gummite, fourmarierite, uranophane, metatorbernite, and autunite.

The above minerals form several assemblages and parageneses:

(a) oxide and sulphide skarn mineralization,

(b) quartz-fluorite-barite with Fe, Cu, Zn, Pb sulphides,

(c) quartz-fluorite,

(d) pitchblende-sulphide-selenide,

(e) uranium-fluorite,

(f) uranium-selenium.

A quartz-fluorite assemblage formed a fluorite deposit within crystalline marbles containing 6,000 m^3 of fluorite, which was mined.

Parageneses (d), (e), and (f) represent uranium mineralizations with accompanying oxidation products, sulphides and selenides.

The principal component of the pitchblende-sulphide paragenesis with selenides (d) is pitchblende. It forms colloform, usually flattened aggregates (Fig. 6). Under the microscope it can be seen that the pitchblende from the Kletno deposit occurs in the four varieties (I, II, III, IV) corresponding to those reported in the literature (Sobolieva and Pudovkina (8)). From variety I to IV the reflectance decreases from 17 to 10 % and so does the microhardness (from 1,025 to 95 kG/mm^2), the colour changes from black to brown, and pitchblende IV displays brown internal reflections. These varieties reflect the different degree of UO_2 to UO_3 oxidation, which increases from variety I to IV. Pitchblende IV is probably the initial phase of the formation of gummite (Banaś (9)).

Pitchblende forms disseminated structures in fluorite or quartz (Fig. 7), sometimes as dendritic, compact, irregular concentrations (Fig. 8), and often as veins (Fig. 9) and as breccias (Fig. 10). There are two generations; fine- and coarse-crystalline pitchblende (Fig. 11), usually together with chalcopyrite which overgrows pitchblende grains, cements their aggregates and together with fluorite, fills the syneresis cracks in the mass of pitchblende (Fig. 12). Less common are pitchblende intergrowths with other sulphides - chalcocite and pyrite. This paragenesis consists of substantial amounts of clausthalite, bohdanowiczite ($AgBiSe_2$), wittichenite, and traces of naumannite, eskebornite, native selenium, and native silver. The selenides and wittichenite showing subtle intergrowth also penetrate into the pitchblende matrix (Fig. 13). Native silver forms inclusions in clausthalite.

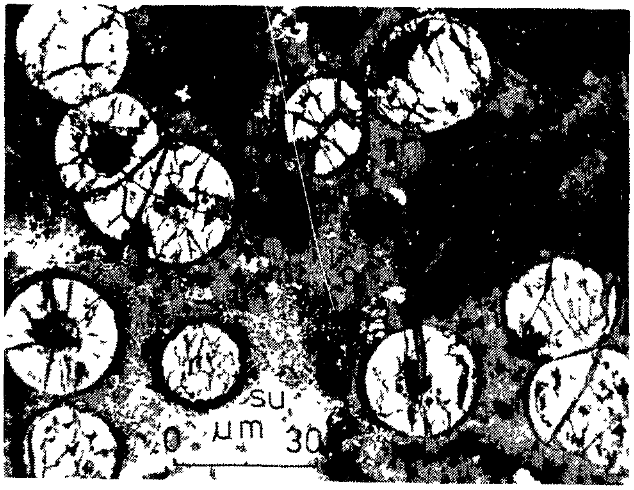

FIG. 7 Pitchblende formıng spherical forms scattered in quartz (q). Quartz intergrown by fluorite (fl), and sulphides (su). Reflected light.

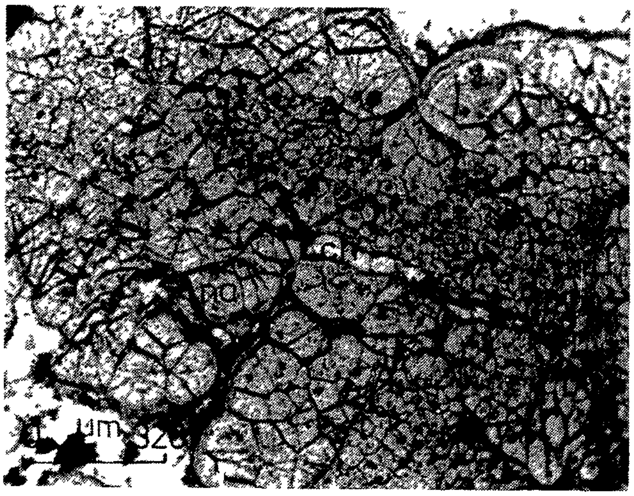

FIG. 8. Compact collomorphic pitchblende (na) occurs in chalcopyrite (ch). The fissures in pitchblende filled by chalcopyrıte and fluorite (black spots). Reflected light.

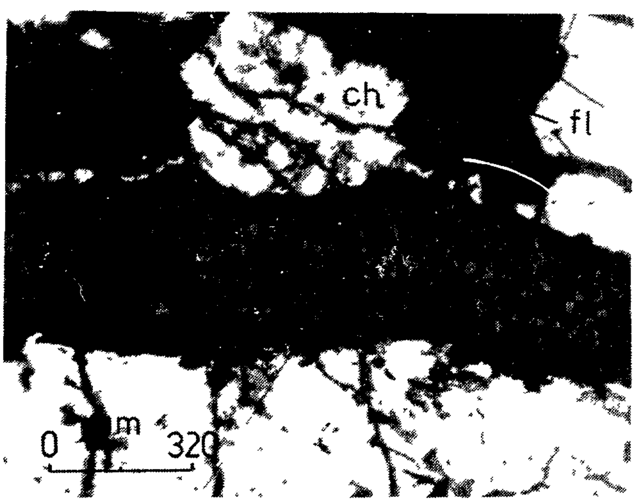

FIG. 9. Vein-form of pitchblende (na) transsecting chalcopyrite (ch), fluorite (fl) accumulations. Reflected light.

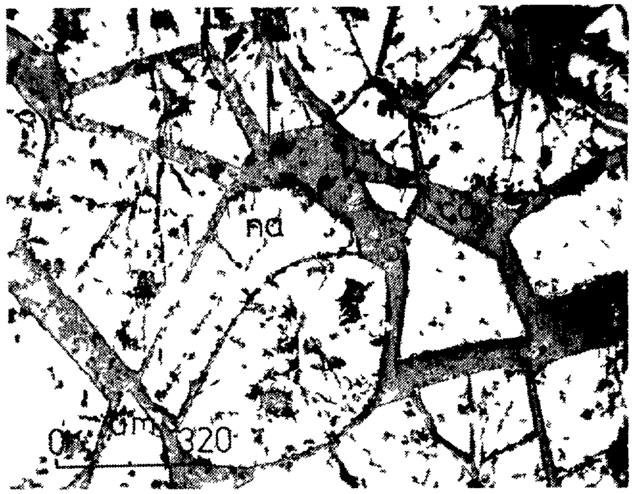

FIG. 10. Fragments of pitchblende (na) cemented by calcite (ca) form a microbreccia structure. Black spots in calcite and pitchblende are fluorite inclusions. Reflected light.

FIG. 11. Two generations of pitchblende. The free spaces within reniform pitchblende I (na) are filled by pitchblende of the second generation (na II), forming fine-crystalline aggregate intergrown by sulphides (su). Fluorite (black veinlets and irregular spots) fills the fissures in pitchblende of both generations and partly replaces it. Reflected light.

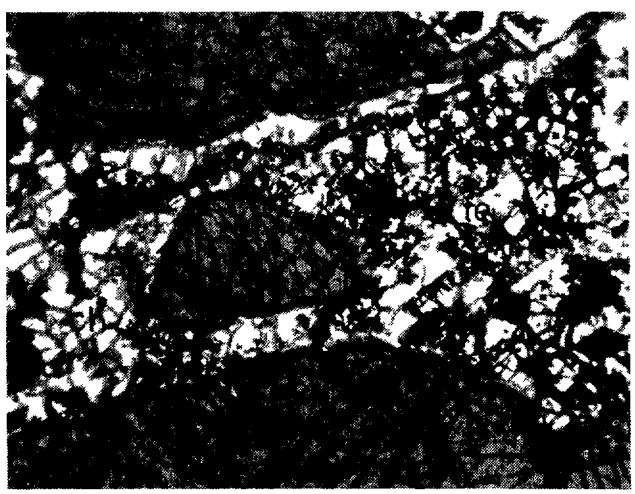

FIG. 12. Vein consisting of partly oxidized chalcopyrite (ch), tetrahedrite (te) and fluorite (black spots) cuts a compact aggregate of pitchblende (na). Reflected light.

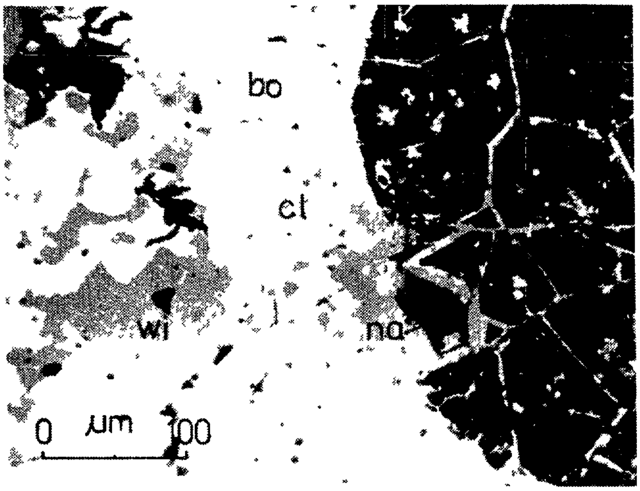

FIG. 13. A collomorphic pitchblende (na) overgrown by: clausthalite, bohdanowiczite and wittichenite (wi). The two selenides (cl and bo) showing similar reflectance are difficult to distinguish on the photograph. The fissures in pitchblende are filled by wittichenite and both selenides. Pitchblende shows the phenomena of metasomatic replacement by these minerals. Reflected light, immersion.

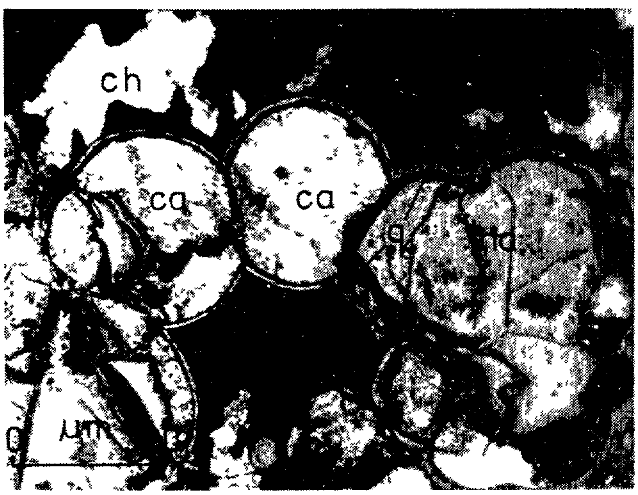

FIG. 14. Digenite-pseudomorphs (ca) after pitchblende (na) in quartz (q). Relicts of chalcopyrite (light spots) are visible in digenite. Deformed pitchblende spherolite is partly replaced by copper-sulphide. Irregular forms of chalcopyrite (ch). Reflected light.

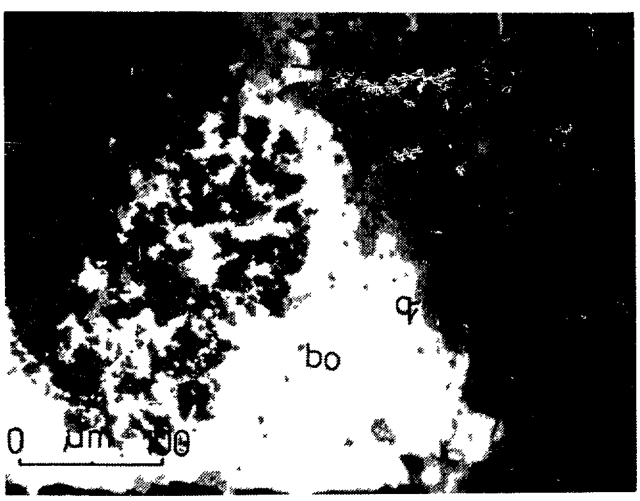

FIG. 15. Replacement of pitchblende (na) by bohdanowiczite (bo). An outline of pitchblende's relict shows the primary spherolitic texture. (q) - quartz; (ca) - chalcocite. Reflected light, immersion.

FIG. 16. Collomorphic pitchblende (na) occurring in quartz (q) changed partly into gummite (gu). The oxidation develops along syneresis cracks and at grain edges of the pitchblende. Reflected light, immersion.

FIG. 17. Process of the oxidation of pitchblende (na). Replacement of pitchblende by fourmarierite (fu) and gummite (gu) is visible on the right side of the photograph. In the centre, a complete pseudomorph of fourmarierite after pitchblende is observed. Transmitted light.

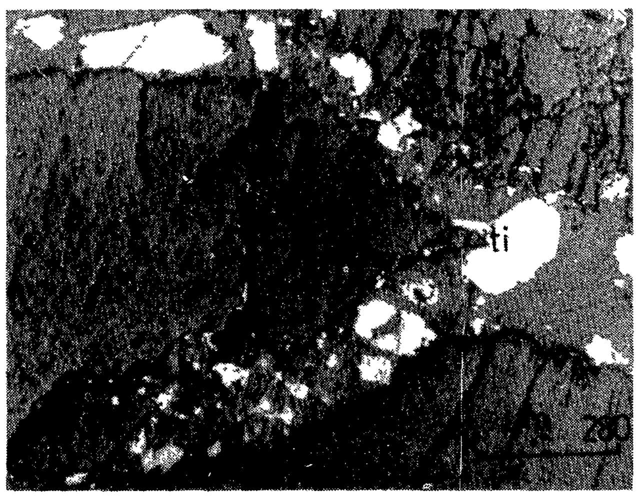

FIG. 18. Veinlet of secondary uranium mineralization with grains of tiemannite (ti) in quartz (q). Reflected light.

Pitchblende is frequently replaced by chalcopyrite, chalcocite (Fig. 14), and selenides, mainly bohdanowiczite, and clausthalite (Fig. 15) (Banaŝ and Mochnacka (10)).

Pitchblende is intensely oxidized and grades zonally into gummite (Fig. 16) or fourmarierite (Fig. 17). Sooty pitchblende, uranophane, metatorbernite and autunite form concentrations at a certain distance from the primary pitchblende. The oxidation zone of uranium minerals reaches to a depth of about 50 m (Banaŝ (11)).

Fairly common is a paragenesis of pitchblende together with fluorite (e). Pitchblende occurs as veinlets together with large, usually irregular concentrations of massive pitchblende within black, disintegrated fluorite. In this case, pitchblende is also intensely oxidized and grades into a gummite conglomerate.

The paragenetic uranium-selenide assemblage (f) consists as a rule of clausthalite, umangite, klockmannite, tiemannite and traces of cinnabar, embedded in veinlets or nests of secondary uranium minerals. Such veinlets usually crosscut quartz-fluorite concentrations (Fig. 18) (Banaŝ (12)).

Pronounced alteration processes have been observed around the uranium mineral aggregates, resulting in irregular concentrations of ferric iron (Fe^{3+}) oxides and rosette-like aggregations of specularite. Fluorite intergrown with pitchblende is black and disintegrated. Quartz acquires the properties of smoky quartz, and the pink colour is typical for carbonates accompanying the pitchblende.

2.4. Discussion

The data collected on the Kletno deposit indicate that polymetallic uranium mineralization is controlled by two basic factors:

(i) the geochemical uranophile environment, and

(ii) the intense tectonic movement leading to the formation of small fracture zones.

The suitable geochemical conditions for the emplacement of uranium minerals have been created by skarns mineralized with magnetite. The uranium occurs in zones of intense cataclastic quartz masses, which were mineralized earlier by light coloured fluorite in the form of veins and nests.

All the mineralogical data imply that polymetallic uranium mineralization in the Kletno deposit is of hydrothermal origin. A deep source is suggested for the mineralizing solutions. The intrusions of granites, tonalites and syenites occurring in the vicinity (within 18 km) of the deposit do not show evidence of the Kletno-type mineralization. It seems feasible, however, that these rocks are the differentiates of a parent magma which was also the source of polymetallic mineralization in the Kletno deposit. It is interesting to note that the magnetite deposit of a similar type at Janowa Góra, only 3 km away from Kletno, contains only traces of uranium.

The source of selenium could not be determined with confidence. It may be sought in selenium-bearing sulphides.

Polymetallic uranium ore is younger than fluorite-quartz sulphide or fluorite mineralization. The origin of the latter from water phase was documented by Thugutt (13).

In the two mineral parageneses, pitchblende-sulphide-selenide and uranium-fluorite, pitchblende seems to be the oldest. It is over- and intergrown by the younger sulphides and selenides, and is replaced by ore minerals and fluorite. In these parageneses, selenides appear to be contemporaneous with sulphides, as they intergrow each other. The uranium-selenium paragenesis, on the other hand, has distinct features of oxidized cap mineralization (Robinson (14)). All the uranium minerals in this assemblage are of a secondary phase, occurring only together with selenides.

The age of polymetallic uranium mineralization from Kletno is an unresolved problem, due to the lack of absolute age dating. The analysis of geological and mineralogical evidences suggests a Late Hercynian age for the mineralization. Table I represents the major characteristics of mineralization in the Kletno deposit. As it appears from these data, the polymetallic uranium mineralization is a modified five-metal formation. In Kletno Ni-Co minerals are absent, and only cosalite contains substantial amounts of Ni. The place of Ni-Co is taken by selenium with its fairly rich mineral assemblages. It appears, therefore, that the polymetallic uranium formation from Kletno is of the U-Ag-Bi-Se type and represents lower crystallization temperatures compared with the classic formations known from Jâchymov (Czechoslovakia) or Kowary (Poland).

3. THE KOWARY DEPOSIT

3.1. General geology

The Kowary deposit is located in the SE part of the metamorphic cover of the Karkonosze Granite. The rocks of this area have been studied extensively. However, there is still a certain disagreement in the interpretation of their age, formation processes, and their regional tectonic pattern. According to Teisseyre (15), the part of the cover hosting the orebody belongs to the so called 'Kowary Gneiss Group', determined by this author as Proterozoic (?) or as granitized Lower Palaeozoic. The 'Rudawy Janowickie Group', adjoining this series to the east and constituting the second component of the eastern metamorphic cover is composed of the Leszczyniec Volcanic Formation and the Czarnôw Schists Formation, both being of Silurian age (Teisseyre (15)).

The Kowary deposit was mined for magnetite and uranium ore. Old chronicles also mention that small amounts of arsenic-silver ore containing Ni, Co, and Zn were exploited here.

The magnetite deposit and the uranium-bearing zones were situated in a rock series referred to as 'the ore-bearing formation' (Fig. 19). The deposit forms a lens of about 2 km length and up to 200 m width, narrowing in the middle to a few dozen metres. It consists of marbles, erlans, schists, skarns, and magnetite lenses. The whole ore-bearing formation is surrounded by gneiss. In the north it has a contact to a granite. The general strike of rocks is approximately concordant with the outline of the granite intrusion. In the eastern part, both the formation and the other metamorphic rocks of the cover, dip at about 70° to S, with a slight deviation to SW or SE. In the western part, the rocks dip - at high angles to N - under the Karkonosze Granite, which covers them like a 'roof' (Fig. 19 and 20) (Mochnacka (16) (17): here see older references for the Kowary deposit).

The ore-bearing formation is cut by several transverse and longitudinal faults. Of particular significance for uranium mineralization is the 'main' fault, located in the western part of the formation, with the fault plane trending NW-SE (Fig. 20).

3.2. Ore-bearing formation

The ore-bearing formation is a series of interbedded rocks grading into each other. In the middle, marbles prevail whereas in the whole ore-bearing formation erlans are the dominant rocks. Erlans show a distinct bedding, small crystal size

TABLE I. MINERAL SUCCESSION OF THE POLYMETALLIC URANIUM MINERALIZATION IN THE KLETNO DEPOSIT.

Minerals	Phases of Crystallization: Hydrothermal	Phases of Crystallization: Supergene	Parageneses
Quartz	———		Pitchblende Sulphides Selenides
Fluorite	———		
Pyrite	———		
Pitchblende	———		
Chalcopyrite	———		
Tetrahedrite	———		
Chalcocite	———		
Clausthalite	———		
Bohdanowiczite	———		
Wittichenite	———		
Native Silver	———		
Naumannite	———		
Eskebornite	———		
Fluorite	———		Uranium-Fluorite
Pitchblende	———		
Specularite	———		
Quartz	———		Uranium-Copper Lead Mercury Selenium
Calcite	———		
Fluorite	———		
Clausthalite	———	- - - - -	
Umangite	———	- - - - -	
Klockmannite	———	- - - - -	
Tiemannite	———	- - - - -	
Cinnabar	———	- - - - -	
Uranophane	———	- - - - -	
Native Gold	———	- - - - -	
Miargyrite	———	- - - - -	
Gummite		———	
Sooty Pitchblende		———	
Fourmarierite		———	
Metatorbernite		———	
Digenite		———	
Native Selenium		———	

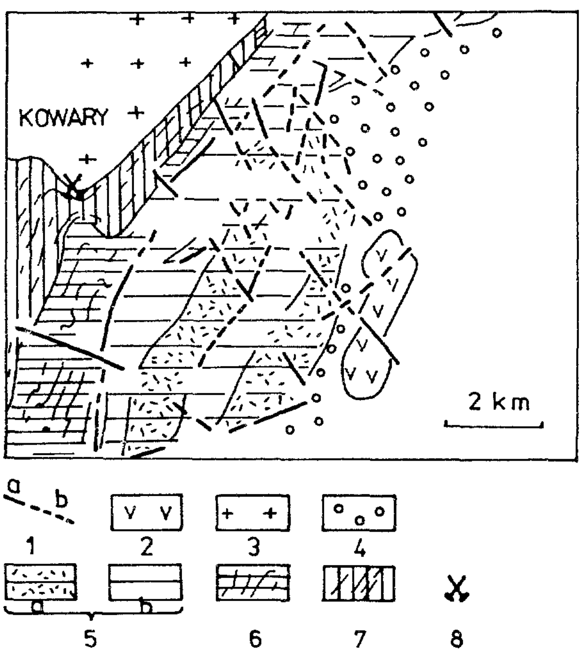

FIG. 19. Geological sketch-map of the Kowary region (after Teisseyre (15). 1. faults, a) observed, b) assumed; 2. Young Palaeozoic volcanites; 3. Karkonosze Granite; 4. Carboniferous sedimentary rocks; 5. Leszczyniec volcanite formation (upper partly Middle Silurian), a) Paczyn Gneiss, b) metavolcanites; 6. Czarnów schist formation (Lower and Middle Silurian); 7. Kowary Gneiss Group (Proterozoic and granitized older Palaeozoic rocks); 8. location of the area shown in Fig. 20).

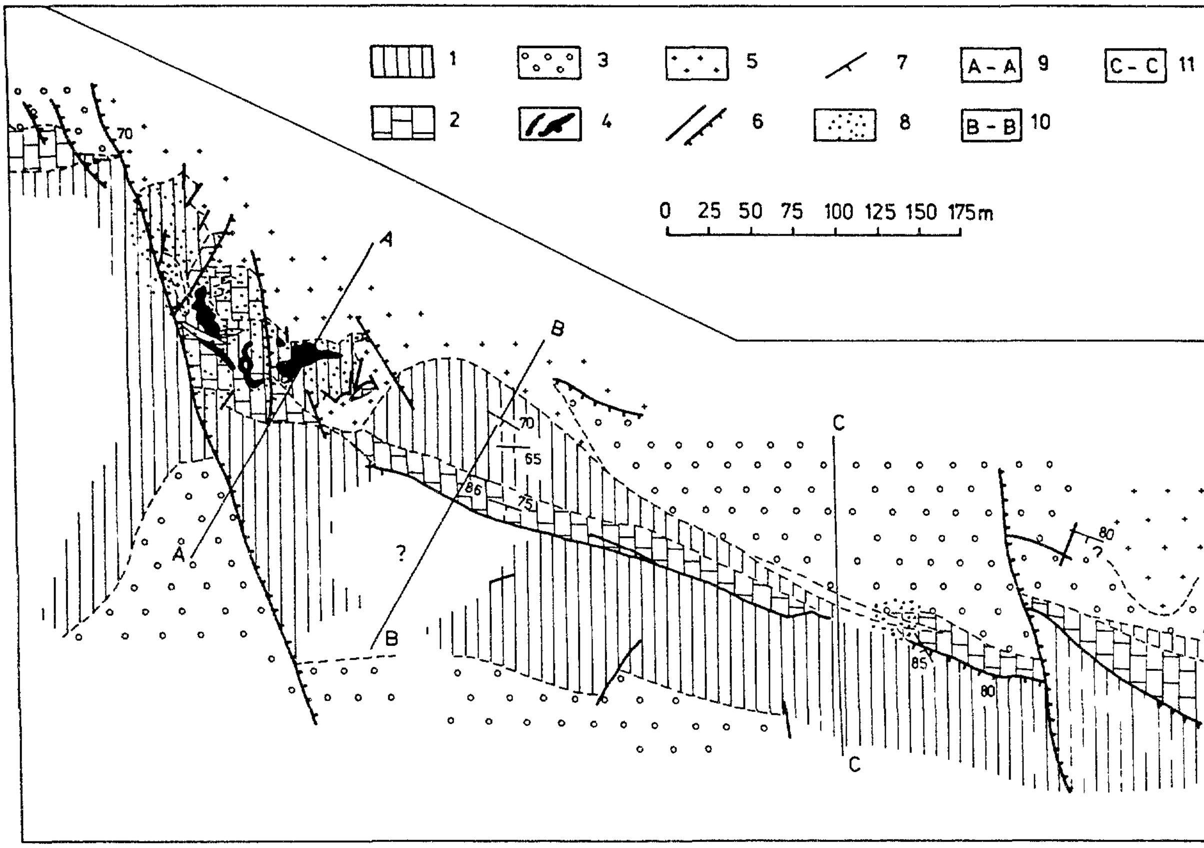

FIG. 20. Geological sketch map of the 118 m level (Kowary Mine). 1. erlans, schists and skarns; 2. marbles; 3. gneiss; 4. magnetite; 5. granite; 6. faults, 7. strike and dip; 8. polymetallic mineralization; 9. cross-section A-A: depth 100 - 550 m, cross-section B-B: depth 550 - 670 m; cross-section C-C: depth 100 - 450 m (Fig. 21).

and varying colours. The main components are feldspars, quartz, pyroxenes (salite, diopside), amphiboles (hornblende, tremolite), biotite, phlogopite, garnets, and minor titanite, epidote (zoisite, clinozoisite), scapolite, and serpentine. The colour of rocks depends on the varying content of individual minerals. In many cases, the schists have a composition similar to erlans. Feldspar-biotite, quartzite, pyroxene-phlogopite, amphibole-biotite, and chlorite schists have been recognized. The marbles are medium- and coarse-crystalline, and show distinct bedding. Calcite predominates, accompanied by serpentine, sometimes diopside, phlogopite, epidote, garnets, humite, and tourmaline.

In places, both marbles and erlans are transformed to skarn, which is a coarse-, inequicrystalline rock characterized by a random structure and a heterogenous pink-green, sometimes dark-green colour. Its principal components are garnets (andradite), pyroxenes (diopside), epidotes (ordinary epidote, clinozoisite, pistacite), amphiboles (hornblende) and sometimes vesuvianite. The subordinate constituents are calcite, feldspars, talc, prehnite, chlorite, titanite and ore minerals, such as pyrite and chalcopyrite. Larger sulphide concentrations were found in places where skarn accompanies magnetite deposits.

Magnetite deposits form lenses and tabular bodies concordant with the host rocks and are usually deformed together with them (Fig. 20 and 21), Zimnoch (18)).

Dikes of granitic, syenitic or pegmatitic composition (Zimnoch (18)) cut both the ore-bearing formation and the enclosing gneiss. They are nearly horizontal.

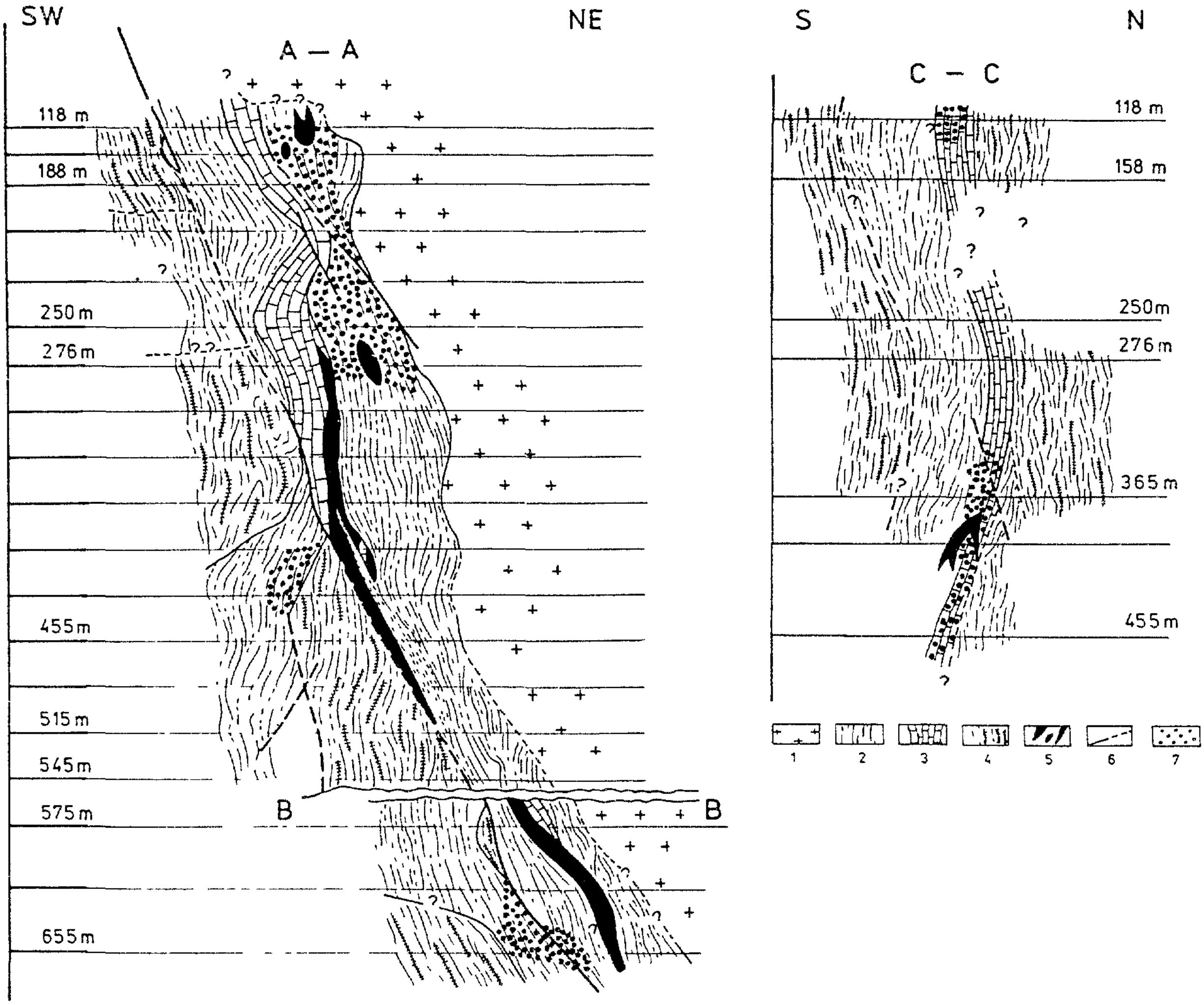

FIG. 21. Geological cross-sections of the region of the Kowary deposit (see also Fig. 20). 1. granite; 2. erlans, schists and skarns; 3. marbles; 4. gneiss; 5. magnetite; 6. faults; 7. polymetallic mineralization.

3.3. Orebodies

Uranium mineralization accompanies, as a rule, polymetallic mineralization, although there occur pitchblende concentrations containing only trace amounts of other ore minerals, or, to the contrary, concentrations of arsenic and cobalt minerals are devoid of uranium minerals.

Polymetallic uranium mineralization is evidently controlled by faults. Uranium-bearing zones are mostly located in the western part of the ore-bearing formation, next to the main fault, and only few occurrences have been reported from the central and eastern parts away from the fault. Major concentrations of uranium minerals were found in the upper horizons. Most suitable conditions for mineralization existed between 150 and 250 m. At about 650 m uranim mineralization disappears, and only a few ore pots were found below (Mochnacka (17)).

The most suitable environment for emplacement of mineralization was the contact between petrographically different rock types.

For mining purposes, two types of deposits were distinguished:

(i) stockwork deposits in the form of pipes, ranging from 5 x 15 m to 15 x 45 m in size, reaching several hundred metres downdip;

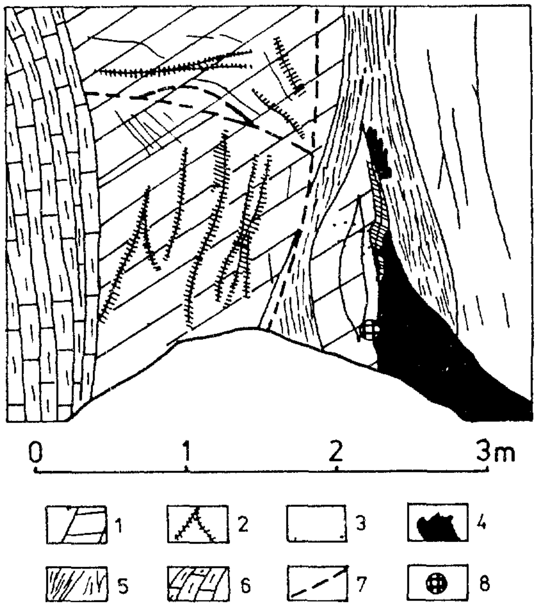

FIG. 22. Section through an ore-bearing vein. 1. calcite vein; 2. veinlets of calcite; 3. ferruginous zone; 4. magnetite with intercalations of crystalline schists; 5. mica-schists; 6. quartzite-schists; 7. faults; 8. sample containing uranium mineralization.

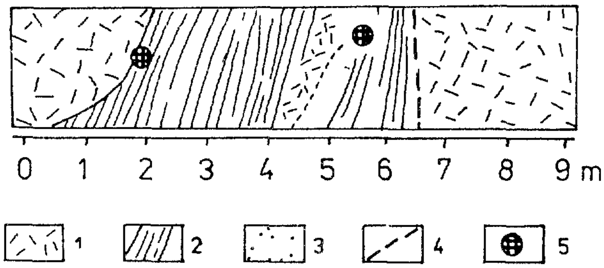

FIG. 23. Polymetallic uranium mineralization in the breccia. 1. breccia; 2. schists; 3. ferruginous zone; 4. faults; 5. samples containing uranium mineralization.

(ii) vein deposits with varying thickness being concordant to fault zones (Fig. 22).

Stockwork-type uranium deposits are characterized by the presence of tectonic breccia (Fig. 23) or networks of quartz-calcite veinlets in which pots of polymetallic uranium minerals are distributed. The size of such pots is difficult to determine, but they can be readily detected with a radiometer. The tectonic breccia is a spotted rock consisting of host rock fragments cemented by quartz, calcite, subordinate barite, and traces of fluorite. In places, quartz is accompanied by feldspars and carbonates (dolomite). The carbonate/quartz ratio decreases with depth. The uranium minerals form pots in the breccia cement. In some uranium zones of this type, a rock appears resembling the host rocks but significantly enriched in quartz, calcite, and potassium feldspars. Occasionally there occur veins of coarse-crystalline quartz and calcite.

Vein deposits are the most common morphological type of uranium ore zones. Carbonate veins of varying thickness (up to several dozen cm) consist of colourless, rusty or pale-pink calcite. This calcite hosts pots of uranium minerals and the accompanying ore minerals.

3.4. Ore mineral assemblage

The principal component of the ore pots is pitchblende accompanied by coffinite, liebigite, arsenopyrite, löllingite, tiemannite, clausthalite, sphalerite, chalcopyrite, pyrite, cinnabar, bornite, covellite, native silver, emplectite,

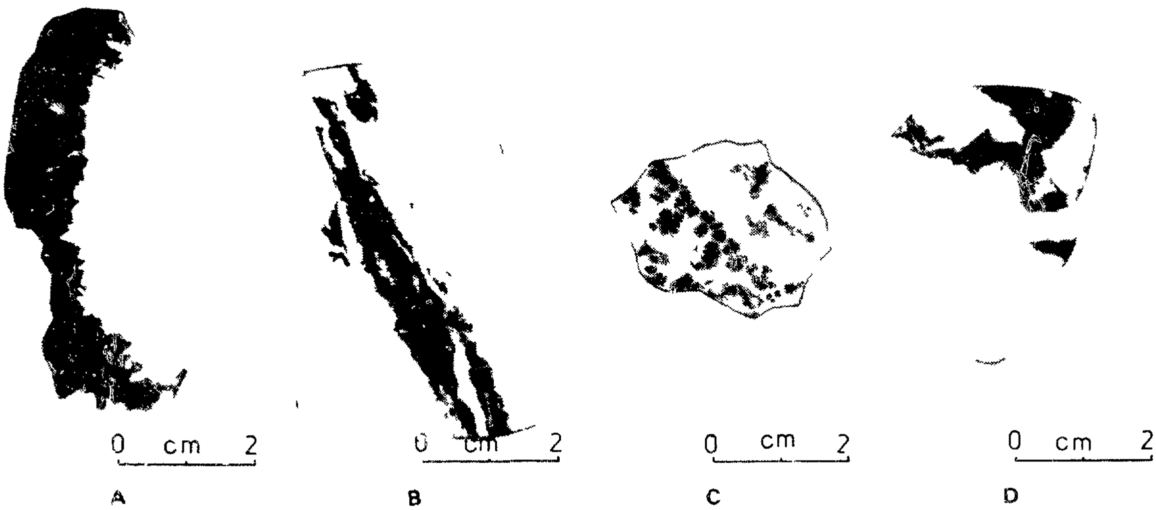

FIG 24. Radiographs showing the structures of pitchblende: A - reniform crusts; B - laminar aggregates· C - concentrations close to dendritic forms; D - irregular aggregates.

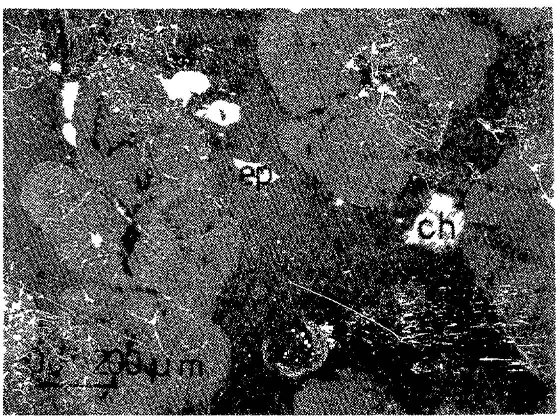

FIG. 25. Individual pitchblende dendrites in calcite. Outward of pitchblende aggregates of chalcopyrite (ch) and emplectite (ep). These minerals occur also in fine but distinct syneresis cracks. Reflected light.

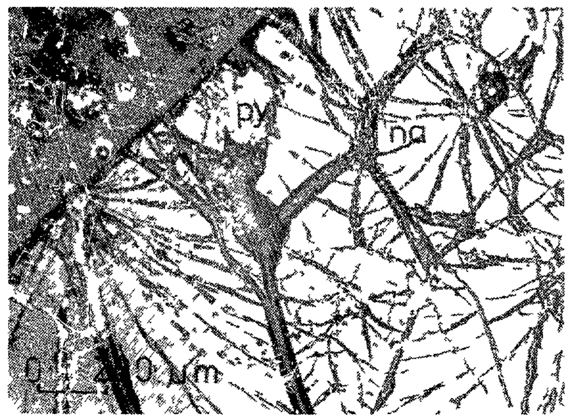

FIG. 26. Pitchblende (na) with distinct syneresis cracks, filled with gangue minerals or pyrite (py). In pitchblende, fine inclusions of pyrite are present; outwards of it, aggregates of pyrite and chalcopyrite are visible. Reflected light.

native bismuth, tetrahedrite, smaltine, rammelsbergite, niccolite, galena, hematite (specularite), stromeyerite, bismuthinite (?), matildite (?), schirmerite (?), native arsenic (?), malachite (Mochnacka (16)). Earlier papers also reported umangite, aikinite, rittingerite, pyrargirite, wittichenite, chalcopyrite, and secondary uranium minerals - uranotil, while the archival data mention gummite, sklodowskite, uranophane, routherfordite, schroeckingerite, autunite and sooty pitchblende.

Ore concentrations have irregular, spotted, occasionally streaky structures, and are directly dependent on the textures of the principal mineral. Pitchblende forms the following structure:

(i) reniform crusts

(ii) laminar concentrations

(iii) concentrations close to dendritic, botryoidal forms

(iv) irregular concentrations (Fig. 24)

Under the microscope, pitchblende is grey-brown, with a reflectance of 16.1 % $\pm$ 1.3 or lower, and sometimes shows untypical internal reflections. According to the data of Soboleva and Pudovkina (8), pitchblende from Kowary can be assigned to two groups, I and II, based on its reflectance and microhardness. Typical are colloform textures with radial cracks or polygonal segments. The cracks are filled with barren minerals or sulphides, which also form inclusions within pitchblende (Fig. 25 and 26). Two generations of pitchblende are often observed in polished sections. Pitchblende II fills the cracks in pitchblende I or replaces it.

Coffinite is the second important uranium mineral. Under the microscope it is grey, showing weak internal reflections in oil immersion. Its microhardness varies from 341 to 458 kG/mm^2, reflectance is about 14 %. Coffinite was found to occur in two forms: as idiomorphic crystals and as massive accumulations. The crystalline variety is more common. Individual crystals form columns up to 0.2 mm in length, and are rectangular or rhembohedral in cross section. If it occurs with clausthalite, coffinite forms fine, idiomorphic crystals which are sometimes corroded by chalcopyrite. It fills up open spaces between the fragments of sphalerite. Occasionally it overgrows pitchblende or fills the cracks.

The content of non-uranium minerals is variable. Chalcopyrite, pyrite and sometimes sphalerite prevail, but arsenopyrite and löllingite are also common. Clausthalite and coffinite are fairly abundant whereas the other minerals appear in small or trace amounts.

Replacement phenomena have often been observed in the assemblage. Pitchblende is replaced by coffinite, sulphides and selenides, and pyrite by sulphides and selenides. Moreover, replacement phenomena typical of secondary zones have been noted (Banaŝ and Mochnacka (10)).

Based on the mineral intergrowths, the mineral succession was established (Table II). The mineralization of the hydrothermal stage was emplaced in four phases:

I - As-Co-Ni minerals
II - pyrite-pitchblende
III - sulphides-selenides
IV - carbonates

Worth mentioning is also phase V, in which secondary minerals were formed. The Kowary deposit was investigated to a depth of 650 m, where it gradually disappears. The study of the distribution of minerals indicates that the oxidation zone reaches a depth of 158 m, while minerals typical for the cementation zone are present to a depth of 250 m.

Macroscopic observation has already revealed significant alteration of wall-rocks and vein components. The most conspicuous feature is the cherry-red or pink colour of the rocks and vein carbonates, imparted by iron oxides. Magnetite in the vicinity of the ore zones has been subject to hematitization. Within the ore pots, hematite occurs as specularite.

Microscopic studies have revealed that breccia adjacent to the ore zones is enriched in potassium feldspar with 'sieve' structures, and contains more quartz than the surrounding rocks. Skarns show advanced decomposition of silicates (sericitization ?), presence of prehnite, presumably related to mineralization, and enrichment in carbonates.

TABLE II. MINERAL SUCCESSION OF HYDROTHERMAL STAGE OF THE KOWARY DEPOSIT.

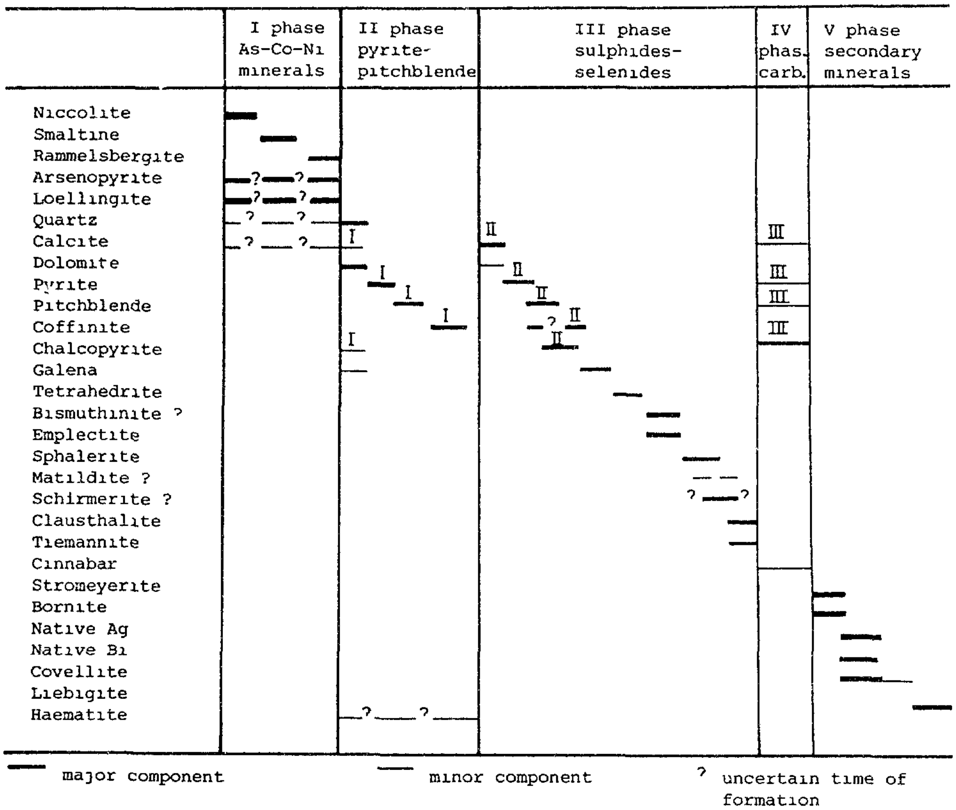

3.5. Conditions of formation and age of mineralization

In earlier papers, the polymetallic assemblage was believed to be high-temperature (Hoehne (19)). However, the presence of pitchblende with syneresis cracks and the conditions of cofffinite formation suggests lower temperatures, ranging between 200°C and 300°C.

The time of emplacement of mineralization can be determined indirectly, defining its relation to skarns which owe their origin to contact metamorphism of the Karkonosze granite. The wall-rock alterations, together with the fact that quartz-carbonate veinlets, genetically related to polymetallic mineralization, penetrate into skarn, prove that mineralization is younger than the granite intrusion and was emplaced after the development of the thermal aureole of granite. Precise data on the age of mineralization were yielded by Pb/U and Pb/Pb datings of pitchblende, made by Lis et al. (20), who obtained two values: 265 and 70 Ma. These data indicate a Permian age for pitchblende which, according to the cited authors, was modified during the Laramidian tectonic phase.

Table III illustrates the formation of polymetallic uranium mineralization related to the geological development of the host rocks.

The oldest rocks are marbles, erlans, schists and magnetite ores. In their present form they do not contain relicts of the primary sedimentary rocks, which were presumably clay, shales, siltstones, marls and limestones, perhaps with pyroclastic rocks (Teisseyre (15)). Iron ores were probably produced by submarine exhalations of the Lahn-Dill type (Zimnoch (18)). The primary rocks were subject to regional metamorphism of the almandine-amphibolite facies (Mochnacka (17), Teisseyre (15)), and ferruginous sediments gave rise to magnetite lenses. This corresponds to the first stage of mineralization in the Kowary deposit (Table III).

TABLE III. DEVELOPMENT OF PRIMARY ORE MINERALIZATION IN THE KOWARY DEPOSIT (SIMPLIFIED)

Age		Variscan Orogeny			Alpine Orogney
		~ 300 Ma ** granite		265 Ma * pitchblende	70 Ma * pitchblende
Processes	Regional Metamorphism (almandine-amphibolite facies)	Intrusion of Karkonosze Granite	Contact Metamorphism (hornblende-hornfels facies)	Hydrothermal Activity	Remobilization
Rocks	Erlans, Schists, Marbles	Granite	Skarns	Breccias, Carbonate Veins	
Mineralization	Magnetite and Associated Minerals		Pyrite, Chalcopyrite, Pyrrhotite (?)	Polymetallic-Uranium Mineralization	Pitchblende
Stages of Mineralization	I		II	III	

* after Lis et al. (20)
** after Przewlocki et al. (22)

The metamorphosed rocks were invaded by granitic magma forming the Karkonosze granite. This intrusion was associated with contact metamorphism corresponding to the hornblende-hornfels facies, as defined by Turner and Verhoogen (21). The result of this metamorphism is skarn, produced by metasomatic alteration of both erlans and marbles. These processes were accompanied by the emplacement of small amounts of sulphides and correspond to the second stage of mineralization (Table III). The age of granite and, indirectly, also of skarn and mineralization was determined by K-Ar and Pb-Sr datings. It was found to be 304 and 292 Ma respectively (Przewlocki et al. (22)). Borucki (23) obtained 299, 310 and 323 Ma for Karkonosze granite by using K-Ar method only.

Dislocations, accompanied by the emplacement of polymetallic uranium mineralization, are later than the granite and skarns. It is the third, youngest stage of mineralization (Table III). The time interval between the emplacement of this mineralization and the formation of the intrusion can be determined by comparing the absolute ages of granite and pitchblende I, the result being about 40 Ma.

4. CONCLUSIONS

The hydrothermal deposits of Kletno and Kowary show several similarities. These are the geological setting, the form of orebodies and the composition of ore minerals.

The mineral parageneses in the two deposits are similar to those occurring in 'five-metal formation' deposits in the meaning of Schneiderhoehn. Taking into account the presence of selenium, the Kowary deposit may be regarded as transitional between a typical 'five-metal formation' and a copper-uranium formation with Ni, Co, and Se, as defined by Kotliar (24). The Kletno deposit shows much greater deviations from the typical five-metal formation and closer similarity to the selenium-copper-uranium formation, differing from the latter in a lower-temperature mineral association. The mineralizing solutions in Kowary were characterized by intermediate temperatures, whereas in Kletno they were of medium- and low-temperature (Fig. 27).

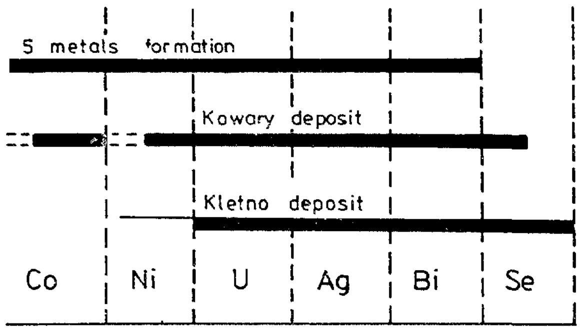

FIG. 27. Comparison of five-metal formation in the described deposits.

The two deposits differ in their relation to magmatism. In Kowary, this relationship is spatially evident, although the time interval between the formation of granite and the emplacement of uranium minerals is nearly 40 Ma years. This is, however, a common phenomenon for a mineralization of this type observed in the Bohemian Massif, as after Legierski (25), uranium mineralization should be associated with some phases of the Variscan orogeny rather than directly with the granite intrusion.

In Kletno, the relationship between mineralization and magmatism is not evident. The lack of datings precludes a precise determination of the age of mineralization. However, the relation to the Variscan tectonites also seems to lend support to the hypothesis concerning the time of emplacement of mineralization in Kowary.

In conclusion, it can be stated that Kowary and Kletno are typical hydrothermal vein deposits which belong to the large family of deposits associated with the Variscan orogeny in Europe.

REFERENCES

(1) OSIKA, R., Metallogenic units of Poland, Bull. Inst. Geol. 237, 13 (1968) 5-12.

(2) SMULIKOWSKI, K., Evolution of the granite gneisses in the Śniesżnik Mts., East Sudetes, Int. Geol. Congr., Rep. of the Twenty First Sess., Norden, Part XIV, Copenhagen (1960) 120-130.

(3) TEISSEYRE, H., Development of geological structure in the region of Ladek and Śnieżnik Kłodzki, Guide to XXX Meeting of Pol. Geol. Soc. in the Kłodzko Area, Wroclaw (1957) 9-13 (in Polish).

(4) TEISSEYRE, H., Development and sequence of tectonic deformations in the eastern part of metamorphic massif of Middle Sudetes, Guide to XLVII Meeting of Pol. Geol. Soc., Warszawa (1975) 51-54 (in Polish).

(5) DON, J., A sequence of the gneisses of Snieznik's Metamorphic Complex, an example of an analysis of linear structures in a contact zone of Radochöw massif, Guide to XLVII Meeting of Pol. Geol. Soc., Warszawa (1975) 51-54 (in Polish).

(6) KASZA, L., Geological structure of the upper part of drainage basin of Biała Ladecka river, Geologia Sudetica 1 (1964) 119-167 (in Polish).

(7) BANAŚ, M., Signs of mineralization in the metamorphic complex of Śnieżnik Kłodzki/Sudetes Mts., Prace Geol. 27, Warszawa (1965) 6-83 (in Polish).

(8) SOBOLIEVA, M.W., PUDOVKINA, I.A., Uranium minerals, Moscow (1957) 408 pp. (in Russian).

(9) BANAŚ, M., Pitchblende from the Metamorphic of Śnieżnik Kłodzki (Sudetes), Bull. Acad. Pol. Sc. Sér. Sc. gêo. gêogr. XII, 3 (1964) 169-175.

(10) BANAŚ, M., MOCHNACKA, K., Some replacement phenomena in polymetallic uranium deposits in the Sudetes, Poland, Geologia II, 1 (1976) 7-17.

(11) BANAŚ, M., Products of Oxidation of Pitchblende from Kletno, Bull. Acad. Pol. Sc. Sêr. Sc. gêol. gêogr. XIV, 1 (1966) 23-26.

(12) BANAŚ, M., New Site of Pb, Hg and Cu Selenides in the Sudetes, Bull. Acad. Pol. Sc. Sêr. Sc. gêol. gêogr. XIII, 4 (1965) 267-271.

(13) THUGUTT, S., Ultramicroscopic examinations of minerals relating to their genesis, Annual of Pol. Geol. Soc. XX, 3 (1951) 245-284 (in Polish).

(14) ROBINSON, S.C., A genetic classification of Canadian uranium deposits, The Canad. Miner. 6 (1958) 174-190.

(15) TEISSEYRE, J.H., Metamorphic rocks of the Rudawy Janowickie and Lasocki Grzbiet ranges, Geologia Sudetica VIII (1973) 7-118 (in Polish).

(16) MOCHNACKA, K., Ore minerals of the polymetallic deposits at Kowary (Lower Silesia), Prace Miner., 4 Warszawa (1966) 7-71 (in Polish).

(17) MOCHNACKA, K., The geology of the polymetallic deposit at Kowary (Lower Silesia), Prace Geol., 40 Warszawa (1967) 7-73 (in Polish).

(18) ZIMNOCH, E., The magnetite series of Kowary, Bull. Ins. Geol. 171 (1961) 7-91 (in Polish).

(19) HOEHNE, K., Über einige arsen-, nickel-, kobalt-, silber-, wismut- und uranerzführende Kalkspatgänge der Grube Bergfreiheit zu Oberschmiedeberg im Riesengebirge, Chemie der Erde 10 (1936) 432-474.

(20) LIS, F., KOSZTOLANYI, CH, COPPENS, R., Etude gêochronologique du gisement polymetallique de Kowary, Pologne, Mineralium Deposit 6 (1971) 95-102.

(21) TURNER, F.J., VERHOOGEN, J., Igneous and metamorphic petrology, McGraw-Hill Book Company, New York (1960) 694 pp.

(22) PRZEWLOCKI, K., MAGDA, W., THOMAS, H.H., Age of some granitic rocks in Poland, Geochim. et Cosmochim. Acta 26 (1962) 1069-1075.

(23) BORUCKI, J., Preliminary Results of Absolute Age Determination (K-A) of the Lower Silesian Granitoidic Rocks, Kwart. Geol. 10, 1 (1966) 1-19 (in Polish).

(24) KOTLIAR, W.N., Geology and genetic types of economic uranium deposits, Moscow (1961) 246 pp (in Russian).

(25) LEGIERSKI, J., Model ages and isotopic composition of ore leads of the Bohemian Massif, Ca. pro Miner. Geol. 18, 1 (1973) 1-23.

(26) SAWICKI, L., TEISSEYRE, H., Geological map, in: Mineral Deposits of Lower Silesia, Ossolineum, Wroctaw (1979) 510 pp.

(27) DON, J., The Sienna synform and the relationship of gneisses to the deformational stages distinguished in the Snieznik metamorphic massif (Sudetes), Geologia Sudetica XVII, 1-2 (1982) 103-124 (in Polish).

VEIN URANIUM DEPOSITS IN GRANITES OF XIAZHUANG ORE FIELD

Li Tiangang, Huang Zhizhang
Uranium Geology Research Institute
Beijing
People's Republic of China

Abstract

VEIN URANIUM DEPOSITS IN GRANITES OF XIAZHUANG ORE FIELD

The Xiazhuang ore field is one of the important uranium districts of China from which substantial uranium resources are known. It lies within the Caledonian orogenic belt, where during the Yenshanian tectonic phase intensive tectono-magmatic activities took place. All uranium ore deposits of this district belong to the vein-type uranium deposits being mainly characterized by a pitchblende-micro-quartz assemblage closely associated with an argillitization-pyritization alteration of the host rock. These deposits are located in a down-faulted block within the Guidong granite massif, which is characterized by a quite perfect granitic differentiation together with an intensive autometamorphism. The granite contains higher uranium and uraninite values. The age of the rock-forming period is 185 to 135 Ma, but the ore-forming period is 85 to 70 Ma. Thus the source of uranium must have been the consolidated granite itself. Fluid inclusion data and stable isotope information show that the ore formation took place mainly between 280 to 150°C under abruptly decreasing pressure conditions and significant escaping of gases.

1. INTRODUCTION

The Xiazhuang uranium district lies in the north of Wengyan county, Guandong province in the south of China covering an area of about 250 km² (Fig. 1). Reconnaissance work started in 1956. After a short time many radioactive anomalies and occurrences were found. In 1957 exploration began, in 1959 it was completed and the development of the first mine and mill complex was started. Exploration, however, is still continuing resulting in a continuous increase of additional uranium reserves. The Xiazhuang uranium district has by now become one of the important uranium production centres in which the uranium occurs in deposits associated with granites. All deposits of this area belong to the hydrothermal vein-type deposits which are either located within granites or, to a lesser extent, within metamorphic rocks, surrounding granites. Uranium mineralization is controlled by structures and favourable lithological units.

2. REGIONAL STRUCTURAL SETTING

In the discussed area three main structural units can be recognized: the Caledonian unit, the Hercynian-Indo-Chinese unit and the Yenshanian unit.

The Caledonian structural unit consists of thick, slightly metamorphosed, terrigenous, detrital sediments which are a sequence of sandstones and shales locally interbedded with carbonaceous shales and layers of phosphatic nodules.

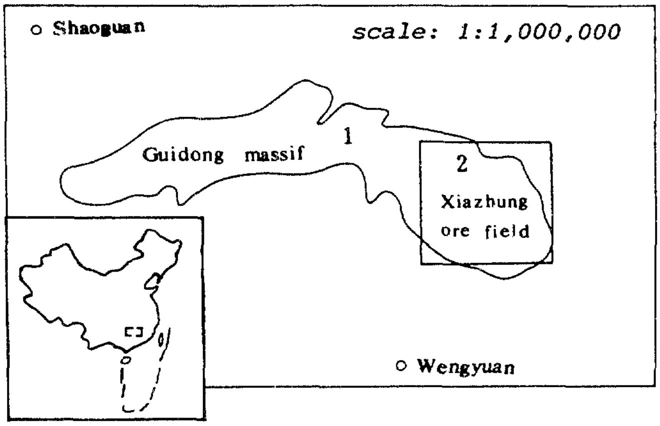

FIG. 1. Location plan of ore field

They are typical miogeosynclinal sediments of Early Palaeozoic age. Average U content is in the range of 3 - 6 ppm. The sediments are slightly enriched in uranium and are favourable source rocks for uranium enriched granites. During a strong deformation phase the whole rock unit was folded into predominantly ENE trending fold belts.

The Hercynian-Indo-Chinese structural unit is a sedimentary unit, deposited under shallow marine conditions, which has a typical platform facies. The lower part of the sequence is composed of transgressive, the rest of regressive clastic sediments, which are all together over 5,000 m thick. Within this unit occur horizons rich in sulphophile elements which led to the formation of several stratabound polymetallic ore deposits in the region. The clastic units within this suit have an average of 2 - 5 ppm U; in carbonates the average is even lower (1 - 4 ppm U). Due to this low average U content these rocks are not considered a favourable source for the formation of uranium enriched granites. The folding was gently leading to wide folds, their trend following the shape of basement blocks.

The Yenshanian structural unit is exposed only locally. It consists largely of sandstones, deposited in intermontane basins, but also of intermediate to acid volcanic rocks and red beds. The basins are now down-faulted and the dip of the sediments is usually low and not steeper than 20°.

The main magmatic activity took place during the Early Yenshanian time resulting in the formation of a granite and subvolcanic dacite-porphyry belt, both having an EW direction. In the Late Yenshanian small acidic bodies and intermediate to basic dikes and dike swarms intruded into the country rocks. Caledonian and Hercynian-Indo-Chinese granites are not exposed in the described area, but are known from adjacent areas.

Faults and fault zones generally have an EW and NE-SW direction. Granites lying in EW direction usually have also EW fracture zones. Except where fold systems run NE-SW and where faults are parallel to these fold axes in basement, the NE-SW fault direction belongs to the Neocathaysian fault system, which controls the distribution of quartz veins and silicified fault zones and which both are closely related to uranium mineralization.

The discussed area has uranium deposits but also important tungsten and polymetallic deposits. Uranium and tungsten sometimes occur together. Uranium deposits tend to be within the so-called transitional phases of granites whereas tungsten deposits tend to be located at the roof of granite intrusions and near contact zones of smaller granites, but mostly within the metamorphic rocks and not too far away from the bigger granite massifs. Granites with uranium affiliation differ from granites with tungsten affiliation in time, size and composition. Polymetallic deposits usually occur in Late Palaeozoic sedimentary units not too far away from big granite intrusions and are often associated with small Yenshanian granodiorite intrusives.

3. GEOLOGICAL FEATURES OF THE URANIUM DISTRICT

3.1. Characteristics of granites of different intrusion phases

The Xiazhuang uranium district lies at the eastern part of the Guidong massif, where its strike direction is changing from EW in the west to NW in the east (Fig. 1). Four intrusion phases can be separated:

3.1.1. Medium to coarse grained porphyritic biotite granites (170 - 193 Ma)

These granites are the oldest and they build up the main body of the massif. Several intrusion phases can be recognized (Fig. 2):

(i) The internal phase which consists of coarse grained porphyritic amphibole-biotite granite and coarse grained porphyritic biotite granite. According to their mineral composition they are monzonite granites with An 30 - 40. Exposure level is about 300 - 400 m above sea level.

(ii) The intermediate phase is a medium grained porphyritic biotite and two mica granite with An 28 - 35. Granites belonging to this phase are exposed between 450 and 900 m above sea level.

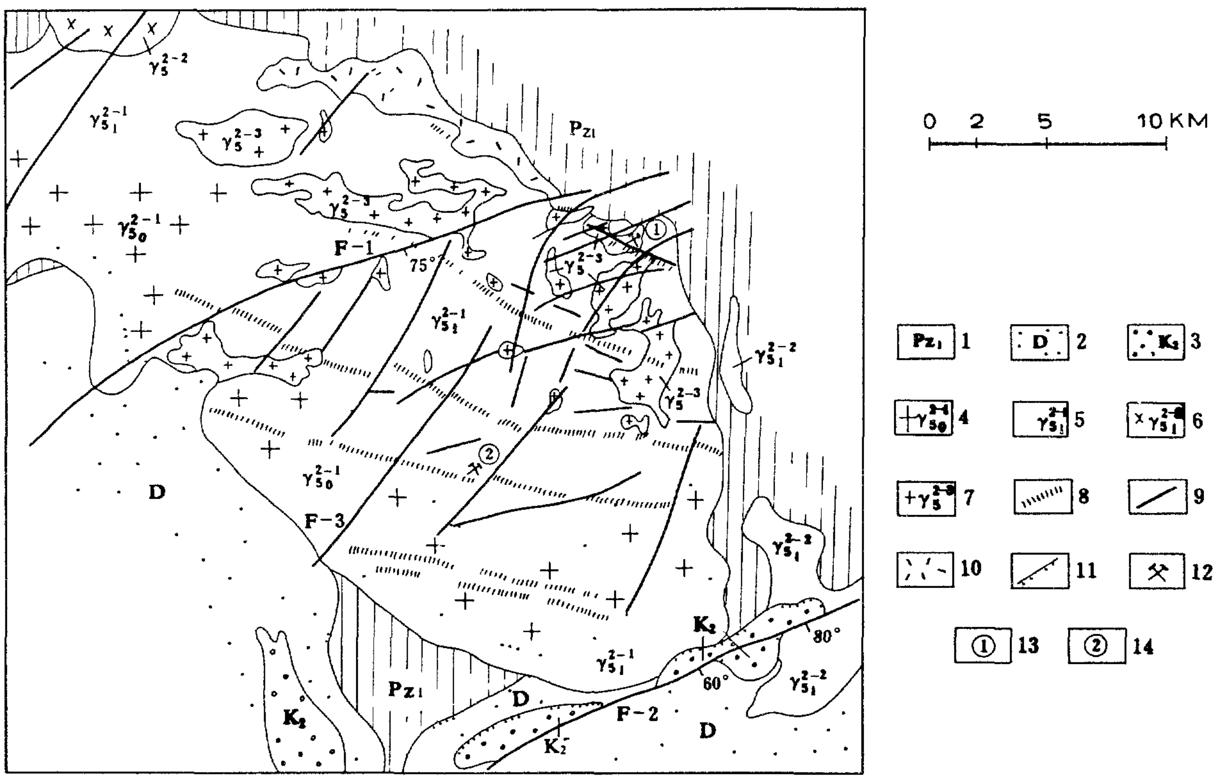

FIG. 2. Geological map of Xiazhuang uranium district. 1. Early Palaeozoic; 2. Devonian system; 3. Late Cretaceous red bed; 4. internal phase; 5. transitional phase; 6. medium-fine grained biotite granite; 7. medium-fine grained two-mica granite; 8. intermediate-basic dike; 9. quartz vein and silicified zone; 10. dacite-porphyry; 11. unconformity boundary; 12. uranium deposit; 13. Zhushanxia deposit; 14. Shijiaowei deposit.

(iii) The so-called marginal phase consists of fine grained muscovite granites, not bigger than several metres to several tens of metres, feldspars having anorthite content of An 6 - 10.

The texture, mineral and chemical composition and trace element content change from the internal phase granites to the marginal phase granites. There is an increase in silica, alkali metals and volatiles (Table I) and a decrease of accessory minerals (Table II). Wolframite and tourmaline, however, increase. The intermediate phase is relatively rich in elements of the iron group, Y, Zr, La, and the marginal phase in Bi, Be, Sn, Pb, Cu, Ga, etc.

The U content in the internal phase is about 6 - 15 ppm, in the intermediate and marginal phase about 10 - 23 ppm. The internal phase contains very little uraninite, the intermediate much more, varying between 0.1 and 7 g/t U.

The main intrusion of the Guidong massif is rich in alkali metals, it is oversaturated by H_2O and Al. The crystallization differentiation in-situ was quite perfect indicating that the intrusion crystallized at medium depth. A strong autometasomatism can be recognized: muscovitization was widely developed and a considerable amount of pneumatolytic minerals appeared together with an increasing U content.

3.1.2. Medium fine grained biotite granites (146 - 158 Ma)

These granites represent the second intrusive phase and occur along the northern margin of the massif in EW direction. They have a seriate texture sometimes with phenocrysts and are characterized by supplementary intrusions without chilled contact features to the host rocks. Besides wolframite, scheelite, Sn, Be and Bi minerals they contain as accessory minerals molybdenite and stibnite. Tungsten-bearing veins are concentrated close to contacts. Higher uranium and uraninite values can be recognized but never leading to higher uranium concentrations (Table III).

3.1.3. Medium fine grained two mica granite, muscovite granite (135 - 145 Ma)

The third phase of granitic intrusion is represented by these types. In general, they occur in the eastern part of the Guidong massif forming small stocks arranged in WNW direction. The two mica and muscovite granites are more acidic carrying more leucocratic and volatile components and also more uranium. Uranium mineralizations are closely associated with these rocks, as most of the deposits lie closely to these granites.

3.1.4. Intermediate to basic dikes

The fourth stage of intrusions is represented by intermediate to basic dikes, mostly diabase but including also odinites, spessartites and microdiorites. They are mainly exposed in the eastern part of the massif, trend usually WNW, less NW and dip steeply. They occur in swarms, which have roughly the same distance to each other. The swarms of dikes are most favourable for the location of uranium mineralizations.

In addition a variety of acid vein-type rocks can also be recognized. Pegmatites and aplites occur anywhere, especially close to the contact between medium

TABLE I. CHEMICAL COMPOSITION OF GUIDONG MASSIF (IN PERCENT)

STAGE	PHASE	AMOUNT OF SAMPLES	SiO_2	TiO_2	Al_2O_3	Fe_2O_3	FEO	MNO	MGO	CAO	Na_2O	K_2O	H_2O	F	CL	TOTAL
1	INTERNAL	10	68.34	0.47	14.61	2.04	2.63	0.16	0.87	1.55	2.95	5.04	0.89	0.27	0.06	99.91
	INTER-MEDIATE	7	72.35	0.19	13.81	1.19	2.14	0.07	0.35	0.90	3.27	5.09	0.61	0.12	0.05	100.14
	MARGINAL	2	75.13	TR.	14.89	0.78	0.82	0.25	0.10	0.58	4.13	4.05	0.41	0.22	0.07	99.41
2		9	72.77	0.11	13.67	2.35	1.92	0.04	0.56	0.93	3.14	5.06	0.57	0.26	0.13	101.29
3		8	73.22	0.11	14.02	0.50	1.22	0.04	0.28	0.69	2.98	5.08	1.01	0.17	0.08	99.51

TABLE II. AVERAGE CONTENT OF ACCESSORY MINERALS

MINERAL IN G/T	PHASE		
	INTERNAL	INTERMEDIATE	MARGINAL
APATITE	517.20	228.85	7.45
ZIRCON	255.05	65.07	4.05
MAGNETITE	1,686.54	2.05	TRACES
PYRITE	219.32	45.92	TRACES
ALLANITE	207.44	3.60	-
SPHENE	737.27	2.15	-
ILMENITE	71.95	1.77	-
TOURMALINE	33.75	264.42	6,244.67
GARNET	0.12	29.65	4,360.0

TABLE III. CONTENT OF U, TH, AND URANINITE OF GRANITES AT VARIOUS STAGES

STAGE	PHASE	U CONTENT (PPM)	TH CONTENT (PPM)	URANINITE (G/T)
1	INTERNAL	6 - 15	37	TRACE
	INTERMEDIATE	10 - 23	32.6	0.1 - 7
2		10 - 25	28	0.3 - 17.4
3		12 - 27	12	0.5 - 12

fine grained two mica granites and muscovite granites and rarely within internal granites of the main massif.

The granite massif of Guidong is an S-type granite (oxygen stable isotope is δO^{18} = + 11.13 to + 11.89 ‰. The rare earth abundance pattern is given in Fig. 3 (δEu = 0.168). This pattern also indicates that it is a perfectly differentiated S-type granite.

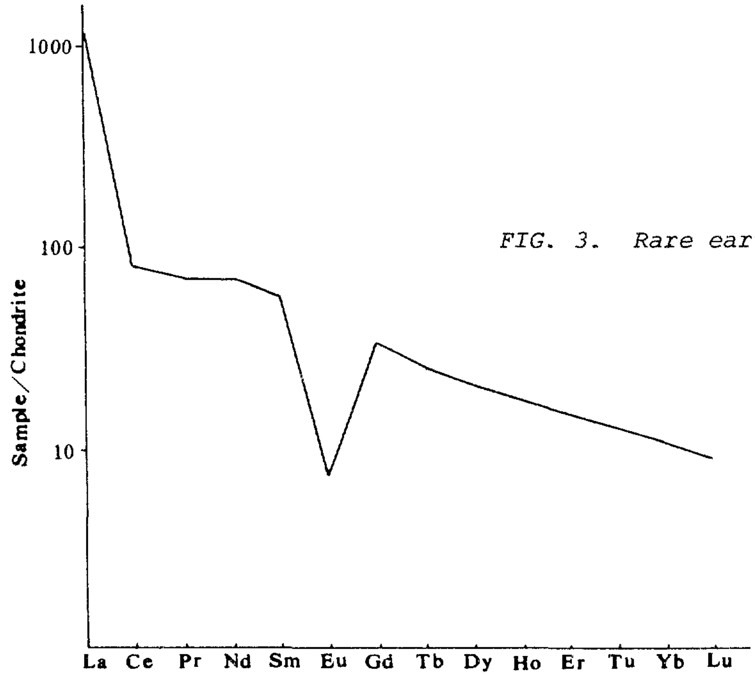

FIG. 3. Rare earth abundance pattern of granite

3.2. Autometamorphism and allometamorphism of the granite massif

This phenomenon occurs most intensively in the eastern part of the massif and is mainly characterized by K-feldspathization and muscovitization. K-feldspathization is best developed in the transitional phase of the main granite body and can be seen in the increase of reddish K-feldspar, reduction and even disappearance of quartz and chloritization of biotite. This feldspathization is usually irregular in form with a transitional contact to the surrounding rock. Still the change is pronounced and can easily be found within 1 - 2 m.

Albitization took place later than K-feldspathization and is more restricted. It is characterized by newly formed, fine grained albite. At some places, like at the Zhushanxia uranium deposit, albitization can form comparatively large albite metasomatic bodies.

Muscovitization appears in the intermediate and marginal phase of the main granite, but also within the later small intrusives. Muscovite has three kinds of origin: muscovitization in the stage of autometamorphism, in the stage of allometamorphism and in the stage of structural hydrothermal activity. All three generations can be superimposed on each other.

(i) During the autometamorphism stage muscovite replaced mainly biotite and less plagioclase. This muscovitization has a regional extent, but seems to be restricted to the uppermost part of the massif and to the intermediate and marginal phase.

(ii) Allometamorphic muscovitization is called the recrystallization of muscovite caused within igneous rocks by younger intrusions. This feature is characterized by the formation of larger muscovite flakes, often associated with pegmatitization. The flakes are sporadically distributed and their size decreases with the distance from the intrusive. The intensity of this type of muscovitization has also a close relationship to the lithology of the younger intrusive. Around biotite granites muscovitization is quite weak and narrow, around two mica and muscovite granites it is strong and extensive. Therefore, medium coarse grained porphyritic biotite granite and medium fine grained two mica granite evolution lead to much more intensive muscovitization compared to the evolution of medium coarse grained porphyritic biotite granite and medium fine grained biotite granite. This may be one of the reasons why the first ones are more favourable for uranium ore forming processes than the second ones.

(iii) Muscovitization caused by structural hydrothermal activities occurs together with silicification along fracture zones and hydrothermal veins.

In addition tourmalinization and chloritization of biotite are also very common.

Autometamorphism and allometamorphism of the granites not only recrystallized the main rock forming minerals but also the various accessory uraniferous minerals. The decrease of accessory minerals by muscovitization is shown in Table IV. Together with the disintegration of accessory minerals, the proportion of easily mobile uranium increases, the leaching ratio of uranium rises. These processes provide the proper conditions of subsequent concentration of uranium in the hydrothermal stage.

3.3. Structural framework of the uranium district and the ore controlling factors

As shown in Fig. 2 the magmatic activity of the Guidong massif is in principal controlled by EW to WNW trending, deep reaching fault systems. The centre of magmatic activity gradually moved from west to east, where the intrusives of the third and fourth stage are concentrated. This centre of magmatism is also the geothermal centre of the area. In case this centre is cut by faults, the conditioning for the movement of hydrothermal solutions has been reached.

In the uranium district of Xianzhuang are two main fault zones (F_1 and F_2 in Fig. 2), both striking 60° - 80° NE, steeply dipping to SE; they are over 50 km long and several tenth of metres wide. The northern zone F_1 consists mainly of silicified cataclastic rocks with white quartz. The southern fault zone F_2 is a compression zone filled with quartz and sometimes with red and grey to black microquartz and is a reversed strike slip fault. Late Cretaceous to Early Tertiary sedimentary basins occur usually at the footwall of this fault zone.

The distance between the two fault zones is about 20 - 22 km and the block between them is down-faulted. Within this down-faulted central block three secondary fault and fracture directions can be differentiated: 20° - 40°, 60° - 80° and 280° - 300°. These secondary structures are several hundred metres to several kilometres in length, commonly composed of silicified mylonites, breccia zones, silicified cataclastites with hydromicatization, white quartz, microquartz of different colour and fluorite. Coarse grained, medium grained and fine grained white quartz is older than microquartz of different colour. The older veins are usually concentrated more to the west of F_3 (Fig. 2), whereas the younger, microquartz veins are concentrated more to the east and seem to reach to a deeper level. Also zoning can be recognized: white quartz veins tend to change to depth into microquartz veins. The quartz within white quartz veins is accompanied by a recrystallization and within the country rock by sericitization of plagioclase and chloritization of biotite. Within the microquartz veins an intensive hydromicatization and pyritization of the wallrock can be recognized. The microquartz is brown to red, or grey to black, fluorite is dark purple and in some cases red calcite occurs together with uranium mineralization.

The distribution of uraniferous hydrothermal veins is concentrated in the down-faulted block between the two fault systems F_1 and F_2. The uranium concentration within the veins can be explained as follows:

TABLE IV. VARIATION OF ACCESSORY MINERALS CAUSED BY MUSCOVITIZATION

SAMPLES OF COARSE-MEDIUM PORPHYRITIC BIOTITE GRANITE	ZIRCON (G/T)	ALLANITE (G/T)	APATITE (G/T)	XENOTIME (G/T)
FRESH	250.8	37.4	437.4	41.9
WEAK MUSCOVITIZATION	211	12	256	-
WEAK MUSCOVITIZATION	185	-	151	-
STRONG MUSCOVITIZATION	28.5	3.7	64.13	7.2

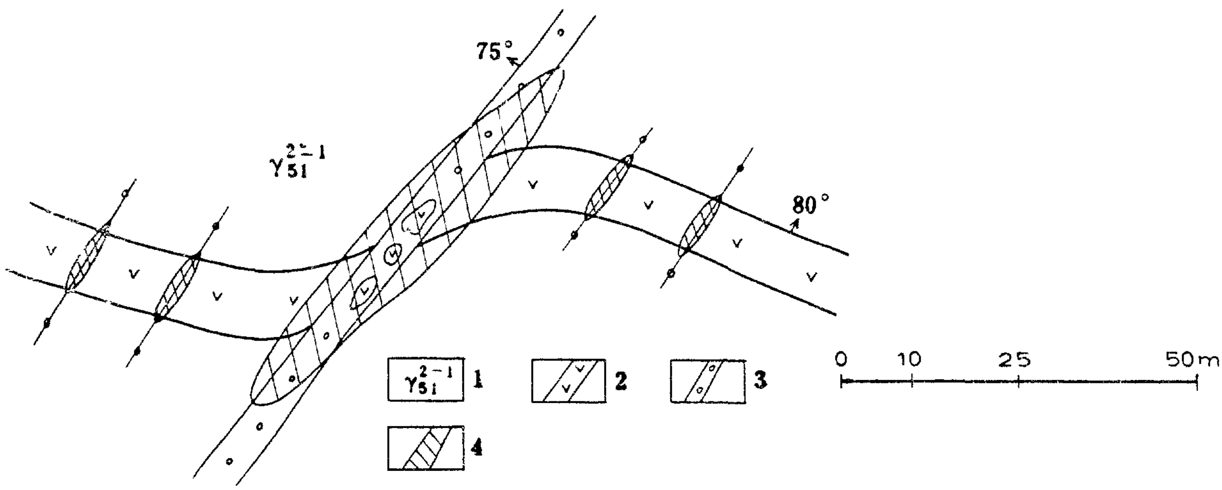

FIG. 4. Sketch map of Shijiaowei deposit; 1. coarse medium grained porphyritic biotite granite; 2. intermediate basic dike; 3. silicified zone; 4. orebody.

(i) Uranium is concentrated where intermediate to basic dikes and alkali metasomatic rocks are intersected by microquartz veins. Fig. 4 shows an example from the Shijiaowei uranium deposit. The size of the deposit depends on the number of intersections, the size and type of silicified zone and the size of the dike.

(ii) The uranium deposits lie in the direct vicinity of contact zones of medium fine grained two mica granites and muscovite granites. The type of structure along the contact controls the ore formation.

(iii) The uranium deposits usually lie at such places, where the strike and dip of the silicified zones change, in silicified zones of en echelon fashion and where two silicified zones intersect each other.

(iv) Most of the deposits are located within the transitional phase of the main granite, where they are strongly affected by muscovitization and K-feldspathization. The internal granitic phase is characterized by the lack of uranium deposits due to less available mobile uranium.

The uranium deposits are vein-like, lenticular or have a columnar to stockwork shape. A typical section through such a deposit, i.e. the Zhushanxia deposit, is given in Fig. 5. The average grade of uranium within these veins ranges from 0.1 to 0.5 % U and the size of the orebodies varies considerably. The vertical extent of orebodies in each single deposit is usually 300 - 500 m. The age of the microquartzite pitchblende veins is 70 - 85 Ma, that of the calcite pitchblende veins 60 Ma.

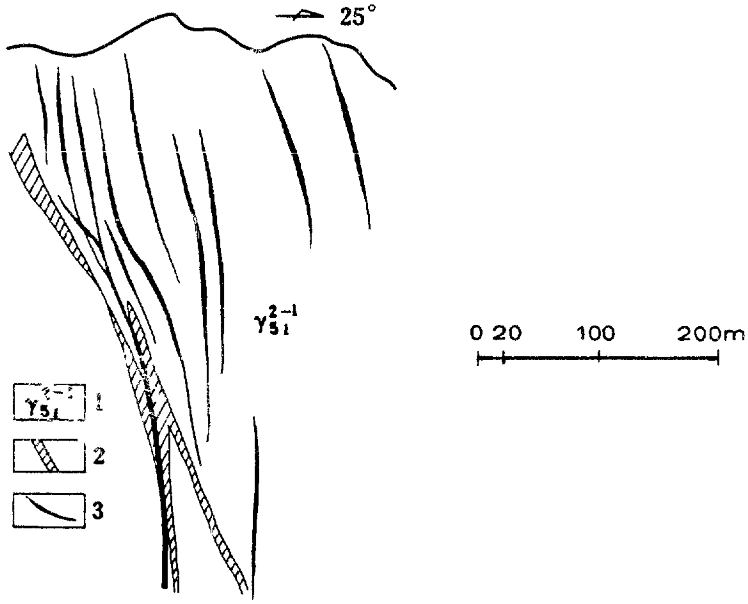

FIG. 5. A transverse profile of Zhushanxia deposit;
1. granite; 2. intermediate basic dike; 3. orebody.

4. HOST ROCK AND NEAR VEIN ALTERATION

4.1. Host rock

The host rock of the uranium ore deposits consists of various granites and intermediate to basic dikes. The most important host rock like medium grained porphyritic two mica granite bodies and spessartites will be discussed.

The medium grained porphyritic two mica granite consists of acidic plagioclase (25.3 %), microcline (32.9 %), quartz (33.5 %), and minor amounts of biotite (4.8 %) and muscovite (3.5 %). Accessory minerals include apatite, zircon, pyrite, tourmaline, ilmenite and uraninite.

The uraninite content in the granite is 6.3 g/t. It occurs either as intergranular grains between or also often as cubes within the rock forming minerals. The grain size of uraninite varies between 0.025 and 0.090 mm. Specific gravity is 8.97, the oxygen coefficient is 2.12. The chemical composition of uraninite is illustrated in Table V.

The dark green spessartite has an isogranular or porphyritic texture. The main minerals are hornblende (52.6 %), intermediate plagioclase (33.1 %) and small amounts of quartz (2.8 %). Apatite, ilmenite, pyrite and epidote are accessories.

4.2. Near vein alteration

Before dealing with the alteration it has to be pointed out that firstly the alteration connected with ore forming processes is superimposed on pre-ore alteration (autometamorphism, allometamorphism) influencing the intensity of near vein alteration, the mineral assemblage and the localization of uranium mineralization. Secondly, the near vein alteration is the product of hydrothermal activities which directly influenced the nature, intensity and mineral assemblage of the alteration. Thirdly, vein is defined here as a silicified zone of microquartz.

TABLE V. CHEMICAL COMPOSITION OF URANINITE

UO_2	78.17 %	Fe_2O_3	1.07 %
UO_3	11.30 %	MnO	0.046 %
ThO_2	2.31 %	MgO	0.05 %
ΣTR_2O_3	1.550 %	CaO	0.34 %
PbO	2.67 %	K_2O	0.169 %
SiO_2	1.77 %	Na_2O	0.13 %
TiO_2	0.24 %	H_2O	0.67 %
Al_2O_3	0.56 %		

TABLE VI. CHEMICAL COMPOSITION OF TWO MICA GRANITE

MAJOR ELEMENTS IN PERCENT			
SiO_2	72.30	MgO	0.34
TiO_2	0.17	CaO	0.73
Al_2O_3	13.97	Na_2O	3.18
Fe_2O_3	1.04	K_2O	5.08
FeO	2.14	P_2O_5	0.12
MnO	0.06	H_2O	0.80

TRACE ELEMENTS IN PPM			
U	28.7	Cu	9
Th	31.2	Pb	16
Zr	71	Zn	43
La	37.9	Mo	1
Ce	72.3	Be	8
Pr	8.3	Ba	177
Nd	44.7	Sr	38
Sm	11.0	V	14
Eu	0.54	Ni	28
Tb	1.19	Nb	35
Yb	2.38	F	70
Lu	0.30	S	30
Y	26		

4.2.1. Characteristics of altered granite

The main host rock is a medium grained porphyritic two mica granite. It is a silica-, potassium-rich and aluminium oversaturated acidic rock (Table VI). Near vein alteration can be recognized in two mineral assemblages: silicification-hematitization association and argillization-pyritization association, the latter one being more extensive and typical.

The argillization resulted from hydrolysis of plagioclase, a process which can be summarized as follows:

(i) hydrolysis of plagioclase caused the formation of hydromica,

(ii) transformation of hydromica into long platy hydromica,

(iii) further alteration into montmorillonite.

The nature of this alteration lies in the removal of Na^+- and Ca^{2+}-cations at the beginning of alteration subsequently followed by the removal of K^+ cations. This replacement is basicly considered an increase in H_3^+O and, therefore, may be attributed to acidic hydrothermal alteration, i.e. hydrogen metasomatism. This alteration resulted in a horizontal zoning:

(i) breccia zone cemented and filled with fine and microcrystalline quartz, dark and red in colour, being the centre of the orebody;

(ii) cataclastic zone of granite with intensive silicification, hematitization and hydromicatization;

(iii) cataclastic granite zone with weak silicification, hematitization and dark-green hydromicatization, 0.5 - 0.8 m wide;

(iv) yellow-green hydromicatized granite, a few metres wide;

(v) weak altered granite.

This zoning has the following features:

- Each zone has transitional relationship
- Silicification and hematitization are usually close to the orebody
- Hydromicatization decreases outward from the centre of the ore zone, the same is valid for the amount of associated pyrite; hydromica changes from the long platy variety into a fragmental one and the colour of the altered rock becomes bright grey.

The variation in chemical composition of the above mentioned various zones of alteration are illustrated in Table VII.

4.2.2. The characteristics of altered spessartite

The mineral assemblage of spessartite alteration can be devided into:

- quartz-hematite-hydromica association
- quartz-hydromica association
- chlorite-carbonate-association

The quartz-hematite-hydromica association (Table VIII) shows a well developed zoning pattern which developed mainly at the intersection of silicified zones, caused by multistage hydrothermal solutions, and early strongly fractured and altered spessartite. The following horizontal zoning can be distinguished:

(i) cataclastic zone of strongly silicified, hematized and hydromicatized rocks (Table VIII, 1). It is characterized by destruction of the rock texture, complete replacement of the rock by quartz, hydromica and minor amount of daphnite and intensive staining of hematite. This zone is 0.1 - 0.2 m wide and forms a part of the orebody;

(ii) weak silicification - hematitization - hydromicatization - daphnitization zone (Table VIII, 2). It differs from the central zone in that the silicification and hematitization weakens and the daphnitization becomes stronger. This zone is about 2 m wide;

(iii) chloritization and uralitization zone (Table VIII, 3). This is the outer zone of alteration, green or grey-green in colour.

TABLE VII. CHEMICAL COMPOSITION OF VARIOUS ALTERED ROCKS

NO.	1	2	3	4	5	HOST ROCK
SiO_2 *	88.08	84.85	78.16	76.16	74.45	72.30
Al_2O_3 *	4.26	7.02	11.51	12.38	12.96	13.97
Fe_2O_3 *	0.90	1.60	0.60	0.58	0.46	1.04
FeO *	0.91	0.93	1.07	1.33	1.48	2.14
MgO *	0.43	0.54	0.61	0.37	0.37	0.34
CaO *	0.19	0.27	0.56	0.56	0.44	0.73
K_2O *	2.86	3.00	5.10	5.12	5.06	5.06
Na_2O *	0.06	0.10	0.28	1.98	2.84	3.18
Cu	15	14	10	9	8	9
Pb	249	51	24	21	19	16
Zn	56	62	43	55	54	43
Mo	21	12	5	4	3	1
S	0.35	0.15	0.12	0.06	0.05	0.003
F	937	1150	1150	1170	130	70
U	0.599	0.036	0.014	0.0047	0.0035	0.0028

* MAJOR ELEMENTS IN %, OTHER ELEMENTS IN PPM

TABLE VIII. CHEMICAL COMPOSITION OF VARIOUS ALTERED ZONES (IN %)

NO.	1	2	3	LAMPRO-PHYRE
SiO_2	68.56	52.43	48.98	49.25
Al_2O_3	12.59	13.53	12.02	12.00
Fe_2O_3	1.46	9.00	2.11	5.24
FeO	3.08	3.48	12.48	12.17
CaO	1.06	1.25	6.34	6.59
MgO	0.86	0.66	2.24	4.41
K_2O	1.86	1.65	1.53	1.04
Na_2O	0.08	0.31	0.91	2.74
U	0.334	0.063	0.004	0.003

5. CHARACTERISTICS OF THE ORE AND THE ORE FORMING PROCESS

Based on the different mineral assemblages of the hydrothermal veins and their relationship to the ore forming process three stages can be recognized.

5.1. White, fine grained quartz stage

This stage can be regarded as the precursor of the hydrothermal activity. It is usually present in the form of breccia and fragments which remained in the silicified zones. Grain size ranges from 0.1 to 1 mm. The uranium content is 1 - 10 ppm U.

5.2. Red, black microcrystalline quartz-pitchblende stage

This stage represents the main ore forming stage. The quartz is impure, containing clay minerals, sulfides and hematite with a grain size of 0.01 - 0.1 mm. The uranium content varies greatly from several tens of ppm to thousands of ppm. Considering the rather long period of hydrothermal evolution during this stage, three generations of mineral associations have been distinguished on the basis of the mineralization sequence.

(i) The red microcrystalline quartz-pitchblende-coffinite generation is widely distributed, representing the major generation of mineralization.

(ii) The black microcrystalline quartz-pitchblende-coffinite-sulfide generation is less well developed than the first one, but can often be seen. It represents an important generation of uranium superimposition and concentration.

(iii) The dark purple fluorite-(calcite)-pitchblende generation has a more limited distribution and is smaller in size than the previous ones.

The primary ore minerals are pitchblende and coffinite. Pitchblende occurs as massive, warty aggregates or is disseminated. Colloidal structures are commonly developed. Pitchblende of massive structure usually is fractured; veined and warty pitchblende exhibit coloidal girdles; disseminated pitchblende shows a spheroidal, girdle and cloud-like texture (Fig. 6, 7, 8). The reflectance of pitchblende is 15.3 % (yellow light), 14.6 % (green light) and 14.1 % (red light). Its specific gravity varies from 7.14 to 7.49 and the microhardness is 630 kg/mm.

The previously mentioned oxygen coefficient of pitchblende (2.41 - 2.57) is much greater than that of the synthetic uranium oxide series of the cubic phase and seems to lie within the interval of the synthetic uranium oxide series of orthorhombic phase ($UO_{2.30}$ - $UO_{2.57}$). The contradiction between oxygen-coefficient and crystal structure shows that pitchblende in hydrothermal uranium deposits is a mixture of UO_2 (cubic phase) and UO_3 (cryptocrystalline phase).

There exists a correlation between Fe_2O_3 and S in pitchblende, therefore, it may be postulated that iron is mainly present in form of FeS_2, minor amounts also occurring in hematite.

It is assumed that unpurities of pitchblende were involved during colloidal precipitation. The chemical composition of various pitchblende samples are given in Table IX.

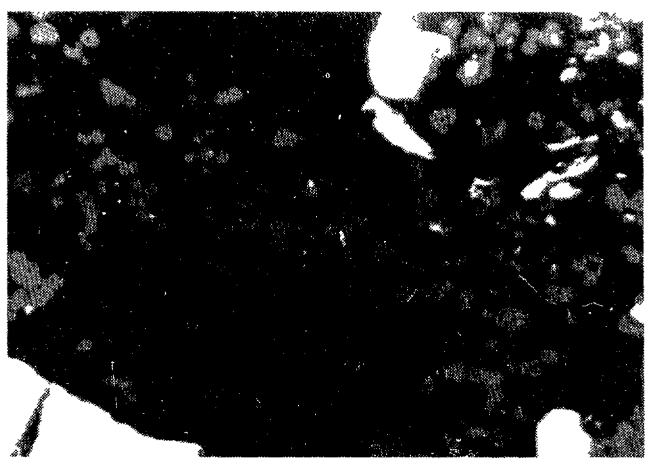

FIG. 6. Dispersed spheroidal pitchblende (grey), coffinite (dark-grey), pyrite (white), microcrystalline quartz (black), reflected light x 800

FIG. 7. Garland-like pitchblende (grey), coffinite (dark-grey), pyrite (white), microcrystalline quartz (black), reflected light x 516

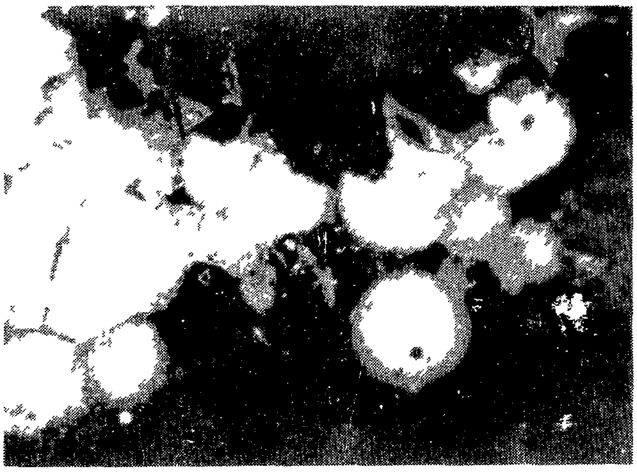

FIG. 8. Spherolite aggregate of pitchblende (grey), galena (white) dispersed in pitchblende, coffinite (dark-grey) replaced pitchblende, reflected light x 520

FIG. 9. Euhedral crystals and aggregates of coffinite (dark-grey), pyrite (white), microcrystalline quartz (black), reflected light x 500.

TABLE IX. CHEMICAL COMPOSITION OF PITCHBLENDE (IN PERCENT)

NUMBER OF SAMPLES	010	003	002	060	022	012	038
UO_2	44.49	36.21	34.61	54.08	51.97	45.01	47.56
UO_3	38.07	47.43	49.23	30.31	38.70	44.17	39.55
ThO_2	0.0052	0.0110	0.0152	0.0060	0.0100	0.0100	0.0080
TR_2O_3		0.001		0.45	0.37	0.37	0.66
PbO	3.22	2.32	2.49	3.76	1.66	1.26	1.60
SiO_2	0.60	1.10	0.70	1.88	2.06	1.00	1.34
Fe_2O_3	2.71	1.28	0.96	0.82	0.48	0.43	0.40
Al_2O_3		0.25		0.31	0.34	0.37	0.66
TiO_2				1.52	1.37	0.62	1.67
MnO	0.40	0.32	0.32	0.79	0.08	0.62	0.65
CaO	5.38	5.08	6.27	4.60	1.40	4.40	3.78
K_2O				0.01	0.04	0.04	0.06
Na_2O				0.06	0.16	0.12	0.11
H_2O^+	0.38	0.38	0.66	1.05	1.86	1.63	1.74
H_2O^-	1.49	1.93	2.08				
UO_x *	2.45	2.53	2.57	2.35	2.41	2.48	2.44

* x = OXYGEN COEFFICIENT

Coffinite is widely distributed, but only in small quantities. It usually precipitated at the periphery of pitchblende and pyrite but also within fine cracks of pitchblende. Sometimes also platy and rhombic varieties (having a size of about 0.01 mm) can be observed within microcrystalline quartz (Fig. 9). Microprobe analyses of coffinite had the following results: U = 58.44 %, Si = 8.67 %, Ca = 0.70 %, Fe = 0.71 %, Pb = 0.85 %. Coffinite usually is younger than pitchblende and it is associated with marcasite.

5.3. Dark purple quartz-carbonate-fluorite stage

This stage is characterized by the appearance of white quartz-comb, banded microquartz, white calcite and fluorite in a variety of colours. It has a lower uranium content and belongs to the post-ore stage.

6. DISCUSSION OF GENESIS OF THE URANIUM DEPOSITS

(i) The rock-forming period is 135 - 185 Ma but the uranium ore-forming period is 70 - 85 Ma. The 'time gap' between rock and ore formation is greater than 50 Ma, which significantly exceeds the time necessary for consolidation of the granite massif. Consequently uranium and hydrothermal solutions could not have originated directly from a granite magma differentiation. The source of the uranium must have derived from the consolidated granite itself. The granite acted as a uranium reservoir and uranium underwent double preconcentration with subsequent mobilization. The first preconcentration of uranium took place during the deposition of basement rocks with the uranium content being up to 3 - 6 ppm U, the second during multistage magmatic reworking and differentiation, the uranium content increasing to 10 - 27 ppm U (uraninite content up to several g/t). Then the uranium-rich granite underwent autometamorphism and tectono-hydrothermal processes leading to mobilization of uranium within the granite.

(ii) Uranium deposits occur around small acidic intrusions and intermediate-basic rocks in down-faulted zones resulting from tension stress within the continental crust. This led to the formation of hydrothermal systems, provided the opportunity for descending and heating of surface water and its involvement into the ore formation process.

(iii) According to fluid inclusion data (Chen Anfu et al., 1980, unpublished) the pre-ore quartz contains 40 - 70 v.% CO_2 inclusions. The gas phase is predominant, but individual liquid CO_2 inclusions can also be observed. Some other inclusions contain complex hydrocarbons. The inclusions of ore stage minerals are characterized by boiling. Inclusions with various gas-liquid proportions coexist in the same visual field. Boiling homogenization temperatures show a high degree of scattering. Three-phase inclusions commonly contain daughter minerals of KCl, NaCl, $CaCO_3$ or NaCl and $CaCO_3$. Post-ore inclusions have a greater proportion of liquid, some of them are also characteristic for boiling.

The temperatures determined by homogenization method varied between 320° and 80°C. The highest temperature of pre-ore inclusions is 320°C, and the lowest one of post-ore inclusions is 80°C. The temperatures of ore stage lie between 280° and 150°C. A gasification temperature exists in both ore and post-ore stages (320° - 260°C). Mineral inclusions formed at this temperature interval can be homogenized to the gas phase.

The pressure of pre-ore stage is 220 - 510 atm, in average 400 atm. The pressure of ore stage and post-ore stage is 10 - 60 atm. Thus the uranium mineralization formed under decreasing temperature and pressure conditions, boiling of ore solutions and a significant escaping of gases from such solutions.

(iv) The salinity of ore solutions has been determined as 16 - 19 wt%. Inclusions with daughter minerals have a salinity of up to 23 - 30 wt%, 300 - 1000 times higher than of ordinary ground water and young hot springs.

(v) As shown in Table X, the main cation within the inclusions from samples of two uranium deposits is Ca^{++} with small amounts of K^+ and Na^+. The highest anion content is HCO_3^-, secondary are F^-, SO_4^{--} and Cl^-. Statistics show that the uranium content in ore has a correlation to CO_2 concentration within ore inclusions (correlation coefficient 0.824). Consequently, carbonate-uranyl or fluorite-carbonate-uranyl complexes in ore solutions might be the major transportation medium of uranium. The solution was intermediate to weak alkaline, became slightly acidic during the ore-stage, and transformed into weak alkaline and alkaline at post-ore stage. Ore formation proceded in a transitional redox environment, but uranium precipitation took place at a little higher oxygen fugacity, which coincided with extensive hematitization in the vicinity of the orebodies.

(vi) All the microcrystalline quartz veins are rich in Au and S. Gold content is in close correlation with U and S (correlation coefficient is 0.970 and 0.982 respectively). The gold in grey-black microcrystalline quartz can reach 295.1 ppb and might exceed that in medium grained two mica granites (0.32 ppb) by more than 900 times. Obviously this

TABLE X. COMPOSITION OF INCLUSIONS

DEPOSIT	PERIOD	AMOUNT OF SAMPLES	K^+	NA^+	CA^{++}	MG^{++}	ΣFE	HCO_3	SO_4^{--}	F^-	CL^-	H_2O	CO_2	CH_4	PH	EH
			G.ION/L									MG	MOLE/L			
1	PRE-ORE	3	0.19	0.37	0.67	0.09	0.05	1.71	0.13	0.22	0.24	5.18	0.46	0.21	7.70	-0.529
	ORE	3	0.05	0.36	1.83	0.18	0.01	2.94	0.81	0.29	0.36	4.97	1.56	0.003	7.51	-0.500
	POST-ORE	3	0.06	0.31	1.03	0.13	0.05	2.48	0.06	0.27	0.18	4.86	0.30	0.006	8.05	-0.554
2	PRE-ORE	2	0.36	0.37	0.90	0.14	0.10	2.53	0.24	0.13	0.15	4.42	1.06	0.016	7.12	-0.511
	ORE	3	0.21	0.17	0.28	0.13	0.06	0.77	0.31	0.44	0.21	4.95	0.84	0.005	6.82	-0.438
	POST-ORE	2	0.52	0.31	2.27	0.36	0.01	1.43	0.62	0.27	0.13	6.32	0.63	0.004	7.44	-0.488

FIG. 10. Diagram showing the relation between δD and $\delta^{18}O$ in water of pre-ore quartz; 1. range of magmatic water; 2. range of hydrothermal water at pre-ore stage.

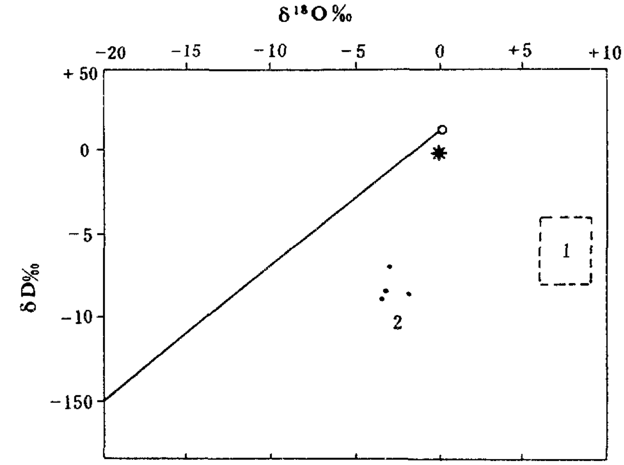

is related to the existence of hydrothermal solutions from a deep-seated source.

(vii) The stable isotope $\delta^{13}C$ value varies between -6.99 and -7.89 ‰ within a narrow range close to the initial $\delta^{13}C$ value (-5 to -8 ‰) reflecting the deep origin of carbon. The $\delta^{34}S$ value in pyrite of veins is at various stages from -4.92 to -15.32 ‰. All these values are negative and tend to increase from older to younger veins. This feature reflects the evolution of deep-circulating hydrothermal solutions.

The $\delta^{18}O$ value in pre-ore quartz is +1.52 to +8.5 ‰. Considering the isotope equilibrium exchange by conversion the $\delta^{18}O$ value in hydrothermal solutions should be -2.97 to -8.85 ‰. The δD values in liquid phase water of inclusions in ore are -54 to -88 ‰. The projection points fall into a transitional area between meteoric and magmatic waters (Fig. 10). This kind of water can be attributed to a mixed water with predominance of meteoric water.

Following all the arguments given above the genesis of uranium deposits may be summarized as follows:

The uranium-rich granite contained a significant amount of uraninite. These granites underwent autometamorphic processes. Then a large-scale down-faulting took place under regional tension. Due to the down-faulting and development of deep reaching structures, a deep reaching circulating hydrothermal system was produced in which ground water migrated downwards and ascended again after heating. The heated ground water extracted continuously uranium and other components from granites during its migration. Uranium was transported mainly in the form of uranyl complexes (carbonate-uranyl and fluorine-carbonate-uranyl complexes and possibly sulphate-uranyl complexes. In addition, the water and various gases of the granite migrated upwards along faults, kept leaching different components from granites, were collected and formed high-salinity solutions which joined the convection system above mentioned. Furthermore, addition of gases and liquids from intermediate to basic magma chambers cannot be excluded. Due to the strong fracturing phase at the ore stage, the pressure of the hydrothermal system decreased abruptly and the ore forming solutions started to boil: a great amount of CO_2 escaped, then carbonate-uranyl complexes were dissociated and the concentration of ore solutions was greatly increased. Silica began to precipitate and uranium was reduced by various reductants resulting in the formation of pitchblende together with SiO_2.

It can be concluded that the decreasing pressure has played a dominant role to precipitate uranium out of the migrating solutions. There were very little changes in temperature, pH, Eh, not playing an important role in the uranium ore formation. Orebodies in the uranium district can occur in any kind of country rocks as long as the structural conditions are favourable. More favourable lithologies, such as intermediate-basic dikes, play a subordinate part in the location of uranium deposits, but may increase the mineralization grade.

ACKNOWLEDGEMENTS

Most data presented in this paper were determined by the Analytical Departments of our Research Institute and a part of them are from Team No. 293, Geology and Exploration Bureau of South China. We are deeply in debt to Dr. Du Letian for reading this paper, Mr. Chen Zuyi and Chen Zhensi for the translation into English and Mrs. Xu Huaile for drawing the figures.

GRANITE-TYPE URANIUM DEPOSITS OF CHINA

Du Letian
Uranium Geology Research Institute
Beijing
People's Republic of China

Abstract

GRANITE-TYPE URANIUM DEPOSITS OF CHINA

The granite-related uranium deposits of China are of acid hydrothermal and alkaline hydrothermal origin. Their geological features, the correlation with each other and their metallogenesis are discussed. The close relationship of the uranium mineralization with the geotectonic history and the existence of a 'carapase of ore formation' as a barrier for precipitation and concentration of uranium from ascending solutions are emphasized.

1. INTRODUCTION

Granite-type uranium deposits (GUD) are defined as hydrothermal deposits which have a spatial and genetic relationship with granites. The term 'hydrothermal' in this paper is used not only for solutions originating from magmas but also for solutions from other sources, particularly meteoric water. Uranium occurrences and deposits of this type are more frequent in China than in other countries. They are similar to those known from France, Spain, Portugal, Czechoslovakia etc.

On the basis of the spatial relationship of these deposits to the granites the following four groups can be distinguished (Fig. 1):

(i) Intragranitic uranium deposits

(ii) Uranium deposits outside of granites within the surrounding rocks like sedimentary, metamorphic and igneous rocks etc. lying not more than tens to thousands of metres away from the granite

(iii) Uranium deposits within down-faulted basins above a granitic basement. These basins are usually of Cretaceous to Early Tertiary age

(iv) Uranium deposits in volcanic depressions on a granitic basement

Granite-type uranium deposits can also be divided into the following types depending on their mineral assemblages and genetic characteristics:

(i) Deposits of acid hydrothermal origin

- microcrystalline quartz-type (MT)
- fluorite-type (FT)
- argillitization-type (AT)

(ii) Deposits of alkaline hydrothermal origin

- sodium metasomatic type (SMT)
- potassium metasomatic type (PMT)

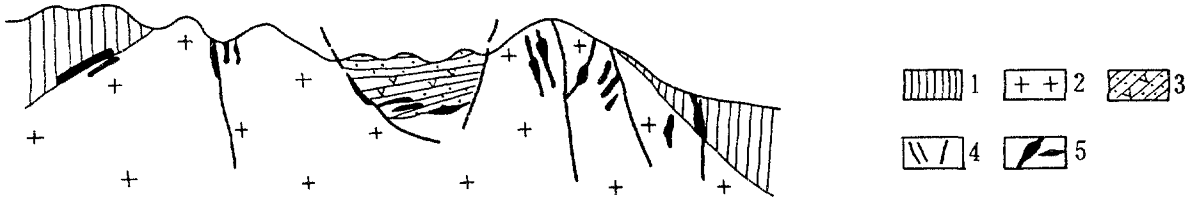

FIG. 1. Summarized schematic profile of granite-type uranium deposits (GUD). 1. sandstone-slate series; 2. granites; 3. down-faulted basins, always with intercalations and covers of acid, intermediate or basic volcanic rocks; 4. silicified faults or mylonitic zones; 5. orebodies.

2. GRANITE-TYPE URANIUM DEPOSITS

2.1. Deposits of acid hydrothermal origin

2.1.1. Microcrystalline quartz-type (MT)

This type of deposits usually occurs within quartz-rich granites. The individual orebodies are closely connected with shear zones (Fig. 2). The uranium mineralization is associated with siliceous filling material. This material exists up to 95 % of microcrystalline quartz (0.01 - 0.1 mm), containing brecciated, altered granite, disseminated colloidal pyrite, goethite and pitchblende thus showing a grey-black to red colour and is opaque. Table I gives the chemical composition of the microcrystalline quartz ore. The uranium content is directly proportional to the pyrite content and the size of the quartz grains (smaller grains: higher uranium content) (Table II). Richer parts of uranium ore formed at the intersections of microcrystalline quartz veins with lamprophyre or diabase dikes. It seems that the presence of mafic dikes favoured the precipitation of uranium (Fig. 3).

Within a number of studied granitic massifs,well developed zones of Na- and K-metasomatic rocks can be recognized. These exposure levels of granites seem to be the roofs of W- and/or Sn-bearing quartz veins. When ore-forming solutions moved into these alkaline metasomatic granites, pitchblende was precipitated around micrograins of pyrite or the uranium was adsorbed by clay minerals.

Hydrothermal wall rock alteration is characterized by hydromica-pyrite metasomatism. Detailed mineralogical studies have revealed that the sequence of alteration is as follows: biotite, feldspar-muscovite-sericite-hydromica or illite (automorph to detrital under the electron microscope) hydromica-montmorillonite interlayer mixture - montmorillonite-kaolinite (from early to late stage as a result of hydrogen metasomatism). This zonal alteration is shown in Fig. 4.

Sometimes the same type of uranium mineralization (MT) occurs in silicified shales, in siliceous limestones, dolomites far away from any granites which have very similar mineralogical characteristics as the veins in granites.

^{206}Pb anomalies frequently existed updip of pitchblende-bearing veins.

2.1.2. Fluorite-type (FT)

The fluorite-type uranium deposits derived from the microcrystalline quartz-type uranium mineralizations and differ from those in respect to the gangue minerals in which fluorite is predominant. This ore-forming fluorite is characterized by a dark violet colour and micrograin size (0.05 - 1 mm). The veins and stockwork structures are completely filled with fluorite without showing any voids.

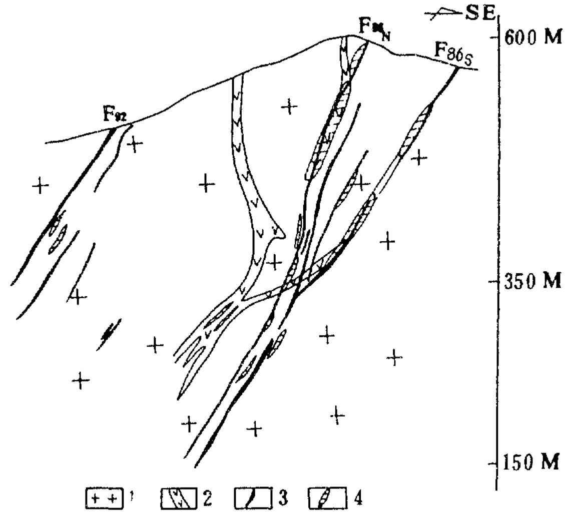

FIG. 2. Schematic profile of a deposit.
1. granite; 2. lamprophyre;
3. silicified faults; 4. orebodies.

TABLE I. CHEMICAL COMPOSITION OF RED AND GREY-BLACK MICROCRYSTALLINE QUARTZ ORE (IN PERCENT)

SAMPLE	1	2	3	4	5	6
STAGE	Q_{4-2}	Q_{4-2}	Q_{4-2}	Q_{4-2}	Q_{5-1}	Q_{5-1}
SiO_2	92.91	94.88	80.0	88.1	85.2	80.8
Fe_2O_3	0.63	0.17	1.36	1.87	6.2	4.5
FeO	1.31	1.32	2.17	1.33	1.5	0.8
Al_2O_3	3.30	2.32	8.08	3.61	2.4	7.9
TiO_2	0.40	0.40	-	-	-	-
MnO	0.20	0.20	-	-	-	-
CaO	0.11	0.04	0.63	0.95	0.5	0.02
MgO	0.32	0.17	-	-	0.74	0.52
P_2O_5	0.04	0.02	-	-	0.1	0.14
K_2O	0.99	0.74	3.28	0.96	0.15	2.25
Na_2O	0.01	0.02	0.23	0.12	0.0	0.0
U	0.16	0.05	0.19	0.15	1.45	0.35
L.I. *	-	-	1.57	1.86	1.93	4.20

* L.I. = LOST IGNITION INCLUDING MAINLY SULFIDES - UNANALYSED

TABLE II. CHEMICAL COMPOSITION OF VARIOUS STAGE QUARTZ (IN PERCENT)

SAMPLE	1	2	3	4	5	6	7	8	9
STAGE *	Q_1	Q_3	Q_{4-1}	Q_{4-2}	Q_{4-2}	Q_{4-2}	Q_{5-1}	Q_{5-2}	Q_6
SiO_2	≥95	≥95	≥95	≥90	87.99	90.32	≥90	—90	≥95
Al_2O_3	0.04	0.96	3.51	1.78	3.81	3.52	1.12	3.15	0.10
Fe_2O_3	0.08	0.16	0.53	0.81	0.46	0.38	0.36	0.18	-
FeO	0.06	0.08	0.18	0.20	0.46	0.20	0.23	0.19	0.07
S	0.009	0.009	0.015	0.015	0.53	0.23	0.006	0.004	0.003
L.I. **	0.74	0.68	1.74	1.18	-	-	1.08	0.64	0.04
U	0.0009	0.0033	0.024	0.023	0.07	0.25	0.012	0.0015	0.002
Th	0.0007	0.0009	0.0012	0.0011	-	-	0.0008	0.0018	0.0006
Th/U	0.8	0.3	0.05	0.05	-	-	0.07	1.2	0.3

* GRAIN SIZE OF QUARTZ SEE TABLE X ** L.I. = LOST IGNITION - UNANALYSED

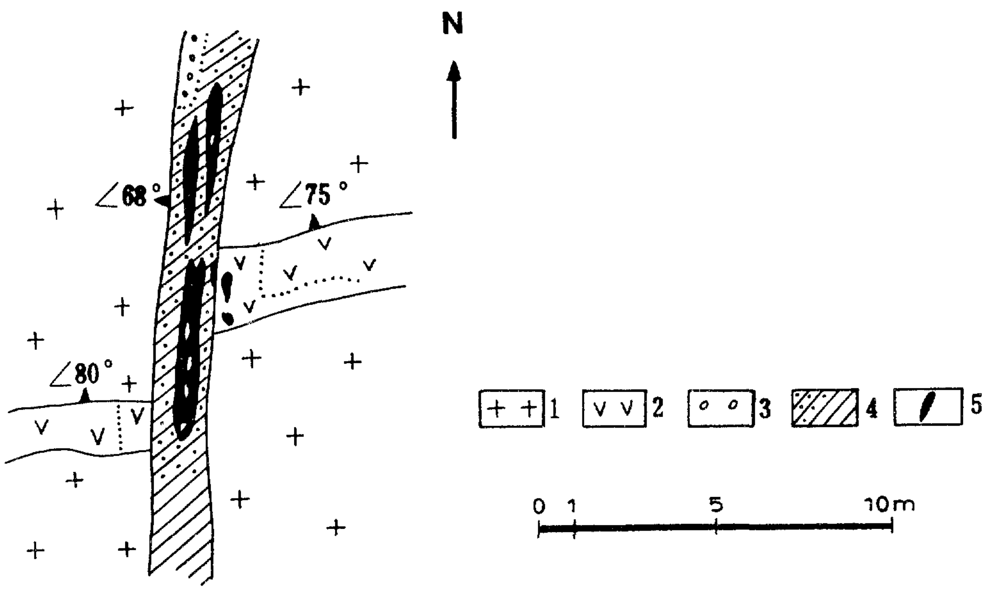

FIG. 3. Cross section of silicified vein with lamprophyre. 1. granite; 2. lamprophyre dike; 3. porcelain-like pre-ore microcrystalline quartz Q_{4-1}; 4. dark, red ore stage microcrystalline quartz Q_{4-2} containing abundant pitchblende pots and impregnations (dotted); 5. lens of massive pitchblende.

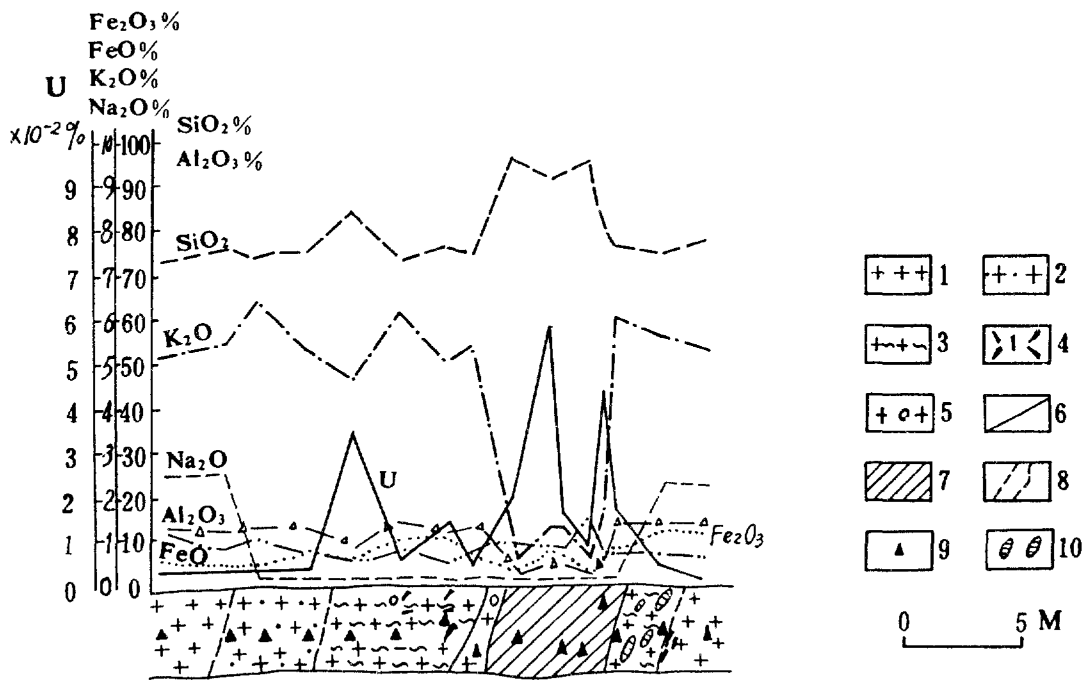

FIG. 4. Variation of chemical composition of altered wall rocks near quartz vein. 1. non-altered granites; 2. montmorillonite-hydromica altered granites; 3. hydromica altered granites; 4. pitchblende pots; 5. crushed granites infiltrated by ore stage quartz Q_{4-2}; 6. boundary of vein; 7. red microcrystalline quartz Q_{4-2}; 8. boundary line of alteration zones; 9. place of samples; 10. impregnation pots of Q_{4-2}.

Metacolloidal pitchblende, finely disseminated within such veins, occurs in close association with pyrite and/or marcasite.

During the hydrothermal process the microcrystalline quartz-type was followed by the fluorite-type and the later one often is superimposed on the first one. This process led quite often to an enrichment of uranium. Ore-forming fluorine (F) was released during hydromica alteration, i.e. the destruction of biotite and muscovite, which are the major fluorine carriers in the wall rocks (Table III). This may be the reason why the fluorite-type uranium deposits developed particularly well in altered two mica granites and volcanic rocks. Here, hydromica metasomatism was intense.

A schematic profile of such a uranium deposit is given in Fig. 5. The close spatial relationship between the orebodies and the two mica granites (γ_5^{2-2}) are obvious. Beryllium halos, often as beryllite, are characteristic for this type of uranium deposits.

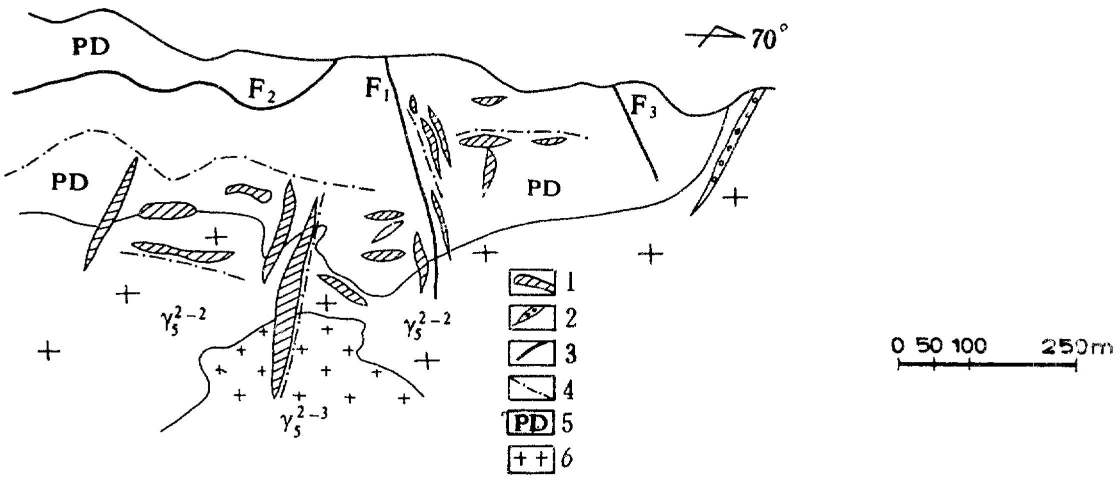

FIG. 5. Longitudinal cross-section of a fluorite-type deposit (FT). 1. orebodies; 2. pre-ore quartz $Q_{1,2,3}$ vein; 3. faults; 4. $Q_{3,4-1}$ veinlets; 5. Lower Palaeozoic sandstone-slate series; 6. granites of various intrusions.

2.1.3. Argillitization-type (AT)

Uranium deposits of this kind (Fig. 6) are important and widespread in China. They are closely connected with W- and Sn-quartz veins and have the following characteristic geological features:

(i) The ore is intensely cataclastic and shows strong hydromica alteration. Pitchblende and pyrite are disseminated in veinlets and the gangue usually is quartz and/or fluorite. The veinlets are about 0.01 to 0.5 mm in width. The three types of deposits (MT, FT, AT) can be separated from each other only by the intensity of cataclastism and alteration (Fig. 7), but the ore-forming mechanism is the same. AT is characterized by the superimposition of uranium mineralization on older greisen and alkaline metasomatic rocks formed during the phase of W, Sn, Nb, Ta mineralization.

(ii) The orebodies show swarms and are aligned in en echelon fashion.

(iii) Autoradiograph and fission track studies of thin and polished sections reveal that uranium is concentrated along fissures of feldspars, along

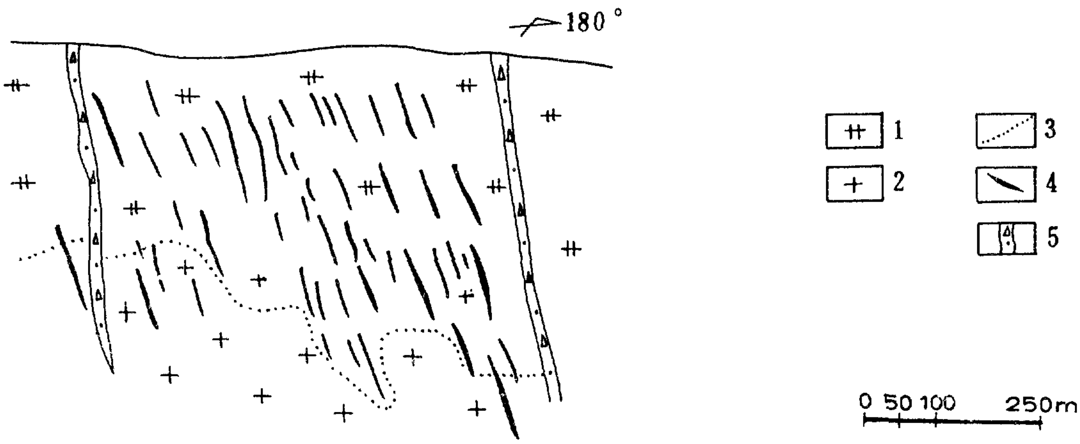

FIG. 6. Schematic profile of a argillization-type deposit (AT). 1. two-mica granite; 2. biotite granite; 3. alteration boundary line, above: red AT, below: green AT; 4. orebodies; 5. mylonite zones.

TABLE III. CONTENT OF FLUOR IN BIOTITE AND MUSCOVITE OF GRANITES (IN PERCENT)

ROCKS	F IN BIOTITE	F IN MUSCOVITE
GRANITE-DIORITES	0.22, 0.55, 0.93	
MEDIUM-COARSE GRAINED PORPHYRITIC BIOTITE MONZONITIC GRANITES	0.62, 0.66, 0.84, 0.95, 1.02, 1.26, 1.32, 1.43	
MEDIUM-FINE GRAINED TWO MICA GRANITES	1.20, 1.08	0.18, 0.19, 0.29
COARSE GRAINED STRONGLY PORPHYRITIC BIOTITE GRANITES	0.85, 0.86, 0.96, 0.99, 1.06	
MEDIUM GRAINED PORPHYRITIC TWO MICA GRANITE	0.45, 0.52	0.06, 0.57
BIOTITE GRANITE	0.42, 0.75, 0.82	
FINE GRAINED MUSCOVITE GRANITE		0.14, 0.16, 0.19, 0.25, 0.25, 0.28, 0.55, 0.56

* DATA FROM WANG YANTIANG ET AL. (UNPUBLISHED)

cleavage planes of biotite, and around fine grains of sulfides such as pyrite, sphalerite, and that it is also adsorbed by clay minerals.

(iv) This type of uranium orebodies (AT) may be subdivided into a red subtype (at shallower depth and in biotite poor rocks, such as alkaline metasomatic granites) and a green subtype (at greater depth and in biotite-chlorite-rich rocks), depending on the abundance of hematite. Chemical composition of such rocks is listed in Table IV.

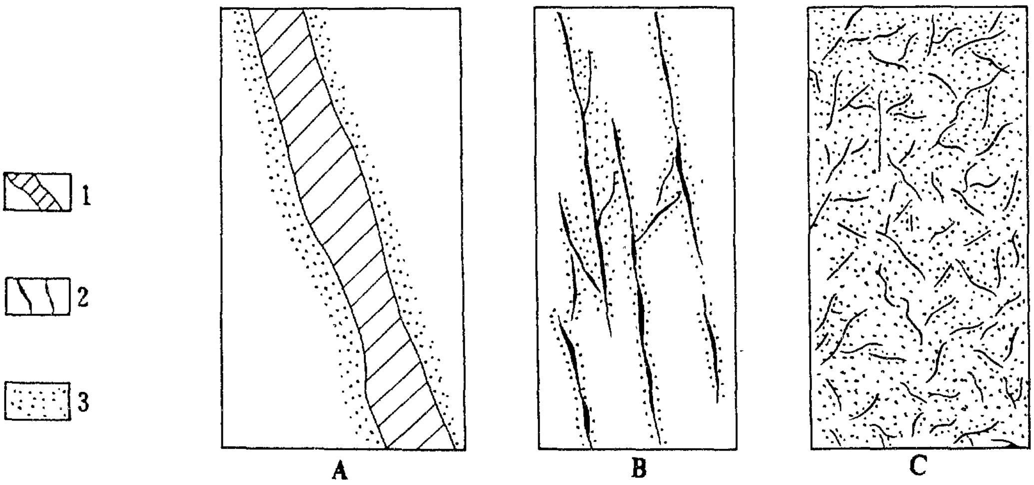

FIG. 7. Comparison of A: microcrystalline-type (MT) mineralization; B: fluorite-type (FT) mineralization; C: argillitization-type (AT) mineralization. 1. ore stage quartz vein (Q_{4-2}, Q_{5-1}); 2. U-bearing violet fluorite veinlets; 3. microveins of ore stage quartz and fluorite and hydromica alteration area (dotted).

TABLE IV. CHEMICAL COMPOSITION OF ARGILLITIZATION-TYPE ORE (IN PERCENT)

SAMPLE	1	2	3	4	5	6	7	8
SiO_2	71.21	72.83	72.45	71.93	73.42	57.54	72.16	71.68
Al_2O_3	13.47	12.75	12.78	12.88	12.29	20.43	13.48	14.19
Fe_2O_3	0.67	0.95	0.89	1.34	1.10	1.82	0.24	0.34
FeO	1.54	1.65	0.83	1.18	1.73	2.41	2.19	1.76
CaO	0.63	0.63	1.25	1.56	0.69	1.94	0.93	1.12
MgO	0.28	0.40	0.28	0.30	0.33	0.63	0.38	0.42
P_2O_5	0.15	0.13	0.14	0.12	0.13	0.18	0.14	0.15
K_2O	5.25	4.50	5.13	5.69	4.88	6.75	5.00	5.68
Na_2O	3.40	2.05	2.20	1.60	2.20	3.05	2.85	3.20
S	0.77	0.04	0.09	0.04	0.06	0.13	0.05	0.0
F	0.25	0.1	0.25	0.15	0.24	0.76	0.14	0.16
U	0.062	0.102	0.15	0.078	0.156	0.527	0.0012	0.0018
L.I. *	1.19	2.36	1.32	2.45	1.54	3.51	1.00	0.88

* L.I. = LOST IGNITION

SAMPLES 1, 2, 3 ARE RED AT (MEDIUM GRAINED PORPHYRITIC TWO MICA GRANITES)
SAMPLES 4, 5, 6 ARE GREEN AT
SAMPLES 7, 8 ARE NON-ALTERED PRIMARY ROCKS

2.2. Deposits of alkaline hydrothermal origin

2.2.1. Sodium metasomatic type (SMT)

This type of uranium ore deposits precipitated out of Na_2CO_3-rich alkaline solutions. The orebodies developed discontinuously along deep fault systems with several 100 km extension. These systems cross different geotectonic units. The ore-forming solutions replaced any kind of rocks by alkaline metasomatism. Many years ago sodium metasomatic type deposits were discovered in China and detailed studies were made (Du Letian (1)). The uranium mineralization of SMT has no significant relationship with magmatism and may appear in any kind of rocks like conglomerates, sandstones, carbonates, migmatites, andesites, rhyolites etc.. Otherwise, the SMT occurs mainly in Archaean, Proterozoic and Lower Palaeozoic rocks. Age datings of a number of uranium deposits of this type from various districts of China range from 1900 to 110 Ma.

The Na-metasomatic-type deposits can be subdivided into deposits

- with dark alkaline minerals such as riebeckite, aegirin etc. which were formed in Fe-rich rocks at higher temperatures, and

- without dark alkaline minerals which were formed in Fe-poor rocks (sialic) at lower temperatures. A schematic cross section of one deposit of this subtype is given in Fig. 8.

The mineralizing process has two stages. The first stage is the formation of Na-metasomatic rocks, in which the uranium is slightly enriched (two to three times background). A favourable environment is generated for the subsequent ore formation as the metasomatized rocks became porous and permeable. Independent of the original composition such rocks consist of albite (An = 0 - 5), chlorite, epidote (rare), hematite, apatite and carbonates. In the second stage a tectonic phase opened the geological system even more and uranium-bearing carbonate solutions had access to the pre-existing metasomatites. Uranium oxides (uraninite and pitchblende) and/or uranium titanites precipitated under lower temperatures and pressure and decreased alkaline conditions than existed during the earlier metasomatic process. The ore is characterized by intense red colour and cataclastism. Microprobe studies revealed that pitchblende is not a pure monomineral, but a mixture of U, Fe, Ti-oxides in which the concentration of these elements vary considerably. The uranium precipitation was accompanied by the formation of goethite, hematite, spherulitic chlorite and leucoxene.

The variation of the mineralogical and chemical composition of the Na-metasomatic rocks and ore is given in Tables V and VI. The Th, Y, Ce, and Zr values are several times higher than background but are not included in the tables.

Sodium metasomatic type uranium ore deposits are known from many shield areas of the world, like Beaverlodge (Canada), Ukraine and Middle Asia (USSR), northern Sweden, Brazil, India, Somalia, etc. The mechanism of ore formation of all such deposits is very similar. The Na_2CO_3 solutions derive from the upper mantle. The uranium has been leached by these ascending solutions from U-bearing rocks by means of alkaline metasomatism.

2.2.2. Potassium metasomatic type (PMT)

Uranium deposits of this type are rare worldwide and, therefore, of special interest. In China one of this type occurs in migmatites of Proterozoic sedimentary origin close to the contact of the Yenshanian migmatic granite complex which has an age of 174 Ma. 2 km away from the deposit passes a silicified fault zone, several hundreds of kilometres long. Medium grained two mica granites having an age of 149 Ma and being associated with fine grained apophyses intruded into the migmatites. This magmatic process was followed by a potassium-rich pegmatite (110 - 100 Ma), a K-metasomatism (92 Ma) and a uranium mineralization phase (47.5 - 42.5 Ma): by U-Pb isotope dating (Geological Team No. 301). Finally, coffinite was formed (20 Ma) (Sun Zhifu, 1981 (unpublished)). As shown in a profile (Fig. 9) the shape of the uranium mineralization is quite complicated in respect to the granite apophyses and the pegmatites.

As a genetic model it is assumed that uranium-bearing K_2CO_3 alkaline solutions ascended along the contact between pegmatites, granites and migmatites and

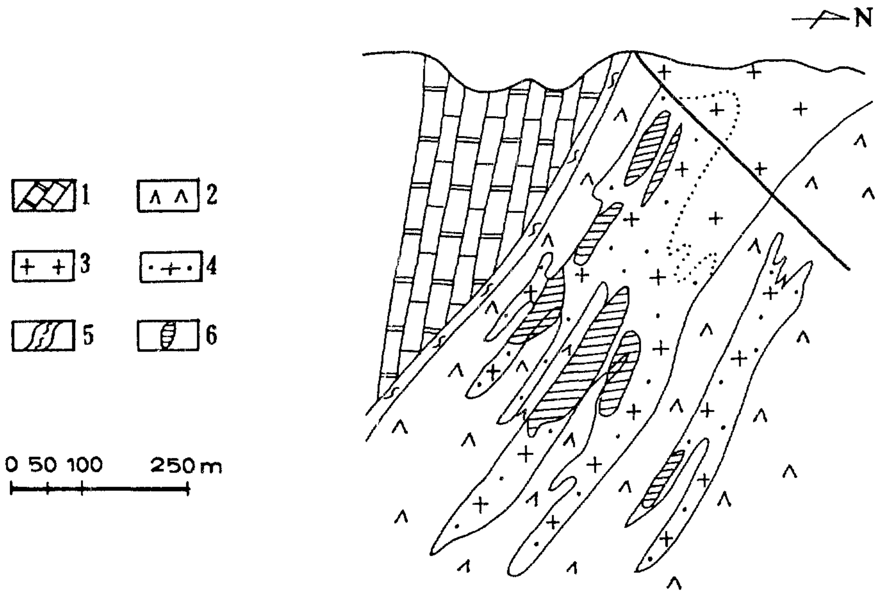

FIG. 8. Schematic profile of a sodium metasomatic-type deposit (SMT). 1. Proterozoic dolomitic limestone; 2. diorite, earlier than granites; 3. medium-coarse porphyritic biotite plagioclase granites (Caledonian); 4. red strongly Na-metasomatic granites; 5. regional deep-reaching faults (mylonites); 6. orebodies.

TABLE V. MINERALOGICAL COMPOSITION OF NA-METASOMATIC ROCKS AND PRIMARY GRANITES (IN PERCENT)

ROCK	1 *	2 **
QUARTZ	35	0 - 3
K-FELDSPAR	23	3
PLAGIOCLASE	37	0 - 2
ALBITE	0.3	74
BIOTITE	4.0	0
CHLORITE	0	7
CARBONATES	0	11
HEMATITE	0	1

* 1 = COARSE PORPHYRITIC BIOTITE PLAGIOCLASE GRANITES
** 2 = NA-METASOMATIC GRANITES MENTIONED ABOVE

TABLE VI. CHEMICAL COMPOSITION OF NA-METASOMATIC GRANITES, ORE AND PRIMARY GRANITES (IN PERCENT, EXCEPT WHERE INDICATED)

SAMPLE	1 *	2 **	3 ***
SiO_2	70.19	62.05	56.37
Al_2O_3	14.23	15.53	14.85
Fe_2O_3	0.85	1.04	1.84
FeO	2.05	1.99	1.68
TiO_2	0.32	0.32	0.39
CaO	1.29	4.26	7.19
MgO	0.06	0.08	0.09
MnO	0.67	0.92	1.00
P_2O_5	0.12	0.22	0.62
K_2O	4.18	0.90	0.21
Na_2O	4.13	7.24	7.60
CO_2	0.19	2.26	4.40
H_2O	0.80	1.10	1.53
U	19 PPM	48 PPM	3.900 PPM
Th	29 PPM	76 PPM	20 PPM

* COARSE PORPHYRITIC BIOTITE PLAGIOCLASE GRANITES (AVERAGE FROM 2 ANALYSES)

** NA-METASOMATIC GRANITES (AVERAGE FROM 9 ANALYSES)

*** URANIUM ORE (AVERAGE FROM 15 ANALYSES)

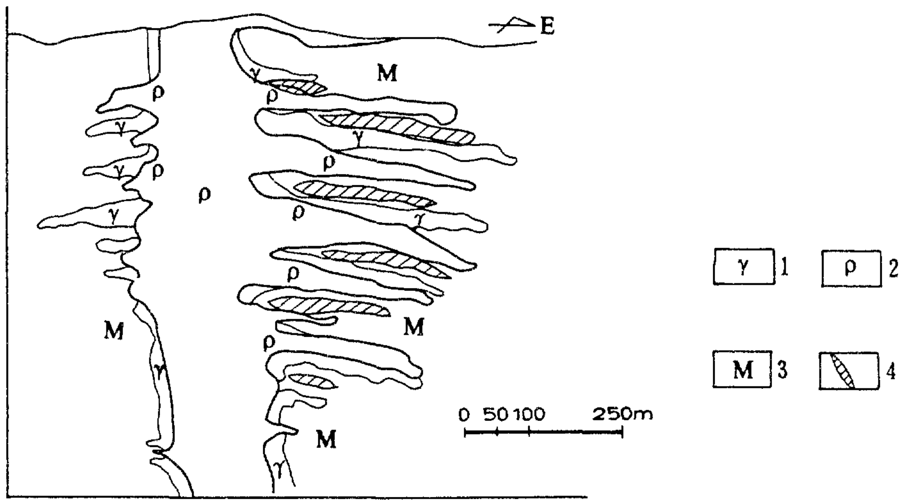

FIG. 9. Schematic profile of a potassium-metasomatic-type (PMT) deposit. 1. fine grained granite; 2. pegmatite; 3. migmatite; 4. orebodies.

TABLE VII. AVERAGE CHEMICAL COMPOSITION OF VARIOUS ROCKS * (IN PERCENT, EXCEPT WHERE INDICATED)

SAMPLE	1	2	3	4	5	6
NO. OF ANALYSES	8	10	21	6	8	6
SiO_2	68.79	55.78	55.65	72.45	58.25	57.46
Al_2O_3	14.91	17.03	15.82	14.25	17.40	16.22
TiO_2	0.41	0.46	0.42	0.13	0.16	0.11
Fe_2O_3	0.28	1.52	2.60	0.30	0.79	6.26
FeO	3.45	3.37	4.32	2.00	0.74	0.59
MnO	0.06	0.05	0.19	0.09	0.05	0.07
MgO	1.49	2.36	1.96	0.42	0.45	0.43
CaO	2.65	2.54	3.53	1.67	3.94	1.11
Na_2O	3.10	0.52	1.79	4.16	2.81	2.48
K_2O	3.85	12.03	8.44	3.67	10.35	8.60
P_2O_5	0.13	0.17	0.16	0.08	0.20	0.11
CO_2	0.25	1.86	2.59	0.12	2.65	0.96
H_2O	0.53	1.86	-	0.53	1.32	-
S **	0.01	0.01	0.03	0.00	0.00	0.06
U **	18 PPM	36 PPM	5,145 PPM	22 PPM	29 PPM	2,880 PPM
TH **	25 PPM	29 PPM	32 PPM	25 PPM	40 PPM	18 PPM

* DATA FROM GEOLOGICAL TEAM NO. 301
** DATA FROM SUN ZHIFU, 1981 (UNPUBLISHED)

SAMPLE 1 - MIGMATITES
SAMPLE 2 - K-METASOMATIC MIGMATITES
SAMPLE 3 - MIGMATITE ORE
SAMPLE 4 - FINE GRAINED GRANITES
SAMPLE 5 - K-METASOMATIC FINE GRAINED GRANITES
SAMPLE 6 - GRANITE ORE

led to the formation of K-metasomatites. These are composed of K-feldspars, chlorite, epidote, hematite, goethite, and carbonates. Chemical composition of such rocks is listed in Table VII. As a result of leaching of quartz these rocks became very porous (Table VIII). The REE, Cu, V and Co content increased but little uranium was introduced during this stage. This stage was followed by intensive cataclastic events, during which uranium was introduced and precipitated into cataclastic contact zones between the various country rocks. Pitchblende and coffinite were precipitated together with sericite and sulfides, concentrating

TABLE VIII. MECHANICAL PROPERTIES OF ROCKS BEFORE AND AFTER K-METASOMATISM *

SAMPLE	1	2	3	4	5	6
NO. OF ANALYSES	4	4	4	4	6	3
SPECIFIC GRAVITY	2.64	2.56	2.69	2.57	2.61	2.46
POROSITY	0.76 %	15.60 %	0.37 %	9.35 %	0.82 %	10.15 %
CRUSHING STRENGTH (DRY)	1,718 KG	584.0 KG	1,328.5 KG	559.5 KG	-	-
CRUSHING STRENGTH (SATURATED)	1,196.5 KG	280.5 KG	886.5 KG	317.0 KG	-	-

* DATA FROM GEOLOGICAL TEAM NO. 301

SAMPLE 1 - FINE GRAINED GRANITES
SAMPLE 2 - K-METASOMATIC FINE GRAINED GRANITES
SAMPLE 3 - MIGMATITES
SAMPLE 4 - K-METASOMATIC MIGMATITES
SAMPLE 5 - PEGMATITES
SAMPLE 6 - K-METASOMATIC PEGMATITES

in clusters of chlorite aggregates or filling fissures within sulfides. Sometimes adular crystals are coated with sooty pitchblende or filling voids where quartz was leached out. Fluid inclusion studies indicate precipitation temperatures of 240° to 306°C, post-ore calcite 145°C. In this context it should be pointed out that the alkaline metasomatism obeys the rule of valence dipolarization in silicate rocks (Du Letian et al. (2)).

3. DISCUSSION OF GENESIS OF GRANITE-TYPE URANIUM DEPOSITS (GUD)

As a result of many studies it can be summarized that known hydrothermal uranium deposits in China have been mostly formed after the intrusion of mafic dikes and/or after the down-faulting of Cretaceous basins (rift opening). All the other hydrothermal deposits with W, Sn, Nb, Ta, REE, Be, Fe, Cu, Mo, Bi, Li, Rb, Cs, Au, Ag, Pb, and Zn mineralizations, excluding some fluorite deposits, were formed before this important event (Table IX).

The development of rift systems, accompanied by down-faulting of basins, led to the intrusion of basic dikes and extrusion of basalts (Chen Zuyi, 1980 (unpublished)), but also to the development of large quartz veins, tens to hundreds of metres wide and tens or more kilometres long, and to the widespread occurrence of hot springs.

To explain the genetic model for the formation of such uranium deposits the following geological parametres are proposed:

(i) Termination of regional large scale sial magmatism

(ii) Increase of thickness of consolidated granitic crust (U source rock) and strengthening of crustal rigidity

(iii) Tension of crust

(iv) Upwarping and diapiring of the upper mantle, which can be demonstrated by geological surveys

(v) Regional geothermal gradients (Chen Zhaobo, 1980 (unpublished)), and locally higher geothermal gradients around the late intrusions (Du Letian, 1978 (unpublished))

(vi) Fault block movement leading to horst-graben structures

TABLE IX. SEQUENCE OF MAGMATIC, HYDROTHERMAL AND METALLOGENETIC ACTIVITIES IN EASTERN CHINA

MAGMATIC SEQUENCE	HYDROTHERMAL ACTIVITY SEQUENCE	METALLOGENIC SEQUENCE
	Q_6	SECONDARY U-MINERALIZATION
	Q_5	U-HYDROTHERMAL MINERALIZATION (90 - 45 MA)
	Q_4	
	Q_3	
	Q_2	(90 - 100 MA)
	Q_1	
2 (BASALTIC, ANDESITIC LAVA AND DIKES)		
DISCORDANCE		
FORMATION OF DOWN-FAULTED BASINS - CRETACEOUS (K_1, K_2)		
DISCORDANCE		
Q^1 (MAFIC DIKES) (YENSHANIAN)		PB, ZN MINERALIZATION
$_5^{3-2}$ (YENSHANIAN)		NB, TA, W, SN MINERALIZATION (102, 130 MA)
$_5^{3-1}$ (YENSHANIAN)	GREISENIZATION	
$_5^{2-3}$ (YENSHANIAN)	ALKALINE METASOMATISM	QUARTZ VEIN-TYPE W, SN MINERALIZATION (141-175 MA)
$_5^{2-2}$ (YENSHANIAN)	ALLOMETAMORPHISM	GRANITE-TYPE NB, TA, W, SN, REE, LI MINERALIZATION (180 - 130 MA)
$_5^{2-1}$ (YENSHANIAN)	AUTOMETAMORPHISM	SKARN MINERALIZATION OF W, SN, FE, CU ... (160 - 188 MA)
$_5^{1-3}$ (YENSHANIAN)		
$_5^{1-2}$ (YENSHANIAN)		
$_5^{1-1}$ (195 - 220 MA)		

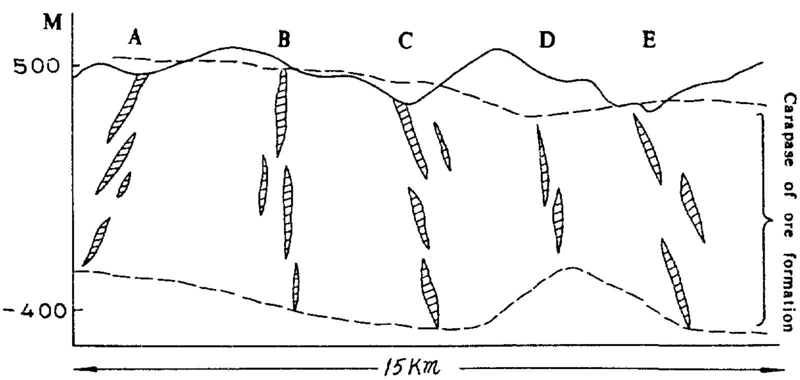

FIG. 10. Schematic longitudinal cross-section of a uranium-bearing silicified fault. A, B, C, D, E - deposits.

In addition it has to be pointed out that the vertical distribution of orebodies is very regular over many districts, which means that ore zones have usually not more than a vertical extension of 300 - 1,000 m, independent of present day relief. This phenomenon is called by the author of this paper the 'carapase of ore formation' describing a limited vertical zone in which ore deposits are developed (Fig. 10). The 'carapase of ore formation' is an important physicochemical factor which controls the vertical localization of orebodies as here the metallogenic conditions suffer severe changes:

- Sudden decrease of pressure along faults and fracture zones affecting ascending hydrothermal solutions

TABLE X. VARIATION IN GRAIN SIZE OF QUARTZ AT VARIOUS STAGES

STAGE	NAME	GRAIN SIZE (MM)
Q_1	COARSE CRYSTALLIZED	> 3
Q_2	MEDIUM CRYSTALLIZED	1 - 3
Q_3	FINE CRYSTALLIZED	0.1 - 1.0
Q_4	MICROCRYSTALLINE	0.01 - 0.1
Q_{4-1}	LIGHT MICROCRYSTALLINE	
Q_{4-2}	DARK MICROCRYSTALLINE (ORE STAGE)	
Q_5	CRYPTOCRYSTALLINE	0.001 - 0.01
Q_{5-1}	DARK CRYPTOCRYSTALLINE (ORE STAGE) *	
Q_{5-2}	LIGHT CRYPTOCRYSTALLINE **	
Q_6	COMB-LIKE AND MICROLITIC	VARIED

* ORE-FORMING DARK VIOLET FLUORITES ARE DEVELOPED IN THIS STAGE
** LIGHT FLUORITES (POST-ORE) ARE ALWAYS ASSOCIATED WITH Q_{5-2}

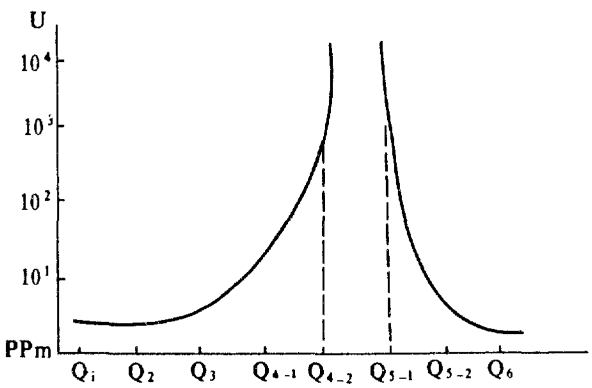

FIG. 11. Variation of U content in quartz versus its stages.

- Rapid cooling and oversaturation of solutions and rapid crystallization of minerals into fine and metacolloidal mineral assemblages

Numerous field observations and studies of sections under the microscope show that the grain size of major gangue minerals like quartz becomes increasingly finer from pre-ore stage (Q_1, Q_2, Q_3) to ore stage (Q_4, Q_5) (Table X), and the U content becomes synchronously higher (Fig. 11).

Chen Anfu et al., 1980 (unpublished), based on detailed studies of inclusions, point out that in the same visual field of a thin section coexisting pure gas inclusions, gas-liquid inclusions and some filled with liquids may be found. These inclusions are extremely small (0.005 - 0.02 mm) with a wide range of variation of homogenization temperature and salinity (8 - 25 wt%). All this indicates that the boiling of hydrothermal solutions may have taken place during the ore-forming process. Migration of U is postulated to have taken place in form of complex ions $(UO_2(CO_3)_2)^{2-}$, $(UF_2(CO_3)_3)^{4-}$ which were dissociated due to the release of CO_2 or HF. Subsequently hydrous oxides of U^{4+} and U^{6+} precipitated in cotton wool fashion showing spherulitic forms. This reaction was proven by experiments (Shen Caiqing, Zhao Fengmin, oral communication, 1982). Based on specific volume method calculation, Chen Anfu et al., 1980 (unpublished) obtained the result, that the pressure of solution was

- in pre-ore stages 194 - 510 atm
- in ore-forming stages 10 - 61 atm
- in post-ore stages 1 - 65 atm

Depth of mineralization was estimated not more than 1 km below surface at that time. As a result of the determination of the homogenization temperature of inclusions the process of ore formation took place under decreasing temperature conditions:

- pre-ore 340°C - 220°C
- ore-forming 295°C - 150°C
- post-ore 190°C - 90°C

The curve of temperature decrease is not smooth but quite irregular.

Shu Shoutian, 1980 (unpublished) determined that the freezing points of fluid inclusions are from -23.4°C to -33.0°C which indicates that the solutions are pure and that they are no suspensions. Jiang Guiyu, 1982 (unpublished) analysed the chemical composition of fluid inclusions and determined the values given in Table XI.

TABLE XI. CHEMICAL COMPOSITION OF INCLUSION FLUIDS

	G.ION/L
K^+	0.2 - 0.5
Na^+	0.2 - 0.6
Ca^{2+}	0.4 - 1.4
Mg^{2+}	0.05 - 0.2
HCO_3^-	0.4 - 3.0
SO_4^{2-}	0.05 - 0.3
F^-	0.1 - 0.5
Cl^-	0.1 - 0.3
pH	7.05 - 8.12
Eh	-0.46 - -0.55 (V)

The 'carapase of uranium ore formation' is a transitional redox zone favourable for the precipitation of pitchblende which consists of a mixture of U^{4+} and U^{6+}. In natural, three basic paragenetic mineral assemblages can be separated:

(i) Pitchblende (U^{4+}, U^{6+}), pyrite (Fe^{2+}, S_2^{2-}), hematite (Fe^{3+}), chlorite (Fe^{2+}, Fe^{3+}), goethite (Fe^{3+}) in the carapase zone of ore formation. A great number of data led to the conclusion, that the most favourable conditions for the precipitation of uranium are neither pure oxidizing nor pure reducing conditions, but a transitional redox barrier where the coexisting system of U^{4+}, U^{6+}, Fe^{3+}, Fe^{2+}, S_2^{2-} is stable (Fig. 12). This means that solutions ascending from depth carried mainly U^{4+} (sometimes with Th^{4+} and Au^+) into the carapase zone of ore formation. The U^{4+} underwent some oxidation resulting in the precipitation of pitchblende (UO_x). Its oxygen coefficient x varied from 2.0 to 3.0. The ratio U^{6+} to U^{4+} in uranium minerals is an indicator of depth of their formation (oxygen fugacity fo_2).

(ii) Uraninite (U^{4+}), pyrrhotite (Fe^{2+}, S^{2-}) formation in strongly reducing environment or at depth

(iii) Secondary uranium minerals (U^{6+}), limonite (Fe^{3+}), jarosite, barite, and gypsum (S^{6+}) at surface and at shallow depth.

In Fig. 13 these findings have been illustrated. For completion of this it should be mentioned that the migration of hexavalent uranium in endogen solutions

Uraninite	Pitchblende	Secondary U minerals
U^{4+}	$U^{4+} + U^{6+}$	U^{6+}
Fe^{2+}	$Fe^{2+} + Fe^{3+}$	Fe^{3+}
$S^{=}$	S^{-}	S^{0} S^{6+}

FIG. 12. Basic paragenetic association of minerals.

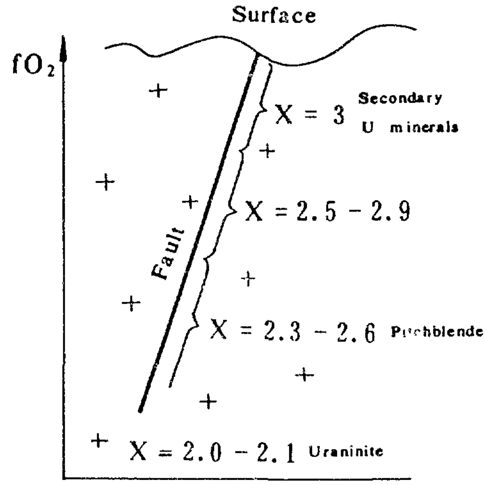

FIG. 13. Relationship of U minerals with depth (fugacity of oxygen fO_2)
X = 2.5 - 2.9 (U containing finely crystallized apatite)
X = 2.0 - 2.1 (dispersed uraninite in granites, which is about 0.03 mm).

has been questioned. Late experiments (Shen Caiqing, 1984 (unpublished)) indicate tetravalent migration of this element.

The results of the determination of the isotopic composition of some minerals are given after Chen Anfu et al., 1980 (unpublished):

- $\delta^{34}S$ = -3 to -15 ‰: in pyrite of ore stage, the sulphur came mainly from wall rocks
- $\delta^{13}C$ = -6.99 to -7.89 ‰ (PDB) (carbonate)
- $\delta^{18}O$ = +1.52 to +8.5 ‰ (standard mean ocean water): early stage quartz corresponding to ^{18}O value of granite, but ^{18}O of H_2O in hydrothermal solutions: -2.97 to -8.85 ‰ which is characteristic for meteoric origin (D = -54 to -88 ‰)

The age of hydrothermal uranium ore is 90 - 65 Ma (from several hundred samples) which corresponds quite well with the late period of crustal tension and mantle upwarping of eastern China.

Fertile granites are characterized by higher uranium content (10 - 30 ppm), lower Th/U ratio (Th/U<3), enrichment of uraninite in rocks (5 g/t and more) and higher U content in zircon of granites. Numerous data are indicating that the fertile granites are derived from a sedimentary (sandstone, shale) sequence of Lower Palaeozoic age. Higher U content (5 - 6 ppm: average value of hundreds of samples) and higher amounts of H_2O^+ (2 - 4 %) in these originally sedimentary rocks have played an important role in the mechanism of autometamorphism and allometamorphism (= contact metamorphism) and the mobilization of uranium within the granites (Fig. 14). The concentration of uranium to form uraninite is considered to be the result of auto- and allometamorphism of granites.

The mechanism of formation of granite-type uranium deposits can be summarized as follows (Du Letian et al. (3)): Hydrothermal solutions of mainly meteoric origin ascended along deep faults and fracture zones leaching silica, fluorine and dispersed uranium (such as in uraninite and zircon) from fertile granites (Fig. 15). These U-pregnant solutions reach the 'carapase of ore formation'

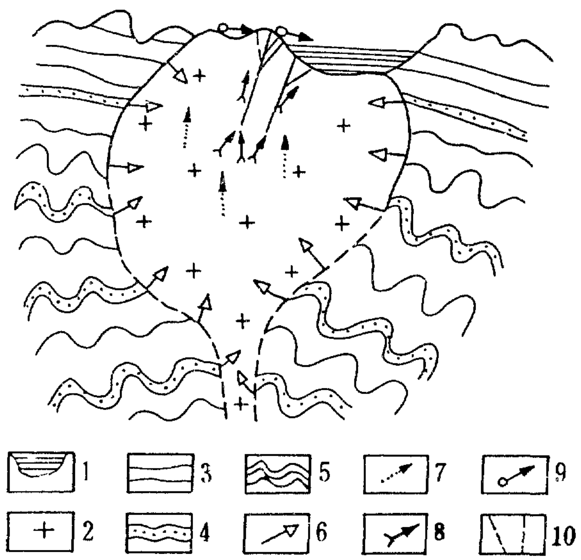

FIG. 14. Transfer and migration of source U at depth. 1. down-faulted basin; 2. granites, 3. slightly metamorphic U-bearing sedimentary series; 4. U-enriched intercalated beds; 5. strongly metamorphosed sedimentary series; 6. U from the sedimentary strata; 7. U mobilized during autometamorphism and allo-metamorphism; 8. U carried by ascending hydrothermal solutions along fracture zones and deep faults; 9. U mobilization by weathering; 10. granitization front.

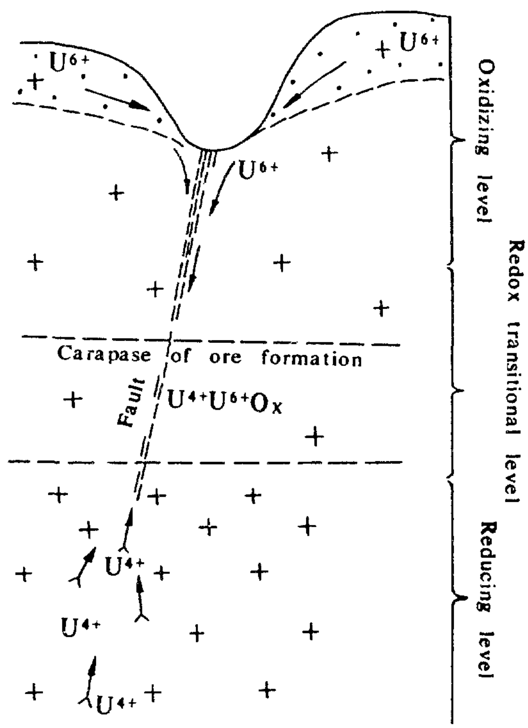

FIG. 15. Genetic model diagram.

where the solutions boil and cool rapidly; U^{6+} is formed by oxidation. Subsequent neutralization caused by wall rock alteration leads finally to the precipitation of hydrous U^{4+} and U^{6+} oxides. This mechanism is initiated by mantle upwarping and by late intrusions generating regional and local geothermal gradients and leading to the heating of meteoric and ground water. This process did not exclude the participation of differentiated alkali-rich solutions from the mantle, which played an important role in the formation of alkaline metasomatic uranium deposits.

ACKNOWLEDGEMENTS

Participants of this work are also: Wang Yanting, Hu Shaokang, Rong Jiashu, Chen Zuyi, Tong Hanshou, Li Tiangang, Hang Zehong, Huang Zhizhang, Zhao Fengmin, Zhang Daishi, Feng Minyue, Sun Zhifu, Cai Gengqing, Xu Ziyang, Cun Xitian, Wang Yuming, Shen Zhuyong, Li Yuexiang, Wang Yuelian. The author is greatly indebted to a number of colleagues in many Geological Teams and research institutes, who have worked together with him in the past many years. They have given large help to the author. The author is also grateful to Mr. Chen Zhenshi and Dr. Helmut Fuchs who read the English manuscript with friendly criticism.

REFERENCES

(1) DU LETIAN, Geochemical principles of alkaline metasomatism, Scientia Sinica (1985) (in press).

(2) DU LETIAN, HUANG ZHIZHANG, The rule of valence polarization in silicate rocks, Geochemistry 3 (1984) (in press).

(3) DU LETIAN et al., Granite-type uranium deposits, Atomic Energy press, Beijing (1982) 75-99 (in Chinese).

URANIUM MINERALIZATION OF COLLAPSE BRECCIA PIPES IN NORTHERN ARIZONA, WESTERN UNITED STATES

K. J. Wenrich
U.S. Geological Survey
Denver, Colorado
United States of America

Abstract

URANIUM MINERALIZATION OF COLLAPSE BRECCIA PIPES IN NORTHERN ARIZONA, WESTERN UNITED STATES

The development of caves within the Mississippian Redwall Limestone of the western United States, accompanied by later upward stoping of overlying Palaeozoic and Triassic rock, resulted in the formation of breccia pipes. The Palaeozoic sedimentary rocks on the Colorado Plateau of northern Arizona are host to hundreds of these breccia pipes. The uranium and copper deposits within these pipes transgress formation boundaries from the Mississippian Redwall Limestone to the Triassic Chinle Formation. These are not classic breccia pipes in that there is no volcanic rock associated with them in time or space; they are the result of solution collapse within the Redwall Limestone. Karst development in the Redwall Limestone began in the Mississippian and apparently either continued to the Triassic, or was at least once again active during that time. The mineralization apparently occurred shortly thereafter, sometime during the Mesozoic. Mining activity in breccia pipes of the Grand Canyon region began during the 19th century and continues today with the operation of the Hack I, II, and III Mines, although the exploited commodity has changed from Cu to U. Although small in size, these pipes occasionally contain fist-size samples with up to 55 wt.% U_3O_8 and can yield 1800 metric tons of U_3O_8 averaging between 0.30 and 0.60 wt. %, such as in the Orphan Mine.

Surface exposure of mineralized pipes commonly contains nodules and concretions of marcasite, pyrite, and goethite, as well as fractures coated with the same minerals, while the primary ore of the unoxidized zones is commonly uraninite within a comminuted sandstone matrix surrounding breccia fragments of overlying formations. Some of the oxidized surface nodules are encrusted with malachite and are exceptionally enriched in Ag. Pyrite is abundant and the organic carbon content of many rocks is occasionally high enough to suggest that it, along with the pyrite, may be a reductant for the uranium. In contrast, it is possible, if uranium were transported as a bicarbonate or carbonate complex, that only a conduit of brecciated rock was necessary to release CO_2, disrupting the equilibrium and causing uraninite to precipitate.

An extensive suite of elements is significantly enriched in the mineralized rock: Ag, As, Ba, Cd, Co, Cr, Cs, Cu, Hg, Mo, Ni, Pb, Sb, Se, Sr, V, Zn, and the rare earth elements. Of these, Pb, Zn, Ag, and particularly As, appear to be the best geochemical indicators of mineralized pipes. The lack of extensive silicification within the breccia, along with the fluid-inclusion filling temperature in calcite of 60° to 110°C, suggest relatively low temperature mineralizing fluids of unknown origin.

The origin of the mineralizing fluids is not as well understood as the origin of the breccia pipes. In any event, any model must address the following:

(i) The pipes are controlled by northeast- and northwest-trending basement structures. In fact, location of these structures is an excellent exploration guide. These structures apparently enhanced dissolution of the Redwall Limestone along these zones of weakness.

(ii) The mineralized pipes commonly occur in localized groups, such as in Hack Canyon (four ore deposits within one square kilometer) and the Bat Cave area of the Hualapai Plateau.

This suggests some control of the fluids by local cavern systems of the Redwall Limestone. Perhaps then, over the past 350 Ma, at least one mineralizing fluid must have ascended the pipe, maybe from the Precambrian basement rocks. On the other hand, another plausible model proposed that the uranium-rich fluids came through one of the aquifer systems from the volcanic rocks to the south, in the Mogollon Highlands, during uplift in the Triassic. Unfortunately, this model does not provide for the systematic movement of mineralizing fluids necessary to account for the clumping of mineralized pipes presumably related by one cave system. Because of the unusual enrichment of so many metals, particularly the epithermal suite of Au, Ag, Hg, As and Cd, within these ore deposits, multiple stages of mineralization appear likely. It is difficult to imagine minerals such as chalcopyrite and arsenopyrite, and the extensive suite of anomalous trace elements, including, in many cases, the rare earths. Th, and such classic epithermal elements as As, Sb, Au, and Ag, forming a deposit solely from low temperature fluids as proposed by Bowles (1). Hydrothermal fluids must have been responsible for much of the mineralization.

1. INTRODUCTION

The Colorado Plateau of northern Arizona is host to hundreds of breccia pipes. Even during periods of a depressed uranium market in the United States, exploration activity for mineralized breccia pipes in north-central and northwestern Arizona has remained high, because of their high grade uranium.

These breccia pipes are not 'classic' breccia pipes, in that there are no volcanic rocks associated in time or space; instead, they are a result of solution collapse within the Redwall Limestone and stoping of the overlying strata; this mechanism was first proposed by Bowles (2). Volcanic activity in northern Arizona was sporadic and confined to the past 6 Ma; the pipes were apparently mineralized by Triassic time. In only one case, the Grand Pipe, is there volcanic rock within a breccia pipe. The pipes and associated mineralization transgress formation boundaries from the Mississippian Redwall Limestone to the Triassic Chinle Formation (Fig. 1). No pipes have been observed during this study nor during those of Huntoon et al. (3), (4), and Billingsley and Huntoon (5) to occur in rock below the base of the Thunder Springs Member of the Redwall Limestone. This solution collapse of the sedimentary rock produced significant brecciation of the rock within the steep walls of the pipes. No pipes have been observed to contain rock from underlying formations; all breccia fragments have been displaced downward in the pipes. As a result, within any given pipe, brecciated rock is surrounded by steeply dipping ring fractures which usually dip outward from the center of the pipe near its base, but becomes more vertical higher in the section until the total displacement of the rock decreases to zero where the pipe manifestation if merely inward-draping beds. In some instances the breccia has been silicified and/or mineralized, and in others it resembles nothing more than quaternary alluvium.

The breccia pipes occur throughout northern Arizona from the Utah border south to the Mogollon Rim, the southern margin of the Colorado Plateau. They are abundant from the edge of the Grand Wash Cliffs (the western margin of the Colorado Plateau), across the Hualapai Indian Reservation, through Coconino National Forest to the Marble Plateau of the Navajo Reservation (Fig. 2). No pipes are known to occur east of the Echo Cliffs. Perhaps the area best known for breccia pipes is the Arizona Strip, extending from the Grand Canyon north to the Utah

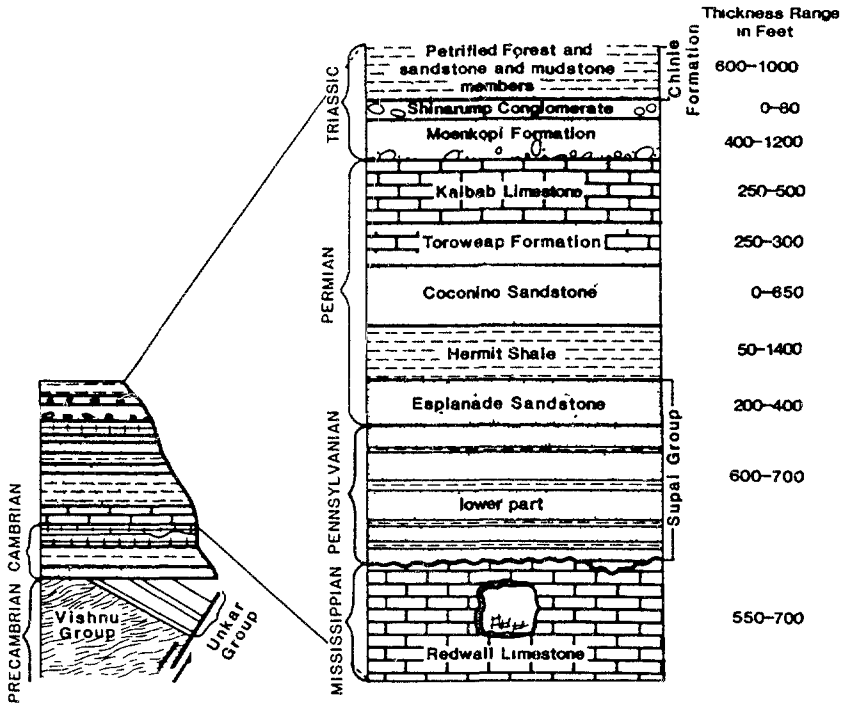

FIG. 1. Stratigraphic column showing rock units found in the Grand Canyon of Arizona. The thickness shown for each unit are those which occur over the area shown in Fig. 2 (thickness measurements from George H. Billingsley, personal communication).

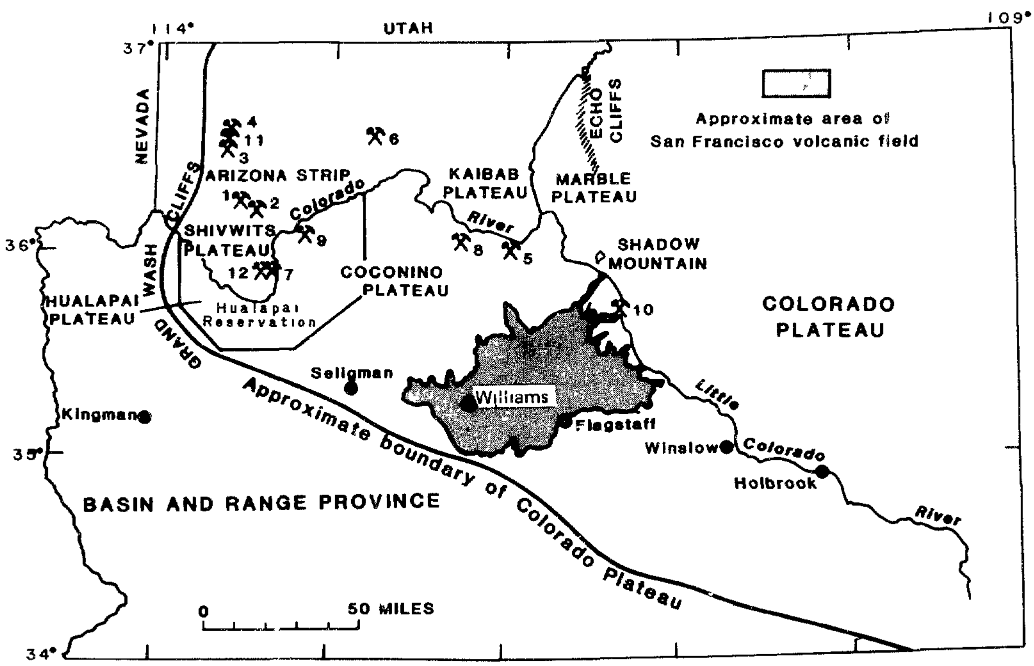

Fig. 2. Index map of northern Arizona showing the location of plateaus, Hualapai Reservation, breccia pipes developed into mines, and the San Francisco volcanic field which buries terrane with high potential for breccia pipes. Numbers refer to the following mines: 1. Copper House, 2. Copper Mountain, 3. Cunningham, 4. Grand Gulch, 5. Grandview, 6. Hack Canyon, 7. Old Bonnie Tunnel, 8. Orphan, 9. Ridenour, 10. Riverview, 11. Savannic, 12. Snyder.

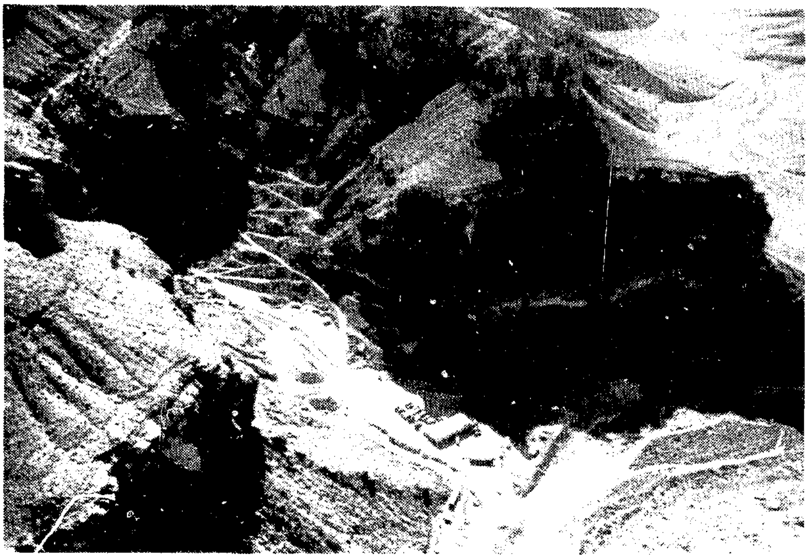

FIG. 3a. Hack Canyon, Arizona. This shows the presently active mining operation at the Hack I pipe (Old Hack Canyon mine is also in the photo to the right of Hack I). The only obvious feature that may suggest a pipe is present, is the typical amphitheater style of erosion characteristic of breccia pipes.

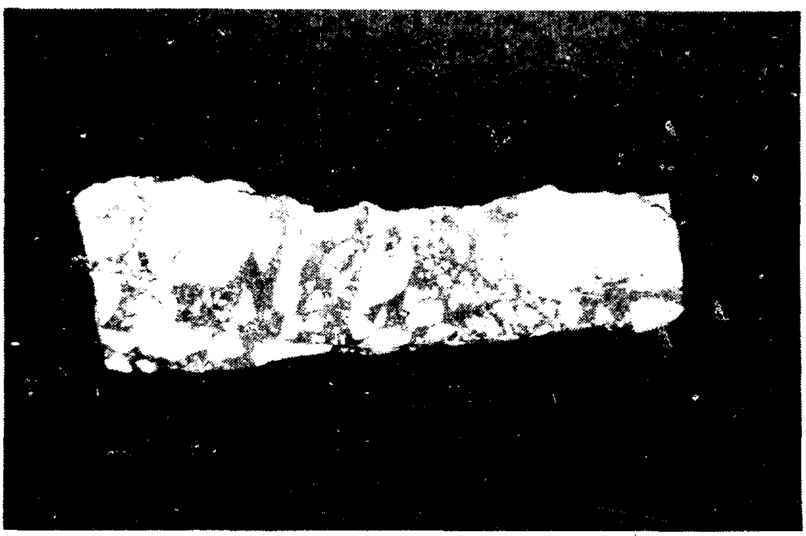

FIG. 3b. Uranium ore from one of the breccia pipes showing uraninite in the matrix surrounding bleached sandstone breccia clasts. The largest clast is 5 cm in length.

FIG. 3c. Kanab North breccia pipe. Development of an underground mine will soon begin within this pipe. Note: (1) the block of red Moenkopi Sandstone (marked with an 'x') that has been down-dropped 225 m into the pipe, and (2) the typical amphitheater style of erosion characteristic of breccia pipes.

border; the flurry of mining ventures, including the Hack Canyon mines, during the early 1980's has brought prominence to the Arizona Strip. Additional pipes undoubtedly exist along the southern margin of the Colorado Plateau, but for the most part are buried beneath the lavas of the San Francisco volcanic field. It is not likely that the pipes extend to the east where the Redwall Limestone thins to zero, between Holbrook and the Four Corners area (McKee and Gutschick (6), p.3), unless the Devonian Martin Formation or Cambrian Muav Limestone have developed an adequate karst for breccia pipes development, which the Muav Limestone has not done where it is exposed in the Western Grand Canyon. Thus, it is possible that pipes extend unrecognized eastward across Arizona, buried beneath the upper Mesozoic sediments.

Pipes located on the eastern edge of the study (Fig. 2) are collared in strata ranging from Permian Kaibab Limestone through the Triassic Chinle Formation; in contrast, pipes on the western edge located along the Grand Wash Cliffs of the Hualapai Plateau, top-out, because of erosion, in the Redwall Limestone or lowermost Supai Group. This latter situation does not provide the potential volume of mineralized rock (at most 175 m of vertical extent) available to the east, where pipes may extend upward as much as 1,000 m between the Mississippian and Triassic rocks.

2. MINING HISTORY

Breccia pipes of northern Arizona were first exploited during the 19th century by miners using burros to transport the ore out of the deep canyons; at this time essentially all ore produced was for copper. By the 1950's the list of named mines included (Fig. 2): The Orphan, Grandview, Riverview, Ridenour, Grand Gulch, Savannic, Cunningham, Copper Mountain, Copper House, Old Bonnie Tunnel, Snyder, and the Hack Canyon Mines. It was not until the 1950's that some of these mines were recognized to contain uranium mineralized rock. Each of these mines is in a breccia pipe with a similar trace-element geochemical signature of the mineralized rock. Each also shows the structural features known to be associated with breccia pipes (Fig. 3a), although the host rock varies from the Mississippian Redwall Limestone (Grandview Mine) up to the Triassic Moenkopi Formation (Riverview Mine). Metals produced from one or more pipes during the past century include Cu, U, Ag, Au, Pb, and Zn (Foord et al. (7)). Uranium ore (Fig. 3b) from mines within these pipes is exceptionally high grade and very similar from pipe to pipe; ore from the Orphan Mine averaged between 0.30 and 0.60 % U_3O_8 (Pierce et al. (8)) and some fist-size samples contained as much as 55 % U_3O_8 (Gornitz et al. (9)). Over 1,800 metric tons of U_3O_8 were removed from the Orphan Mine before it was closed in 1969; apparently 'large amounts of ore' still remain in the mine as the owner has been considering reactivation of the mine (O'Neill et al. (10)). Surface samples from the Riverview Mine yield over 2 % U_3O_8 (unpublished data, Wenrich and Sutphin, 1981). At present the only mines in production are the Hack I (Fig. 3a), II, and III (adjacent to the old Hack Canyon Mine), with the new Pidgeon Mine in the final stage of development and the Kanab North Pipe (Fig. 3c) soon to begin development. These mineralized pipes have reserves similar to the Orphan Mine. Several other targets are in the exploration stage with grade in excess of 0.5 % U_3O_8. These mines have been operated essentially for their uranium content, although silver could be a viable by-product; the Orphan mine produced 81,000 oz of Ag during 1963 through 1966 (USGS file material). Analyses of uranium-mineralized rock from breccia pipes throughout the Grand Canyon region routinely yield silver concentrations of 10 to 100 ppm, with samples containing as much as 1,150 ppm (35 ounces/ton) (unpublished data, Wenrich, 1981-1983). At present silver is not being recovered from the Hack Canyon ore because of mill design. Also present in significant quantities, but not economic in today's market, are Co, Cu, Ni, Pb, and Zn.

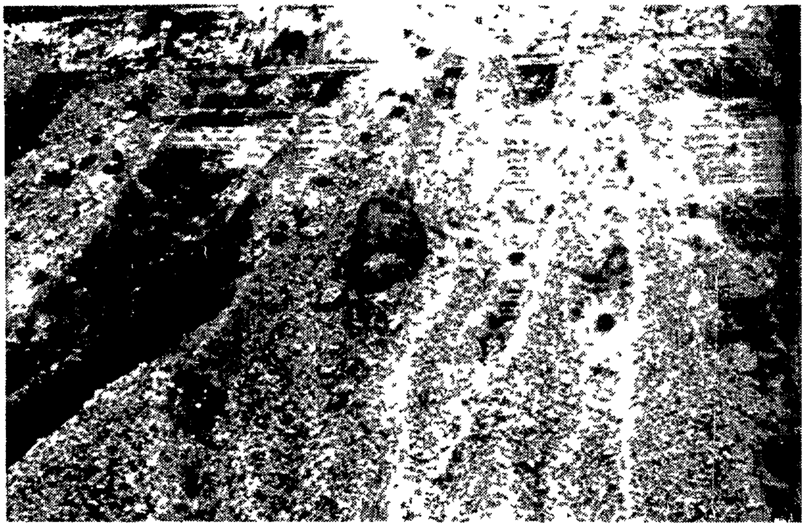

FIG. 4a. Breccia pipe exposed in the Hermit Shale. Note the bleaching of the Hermit adjacent to the resistant pinnacle of breccia. Pipes exposed along the canyons, such as this one just north of the Colorado River, are easy to recognize because of their vertical sides.

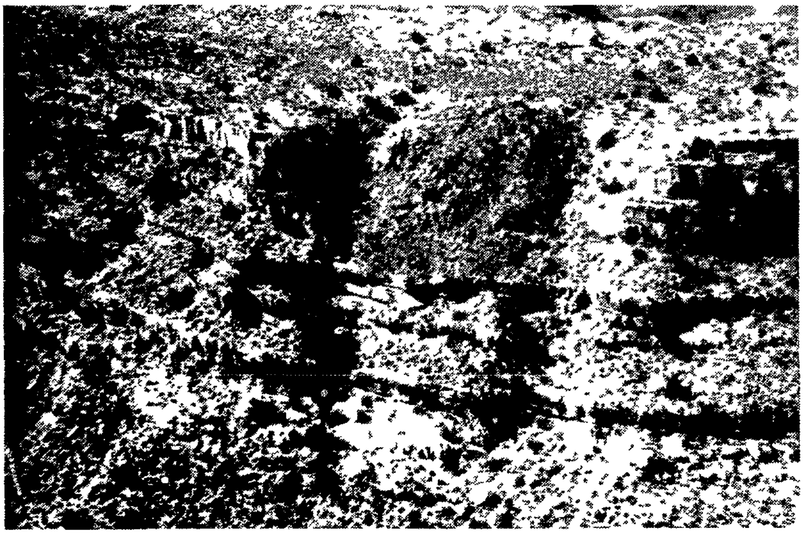

FIG. 4b. Many pipes are expressed on the surface as a small plug of limonite stained breccia surrounded by a ring fracture representing the margin of the pipe. Note the bleaching of the undeformed country rock.

FIG. 4c. The Grand Pipe is located just north of the Colorado River near the western edge of the Colorado Plateau, and is one of many shallow structural basins (note the inward dipping beds) on plateaus thought to be surface expressions of the upper parts of breccia pipes. The pipe is about 0.7 km in diameter - this is one of the largest in northern Arizona.

3. FIELD RECOGNITION OF BRECCIA PIPES

Although breccia pipes are easily recognized within canyons where their third dimension is exposed (Fig. 4a), large expanses of northern Arizona are comprised of undissected high plateaus. Recognition of pipes in these areas is particularly important because mining access to the plateaus is significantly better than in the canyons. In addition, pipes exposed in canyon walls have commonly lost much of their rock, including mineralized rock, to erosion. Some pipes are obvious on the surface where a central plug of limonite-stained breccia is encircled by a ring fracture (Fig. 4b). Shallow structural basins, delineated by inward tilted beds, representing the upper part of the pipe, are thought to be surface expressions of breccia pipes on the adjacent plateaus (Fig. 4c). This assumption is supported by the occasional exposure of a breccia pipe in a canyon wall with a shallow structural basin lying directly above on the plateau surface (Fig. 5).

FIG. 5. Photograph of a pipe exposed in a canyon wall and also as a structural basin on the overlying plateau. Such examples support the assumption that shallow structural basins are probably surface manifestations of breccia pipes.

Mapping of collapse features as breccia pipes on the high plateaus is complicated by the karst development in the Kaibab Limestone and collapses formed by solution of gypsum in the underlying Toroweap Formation, and the Harrisburg Member of the Kaibab Limestone. It has generally been assumed that collapse features resembling ordinary sink holes, that is, with vertical walls, no tilted beds, and a flat-bottomed hole containing uncemented rubble, are recent karst development. In contrast, collapse features with tilted beds, brecciation and alteration have been assumed to be good candidates for breccia pipes. Unfortunately, recent evidence indicates that these collapses may not necessarily have breccia pipes beneath them, suggesting that geochemical and geophysical exploration techniques should be used before drilling.

Nevertheless, detailed mapping of all such collapse features is necessary because the pipes are not sufficiently understood to allow a good visual distinction of breccia pipes from more recent karst development. In addition, it is possible that all the mineralizing fluids required for ore formation was a conduit and brecciated rock. The decrease in confining pressure encountered by the mineralizing fluids when entering the conduit of brecciated rock may remove CO_2 from solution. This could be a significant contribution to uranium precipitation if uranium was transported as a bicarbonate or carbonate complex. This is a possibility because abundant calcite is associated with mineralized pipes. It is remotely possible that a mineralized breccia needs not to be a pipe extending all the way down to the Redwall; even brecciation resulting from Kaibab or Toroweap solutioning could host mineralization. Nevertheless, field evidence does not support this. Hence, until the extent and genesis of the mineralizing fluids is understood it is essential for breccia pipe exploration that all collapse features be mapped and distinguished by any different geologic characteristics.

Collapse features occur in moderate concentration across northwestern Arizona. A detailed map (Fig. 6) of those located on the Marble Plateau provides a good example of their density when mapped in detail (dashed line surrounds the area mapped in detail). This density is not unique to the Marble Plateau, but extends westward where a similar concentration has been mapped on the Hualapai Indian Reservation (Wenrich (11)). Over 250 collapse features have been added in the last two years to those mapped by Huntoon et al. (3), (4) and Billingsley and Huntoon (5) on the Hualapai Reservation. Detailed recognition criteria for collapse features are discussed in Wenrich (12); Fig. 6 shows collapse features, defined as areas with:

(i) concentrically-inward dipping beds,

(ii) circular patches of brecciated rock,

(iii) circular outcrops of bleached or heavily limonite-stained rock,

(iv) circular topography and/or

(v) circular vegetation changes.

In most collapses shown on Fig. 6 more than one of the criteria are present. Sink holes are not included. Two exploration problems are apparent when breccia pipes are mapped: first, collapse features are extremely difficult to recognize in densely wooded areas, and second, mineralized rock is more readily located when the third dimension of the pipe is exposed along canyon walls.

4. MINERALIZATION OF THE BRECCIA PIPES

Dissolution of the Redwall Limestone began during Mississippian time, creating an extensive karst terrain. The Pennsylvanian Supai Formation was deposited onto this terrain, sometimes into channels as deep as 100 m (Billingsley (13)). Because the breccia pipes include strata up through the Triassic Chinle Formation, it is probably safe to assume that the karst development in the Redwall, and hence breccia pipe formation, continued until, or at least occured again, in the Triassic. Mineralization most likely occurred subsequent to this time; uraninite (Fig. 7a and 7b) assumed to be primary ore, occurs within the Triassic Moenkopi Formation at the Riverview Mine. No pipes have been observed to extend into rocks younger than the Chinle Formation. A minimum age of 141 Ma was determined for uranium mineralization in the Orphan Mine by U/Pb dating (Gornitz et al. (9)). Preliminary U/Pb isotope data for samples from the Hack breccia pipes suggest a main period of mineralization at about 200 Ma ago (Ludwig, 1983, oral commun.). Such an age is in agreement with the geology: mineralized rock has been observed through the Triassic strata, but never into Jurassic rock.

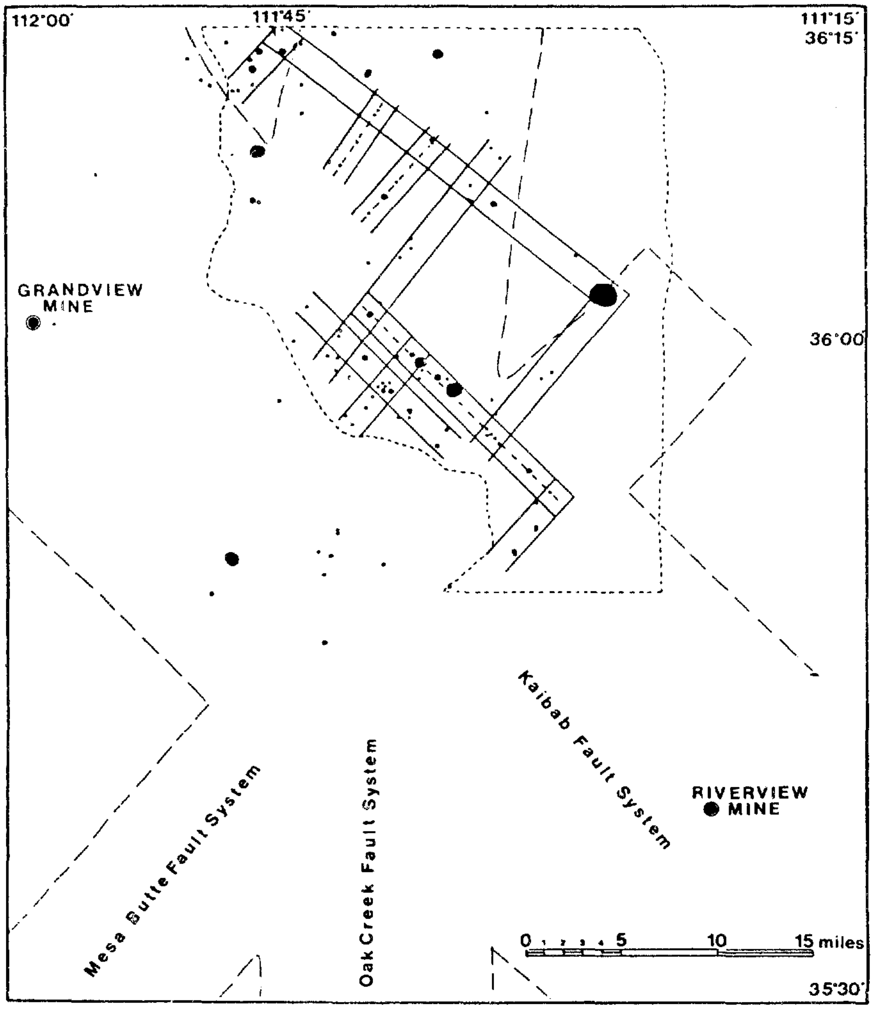

FIG. 6. The occurrence of breccia pipes located on the Marble Plateau appears to be controlled by NW- and NE-trending zones apparently related to basement structures. Within this area, outlined by a dashed line, 78 of the 94 (83 %) collapse features fall within these zones that cover only 23 % of the total surface area (Sutphin et al. (16)). This is an example of the density of collapse features in northern Arizona (only the area outlined by the dashed line is mapped in detail).

The alteration of the rock surrounding the breccia pipes in some cases facilitates recognition of the pipes. Bleaching of the host formation is normally the most conspicuous alteration, particularly where the host is a red-bed member of the Supai, Hermit or Moenkopi Formations (Fig. 4b). Minor silicification occurs in some pipes, producing erosional pinnacles (Fig. 8a).

Surface expression of pipe mineralization is generally restricted to supergene copper minerals, minor increases in gamma radiation, barite, calcite, goethite, and more rarely pyrite or marcasite, commonly located along the ring fracture of the pipe. In some places the Fe mobilization has been sufficiently extensive to form well-developed Liesegang banding. The greatest concentrations of gamma radiation commonly occur in comminuted rock or in fracture zones. Most pipes which have been mineralized by economic grades of uranium contain a 'pyrite cap'; hence the presence of goethite on the surface is deemed a good pathfinder for mineralized pipes. The goethite is an oxidation alteration of the pyrite and/or marcasite. Goethite occurs as:

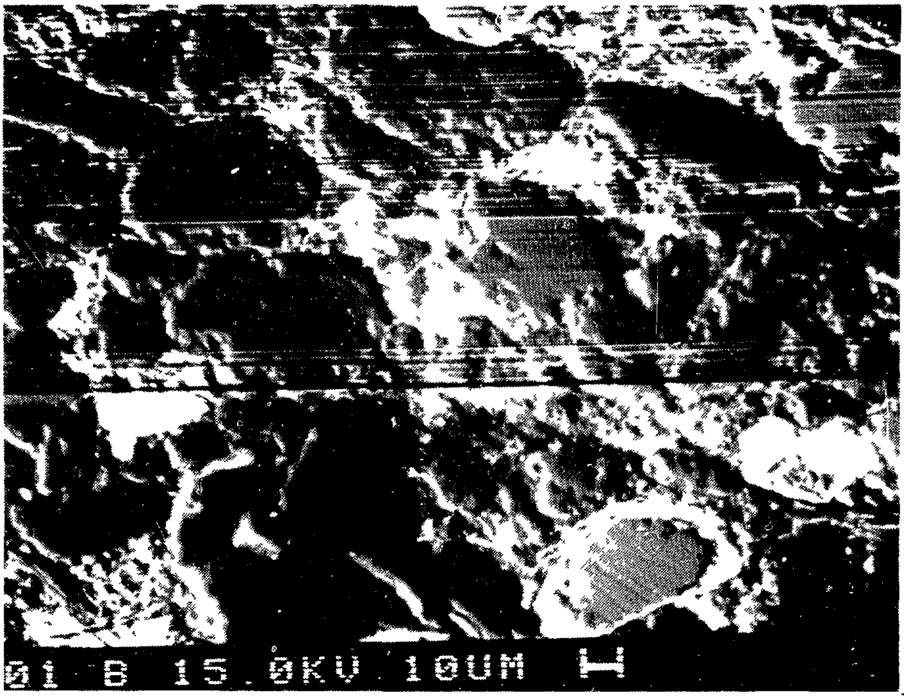

FIG. 7a. Backscattered-electron image, from an electron microscope, of a fine-grained sandstone containing 1.4 % U from the Riverview Mine. The higher the atomic number of the elements within each phase, the lighter the image tone.

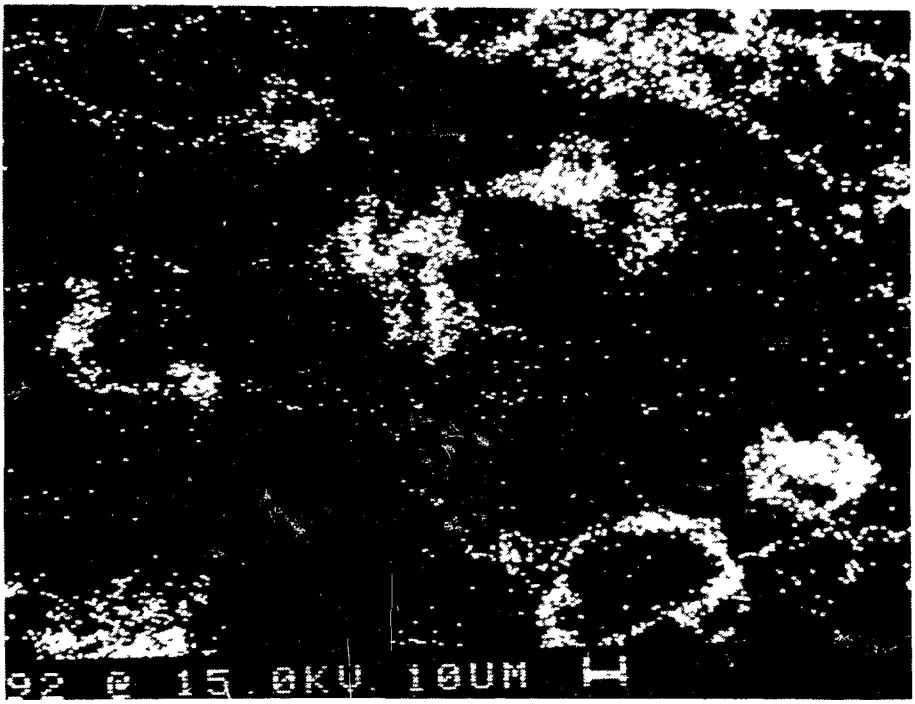

FIG. 7b. Uranium X-ray map of the same area as Fig. 7a. The uranium (represented by the white dots) is present as uraninite, in some places surrounding detrital apatite grains.

(i) pseudomorphs after pyrite cubes,

(ii) concretions which range from being totally goethite to some that are almost entirely pyrite,

(iii) botryoidal masses, and

(iv) boxwork fracture fillings.

The pyrite occasionally occurs as framboids associated with covellite.

Copper mineralization at the surface of pipes commonly occurs as supergene minerals such as malachite, brochantite, chrysocolla, and azurite. Where less oxidized zones are exposed, nodules rich in the copper sulfides, bornite, chalcocite, covellite, chalcopyrite, enargite, tennantite, digenite and djurleite can be seen (Fig. 8b). In relatively unoxidized samples, primarily collected from mines or drill core, galena, and sphalerite are common. Other potential ore minerals reported by Kofford (14) and Gornitz and Kerr (9) are molybdenite, skutterudite, siegenite, bravoite, rammelsbergite, niccolite, and arsenopyrite. Both uranium and copper minerals commonly occur on the surface associated with goethite/pyrite concretions; these perhaps represent the remains of the pyrite cap associated with the uranium ore in unoxidized mineralized pipes. Microprobe analyses indicate that most uranium is present as uraninite. Some uraninite surrounds apatite grains (Fig. 7b).

The geologic and geochemical controls on the mineralization of these breccia pipes are poorly understood at present. There is little doubt that the pipe location is controlled by northwest and northeast trending fracture zones (Sutphin et al. (15), Sutphin and Wenrich (16)); nevertheless insufficient detailed mapping of mineralized breccia pipes is available to determine specific controls on those which are mineralized. It is known, however, that those pipes which are mineralized occur in clusters, as do the pipes themselves. This is perhaps suggestive that the fluids used Redwall Limestone cavern systems as channelways, moving into those pipes connected by one cavern. This grouping is especially obvious in the area of Hack Canyon where the Hack I, II, III, and Old Hack Canyon Mines (four separate pipes) all occur within a square mile of each other. Another interesting group of mineralized pipes can be seen in the Bat Cave Tower area, in the northwestern corner of the Hualapai Reservation. These are essentially the only mineralized pipes on the Hualapai Plateau; they all appear to be spatially associated with the Surprise Canyon Formation, a Mississippian deposit of organic-rich shales, sandstones, and conglomerates, recently recognized by Billingsley and Beus (17), filling ancient channels cut into the Redwall Limestone during the Mississippian. This once again suggests control of mineralization by the Redwall Limestone, which caps the Hualapai Plateau. The organic-rich Surprise Canyon Formation may provide one of the only reductants available on the Hualapai Plateau to precipitate uranium; interestingly though, there are no visible copper minerals associated with these pipes on the Hualapai Plateau.

5. GEOCHEMISTRY

An extensive anomalous suite of elements is anomalously concentrated in mineralized rock within the breccia pipes. Silver, As, Ba, Cd, Co, Cr, Cs, Cu, Hg, Mo, Ni, Pb, Sb, Se, Sr, V, Zn and some of the rare-earth elements are consistently enriched in mineralized samples regardless of whether they are from pipes having minor anomalous radiation exposed on the surface, or whether they are from mines within the breccia pipes.

Histograms (Fig. 9a - 9f) plotted for individual samples illustrate which elements are enriched or depleted in these pipes, relative to average crustal

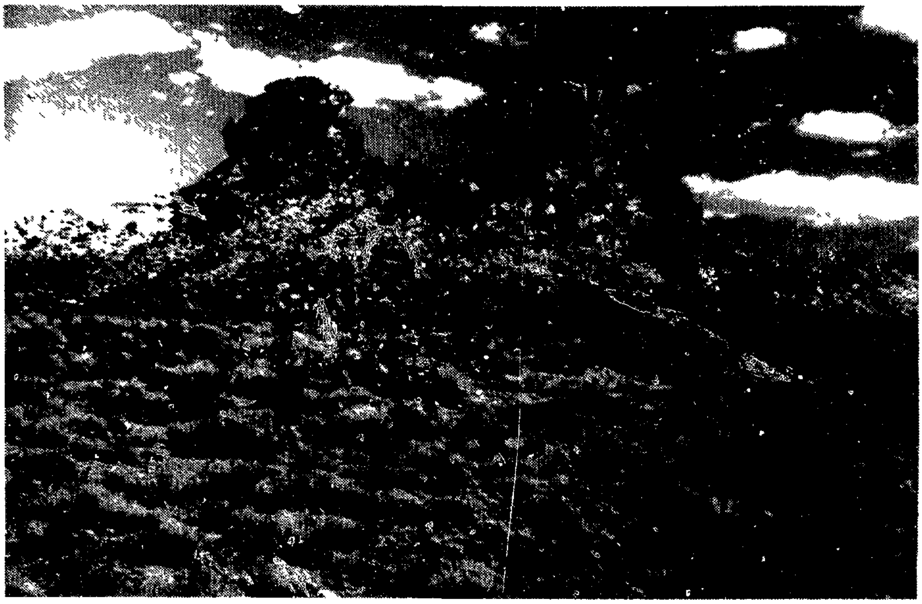

FIG. 8a. Silicified pinnacles of breccia on the Marble Plateau. This collapse occurs within the Chinle Formation and these pinnacles, located along the margin of the collapse, were referred to by Barrington and Kerr (24) as silica plugs, but were not considered by them to be a part of the collapse. They are part of the collapse, and were probably produced by increased silica movement along the ring fracture.

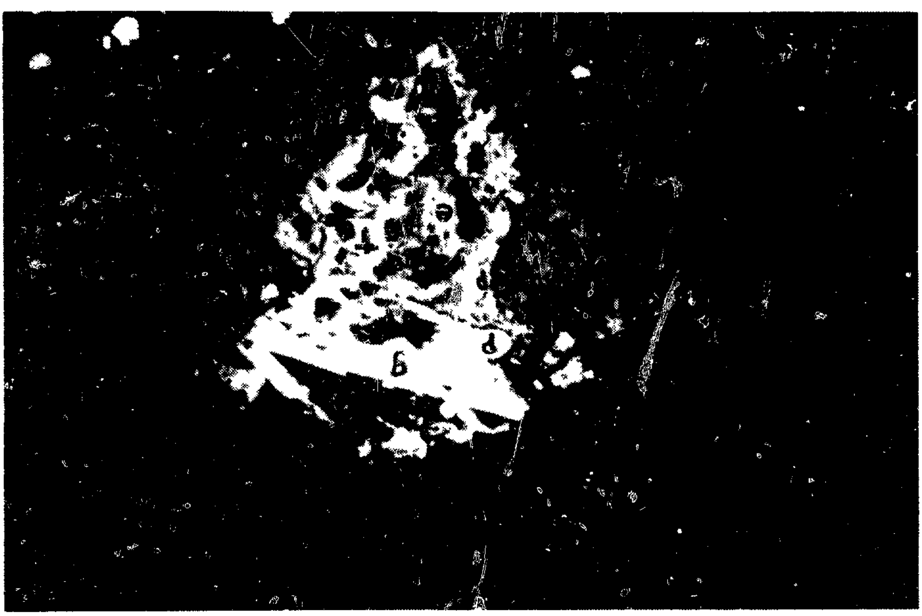

FIG. 8b. Reflected light photomicrograph showing the association of galena(g), sphalerite (s), pyrite (p), tennantite (t), and enargite (e).

TABLE I. GEOCHEMICAL DATA FOR MINERALIZED BRECCIA PIPES IN NORTHERN ARIZONA (30 SAMPLES FROM 22 PIPES). ELEMENTS ARE LISTED IN DECREASING ORDER OF ENRICHMENT. DATA BELOW THE DETECTION LIMIT WERE REPLACED WITH THREE-FOURTHS OF THE DETECTION LIMIT VALUE FOR CALCULATING THE AVERAGE CONCENTRATION (ALL VALUES IN PPM EXCEPT WHERE INDICATED).

SAMPLES > AVERAGE CRUSTAL ABUNDANCE	MAXIMUM CONCENTRATION	MINIMUM CONCENTRATION	AVERAGE
Cu	150,000	3	32,000
As	14,000	9	2,730
Se	905	0.1*	77
Mo	2,000	5	249
U	16,600	11.4	2,488
Ag	170	2*	44.6
Co	266	0.7	71.8
Zn	17,000	20*	1,672
Pb	6,300	4*	863
Ni	1,100	2*	134
Cd	180	4*	42
Ta	120	0.6	48
Sb	103	1.9	39
V	40,000	2*	1,377
Hg	3.5	0.03	0.58
Si	28.3 %	0.01 %*	2.23 %
Fe	47 %	0.32 %	9.48 %
Be	14	2*	5.2
Th	52	4.5	237
Nb	26	4	9.8
Cs	170	1	17.4
Ba	5,100	7	762

* DETECTION LIMIT FOR THAT ELEMENT

abundance for the respective rock type. The element concentrations were divided by the average crustal abundance for that element (Turekian and Wedepohl (18)) in sandstone or limestone, whichever was the host for the respective sample. Each bar on the histograms represents an individual sample. The samples are in the same order for each element. Table I lists the elements in order of enrichment and shows the maximum, minimum, and average concentration for each element from the suite of 30 samples (22 pipes). The elements are divided into groups of chemically similar elements and arranged in increasing atomic number.

It is interesting that, although there are no consistent trends, the elements which are the most enriched are the heavier elements in each group; this is particularly pronounced among the 3-d transition metals (Fig. 9c). The alkalies and alkaline earths also leave a similar, but not as pronounced, signature (Fig. 9a and 9b).

Some Th as well as rare-earth elements were transported by the mineralizing fluids, but apparently not to the extent that U was. In some pipes, such as the Ridenour Mine, the rare-earth elements are so enriched that neutron activation analysis is not necessary. In these pipes, they are present in concentrations above the detection limit for determination by induction-coupled argon plasma optical emission spectroscopy (ICP). Background samples of sandstone and limestone units in the Grand Canyon Region contain even lower rare-earth concentrations than Turekian and Wedepohl (18) averages, thus suggesting an even greater enrichment of the rare-earth elements by mineralizing fluids than shown in Fig.9f. Nevertheless, not all uranium enriched samples contain high rare-earth element concentrations; those that do, appear to be the higher-grade samples. Th is

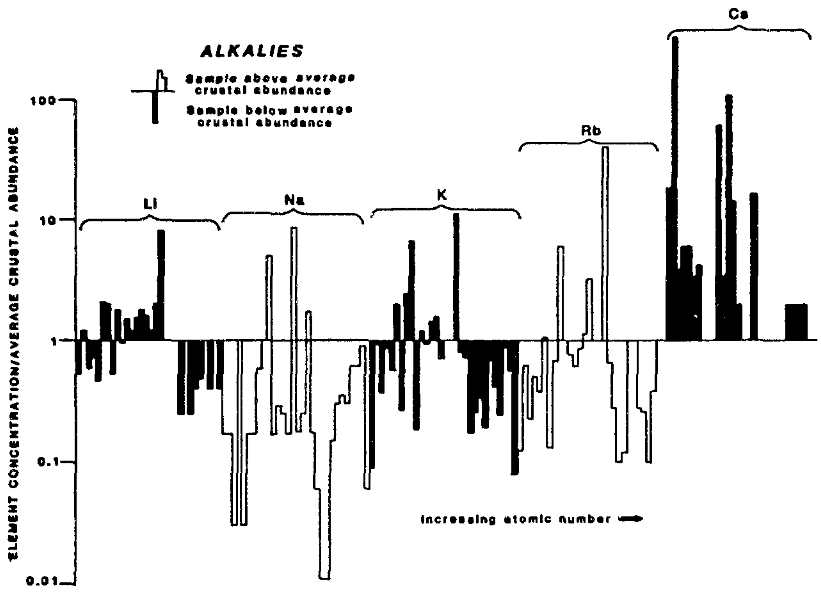

FIG. 9a

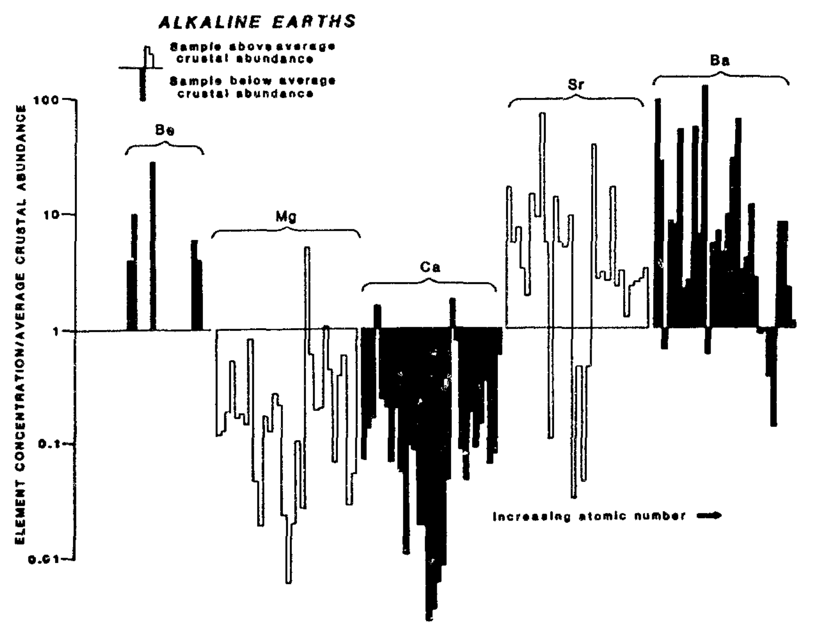

FIG. 9b

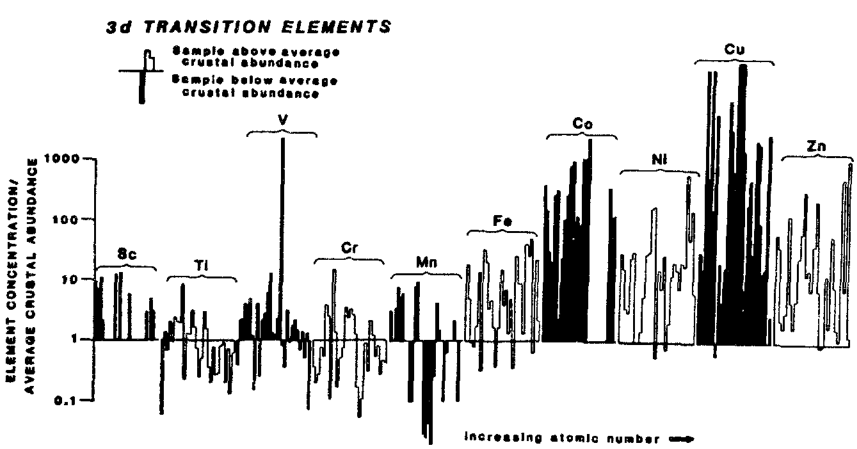

FIG. 9c

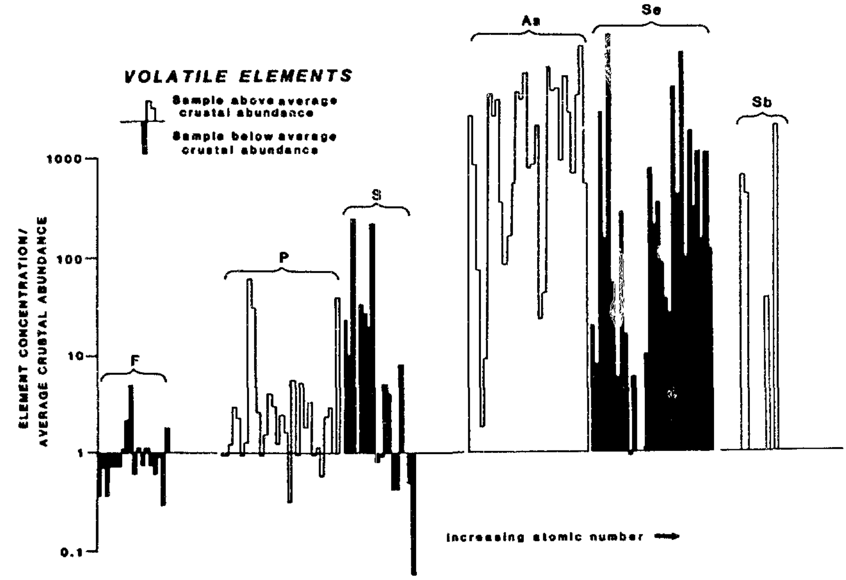

FIG. 9d

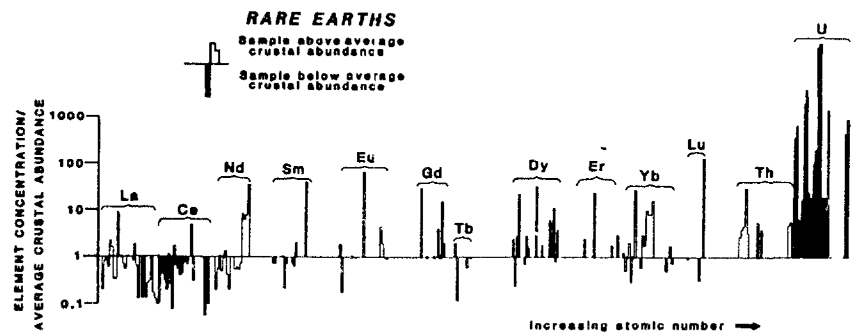

FIG. 9e

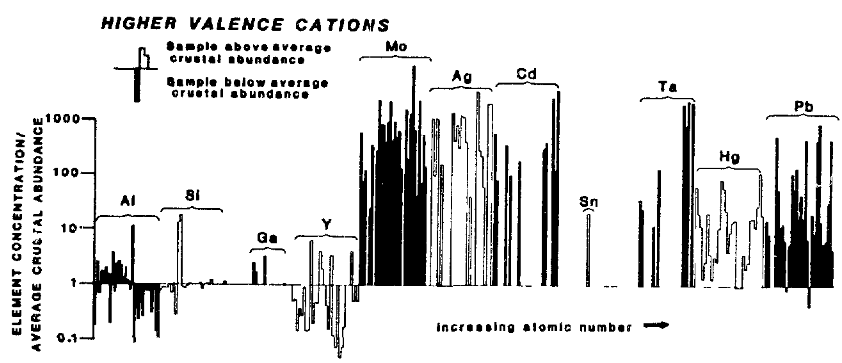

FIG. 9f

FIG. 9a - 9f. Histograms of the elements as compared to their average crustal abundance (Turekian and Wedepohl (18)). Each bar represents an individual sample collected from breccia pipes in northern Arizona. Elements are arranged in increasing atomic number. If an element was less than the detection limit and the detection limit was greater than the average crustal abundance, a bar was not plotted for that sample. This causes some elements, such as Sc and Be, to appear consistently enriched unless the graph is carefully studied because no samples will show a depletion; they will instead have no data plotted.

occasionally enriched, although Th concentrations are not high (ranging up to 52 ppm). This is particularly significant considering that the Th/U ratio is usually less than 0.5, they are significantly greater than the average crustal abundance of 1.7 ppm for sandstones and limestones.

Silver concentrations are sufficiently anomalous (Fig. 9e) to be of economic interest in some pipes, as it was in the Orphan mine (USGS file material). One nodule rich in copper sulfides contained 1,150 ppm (35 oz/ton) silver. Silver concentrations routinely exceed 4 ppm for samples collected from areas with gamma radioactivity exceeding 2.5 times background. Microprobe analyses have shown the Ag to be concentrated in the copper sulfide phases, specifically in high grade specks (perhaps inclusions of native Ag) and disseminated in tennantite, in concentrations up to 2,000 ppm. With the exception of the Copper Mountain breccia pipes, those samples highest in silver from this study have all

TABLE II. CHEMICAL COMPOSITION OF AU-RICH SAMPLES FROM THE COPPER MOUNTAIN MINE. (ALL VALUES IN PPM EXCEPT WHERE INDICATED)

SAMPLE	AU ADIT (G)	AU ADIT (F)	UPPER ADIT 44
U	405	304	10
AU	150	30	0.5
HG	50	45	300
AG	700	200	24
CU	0.37 %	0.16	1,800
PB	5,200	4,800	0.4
ZN	26 %	23	< 2
CD	1,200	1,400	< 50
W	100	50	0.63
S	0.02 %	0.21	-

yielded Au determinations of <0.05 ppm. Nevertheless, significant Au concentrations, as high as 150 ppm, have been found in the 'Au adit' of the Copper Mountain mine (Wenrich and Silberman (19)). Two radioactive samples (20 and 40 times background respectively) of brecciated, oxidized sandstone, rich in hemimorphite and smithsonite, from this adit, and another sample of hematite, malachite, and chalcocite impregnated sandstone from a higher level adit contained high concentrations (Table II) of Au, Hg, Cd, and W along with many elements commonly anomalous in mineralized breccia pipes from northern Arizona: Ag, As, Co, Cu, Mo, Ni and Pb.

Preliminary oxygen isotope ratio data for detrital quartz in the Copper Mountain Pipe suggest that samples strongly mineralized with Au and Ag have $\delta^{18}O$ 0.9 to 1.5‰ lighter than non or less mineralized samples. The strongly developed epithermal suite (Au, Ag, Hg, Cd, and As) and ^{18}O depletion of originally detrital quartz is suggestive of at least moderately high temperature hydrothermal fluids involved in the mineralization of the Copper Mountain system.

In addition to Ag those elements which are strongly enriched in radioactive samples are As, Pb and Zn (Fig. 9c, 9d, 9e). These elements make excellent pathfinders for mineralized breccia pipes. Many of the other elements discussed above are routinely enriched in mineralized pipes and are commonly useful as geochemical indicators.

The organic carbon content of some of the breccia pipes, particularly those in the Chinle and Moenkopi formations, is moderately high (averaging about 0.30 %) as compared to average sandstones and limestones, particularly in those samples containing framboidal pyrite. The presence of framboidal pyrite may suggest that biogenic processes acted as the reductant for the formation of pyrite and perhaps likewise the uraninite, as areas of increased radioactivity are usually in relatively close association with pyrite.

A strong depletion in Ca, Mg, and Na seems to occur in the uranium mineralized zones, whereas there is a strong enrichment in Sr, Ba, and Cs (Fig. 7a and 7b). O'Neil et al. (20) have shown that in an epithermal mineralizing system formed by the interaction of a cooling shallow intrusion and local meteoric water, the altered rocks are depleted in Na, Ca, and Mg, and enriched in K and Rb. Ba is frequently enriched in epithermal hydrothermal systems. Although there is no significant enrichment in K and Rb the breccia pipes are not depleted in these elements to the extent that Na, Ca, and Mg are. Furthermore, even though Cs is known to concentrate in clays from ground water, its concentration is orders of magnitude higher in thermal waters than in ground water; rocks altered by hydrothermal fluids in Yellowstone National Park are enriched in Cs (Keith et al. (21)). A Cs-rich analogue of carnotite, margaritasite, has been shown to form from 200°C temperature waters (Wenrich et al. (22)). In contrast, a fluid-inclusion filling temperature of calcite from the Orphan Mine was determined to be 60 to 110°C (Gornitz and Kerr (9)).

Rocks from surficial (oxidized) radioactive zones are somewhat in isotopic disequilibrium. For a given grade of material, the U concentrations are not as high as would be expected from the equivalent U values determined from gamma-ray measurements. Apparently, the oxidized surface exposures are enriched in the gamma-emitting daughter products, perhaps Ra. The K and Th contributions to the gamma radioactivity in the breccia pipes is minor in contrast to the U (Pitkin, 1983, oral commun.).

6. GENESIS OF THE BRECCIA PIPES AND MINERALIZING FLUIDS

The origin of the mineralizing fluids for the breccia pipes of northern Arizona is not as well understood as the origin of the breccia pipes themselves. It was first suggested by Kofford (14) that these pipes were diatremes; because there is no evidence for associated igneous activity Gabelman (23) proposed a cryprovolcanic explosion which did not reach the surface. Nevertheless, there appears to be little doubt at present that the pipes formed by solution collapse within the Redwall Limestone and stoping of the overlying strata; this collapse mechanism was first proposed by Bowles (2).

Theories for the source of the mineralizing fluids are more numerous and less understood:

(i) Kofford (14) believed the mineralization formed by 'telescoped hydrothermal deposition' followed by 'post-deposition mobilization and enrichment, mainly through bacteriologic processes'.

(ii) Gornitz et al. (9) also believed the origin was hydrothermal, but they suggested that a direct unmixed magmatic source is improbable.

(iii) Bowles (2) believed that a mixing of waters was important but that neither water was hydrothermal. 'Ground water carrying high-valence Cu and U ions then entered the pipe from the lower sandstone aquifers of the Supai. Mixing of the ground water in the pipe with ground water from aquifers in the Supai caused Fe, Cu, and U ions to be reduced, and pyrite, chalcopyrite, and uraninite were precipitated in the pipe above the point of recharge by aquifers in the Supai.'

(iv) O'Neil et al. (10) believed the ore deposits formed by the mixing of three compositionally different ground-water solutions. 'The breccia pipes constituted conduits through which differing solutions could flow; oxidizing, uranium-bearing ground water from the upper Supai Group thereby mixed with reducing ground water from the Redwall Limestone'.

It is possible that the uranium mineralizing fluids were heated ground waters in the temperature range of 60 - 110°C (Gornitz and Kerr (9)). The source for the uranium may have been the volcanic rocks associated with the Mogollon Highlands to the south, which were uplifted during the Triassic and remained elevated until the Late Eocene. This would coincide with the U/Pb age determination for uraninite of 200 Ma. These fluids then moved through an aquifer, such as the Supai Formation, Coconino Sandstone, or Chinle Formation, to northern Arizona. Although the Chinle Formation is considered a favourable source for the uranium by many geologists it was not considered highly probable during this study because those non-pipe uranium deposits occurring in the Chinle are generally not as enriched in most metals as other formations lower in the breccia pipe. In addition, if the waters descended from the Chinle Formation it might be reasonable to expect those collapse features which bottom in the Kaibab Limestone or Toroweap Formation to also be mineralized and they are not. Oxygen isotope studies are in progress to determine whether the fluids traveled up or down the pipes.

The Precambrian basement cannot presently be ruled out as a source for the uranium, although Pb isotopes (Ludwig, 1983, personal commun.) suggest it was not. Nevertheless, the Precambrian is an appealing source because the pipes are definitely controlled by northeast- and northwest-trending basement structures (Fig. 6) which enhanced dissolution of the Redwall Limestone along these zones of weakness. In addition, the mineralized pipes occur in localized groups suggesting some control of the fluids by local cavern systems of the Redwall Limestone. Thus, any model for the source of the fluids must provide for more than random movement of waters from an aquifer into pipes. The fluids apparently were controlled by the cavern system and may have used it as a channelway.

The large suite of associated elements and particularly the Au found at the Copper Mountain pipe suggest multiple stages of mineralization. It appears that the Au mineralization occurred at considerably over 100°C, which places it as a separate mineralizing event from that of the uranium. It is possible that some of the other elements, such as Pb and Zn, may have been from a third mineralizing episode.

Although much isotopic and fluid-inclusion filling temperature data are still needed to determine the origin of these mineralizing fluids for the breccia pipes, it can certainly be stated that they are not typical ground water Colorado Plateau uranium deposits. The depletion and enrichment of alkalies and alkaline earths are similar to that of epithermal systems, yet the degree of silicification is not. Although some silicification within the central core of the pipes does result in resistant pinnacles (Fig. 8a), the rock rarely resembles the silicified breccia associated with epithermal systems. Nevertheless, it is difficult to imagine this suite of anomalous trace elements, which includes some of the relatively immobile (in low temperature ground water) rare earths and Th, as well as such classic epithermal elements as As, Sb, Ag, and Au, forming solely from a low temperature source.

ACKNOWLEDGEMENTS

This research was supported by the U.S. Bureau of Indian Affairs and the Hualapai Indian Tribe. Much of this study was completed with the excellent field assistance of Hoyt B. Sutphin. Data compilations were made by George M. Bedinger and Stephen P. Schwarz. Suggestions made by Miles L. Silberman, Ken Ludwig and Gil Bowles are greatly appreciated.

REFERENCES

(1) BOWLES, C.G., Economic implications of a new hypothesis of origin of uranium- and copper-bearing breccia pipes, Grand Canyon, Arizona, *in:* J. Campbell (editor), Short Papers of the U.S. Geol. Survey Uranium and Thorium Symposium 1977, U.S. Geol. Survey Circular 753 (1977) 25-27.

(2) BOWLES, C.G., Uranium-bearing pipe formed by solution and collapse of limestone, U.S. Geol. Survey Professional Paper 525-A (1965) 25-27.

(3) HUNTOON, P.W., BILLINGSLEY, G.H., Jr., CLARK, M.D., Geologic map of the Hurricane fault zone and vicinity, Western Grand Canyon, Arizona, Grand Canyon Natural History Association (1981)

(4) HUNTOON, P.W., BILLINGSLEY, G.H., Jr., CLARK, M.D., Geologic map of Lower Granite Gorge and Vicinity, Western Grand Canyon, Arizona, Grand Canyon Natural History Association (1982)

(5) BILLINGSLEY, G.H., Jr., HUNTOON, P.W., Geologic map of Vulcans Throne and Vicinity, Western Grand Canyon, Arizona, Grand Canyon Natural History Association (1983)

(6) McKEE, E.D., GUTSCHICK, R.C., History of the Redwall Limestone of Northern Arizona, Geol. Soc. America Mem. 114 (1969) 726 pp.

(7) FOORD, E.E., McKEE, E.D., BOWLES, C.G., Status of mineral resource information for the Shivwits Plateau, Parashant, Andrus and Whitmore Canyons, and Kanab Canyon areas, Grand Canyon, Arizona, U.S. Geol. Survey Administrative Report for the National Park Service (1978) 30 pp.

(8) PIERCE, H.W., KEITH, S.B., WILT, J.C., Coal, oil, natural gas, helium, and uranium in Arizona, The Arizona Bureau of Mines Bulletin 182 (1970) 289 pp.

(9) GORNITZ, V., KERR, P.F., Uranium mineralization and alteration, Orphan Mine, Grand Canyon, Arizona, Econ. Geol. 65 (1970) 751-765.

(10) O'NEIL, A.J., NYSTROM, R.J., THIEDE, D.S., National uranium resource evaluation, Williams Quadrangle, Arizona, U.S. Department of Energy Open-File Report GJQ-009 (1981) 56 pp.

(11) WENRICH, K.J., Mineralization of breccia pipes in northern Arizona, Econ. Geol. (1984) (in press).

(12) WENRICH, K.J., Exploration guides for breccia pipes in northern Arizona, GSA Bulletin (1984) (in press).

(13) BILLINGSLEY, G.H., A synopsis of stratigraphy in the Western Grand Canyon, Museum of Northern Arizona Research Paper 16 (1978) 26 pp.

(14) KOFFORD, M.E., The Orphan ore deposits, unpubl. mine report (1956).

(15) SUTPHIN, H.B., WENRICH, K.J., VERBEEK, E.R., Structural control of breccia pipes on the southern Marble Plateau, Arizona, Geol. Soc. Am. Abstr. with Programs, 15, no. 5 (1983) 376 pp.

(16) SUTPHIN, H.B., WENRICH, K.J., Structural control of breccia pipes on the southern Marble Plateau, Arizona, U.S. Geol. Survey Open-File Report 83-908, scale 50,000 (1983).

(17) BILLINGSLEY, G.H., BEUS, S.S., Surprise Canyon Formation, A Late Mississippian Rock Unit in the Grand Canyon, in: U.S. Geol. Survey Bull., Contributions to Stratigraphy (1985) (in preparation).

(18) Turekian, K.K., WEDEPOHL, K.H., Distribution of the elements in some major units of the earth's crust, Geol. Soc. Am. Bull. 72 (1961) 175-191.

(19) WENRICH, K.J., SILBERMAN, M.L., Potential precious and strategic metals as byproducts of uranium mineralized breccia pipes in northern Arizona, AAPG Abstracts with Programs, Rocky Mountain Section (1984) (in press).

(20) O'NEIL, J.R., SILBERMAN, M.L., FABBI, B.P., CHESTERMAN, C.W., Stable isotope and chemical relations during mineralization in the Bodie Mining District, Mono County, California, Econ. Geol. 68 (1973) 765-784.

(21) KEITH, T.E.C., THOMPSON, J.M., MAYS, R.E., Selective concentration of cesium in analcime during hydrothermal alteration, Yellowstone National Park, Wyoming, Geochim. et Cosmochim. Acta 47 (1982) 795-804.

(22) WENRICH, K.J., MODRESKI, P.J., ZIELINSKI, R.A., SEELEY, J.L., Margaritasite: a new mineral of hydrothermal origin from the Pena Blanca Uranium District, Mexico, Am. Mineralogist 67 (1982) 1273-1289.

(23) GABELMAN, J.W., The origin of collapsed plug pipes, Mines Mag. 47 (1975) 67-72, 79-80.

(24) BARRINGTON, J., KERR, P.F., Collapse features and silica plugs near Cameron, Arizona, Geol. Soc. Am., Bull. 74 (1963) 1237-1258.

METALLOTECTONIC CONTROL OF THE URANIUM MINERALIZATION IN VEIN-TYPE DEPOSITS OF CENTRAL IRAN (ANARAK DISTRICT)

M. R. Espahbod

Atomic Energy Organization of Iran

Tehran

Iran

Abstract

METALLOTECTONIC CONTROL OF THE URANIUM MINERALIZATION IN VEIN-TYPE DEPOSITS OF CENTRAL IRAN (ANARAK DISTRICT)

The investigated area lies in Central Iran and belongs geologically to the Central Iran Fold Belt. The Talmesi-Meskani Intermountain Basin lies within this belt and is built up by Cretaceous and Tertiary sediments and volcanics. The basin was subject to intense faulting and folding. Cu, Ni, Co, U mineralizations occur within shear and breccia zones of andesite porphyrites and trachyandesites. These volcanic rocks only serve as host as the uranium derived from late stage two mica granites which underwent intense albitization. The Talmesi and Meskani copper mines are multistage hydrothermal uranium occurrences within well developed shear and fracture zones.

1. INTRODUCTION

In the Talmesi-Meskani copper mines area uranium mineralizations occur in porphyritic andesite and trachyandesite. The uranium mineralization is associated with a relatively high K_2O content. The volcanic host rocks are of Eocene age and belong to the Shoshonitic Series. They consist of plagioclase with mafic and accessory minerals of which apatite and magnetite are predominant. The texture is porphyritic.

The investigated area in general belongs to the Central Iran Fold Belt which is part of the Mediterranean Fold Belt and is situated within the Baikalian Anarak-Khur Massif (Stocklin (1), Davoudzadeh (2)). The area is limited by the Nain-Zevar Melange Series which are Upper Cretaceous sediments with intercalated ultrabasic sequences (Alpine Ophiolitic Sutur Zone). The curvature of the Great Kavir Fault system on the western and northwestern part of the Anarak Massif, which is connected with alpine orogenic movements, represents a different style of structure.

The Talmesi-Meskani Intermountain Basin, which is the target for uranium exploration, was folded into a central syncline with anticlines on both sides. Later faulting caused the formation of horst and graben structures (Fig. 1). Folding and faulting occurred during middle and late alpine orogeny. The oldest rocks of this basin are muscovite-chlorite schists which are mostly confined to structural zones. In Early Eocene time the rocks of Cretaceous age of limestone have been intruded by andesites and trachyandesites. They are succeeded by marly sandstones of Eocene-Oligocene age and red beds of molassic character of Late Oligocene age. These units are associated with evaporites, interbedded limestones and argillaceous sandstones (Table I).

TABLE I. STRATIGRAPHY OF THE AREA AROUND THE TALMESI-MESKANI DEPOSITS (CENTRAL IRAN)

	THICKNESS	LITHOLOGY
NEOGENE		CONGLOMERATE
OLIGO-MIOCENE	> 500 M	FOSSILIFEROUS LIMESTONE
EOCENE-OLIGOCENE	> 2.000 M	EVAPORITES AND RED BEDS
EOCENE	> 2.500 M	ANDESITES, TRACHYANDESITES, CONGLOMERATES, NUMMULITIC LIMESTONES, GYPSIFEROUS MARL
PALEOCENE	> 250 M	CONGLOMERATE, KERMAN CONGLOMERATE COARSE GRAINED SANDSTONE
CRETACEOUS (UPPER)	> 500 M	ULTRABASIC ROCKS, LIMESTONE
CRETACEOUS (UPPER, MIDDLE)	> 50 M	FOSSILIFEROUS LIMESTONE, SILTSTONE, BASAL CONGLOMERATE
JURASSIC - UPPER PROTEROZOIC	> 2.000 M	METAMORPHIC SCHISTS, DOLOMITE, MARBLE

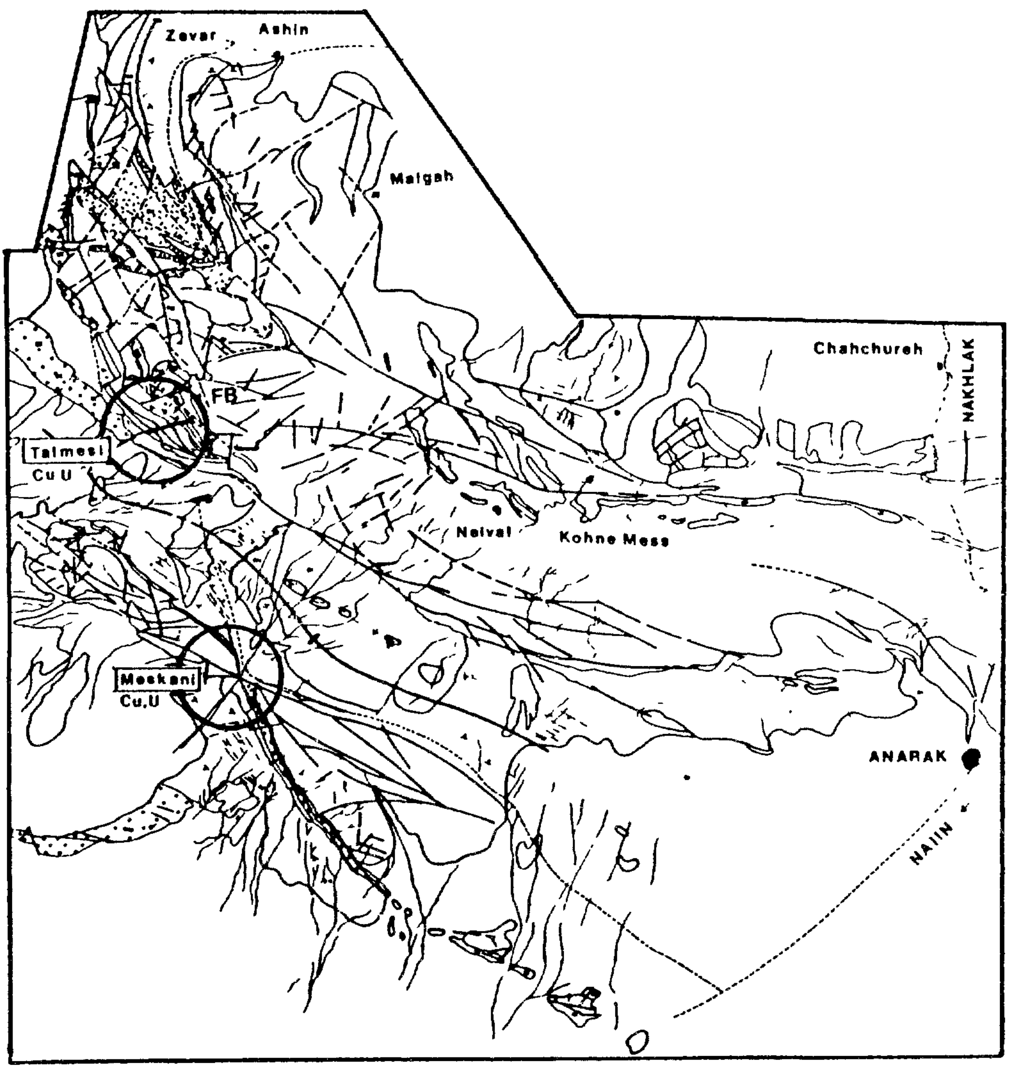

FIG. 1. Geological and tectonic pattern of the investigated area.

2. STRUCTURAL FEATURES

2.1. General

The area under consideration was subject to intense tectonic movements of alpine style, which led to large scale shear zones and structures in en echelon fashion. The main direction of these zones is NW-SE and NE-SW but trends with directions of NNW-SSE, EW and NS are also present. The whole structural pattern is characterized by a series of horst-graben. Two styles of tectonism can be recognized.

(i) faulting: major fault systems and their associated smaller faults

shearing and joining in form of rectangular cross cuttings and openings

(ii) folding: regional fold systems

diaclase and small dislocations along axial planes of folds

2.2. Major faults

These major fault systems are mostly nominal faults with NW-SE directions. In the Zevar area (northwestern part of Talmesi Mine) these are intersected by NS running faults and monoclines of the Western Great Kavir fault system (Doruneh Fault). At the Talmesi Mine Area the Talmesi main fault with its strike-slip displacement is striking N 40 W and N 60 W and runs for over several km parallel to the Meskani main fault zone.

2.3. Secondary faults

The NE-SW trending secondary faults have intersected the above mentioned main fault structures which resulted in strong brecciation of such zones. These NE trending structures are usually not normal but they are inversed faults with a general dip to the SE. For example fault FB (Fig. 1) is crossing the whole geological section of the western part of the Talmesi Mine, it is trending NE, dipping with 55° to the SE and can be recognized for about 3 km (Espahbod et al. (3)). Further west similar faults running parallel can easily be distinguished.

In the Meskani Copper Deposit, about 7 km to the SE of the Talmesi Mine the same tectonic features can be recognized. The general directions are N 20 W and N 60 W (Fig. 1). The small secondary faults, often branching out of the bigger ones, follow the same directions.

2.4. Relative ages of the fault systems

In the Anarak area the faults are the result of compressional stress, and only locally there is evidence of some tensional stress leading to open structural features.

A first tectonic phase can be recognized in the muscovite-chlorite schists and evaporitic beds of the units of Jurassic age. The main tectonic event, however, was the Laramide tectonic phase, during which the basement consisting of

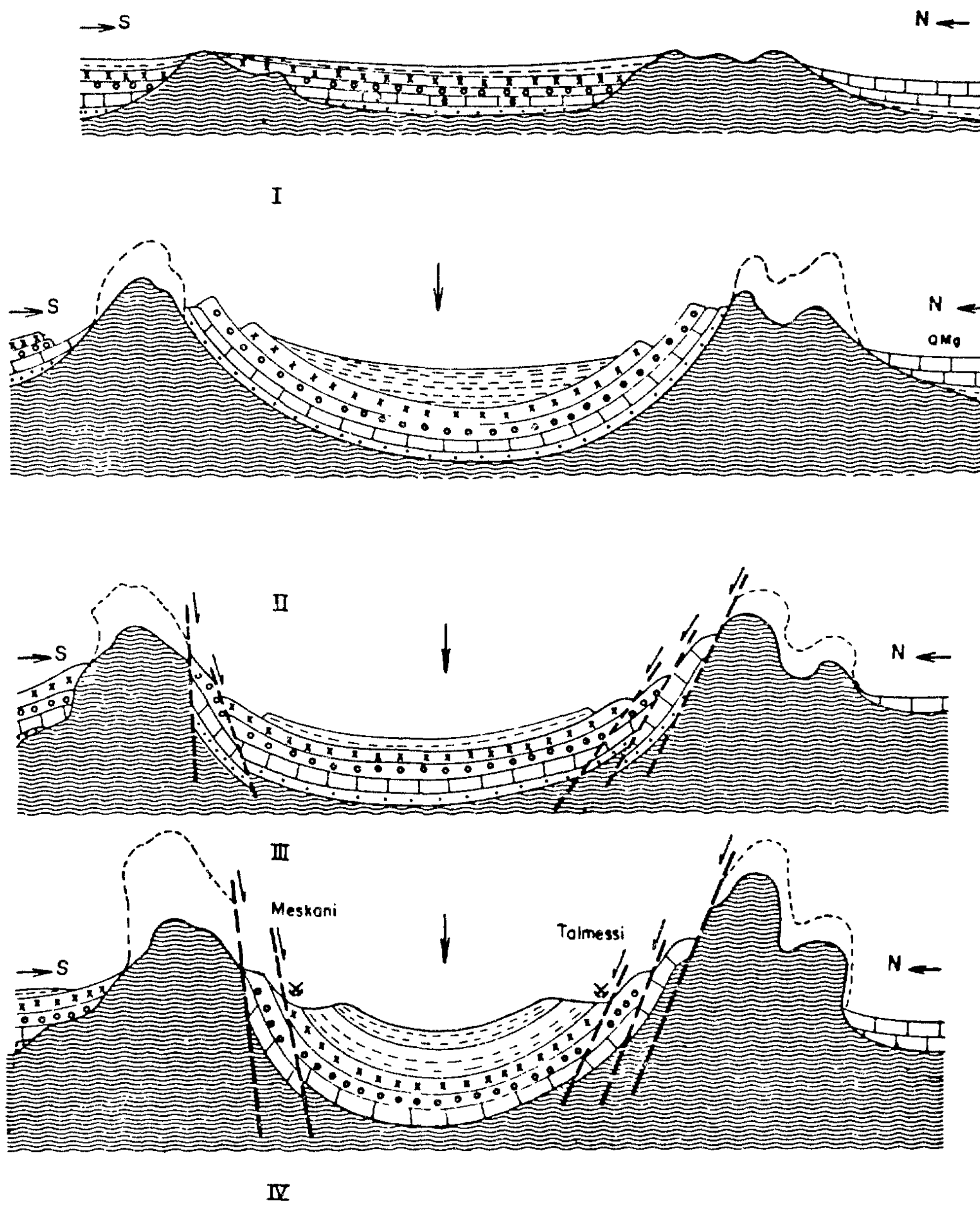

FIG. 2. Different stages of tectonic evolution in Talmesi-Meskani Basin

metamorphic schist was compressed and pushed upwards. With increasing lateral stress, the whole complex has undergone strong folding leading to the development of tight syncline and anticlines. This folding phase was then succeeded by a block faulting phase leading to the formation of horst and graben structures (Fig. 2). These tectonic events occurred from the Eocene until Late Miocene.

3. METALLOGENESIS

Andesitic porphyrites and trachyandesites of Eocene age are the main rock units outcropping in the described area. About 70 km east of the Talmesi Mine has been recognized an acidic two mica granite (Kali-Kafi Copper Mine) with a strong differentiation from granite to either granodiorite and diorite or grano-syenite and alkali syenites. Small granitic bodies of same provenience exist also a few km north of Talmesi Mine (Safiabad Deposit). The mineralization of Cu, Ni, Co, U, Hg, Bi, As, Au occurs within shear zones and breccia zones of andesite porphyrites and trachyandesites, but these rocks only serve as host rocks.

Latest results show that the mineralization especially the uranium mineralization is directly connected with the late stages of the granitic intrusions especially with the small intrusions or the formation of subvolcanic stocks. The primary uranium mineralization derived from the two mica granite, containing large amounts of zircon, apatite and titanite. Parts of these granitic rocks have undergone a strong metasomatism leading to intense albitization (Plyaskin et al. (4)). The primary mineralization of ore minerals from Cu, Pb, Mo, U, Au (like chalcopyrite, bornite, molybdenite, pitchblende, coffinite) are the result of multi-stage hydrothermal processes in connection with the formation of intrusive and extrusive bodies in the Anarak region. The locally recognized primary Ni and Co mineralization are closely related to small mafic intrusions. In the Talmesi and Meskani Copper mines also secondary minerals like native copper, nickel arsenides, autunite, metazeunerite and uranospinite can be recognized within the superficial oxidation zone.

3.1. Uranium mineralization in connection with the fracture system

As already mentioned the studied area has undergone various tectonic events. Especially the area of Talmesi-Meskani shows a concentration of faults and shear zones. Besides large scale faults there are numerous small faults, fractures and fissures, which mainly occur where regional faults intersect each other. In such

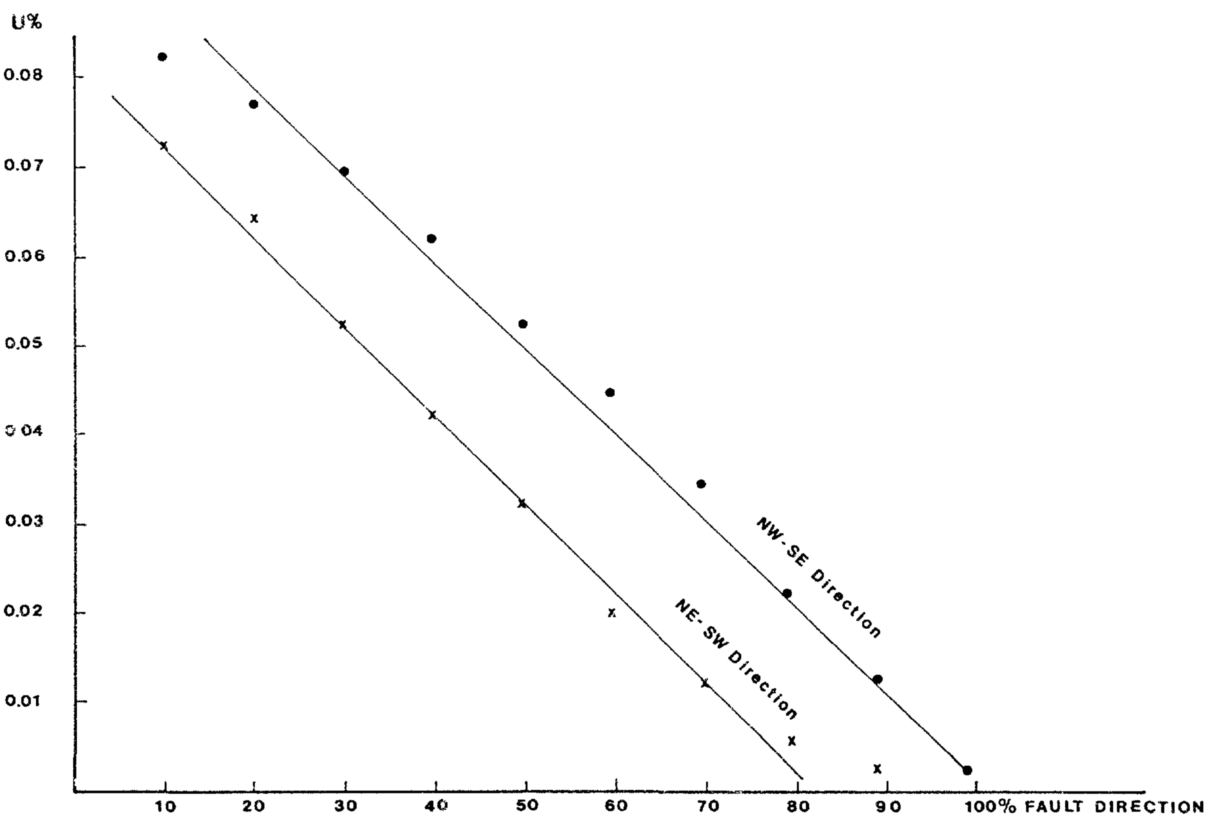

FIG. 3. Correlation between U% and faults direction in Talmesi-Meskani Deposit.

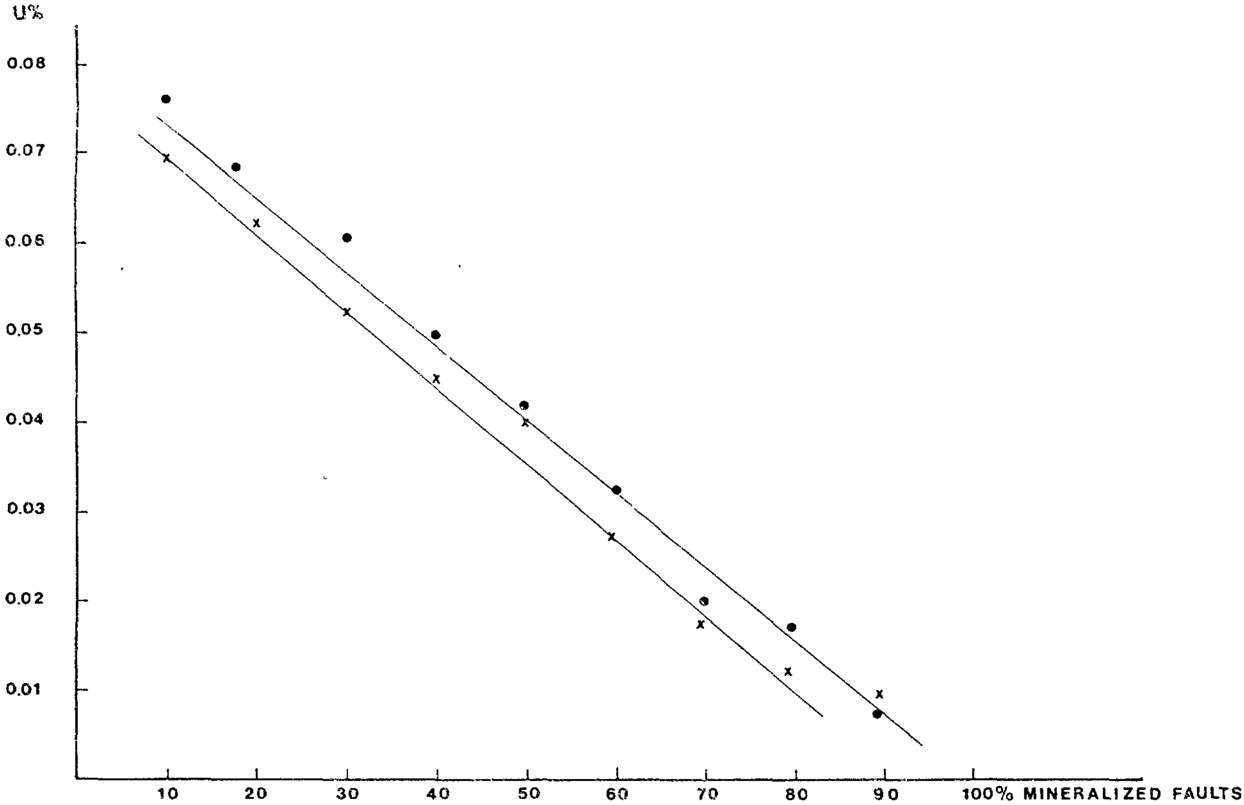

FIG. 4. Correlation between U% and mineralized faults in %.

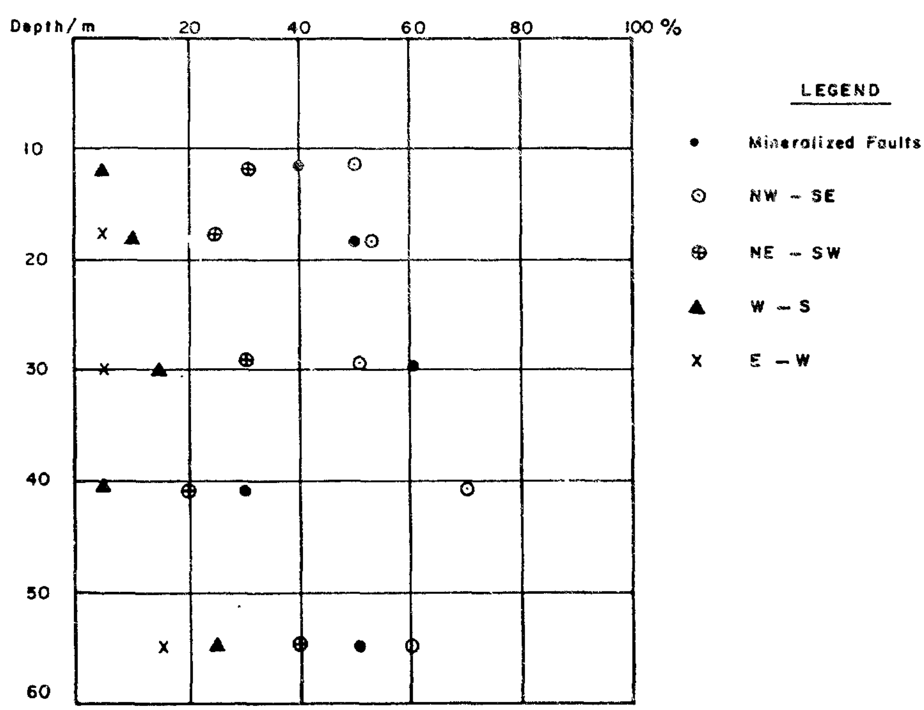

FIG. 5. Diagram representing the mineralized faults and their directions from surface to depth in Talmesi copper mine.

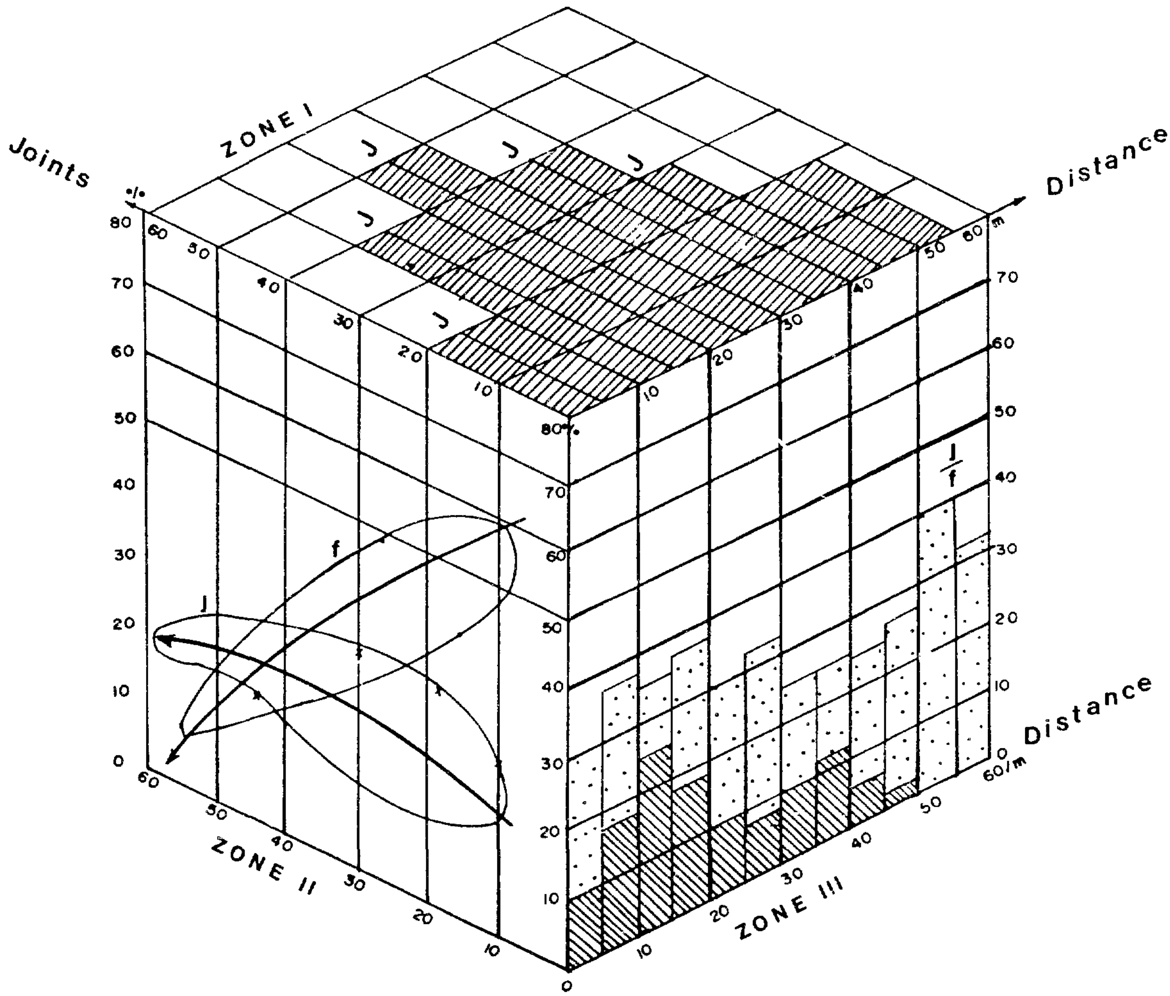

m	J/F %	J/NW-SE%	D/J	J/NE-SW%
12	30	22	30°	12
18	40	30	41°	10
30	45	40	40°	15
42	40	42	45°	20
55	50	50	50°	25
75	63	52	48°	30
93	60	–	–	–

FIG. 6. Three dimensional diagram, representing log normal distribution of joints (I), ratio of joint/fault and direction of joints (II,III).

areas also stock work structures or breccia zones can be recognized. Mineralizing solutions migrated along these strongly tectonized rocks and uranium precipitated in fissures and fractures of some cm to several m length. Present studies indicate that the main mineralization phase is post tectonic as there is no evidence for syntectonic mineral concentrations. At Talmesi the main direction of the usually subvertical mineralized fracture zones is NW-SE, other directions are NE-SW, EW and NS (Fig. 3). About 500 faults have been studied of which about 40 % are mineralized. A greater part of the rest seems to have been mineralized but the uranium has been leached out and most likely again precipitated at depth.

A detailed survey at Talmesi deposit shows quite clearly that the amount of mineralized structures increases to depth (Fig. 3), but there exists no clear correlation between uranium grade and the two main fault directions (Fig. 4). In both mines, i.e. Talmesi and Meskani, there seems to exist no preferred grade or natural cut off of mineralization as shown in Fig. 5: the lower the grade the more mineralized faults. In addition this figure indicates that the average grade at Talmesi Mine is slightly higher than at Meskani Mine.

Based on these findings it is assumed that the oxidation zone at Talmesi Mine is less deep than at Meskani Mine and that at Meskani Mine the average grade of uranium may increase below the deeper developed oxidized or leached zone. To summarize the relationship between faults and joints a three dimensional diagram has been drawn (Fig. 6). The distribution of the joint systems are relative assymetric (zone I). The concentration of joints in percent increases somewhat to depth but the concentration of faults decreases considerably to depth (zone II). The ratio of joints to faults (J/F) has a log normal distribution in respect to the concentration of joints (zone III).

3.2. The age of uranium mineralization in relation to the tectonics

Primary uranium oxides and silicates occur as vein-filling or coatings of fractures or joints around copper and nickel ore. Pitchblende and coffinite are predominant. The mineralization is the result of hydrothermal processes and is of Palaeogene age. A strong remobilization of uranium, however, occurred at late alpine tectonic phase or may be even at a post alpine tectonic phase. Circulating waters which were strongly oxidizing desolved uranium at surface and precipitated uranium at depth (Sarcia (5), Ziegler (6)).

4. CONCLUSIONS

As a result of uranium exploration in the area of the Anarak Polymetallic Zone of Central Iran the following results can be summarized. Hydrothermal activities preconcentrated U, Cu, Ni, Co, Mo along shear zones, but late tectonic movements could have remobilized and reconcentrated uranium and associated elements, which may have led to subeconomic or even economic uranium deposits.

In spite of the fact that there also exists disseminated and impregnated uranium minerals within the host rock it is assumed that the main introduction of uranium has been along shear and fracture zones from source areas of granitic material, which are quite a distance away from the present uranium concentrations.

REFERENCES

(1) STOCKLIN, J., Structural history and tectonics of Iran: A review, Am. Assoc. Petrol. Geol. 52 (1968) 1229-1258.

(2) DAVOUDZADEH, M., Geology and Petrography of the Area north of Nain, Central Iran, Geol. Survey Iran 14 (1972) 66-69.

(3) ESPAHBOD, M.R., GHERTASI, M., BADIZADEGAN, M., ESPHAHANI, M., The investigation of geology and metallogeny of uranium in Talmesi-Meskani deposits (in persian), Atomic Energy Organization of Iran 1 (1982) 10-75.

(4) PLYASKIN, V., KRIVYAKIN, B., KRYATOV, B., MOROZOV, L., PROVOLIEV, S., Report on detailed geological prospection in Anarak area (Central Iran), Technoexport 8 (1982) 10-300.

(5) SARCIA, J.A., Iran-France Technical Cooperation, Sarcia Mission April - July 1959, Technical Report (1959) unpublished.

(6) ZIEGLER, V., A general view of some mineralization in Anarak area, Commissariat a l'Energie Atomique, internal report, Geol. Survey Iran (1961) 180 pp.